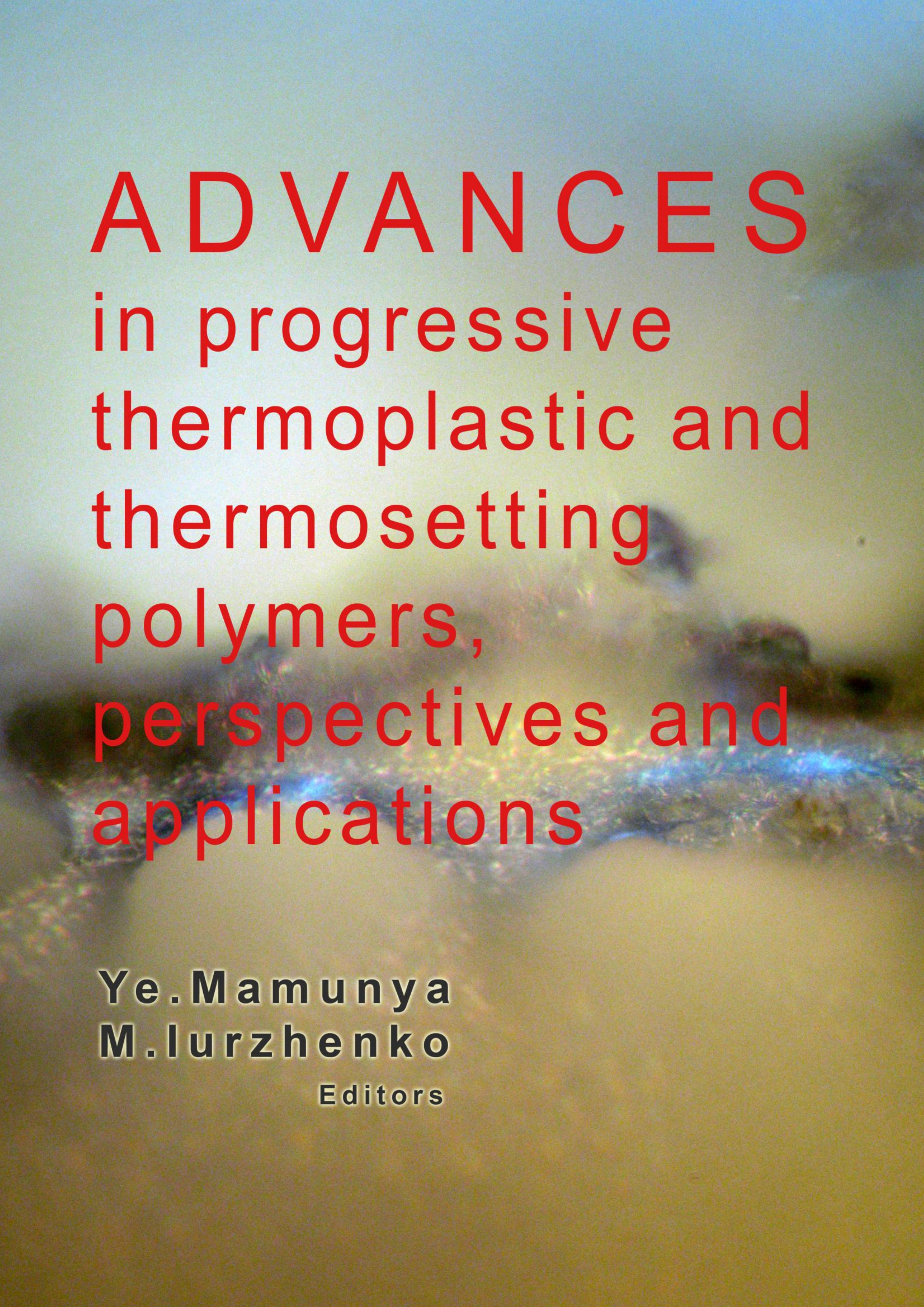

ADVANCES in progressive thermoplastic and thermosetting polymers, perspectives and applications

Ye. Mamunya
M. Iurzhenko
Editors

“If you have no fundamental investigations today you will have nothing to apply tomorrow...”

Prof. N. Bogolyubov,
Director of JINR - Dubna (1966—1988)

Advances in progressive thermoplastic and thermosetting polymers, perspectives and applications

Edited by Ye.Mamunya, M.Iurzhenko

Open access:

Tehnopress editura
http://www.tehnopress.ro

CCUE NASU in IMC NASU
http://www.macromol.kiev.ua/CCUE/

Contributors

AGAPIE Bogdan, PhD student at the Department of Physics and Structure of Polymers of the Institute of Macromolecular Chemistry “Petru Poni” (Romania).

BARANTSOVA Antonina, PhD in Polymer Chemistry, Senior staff scientist at the Department of Chemistry of Oligomers and Netted Polymers of the Institute of Macromolecular Chemistry of the National Academy of Sciences of Ukraine (Ukraine).

BARDASH Liubov, Leading engineer at the Department of Chemistry of Heterochain Polymers and Interpenetrating Polymer Networks of the Institute of Macromolecular Chemistry of the National Academy of Sciences of Ukraine (Ukraine).

BOITEUX Gisèle, Dr.Hab. in Physics, Director of Research CNRS, Université de Lyon, Université Lyon 1, «Ingénierie des Matériaux Polymères», UMR CNRS 5223, IMP@LYON1 (France).

BOIKO Vitaliy, PhD in Polymer Chemistry, Senior staff scientist at the Department of Chemistry of Oligomers and Netted Polymers of the Institute of Macromolecular Chemistry of the National Academy of Sciences of Ukraine (Ukraine).

BUSKO Nataliya, PhD in Polymer Chemistry, Senior staff scientist at the Department of Chemistry of Oligomers and Netted Polymers of the Institute of Macromolecular Chemistry of the National Academy of Sciences of Ukraine (Ukraine).

FAINLEIB Alexander, Professor in Polymer Chemistry, Dr.Hab. in Polymer Chemistry, PhD in Polymer Chemistry, Leading research scientist at the

Department of Chemistry of Heterochain Polymers and Interpenetrating Polymer Networks of the Institute of Macromolecular Chemistry of the National Academy of Sciences of Ukraine (Ukraine).

GAINA Constantin, PhD in Chemistry of the Institute of Macromolecular Chemistry “P. Poni”, Senior researcher at the Department of Polyaddition and Photochemistry of the "Petru Poni" Institute of Macromolecular Chemistry of the Romanian Academy (Romania).

GAINA Viorica, Doctor in Chemistry, Senior researcher at the Department of Polyaddition and Photochemistry of the "Petru Poni" Institute of Macromolecular Chemistry of the Romanian Academy (Romania).

GRANDE Daniel, Dr.Hab in Polymer Chemistry and Physico-Chemistry, PhD in Polymer Chemistry, CNRS Researcher, Adjunct-Director of the “Complex Polymer Systems” Laboratory at the Institut de Chimie et des Matériaux Paris-Est, UMR 7182 CNRS–Université Paris-Est Créteil.

GRIGORYEVA Olga, PhD in Polymer Chemistry, Senior research scientist at the Department of Chemistry of Heterochain Polymers and Interpenetrating Polymer Networks of the Institute of Macromolecular Chemistry of the National Academy of Sciences of Ukraine (Ukraine).

GRISHCHENKO Volodymyr, PhD in Polymer Chemistry, Leading staff scientist at the Department of Chemistry of Oligomers and Netted Polymers of the Institute of Macromolecular Chemistry of the National Academy of Sciences of Ukraine (Ukraine).

GUSAKOVA Kristina, PhD in Polymer Chemistry, Junior research scientist at the Department of Chemistry of Heterochain Polymers and Interpenetrating Polymer Networks of the Institute of Macromolecular Chemistry of the National Academy of Sciences of Ukraine (Ukraine).

IURZHENKO Maksym, Doctor in Polymer Physics, Senior staff scientist at the Department of Polymer Composites of the Institute of Macromolecular Chemistry of the National Academy of Sciences of Ukraine (Ukraine).

LEBEDEV Eugene, Academician, Professor, Dr.Hab. in Polymer Chemistry, PhD in Polymer Chemistry, Director of the Institute of Macromolecular Chemistry of the National Academy of Sciences of Ukraine (Ukraine), Head of the Department of Polymer Composites.

LEVCHENKO Volodymyr, Doctor in Polymer Physics, Staff scientist at the Department of Polymer Composites of the Institute of Macromolecular Chemistry of the National Academy of Sciences of Ukraine (Ukraine).

MAMUNYA Yevgen, Dr.Hab. in Polymer Physics, PhD in Polymer Chemistry, Leading staff scientist at the Department of Polymer Composites of the Institute of Macromolecular Chemistry of the National Academy of Sciences of Ukraine (Ukraine).

MYSHAK Volodymyr, PhD in Polymer Chemistry, Senior staff scientist at the Department of Polymer Composites of the Institute of Macromolecular Chemistry of the National Academy of Sciences of Ukraine (Ukraine).

NECHIFOR Marioara, PhD in Polymer Chemistry, Senior scientist at the Department of Photochemistry of the "Petru Poni" Institute of Macromolecular Chemistry of the Romanian Academy (Romania).

PRISACARIU Cristina, PhD in Chemistry, Senior Scientist II at the Department of Physics and Structure of Polymers of the Institute of Macromolecular Chemistry “Petru Poni” (Romania).

SCORTANU Elena, PhD in Chemistry, Senior Scientist II at the Department of Physics and Structure of Polymers of the Institute of Macromolecular Chemistry “Petru Poni” (Romania).

STAROSTENKO Olga, PhD in Polymer Chemistry, Research scientist at the Department of Chemistry of Heterochain Polymers and Interpenetrating Polymer Networks of the Institute of Macromolecular Chemistry of the National Academy of Sciences of Ukraine (Ukraine).

TANASA Fulga, PhD in Chemistry, Senior researcher at the Laboratory of Polyaddition and Photochemistry of the “Petru Poni” Institute of Macromolecular Chemistry of the Romanian Academy (Romania).

URSACHE Oana, PhD student at the Institute of Macromolecular Chemistry “Petru Poni” of the Romanian Academy (Romania).

ZANOAGA Madalina, PhD in Technical Science, Senior researcher at the Laboratory of Polyaddition and Photochemistry of the “Petru Poni” Institute of Macromolecular Chemistry of the Romanian Academy (Romania).

Contents

HYBRID POLYMER MATERIALS

POLYMER NANOMATERIALS

Preface

Demand of polymeric materials is very high for the up-to-date stage of techniques and newest technologies development. As a result, the yearly growth of the world consumption of polymers is observed. Development of polymer technologies shifts towards the design of functional polymer systems able to provide specific properties (optical, electrical, magnetic, thermal, transport, biological, sensor, etc.). This trend becomes one of the main goals of polymer chemistry, conjugated with investigations on new routes of synthesis and building-up specific structures of functional materials that provide high values of the desired characteristics. Very often such materials have unusual properties compared to conventional polymers, but nevertheless they have to be prospective for some applications.

From this point of view this book reflects the recent trends in the design and synthesis of novel high performance polymeric materials having high thermal resistance, electronic or ionic conductivity, enhanced mechanical properties and other desired characteristics. All these properties are the result of the research on new pathways of obtaining specific morphological structures. The content of the book is divided into three subject parts, namely *Polymer Materials*, *Hybrid Polymer Materials* and *Polymer Nanomaterials*, which include the following chapters:

Chapter 1. **Aromatic Polyamides as High Performance Polymers**

Marioara NECHIFOR

Aromatic polyamides are members of a relevant class of thermally stable polymers that in the past decades have attracted great interest of many research groups, at both academic and industrial level, not only as high performance materials but also for their peculiar conformational structure and superior chemical and physical (especially thermal, mechanical and electrical) properties. The presence of both aromatic and amide groups, differently linked and oriented along the chain, allows the preparation of a wide variety of polyamide structures, ranging from rigid to flexible ones, and endows these engineering polymers with high performance characteristics useful for advanced technologies. Recent literature reports and patents involving aromatic polyamides in high-technology applications, such as electrochromic, luminescent and photosensitive materials, reverse osmosis, gas separation or ion-exchange membranes, optically active materials, nanocomposites, fire-resistant materials, biomaterials, etc relieve the scientific interest for the study, design, synthesis, characterization and applications of these versatile thermally stable polymers.

Chapter 2. **Copolyamides – Versatile Engineering Polymers**

Madalina ZANOAGA, Fulga Mihaela TANASA

Copolyamides are a subject of long lasting interest due to their variety, complex structures, high performance properties, commercial importance, long term use and versatility as engineering polymers. This chapter briefly reviews the main methods of synthesis and fields of application of these polymers, emphasizing their role in the development of fundamental knowledge database (new synthetic methods and protocols) and engineering.

Chapter 3. **Block Copolymers and Composite Polymeric Materials on Their Base**

Volodymyr GRISHCHENKO, Nataliya BUSKO, Antonina BARANTSOVA, Volodymyr MYSHAK, Madalina ZANOAGA, Fulga TANASA

A series of novel thermoplastic diene-styrene and diene-acrylate block copolymers (BCPs) based on an aliphatic copolyamide and an oligodiene having isocyanate end groups was prepared. The synthesis and properties of BCPs obtained by photoinitiated radical polymerization using oligomeric azo- and polyazoinitiators have been investigated. The distributions of molecular weight and viscosity of the BCPs were determined. The morphology, thermal and dynamic - mechanical behavior were investigated by IR spectroscopy, differential scanning calorimetry, dynamic mechanical analysis and small angle X-ray scattering. New polymeric blends based on BCPs and polyethylene waste were obtained and subsequently characterized.

Chapter 4. **Polymeric Materials on the Base of Oligomers with Terminal Functional Groups**

Volodymyr GRISHCHENKO, Antonina BARANTSOVA, Vitaliy BOIKO, Nataliya BUSKO

A progressive method of polymer synthesis without solvents, through a stage of an isocyanate prepolymer (liquid rubber), was developed. On this base, a range of polymeric composites with controlled characteristics and required physical-mechanical properties can be developed. It is a result of using carbochain oligomers with different end groups which can be obtained with the help of specially synthesized initiators for radical polymerization. Using the liquid rubbers with different functional end groups, polymeric materials with properties ranging from sticky adhesives, mild elastic adhesives to strong abrasive-resistance materials resistant over a wide temperature interval, were prepared.

Chapter 5. **Polyurethanes and Their Derivatives**

Cristina PRISACARIU, Elena SCORTANU, Bogdan AGAPIE

This chapter presents new ideas in the fundamentals of conventional and novel PUs and PUUs which can be tailored, by both chemistry and processing, to yield products in a wide variety of forms and which allow the processor to control the nature and the properties of the end product. This review summarizes a series of researches made in the last years on the synthesis, and properties of PUs and PUUs and their sensitivity to molecular structure.

The dibenzyl system represents the simplest biaromatic system able for rotational isomerism which allows multiple spatial arrangements, with different reciprocal influences of the functional groups situated in the two rings. The possibility of introducing this system to a macromolecular chain and its influence on some properties of the polymer obtained was studied of the cases of polyurethanes, polyureas, poly(parabanic acids) and polyimides. Some practical applications of polymers with dibenzyl structures are presented.

Chapter 6. **Recent Developments in Generation of Porous Polymer Materials**

Kristina GUSAKOVA, Olga GRIGORYEVA, Olga STAROSTENKO, Alexander FAINLEIB, Daniel GRANDE

The present chapter summarises the main ways and up-to-date advances on generation of porous materials based on thermostable polymers. The main attention has been paid to basic principles and recent developments of pore generation techniques mainly for film-forming polymer materials suitable for application as membranes, absorbents, filters, etc. Effect of pore generation methods on chemical structure and morphological peculiarities as well as on physical-chemical properties of porous polymers produced have been analysed and summarized.

Chapter 7. **Modern Trends in Progress of Hybrid Organic-Inorganic Polymer Systems**

Maksym IURZHENKO, Yevgen MAMUNYA, Gisele BOITEUX, Eugene LEBEDEV

Hybrid organic-inorganic systems (HOIS) are a new class of polymer materials, high interest to which appeared in recent years. It is explained by their peculiar structure, which includes organic and inorganic units, and, accordingly, possesses their common properties. Such combination provides the opportunity to obtain materials with predefined properties, which are regulated by variation of chemical composition of organic and inorganic components. Considering onrush of up-to-date technology, that require new materials with specific properties, their application area is constantly expanding. Overall, it is often that new hybrid organic-inorganic polymer systems show characteristics, which far exceed the corresponding characteristics of the existing analogs.

Chapter 8. **(Bis)Maleimides for Organic-Inorganic Hybrid Materials**

Viorica GAINA, Oana URSACHE, Constantin GAINA

Remarkably, strategies of hybridization apply to all families of materials: not only to polymers but also to cements and materials for electronics or medical uses. Hybridization intensifies the need for multidisciplinary cooperation: molecular biologists, chemists, chemical engineers, mechanical engineers, electronic engineers and physicists have to collaborate. Thus hybrid materials constitute a composite field of research requiring the knowledge and the know-how of various disciplines. Organic-inorganic hybrid materials offer the opportunity to combine the desirable properties of organic polymers, such as, for example, processability, toughness, and impact strength, with the desirable properties of inorganic materials, such as, for example, high temperature stability, durability, and high modulus.

Since microsynthesis has been successful applied in making computer components, materials scientists have aimed to go beyond the microscale and to build up materials atom by atom (that is at the nanoscale: less than 100 nanometers) in order to make complex materials that can function as devices or micromachines. Again biological systems provided the model.

Chapter 9. **Thermoplastic Polymers Containing Nanofillers**

Volodymyr LEVCHENKO, Yevgen MAMUNYA, Gisele BOITEUX, Eugene LEBEDEV

Polymer nanocomposites filled with nanofillers are intensively investigated during last years due to their valuable properties and the perspectives of application in the various areas. Their physical and electrical characteristics can be close to the properties of those for the nanofiller, whereas the mechanical properties and processing methods are typical for the plastics. The electrical properties of such nanocomposites based on polymers filled with conductive nanofillers are of great interest both for science and technology. In recent years, different kinds of nanoparticles are frequently used together as combined nanofiller to prepare multi-component polymer nanocomposites, in order to study the synergistic effects of different nanofillers. Such combination of two fillers may result in a successful integration of properties of the components in new nanomaterials based on thermoplastics which reveal new valuable characteristics.

Chapter 10. **Thermosetting Cyanate Ester Resins Filled with CNTs**

Alexander FAINLEIB, Liubov BARDASH, Gisele BOITEUX, Olga GRIGORYEVA

In this chapter, a review on synthesis, structure and properties of the novel nanocomposites based on high performance thermosetting polymer matrix, polycyanarate, from Cyanate Ester Resins and the nanofiller, Carbon Nanotubes, is given and the own results of the authors are discussed.

Hence, the content of this book includes different aspects of design and synthesis of polymer materials with specific properties. The variety of effects existing in such systems is caused by the complexity of chemical processes and their kinetic regularities occurring along with the development of chemical structure and formation of the morphological structure. This book brings together some recent advances of research performed during last years in the Institute of Macromolecular Chemistry of the National Academy of Sciences of Ukraine (Kyiv, Ukraine) (partially in collaboration with the Laboratory of Polymer Materials and Biomaterials of CNRS, Université Claude Bernard Lyon 1, and the “Complex Polymer Systems” Laboratory at the Institut de Chimie et des Matériaux Paris-Est CNRS–Université Paris-Est Créteil, France) and in the Institute of Macromolecular Chemistry "Petru Poni" of the Romanian Academy (Iasi, Romania). The societal need for novel hi-tech, easy-to-use, even low cost or non-polluting materials led to an impetuous development of polymer materials science to identify the optimum in the structure-properties-application relationship and to find the best ways (resources, technologies, equipments) to achieve it. We do believe that systematization of accumulated scientific results in the field of design and synthesis of novel progressive high performance polymeric materials will promote further development of existing conceptions, and this book will be found useful by researchers working with dedication in this field of polymer science.

This book is in open access that means the possibility to read, to print and to distribute it (entirely or partially) freely, on the mandatory condition that the original source will be properly cited. The chapters of this book may be republished and used by authors in other publications and using any media, providing the indication of the original source. Copying without indication of this book as the original source is forbidden.

The authors are exceptionally responsible for the information contained in their contributions, citation of original publications, use of materials from different sources, accuracy of text and graphic materials. No responsibility is accepted by editors and publisher concerning the aforesaid points regarding the book.

Acknowledgement. The editors would like to express great gratitude to Dr. Madalina Zanoaga, Dr. Marioara Nechifor and Dr. Fulga Tanasa for their substantial contribution to the preparation of the manuscript for publication.

Editors: Yevgen Mamunya

Maksym Iurzhenko

Polymer
Materials

Chapter 1

Aromatic Polyamides as High Performance Polymers

Marioara Nechifor

„Petru Poni“ Institute of Macromolecular Chemistry, Iasi, Romania

Summary

Aromatic polyamides are members of a relevant class of thermally stable polymers that in the past decades have attracted great interest of many research groups, at both academic and industrial level, not only as high performance materials but also for their peculiar conformational structure and superior chemical and physical (especially thermal, mechanical and electrical) properties. The presence of both aromatic and amide groups, differently linked and oriented along the chain, allows the preparation of a wide variety of polyamide structures, ranging from rigid to flexible ones, and endows these engineering polymers with high performance characteristics useful for advanced technologies. Recent literature reports and patents involving aromatic polyamides in high-technology applications, such as electrochromic, luminescent and photosensitive materials, reverse osmosis, gas separation or ion-exchange membranes, optically active materials, nanocomposites, fire-resistant materials, biomaterials, etc relieve the scientific interest for the study, design, synthesis, characterization and applications of these versatile thermally stable polymers.

Notations and acronyms

3,4′-ODA	3,4′-oxydianiline
DMAc	*N*,*N*-dimethylacetamide
DMF	*N*,*N*-dimethylformamide
CT	charge-transfer
CV	cyclic voltammetry
EC	electrochromic
EL	electroluminescent
HOMO	highest occupied molecular orbital
HMPA	hexamethylphosphoramide
GPC	gel permeation chromatography
IL	ionic liquid
ITO	indium-tin oxide
LOI	limiting oxygen index
LUMO	lowest unoccupied molecular orbital
MPDA	*m*-phenylenediamine
Mw	weight-average molecular weights, g/mol
Mn	number-average molecular weights, g/mol
MW	microwave radiation
NMP	*N*-methyl-2-pyrrolidone
NF	nanofiltration
PF	polyfluorene
PL	photoluminescence
PMPI	poly(*m*-phenylene isophthalamide)
PPBA	poly(*p*-benzamide)
PPDA	*p*-phenylenediamine
PPPT	poly(*p*-phenylene terephthalamide)
PPV	poly(1,4-phenylenevinylene)
Py	pyridine
RO	reverse osmosis
Td_5	temperature at which 5% weight loss occurred, recorded by TGA, °C
Td_{10}	temperature at which 10% weight loss occurred, recorded by TGA, °C
Tg	glass transition temperature, °C
TFC	thin film composite
TGA	thermogravimetric analysis
Tm	melting temperature, °C
TMA	thermomechanical analysis
TPA	triphenylamine
TPC	terephthaloyl dichloride
TPP	triphenylphosphite
Ts	softening temperature, °C

1. Introduction

The development of high performance/high temperature polymers begun during the 1960s in order to satisfy the thermal stability requirements of the aerospace, automotive, military and electronic industries where high strength and dimensional stability are required at high temperatures. These polymers are characterized by specific properties, such as high thermooxidative and thermal stability, high glass transition temperatures, outstanding mechanical properties (tensile and impact strength), excellent resistance to solvents and radiation, high conductivity, low specific density, high electrical or sound insulation properties, superior flame resistance allowing exposure at elevated temperatures and good resistance in harsh environments. Aromatic polyamides are a subject of lasting and growing interest because of their variety, complex internal structures, commercial importance, versatility and long-term use, and various synthesis methods. They have gained a respected place among polymeric materials and, although they have been outperformed in some applications by newer better-suited formulations, they remain important in both volume and in their ability to meet specific needs.

Wholly aromatic polyamides, as representative members of high performance polymeric materials, have been used as heat-resistant and high-tensile strength chemical fibers in aerospace and military applications, for bulletproof vests, welders' protective shields, flame-resistant and heat protective clothing, industrial filters, sport fabrics, optical fiber cable systems, advanced polymer matrix composites, reinforcement of rubbers, concrete and thermoplastic pipes, insulation films for electrical motors and transformers, conveyor belts and circuit boards, advantageous replacements for metals or ceramics in currently used goods, in asbestos substitutes and many others or even as new materials in novel technological applications.

However, wholly aromatic polyamides are characterized by the rigidity of the backbone and strong intermolecular interactions through hydrogen bonding, which result in poor solubility in common organic solvents and extremely high melting or glass transition temperatures, which lie above their decomposition temperatures. These properties make them generally intractable or difficult to process and therefore their applications are restricted. Consequently, recent basic and applied research has focused on enhancing their processing characteristics and solubility in order to extend the technological applications of these materials.

This current chapter sets out to review the design, synthesis, characterization and potential applications of new aromatic polyamide structures reported in the literature during the last decade.

2. Commercial aromatic polyamides

Aromatic polyamides are produced commercially for two major end uses: (1) flame and heat resistant polymers in the form of fibers, films, molding powders, and papers, and (2) polymers with extended chains for high strength, high modulus fibers. The polymers belonging to the second class give liquid crystalline solutions, which make possible the direct formation of highly oriented, high strength fibers. Aramid fibers of this type are useful in cut resistant clothing, ballistics protection, asbestos replacement, ropes and cables, and reinforcement of resins and rubber.

Aromatic polyamides were first introduced in commercial applications in 1967, with a *meta*-aramid fiber produced by DuPont under the trade name Nomex (PMPI). According to the US Federal Trade Commission, aramid fibers are synthetic polymers in which at least 85% of the amide (-CO-NH-) linkages are attached directly between two aromatic rings. Nomex fiber, which handles similarly to normal textile apparel fibers, is characterized by the manufacturer as an “inherently flame-resistant, high-temperature fiber that will not melt, drip or support combustion in air. It also delivers outstanding resistance to a broad range of chemicals and is offered in paper, felt, fabric and fiber forms”. Due to all-*meta* orientation of the phenylene rings, PMPI has a non-linear structure, which leads to a simultaneous reduction of its cohesive energy and crystallization tendency. Because of its high thermal and mechanical resistance, PMPI is used extensively in the production of protective apparel, air filtration, thermal and electrical insulation as well as a substitute for asbestos.

The first commercialized all-*para* oriented aramid was PPBA (marketed by Du Pont under the Fiber B trading name). Probably due to economic reasons or because PPBA is only about one-half as strong as PPPT *[Preston, 1988]*, its production lasted for a short time. The polymer was prepared by a low-temperature solution method using polar aprotic solvents (DMAc or NMP containing LiCl), which yielded a stiff, semicrystalline polymer soluble only in the same solvents used for its preparation. Films and fibers were obtained from these polymer/solvent systems, which exhibited lyotropic behavior. PPBA was replaced on the market by PPPT in 1973 under the trade name of Kevlar, probably the best known of the wholly aromatic class of polyamides. Compared with the best of the aliphatics, it provides a doubling or tripling of strength and more than.

The synthesis of PMPI and PPPT was performed at low temperatures in a solution of TPC, MPDA and PPDA, respectively, in HMPA. Later, the solvent was successfully replaced by a NMP/$CaCl_2$ system. PPPT presented a lower insolubility than PPBA and could be transformed into fibers by spinning from lyotropic solutions in concentrated sulfuric acid at high temperatures. The macromolecular chains in Kevlar are highly oriented with strong inter-chain bonding, which results in a unique combination of properties. It is well understood that the microstructure of Kevlar is the main reason for its outstanding properties. These fibers present an inherently extended rigid chain structure caused by the interplay of *para*-linked benzene rings and partial double-bond character of the *trans*-amide linkages. In addition to the rigid chemical structure, the hydrogen-bonding network in aromatic polyamides plays an important role in their thermomechanical properties. The combination of the high persistence length and inter-chain attraction leads to materials with high mechanical strength and excellent thermal resistance. Unlike PMPI with its crystalline/amorphous regions, PPPT is considered a crystalline material, interrupted only by imperfections. Kevlar forms hydrogen bonded sheet-like structure due to highly favorable intramolecular hydrogen bonds. The sheets stack together radially, as determined by wide-angle X-ray diffraction studies. Kevlar *para*-aramid fiber possesses a remarkable combination of properties that has led to its adoption in a variety of end-uses since its commercial introduction in the early 1970's. Because all-*para* aramids are characterized by melting temperatures higher than their thermal decomposition ones, liquid crystalline mesophases of the above polymers can be obtained only in solution. Their processing from the partially ordered state (the lyotropic mesophase) leads to materials characterized by superior mechanical properties (high elastic modulus, high tenacity, etc.).

Another aramid fiber is a copolymer synthesized from TPC, PPDA and 3,4′-ODA, and commercialized since 1987 under the trading name Technora, with a TPC/PPDA/3,4'-ODA mole ratio of 100/50/50. Copolymerization has provided the opportunity for improved solubility, increased thermal stability as well as better fiber properties. Technora was processed by dry-jet wet spinning from NMP solution. Recent reports have evidenced that the physical properties of Technora fibers such as tenacity, elongation, and modulus depend on the molar ratio of the two diamines, and there is an optimum composition for obtaining excellent physical properties. Technora fibers are used in ropes, hoses, optical cables, sails for windsurfing boards, etc. *[Preston, 1988; Vollbracht 1989; Gaymans, 2003; Fink, 2008]*. The chemical structures of the earliest, simplest, and best-known commercial aramids are presented in Scheme 1.

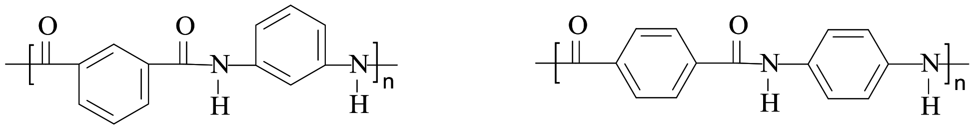

PMPI, Nomex **PPPT, Kevlar**

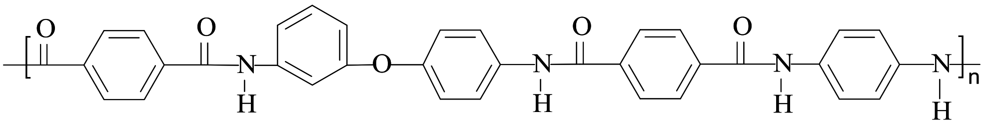

ODA/PPPT, Technora

Scheme 1. The structure of the commercial aromatic polyamides

3. Synthesis of the aromatic polyamides

Although the thermal polymerization is a well-known industrial process for the synthesis of aliphatic polyamides with high molecular weights, it is difficult to obtain aromatic polyamides with high molecular weights by molten PC. This has been mainly explained by the lower reactivity of aromatic diamines compared with that of aliphatic diamines (the resonance effect of phenyl groups). The high reaction temperatures usually result in low molecular weight polymers due to extensive side reactions, such as decarboxylation of aromatic diacids and oxidation or sublimation of aromatic diamines. Consequently, there have been developed different PC reactions at low temperatures, which avoid the thermal degradation of the monomers and resulted polymers. There are two conventional methods for the synthesis of aromatic polyamides. One is the low-temperature solution polymerization, which involves aromatic dicarboxylic acid chlorides and aromatic diamines (the Schotten-Baumann reaction). This approach is the most versatile method for preparing aromatic polyamides even though the use of acid halides is environmentally undesirable. There are two principal types of low-temperature PC: the two-phase process, known as interfacial PC, and a single liquid phase process or solution PC. The other is the high-temperature solution polymerization, a direct condensation reaction between aromatic dicarboxylic acid and aromatic diamines, which is performed in the presence of condensing agents.

Low-temperature solution PC takes place in amide type solvents, such as NMP, DMF, DMAc, and HMPA. The solvating power of these organic solvents is greatly increased by the addition of solubility promoters, such as lithium chloride, calcium chloride or a mixture of both, because the cations interact with the amide groups, diminishing the strength of the inter-chain hydrogen bonds. The concentrated polymer solutions thus obtained could be used for wet spinning of fibers or casting films. PPPT and PMPI are prepared industrially by this method, also Tehnora, but in the absence of inorganic salts. An alternative route to this method uses silylated aromatic diamines with a higher reactivity than that of parent ones. The reaction is performed *in situ* to avoid the isolation and purification of the moisture sensitive silylated diamines.

Interfacial PC is a rapid and irreversible polymerization occurring at the interface between an inert immiscible organic solvent containing a diacid chloride and water containing an aromatic diamine, a base and a surfactant. Due to asymmetric solubility, a very fast reaction takes place on the organic side and the polymer precipitates quickly, forming a thin dense film. The film thickness may be of the order of tens of nanometers up to several microns, and is affected by the monomer concentration as well as the ratio between reactant concentrations. The film growth rate increases until diffusion of monomers through the film starts to be limited. The termination of the reaction is explained by slower diffusion of diamines through the film as well as by hydrolysis of the acid chlorides that blocks the diamines and competes with the polymerization. The rate of polymer production depends mainly on the solvent, monomer concentration and interfacial area available for reaction. The success of the method in producing defect-free ultrathin films is due to two effects, self-sealing and self-termination because of the growing resistance of the film. Unlike solution PC, the reagents need not to be pure or in stoichiometric amounts, but the resulted polymers have broad molecular weight distributions that are considered to be unsuitable for fibers or film-forming materials. Even the proper choice of the PC conditions, such as the organic solvent type, solvent volume, monomer concentration, and stirring rate, leads to aromatic polyamides with properties similar with those prepared *via* solution PC methods, the interfacial PC has not commercial importance *[Elias, 2007; Garcia et al., 2010]*.

High-temperature solution PC has proved to be more efficient and convenient compared with low-temperature PC. This method avoids the tedious and difficult synthesis and handling of aggressive, highly toxic, heat sensitive or easy hydrolysable diacid chlorides. Since 1975, when Yamazaki and colab. have reported the phosphorylation PC, this reaction has been applied extensively to polyamide synthesis because of its effectiveness. This technique employs activating/condensing agents, which are reagents that enable the *in situ* activation of the aromatic acid *[Yamazaki et al., 1975]* or aromatic diamine *[Aharoni et al., 1984]*. The reaction systems include, generally, the aromatic reagents, activating agent (the most widely used is TPP), solvents (*i. e.*, NMP and Py), as well as alkaline salts (LiCl or/and $CaCl_2$). The temperature depends on the reaction system, but it is much lower compared with melt PC (usually at the boiling temperature of the solvent or mixture of solvents). The drawbacks of this method are the high purity of the monomers and the side reactions evolving at the high temperatures used.

There are several alternative polymerization methods reported in the literature, such as the direct PC of aromatic diacids with aromatic diisocyanates, aromatic diacids with diamines in the presence of thionyl chloride as activating agent, aromatic diacids with the formamidinium salts of aromatic diamines or using aromatic diamines with aromatic diacid phenyl esters, aromatic diamines with dihaloaryl compounds by a palladium-catalyzed carbonylation-PC, etc.

In the recent years, alternative routes to this synthetic method use either MW as nonconventional energy source or ILs as environmental friendly solvents to promote the condensation of aromatic acids and diamines under Yamazaki conditions. Following the first approach, the reaction time is shortened from 3-4h to approx. 2-3min. The second one avoids the harmful solvents used either in low- or high-temperature PC. Both methods applied to polymers having identical structures lead to polymers with inherent viscosities comparable with those obtained using conventional heating system or common organic solvents.

4. Aromatic polyamides with special properties

As stated above, wholly aromatic polyamides are characterized by high melting and glass transition temperatures and restricted solubility in the most organic solvents. Poor processability of these polymers has been a limiting factor for their wider use. Expanding their applications involves improving the processing characteristics of these relatively intractable polymers. Intense efforts and numerous studies have aimed at various modifications of these rigid-rod polymers and their converting into fusible and/or soluble analogues. There are several methods reported in literature and employed to enhance the polymer processability and all of them consist in introduction of specific functional groups into the backbone or side chain in order to destroy inter-chain hydrogen bonds, to interrupt the symmetry and to reduce the rigidity and crystallinity of macromolecular chains. There have been demonstrated that the chemical, thermal and mechanical properties of the resulted polymers are lower compared with the corresponding unsubstituted analogues.

Some of the successful approaches used to increase the solubility are as follows: introduction of flexible segments, bulky pendant groups, non-coplanar or heterocyclic structures into the polymer chain, replacing symmetrical aromatic rings by unsymmetrical ones, etc. There are two distinct locations where a side substituent may be attached: (a) the hydrocarbon part of the monomer segment, and (b) the amide link, specifically to the nitrogen atom of the link. If the attachment is on the non-amidic part, then the substituent is usually part of the monomer; if on the amide link, then the substituent is usually added after polymerization. Considering non-amidic locations first, some instances have already been noted of monomers possessing alkyl pendant groups that are non-reactive and have little or no effect on the progress of the polymerization. The purpose of providing such an inert addition is generally to affect the size and molecular packing of the crystalline regions. Other, more reactive, pendant groups may be introduced to allow bonding to other compounds or to provide functionality for such purposes as dyeing, flame retardancy, optical activity, electrochromism and photoluminescence, photoreactivity, etc., or to improve physico-chemical properties in order to achieve tailored macromolecules for specific end applications. Similarly, it has been suggested that *N*-substitution of aromatic amide groups strongly decreases the stiffness of the polyamide chain, increasing at the same time its solubility in common organic solvents, owing to its capability of destroying hydrogen bonding. Good solubility, moderate *Tg* or *Ts* values, and good thermal stability make these functionalized polyamides as promising high-performance polymers.

4.1 Electrochromic and luminescent aromatic polyamides

Triarylamine derivatives are well known for their photo and electroactive properties and have attracted considerable interest as photoconductors and hole-transport materials for use in multilayer organic EL devices due to their relatively high mobility and low ionization potential. The feasibility of spin-coating and ink-jet printing processes for large-area EL devices and possibilities of various chemical modifications (to improve emission efficiency and allow patterning) make polymeric materials containing TPA units very attractive. To enhance the hole injection ability of polymeric emissive materials, several hole-transporting units having an emissive π-conjugated core, such as triarylamine, carbazole or phenoxazine groups, are deliberately introduced into the main chains or grafted as side chains or attached onto the polymer chain-ends or the outer surface of dendritic wedges. The introduction of these bulky pendent groups into the structure of the aromatic polyamides interrupts the inter-chain hydrogen bonding and reduces the chain-packing efficiency. Therefore, the solubility is enhanced while maintaining high *Tg*'s or *Ts*' through decreased segmental mobility resulted from steric hindrance.

The characteristic structural feature of TPA is the nitrogen atom, the electroactive site of TPA, which is linked to three electron-rich phenyl groups in a propeller-like geometry. TPA can be easily oxidized to form stable radical cations, and the oxidation process is always associated with a noticeable change of color. The anodic oxidation pathway of TPA leads to an unstable electrogenerated TPA cation radical, which forms a dimer (tetraphenyl-benzidine) by tail-to-tail (*para*-positions) coupling reaction, along with the loss of two protons per dimer. When the phenyl groups have electron-donating substituents at their *para*-positions, the coupling reactions are greatly prevented by generating stable cationic radicals and lowering the oxidation potential.

TPA-based polymers are not only widely used as hole-transport layers in EL devices, but also show interesting EC behavior. Electrochromism is a phenomenon in which electroactive materials present a reversible change in optical properties when they are electrochemically oxidized or reduced. EC materials, both organic and inorganic, have promising applications such as automatic antiglazing mirrors, smart windows, EC displays, and chameleon materials. EC applications based on π-conjugated polymers have received increased attention owing to their ease of color-tuning, fast switching times, and high contrast ratios *[Liou et al., 2006a, 2008]*.

Two series of TPA-based polyamides with strong fluorescence emissions in the blue region and high quantum yields up to 64% (**PA1**) and 40% (**PA2**) have proved that incorporating a *para*-methyl/methoxy-substituted TPA group into the polymer backbone not only enhanced the processability of the rigid polymer backbone while maintaining good thermal stability but also provided stability for the EC characteristics: lower HOMO values, excellent electrochemical stability and EC characteristics, changing color from the pale yellowish neutral form to the pale blue oxidized form (Scheme 2) *[Liou et al., 2006b, 2006c]*. All these aromatic PAs were highly soluble in polar solvents and afforded transparent and flexible films. Consequently, they are potential candidates for practical applications by spin- or dip-coating processes. They exhibited good thermal stability with insignificant weight loss up to 380°C (**PA2**) and 400°C (**PA1**) in nitrogen. The Td_{10}'s in nitrogen and air were recorded in the range of 460-500 and 455-485°C, respectively, for polyamides **PA2** and of 482–580 and 476–568°C, respectively, for polyamides **PA1**. Their *Tg′*s were observed in the range of 267-307°C (**PA2**) and 252–309°C (**PA1**). These polymers exhibited strong UV–vis absorption bands at 352–370nm (**PA1**) and 360-370nm (**PA2**) in NMP solutions, which were assignable to the $\pi\rightarrow\pi^*$ transition resulting from the conjugation between the aromatic rings and nitrogen atoms. Their PL spectra in NMP solution and polymer thin film showed maximum bands at 439-535nm (**PA1**) and at around 465nm (**PA2**) in the blue region. These methyl/methoxy-substituted TPA polyamides have great potential as new blue light emitting hole-transporting and EC materials because of their proper HOMO values and excellent electrochemical and thermal stability.

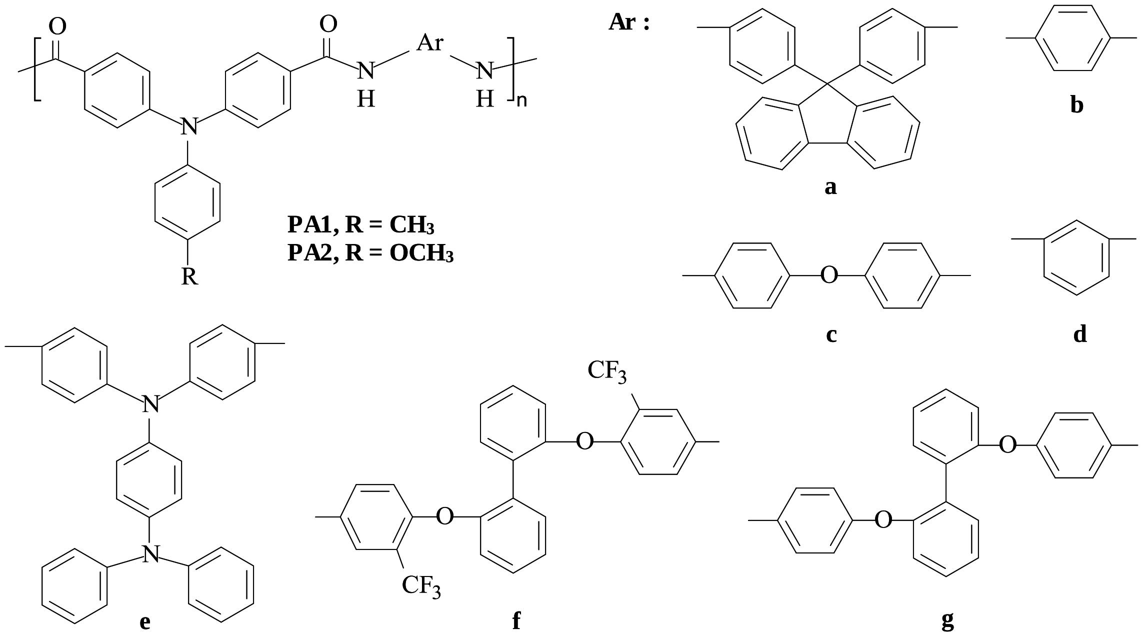

Scheme 2. Structures of polyamides **PA1(a-g)** and **PA2(a-g)**

Continuing with the electron-rich TPA core, three *N*,*N*,*N′*,*N′*-tetraphenyl-*p*-phenylenediamine derivatives were used to prepare three series of novel EC aromatic polyamides with pendent TPA units (Scheme 3) *[Chang et al., 2008; Liou and Chang, 2008; Su et al., 2005]*. The *N*,*N*,*N′*,*N′*-tetraphenyl-*p*-phenylenediamine is an anodic EC compound, and emits different colors depending on the oxidation state. All polymers were amorphous with good solubility in organic solvents, such as NMP and DMAc, and could be solution-cast into tough and flexible polymer films with good mechanical properties. These aromatic PAs had useful levels of thermal stability associated with relatively high *Ts*, Td_{10} in excess of 510°C, and char yields at 800°C in nitrogen higher than 63% (Tables 1 and 2).

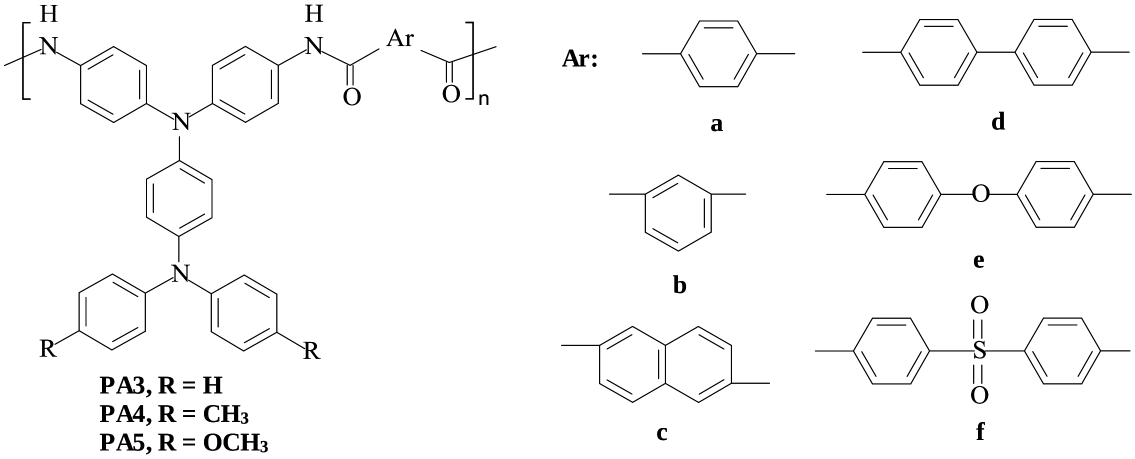

Scheme 3. Structures of polyamides **PA3-5(a-f)**

They exhibited in NMP solutions strong UV-vis absorption peaks at 307–358nm (**PA3**) and 308-351nm (**PA5**) and PL peaks around 532–590nm (**PA3**) and 434-485nm (**PA5**) in the green region (Tables 3 and 4).

Table 1. Inherent viscosities and thermal properties of polyamides **PA3(a-f)** *[Reprinted with permission from Su et al., 2005. Copyright 2005, Wiley Periodicals, Inc.]*

Polymer	η_{inh} [a] (dl/g)	*Tg* (°C)	*Ts* (°C)	Td_5 (°C)	Td_{10} (°C)	Char yield[b] (%)
PA3a	0.60	276(295)[c]	273(297)	514	574	68
PA3b	0.27	265(289)	260(271)	500	562	77
PA3c	0.52	276(307)	261(315)	525	592	80
PA3d	0.88	290(302)	283(304)	530	591	75
PA3e	0.53	263(273)	248(269)	504	546	71
PA3f	0.53	287(295)	280(292)	486	549	67

[a] Measured at a polymer concentration of 0.5g/dL in DMAc at 30°C; [b] At 800°C in nitrogen; [c] The values in parentheses belong to unsubstituted analogues polyamides having the structure:

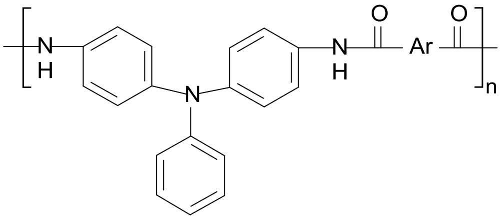

The cutoff wavelengths (absorption edge) evidenced in UV–vis transmittance spectra are also indicated in Tables 3 and 4 and were located in the range of 431–533nm (**PA3**) and 408-455nm (**PA5**). The cutoff wavelengths increased with increasing electron affinity of the corresponding diacid residue, and this suggested that the coloration of the polymer films was caused by CT interactions. The Stokes shifts [PL wavelength (λ_{PL}) - absorption wavelength (λ_{abs})] of the PAs in solution or film were around 200nm or even higher. This phenomenon could be attributed to the CT interactions between intrinsic electrondonating TPA-containing diamine and various aromatic dicarboxylic acids as electron-acceptor moieties.

Table 2. Inherent viscosities and thermal properties of polyamides **PA5(a-f)** *[Reprinted with permission from Liou and Chang, 2008. Copyright 2008, American Chemical Society]*

Polymer	η_{inh}[a] (dl/g)	*Tg* (°C)	*Ts* (°C)	*Td$_5$* (°C)	*Td$_{10}$* (°C)	**Char yield**[b] (%)
PA5a	0.31	248	242	480	510	69
PA5b	0.37	267	274	485	520	71
PA5c	0.49	266	255	495	530	71
PA5d	0.80	282	282	470	520	68
PA5e	0.60	248	233	495	530	67
PA5f	0.33	269	259	480	510	63

[a] Measured at a polymer concentration of 0.5g/dL in NMP at 30°C; [b] At 800°C in nitrogen.

Table 3. Optical properties for the aromatic polyamides **PA3(a-f)** *[Reprinted with permission from Su et al., 2005. Copyright 2005, Wiley Periodicals, Inc.]*

Polymer	$\lambda_{abs,max}$[a] (nm)	$\lambda_{abs,onset}$[a] (nm)	λ_{PL}[b] (nm)	λ_0[c] (nm)
PA3a	358(317)	422(469)	556	508
PA3b	349(341)	409(429)	546	464
PA3c	310(331)	449(477)	590	512
PA3d	307(322)	435(450)	557	494
PA3e	348(341)	398(421)	532	446
PA3f	321(324)	467(494)	572	533

[a] UV–vis absorption measurements in NMP. The values in parentheses are for polymer films; [b] PL spectroscopy measurements in NMP; [c] Cutoff wavelengths from the transmission UV–vis absorption spectra of polymer films.

The electrochemical behavior of the polyamide **PA3,4** and **5** series was investigated by CV conducted by film cast on an ITO-coated glass substrate as the working electrode in dry CH_3CN containing 0.1M of tetrabutylammonium perchlorate as electrolyte under nitrogen atmosphere. By comparison the typical cyclic voltammograms for polyamides **PA5d** (with 4,4′-dimethoxysubstituents) and **PA3d** (without 4,4′-dimethoxysubstituents) some conclusions were drawn.There were two reversible oxidation redox couples at $E_{1/2}$ values of 0.48 (E_{onset}=0.36) and 0.84V for **PA5d** and 0.57 (E_{onset}=0.44) and 0.95V for **PA3d** in the oxidative scan. Because of the stability of the films and the good adhesion between the polymer and ITO substrate, polyamide **PA4g** exhibited excellent reversibility of EC characteristics in 1000 continuous cyclic scans between 0.0 and 0.98V, changing color from colorless to green and then blue at electrode potentials ranging over 0.48 and 0.84V. Comparing electrochemical data, the authors found that polyamide **PA5d** was more easily oxidized than polyamide **PA3d** (0.48 *vs* 0.57V). The first electron removal for polyamide **PA5d** was assumed to occur at the N atom on the pendent 4,4′-dimethoxytriphenylamine groups, which was more electron-richer than the N atom on the main chain TPA unit. The introduction of electron-donating 4,4′-dimethoxytriphenylamine not only greatly prevented the coupling reaction but also lowered the oxidation potentials of the electroactive polyamides **PA5** as compared with the corresponding polyamides **PA3** without methoxy substituent. The energy of the HOMO and LUMO levels of the investigated polyamides could be determined from the oxidation onset or half-wave potentials and the onset absorption wavelength of polymer films, and the results are listed in Tables 5 and 6.

Table 4. Optical properties for the aromatic polyamides **PA5(a-f)** *[Reprinted with permission from Liou and Chang, 2008. Copyright 2008, American Chemical Society]*

Polymer	**λ, solution** (nm)		**λ, film** (nm)			
	abs_{max}	**PL_{max}** [a]	**λ_0** [b]	**abs_{max}**	**abs_{onset}**	**PL_{max}** [a]
PA5a	351	452	421	357	453	-
PA5b	311	443	445	363	484	-
PA5c	313	434	445	329	488	-
PA5d	308	444	441	327	473	-
PA5e	351	485	408	352	420	-
PA5f	333	439	455	335	506	-

[a] They were excited at the abs_{max} for both films and solutions; - :No discernible PL_{max} was observed; [b] The cutoff wavelength from the UV-vis transmission spectra of polymer films.

EC of polyamides thin films was examined by an optically transparent thin-layer electrode coupled with UV-vis spectroscopy. All these PAs exhibited similar EC properties, and similar EC transmittance spectra. When the applied potential increased positively from 0 to 0.70V, the peak of transmittance at 348nm, characteristic for neutral form of polyamide **PA5d**, decreased gradually. Two new bands grew up at 430and 1035nm due to the first stage oxidation. When the potential was adjusted to a more positive value of 0.98V, corresponding to the second step oxidation, the peak of characteristic absorbance decreased gradually and one new band grew up at 850nm. Meanwhile, the film changed from original colorless to green and then to a blue oxidized form. Polymer **PA5d** exhibited high contrast of optical transmittance change (Δ*T* %) up to 60% at 430nm and 73% at 1035nm for green, and 86% at 850nm for blue.

Table 5. Electrochemical properties of the aromatic polyamides **PA3(a-f)** *[Reprinted with permission from Su et al., 2005. Copyright 2005 Wiley Periodicals, Inc.]*

Polymer	**Oxidation**[a] (V)		**ΔE**[b] (eV)	**HUMO**[c] (eV)	**LUMO**[d] (eV)
	first	**second**			
PA3a	0.58	0.96	2.64	4.89	2.25
PA3b	0.58	0.96	2.89	4.89	2.00
PA3c	0.58	0.95	2.60	4.89	2.29
PA3d	0.63	1.00	2.76	4.94	2.18
PA3e	0.63	1.00	2.95	4.94	1.99
PA3f	0.65	1.03	2.51	4.96	2.45

[a] *vs* Ag/AgCl in CH_3CN; [b] The data were calculated from polymer film by the equation: $\Delta E = 1240/\lambda_{onset}$; [c] The HOMO energy levels were calculated from CV and were referenced to ferrocene (4.8eV); [d] LUMO= HOMO -ΔE.

Table 6. Electrochemical properties of the aromatic polyamides **PA5(a-f)** *[Reprinted with permission from Liou and Chang, 2008. Copyright 2008, American Chemical Society]*

Polymer	**Oxidation**[a] (V)				**HUMO**[c] (eV)		**LUMO**[d] (eV)	
	first		**second**		**$E_{1/2}$**	**E_{onset}**	**$E_{1/2}$**	**E_{onset}**
	$E_{1/2}$	**E_{onset}**	**$E_{1/2}$**	**E_g**[b] (eV)				
PA5a	0.50	0.38	0.82	2.74	4.86	4.74	2.12	2.00
PA5b	0.49	0.36	0.86	2.56	4.85	4.72	2.29	2.16
PA5c	0.49	0.36	0.86	2.54	4.85	4.72	2.31	2.18
PA5d	0.48	0.34	0.84	2.62	4.84	4.70	2.22	2.08
PA5e	0.48	0.36	0.84	2.95	4.84	4.72	1.89	1.77
PA5f	0.47	0.37	0.85	2.45	4.83	4.73	2.38	2.28

[a] *vs* Ag/AgCl in CH_3CN; [b] The data were calculated from polymer film by the equation: $E_g = 1240/\lambda_{onset}$; [c] The HOMO energy levels were calculated from CV and were referenced to ferrocene (4.8eV); [d] LUMO =HOMO-Eg.

Electrochromic aromatic PAs presented in Scheme 4 have a great potential for use in opto-electronic applications *[Hsiao et al., 2009]*. They had *Tg*'s of 269–296°C, Td_{10} higher than 544°C, and char yields at 800°C in nitrogen greater than 62%. The dilute solutions of these PAs in NMP exhibited strong absorption bands centered at 316–342nm and PL maxima around 362–465nm in the violet-blue region. CV of the polyamide films cast onto ITO-coated glass substrate exhibited two reversible oxidation redox couples at 0.57–0.60V and 0.95–0.98V *versus* Ag/AgCl in CH_3CN solution. The PA films revealed excellent electrochemical and EC stability, with a color change from a colorless or pale yellowish neutral form to green and blue oxidized forms at applied potentials ranging from 0.0 to 1.2V. These anodically coloring polymeric materials showed interesting EC properties, such as high coloration efficiency (CE=216cm^2/C for the green coloring) and high contrast ratio of optical transmittance change (ΔT%) up to 64% at 424nm and 59% at 983nm for the green coloration, and 90% at 778nm for the blue coloration. The electroactivity of the polymers remained intact even after cycling 500times between their neutral and fully oxidized states.

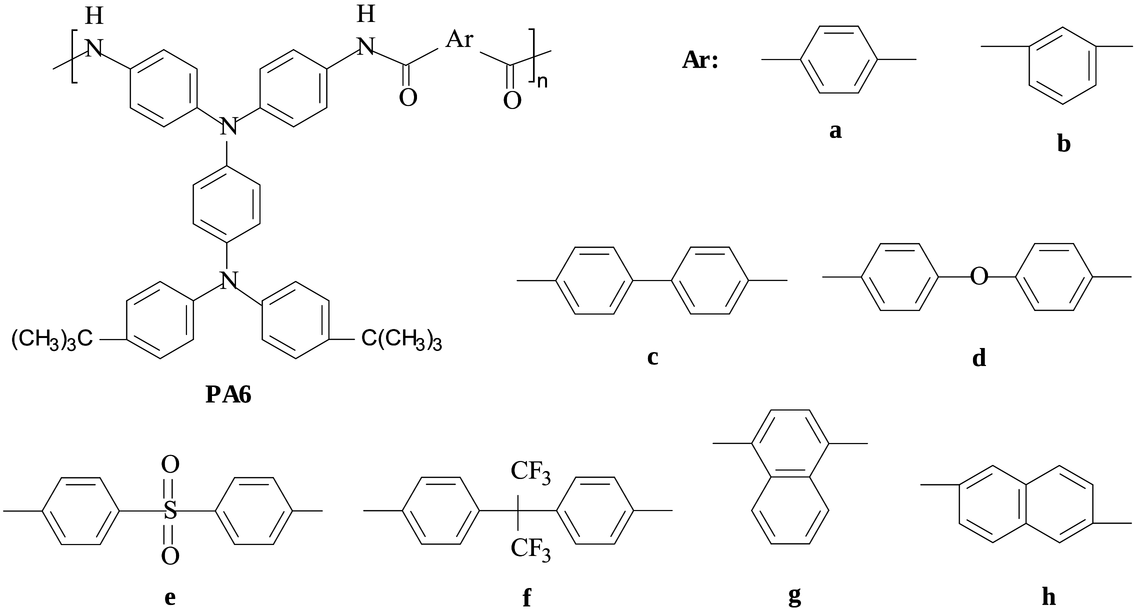

Scheme 4. Structures of polyamides **PA6(a-h)**

A series of TPA-containing aromatic polyamides having a crank and twisted noncoplanar structure is outlined in Scheme 5 *[Liou, 2006d]*. These polymers had inherent viscosities of 0.14–0.64dL/g and useful levels of thermal stability associated with relatively high *Tg*′s (174–311°C). They exhibited strong UV–vis absorption bands at around 300nm in NMP solutions. The PL spectra of these polymers in NMP solutions showed maximum peaks around 396–479nm. Their hole-transporting and EC properties were examined by electrochemical and spectroelectrochemical methods. Cyclic voltammograms of the polymer films cast onto an ITO-coated glass substrate exhibited two reversible oxidation redox couples at potentials of 0.70–1.01V *vs* Ag/AgCl in CH_3CN solution. The polymer films revealed EC characteristics, with a color change from neutral pale yellowish to green and then to a blue oxidized form at applied potentials ranging from 0.00 to 1.75V.

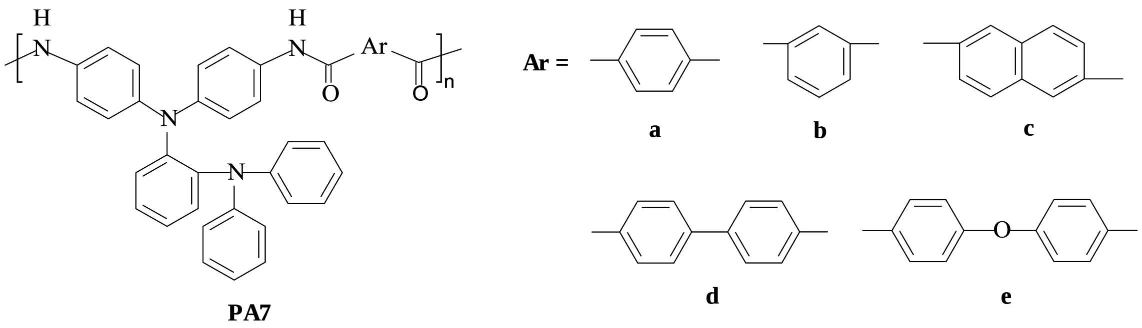

Scheme 5. Structures of polyamides **PA7(a-e)**

Carbazole is another well-known hole-transporting and EL unit. Polymers containing carbazole moieties in the main chain or side chain have attracted much attention because of their unique properties, which allow various optoelectronic applications as photoconductive, EL and photorefractive materials. From a structural point of view, carbazole differs from diphenylamine in its planar structure because it can be further imagined as bonded diphenylamine; therefore, the thermal stability of materials with carbazolyl units was improved. In addition, carbazole can be easily functionalized at the (3,6), (2,7) or *N*-positions and then covalently linked into polymeric systems, both in the main chain as building blocks and in the side chain as pendent groups.

Some aromatic PAs with pendent *N*-phenylcarbazole units are potential candidates in the development of dynamic EC and EL devices due to their proper HOMO value, excellent thermal stability and reversible electrochemical behavior (Scheme 6) *[Liou et al., 2006a]*.

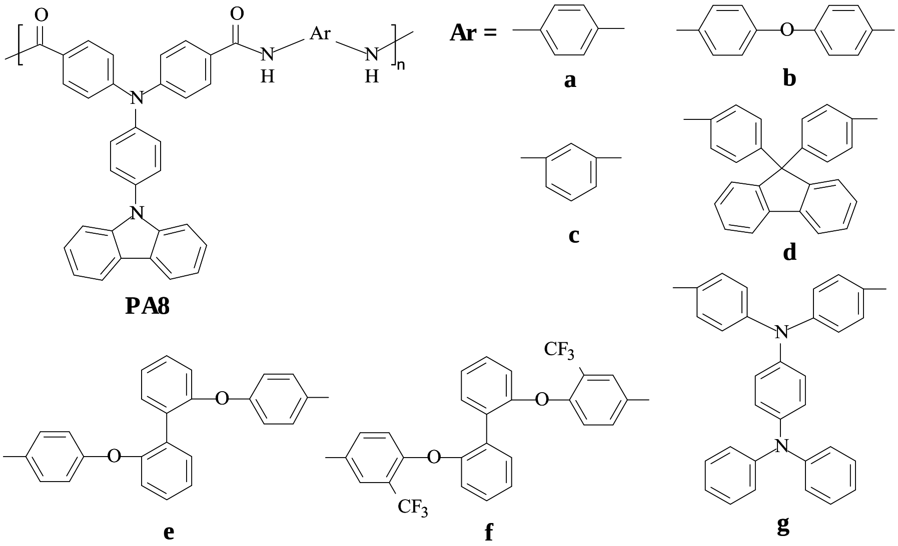

Scheme 6. Structures of polyamides **PA8(a-g)**

These blue-light emitting materials with inherent viscosities of 0.36-0.61dL/g were amorphous and gave flexible, transparent, and tough films with good mechanical properties (e.g., flexibility). They had good thermal stability, as indicated by high *Tg*'s (269–322°C), and Td_{10} values between 556 and 618°C in N_2 atmosphere These polymers exhibited strong UV-vis absorption maxima at 340-361nm, and their PL showed emission peaks around 449-465nm with quantum yields up to 46% in NMP solution. Cyclic voltammograms of polyamide films prepared by casting polymer solution onto an ITO-coated glass substrate exhibited one reversible oxidative redox couples at potentials of 1.11-1.18V *vs* Ag/AgCl in acetonitrile solution due to oxidation of main-chain TPA unit. The polymer films revealed excellent stability of EC characteristics for the radical cations generated, changing color from original yellowish to deep blue.

In a similar work, the authors *[Yen and Liou, 2008]* synthesized and described the photophysical and EC characterization of green-light-emitting polymers bearing anthrylamine chromophores (Scheme 7).

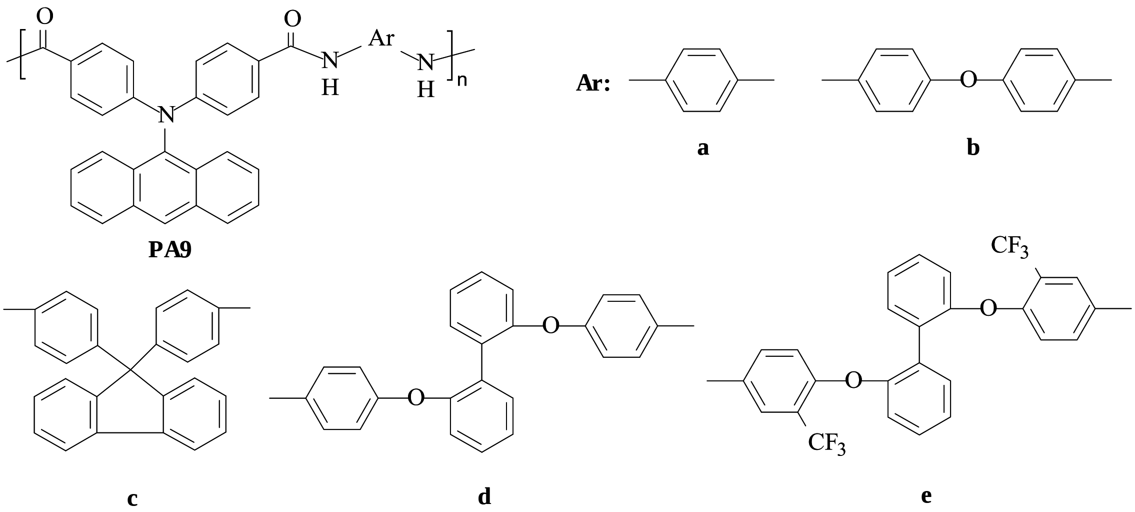

Scheme 7. Structures of polyamides **PA9(a-e)**

These aromatic PAs were amorphous and had significantly high thermal stability evidenced by high *Ts*' (290–300°C), Td_{10} higher than 550°C, and char yields over 60% at 800°C in nitrogen. The polymers show good solubility, and **PA9d** and **PA9e** are even soluble in THF. These aromatic PAs exhibited highly PL quantum yield in NMP solution, ranging from 55.2% for **PA9a** to 73.9% for **PA9e** due to the introduction of anthrylamine chromophores. Cyclic voltammograms of the polyamide films cast onto an ITO-coated glass substrate exhibited one oxidation and reduction couples (E_{onset}) around 1.10 and -1.50V *versus* Ag/AgCl in CH_3CN and DMF solutions, respectively. All polymers exhibited high optical transparency as indicated by the UV–vis transmittance measurement with cut-off wavelengths between 423 and 433nm, and exhibited a green emission maximum around 478–484nm in the solid state. Owing to their relatively high quantum efficiency, these novel anthrylamine-based polyamides could be considered as new candidates for organo-processable high-performance polymers for green-light emitting materials.

Fluorescent aromatic PAs having bulky dansyl (**PA10**) or fluorene (**PA11**) pendant groups connected to the main chains through a urea group, a well-known binding site in supramolecular chemistry, showed yellowish-green or blue fluorescence in solution and solid state depending on the signaling unit, with the former corresponding to the dansyl and the latter to the fluorene residue (Scheme 8) *[San-José et al., 2008]*.

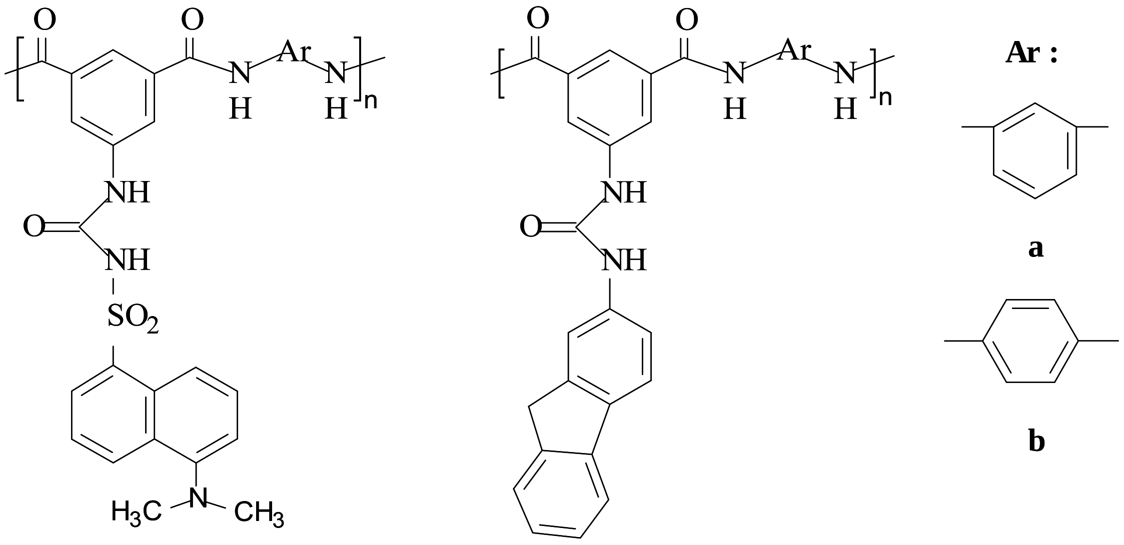

PA10 **PA11**

Scheme 8. Structures of polyamides **PA10(a,b)** and **PA11(a,b)**

These PAs are amorphous and soluble in polar aprotic solvents and proved film-forming capability. The polar amide, urea, and sulfonamide groups gave rise to a high water sorption (7.5-10.0%) and the number of water molecules per repeating unit ranged between 2.3 and 3.0. The *Tg*'s of the polymers varied between 174 and 331°C, and the decomposition temperatures had moderate values (274-290°C) due to the low thermal stability of the urea group.

Two series of aromatic PAs having noncoplanar biphenylene units in the main chain and phenyl (**PA12**) or bulky naphthyl pendant group (**PA13**) at 2,2′-disubstituted position (Scheme 9) exhibited strong UV-Vis absorption bands at 262-353nm in NMP solution, and their fluorescence emission maxima appeared at 440-462 and 442-459nm, respectively, in the purple to blue region *[Liou et al., 2007]*. The thin films of aromatic PAs without TPA units showed high optical transparency from UV-Vis transmittance measurements with cutoff wavelength in the range of 323-345nm.They were readily soluble in organic solvents such as NMP, DMAc, DMSO, DMF and *m*-cresol, and PAs derived from diamines **d-g** were even soluble in THF. These polyamides had inherent viscosities in the range of 0.17-1.09dL/g, and their *Mw* and *Mn* were recorded in the ranges 13000-31000g/mol, and 12000-23000g/mol, respectively, relative to polystyrene standards. They showed excellent thermal stability associated with high *Tg*'s between 229 and 292°C and Td_{10}=495-600°C in nitrogen. The polyamide **PA13d** derived from the diamine with TPA moieties revealed excellent EC contrast and coloration efficiency, changing color from the pale yellowish neutral form to green then to the blue oxidized forms when scanning potentials positively from 0.00 to 1.30V.

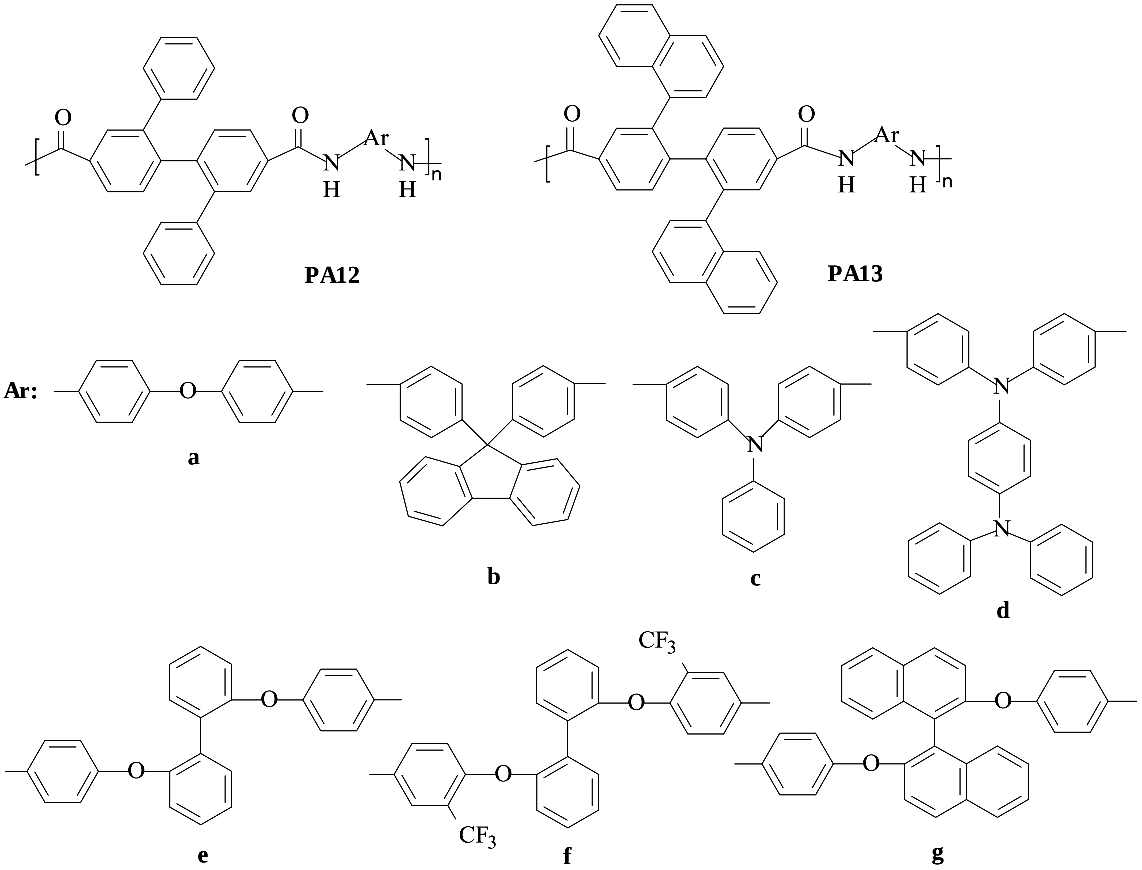

Scheme 9. Structures of polyamides **PA12(a-g)** and **PA13(a-g)**

The polymers with structures evidenced in Scheme 10 showed good thermal properties associated with *Tg* in the range of 221–257°C and Td_{10} in air between 393 and 408°C *[Nechifor, 2009]*. They were soluble in polar aprotic solvents and had film-forming properties. UV illumination (λ >300 nm) of the polymer films induced crosslinking between polyamide molecules through a [2+2] photocycloaddition at the C=C bond of coumarin moieties, which induced insolubilization of the polymers. All aromatic coumarinated PAs are highly fluorescent. The emission spectra of the polymer solutions showed only one band with a maximum located at 387nm, irrespective of the structure of aromatic diamine moiety, which means that the PL maximum corresponding to coumarin chromophore in the backbone could not be detected by exciting with absorbance maximum. The fluorescence spectra of polymer films showed red shifts of 18nm in the emission maxima and are characteristically broader as compared with those in dioxane solution.

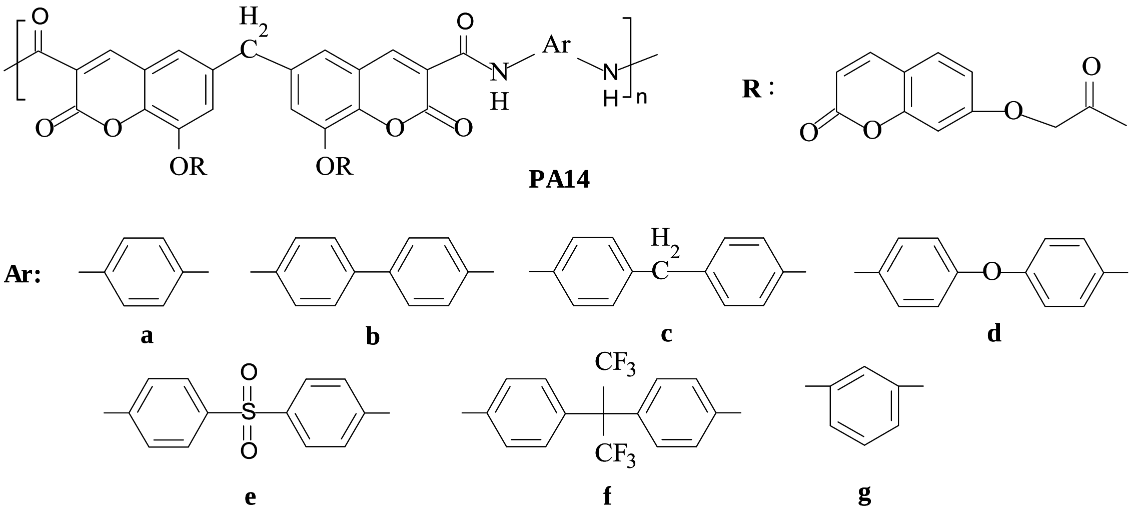

Scheme 10. Structures of polyamides **PA14(a-g)**

4.2 Photosensitive aromatic polyamides

In recent years, there has been widespread research in the synthesis and applications of photosensitive polymers. These polymers are extensively used as photoresists for the manufacture of numerous industrial products, for instance, integrated circuits, printing materials, coatings, paint, compact discs, cathode ray tubes, etc. Photosensitive polymers containing photo-cross-linkable groups have gained a considerable interest in recent years and are widely used for several applications in the field of microlithography, printing materials, photocurable coatings, liquid crystalline and nonlinear optical materials, energy exchange materials, photosensitizers, etc. Polymers with α,β-unsaturated carbonyl groups either in the backbone or in pendent position have attracted particular attention because of their excellent photoreactivity at UV absorption wavelengths. These polymers with properties of high photosensitivity, film forming ability, good thermal stability, good solubility before radiation, resistance towards solvents after cross-linking are essential requirements for practical use of the photopolymers as negative photoresist materials. The photosensitivity of these materials is mainly attributed to the π electron density of the photoactive chromophore (*i.e.* -CH=CH-C(=O)-). Among many promising photosensitive groups, the cinnamate, chalcone, cinnamylidene, abietate, maleimide, thymine and coumarin derivatives have been studied for the synthesis of photo-cross-linkable polymers due to their high sensitivity to UV radiation.

Polyisophthalamides with pendant cinnamoyl units introduced through amide or ester bonds were prepared through a direct reaction between carbonyl groups from *O*-cinnamoyl-5-hydroxyisophthalic acid or *N*-cinnamoyl-5-

aminoisophthalic acid and two aromatic diisocyanates without use of any condensing agents (Scheme 11) *[Onciu and Rusu, 2002]*. The synthesis was carried out in NMP, and in the presence of 4-dimethylaminopyridine as catalyst.

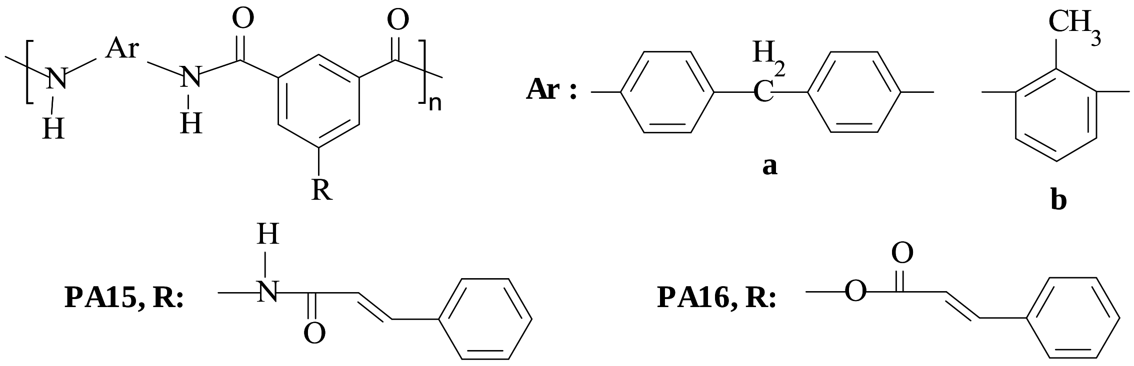

Scheme 11. Structures of polyamides **PA15(a,b)** and **PA16(a,b)**

Irradiation at λ=313nm of these polymers led to spectroscopic changes attributed to the photoisomerization and saturation of the ethylenic double bonds and photo-Fries rearrangement of the cinnamoyl groups. Both thermal stability and solubility depended on the structure of the binding as well as the presence of functional pendant groups (Table 7). The polymers can be especially used for membranes and composites.

Table 7. Thermal and spectroscopic data for polymers **PA15** and **PA16** *[Reprinted with permission from Onciu and Rusu, 2002. Copyright 2002, Society of Chemical Industry]*

Polymer	η_{inh}[a] (dl/g)	Td_{10}[b] (°C)	**Weight loss**[b] **at 400°C** (%)	λ_{max} (nm)	
				solution	**film**
PA15a	0.73	382	9	296	288
PA15b	0.69	408	6	295	286
PA16a	0.64	405	11	289	286
PA16b	0.61	418	7	288	282

[a] Measured at a concentration of 0.5g/dL in NMP, at 25±0.1°C; [b] TGA was performed in air at a heating rate of 10°C/min.

Two series of structurally different polyamides were synthesized by direct polycondensation of three aromatic dicarboxylic acids with two diamines prepared by the attachment of cinnamoyloxyethyl and 4-dimethylamino-cinnamoyloxyethyl group through an ester bridge to 3,5-diaminobenzoic acid (Scheme 12) *[Rusu and Nechifor, 2003; Rusu and Onciu, 2005a]*. The polyamides were soluble at room temperature in aprotic solvents, such as NMP, DMF, DMSO, DMAc, THF and pyridine and afforded transparent, flexible and tough films by solution casting. The polyamides **PA18(a-c)** had Td_{10}'s lower than **PA17(a-c)** due to the presence of *p*-dimethylamino substituent to the cinnamoyl unit. The Td_{10} values of the polymers **PA17(a-c)** can be associated to the decomposition of the ester moieties present in the pendant side chains. The presence of the (4-dimethylamino)cinnamoyloxyethyl pendant groups increased the disorder in the main chain and reduced the inter-chain interactions through hydrogen bonds by comparison with unsubstituted PAs. The unsubstituted PAs, such as PMPI and poly(*m*-phenylene terephthalamide) have *Tg* of 276°C and 238°C, respectively. The *Tg*'s of the polyamides **PA17** and **PA18** ranged between 182 and 219°C and are lower than that of unsubstituted PAs.

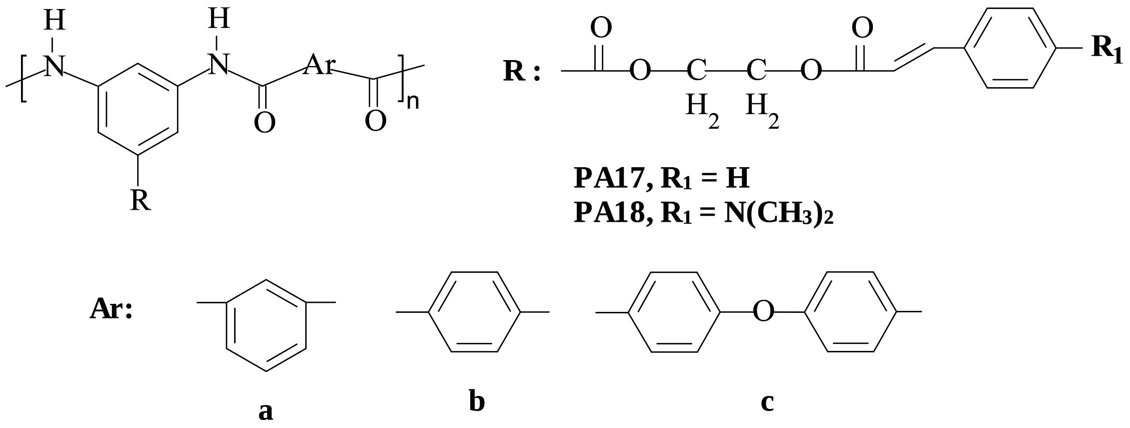

Scheme 12. Structures of polyamides **PA17(a-c)** and **PA18(a-c)**

According to UV absorption spectra, the polymers exhibited a typical absorption band at around 279nm in the case of polymers **PA17** and about 356nm in the case of polymers **PA18** due to the $\pi \rightarrow \pi^*$ transitions of C=C from the pendant cinnamoyl moiety in DMSO solutions. The changes in the UV spectra upon irradiation were evidenced by a decrease in the intensity of the maximum absorption bands. In the initial stage these modifications are characterized by the appearance of two isosbestic points at about 264 and 313nm (**PA**17), and about 318nm and 385nm (**PA**18), their presence being associated with an exclusive *trans–cis* photoisomerization reaction of the double bond in cinnamoyl moiety. The spectral change on prolonged irradiation, namely the disappearance of the isosbestic points, was associated to the formation of the cyclobutane ring by photocycloaddition of C=C double bonds which destroys conjugation in the entire π-electron system. This behavior indicated that the cross-linking of the polymer chains occurred.

A derivative of 3,5-diamonobenzoic acid comprising an ethylene-cinnamide group as substituent was prepared and successfully used as a condensation monomer in reaction with aromatic dicarboxylic acids for the synthesis of certain aromatic PAs (Scheme 13) *[Onciu, 2007a]*. As expected, the presence of the bulky and extended cinnamide unit in the side chain renders the polymers soluble and photosensitive. All PAs had good solubility in polar aprotic solvents and could be cast into strong, homogeneous, and flexible films.

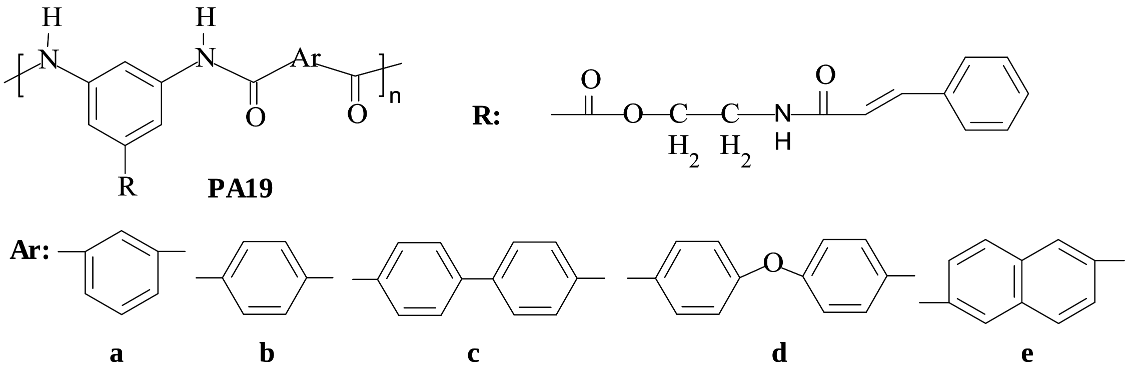

Scheme 13. Structures of polyamides **PA19(a-e)**

The polymers had *Mw* and *Mn* in the range of 39000–72700g/mol and 18800–29000g/mol, respectively, and polydispersity index varying between 1.93 and 2.51. The polymers had moderate *Tg* values (225–245°C) and relatively high hydrophilicity. Cinnamoyl-based polyamides in the solid state were found to undergo the [2+2] cycloaddition of the vinylene C=C double bonds in addition to the *trans–cis* photoisomerization of the cinnamoyl species during UV illumination. Good solubility, moderate *Tg* values, film forming ability and their photocrosslinkable properties leading to insolubilization make these polyamides suitable for microelectronics applications.

Some other photosensitive polyamides with two cinnamoyl moieties *per* repeating structural unit of polymer backbone were prepared by triphenyl phosphite-activated PC reaction of 4,4′-methylene-dicinnamic acid with various aromatic diamines containing aryloxy groups (Scheme 14) *[Nechifor, in press]*. The resulting polymers were amorphous and soluble in aprotic solvents due to the presence of flexible aliphatic and aryl ether linkages in the main chains. Inherent viscosity and GPC measurements relieved that polyamides with high molecular weights were obtained, and good thermal stability was evidenced by TGA. These polymers showed good film forming ability and low water absorptions. All the polyamides underwent a free-photosensitizer photocycloaddition reaction upon the UV light irradiation (λ>280nm) both in solution and film state. Flexible methylene and aryl ether linkages inserted into aromatic main chains bring about a beneficial structural modification to linear PAs because they provide a considerable lower energy of internal rotation, which results in improving the overall flexibility of the polymer backbones. Consequently, these polymers generally revealed an enhanced solubility with respect to conventional aromatic PAs. Simultaneously, these flexible linkages usually tend to lower *Tg*. The *Tg*’s values of these polyamides were observed in the range 214–239°C, depending on the structure of the diamine component and increased with increasing rigidity, symmetry and steric hindrance of the polymer backbone.

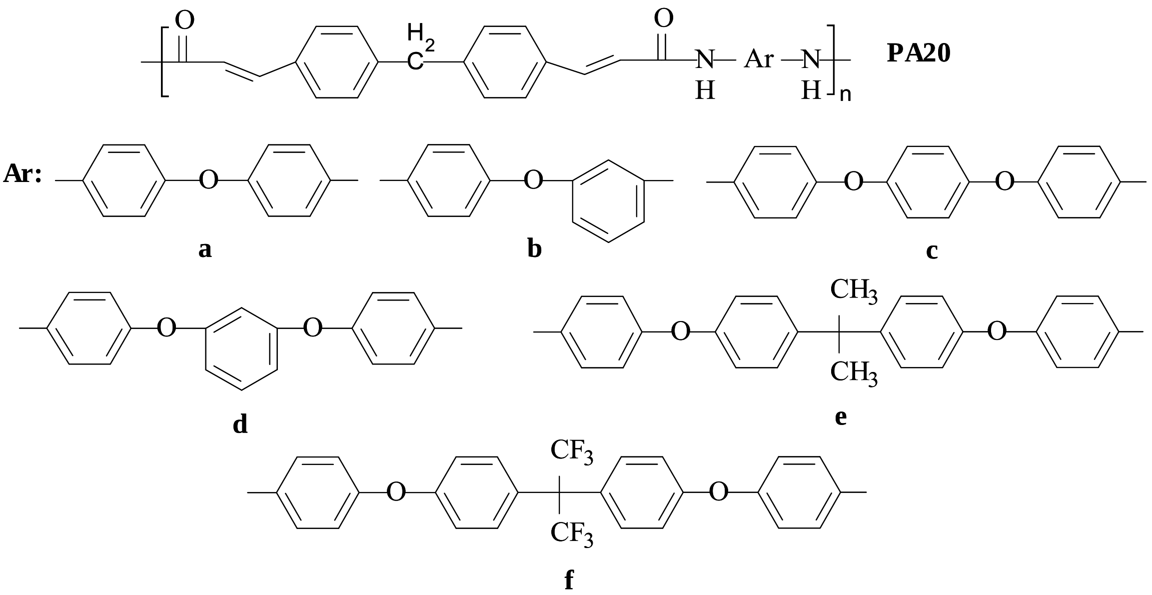

Scheme 14. Structures of polyamides **PA20(a-f)**

Another chromophore introduced into the structure of aromatic PAs is chalcone. The chalcone unit is well known for its rigid-rod nature and transfers this characteristic to the pendant group of the polyamide structure. The steric hindrance from the chalcone unit increases aplanarity of the styryl phenyl ring and supresses the *trans-cis* isomerization. The presence of an extended segment (*e.g.* oxyethylene) at the position 4 of chalcone unit favoures aplanarity (Scheme 15) *[Rusu and Onciu, 2005b, 2005c]*.

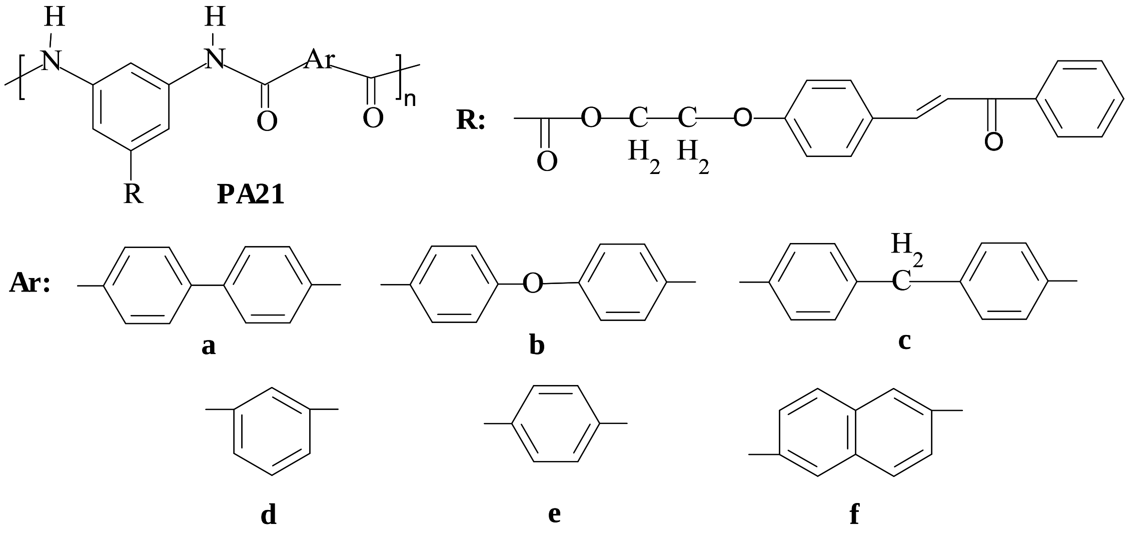

Scheme 15. Structures of polyamides **PA21(a-f)**

Simultaneously, the presence of the chalconyloxyethyl groups in the polyamide structure increased the disorder in the main chain because they screened off H-bonds between polymer chains and/or enlarged the spaces between polymer chains. As a consequence the polymer's free volume increased resulting in decreased *Tg*'s. On the other hand, the size of the chalconyloxyethyl pendant groups restricts the mobility of the polymer chain and contributes to an increase in *Tg*. Moreover, the *meta*-linked phenylendiamine segments seemed to increase the flexibility because of the different possible positions of this group in the chain, resulting in a decrease of *Tg*. The presence of the voluminous chalconyloxyethyl unit and *m*-linked amino groups in monomer structure gave to all polymers an amorphous character and film-forming property. The chalcone group of the polymer easily underwent intermolecular cycloaddition by UV irradiation and, as a consequence of the photo-cross-linking of polymer chains, insolubility of the polyamide films in usual organic solvents increased. The polyamides were stable up to the temperature above 316°C and the pendant groups contributed by their size and rigidity to a *Tg* value around 230°C.

Another alternative route to the cinnamate chromophore is the coumarin chromophore, because it is known to undergo [2+2] cycloaddition on UV irradiation. Polymers with coumarin moieties have been useful in many fields, such as fluorescence materials and laser dyes, nonlinear optical materials, photorefractive materials, photoresists, energy-transfer materials, alignment agents for liquid crystals, biological materials, electroluminescent materials, etc. The PAs illustrated in Scheme 16 were highly soluble at room temperature in polar aprotic solvents such as DMF, DMAc, NMP, DMSO and dioxane and in less polar solvents like Py, *o*-chlorophenol, methanesulfonic acid and *m*-cresol *[Onciu, 2007b]*.

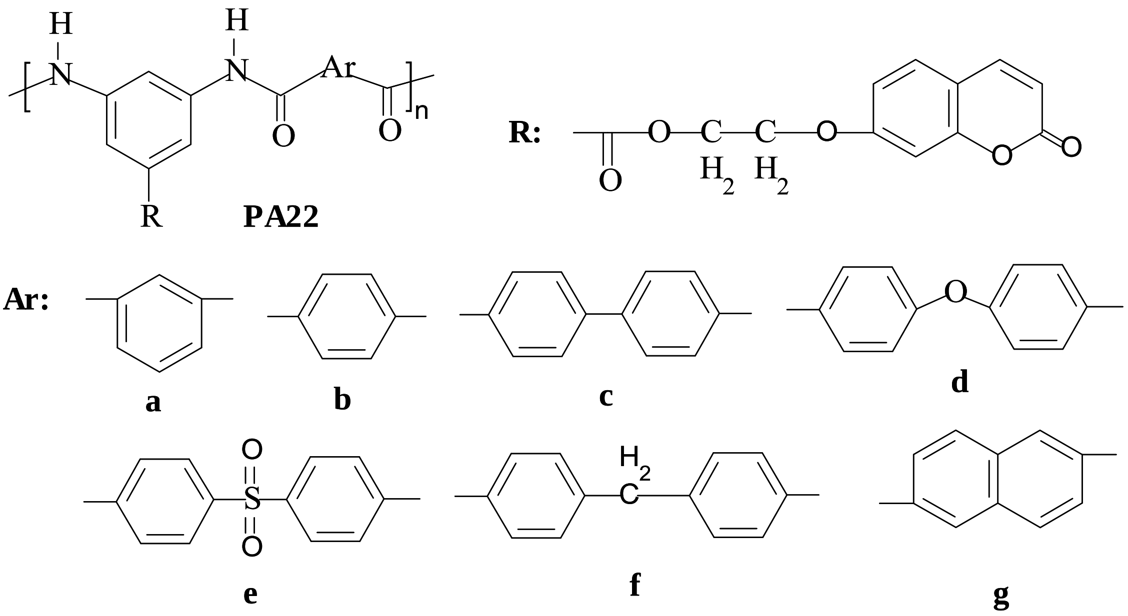

Scheme 16. Structures of polyamides **PA22(a-g)**

All the PAs were highly amorphous, their DSC curves showed no endotherms in the region 20-250°C that could be assigned to melting. They exhibited reasonable thermal stability and started to decompose from the weaker ester linkages at around 275°C. *T*g's ranged between 191 and 223°C and decreased with decreasing rigidity and symmetry of the polymer backbone. In the UV-visible spectra, the coumarinated PAs revealed a maximum absorption at around 320nm, which diminished significantly with increasing UV exposure time, exhibiting the cross-linking (dimerization) between the coumarin moieties in the side chains and transformation of the polymer film from soluble to insoluble. High solubility and film forming properties, high photosensitivity, moderate *Tg*`s values and relative high hydrophilicity and thermal stability made these coumarinated polyamides promising polymeric materials.

4.3 Optically active aromatic polyamides

Optically active polymers are of particular interest due to their specific properties and successful uses as stationary phase in chromatographic separation of enantiomers, chiral media for asymmetric synthesis, chiral liquid crystals in ferroelectric and nonlinear optical devices, optical switches, biodegradable and biomedical devices, drug delivery agents, etc. These applications have generated more effort to improve different synthetic procedures of optically active polymers, but, generally, their synthesis involves either the PC reaction of optically active monomers or asymmetric polymerization, which generates optically active polymers from optically inactive monomers. The aromatic PAs reported within this review are polyisophthalamides prepared from optically active monomers **M(23-28)**, which introduce the chiral element into the side chains of the polymers **PA(23-28)**.The polymers illustrated in Scheme 17 presented chiroptical properties conferred by the presence of pendant *L*-alanine (**PA23** and **PA25**) *[Mallakpour and Rafiee, 2008a, 2008b, 2009]*, *L*-leucine (**PA24** and **PA27**) *[Mallakpour and Dinari, 2009; Mallakpour and Meratian, 2009]*, *S*-valine (**P26**) *[Mallakpour and Kolahdoozan, 2008]* or methionine core groups (**PA28**) *[Mallakpour and Seyedjamali, 2008, 2009]* and evidenced by their optical rotation [α].

Some of the polyamides in Scheme 17 were prepared by four different methods, all of them based on Yamazaki phosphorylation reaction, as follows: by conventional heating (method A), by MW (method B), in the presence of ILs (method C) and in the presence of ILs and using MW (method D). The authors studied the influence of different conditions on reaction yields and some properties of polymers, such as the inherent viscosity and optical rotation.

An alternative to conventional heating is microwave heating for activation of polymerization reactions. This quite new form of energy transfer offers many discrete benefits over traditional heating, such as volumetric, fast, directly selective, instantaneous, and controllable heating. It offers a clean, cheap, and convenient method of heating, which often results in higher yields and shorter reaction times.

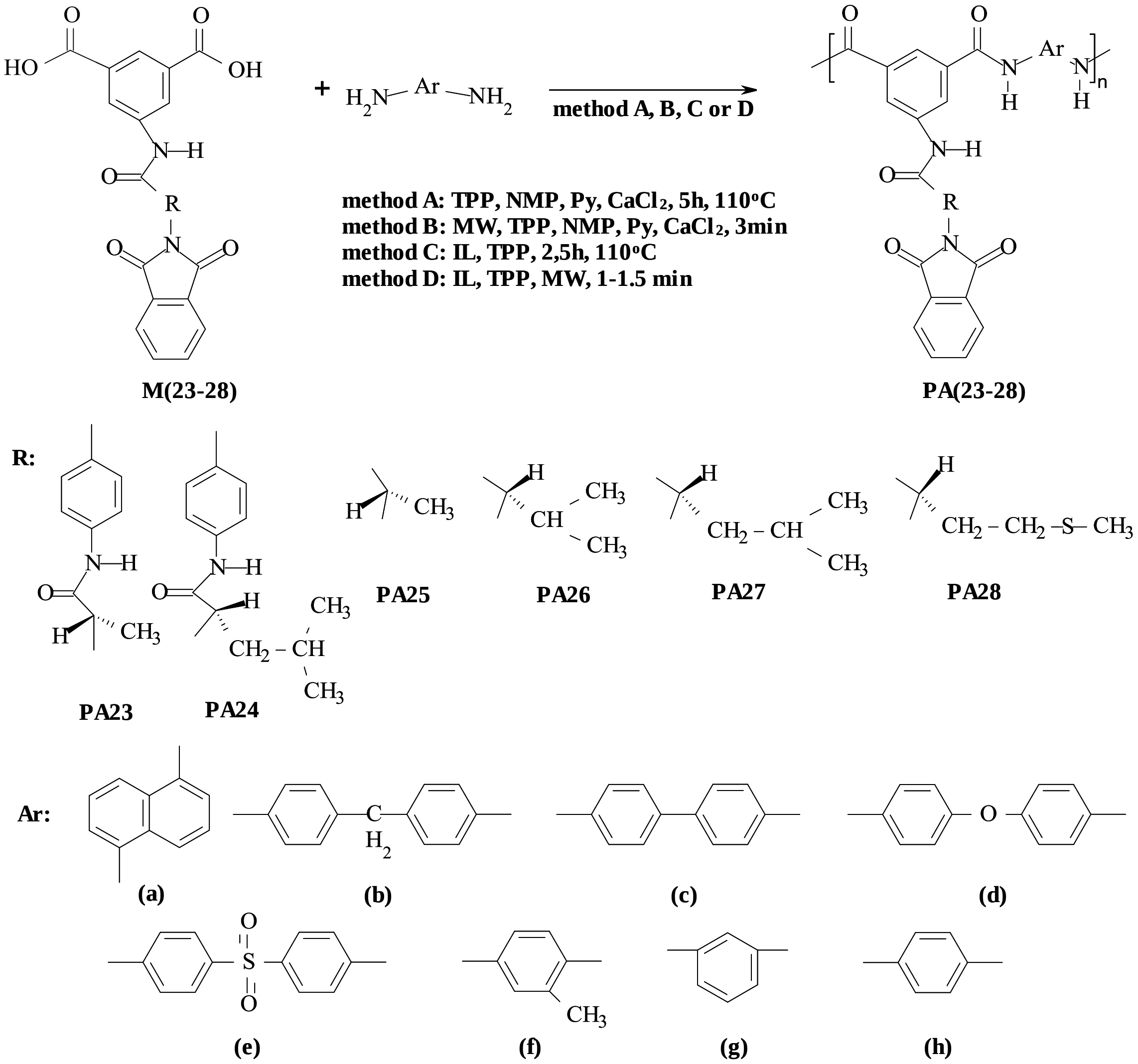

Scheme 17. Structures of polyamides **PA23-PA28(a-h)**

There is a great require for the introduction of new methodologies for polymerization reactions using environmentally eco-friendly media, which could replace the traditional volatile, flammable, toxic, quite hazardous and harmful common organic solvents. ILs have recently gained recognition as possible environmentally friendly alternative solvents in various chemical processes. ILs possess a unique array of physico-chemical properties such as high electrical conductivity, high thermal stability, large electrochemical window, low nucleophilicity and capability of providing weekly coordinating or noncoordinating environment, very good solvents properties for an extensive diversity of organic, inorganic, organometallic and polymeric compounds. In some cases, the solubility of certain solutes in ILs can be several orders of magnitude higher than that in traditional solvents. The ILs are also suitable for microwave chemistry and it is expected that their high polarity to be an efficient substrate for quick heating under microwave irradiation. The significant advantages of using ILs and MW are avoiding volatile and toxic organic solvents and drastic reduction of reaction time.

The specific rotations of polymers **PA(23-28)** based on different diamines showed random changes. These observations are the result of different polymer structure and inherent viscosity. The yields and inherent viscosities of the polymers obtained by MW *versus* thermal heating are comparable, with remarkable reduction of reaction time due to homogeneous heating.

The presence of thermostable phthalimide heterorings as pendent group might compensate any loss of thermal properties that could be caused by incorporation of aliphatic spacers. At the same time, the phthalimide linkage in the polymer side chain significantly improved the solubility of the polymers because the introduction of pendent bulky groups along the polymer backbone results in a less ordered polymer matrix by disturbing the strong inter-chain forces and inherent macromolecular rigidity and consequently increasing the solubility characteristics without affecting thermal properties largely. All the polyamides in Scheme 17 are readily soluble in organic solvents, such as DMF, DMAc, DMSO, NMP, Py, THF, and in H_2SO_4 at room temperature and some of them are capable to give thin flexible films by casting from their solutions. On the other hand, the effect of the benzamide group on the Td_5 and Td_{10} values could be appreciated when polyamides **PA23** and **PA24** were compared with polyamides without benzamide unit **PA25** and **PA26** while the other part of the polymer structure was maintained the same. These polyamides showed higher Td_5 and Td_{10} values, and they are more thermally stable than those without benzamide group.

Char yield can be applied as criterion for estimating LOI of the polymers in accordance with Van Krevelen and Hoftyzer equation *[Van Krevelen and Hoftyzer, 1976]*:

$$\mathrm{LOI} = 17.5 + 0.4\ \mathrm{CR} \tag{1}$$

where CR is the char yield obtained by TGA.

These polymers had LOI values higher than 35 and, consequently, they can be classified as self-extinguishing polymers.

Because these optically active polymers have amino acids in the polymer architecture, they are expected to be biodegradable, and therefore are classified as environmentally friendly polymers. These properties, associated with an easy processability, make these polymers potential candidates for practical applications in the area of films, coatings, engineering plastics, polymer blends, and composites.

4.4 Aromatic polyamides with membrane properties

The development of polymeric membranes having advanced or novel functions in the various membrane separation processes of liquid and gaseous mixtures (gas separation, reverse osmosis, pervaporation, nano-, ultra- and microfiltration) and in other important applications of membranes such as biomaterials, catalysis or lab-on-chip technologies has been focused on novel processing technologies of polymers for membranes, the synthesis of novel polymers with well-defined structure as "designed" membrane materials, advanced surface functionalization of membranes, the use of templates for creating "tailored" barrier or surface structures for membranes and the preparation of composite membranes for the synergistic combination of different functions by different (mainly polymeric) materials.

Aromatic PA membranes were first developed by DuPont in a hollow fiber configuration. Like the cellulosic membranes, these membranes have an asymmetric structure with a dense and porous substructure, and are subject to compaction at high pressures and temperatures. Unlike cellulosic membranes, PA membranes can withstand higher temperatures and have better resistance to hydrolysis and biological attack. Usually, they operate over a pH range of 4 to 11, but at the extremes of this range, they can undergo irreversible degradation. They have better salt rejection characteristics than cellulosic membranes as well as better rejection of water-soluble organics. A major drawback of polyamide membranes is their degradation by oxidants, such as free chlorine.

4.4.1 Gas separation membranes

Gas separation membranes are increasingly being used for applications such as hydrogen recovery, nitrogen generation and carbon dioxide removal. Membrane technology is seen as a route to cost-effective, energy-efficient, environmentally benign processes in various industries. Many polymers have been investigated as gas separation membrane materials, but only a few have found commercial applications. These include rubbery polymers, such as poly(dimethylsiloxane), and glassy polymers, such as polysulfone, poly(phenylene oxide), cellulose acetate and polyimides. To be useful, a membrane material must offer high permeability as well as good selectivity for a desired separation. Unfortunately, polymers that exhibit good selectivity generally have low permeability and *vice versa*.

Aromatic PAs offer excellent thermal and mechanical properties, good chemical resistance, and are easily spun into hollow fibers appropriate for gas separation modules. Because PAs commonly have high cohesive energy density and show a strong propensity for very efficient polymer chain packing, they normally exhibit low permeability to small molecules. Wholly aromatic PAs, such as PPPT (Kevlar) and PMPI (Nomex), exhibit extremely low gas permeabilities. Recent studies have demonstrated that both permeability and selectivity can be enhanced by incorporation of bulky pendent groups in glassy membrane-forming polymers that renders them highly amorphous and moderately permeable.

The productivity of a membrane is expressed in terms of its permeance, a measure of the amount of permeate that passes through a certain membrane area in a given time for a particular pressure difference. Permeance multiplied by thickness gives the permeability *P* (more strictly called the permeability coefficient), which is a characteristic of the material. Values of *P* are often quoted in units of Barrer (1 Barrer=10^{-10}[cm^3(STP) cm]/[cm^2 s cmHg]). For an ideal mixture of two gases, A and B, involved in a separation process, the selectivity, $\alpha_{A/B}$, is defined as the ratio of their permeability coefficients: $\alpha_{A/B} = P_A/P_B$.

A series of aromatic PAs shown in Scheme 18 exhibited an outstanding permeability to gases, comparable or even higher than of glassy, engineering thermoplastics, with an acceptable selectivity of technical gas pairs, such as O_2/N_2, H_2/CH_4 and CO_2/CH_4 *[Espeso et al., 2006]*.

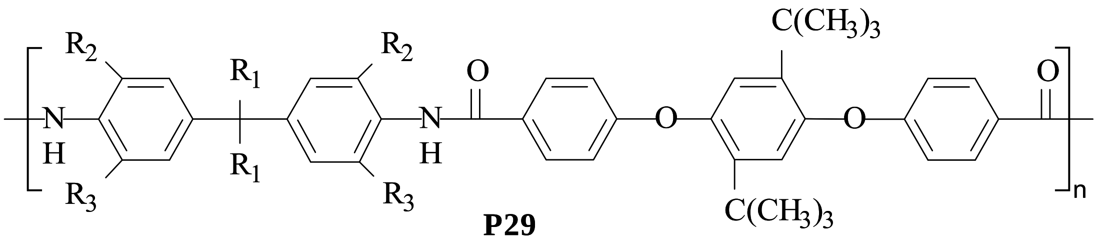

P29

PA29a: $R_1 = CH_3$, $R_2 = H$, $R_3 = H$ **PA29b: $R_1 = CH_3$, $R_2 = CH_3$, $R_3 = H$**

PA29c: $R_1 = CH_3$, $R_2 = CH_3$, $R_3 = CH_3$ **PA29d: $R_1 = H$, $R_2 = CH_3$, $R_3 =$ *t*-Bu**

PA29e: $R_1 = CF_3$, $R_2 = H$, $R_3 = H$

Scheme 18. Structures of polyamides **PA29(a-e)**

Gases permeated much faster through these polyamides than through Trogamid, an amorphous aliphatic–aromatic PA with a non-regular chemical structure, which is probably the commercial PA that offers the highest permeability to gases. The ideal separation factor α of all polyamides **PA29** had higher values than Trogamid, evidenced for the gas pair CO_2/CH_4. For example, Trogamid has α_{CO_2/CH_4}=18.3 and polyamide **PA29e** has α_{CO_2/CH_4}=25.24. The results confirmed that the presence of a growing number and growing size of substituents might substantially improve the free volume and the permeability. An additionally advantage of polyamides **PA29** was their good solubility in organic solvents, so they could transformed into defect-free films with excellent mechanical properties.

Other reports dealt with the synthesis, the thermal and gas transport properties, permeability, and selectivity of benzophenone and hexafluoroisopropylidene containing aromatic polyisophthalamides (Scheme 19) and copolyamides (Scheme 20) derived from the copolymerization of isophthalic (ISO) and 5-tertbutylisophthalic (TERT) acids with 4,4′-diaminebenzophenone (DBP) or 2,2-bis(4-aminophenyl) hexafluoropropane (HFP), in different DBP/TERT or HFP/TERT molar ratio *[Carrera-Figueiras and Aguilar-Vega, 2005, 2007]*.

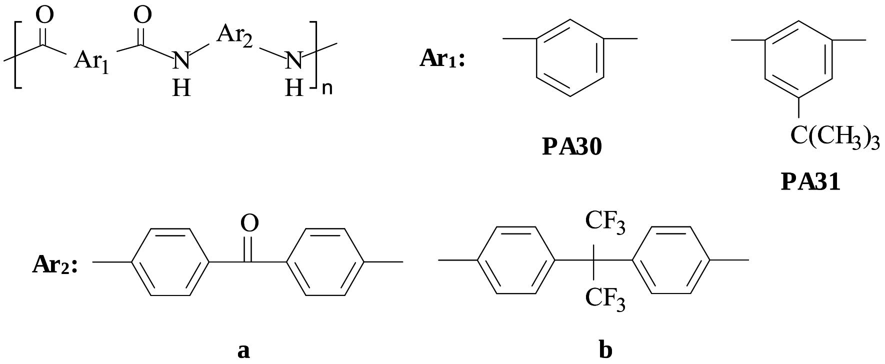

Scheme 19. Structures of polyamides **PA30(a,b)** and **PA31(a,b)**

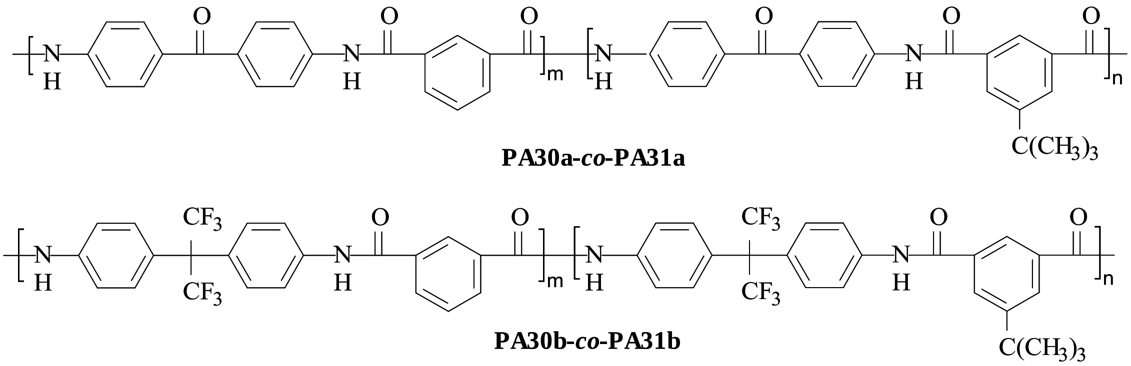

Scheme 20. Structures of copolyamides **PA30a-*co*-PA31a** and **PA30b-*co*-PA31b**

The results indicated that the *Tg*'s of the copolyamides **PA30a-*co*-PA31a** and **PA30b-*co*-PA31b** increased as the concentration of DBP/TERT and HFP/TERT, respectively, increased. The gas permeability coefficients for **PA30a** were around 10^{-2} Barrers for O_2, which situated this polymer as a barrier polymer. It was also found that permeability coefficients of polyamides **PA30a** and **PA31a,** and copolyamides **PA30a-*co*-PA31a** were independent of pressure for He or decreased slightly particularly with O_2, CO_2, and N_2. It was seen that **PA31a** was up to 15 times more permeable than **PA30a**, depending on the gas being considered. This behavior was assigned to the presence of the bulky lateral substituent, the tert-butyl group, in **PA31a** and **PA30a-*co*-PA31a** copolyamides. The selectivity of gas pairs, such as He/O_2 and He/CO_2, decreased slightly with the addition of DBP/TERT. As concern the polyamides **PA30b** and **PA31b** and copolyamides **PA30b-*co*-PA31b**, their gas permeability coefficients were independent of pressure or decreased slightly particularly with CO_2, N_2, and CH_4. It was seen that HFP/TERT is 2–6 times more permeable than HFP/ISO, depending on the gas being considered. This was assigned to the presence of the bulky lateral substituent, *t*-butyl group in **PA31b** and **PA30b-*co*-PA31b** copolyamides. This bulky substituent increased fractional free volume and inter-chain spacing; as a consequence, the gas permeability and diffusion coefficients generally increased. The experimental results for the gas permeability coefficients and permselectivity for the copolyamides was well represented by a logarithmic mixing rule of the homopolyamides permeability coefficients as a function of their volume fraction. The selectivity of gas pairs, such as O_2/N_2, CO_2/CH_4, and N_2/CH_4 decreased slightly with the addition of HFP/TERT. The temperature dependence of permeability for all homo-polyamides and copolyamides could be described by an Arrhenius type equation.

The effect of nitrile group on the gas permeability and permselectivity of the polymers depicted in Scheme 21 revealed that increasing content of nitrile group led to an increase of the gas permeability and a decrease of permselectivity of the aromatic polyamides *[Choi et al., 2000]*. In addition, the non-linearity of the polymers increased the permeability. An increase in chain spacing, measured by X-ray diffraction, also supported the increase in gas permeability with increasing the nitrile group content. The chain linearity of aromatic PAs also affected their gas permeability. The gas permeability of *meta*-substituted aromatic PAs was higher than that of *para*-substituted ones, indicating that the non-linearity of the chain decreased the permselectivity.

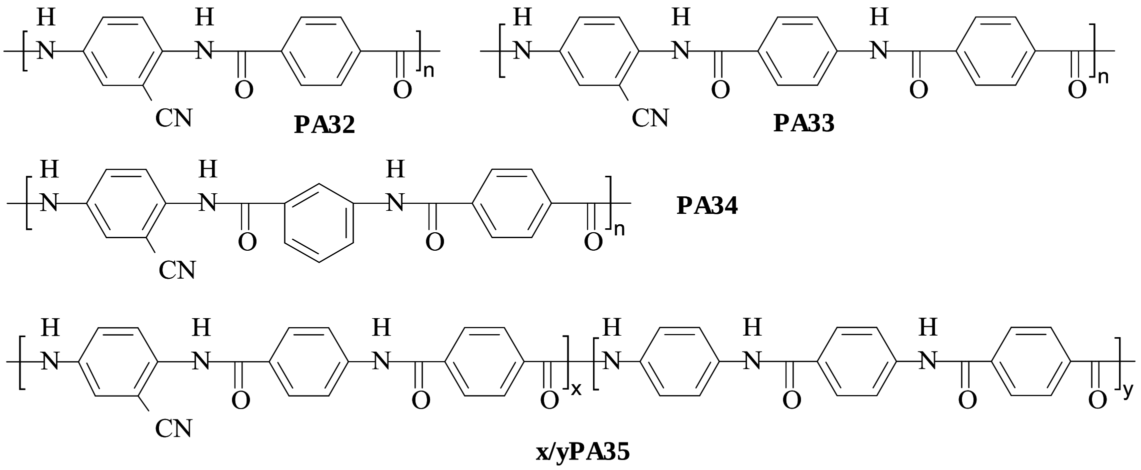

Scheme 21. Structures of polyamides **PA32-35**

These aromatic PAs can be used as ultra-high gas purification membranes despite of their lower gas permeability, because they have high permselectivity and good mechanical properties for preparation of ultra-thin films.

A series of polydimethylsiloxane-grafted aromatic PAs, which consisted of different polydimethylsiloxane (PDMS) segment lengths, were prepared in order to clarify the effect of PDMS segment length on the permeation properties of the copolymer membranes (Scheme 22) *[Nagase et al., 2007]*. The *Mn*'s of all the copolymers were in the order of 10^4, which were high enough to prepare mechanically strong and insoluble membranes in several organic solvents. Gas permeability coefficients of the copolymer membranes for N_2, O_2, H_2, CO_2, CH_4 and C_2H_6 were evaluated and compared with those of PDMS cross-linked membrane. It was noticed that the gas permeability coefficients of PDMS-grafted copolymer membranes increased as the PDMS segment length became longer. Furthermore, the difference of the gas permeabilities for each gas would be due to the surface property of the copolymer membranes. In the gas permeation through such high permeable copolymer membranes, the solubility of gases in the membrane surface would dominate the gas permeability, because the diffusivity in the membrane is very high and the difference of diffusivities of each gas becomes small. It was found from these results that PDMS-grafted copolymer membranes possessed highly hydrophobic surface, which was effectively covered with PDMS side chain, where the organic gas permeabilities of methane and ethane became significantly high.

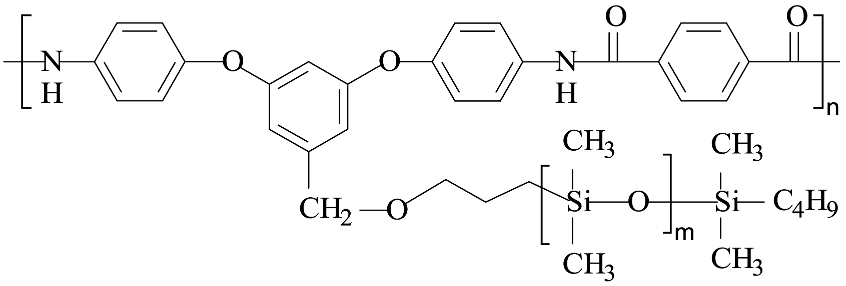

PA36a: m = 6.2

PA36b: m = 12.5

PA36c: m = 15.7

Scheme 22. Structures of polyamides **PA36(a-c)**

4.4.2 Reverse osmosis and nanofiltration membranes

Reverse osmosis and nanofiltration membranes have been increasingly used in water treatment and wastewater reclamation in the last few decades, because they are capable of removing a broad range of contaminants in one treatment step due to the great technological advancement and cost reduction. RO by polymeric membranes is considered as the simplest and most efficient technique for seawater desalination purposes. For the development of these polymeric RO membranes, two different techniques have been used: the phase inversion method for asymmetric membranes, and the interfacial polymerization for TFC membranes.

Modern RO and NF membranes for water purification are predominantly TFC polyamide membranes. A typical composite polyamide membrane consists three layers: a thin top selective polyamide layer (~50-200nm), a microporous polysulfone support layer (~50μm) backed by a nonwoven fabric (polyester) layer (~200μm) for mechanical strength. Such composite design allows separate optimization of performance and mechanical stability. The top dense skin layer is the most critical layer, as the performance of a composite membrane is essentially determined by its physiochemical properties (such as permeability, selectivity, surface roughness, and hydrophobicity). Fully aromatic crosslinked PA is the polymer of choice for the active layers of most RO and many NF membranes and it is prepared by interfacial polymerization. The polysulfone support is first soaked with an aqueous solution of MPDA, and then brought into contact with a solution of trimesoyl chloride in organic solvent (e.g., hexane) (Scheme 23) *[Roh and Khare, 2002; Tarboush et al., 2008]*.

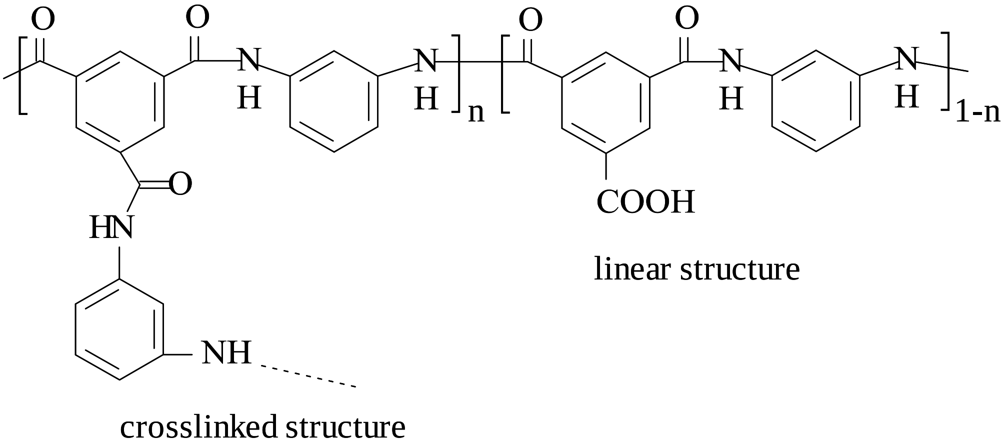

PA37

Scheme 23. Structure of polyamide **PA37**

Permeation measurements conducted on the polyamides **PA37** and PMPI revealed that the network polyamide evidences higher water flux as well as salt rejection compared to the linear polyamide. The higher water flux was attributed mainly to the higher hydrophilicity (arising from the hydrolysis of unreacted carboxylic acid groups in the structure) of the network polyamide. Hydrophilicity was found to overwhelm other factors such as the film thickness and chain mobility. On the other hand, the high rejection was found to be due to a combination of high hydrophilicity, greater negative charge, and greater rupture strength of the network polyamide.

Several ternary copolyamides were prepared from aromatic diamine (*m*-phenylenediamine, 3,3′- or 4,4′-diaminodiphenylsulfone), aromatic diamine with carboxyl or sulfonic group (3,5-diaminobenzoic acid, 2,4-diaminobenzene sulfonic acid), and iso or terephthaloyl chloride (Scheme 24) *[Konagaya and Tokai, 2000]*. The flat asymmetric membranes of the copolyamides prepared from terephthaloyl dichloride and mixed diamine components of 3,3'-diamino diphenylsulfone and 3,5-diaminobenzoic acid showed good RO performance, and high chlorine resistance.

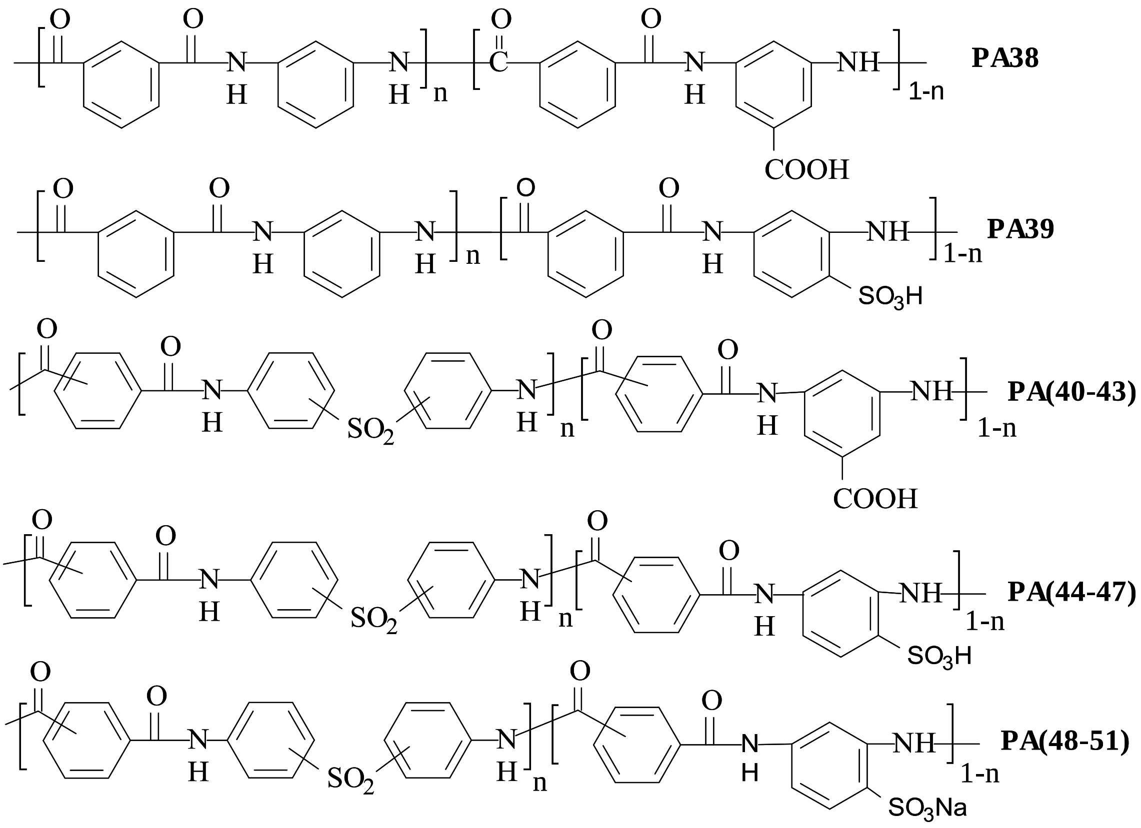

Scheme 24. Structures of polyamides **PA(38-51)**

Flux rate of product water (FR) and salt rejection (Rj) represent a RO performance of an asymmetric membrane. FR means an amount of product water (L/m^{2}day) that permeates through a membrane, when 25°C saline water containing 35.000 ppm of sodium chloride has been supplied to the common continuous pump-type RO apparatus under the pressure of 55kg/cm^2. Rj means a percentage (%) of the difference in sodium chloride concentration between the feed and the permeate to the sodium chloride concentration of the feed. The RO performance of the polyamides was improved, as indicated by a salt rejection between 68.0 and 97.3% and flux rate values ranging from 55 to 142 L/m^2 day, in comparison with Nomex aramid, which has Rj of 61.5% and FR of 84L/m^{2}day.

Polyamide nanocomposite films of about 400–800nm thickness coated over porous polysulfone support *via* interfacial polymerization to produce thin film nanocomposite membrane with enhanced properties were prepared from MPDA and trimesoyl chloride in *n*-hexane. Two types of nanocomposite films were prepared by incorporating two types of silica nanoparticles *in situ* into the polyamide films *[Jadav and Singh, 2009]*. The nanocomposite membranes exhibited superior thermal stability than the pure polyamide membranes. Higher silica loading into the polymer resulted into a thicker nanocomposite membrane film formation. At the same time, these nanocomposite membranes had relatively large pore sizes as well as higher pore number density, as determined by the analysis of membrane permeation data of aqueous solutions of organic solutes and sodium chloride at pressures ranging from 50 to 400psig. Depending on the silica content, the average pore radii membranes varied from smaller radius of 0.34nm to fairly larger radius of 0.73nm. Excellent membrane performance in terms of separation efficiency and productivity flux was observed for the nanocomposite membranes containing about 1–2 wt. % silica.

5. Conclusion

In the past three decades, significant synthetic efforts have been devoted to the development of novel aromatic polyamide materials with an optimal balance between processability and thermal/mechanical properties with emphasis on the modifications of chain structures, and some of them have been extended to commercial development. The interest towards aromatic polyamides was in the early years motivated by the desire to have highly thermostable polymers, which are soluble, hence easily processable at the same time. Now, this goal already attained, the interest is even stronger to achieve tailored macromolecules for specific end applications.

The intention of this brief overview was to provide information on the design, synthesis, properties of some representative high performance aromatic polyamides and their applications as electroluminescent, electrochromic, optically active, photosensitive and membrane materials.

The increasing number of articles published in the last decade proves that aromatic polyamides attract more and more attention, for both scientific and technical reasons.

6. References

Aharoni S. M., Hammond W. B., Szobota J. S., Masilamani D. (1984) Reactions in the presence of organic phosphites, II: Low-temperature amidation in solvent. *J. Polym. Sci. Polym. Chem. Ed.* Vol. 22, No 10, pp. 2579-2599.

Carrera-Figueiras C., Aguilar-Vega M. (2005) Gas permeability and selectivity of hexafluoroisopropylidene aromatic isophthalic copolyamides. *J. Polym. Sci. B: Polym. Phys.*, Vol. 43, No 19, pp. 2625–2638.

Carrera-Figueiras C, Aguilar-Vega M. (2007) Gas permeability and selectivity of benzophenone aromatic isophthalic copolyamides. *J. Polym. Sci .B: Polym. Phys.* Vol. 45, No 15, pp. 2083–2096.

Chang C. W., Chung C. H., Liou G. S. (2008) Novel Anodic Polyelectrochromic Aromatic Polyamides Containing Pendent Dimethyltriphenylamine Moieties. *Macromolecules*, Vol. 41, No 22, pp. 8441-8451.

Choi H. S., Jo W. H., Oh T. J., Kang Y. S., Park H. C. (2000) Effects of the Nitrile Group Substitution on the Gas Separation Properties of Aromatic Polyamide Membranes. *Fibers and Polymers*, Vol.1, No 2, pp. 111-115.

Elias H. G. (2007) *Macromolecules. Industrial polymers and synthesis*, Wiley-VCH, Weinheim, Germany.

Espeso J. F., Lozano A. E., Ferrero E., de la Campa J. G., de Abajo J. (2006) Effect of substituents on the permeation properties of polyamide membranes. *J. Membr. Sci.*, Vol. 280, No 1-2, pp. 659–665.

Fink J. K. (2008) *High performance polymers*, William Andrew Inc., Norwich, USA.

Garcia J. M, Garcia F. C., Serna F., de la Peña J. L. (2010) High-performance aromatic polyamides. *Progr. Polym. Sci.*,Vol. 35, No 5, pp. 623–686

Gaymans R. J. (2003) Polyamides, In: *Synthetic methods in step-growth polymers*, John Wiley & Sons, Inc., Hoboken, USA.

Hsiao S. H., Liou G. S., Wang H. M. (2009) Highly Stable Electrochromic Polyamides Based on N,N-Bis(4-aminophenyl)-N′,N′-bis(4-tert-butylphenyl)-1,4-phenylenediamine. *J. Polym. Sci.: Part A: Polym. Chem.*, Vol. 47, No 9, pp. 2330–2343.

Jadav G. L., Singh P. S. (2009) Synthesis of novel silica-polyamide nanocomposite membrane with enhanced properties. *J. Membr. Sci.*, Vol. 328, No 1-2, pp. 257–267.

Konagaya S, Tokai M. (2000) Synthesis of ternary copolyamides from aromatic diamine (*m*-phenylenediamine, diaminodiphenylsulfone), aromatic diamine with carboxyl or sulfonic group (3,5-diaminobenzoic acid, 2,4-diaminobenzenesulfonic acid), and iso or terephthaloyl chloride. *J. Appl. Polym. Sci.*, Vol. 76, No 6, pp. 913–920.

Liou G. S., Hsiao S. H., Huang N. K., Yang Y. L. (2006a) Synthesis, Photophysical, and Electrochromic Characterization of Wholly Aromatic Polyamide Blue-Light-Emitting Materials. *Macromolecules*, Vol. 39, No 16, pp. 5337-5346.

Liou G. S., Huang N. K., Yang Y. L. (2006b) Blue-Light-Emitting and Anodically Electrochromic Materials of New Wholly Aromatic Polyamides Derived from the High-Efficiency Chromophore 4,4′-Dicarboxy-4′′-methyltriphenylamine. *J. Polym. Sci.: Part A: Polym. Chem.*, Vol. 44, No 13, pp. 4095-4107.

Liou G. S., Huang N. K., Yang Y. L. (2006c) New soluble triphenylamine-based amorphous aromatic polyamides for high performance blue-emitting hole-transporting and anodically electrochromic materials. *Polymer*, Vol. 47, No 20, pp. 7013-7020.

Liou G. S., Yang Y. L., Su Y. O. (2006d) Synthesis and Evaluation of Photoluminescent and Electrochemical Properties of New Aromatic Polyamides and Polyimides with a Kink 1,2-Phenylenediamine Moiety. *J. Polym. Sci.: Part A: Polym. Chem.*, Vol. 44, No 8, pp. 2587–2603.

Liou G. S., Fang Y. K., Yen H. J. (2007) Synthesis and Properties of Noncoplanar Rigid-rod Aromatic Polyamides Containing Phenyl or Naphthyl Substituents. *J. Polym. Res.*, Vol. 14, No 2, pp. 147-155.

Liou G. S., Chang C. W. **(**2008) Highly Stable Anodic Electrochromic Aromatic Polyamides Containing *N*,*N*,*N′*,*N′*-Tetraphenyl-*p*-Phenylenediamine Moieties: Synthesis, Electrochemical and Electrochromic Properties. *Macromolecules*, Vol. 41, No 5, pp. 1667-1674.

Mallakpour S., Rafiee Z., (2008a) Safe and fast polyamidation of 5-[4-(2-phthalimidiylpropanoylamino)-benzoylamino]isophthalic acid with aromatic diamines in ionic liquid under microwave irradiation. *Polymer*, vol. 49, No 13-14, pp. 3007–3013.

Mallakpour S., Rafiee Z. (2008b) Use of ionic liquid and microwave irradiation as a convenient, rapid and eco-friendly method for synthesis of novel optically active and thermally stable aromatic polyamides containing *N*-phthaloyl-*L*-alanine pendent group. *Polym. Degrad. Stab.* Vol. 93, No 4, pp. 753-759.

Mallakpour S., Rafiee Z. (2009) Microwave-induced synthesis of new optically active and soluble polyamides containing pendent 4-(2-phthalimidiylpropanoylamino) benzoylamino-groups. *Amino Acids*, Vol. 37, No 4, pp. 665–672.

Mallakpour S., Dinari M. (2009) Preparation of thermally stable and optically active organosoluble aromatic polyamides containing *L*-leucine amino acid under green conditions. *Polym. Bull.*, Vol. 63, No 5, pp. 623–635.

Mallakpour S., Meratian S. (2009) Preparation and Characterization of Thermostable Chiral Extended Polyamides Bearing *N*-Phthaloyl-*L*-leucine Pendent Architectures in Green Media. *J. Appl. Polym. Sci.*, Vol. 111, No 3, pp. 1209–1215.

Mallakpour S., Kolahdoozan M. (2008) Synthesis and properties of novel soluble aromatic polyamides derived from 5-(2-phthalimidyl-3-methyl butanoylamino)isophthalic acid and aromatic diamines. *React. Funct. Polym.*, Vol. 68, No 1, pp. 91–96.

Mallakpour S., Seyedjamali H. (2008) One-pot polyamidation reaction of optically active aromatic diacid containing methionine and phthalimide moieties with aromatic diamines under microwave irradiation and traditional heating. *Eur. Polym. J.*, Vol. 44, No 11, pp. 3615–3619.

Mallakpour S., Seyedjamali H. (2009) Ionic liquid catalyzed synthesis of organosoluble wholly aromatic optically active polyamides. *Polym. Bull.*, Vol. 62, No 5, pp. 605–614.

Nagase Y., Ando T., Yun C. M. (2007) Syntheses of siloxane-grafted aromatic polymers and the application to pervaporation membrane. *React. Funct. Polym.*, Vol. 67, No 11, pp. 1252–1263.

Nechifor M. (2009) Synthesis and properties of some aromatic polyamides with coumarin chromophores. *React. Funct. Polym.*, Vol. 69, No 1, pp. 27–35.

Nechifor M. (2010) Polymeric materials with self-photocrosslinking capability, In: *Functional Polymeric Materials Designed for Hi-Tech Applications,* Transworld Research Network, Kerala, India.

Nechifor M. (in press) Synthesis and properties of novel aromatic polyamides with non-conjugated bichromophoric units in the main chains. *J. Polym. Res.,* DOI 10.1007/s10965-011-9669-4.

Onciu M., Rusu E. (2002) Synthesis and characterization of some polyamides incorporating modified isophthalic acid units. *Polym. Int.,* Vol. 51, No 6, pp. 488-492.

Onciu M. (2007a) Synthesis and Properties of New Polyamides Based on a Hydroxyethyl Cinnamide Extended from 3,5-Diaminobenzoic Acid. *J. Appl. Polym. Sci*., Vol. 103, No 3, pp. 2013–2020.

Onciu M. (2007b) Synthesis and characterization of novel aromatic polyamides containing pendent coumarin groups. *J. Optoel. Adv. Mater*., Vol. 9, No 4, pp. 1014 – 1018.

Preston J. (1988) Aromatic polyamides, In *Encyclopedia of Polymer Science and Engineering,* Wiley Interscience, New York, USA.

Roh I. J., Khare V. P. (2002) Investigation of the specific role of chemical structure on the material and permeation properties of ultrathin aromatic polyamides. *J. Mater. Chem.,* Vol. 12, No 8, pp. 2334–2338.

Rusu E., Nechifor M. (2003) Polyamides with pendant cinnmoyloxyethyl units. *High Perf. Polym*., Vol.15, No 2, pp. 197–206.

Rusu E., Onciu M. (2005a) Synthesis and properties of new polyamides based on 2-(4-dimethylaminocinnamoyloxy)ethyl-3,5-diaminobenzoate. *Des. Monom. Polym.*, Vol. 8, No. 1, pp. 37–47.

Rusu E., Onciu M. (2005b) Aromatic polyamides containing chalconyl substituted *m*-phenylenediamine segments. *Polimery*, Vol. 50, No 11—12, pp. 797-804.

Rusu E., Onciu M. (2005c) Polycondensates of 2′-(Chalcone-4-Oxy)-Ethyl-3,5-Diaminobenzoate with Some Aromatic Dicarboxylic Acids. *J. Macromol. Sci. Part A: Pure Appl. Chem.,* Vol. 42, No 8, pp. 1025–1036.

San-José N., Gómez-Valdemoro A., Estevez P., García F. C., Serna F., García J. M. (2008) Fluorescent aromatic polyamides with urea binding sites and fluorene or dansyl signaling units. *Eur. Polym. J.,* Vol. 44, No 11, pp. 3578–3587.

Su T. H., Hsiao S. H., Liou G. S. (2005) Novel Family of Triphenylamine-Containing, Hole-Transporting, Amorphous, Aromatic Polyamides with Stable Electrochromic Properties. *J. Polym. Sci.: Part A: Polym. Chem.,* Vol. 43, No 10, pp. 2085–2098.

Tarboush B. J. A., Rana D., Matsuura T., Arafat H. A., Narbaitz R.M. (2008) Preparation of thin-film-composite polyamide membranes for desalination using novel hydrophilic surface modifying macromolecules. *J. Membr. Sci.,* Vol. 325, No 1, pp. 166–175.

Van Krevelen D. W., Hoftyzer P. J. (1976) *Properties of polymers*. Elsevier Scientific Publishing Company, New York, USA.

Vollbracht L. (1989) Aromatic polyamides In *Comprehensive polymer science,* Pergamon Press, New York, USA.

Yamazaki N., Matsumoto M., Higashi F. (1975) Studies on reactions of the N-phosphonium salts of pyridines. XIV. Wholly aromatic polyamides by the direct polycondensation reaction by using phosphites in the presence of metal salts. *J. Polym. Sci. Polym. Chem. Ed.* Vol. 13, No 6, pp. 1373-1380.

Yen H. J, Liou G. S. (2008) Novel thermally stable triarylamine-containing aromatic polyamides bearing anthrylamine chromophores for highly efficient green-light-emitting materials. *J. Polym. Sci.: Part A: Polym. Chem.,* Vol. 46, No 22, pp. 7354–7368.

Chapter 2

Copolyamides – Versatile Engineering Polymers

Madalina Zanoaga, Fulga Mihaela Tanasa

"Petru Poni" Institute of Macromolecular Chemistry Iasi, Romanian Academy

---

Summary

Copolyamides are a subject of long lasting interest due to their variety, complex structures, high performance properties, commercial importance, long term use and versatility as engineering polymers. This chapter briefly reviews the main methods of synthesis and fields of application of these polymers, emphasizing their role in the development of fundamental knowledge database (new synthetic methods and protocols) and engineering.

Notations and acronyms

ADETA	nylon salt of adipic acid and diethylenetriamine (DETA)
AH	nylon salt of adipic acid and hexamethylenediamine (HMD), or hexamethylenediamine adipate
AN2	nylon salt based on adipic acid and 1-(2-aminoethyl) piperazine (N2).
BA	3,5-diaminobenzoic acid
CL	ε-caprolactam
coPA	copolyamide
DETA	diethylenetriamine
DMAc	dimethylacetamide
4T	tetramethylene terephthalamide
HDD	hydrogenated distilled dimerized polymeric fat acids
HFA	4,4’-(hexafluoroisopropylidene)dianiline
HMA	hot melt adhesive
HMD	hexamethylenediamine; 1,6-diamino hexane
LL	λ-laurolactam
N2	1-(2-aminoethyl) piperazine
NMP	*N*-methylpyrrolidone
NW	nonwoven
PA	polyamide (nylon)
PA 6	polyamide 6, poly-ε-caprolactam
PA 4,6	polytetramethylene adipamide
PA 6,6	polyhexamethylene adipamide
PA 12	polydodecanamide; polylaurolactam
PP	polypropylene
PTT	poly(trimethyleneterephthalamide)
6T	hexamethylene terephthalamide
SH	nylon salt of sebacic acid and hexamethylenediamine (HMD), or hexamethylenediamine sebacate
T_{BD}	temperature of beginning of decomposition, °C
T_c	temperature of crystallization, °C
T_g	glass transition temperature, °C
T_m	temperature of melting, °C
TERT	5 t-butylisophthalic diacid
TPE	thermoplastic elastomer
wt.	weight

1. Introduction

Polyamides have been used since the 1930s – the dawn of the synthetic polymers age. The development of polyamide technology established many of the principles and experimental protocols for polymerization in general, laying the groundwork for the great array of materials that have followed.

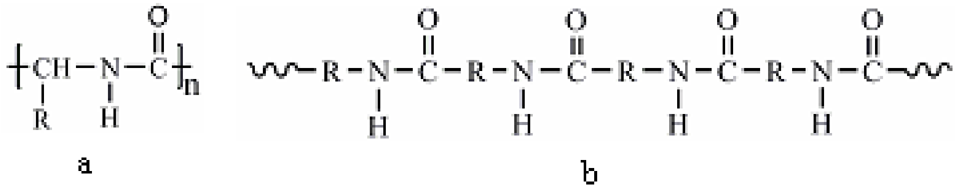

Figure 1. The general structure of a polyamide: a) a repeating structural unit; b) fragment of a macromolecular chain

Polyamides (PAs) continue to have a well established and respected place among polymeric materials and, although they were replaced in some applications by novel better-suited formulations, they still remain important in both volume and their ability to meet specific needs. In fact, some of the competition has been internal, in terms of designing new types of polyamides with superior properties that have sometimes edged out the classic ones.

It may be said about polyamides that they are polymeric materials of great practical utility. In terms of engineering, polyamides embody reaction engineering in its most general sense, where a combination of chemical and physical transformations is designed to yield in useful products.

Along with its essential role in joining small molecules into large ones, the amide bonding dictates most of the properties of the polymer due to its polar nature. Amide groups participate in hydrogen linkage which restricts inter-chain mobility, resulting in strength and in strength retention as temperature increases. In most polyamides, hydrogen bonding pulls many of the chains into ordered crystalline regions, which further augment the strength and melting point of the polymer. Hydrogen linkage also occurs between polyamide and water and other polar absorbed substances. If in the crystalline region the polyamides are aligned in the same direction, the polymer displays notable behaviour under electrical stimuli. Augmenting the effect of the amide dipole, the more recent incorporation of aromatic monomers, particularly where conjugation between the benzene double bonds and the acyl double bond in the amide link occurs, adds further to the strength and temperature-resistance of the polymer, as well as other useful properties.

The two original polyamides, nylon 6,6 and nylon 6, were invented in the 1930s, but their origins were in the 1920s when Herman Staudinger developed the concept of natural polymers as large molecules comprising repeating small units or segments. On this basis, Wallace Carothers, working for

DuPont, reasoned that synthetic polymers could be made by the chemical bonding of small molecules, and he eventually settled on diamines and diacids as the molecules of choice, reacting them with each other to produce amide linkages and large molecules consisting of 100 and more repeating units *[Marchildon, 2001]*.

Copolyamides (coPAs) were created on the same basis due to the need to obtain some balance of properties not attainable with a single polyamide or attainable only with a polyamide requiring a monomer that was not readily available.

From this point on, novel polyamides and copolyamides were continuously designed, obtained and characterized, tailored for specific applications. Copolyamides were the answer to an up-to-date problem: diversifying the structures and expanding the range of applications, while using available raw materials and existing technologies. Low melting points and reduced melt viscosities, modified crystallinity, electric and mechanic properties, adhesion characteristics, enhanced solubility and processability, all these were possible to achieve due to the design of copolyamides composition, co-monomers ratio respectively *[Feldman and Marculescu, 1977]*. In example, two different polyamides are highly crystalline, opaque, hard, insoluble and have high thermal stability, whilst the copolyamide resulted from both type of structural units may have amorphous character, may be transparent, soluble in common organic solvents, easy fusible, even plastic or thermoplastic.

First patents on copolyamides date from late 1930s – early 1940s: in 1937, Wallace Carothers presented the fist copolyamide obtained starting from hexamethylenediamine, diethylenetriamine and adipic acid *[Carothers, 1937; 1938a, 1938b, 1938c]*; in 1938-1939, Hubert, Ludewig and Schlack obtained glassy transparent, soluble and highly adhesive copolyamides based on ε-caprolactam, diacids and diamines *[Hubert et al., 1939; Schlack, 1938]*; in 1942, Baker and Fuller presented series of binary copolyamides made of adipic and sebacic acids, and hexamethylenediamine and decamethylenediamine, respectively *[Baker and Fuller, 1942]*.

2. Synthesis and structure–property relationships

2.1 General considerations

PAs and coPAs are used neat in fibres, films and engineering plastics and may contain fillers in some engineering plastics applications *[Daebel et al., 1998; Hofmann, 1998; Jacobs and Zimmermann, 1977; Kohan, 1995; Preston, 1989; Vollbracht, 1989; Zimmerman, 1989]*. Reinforced PA accounts for about 80% of the engineering plastic market. In the case of the reinforced structures the filler is glass fibers, particles like talc, kaolin, metal powders, carbon nanotubes, as well as wood chips, lignocellulosic fibres, mica, silicates, etc.

For engineering plastics applications, dimensional stability at high temperatures is often sought. Solvent resistance to hydrocarbons is also important for use in automotive applications. The processing of engineering plastics is achieved by injection molding and, to a lesser extent, by extrusion; to ensure good processability, a low melt viscosity is required and rapid crystallization is important, as well.

Semicrystalline partial aromatic PAs and coPAs have a very high melting temperature, often too high for melt synthesis and melt processing. Amorphous partial aromatic PAs and coPAs do not have a melting temperature and can, thus, be synthesized and processed at lower temperatures. They are transparent and have good solvent resistance and relatively low water absorption.

Wholly aromatic PAs can be processed from solution into film and fibres. These polymers have very good dimensional stability and excellent heat stability. All *para* wholly aromatic PAs form liquid crystalline solutions and fibres can be obtained, which are highly oriented and which have a *para*-crystalline structure. These all-aromatic PA fibres have a very high modulus and fracture strength.

2.2 Main methods of polyamides and copolyamides synthesis

The most well-known and widely used types of PAs are usually obtained by polycondensation (in molten state, in solution, interfacially, and even in solid state) and polyaddition reactions (i. e., lactams ring opening polymerization).

Common liniar PAs can be obtained by polycondensation, as follows:

–CO–NH–R–CO–NH–R′–CO–NH–R–CO–NH– (1)

–NH–CO–R–CO–NH–R′–NH–CO–R–CO–NH– (2)

where R = $(CH_2)_x$

Type (1) is produced by the self polycondensation of ω-aminoacids or their corresponding esters, while type (2) results from the polycondensation of diacids and diamines, or their derivatives, respectively (esters, nitriles, acid chlorides, isocyanates, etc.) (Fig. 2) *[Floyd, 1961; Gaymans, 2003]*.

A special mention has to be done for the case of fatty PAs obtained directly from fatty oils (i.e., soy bean or tall oil) by their polymerization under high temperature and inert medium, in the presence of specific catalysts; this is possible due to their high content of unsaturated bonds able to undergo intermolecular polymerization processes *[Cowan et al., 1948]*.

Hydrolytic processes involved in PAs and coPAs synthesis are kinetics driven and their yields depend on concentration of monomers and temperature *[Gaymans, 2003]*. For the case of synthesis of PA 6 in aqueous medium, the equilibrium constant K has been found to be independent of the water concentration, but the dielectric constant of the medium and the degree of ionization of end groups increases with the increasing amount of water. This is likely to influence the end groups activity coefficient, depending on whether polycondensation involves reactions of predominantly neutral or ionized species. By removing the water, the equilibrium is shifted towards higher molecular weights, but under high anhydrous conditions and elevated temperatures significant degradation reactions take place, yielding in Schiff bases which give coloured PAs (Fig. 3), branched macromolecules or even cyclization of end groups (as in the case of diaminobutane end group in the polymerization of PA 4,6 (Fig. 4).

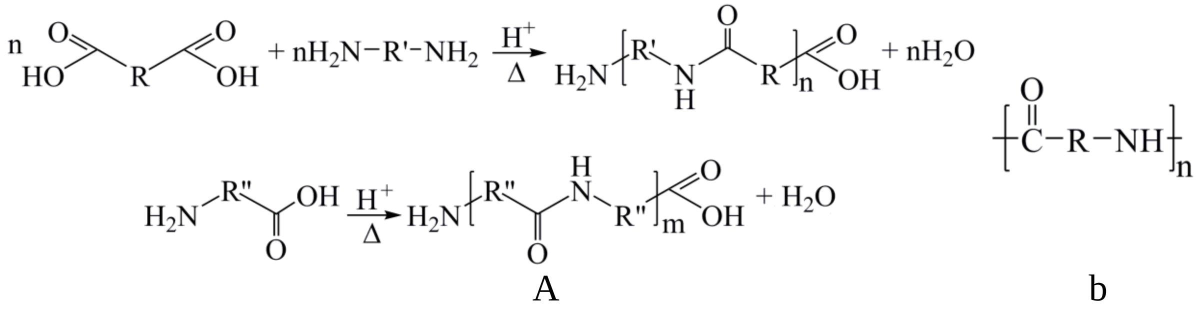

Figure 2. Typical syntheses of polyamides: a) reaction between a diacid and a diamine; b) the polycondensation of an aminoacid

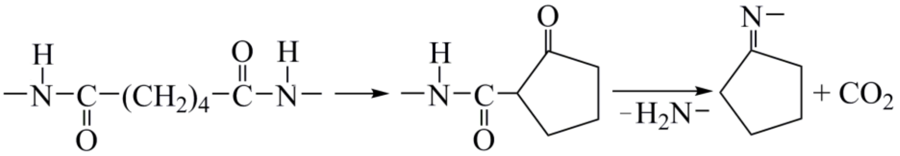

Figure 3. Schiff base formation

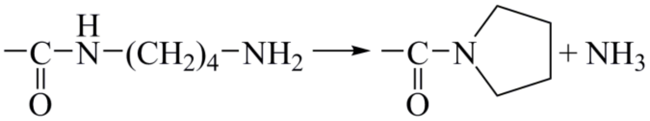

Figure 4. Cyclization of the diaminobutane end group during PA 4,6 synthesis

Reactions of acid chlorides with amines evolve with the formation of hydrochloric acid, as by product (Fig. 5), which can form amine salts with the unreacted amine groups, reducing the yield in PA *[Preston, 1989; Vollbracht, 1989]*.

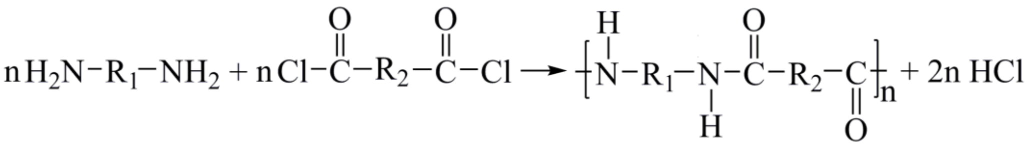

$$n\,H_2N-R_1-NH_2 + n\,Cl-\overset{O}{\overset{\|}{C}}-R_2-\overset{O}{\overset{\|}{C}}-Cl \rightarrow \left[\overset{H}{\overset{|}{N}}-R_1-\underset{H}{\underset{|}{N}}-\overset{O}{\overset{\|}{C}}-R_2-\underset{O}{\underset{\|}{C}}\right]_n + 2n\,HCl$$

Figure 5. Typical reaction of diamines and acid chlorides

To prevent this secondary reaction, acid binders, which are more reactive than the amines, are added in the reaction mixture. The basicity of the aromatic diamine is rather low and acid binding can be achieved even with solvents such as *N*-methylpyrrolidin-2-one (NMP) and dimethylacetamide (DMAc). The whole *para* aromatic amide poly(*p*-phenyleneterephthalamide) can be synthesized in DMAc. To prevent precipitation of the polymer, a salt, such as calcium chloride or lithium chloride, can be added.

Similarly, a reaction between acid chlorides and silylated diamines (Fig. 6) can yield into aromatic or aliphatic, even star-shaped, PAs *[Kricheldorf and Denchev, 1998; Oishi et al., 1987]*:

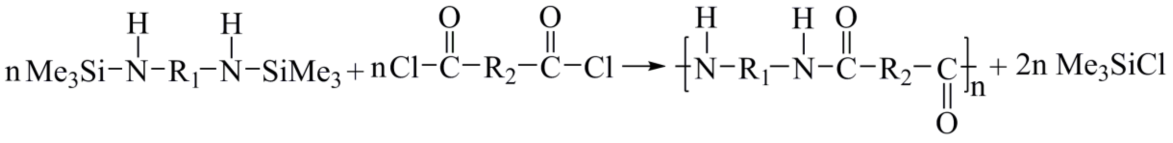

$$n\,Me_3Si-\overset{H}{\overset{|}{N}}-R_1-\overset{H}{\overset{|}{N}}-SiMe_3+n\,Cl-\overset{O}{\overset{\|}{C}}-R_2-\overset{O}{\overset{\|}{C}}-Cl \longrightarrow \left[\overset{H}{\overset{|}{N}}-R_1-\overset{H}{\overset{|}{N}}-\overset{O}{\overset{\|}{C}}-R_2-\underset{O}{\underset{\|}{C}}\right]_n+2n\,Me_3SiCl$$

Figure 6. Reaction of silylated diamines and acid chlorides

Interfacial polycondensation takes place at the interface of two distinct phases (the aqueous solution of diamine and the phase of the diacid or diacid chloride dissolved in an organic solvent). If the process evolves under stirring, the active surface is much wider and the rate of polymerization is higher. By this methods, high molecular weight PAs can be produced, such as PA-2,10; 4,10; 6,10; 10,10, as well as coPAs. In this case, diacids and diamines showed a modified reactivity, due to the non-equilibrium reaction conditions and low temperature (which prevents any other subsequent transamidation). Under these conditions, hexamethylenediamine is more reactive than ethylenediamine, while acid chloride of terephthalic acid is more reactive than that of tetrachloroterephthalic acid. It was also proven that thermal and mechanical properties of copolyamides obtained in equilibrium and non-equilibrium conditions (interfacial policondensation) are of comparable performance. Still, due to the temperature regime, which is different in each case in relation to polymer glass transition temperature, copolyamides obtained by interfacial policondensation have a higher degree of crystallinity. The most important factors that influence this type of polycondensation have been studied in detail *[Morgan, 1977; Zydowicz et al., 2001]*.

Ring-opening polymerization is a specific method for lactams; cyclic dimers can also occur and they take part in the polymerization. Being a hydrolitic process, it is influenced by temperature and presence of water. The polymerization of PA is carried out between 220-280°C and water is added to initiate the ring-opening reaction. At a high water content, the degree of polymerization is low but the rate of ring opening (initiation) is high. At low temperatures, the degree of polymerization is higher but the rate of polymerization is lower (Fig. 7) *[Gaymans, 2003]*.

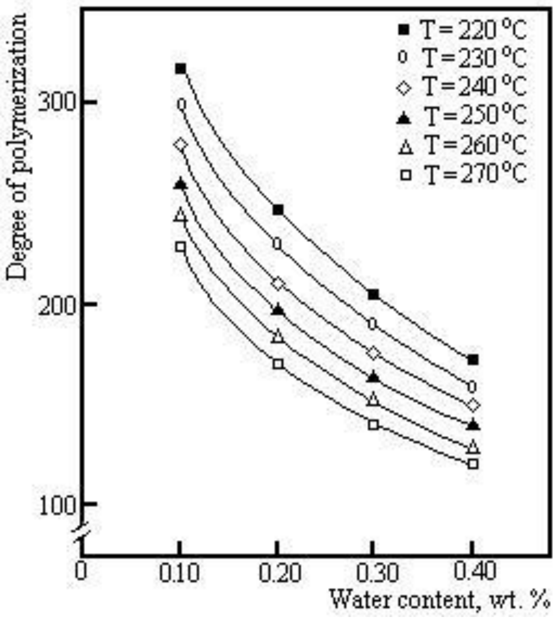

Figure 7. Influence of water content (wt.%) on the degree of polymerization (Pn) at different temperatures (equilibrium) *[after Gaymans, 2003]*

For the low molecular weight PAs, the ring stability of the lactam is unfavorable for melt polymerization. But for the seven-membered lactam rings and the larger ones the melt polymerization and melt processing are possible *[Dubois et al., 2009; Jacobs and Zimmermann, 1977; Zimmerman, 1989]*.

Transamidation is a direct acid-catalyzed interchange reaction between two amide groups and the effects depend on types of polyamides involved in the reaction *[Kricheldorf and Denchev, 1998]*.

Solid-state polymerization is applied for PAs as well as for coPAs and is carried out at temperatures just below the melting temperature of the polymer *[Jacobs and Zimmermann, 1977; Zimmerman, 1989]*. This method offers some advantages: water removal, limited thermal degradation, equilibrium molecular weights are higher than in molten-state due to lower reaction temperature and higher chain-end concentration in the amorphous phase (while most of macromolecular chains are in the crystalline phase). The starting materials for solid-state polymerization can be monomers (PA salts), prepolymers and polymers. Solid-state polymerization is carried out on granules at 10–40°C below their melting temperature for 24 h; the size of the granules seems to have little effect on the reaction rate. The process can be carried out in a high vacuum with a nitrogen sweep; however, at high temperatures (T>220°C), in the absence of water, the polymer becomes colored due to degradation reactions. The use of superheated steam prevents granules from turning yellow and the steam does not seem to reduce the reaction rate *[Oishi et al., 1987; Zimmerman, 1989]*.

There is a wide variety of synthetic protocols for specific PAs and coPAs, and the literature is abundant on this issue due to the necessity of modulating the product properties according to its specific application demands.

2.3 Structure-properties relationship in copolyamides

It is well established that the nature and ratio of monomers, reaction conditions, crystallization, amount of hydrogen bonds, long distance order of macromolecules, etc., have a great influence on the properties of PAs and coPAs. Based on theoretical and experimental data, it was concluded that co-polymerization is a very effective tool for obtaining coPAs with low crystallinity and other favourable properties that derive from it, such as: low melting temperatures, low density, enhances solubility or sensitivity towards solvents, increased elasticity and flexibility, transparency, adhesion properties, etc. *[Brown, 1999]*. These characteristics are valuable for different specific applications where thermosensitive materials are involved *[Harman, 1989; Hu et al., 1989; Loeb, 1978; Peerman and Kanten, 1980]*. Thermoplastic coPAs properties and areas of application can be modulated through their molecular weight, as follows:

- low molecular weight coPAs are used for low temperature applications and simple, cheap technology is involved;
- medium molecular weight coPAs need a more complex technical support for applications;
- high molecular weight coPAs applications require hi-tech very sophisticated devices *[Bateman, 1978; Ebnesaijjad, 2008; Floyd, 1961; Petrie, 2007; Tremblay, 2010]*. Consequently, a different range of values is obtained for main properties of each type of coPAs *[Petrie, 2007]*, as presented in Table 1.

Table 1. Main properties of thermoplastic coPAs versus molecular weight *[after Petrie, 2007]*

Property	Molecular weight		
	Low	**Medium**	**High**
Melting temperature, °C	95-180	95-200	135-200
Melt viscosity, poise – 160°C – 210°C – 260°C	 5 - Solid 1 - 10 ---	 120 - Solid 20 - 110 5 - 25	 --- 250 - 50,000 20 - 1000
Tensile strength, N/m^2	$(1.1 \div 11)\cdot 10^6$	$(3.10 \div 20.68)\cdot 10^6$	$(23.44 \div 44.80)\cdot 10^6$
Elongation at break, %	5-100	25-1000	200-600

Crystallization of coPAs strongly depends on the mixture composition and reaction conditions. In the case of PA 4,6/PA 6I (6I is polyhexamethylene isophthalamide) obtained by melt polymerization (90 min, 315°C) their amorphous structures become exclusives for 70% PA-6I, confirmed by their transparency at room temperature and absence of crystallization temperature or heat *[Eersels et al., 1996]*. Further processing of copolyamides as fibres (stretching, thermal treatments in hot air, nitrogen, steam or infrared radiation) enhanced the crystallinity and, subsequently, an increased dimensional stability and degree of lateral order (DLO) were registered *[Champan et al., 1977]*. Properties of these coPAs allow the production of monofilaments, short and long fibres, cables, etc.

Another important characteristics affected by crystallinity are mechanic properties and the flame resistance. In example, copolyamides as PA 6T,6I (6T is polyhexamethylene terephthalamide) showed higher dimensional stability (contraction in boiling water is 8%, which indicates DLO values over 70%), enhanced resistance to wear and impact, as well as an increased resistance to flame and adhesive properties towards rubber, when compared to PA 6,6 and PET *[Kehayoglou, 1983]*.

Copolyamides based on PA 6,12 and LL (laurolactam) showed a lower crystallinity and melting temperature (Fig. 8 and 9), enhanced flexibility and transparency due to the addition of LL and type of synthesis (centrifugal anionic copolymerization) *[Ramanathan, 2000]*, *[Rusu, 2003]*. Up to 20% LL, macromolecular order is rather high due to the effects exerted by PA-6 segments which are predominant, involved in hydrogen bonds and strong dipol-dipol interactions and constrain PA-12 sequences to exist only in the amorphous phase of the polymer. Other studies proved that the degree of crystallinity decreases along with the increasing amount of LL up to 50% (mol), but after this value the effect is opposite *[Arvanitoyannis and Psomiadou, 1994; Goodman and Kehayoglou, 1983;Udipi et al., 1997]*.

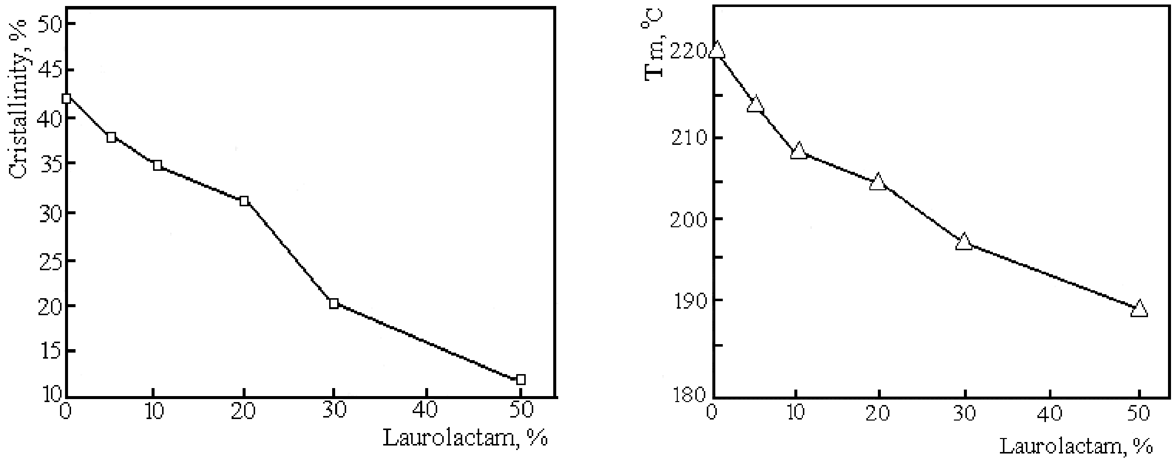

a b

Figure 8. Influence of LL amount on: a) crystallinity (by X-ray diffraction); b) melting temperature *[after Rusu, 2003]*

Amorphous or low crystalline copolyamides having low melting temperature and enhanced solubility (solubility in aliphatic alcohols gives the possibility to obtain stable solutions and even transparent films) are of special interest due to their potential for thermosensitive materials applications. There are many examples in the literature showing a wide variety of synthetic protocols and structures. Copolyamides PA 6,6/6 which contain 40-65% CL (ε-caprolactam) have melting point of about 180°C and are soluble in hot methanol, although PA 6 or PA 6,6 are not. Ternary copolyamides based on hexamethylenediamine, CL and dicarboxylic acids showed transparency over a wide window of compositions *[Ramanathan, 2000]*.

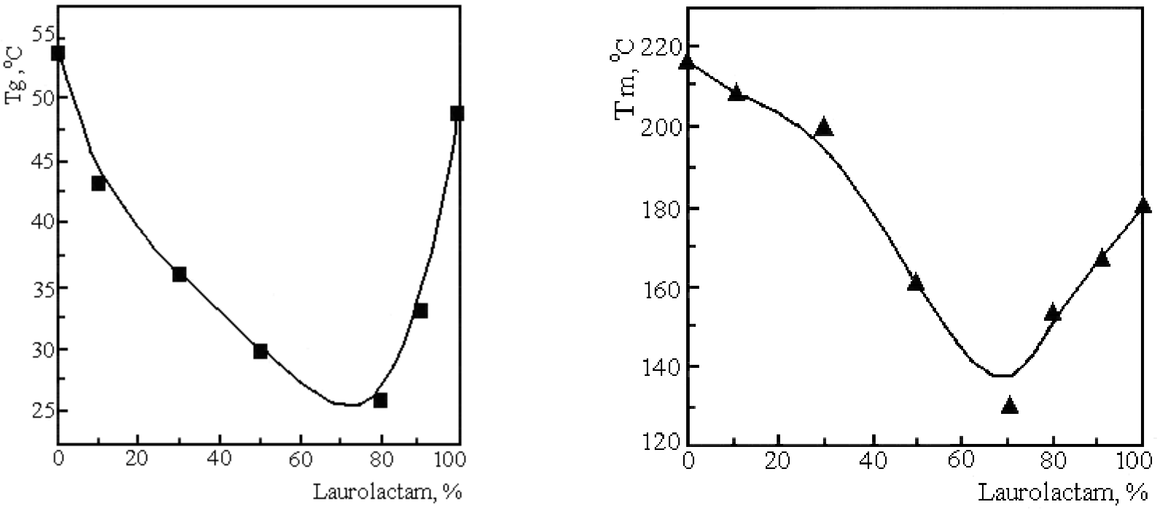

a b

Figure 9. Influence of LL amount on: a) glass transition temperature (T_g); b) melting temperature (T_m) *[after Ramanathan, 2000]*

Polyamides and copolyamides water absorption is another property affected by the degree of crystallinity; it increases exponentially with amide groups content. Water drastically lower T_g, but the fracture strength is little affected due to the value of the higher modulus compared to a dry sample. Since first percents of water are absorbed without increasing polymer volume, it may be considered that this water is distributed in the free space between macromolecular chains, with the specification that water molecules penetrate first the amorphous phase where break hydrogen bonds and favour the formation of new feeble bonds (Fig. 10) *[Goetz, 2003; Peerman, 1967]*.

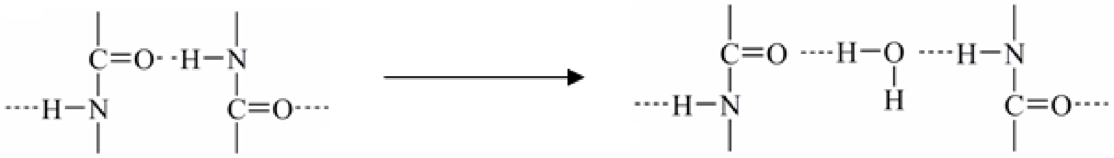

Figure 10. The water molecule intercalation and the formation of new feeble bonds *[after Peerman, 1967]*

A water content higher than 3% has a negative impact on the processability of copolyamides: processing these materials at temperatures above 100°C produces a foaming phenomenon into the melted polymer, which generates pores and other defects (Fig. 11) that bring down mechanical and adhesion properties *[Albrecht et al., 2003]*.

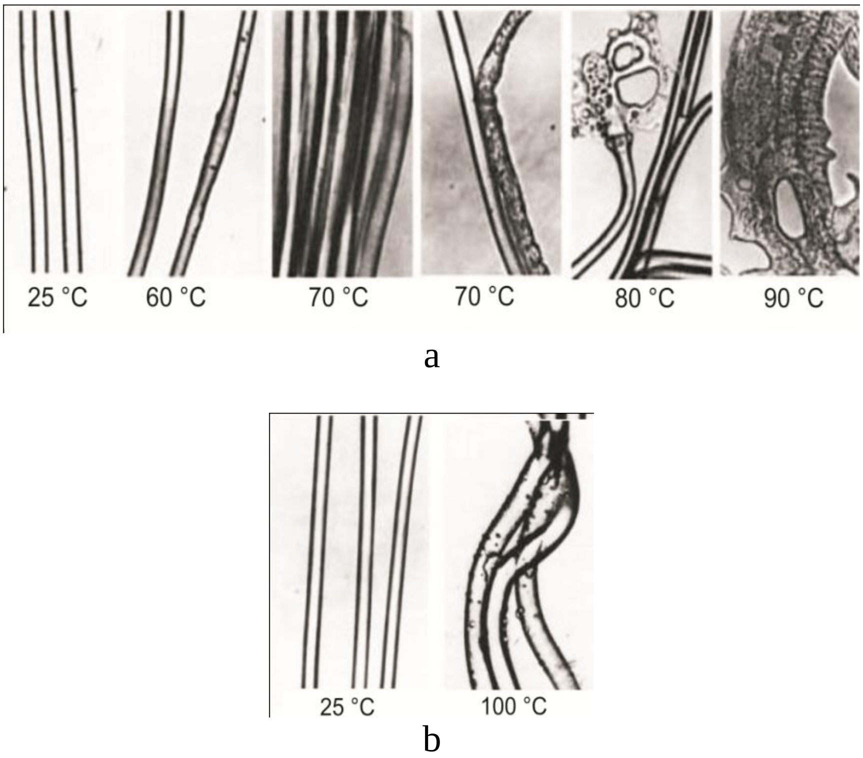

Figure 11. Copolyamidic fibres treated with water at different temperatures: a) Grilon K 140; b) Grilon K 115 *[after Albrecht et al., 2003]*

Low melting point copolyamides are a class of polyamide that must suffer enough disruption of hydrogen bonding to significantly lower their crystallinity and melting point, but retain enough internal bonding to keep them strong enough for their intended end use. Zytel 61® was an early offering of the DuPont company and consisted of a terpolymer of polyamides 6/6,6/6,10; this coPA was completely amorphous (crystallinity of about 10%), it had no sharp solid-liquid transition and was soluble in alcohol. Its main application was in conservation, used as solution to protect paper and other art objects *[Marchildon, 2001]*.

It is well known that classic ternary copolyamides are mostly used as hot-melt adhesives in light industry for clothing manufacturing *[Crusos and Zanoaga, 1992; Crusos et al., 1999, 2001a; Poessnecker et al., 2003; Zanoaga, 2001a, 2001b; Zanoaga and Melinte, 2008a]*, where they have to satisfy a number of requirements: high bond strength, resistance to dry-cleaning solvents, resistance to washing temperature up to 80°C, low melting point to allow application to thermo-sensitive fabrics. There were various formulations reported in the field, most of them based on PA 6, PA 11, PA 12 with HMD (1,6-hexane diamine) *[Raabe and De Jong, 1978]* or mixtures of diamines and diacids *[Poessnecker et al., 2003]*, or even PA 6 and PA 6,6 with various additives such as castor oil, acetic anhydride or formaldehyde in order to lower the melting point *[Besshaposhnikova et al., 2004]*.

Some new copolyamides based on short aliphatic diamine (such as HMD), aliphatic dicarboxylic acids (adipic and sebacic acid) and CL were synthesized by melt polycondensation and displayed a most interesting behaviour in alcohols and high stability in usual solvents, as well as hot-melt adhesive properties *[Crusos et al., 1983, 1985, 2001a; Zanoaga, 2001a, 2001c; Zanoaga and Tanasa 2010a]*. The reaction mixtures are presented in Table 2 and polymers properties are showed in Table 3. An indication on the high molecular weight of copolyamides was afforded by the toughness and ability to form fibres drawn directly from melt phase. A most remarkable behaviour towards alcohol was noticed for copolymers: at temperatures above 100°C, under pressure, they yield in viscous solutions which become gels upon cooling. Thermal characterization of these coPAs evidenced their low melting temperatures (125-174°C) and good thermal stability up to 400°C.

Table 2. Reaction mixtures and polymers yields *[after Zanoaga, 2001a]*

Polymer	**Reagents, g**					**Water soluble extract, %**	**Yield, %**
	CL	**HMD**	**AA**	**SA**	**Water**		
A0	9	4.16	1.12	5.72	10	5.21	94.79
A1	9	4.16	-	7.28	10	17.98	82.02
A2	9	4.16	5.23	-	10	21.32	78.68

where: AA – adipic acid; SA – sebacic acid

Table 3. Main properties of copolyamides *[after Zanoaga, 2001a]*

Polymer	**Aspect**	**Toughness**	**Viscosity, dl/g**	**Water absorption, %**	**Density, g/cm^3**	**Crystallinity, %**
A0	Light yellow, translucent	Very resistant, spinnable	0.83	6.82	1.110	67
A1			0.59	6.92	1.065	59
A2			0.98	22.65	1.133	46

A specific formulation from the above mentioned copolyamides was patented by *„Petru Poni” Institute of Macromolecular Chemistry* in Iasi, Romania, under the trade name Aderom (melting temperature 125-135°C, powders with particles size of 1-400μm). The product was successfully tested as a hot-melt adhesive in the light industry, mainly for affixing various accesories *[Buruiana et al., 2007; Zanoaga, 2001b, 2006, 2007; Zanoaga and Harnagea, 2005, 2008b; Zanoaga and Melinte, 2008a; Zanoaga and Tanasa, 2002, 2010b; Zanoaga et al., 2004a, 2004b]*. The level of performance was comparable with that of well know adhesives Sarpifan (Stockhausen, Germany), Schaetttifix

(Shaetti, Switzerland), Platamid (Plate Bonne, Germany), Vestamid (Huls, Germany) or Abifor (Billeter, Switzerland).

Thermoplastic elastomers (TPEs) are a class of block copolymers in which periodic crystallizable "hard" segments are interspersed with "soft" segments, each of the latter consisting of a long block of non-crystallizing polymer. The most common choice for the soft segments is a polyether, formed from three-carbon or four-carbon monomers, these monomers being either diols or cyclic oxides. Each hard segment is a relatively short length of a polymer with capability to bond (generally, through hydrogen bonding) with other hard segments. Polyamides and copolyamides are very good candidates. Under stress, the soft segments of the solid TPE extend greatly, but are eventually restrained by the mutually bonded hard segments. On the release of stress, the soft segments retreat into their random configuration. At a sufficiently high temperature the hard segments debond and the polymer becomes a uniform melt, processable as any other linear polymer. In particular, the poly(ether-block-amide)s constitute an important family of TPEs, bridging the gap between thermoplastics and rubber. Important members of this class of block copolymers are based on poly(lauryl lactam), PA 12, poly(tetramethylene ether) glycol and adipic acid (Pebax®, Vestamid®), PA 6 and trimers of HMD and terephthalic acid (T6T, T6T6T) *[Marchildon, 2001]*, *[Degussa AG, 2011b]*.

3. Applications of copolyamides

Due to their excellent properties, copolyamides are used in a wide range of industrial applications, varying from apparel industry to electronics and electrotechnics, automotive and aerospace industries, defense, healthcare products, waste recovery and recycling, etc. They can be employed as fibers, pastes, particles or solutions, acting as fibers or fibers modifiers, hot-melt adhesives, conductive binders, thermoplastic matrices for composites with various fillers (metal particles, wood waste, lignocellulosic fibers, carbon nanotubes, etc.), protective coatings, etc.

In the following sections, a survey on various applications of copolyamides is presented.

3.1 Copolyamides in the light industry

3.1.1 Copolyamides as fibers and fiber modifiers

In the light industry, coPAs can be found as fibres and fibres modifiers and as hot-melt adhesives. When it comes to the development of synthetic fibres production, it is of interest to note the increasing demand and, subsequently, production. Therefore, new types of copolyamidic fibres have been designed in order to meet the new demands (good balance between moisture absorption and elimination, vapour permeability, thermal properties, etc.).

Copolyamidic fibres for textiles with high tenacity and elasticity at low temperatures were obtained from copolyamides modified by incorporation of elastic segments into their structure *[Farana et al., 2005]*. Modification was carried out by using the urea-prepolymer, prepared from 1.6-hexamethylenediisocyanate and poly(oxypropylenediamine), as activator for the anionic copolymerisation of ε-caprolactam (CL) with λ-laurolactam (LL). Copolyamide fibres with a diameter 70 to 80 μm by melt spinning method were obtained (Fig. 12).

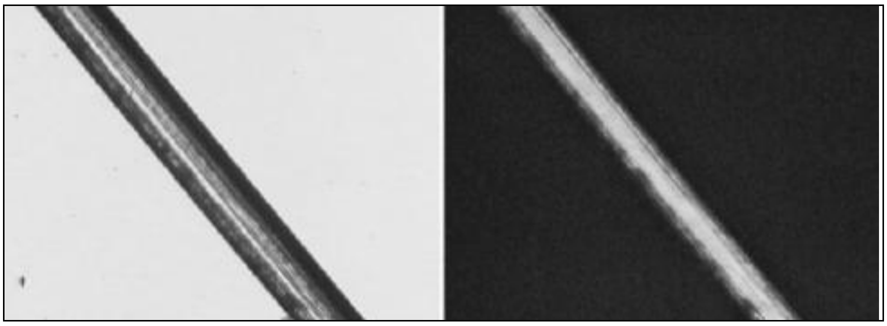

Figure 12. Microphotographs of copolyamidic fibres: a) in white light, b) in polarized light *[Farana et al., 2005; reprinted by permission of Fibres & Textiles in Eastern Europe]*

The mechanical properties of these fibres, such as tensile strength, elongation, impact notched strength, are superior to those of commercial polyamides (PA 6 and PA 12). Another interesting feature of these new fibres is the fact that they may undergo fibrillation during drawing.

Another method for fibres modification is their additivation with compatible products. Thus, various coPAs based on CL and other reagents were synthesized and applied as compatible modifiers for PA 6 fibres in order to improve their sorption and electric properties *[Krištofic, 1999; Krištofic and Ujhelyiová, 2006; Krištofic et al., 2000a, 2000b]*. The new coPAs were synthesized starting from CL, adipic acid and diethylenetriamine (DETA), by the poly(addition-condensation) reaction, in two steps: I - synthesis of the linear alkaline copolyamides; II - cyclization of the alkaline copolyamide on the polyamideimidazoline (Fig. 13). The properties improvement is due to the introduction of a sufficient polar functional groups, namely secondary NH groups (or N atoms, also), into the PA 6 macromolecular chains.

The obtained coPAs were used as additives (10-50%) for fibre-forming PAs. These fibres are able to absorb from 10 to 50% wt. of such coPA additives without any negative influence on the processability of their blend melt, i.e. during the spinning and drawing processes of PA 6. Moisture sorption of the additivated PA-6 fibres was increasing with a higher coPA content. The highest efficiency was achieved for PA 6 fibres modified with 30 and 50% of the coPA with a higher content (30.6 mass %) of the nylon salt ADETA (nylon salt prepared from adipic acid and diethylenetriamine) by a poly(addition-condensation). The content of the low molecular compounds in coPAs is comparable to that of the homopolymer PA-6 (8-12 wt.%), according to the reaction temperature. The melting temperatures of coPAs are lower in comparison with the PA 6 (~220°C). The higher amount of the comonomer ADETA lowers essentially the melting temperature of the coPAs.

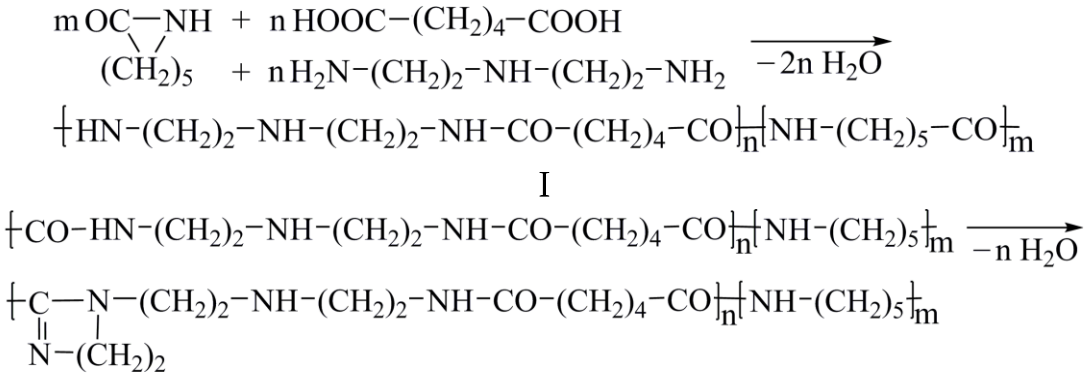

Figure 13. The two-step poly(addition-condensation) reaction I: - synthesis of the linear alkaline copolyamides; II - cyclization of the alkaline copolyamide on the polyamideimidazoline *[after Krištofic et al., 2000a]*

Strength of the additivated fibres decreased with the growing coPA content, while the elastic deformation had an upward tendency. The elongation of modified fibres was also improved; the sorptive and electrical properties of modified PA 6 fibres containing 20% coPA are substantially better when compared to non-modified PA 6 fibres.

CoPAs of high molecular weight were obtained by employing other salts in their composition. In example, using CL and various amounts of a nylon salt (AN2) based on adipic acid and 1-(2-aminoethyl) piperazine (N2) (the nylon salt acted as activator of the polyaddition reaction), copolyamides with properties comparable to PA 6 were synthesized *[Krištofic and Ujhelyiová, 2009]*. Melting temperatures of the coPAs are lower in comparison with PA 6 and decrease proportionally to the amount of the nylon salt. The glass transition temperature (T_g) was slightly affected. The crystallization temperature (T_c) of coPA decreased along with the amount of comonomer. These new coPAs are excellent compatible additives for PA 6 and can be synthesized within a much shorter time (2-3 h) than PA 6 (> 16 h).

Modification of PA 6 fibres with coPAs containing tertiary nitrogen from piperazine derivatives determined a higher water (vapours) sorption *[Krištofic et* *al., 2000a]*. Comonomers decrease the enthalpy of fusion (ΔH_m) of the copolyamide, compared with PA 6. This results from a lower regularity of macromolecules and steric arrangement of the piperazine ring. Comonomers do not influence significantly the thermal properties of polymers, but they do affect the kinetics of crystallization. The higher concentration of NH groups and N atoms in polyamideimidazoline brings about a high affinity towards water, which leads to its solubility in water.

Other copolyamidic modifiers for PA 6 fibres were reported to be composites with copolyamide matrices and various nanoclays and layered silicates *[Krištofic et al., 2005a, 2007, 2010; Ryba et al., 2010; Vass et al., 2008]*. Binary and ternary high molecular weight semicrystalline coPAs, containing layered silicates (i.e., 0.25–1% Bentonite 11958 or Cloisite 15A), were prepared (Fig. 14) and used as modifiers for the PA-6 fibres.

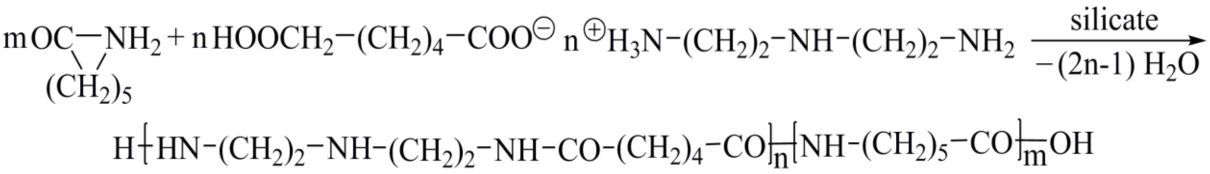

Figure 14. Synthesis of coPA modifier from CL and nylon salt in the presence of layered silicate *[after Krištofic et al., 2005a]*

The modified PA 6 fibres exhibited standard or better properties. These new coPAs reduced the tensile strength of modified fibres, due to the orientation of new composite fibres, and improved sorption properties of modified fibres due to their higher hydrophilicity. Melting temperatures of modified PA 6 fibres are lower as effect of modifiers lower melting temperatures. Ultraviolet protection factor, fibres orientation factor, hydrophilicity and barrier properties depend on the type of layered silitate used for composites; in terms of improving these characteristics, Cloisite 15A proved to be more effective.

CoPAs based on CL and various amounts (5, 10 or 15 wt.%) of ADETA nylon salt were prepared by the same poly(addition-condensation) reaction and used to modify polypropylene fibres *[Krištofic et al., 2001, 2005b]*. These fibres were modified with 4, 8, and 12 wt.% coPAs and were obtained by spinning method. The properties of modified polypropylene fibres depend on the amount of coPAs: the higher the content of coPA, the higher the degree of elasticity and sorption of water vapour. Polypropylene modified fibres have better hydrophobicity, dyeability and electrical properties. Concerning mechanical properties, it was observed that the tensile strength of the modified polypropylene fibres was affected only at the highest amount of coPA (12 wt.%), due to the lower compatibility of two components.

Polypropylene (PP) fibres were also modified with coPA-based composites containing organically modified montmorillonite (bentonite)

[Krištofic et al., 2011]. CoPA matrix was prepared from CL, nylon salt of adipic acid and DETA and nylon salt of adipic acid and 1-(2-aminoethyl) piperazine. PP fibres modified with 4, 8 and 12 wt.% of these composites, can be spun even without a compatibiliser by the standard melting process and drawn at high drawing ratios. Mechanical properties of the modified PP fibres, i.e. tenacity and Young's modulus, are better mainly at lower amounts of modifier and at higher drawing ratios. The electric properties of the modified PP fibres were improved along with the increasing amount of coPA. The sorption properties of the modified PP fibres, i.e. the sorption of water vapour and disperse dyestuffs, are much better in comparison with non modified polypropylene fibres.

CoPAs with other special applications were reported. Thus, poly(trimethyleneterephthalamide) (PTT) was blended with a coPA of a specific composition to produce new acid-dyeable fibres *[Wang and Hu, 2009]*. The coPA consisted of HMD and adipic acid and the trifunctional diethylenetriamine (DETA). The last provided amine ends in excess to that required for polymerization. The study demonstrated optimum results with weight ratio PTT:coPA = 95:5 and with the DETA constituting 25 mol.% of the coPA. The dyeability of the modified PTT fibres was fairly good. The dye-uptake increased when the copolymer content and the DETA concentration were higher. Due to the fact that coPA and PTT are immiscible, a compatibilizer (Surlyn®) was required. The desired dye uptake was achieved and with little adverse effect on mechanical and thermal stability. When the sum of the coPA and the compatibiliser is bellow 0.10 weight fraction the deterioration of mechanical properties does not affect the regular applications of PTT fibres.

CoPA yarns with visual effect of bulking, made of a bicomponent effect yarn where each component comprised of a fibre-forming polyamide having different shrinkages, have been reported *[Lintecum et al., 2003a, 2003b]*. This differential shrinkage was achieved by using different polymers or similar polymers having different relative viscosities. The bicomponent yarn was made up of nylon 6,6 copolymerized with 30% poly-2-methylpentamethylene-adipamide (MPMD), as the high relative viscosity (η_{rel}) component, and nylon 6,6 as the low η_{rel} component. The obtained polymer yarns exhibited an enhanced visual effect, including a stratified effect, which improves visual impact of products obtained using this bicomponent yarn.

3.1.2 Copolyamides as hot melt adhesives

Copolyamides are widely used as hot melt adhesives (HMAs) in the light industry for the manufacture of clothing, footwear, nonwovens, carpets etc. Using of these hot melt adhesives leads to short production times and lower unit costs. At the same time, from production to application, these HMAs are characterized as environmentally friendly. Low activation or application temperature adhesives are of interest to end users because of a number of potential advantages including: protecting heat sensitive substrates from thermal damage; increasing productivity; workers safety; reducing scrap and waste; lowering energy costs; allowing greater design and process flexibility.

The low melt coPA adhesives discussed in this category are nylon types and are commonly derived from building blocks such as PA 6 and PA 6,6. By adjusting the ratios of monomers, coPA adhesives can be designed to combine low fusion points and excellent resistance to laundering and dry-cleaning. So, by selecting and combining the proper raw material ratios, melting points between 60°C and 150°C are possible *[Halbmaier, 1998]*. These products can be applied by different techniques: wide webs, spraying, films slots, gravure, rolls. They are important because they provide flexibility in product design and technological approach, at competitive costs.

Novel HMAs obtained by individual copolymerization of PA 6, PA 11 and PA 12 with HMD polymers of various aliphatic diacids have been reported *[Raabe and De Jong, 1978]*. No component accounted for more than 40 or less than 15wt.% of the copolymer. The polymers have melting points of 110°C.

Other coPAs based on CL and HMD with a mixture of polymeric fat acids and an aliphatic co-dicarboxilic acid having 20-22 carbon atoms were prepared and characterized *[Peerman and Kanten, 1980]*. The coPAs may be described as 6,HDD/6,10/6 or 6,HDD/6,12/6 depending on the co-dicarboxylic acid employed (HDD hydrogenated distilled dimerized polymeric fat acids). Melting temperature of these hot melt adhesives are 94-105°C.

A large scale batch of the copolyamide 6,HDD/6,12/6 (50/25/25) was also prepared for subsequent formation into a reticulated web. The aqueous suspensions of this coPA were produced at 30% resin solids and were printed on to various fabrics with a dot adhesive patern at a density of 21 g/m^2.

In order to achieve melting points below in the range 79–121°C, hot melt adhesives were synthesized by copolymerization of PA 6 and PA 12 and a mixture of diacids and diamines *[Poessnecker et al., 2003]*. The diacids that were tested included both aliphatic and aromatic, while the diamines included 2-methylpentamethylenediamine (MPMD), HMD and piperazine.

Good adhesion properties in molten state were reached by modifying a coPA based on a mixture of CL:PA6,6 salt=60:40 (wt.%) with various additives: castor oil, acetic anhydride, acrylamide, polyethylene, formaldehyde) *[Besshaposhnikova, 2004]*. Initially, coPA had a melting temperature of 160-165°C, but it decreased to 140°C after using additives. They act by disturbing hydrogen bonds between amide groups. An additive content higher than 5% weakens the peel strength of the HMA.

A series of novel HMAs with copolyamidic structure was synthesized during a collaboration between *“Petru Poni” Institute of Macromolecular Chemistry*, Iasi, and *Institute for Research on Synthetic Fibres*, Savinesti

(Romania), under the registered trade name Aderom *[Crusos and Zanoaga, 1989; Crusos et al., 1983, 1995, 1999; Zanoaga, 2001a]*. These adhesives are ternary statistic coPAs (6/6,10/6,6) obtained directly from monomers (30-75% HMD, 10-50% CL, 10-30% adipic and sebacic acids) by melt polymerization, without neutral/nylon salt synthesis. Depending on reactants ratio, the melting temperatures of these polymers are in the range 125-175°C. The copolyamidic polymer Aderom was obtained as wire, granules and web (Fig. 15) and it is recommended for the production of auxiliary thermoadhesive materials (fusible linings) for thermo–sensitive materials (textiles, leather, leather substitutes).

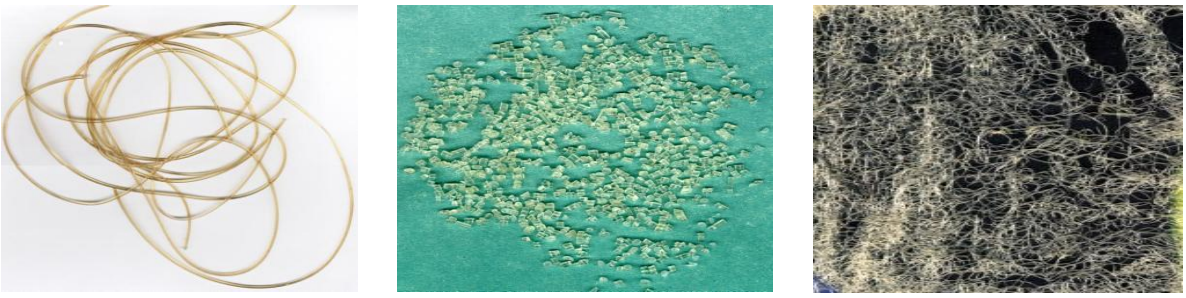
a b c

Figure 15. Aderom conditioned as: a – wire; b – granules; c – filament web

It was also reported a method of producing hot melt adhesive pastes based on coPAs with low melting point and improved bonding *[Crusos and Zanoaga, 1992]*. Pastes were manufactured by dispersing (10-30):10-50):30-75):(20-50) adipic acid–CL–HMD–sebacic acid copolymer 20-30% in 60-80% water and 5-20% dispersing agents, homogenizing agents, stabilizers and swelling agents. Dispersions have superior stability. The suspensions were printed on to various fabrics with a dot adhesive patern at a density of 22-25 g/m^2 and were tested in apparel and nonwoven industry. Melting temperature of these hot melt adhesive pastes are at 110 up to 125°C.

Copolyamidic HMAs with melting temperatures of 125-135°C were tested with good competitive results in light industry, as powders or pastes, for apparel, footwear and nonwovens *[Buruiana et al. 2007; Crusos et al., 2001b; Zanoaga, 2001b, 2007; Zanoaga and Tanasa, 2010; Zanoaga et al., 2004a, 2004b]*.

If the copolyamide (20-50% SH salt, 5-30% AH salt, 21% CL) is blended with 5-50% polyethylene, a novel series of HMAs was obtained, which have a high adhesive strength and good detergent and dry-cleaning resistance *[Crusos et al., 1985]*. These compositions can be used as hot melt adhesives for the preparation of cleaning-resistant laminated materials which have a particularly high wash resistance.

HMAs can be also affixed as fibres, not only as monocomponent fibres, which are made exclusivelly from a HMA polymer, but also as bicomponent fibres. These fibres are used in the light industry to improve the quality of finished garment, solve a few of production problems, contribute to the design of new production techniques. CoPA hot melt adhesive fibres can be obtained from copolyamide resins based on CL, HMD, adipic acid, sebacic acid, terephthalic acid and/or dimethyl terephthalate *[Crusos et al., 2001a]*. These coPAs are used to produce fusible fibres and nets (webs) for the apparel, footwear and nonwovens production or for other different substrates.

Other types of HMA fibres are Grilon® yarns *[EMS-Griltech, 2001a]* and Vestamelt® *[Degussa AG, 2011a]*, *[Evonik, 2011a]*. Grilon yarns are low melt nylon, coPA (copolyamide) and low melt polyester, coPES (copolyester) multifilaments used for technical applications in the textile industry worldwide.

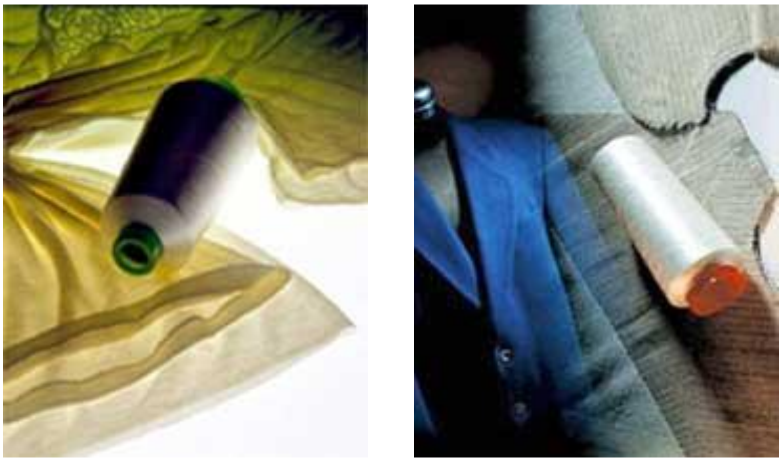

Figure 16. Grilon HMA yarns *[after EMS-Griltech, 2001a]*

These low melting fusible yarns are available in various melting points and counts. They can be stitched, knitted or woven. It is thus possible to use them precisely and effectively where needed.

The possibilities of fusible fibres in the textile industry seem to be endless: from replacing or eliminating slow and expensive sewing operations, up to a new concept of using foils to produce metallic embroidery *[Albrecht et al., 2003]*. Materials containing fusible filaments or fibres, such as PA 6/coPA or PA 6,6/coPA bicomponent fibres, marketed under the trade marks of Grilon (available from EMS-Griltech) have been reported to be used into the upper footwear *[Dua, 2005]*. These materials are heated so that the fusible filaments melt together with others to form fused areas. Compared to unfused areas, the fused ones are characterized by improved properties that include greater stretch resistance, stability, support, abrasion resistance, durability and stiffness, for example. In addition, the fused areas generally provide air-permeability without significantly increasing the weight of the footwear.

Fusible separation yarns based on coPAs are multifilaments of low melt polymers that will melt, shrink and "disintegrate" in invisible particles, under the effects of heat (steam, hot air, infra-red rays). This new class of coPAs is characterised by a good tensile strength in the dry state; these copolyamides can be knitted, woven or stitched *[EMS-Griltech, 2011b]*.

These fibres replace efficiently the traditional and costly "hand separation thread" process of knitted articles from the knitting sector, by a quick, clean, safe and effective thermoplastic separation; even more, they can create a fantasy holes effect (Fig. 17.) *[EMS-Griltech, 2011c]*.

The use of these fibres in light industry will bring benefits: shortening production times, reducing unit costs, improving quality, developing new production process, enhancing creativity.

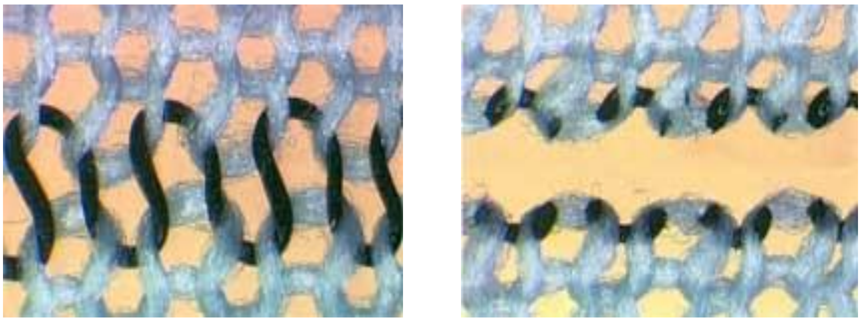
a b

Figure 17. Fusible separation yarns: a) before separation b) after separation *[after EMS-Griltech, 2011c]*

Preferred coPAs in this field of applications are derived from: nylon 6/6,6/12; 6/6,9/12; 6/6,10/12; 6/6,6/11; 6/6,9/11; 6/6,10/11. A process for the production of coPA filaments based on the terpolymers (6/6,6/12,10; 6/6,6/12, 6/6,6/9,10; 6/6,9/12; 6/6,10/12; 6/9,9/12; 6/9,10/12; 6/6,6/11), by spinning and stretching, has been reported *[Schmid and Griehl, 1980]*. Filaments are made of at least three polyamide forming, unbranched, saturated monomer components (CL, LL, adipic acid, aminocaproic acid, salt of diamine and dicarboxylic acid, such as AH). These components together have an average groups frequency amide: methylene of 1:6.4-7.4 (alternatively, methylene:amide = 1:0.156-0.135) and are each present in amount of 10-60 mol%. The melting points of these coPAs are mostly in the range of 100-150°C.

3.1.3 Copolyamides in the nonwovens industry

Nowadays, the nonwovens (NWs) industry – as a significant part of the light industry – is best characterized as a branch that has accomplished a rise in product quality which the user can „see and feel". Its range of products has become ever larger. This has been achieved by creative work and successful cooperation with the suppliers of raw and auxiliary materials, as well as the manufacturers of equipment. Based on this cooperation, there are good prospects for novel products. Future developments will continue to focus on the best functionality and lowest consumption of resources.

NWs are manufactured for disposables and for nondisposables (stronger material), which have different functions: moisture impermeability, absorption of liquids, drainage, combustion inhibitors, bacterial barriers and sterility, combining strength and elasticity with softness and smoothness.

In this field, polyamides and copolyamides may be used as fibres (such as PA 6, PA 6,6) for producing nonwovens for panties, top clothes, underware, lining and backing fabrics, as well as furnishing fabrics, carpets, artificial suede or flock fibres, technical fabrics *[Albrecht et al., 2003]*.

They can also be used as binders, in fact as hot melt adhesives (adhesives fibres or powders). The use of adhesive fibres, such as coPAs, is one of the most elegant and convenient methods to consolidate nonwoven structures. Adhesive fibres are easy to apply by blending with other fibres, then the mixture can be manufactured into a nonwoven structure without additional process steps or equipment.

Various commercial hot melt adhesive fibres based on coPAs are known at present. These fibres are available either as monocomponent fibres (i.e. Griltex, Grilon K 115, Grilon K 140, from EMS-Griltech), which are made from 100% of a hot melt adhesive polymer, or as bicomponent fibres (i.e. Grilon BA 115, Grilon BA 140; Grilon BA 165, also from EMS-Griltech). NWs bonded with both types of fusible fibres (20% HMA fibres) are presented in Fig. 18.

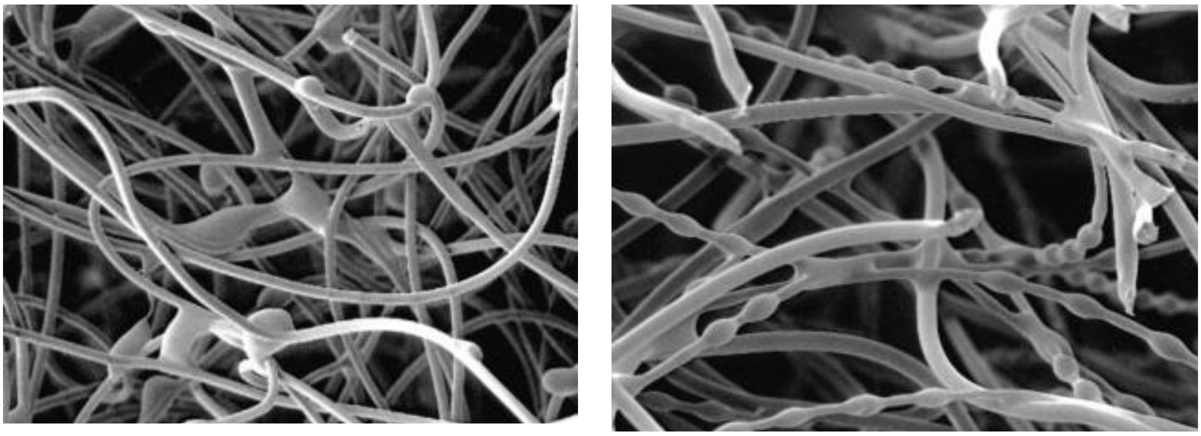
a b

Figure 18. Nonwoven bonded with: a) monocomponent HMA fibres; b) bicomponent HMA fibres *[after Albrecht et al., 2003]*

Fusible coPA fibres impress by offering very high specific adhesive strength and good resistance to mechanical loading and solvents. An other very interesting feature of these fibres is the possibility to further reduce the softening temperature with moisture. Steam, as the medium for the fusing process, is therefore used.

In case of fusible bicomponent fibres, the fibre sheath consists of a coPA which has a lower melting point compared to the core component (PA 6). These yarns has been successfully used for obtaining nonwoven materials or other various technical applications in the textile industry worldwide.

It must be mentioned that HMA coPAs can also be applied as powders onto or into a nonwoven. But, in the powder-bonding process, the powders are scattered into the nonwoven and require additional equipment and the fusing has to be initiated immediately after applying the adhesive. Such HMA powders were reported to be obtained as fatty copolyamides based on 5-20% linoleic acid into a mixture of 20-25% adipic acid, 15-20% HMD, 30-40% CL *[Crusos et al., 1999]*. The polymer granules have a light yellow color and a certain transparency (Fig. 19), melting temperatures of 150-165°C and excellent adhesive properties. These polymers were successfully tested and used as fusible powders for technical nonwoven materials *[Crusos and Zanoaga, 1993]*. Thermoplastic coPA resins exhibit improved low temperature flexibility and outstanding adhesion to various surfaces as textiles (NWs included), metals and plastics.

Figure 19. HMA fatty copolyamide granules

Aderom adhesive with a low melting temperature was used as powder *[Crusos and Zanoaga, 1989; Crusos et al., 1995]* with granulation of 100-400μm, for deposition onto NW materials (amount of applied polymer powder was 800-1000g/m^2) in order to obtain new materials for different applications, such as interlinings for apparel industry.

A tipical plant for application, sintering and heat sealing polymer powder is presented in Fig. 20. Some of the resulting products are presented in Fig. 21 *[Zanoaga, 2007]*, *[Zanoaga and Tanasa, 2003]*.

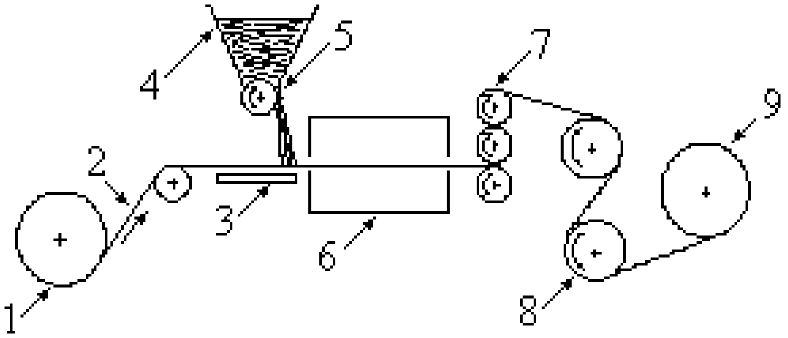

Figure 20. Plant for application, sintering and heat sealing of thermoadhesive powder: 1-roll with nonwoven or fabric material; 2-conveyor belt; 3-electrostatic attraction; 4-powdered HMA hopper; 5-rotating brush; 6-sintering heater; 7-smooting rolls; 8-cooling roll; 9-interlining *[after Zanoaga and Tanasa, 2003]*.

Researchers from *"Petru Poni" Institute of Macromolecular Chemistry*, Iasi, Romania, have also reported on the process of obtaining multi-layer nonwoven technical materials by themal bonding method using as adhesive a coPA with a low temperature melting *[Zanoaga and Tanasa, 2010]*.

Figure 21. NW interlinings for apparel industry

For these technical materials, recycled textile fibres (natural and/or synthetic) were used in order to offer a new route to recover and up-cycle textile waste. Number of web layers were 3 up to 7. The novel technical materials were different by their mass per unit area (650-6500 g/m^2), thickness (8-40 mm), the amount of the deposited adhesive powder (12-85 g/m^2) and by fibrous blend components (first time used textile fibres or fibres recovered from textile industrial waste). The breaking strength values of the multi-layer nonwovens were 6 N/5cm for composites based of new textile fibres and 2-3 N/5 cm for composites of recycled/waste fibres. So, the composite systems exhibited satisfactory values of adhesion between the nonwoven layers.

A typical technological process line of obtaining bulky nonwoven textile fibre composites (BNTFCs) using HMAs powders is presented in Fig. 22.

Although slight differences in properties of the web were observed, it should be noted that the amount of recycled content of fibers was considerable high. Even though the webs with high recycled content were slightly weaker, they were softer and may be better used for some specific products.

The investigation presented a method for achieving a new composite structure based on low quality and value textile waste, that could not be used directly in the apparel industry, but which have a high potential in the manufacturing of composite nonwovens, that are quite promising materials for insulation.

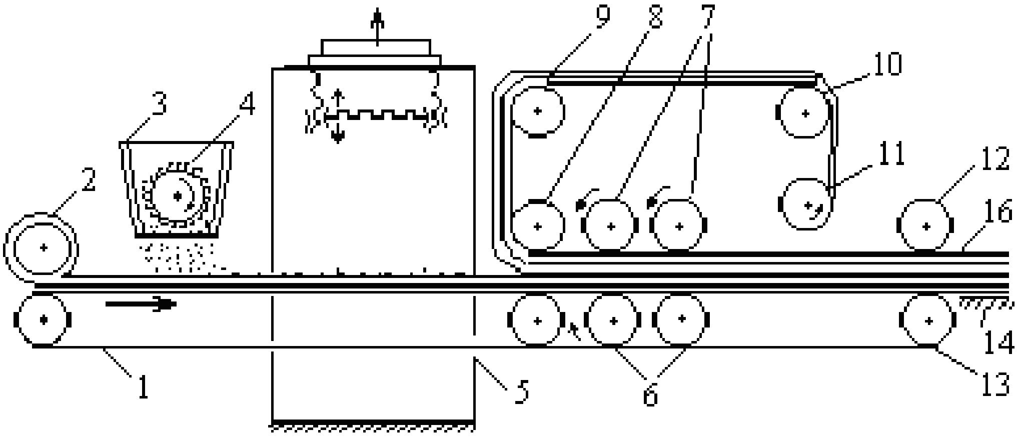

Figure 22. The process line of producing multi-layer nonwovens with HMAs: 1-conveyor belt; 2-roll with the NW material; 3-powdered HMA hopper; 4-powder distribution cylinder; 5-sintering heater; 6-7-pressure-cooling cylinders; 8-9-10-guide cylinders of NW; 11-roll with another NW material; 12-13-delivery calendars; 14-fixed mass; 16-bulky nonwoven textile fibre composites (BNTFCs) *[after Zanoaga and Tanasa 2010b]*

The presented results are preliminary and further experiments will focus on scaling up and optimization of process parameters, such as binder ratio, blend uniformity, curing time, temperature and pressure. Subsequent investigations will be devoted to the phono- and thermo- insulating properties of these bulky composite materials, prior to their testing for various applications in civil and industrial engineering, mechanical engineering, protection equipment etc.

The sequence of technological operations concerning obtaining of bulky nonwoven textile fibre composites is presented in Fig. 23.

A new way to obtain other NWs comprising thermoplastic fibres (th) and two types of bonding fibres with different fusion temperatures (T_m): $T_m(th)>T_m(1)>T_m(2)$ has been presented *[Dijkema and Visscher, 2009]*. As thermoplastic fibres were used PA, PET, PP, polyoxymethylene, etc., while the bonding fibres were usually synthetic fibres such as: PE, PP, coPAs, copolyesters, etc. Nonwovens, tufted nonwovens and articles containing NWs were manufactured. The nonwovens maintained their structural integrity up to a high degree because the solidified melt of the bonding fibres ties together thermoplastic fibres, thereby stabilizing the structure of the nonwoven structures. The high dimensional stability and structural integrity of the nonwovens are advantageous in a multitude of articles, i.e. filters for industrial (dust, soot, pollen or gas filters) or medical (bacterial or viral filters, filters for exchanging heat and moisture) applications. The combination of high dimensional stability and structural integrity properties of the tufted nonwoven is advantageously for tufted carpets, home textiles, pillows, cushions, textiles in automobiles, trains or airplanes, as well as for outdoors applications, such as artificial turf or playing surfaces.

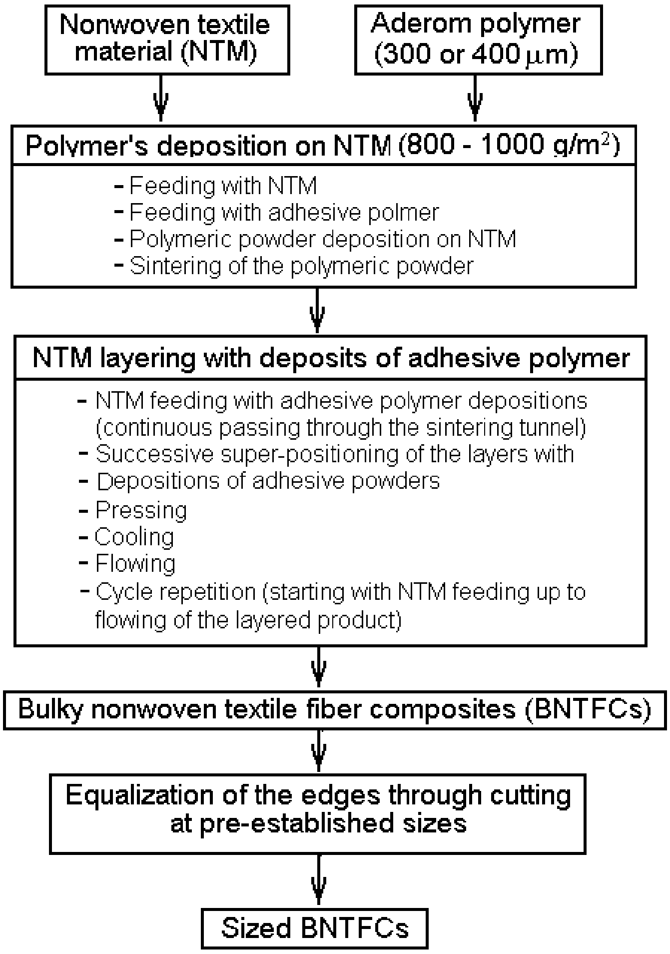

Figure 23. The sequence of technological operations of producing multi-layer nonwoven materials by Aderom powder deposition *[after Zanoaga and Harnagea, 2008b]*

NWs are also used as carpet backings and the manufacture of a nonwoven primary carpet backing with a multi-layer structure have been described *[Coolen and Johnson, 2001]*. Nonwoven backing comprising thermoplastic polymer filaments or fibres was bonded by means of a thermoplastic coPA binding agent. Fusible or bicomponent fibres (the core/sheath or the side-by-side type) and filaments were used as bonding agents for thermally bonded. The other forms of the binder coPA, i.e., powder, emulsion or fibrides, can be added to the unbonded filaments or fibres to obtain the nonwoven. A carpet comprising the nonwoven backing exhibit increased strength and elongation.

The process to produce synthetic NWs wipes made of fibre webs was reported *[Gorley et al., 2005]*. The wipes may consist of a single layer of nonwoven web, or of a laminate material containing spunlaid-meltblown-spunlaid webs. Various fibre types based on co-PA were used, such as monocomponent fibres, bicomponent fibres, biconstituent fibres (thermoplastic fibres that are comprised by a blend of two or more thermoplastic polymers) and combination thereof. The resulting 100% synthetic nonwoven webs have not only a good strength in the machine and cross directions, but may also be soft and have a high sorption capacity, without the integration of non-synthetic fibres, such as wood pulp. The wipes can be used in a variety of applications, such as surface cleaning and absorbent products.

Nowadays, nonwovens are part of our life. Due to their tailor-made characteristics, they are highly suitable to meet a wide diversity of practical requirements. Thus, nonwovens may be considered up-to-date products.

3.1.4 Other applications in light industry

Copolyamides can be used as finishing products for leather and leather substitutes. Preferred leather substitutes are those based on polyurethane, polyacrylate or polyamide. Finishing materials have the following properties: high gloss, smooth pleasant handle.

A series of coPAs was prepared by melt polycondensation of the ingredients (10-32% of the AH salt; 30-45% CL; 28-45% of the salt of A and bis-(4-amino-cyclohexyl)-2,2-propane) *[Fisher et al., 1978]*. A particular advantage of these coPAs is their sealing effect counteracting the migration of dyes, plasticizers and fats; other advantages are good mechanical properties and the stability of the solutions.

A special mention has to be done for coPAs as waste recovery and recycling products. It was reported that novel coPAs, based on raw materials resulted by degradation of clean PA 6 waste, were synthesized *[Wesolowski and Grzebieniak, 2004]*. Resulting waste from the PA-6 fibres manufacture were degraded in a controlled manner. The degradation process conditions were fixed to obtain low molecular oligomeric degradation products, which were used in the synthesis of new coPAs of Polmid type. Polmid copolyamides are obtained from CL and salts of dicarboxylic acids with diamines and their properties were tailored by selecting adequate synthesis condition (process time, pressure phase, vacuum period). Properties of coPAs obtained from waste degradation products are similarly with properties of standard Polmid polymers.

Today, it is difficult to imagine the modern light industry without these highly specialized materials based on coPAs, not only because they offer a wide range of products, but because they are also the answer to many technological issues which otherwise would not be economically feasible.

3.2 Copolyamides for membranes

The reverse osmosis (RO) through synthetic membranes has significantly attracted researchers attention as an economic process in the filed of water desalination, ultra-pure water production, water purification, waste water treatment. Thin film composite (TFC) membranes consist in three structural components: (1) top ultra-thin skin copolyamide layer; (2) middle polysulfone porous support; (3) bottom non-woven polyester fabric. In these structures, the active skin layer is the key component, it controls mainly the separation properties of the membrane, while the support layer gives membrane the required mechanical properties.

Materials used to produce the skin layer included various polymers, such as PAs and coPAs. At present, coPAs are one of the most important reverse osmosis ultrafiltration membrane materials *[Li et al, 2008; Trigo-López et al., 2009]*. When coPAs are employed as active thin layer, membrane shows high salt rejection, high water permeability and high fouling tolerance. These membranes can be used for the desalination of sea water or brackish water, the purification of contaminated water to produce dinking water or industrial water; their applications may also include concentration, removal or recovery of various substances from aqueous solutions, for example the concentration of food stuffs or the separation/concentration of biological or pharmaceutical products.

Semipermeable membranes and hollow filaments were obtained from various formulations of aromatic heterocycle-containing coPAs *[Elfert et al., 1980]* based on different monomers presented in Table 4.

Table 4. Monomers used for coPA-based semipermeable membranes *[after Elfert et al., 1980]*

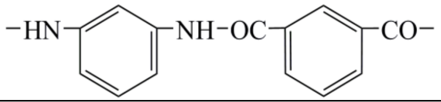	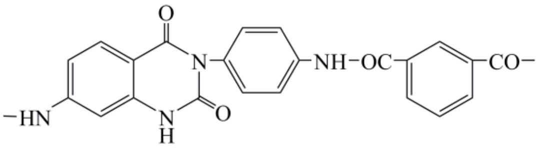
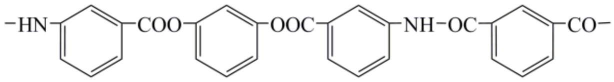	
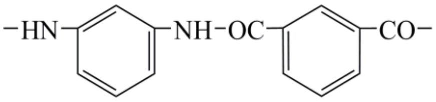	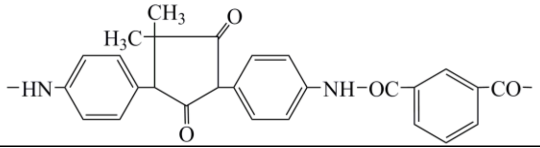
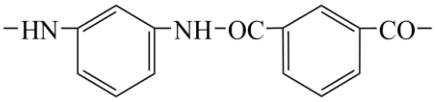	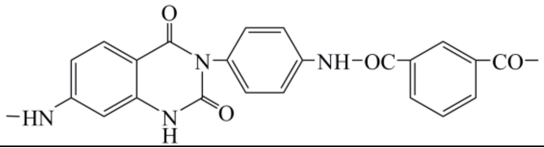

These semipermeable membranes have a high chemical and thermal resistance, are characterised by high permeability to water coupled with a high selectivity. The membranes shown a water absorption capacity of 4.5-11% by weight (as measured on ≈ 40μm thick symmetrical films, at room temperature and relative air humidity 65%) and a high throughflow of 130-200 l/m^2d for a desalination level of 94.6-99.5%.These new coPAs are particularly suitable for membranes production and their application for inverse osmosis and ultrafiltration.

Regular coPAs can also be used as desalination membranes *[Vogl and Stevenson, 1977]*. They were prepared by reacting an aliphatic diester with an excess of an aliphatic diamine, and subsequently reacting the intermediate diamine product with an aliphatic diacid chloride, through conventional solution polymerization or interfacial polymerization techniques. The resulting permselective membranes may be used in conventional RO processes, either as free film or, more commonly, as film mounted or deposited on a porous support material.

A special procedure, interfacial polymerization of coPA membranes on microporous supports, was reported to yield in thin films because the reaction is self-limiting and controlled by diffusion *[Sundet, 1991]*. The coPA was obtained from *m*-phenylene diamine with cyclohexane-1,3,5-tricarbonyl chloride and either aromatic or aliphatic diacyl chlorides. The composite membranes are suitable for use in the RO processes, such as the desalination of aqueous solutions.

Same method was employed to produce thin film composite coPA membranes based on piperazine and 3,5-diaminobenzoic acid (BA), using a polysulphone as microporous support *[Ahmad et al., 2003]*. Incorporation of BA induced an improved product rate (PR), an increased pure water permeability constant and solute transport parameter. The rejection ability of NaCl and Na_2SO_4 dropped at a higher ratio of BA and piperazine. This implies that anionic surface charge density was introduced that counterbalanced the loss of rejection due to the poor steric. Membranes with a higher content of BA produced a loose and defected skin layer. Both pure water parameter (PWP) constant and solute transport parameter increased at higher BA:piperazine ratio.

Using piperazine, BA and trimesoyl chloride, coPA membranes onto polysulphone support were obtained *[Ahmad et al., 2002]*. By incorporating BA in the diamine mixture, it was recorded an increase in hydraulic permeance and flux, but also a loss in the rejection of NaCl and Na_2SO_4 of these membranes. Higher concentration of BA produced a loose skin layer with defects, but small amounts of BA can improve the flux and rejection of Na_2SO_4. However, the retention ability for NaCl was reduced indicating a loose structure of skin layer. The effect of BA on retention of Na_2SO_4 is less significant than that of NaCl, which implies that anionic surface charge density increased and counter-balanced the loss of rejection due to the poor steric hindrance of thin film layer.

Membranes from the same family of coPAs were tested with good results for nanofiltration *[Ahmad et al., 2004]*. It was demonstrated the increased hydrophilicity of membranes and product rate. The membranes rejection ability towards divalent ions was excellent compared to monovalent ions and the rejection of multivalent ions was over 96%, at a low operating pressure (450 kPa). The modified membranes had an increased negative charge compared to the unmodified membrane and they can be used for pre-treatment in the desalination plant.

It is know that the Nomex-type aromatic polyamides with the structure of poly(*m*-phenylene isophthalamide), which have been used as a membrane-forming material, has good RO performance and mechanical properties, but lower resistance to chlorine. In RO systems, resistance to chlorine is especially important since active species of Cl^+ are often added to water for microorganisms control and to prevent membrane fouling by microbiological growth.

New copolyamides with complex structures were designed and synthesized in order to overcome this disadvantage. In example, ternary coPAs based on aromatic diamine (m-phenylenediamine, diaminodiphenylsulfone), aromatic diamine with carboxyl or sulfonic group (3,5-diaminobenzoic acid, 2,4-diaminobenzenesulfonic acid), and iso- or terephthaloyl chloride were obtained (Fig. 24) *[Konagaya and Tokai, 2000]*.

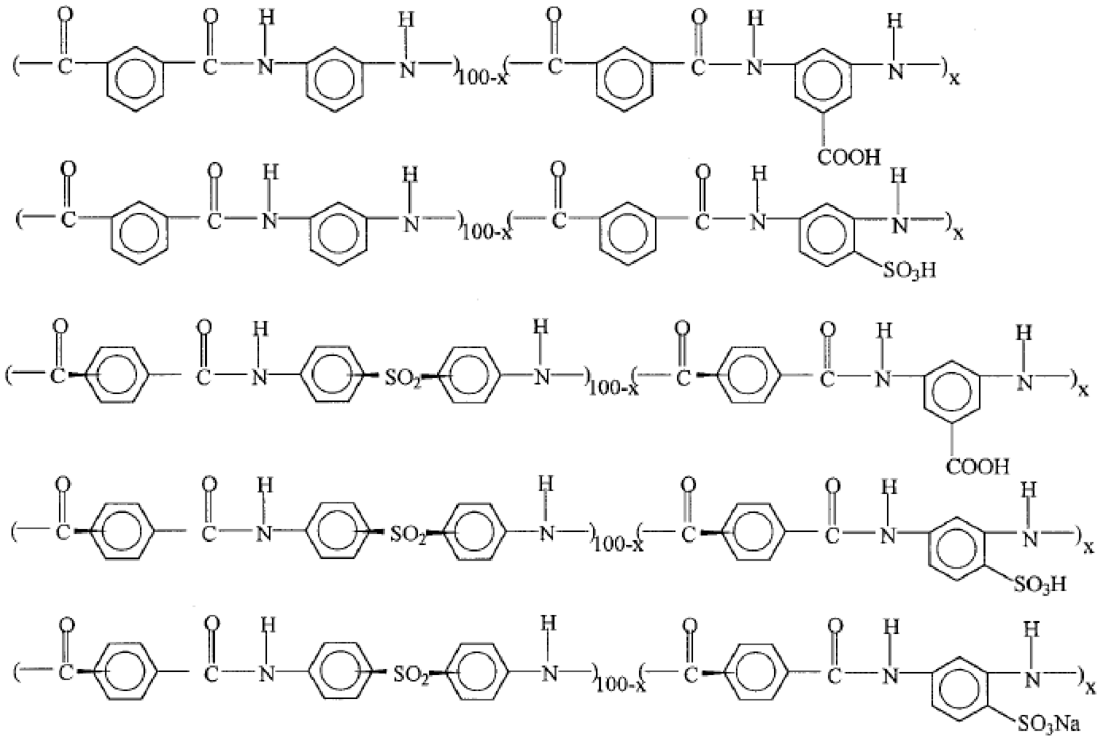

Figure 24. Structures of some new Nomex-type aromatic coPAs *[after Konagaya and Tokai, 2000]*

The flat asymmetric membranes prepared from terephthaloyl dichloride and mixed diamine components of 3,3′-diaminodiphenylsulfone and 3,5-diaminobenzoic acid showed good RO performance, but also high chlorine resistance.

Other coPAs of the same class were synthesized from aromatic diamines (*m*-phenylenediamine, diaminodiphenylsulfone), aromatic diamine with carboxyl or sulfonic group (3,5-diaminobenzoic acid, 2,4-diaminobenzene-sulfonic acid) and iso- or terephthaloyl chloride (Fig. 25), by low temperature solution polycondensation *[Konagaya et al., 2000]*.

The obtained copolyamides are random copolymers, which have good solubilities in organic solvents and good mechanical properties, even in water. Long term test of chlorine resistance showed that membranes produced from these coPAs are very stable.

In the case of membranes obtained from aromatic coPAs synthesized from iso- or terephthaloyl chloride and 3,3′-diaminodiphenylsulphone (coPAs 3I and 3T) *[Konagaya et al., 2001]*, it was recorded a lower permeability compared to Nomex membranes, due to the assymetric flat membranes. Using modified comonomers (3T-MC30), improved results were obtained: good potential for sea water desalination and enhanced resistance towards chlorine.

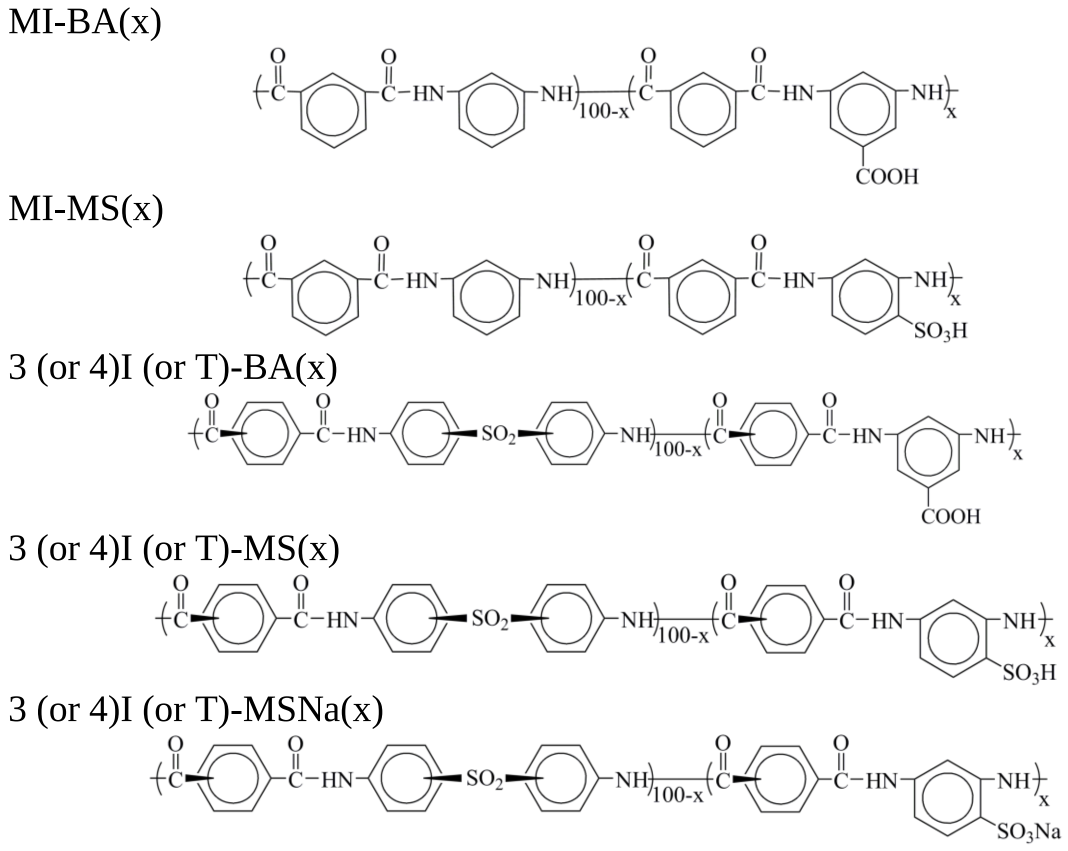

Figure 25. Structures of copolyamides based on: M – *m*-phenylenediamine; IPC – terephthaloyl and isophthaloyl chlorides; BA – 3,5-diaminobenzoic acid; MS – 2,4-diamiobenzenesulfonic acid, MSNa – 2,4-diaminobenzenesulfonate sodium salt *[after Konagaya et al., 2000]*

The separation of gases by polymeric membranes is used in a wide variety of applications, such as the removal of helium from natural gas, hydrogen recovery from ammonia, carbon dioxide recovery from natural gas and biogas, or concentration of oxygen from air among others.

The ideal polymeric material for gas separation applications should be highly permeable and selective, having at the same time high thermal and mechanical stability. Aromatic coPAs seem to be a very good candidate for this type of applications.

Various formulations of PAs and coPAs, obtained by the direct polycondensation of isophthalic homopolyamides and copolyamides (Fig. 26), were reported *[Carrera and Aguilar, 2005]*. The reaction was carried out in a 1:1 mol ratio between the diamine and the diacid for the homopolyamides or mixture of diacids for the copolyamides.

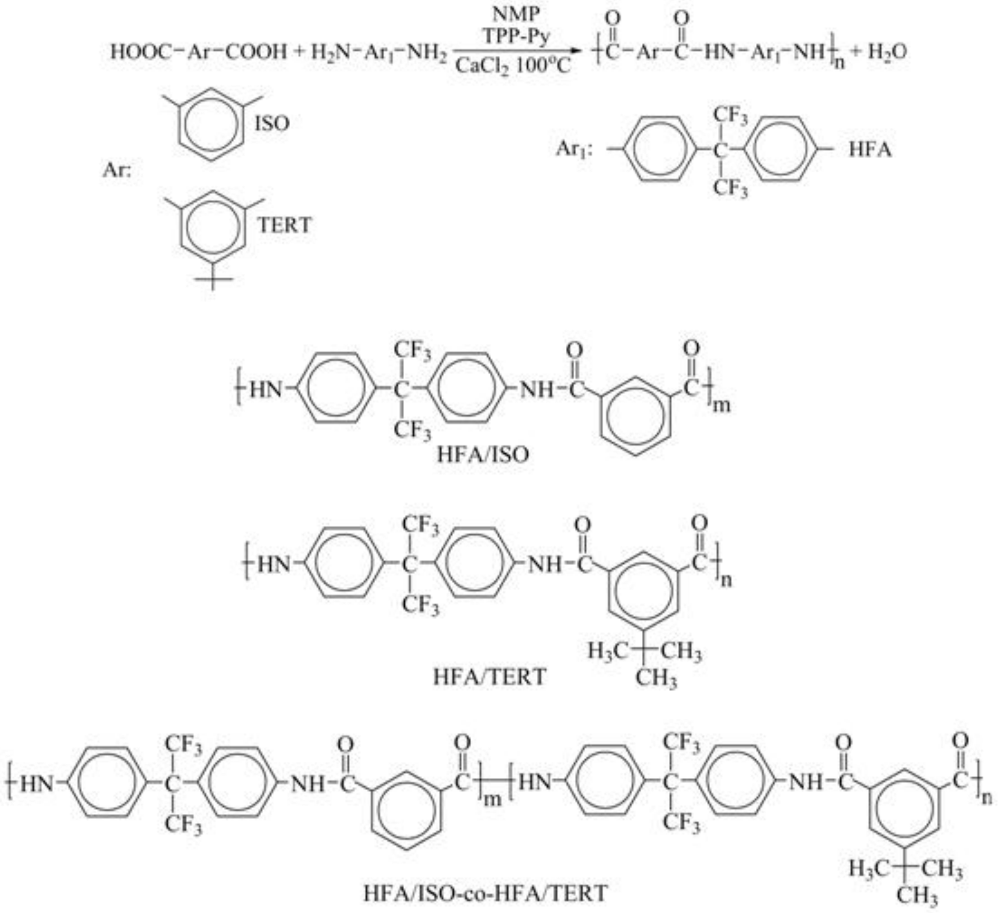

Figure 26. Synthesis and structures of highly aromatic coPAs *[after Carrera and Aguilar, 2005]*

The copolymerization of these highly aromatic aramides allows a control of their properties that follows closely simple rules of mixing. The highest gas permeability coefficients were found for the PAs and coPAs that had the largest amounts of the *tert*-butyl group in their structure. Gas permeability coefficients increased with temperature. This fact enables these polymers to be used as membranes for gas separation.

Some of the best results in filtration processes were obtained using membranes from electrospun no-beads nanofibers. Fibers obtained from copolyamide 6/6,6/10,10 showed remarkable tensile strength and elongation at break and the corresponding membrane was uniform *[Li et al. 2006]*.

The concentration of spinnable solutions of coPA 6/6,6/10,10 was in the range of 6-14 wt%. Higher solution concentrations favored the formation of uniform ultrafine fibres without beads. The average diameter of the electrospun fibres is of 368 nm and increased with the increase of the solution concentration and slightly decreased with the increasing voltage and the needle tip-to-collector distance.

The next generation of membranes should overcome the energy and cost required to force water through semipermeable media. One possible way is for the new membranes to develop continuous pores of a given radius, surrounded by non-polar atoms, that withstand lower resistance towards water, but impede the passage of ions.

3.3 Copolyamides applications in automotive industry

In the automotive industry, as in many others, plastics – PAs and coPAs included - replace metal in various applications and help lower vehicle weight. Copolyamides were, despite their higher price, preferred to copolyesters due to their benefits. Copolyamides surpass copolyesters in heat resistance, at equal physical properties, by 10-15°C. The possibility to use lower melting point products is of significant advantage when temperature-sensitive substrates are used. The higher price is, in large part, compensated by the improved specific bonding, i.e. reduced use of material.

Nowadays, many copolyamide formulations have been patented and are in use with excellent results. Radiator agents prevent the cooling water from freezing or overheating and protect the system from deposits and corrosion. For the oil circuit, they enable the optimum component design and low cost production. In breaks, these materials ensure reliable response at all times and protect the system from corrosion. Used in fuel circuit and for emissions reduction, they help enhance performance, reduce fuel consumption and emissions, and keep deposits from building up in the engine. As for the driving comfort, PAs and coPAs enhance chassis safety and comfort, reduce vibrations and insulate engine noise to ensure a calm and pleasant atmosphere inside the vehicle.

3.3.1 Hybrid car components

Hybrid car components made of metal and plastic, flat parts like front-end support structures, roof and rear hatch reinforcing structures, not to mention compact injection molding-sheathed components in joined areas of a vehicle's body structure, are increasingly being used to to minimize the use of metal and improve lightweight design systems. If conventional mechanical anchors for the polymers are replaced with material bonds using a copolyamide adhesion promoter, the resulting components offer considerably improved mechanical properties and also reduce the amount of material required *[Risthaus, 2011]*.

A common material combination is galvanized steel DX56D overmolded with PA6 GF30. However, the lack of adhesion between metal and polymer is a drawback. Hybrid components get their rigidity only through the mechanical anchoring of the polymer.

New adhesion promoter systems, based on the copolyamide Vestamelt® X1333 from Evonik Degussa GmbH *[Evonik, 2011b]*, allow material bonding between the different materials, i.e., polymer and metal.

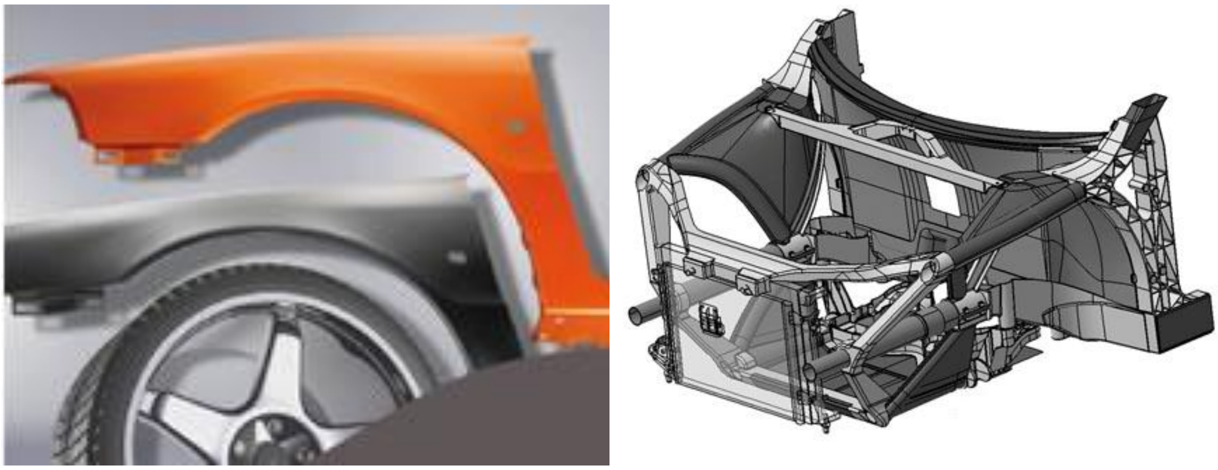

Figure 27. Hybrid car components *[after Risthaus, 2011]*

The considerably improved mechanical properties afford new levels of freedom in the design and dimensioning of hybrid components.

3.3.2 Filters

The introduction of the EURO V standard for cars emissions and the necessity to use new filters for diesel vehicles created a serious demand for such filter systems with improved performance level (Fig. 28).

When a certain amount of 5-15% wt. of a copolyamide powder (Vestamelt 730-P1) is added to the extrusion material comprising SiC, and this polymer, after the extrusion, is burnt out again at approx. 350°C, this yielded into a porous structure with significantly improved filtering properties as a result of an enormous increase in the BET values of >350 m^2/l to about 800 m^2/l *[Risthaus and Woenicker, 2009]*. Preference is given to using copolyamide powders which have a particle size distribution in the range of 0-200 μm, preferably in the range from 0 to 80 μm. The burning out of the polymeric components significantly altered the surface structure of the SiC material, more linear elements and channels formed within the monolithic SiC structure, which enhanced the filter performance and, hence, improved the efficiency of the filter cartridge. The incorporation of the polyamide powder and subsequent hydrolysis can significantly lower the exhaust gas backpressure, which results in a significantly better filter action.

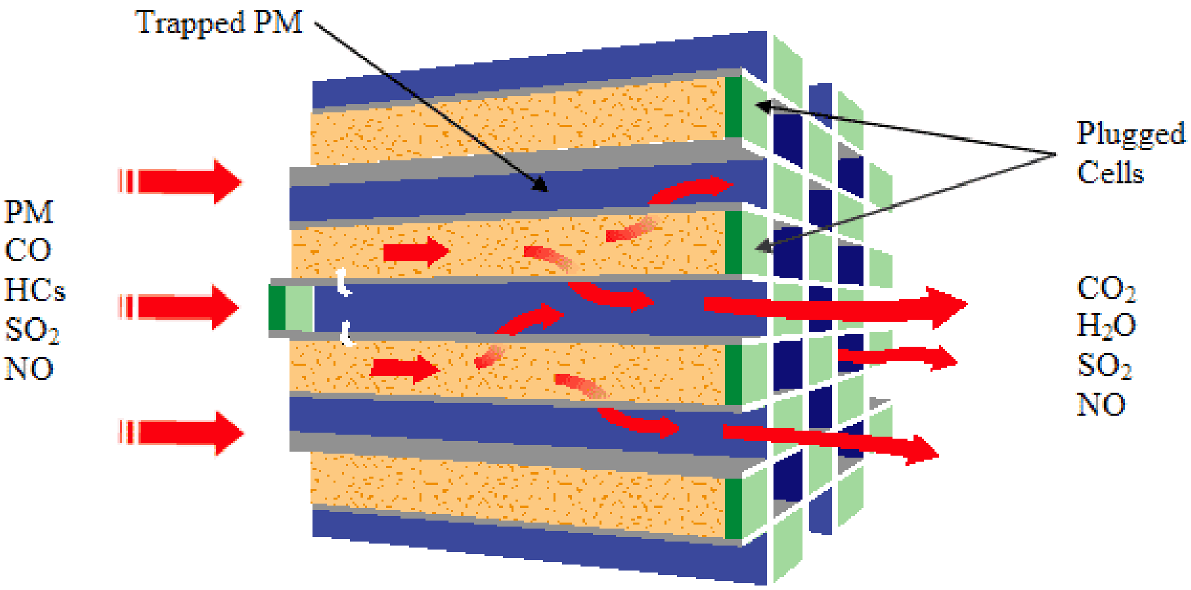

PM=particulate matter, CO=carbon monoxide, HCs=hydrocarbons, SO_2=sulphur dioxide, NO=nitrogen monoxide, CO_2 =carbon dioxide, H_2O=water

Figure 28. Scheme of a Diesel particulate filter *[after “Diesel Retrofit Technology for Clean Air”, http:// www.meca.org/galleries/default-image/diesel_particulate_filter.gif]*

The proton exchange membrane fuel cells (PEMFCs) are widely used for applications in automotive, stationary and portable electronics due to its high energy conversion efficiency and environmentally friendly energy generation. Proton exchange membrane (PEM) is a crucial component in PEMFCs for transferring protons from the anode to the cathode as well as separating the fuel from oxidant. A series of sulfonated copolyamides (SCPAs) and evaluated them as a potential PEM materials *[Jo, 2008]*. Although promising, SCPAs having a sulfonation degree (SD) higher than 70% showed instability in water. In order to improve water stability of SCPAs having higher SD, he synthesized a series of fluorine substituted SCPAs. The fluorine substitutions into the ionomer reduced the water uptake, thereby improving mechanical stability of the membrane.

Other sulphonated random copolyamides, having the sulfonation degree (SD) of 20-50 mol %, were synthesized starting from 4,4’-(hexafluoroisopropylidene)dianiline (HFA) and 2,4-diaminobenzenosulfonic acid (DABS) as comonomers *[Perez-Padilla et al., 2011]*. The mixture of diamines is reacted by polycondensation with isophthalic diacid (ISO) in order to produce random copolymers poly(hexafluoroisopropylidene-co-2,4-diaminobenzensulfonic)isophthalamides (HFA-co-DABS/ISO) (Fig. 29). The SD was controlled by adjusting the ratio of diamines HFA and DABS (HFA/ DABS).

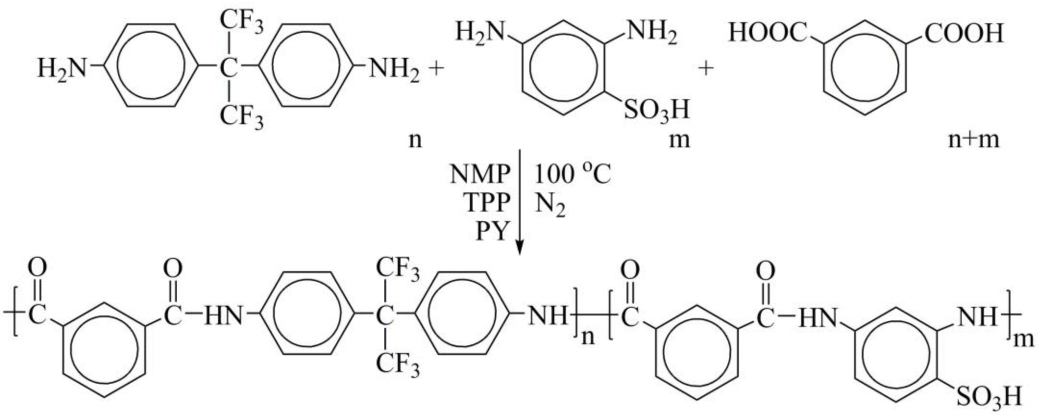

Figure 29. Synthesis of random copolyamides HFA-co-DABS/ISO *[after Perez-Padilla et al., 2011]*

Thermal stability of coPAs showed the onset of decomposition at 320°C for the ionic moieties and above 600°C for the nonsulfonated part of the copolymers. The membranes obtained from copolyamides HFA-co-DABS/ISO showed an increase in ion exchange capacity (IEC) and an enhanced proton transfer capacity, with the increasing degree of sulfonation. These membranes should be considered good candidates for proton exchange membranes (PEM) for fuel cells, with improved thermal stability as compared to the ones currently in use (i.e., Nafyon 115).

3.3.3 Prefabricated components

Copolyamides for injection-moulding, extrusion, blow moulding and compression moulding processing are required for automotive industry. The use of semi-aromatic coPAs based on tetramethylene terephthalamide (4T) and hexamethylene terephthalamide (6T) units, where PA 4T/6T ratio was 50/50, 40/60, 30/70, for car parts production has been reported *[Rulkens and Crombach, 2004]*. These copolyamides have the melting points over 300°C and a high cristallinity. They are suitable for electric and electronic components, film and fibres, too.

Synthesis and characterization of novel terephthalic acid coPAs were patented *[Mok and Pagilagan 1995]*. Partially crystalline copolyamides were obtained from terephthalic acid or a mixture of terephthalic acid and isophthalic acid, containing less than 40% of isophthalic acid, and a mixture of hexamethylene diamine and 2-methyl pentamethylene diamine. The copolyamides have melting points of 280-330°C and may be moulded into various articles by using injection moulding technology: valves, tanks, containers, washers and the like for automotive end-uses; into articles for electrical end-uses, e.g. parts requiring resistance to temperatures of 260°C or above; articles where retention of mechanical properties under the influence of heat, moisture, hydrocarbons, alcohols is very important. These coPAs may be also spun into fibres or formed into films, and used in a wide variety of end-uses especially where high temperature properties are required.

Grivory HT is a member of a group of engineering plastics (EMS GRIVORY) *[EMS-GRIVORY 2011]*; it is a semicrystalline thermoplastic construction material based on copolyamide PA-6T/6I and PA-6T/6,6, characterized by a high performance profile. Technical injection moulded parts made of this material have impressive dimensional stability, even at high temperature, as well as stiffness and strength; low tendency to warp, good surface quality and resistance to chemicals; efficient and cost-effective manufacture. In automotive industry, it is used for electric and electronic parts, different innards for under-bonnet applications (chassis, brakes, clutch), interior and exterior construction elements, as well as lighting.

Badamid® from Bada Company (Germany) is a product group *[Bada AG, 2011]* consisting of thermoplastic construction materials based on polyamides and copolyamides (PA 6, PA 6,6, copolyamide PA 6,6/6 and partly aromatic PA6/PA6T) feature outstanding, versatile properties. Besides their exceptional mechanical strength and high thermal resistance, they also demonstrate good toughness at low temperatures and favourable friction and abrasion behaviour, and can be further processed by all conventional moulding processes. Their application in a variety of technical sectors includes machine elements, the electric, electronic and automotive industry, etc. Advanced modifications to customer specification in respect of reinforcement, toughness, ease of processing, flammability and colour can be realized with excellent results.

3.3.4 Hot melt adhesives for automotive applications

Hot melt adhesive properties of coPAs are used in automotive industry, as well, for interior finishing materials, fixing interior trim and seat heaters, etc. Vestamelt® hotmelt adhesives are used by the automotive industry because they can be applied to substrates by means of typical processes *[Degussa, 2011]*. Hybrid components made with an adhesion promoter based on PA 12 by Evonik Industries *[Evonik Ind., 2010]* can absorb a greater amount of force in panels of the same thickness and they are lighter given the same level of performance. One special application: the reliable bonding of paper to aluminum for the construction of fuel filters. Griltex® copolyamides *[EMS-Griltech, 2011b]* also meet the requirements of the automotive industry in terms of bonding strength, heat resistance and emissions. The lower amount of adhesive also results in a better, more even surface structure. Further advantages are high transparency as well as the very good hydrolysis resistance. Arkema Inc. *[Arkema Inc., 2011]* manufactures polyamides and copolyamides for various automotive applications: Rilsan® for fuel lines, coiled air hoses for trucks, electrical components, etc.; Platamid® heatseal copolyamides for bonding of fabrics in the textile industry (garments and automobile interior fittings); Rilsan® for protection of automotive parts (spline shafts, brake hoses), water pipes; Rilsan® powder coating with added surface protection against bacterial growth.

4. Conclusions and future development trends

Engineering polymers, such as PAs and coPAs, will be of major importance in the development of different industry branches. They have been developed – and this is an on-going trend – for applications that until now have been unavailable with regular polymers due to their insufficient characteristics. High performance polymers previously available have never fully succeeded due to their unfavourable price/performance ratio.

Copolyamides and their derivatives are unique materials insofar as their chemical, thermal and mechanical behavior is concerned. New copolyamides continue to be developed. The biggest step so far has been the incorporation of monomers containing aliphatic and/or aromatic rings. These structures have helped to keep copolyamides in the midst of the general effort to insert polymers into applications that currently use metals and ceramics, applications that generally feature high-temperature and/or other extreme conditions. Other uses have entirely different requirements, for which copolyamides have been also tailored, sometimes by actually tempering the very coherence and stiffness of the base polymer. While the number of possible monomers is limited (not least by economics), the number of monomer combinations is limitless. The search for new copolymer formulations will continue to be worthwhile both for academics and industry specialists.

As a consequence, fundamental and applied research is being carried out to expand their processability in order to broaden the area of application associated with these materials. From a research point of view, these goals have been partly achieved, although further research is still needed.

Some of the effort that goes into developing polymers might be wisely redirected into developing ways to make cheaper monomers. Increasing attention is being paid to the source of monomers. Materials that are derived from vegetable or animal sources rouse interest over fossil ones.

Innovative technologies and adding value are other possible keys to the future success of copolyamides.

Moreover, researchers try to exploit the high performance properties of the copolyamides in new fields, such as smart materials, hybrid materials, biodegradable materials, etc.

Under these circumstances, the ultimate challenge for scientists in the field is to find answers to global problems, such as climate protection, energy efficiency, healthcare, nutrition and mobility – a contribution to a better future for all of us and for coming generations.

5. References

Ahmad A. L., Ooi B. S., Choudhury J. P. (2002) Preparation and characterization of interfacial polymerised membrane from 3,5-diaminobenzoic acid. *Songklanakarin J. Sci. Technol.*, Vol. 24 (Suppl.), pp. 807-814.

Ahmad A. L., Ooi B. S., Choudhury J. P. (2003) Preparation and characterization of co-polyamide thin film composite membrane from piperazine and 3,5-diaminobenzoic acid. *Desalination*, Vol. 158, No 1-3, pp. 101-108.

Ahmad A. L., Ooi B. S., Mohammad A. W., Choudhury J. P. (2004) Development of a highly hydrophilic nanofiltration membrane for desalination and water treatment. *Desalination*, Vol. 168, No 5, pp. 215-221.

Albrecht W., Fuchs H., Kittelmann W. (Eds) (2003) *Nonwoven fabrics* Wiley-VCH, Verlag GmbH & Co. KGaA, Weinheim, Germany.

Arkema Inc. (2011) Arkema Group retrived from http://www.arkema-inc.com/

Arvanitoyannis I., Psomiadou E. (1994) Composition of anionic copolyamides (Nylon 6/Nylon 12) with short glass E-fibres – Preparation and properties. *J. Appl. Polym. Sci.*, Vol. 51, No 11, pp. 1883-1899.

Badamid (2011) retrieved from http://www.bada.de/en/index.php?seite_nr=14

Baker W. O., Fuller, C. S. (1942), Macromolecular disorder in linear polyamides. Relation of structure to physical properties of copolyamides. *J. Am. Chem. Soc.*, Vol. 64, pp. 2399-2407.

Bateman D. L. (1978) *Hot melt adhesives*, 3rd Edition, Noyes Data Co., New Jersey, USA.

Besshaposhnikova V.I., Artemenko S.E., Polushenko I.G. (2004), Copolyamides with low melting points for articles in light industry. *Fibre Chemistry,* Vol. 36, No 1, pp. 59-61.

Brown R. (Ed.), (1999) *Handbook of polymer testing*, Marcel Dekker, New York, USA.

Buruiana E.C., Zanoaga M., Mihai A. (2007) Performance composites and laminates with special properties for footwear, *Proceedings of The 5th International Conference on the Management of Technological Changes − MTC*, 25-26 August 2007, Alexandropolis, Greece.

Carothers W. H. (1937) Polyamides from amino acids. US Patent 2071253.

Carothers W. H. (1938a) Linear polyamides and their production. US Patent 2130523.

Carothers W. H. (1938b) Diamine-dibasic acid salts. US Patent 2130947.

Carothers W. H. (1938c) Polyamide fibers and methods of making. US Patent 2130948.

Carrera-Figuiras C., Aguilar-Vega M. (2005) Gas permeability and selectivity of hexafluoroisopropylidene aromatic isophthalic copolyamides. *J. Polym. Sci. Part B: Polym. Phys.*, Vol. 43, No 19, pp. 2625–2638.

Chapman R. D., Holmer D. A., Pickett Jr. O. A., Saunders J. H. (1977) Dimensionally stable 6TA/6IA fibers. US Patent 4022756.

Coolen P. T., Johnson S. T. (2001) Nonwoven backing and carpet comprising same. US Patent 6207599 B1.

Cowan J. C., Falkenburg L. B., Teeter H. M., Skell P.S (1948), Polyamides from polymeric fat acids. US Patent 2450940.

Crusos A., Ungureanu C., Rez T., Murariu G., Zanoaga M. (1983) Procedeu de obţinere a unor termoadezivi de tip copoliamidic. Romania Patent 82985.

Crusos A., Zanoaga M., Luncasu M. (1985) Procedeu de obtinere a unor termoadezivi de tip copoliamida-polietilenă. Romania Patent 89603.

Crusos A., Zanoaga M. (1989) Procedeu de obtinere a unor pulberi adezive pe baza de polimer copoliamidic. Romania Patent 97989.

Crusos A., Zanoaga M. (1992), Procedeu de obtinere a unor paste termoadezive pe bază de copoliamide. Romania Patent 101323.

Crusos A., Zanoaga M. (1993) Copoliamide. Relatii structura–proprietati. II. Influenta acizilor grasi în sistemul de reactie. *Materiale Plastice,* Vol. 30, No 2, pp. 135-139.

Crusos A., Crusos G., Zanoaga M., Tataru D., Bordei A., Dobinda V. (1995) Metoda de macinare criogenica pentru transformarea diferitelor produse din granule in pulberi fine si foarte fine. Romania Patent 112252.

Crusos A., Zanoaga M., Dobândă V. (1999) Procedeu de obţinere a unor termoadezivi copoliamidici. Romania Patent 114260 B1.

Crusos A., Zanoaga M., Crusos C., Dobinda V. (2001) Procedeu de obţinere a unor termoadezivi filabili de tip hot-melt, pe bază de copoliamide. Romania Patent 114800.

Crusos A., Zanoaga M., Stoleriu A., Preda C. (2001) Copoliamide. Relatii intre structura şi proprietati. Unele aspecte ale comportarii termice. *Industria Textilă,* Vol. 52, No 4, pp. 167-171.

Daebel H., Götz W., Oenbrink G., Roerdink E., Roh-Liebenau U., Schenkels F. A. M. (1998) In: *Kunststoff handbuch*, Vol. 3/4: *Polyamide*, Bottenbruch L. and Binsack R. (Eds.), Hanser Verlag, Munich, Germany, p. 803.

Degussa AG (2011a) In: *High performance polymers,* retrieved from http://www.degussa-hpp.com/dl/brochure/vestamelt_doubledot_eng.pdf

Degussa AG (2011b) In: *Handling and processing of VESTAMID,* retrieved from http://www.daicel-evonik.com/catalog/nylon12/pdf/vestamid_handling_eng.pdf

Dijkema J., Visscher E. J. (2009) Nonwovens, tufted nonwovens, and articles containing the same. US Patent 0152191 A1.

Dua B. (2005) Footwear incorporating a textile with fusible filaments and fibers. US Patent 6910288 B2.

Dubois P., Coulembier O., M. Raquez J. (2009) Polyamides Chapter 7, In: *Handbook of ring-opening polymerization*, Dubois P., Coulembier O. and Raquez J. M. (Eds.), Wiley-VCH Verlag GmbH&Co., Weinheim, Germany, 165.

Eersels K. L. L., Aerdts A. M., Groeninckx G. (1996) Transamidation in melt-mixed aliphatic and aromatic polyamides. 2. Molecular characterization of PA 46/PA 6I blends. *Macromolecules*, Vol. 29, No 21, pp. 1046-1050.

Ebnesaijjad S. (Ed) (2008) *Adhesives technology handbook*, 2nd Edition, William Andrew Inc., New York, USA.

Elfert K., Wolf G. D., Bentz F., Kunzel H. E. (1980) Semipermeable membranes of heterocyclic copolyamides. US Patent 4221903.

EMS-GRILTECH (2011a) In: *Grilon EMS – Bonding yarns*; retrieved from http://www.districo.com/page_gb/bondingyarn.htm.

EMS-GRILTECH (2011b) In: *Thermoplastic Adhesives and Technical Fibers for High Performance*, retrieved from http://www.emsgriltech.com.

EMS-GRILTECH (2011c) In: Fusible yarns - Grilon*® EMS,* retrieved from http://www.districo.com/page_gb/fusibleyarn.htm.

EMS-GRIVORY (2011) Grivory HT Enhenced performance at high temperatures retrieved from http://www.iplatech.com/product/.

Evonik-Degussa GmbH (2011a) *Vestamelt® - Thermoplastic copolyamide hotmelt adhesives*, retrieved from http://www.degussa-hpp.com/dl/brochure/vestamelt_pastedot.

Evonik-Degussa GmbH, (2011b) *Vestamelt® - Curable copolyamide hotmelt adhesive,* retrieved from http://adhesives-sealants.evonik.com/sites/dc/ Sealants/.

Evonik Industries (2010) In: Hybrid components with Vestamelt® copolyamide adhesion promoters, retrieved from http://www.radtech-europe.com/files_content/.

Farana J., Boryniec S., Dutkiewicz S. (2005) Fibres made of copolyamides modified with polyetheramines. Studies of the supramolecular structure. *Fibres & Textiles in Eastern Europe*, Vol. 13, no 5 (53), pp. 118-121.

Feldman D., Marculescu B. (1977) Copoliamide. *Industria usoara,* Vol. 24 No 10, pp. 436-441.

Fisher K., Horn P., Eckert G., Leppmeier F. (1978) Copolyamide and its use for finishing leather and leather substitutes. US Patent 4126414.

Floyd D. E. (1961) *Polyamide resins*, Reinhold Publishing Co., New York, USA.

Gaymans R. J. (2003) Polyamides, Chapt. 3, In: *Synthetic methods in step-growth polymers*, Rogers M. E. and Long T. E. (Eds.), Wiley-Interscience, John Wiley & Sons, Hoboken, New Jersey, USA, p. 135.

Goodman I., Kehayoglou A. H. (1983) Anionic copolymers of caprolactam with laurolactam (nylon 6/12 copolymers)–II. Crystallisation, glass transitions and tensile properties, *Eur. Polym. J.*, Vol. 19, No 4, pp. 321-325.

Goetz W. (2003) Polyamide for flexible packing film, *Proceedings of 2003 European PLACE Conference*, 12-14 May 2003, Rome, Italy.

Gorley R. T., Pung D. J., Sherry A. E. (2005) 100% Synthetic nonwoven wipes. US Patent 0133174 A1.

Halbmaier J. G. (1998) Low melt, high performance textile adhesives, *Proceedings* of *TAPPI Hot Melt Symposium,* 28 June-1 July 1998**,** Atlanta, USA.

Harman N. W. (1989) Long open assembly time vinyl-bonding polyamide from dimer acid. US Patent 4853460.

Hofmann H. (1998), In: *Kunststoff Handbuch*, Vol. 3/4: *Polyamide*, Bottenbruch L. and Binsack R. (Eds.), Hanser Verlag, Munich, Germany, p. 57.

Hu A. T., Tsai R.-S, Lee Y.-D. (1989) Preparation of block copolyestheramides and their properties as hot melt adhesives. *J. Appl. Sci*., Vol. 37, No 7, pp. 1863-1876.

Hubert E., Schlack P., Ludewig H. (1939) Polyamides and polyurethanes - materials for records. US Patent 277948.

Jacobs D. B., Zimmermann J. (1977) Polymerization processes, In: *High polymers*, Vol. 29, Schieldknecht C. E. and Skeist I. (Eds.), Wiley-Interscience, New York, USA, p. 424.

Jo T. S. (2008) Synthesis of partially fluorinated sulfonated copolyamides and their applications in proton exchange membranes fuel cells, Graduate Seminar CHE 101, 2008; retrieved from http://radchem.nevada.edu/classes/chem491/abstracts/.

Kehayoglou A. H. (1983) Anionic copolymers of cprolaactam with laurolactam (nylon 6/12 copolymers)–I. Preparation and general properties. *Eur. Polym. J.*, Vol. 19, No 3, pp. 183-188.

Kohan M. I. (1995) *Nylon plastics handbook*, Hanser, New York, USA.

Konagaya S., Tokai M. **(**2000) Synthesis of ternary copolyamides from aromatic diamine (m-phenylenediamine, diaminodiphenylsulfone), aromatic diamine with carboxyl or sulfonic group (3,5-diaminobenzoic acid, 2,4-diaminobenzenesulfonic acid), and iso- or terephthaloyl chloride. *J. Appl. Polym. Sci.*, Vol. 76, No 6, pp. 913–920.

Konagaya S., Kuzumoto H., Watanabe O. **(**2000) New reverse osmosis membrane materials with higher resistance to chlorine. *J. Appl. Polym. Sci.,* Vol. 75, No 11, pp. 1357–1364.

Konagaya S., Tokai M., Kuzumoto H. (2001) Reverse osmosis performance and chlorine resistance of new ternary aromatic copolyamides comprising 3,3′-diaminodiphenylsulfone and a comonomer with a carboxyl group. *J. Appl. Polym. Sci.,* Vol. 80, No 4, pp. 505–513.

Kricheldorf H. R., Denchev Z. (1998) Interchange reactions in condensation polymers and their analysis by NMR spectroscopy, In: *Transreactions in condensation polymers*, Fakirov S. (Ed.), Wiley-VCH, New York, USA, p. 1.

Krištofic M., Marcincin A., Borsing E. (1999) Preparation, properties and application of modified fibres with piperazine rings. *Polym. Adv. Technol.,* Vol. 10, No 3, pp. 179-186.

Krištofic M., Marcincin A., Ujhelyiová A., Murarova A. (2000a) Modification of PA 6 fibres with alkaline copolyamides. *Chem. Papers,* Vol. 54, No 1, pp. 53-58.

Krištofic M, Marcincin A, Ujhelyiová A. (2000b) The DSC study of PA 6, polyamides and copolyamides. *J. Therm. Anal. Calorim.,* Vol. 60, No 2, pp. 357-369.

Krištofic M., Hricova M., Ujhelyiova A. (2001) Modification of PP fibres with alkaline copolyamides. *Macromol Symp.,* Vol. 170, pp. 291-299.

Krištofic M., Karabcova N., Alexy P., Ryba J., Vassova I. (2005a) Modification of PA 6 by comonomers and layered silicate. *Fibres & Textiles in Eastern Europe,* Vol. 13, No 6 (54), pp. 33-35.

Krištofik M., Naciniakove Z., Legen J., Ryba J. (2005b) Polypropylene fibres modified by copolyamides. Part I. Preparation of modified fibres and their properties. *Vlakna a textil,* Vol. 12, No 3, pp. 104-110.

Krištofic M., Ujhelyiová A. (2006) PA 6, copolyamides of ε-caprolactam with nylon salt of diethylenetriamine + adipic acid and their thermal properties. *Fibres & Textiles in Eastern Europe*, Vol. 14, No 4 (58), pp. 21-24.

Krištofic M., Dulikova M., Vassova I., Ryba J. (2007) PA 6/copolyamide /layered silicate fibres. *Fibres & Textiles in Eastern Europe*, Vol. 15, No 5-6 (64-65), pp. 34-36.

Krištofic M., Ujhelyiová A. (2009) Thermal properties of poly-ε-caprolactam and copolyamides based on ε-caprolactam. *J. Therm. Anal. Calorim*. Vol. 98, No 1, pp. 145-150.

Krištofic M., Ujhelyiová A., Ryba J., Vassova I. (2010) Structural and physiologic properties of PA 6 fibres functionalized with copolyamides and nanoclays, *Proceedings of 7th International Conference – TEXSCI 2010,* 6-8 September 2010, Liberec, Czech Republic.

Krištofic M., Vassova I., Ujhelyiová A., Ryba J. (2011) Functionalisation of polypropylene. Part I. Mechanical, electric and sorptive properties of PP fibres modified with concentrates consisting of copolyamides and nanoclay. *Fibres & Textiles in Eastern Europe,* Vol. 19, No 2 (85), pp. 18-22.

Li L., Zhang S., Zhang X., Zheng G. (2008) Polyamide thin film composite membranes prepared from isomeric biphenyl tetraacyl chloride and m-phenylenediamine. *J. Membr. Sci.,* Vol. 315, No 1-2, pp. 20–27.

Li Y., Huang Z., Lur Y. (2006) Electrospinning of nylon-6,66,1010 terpolymer. *Eur. Polym. J.*, Vol. 42, No 8, pp. 1696-1704.

Lintecum B.M., Shoemaker R.T., Anderson Jr. C.R. (2003a) Bicomponent effect yarns and fabrics thereof. US Patent 0187140 A1.

Lintecum B.M., Shoemaker R.T., Anderson Jr. C.R. (2003b) Bicomponent effect yarns and fabrics thereof. US Patent 6548429 B2.

Loeb M. L. (1978) Polyamide resins and method for manufacture. US Patent 4072641.

Marchildon K. (2001) Polyamides – Still strong after seventy years. *Molec. React. Eng.,* Vol. 5, No 1, pp. 22-54.

Mok S. L., Pagilagan R. U. (1995), Terephthalic acid copolyamides. US Patent 5378800.

Morgan P. W. (1977) Synthesis and properties of aromatic and extended chain polyamides. *Macromolecules,* Vol. 10, No 6, pp. 1381-1390.

Oishi Y., Kakimoto M.-A., Imai Y. (1987) Novel synthesis of high molecular weight aramids from N-silylated aromatic diamines and aromatic diacid chlorides. *Macromolecules,* Vol. 20, No 3, pp. 702-703.

Peerman D. E., Kanten G. (1980) Polyamide adhesive for bonding fabrics. US Patent 4217256.

Peerman D.E. (1967), Polyamides from fatty acids, In: *Encyclopedia of polymer science and technology*, Vol. 10, Mark H. F. Gaylord N. G. and Bikales N. M. (Eds.), Interscience Div., Wiley & Sons, New York, USA. p. 597.

Perez-Padilla Y., Smit M.A., Aguilar-Vega M. J. (2011) Preparation and characterization of sulfonated copolyamides based on poly(hexafluoroisopropylidene)isophthalamides for polymer electronic membranes. *Ind. Eng. Chem. Res.*, Vol. 50, No 16, pp. 9617-9624.).

Petrie E. M. (2007) Synthetically designed hot-melt adhesives – polyamides and polyesters, In: *SpecialChem*, retrieved from /www.specialchem4adhesives.com/

Poessnecker G., Spindler J., Kinkelin E. (2003) Low-melting copolyamide and their use as hot-melt adhesives. US Patent 6590063 B2.

Preston J. (1989) Aromatic polyamides, In: *Encyclopedia of Polymer Science and Engineering*, Vol. 11, Mark H. F., Bikales N. M., Overberger C. G. and Menges G. (Eds.), Wiley-Interscience, New York, USA, p. 381.

Raabe F., De Jong E. (1978) Copolyamides containing caprolactam, laurolactam and 11-aminoundecanoic acid. US Patent 4093492.

Ramanathan L. S. (2000) Studies on particle forming polycondensation and ring opening polymerization processes, *Thesis*, Division of Polymer Chemistry National Chemical Laboratory, Pune, India.

Risthaus M. (2011) Hybrid: stronger and lighter, retrieved from http://www.chemanager-online.com.

Risthaus M., Woenicker H.-J. (2009) Copolyamide powder as a pore former in regenerable ceramic particulate filters. US Patent 2009/0255402 A1.

Rulkens R., Crombach R. C. B. (2004) Copolyamide based on tetramethylene terephthalamide and hexamethylene. US Patent 6747120 B2.

Rusu G. (2003) Copolimerizarea anionica a ε-caprolactamei cu laurolactama prin procedeul de formare rotationala, *Materiale Plastice*, Vol. 40, No 1, pp. 31-36.

Ryba J., Ujhelyiová A., Krištofic M., Vassova I. (2010) Thermal properties of PA 6 and PA 6 modified with copolyamides and layerd silicates. *J. Therm. Anal. Calorim*., Vol. 101, No 3, pp. 1027-1037.

Schlack P. (1938), Verfahren zur herstellung verformbarer hockmolekularer polyamide. German Patent 748253.

Schlack P., Kunz K. (1952), *Chemische textilfasern, filme und folien, grundlagen und technologic* (R. Pummerer, ed.) Ferdinand Enke Verlag, Stuttgart, Germany.

Schmid E., Griehl W. (1980) Ternary polyamide filaments. US Patent 4225699.

Sundet S. A. (1991) Microporous support layer with interfacially polymerized copolyamide membrane thereon. US 5015382.

Tremblay S. (2010) *Advances in hot melt technology,* retrieved from http://www.henkelna.com/.

Trigo-López M., Estévez P., San-José N., Gómez-Valdemoro A., García F. C., Serna F., De la Peña J. L., García J. M. (2009) Recent Patents on Aromatic Polyamides. *Recent Patents on Materials Science*, Vol. 2, No 3, pp. 190-208.

Vass I., Krištofic M., Ryba J. (2008) Properties of polyamide 6 fibres modified by silicate nanopaticles. *Hungarian Journal of Industrial Chemistry Veszprem*, Vol. 36, No 1-2, pp. 155-157.

Vogl O. F., Stevenson D. R. (1977) Regular copolyamides as desalination membranes. US Patent 4002563.

Vollbracht L. (1989) Aromatic polyamides, In: *Comprehensive polymer science*, Vol. 5: *Step polymerization*, Allan G., Bevington J. C., Eastmond G. C., Ledwith A., Russo S. and Sigwald P. (Eds.), Pergamon, Oxford, UK, p. 373.

Wang L.-J., Hu Z.-H. (2009) Synthesis and application of a basic copolyamide as an acid-dyeable PTT fiber additive. *Text. Res. J.*, Vol. 79, No 12, pp. 1135-1141.

Wesolowski J., Grzebieniak K. (2004) Research on the degradation of PA 6 waste and utilisation of the degradation products for the synthesis of copolyamide resins. *Fibres & Textiles in Eastern Europe,* Vol. 12, No 1 (45), pp. 66-69.

Zanoaga M. (2001a) Novel thermoplastic copolyamides based on caprolactam, 1,6-hexane diamine. Synthesis and study of properties, *Proceedings of 12th Romanian International Conference on Chemistry and Chemical Engineering - RICCCE,* 13-15 September 2001, Bucureşti, Romania.

Zanoaga M. (2001b) Les caracteristiques et les possibilites d'utilisation d'un polymere polyamidique comme hotmelt. *Chemical Bulletin of "Politehnica" University – Timisoara*, Vol. 46, No 1-2, pp. 177-180.

Zanoaga M. (2001) Aspects concerning the modifications of a thermoplastic polymer with filler agents, *Proceedings of International Conference on Materials Science and Engineering,* 1-2 March 2001, Braşov, Romania.

Zanoaga M., Tanasa F. (2002), A new thermoplastic matrix for composites based on recycled and recovered materials. I. Synthesis and characterization, *Proceedings of Second International Conference on Ecological Chemistry,* 11-12 October 2002, Chisinau, Rep. Moldova.

Zanoaga M., Tanasa F. (2003), Performant nonwovens – 'sandwich' composite structures with novel thermoplastic matrices, *Proceedings of 7th International Conference on Frontiers of Polymers and Advanced Materials – ICFPAM,* 10-15 June 2003, Bucharest, Romania.

Zanoaga M., Harnagea F., Rosculet V. (2004a) A copolyamide – as a possible hot melt adhesive for light industry, *Proceedings of 7th European Adhesion Conference - EURADH 2004*, 5-9 September 2004**,** Freiburg im Breisgau, Germany.

Zanoaga M., Harnagea F., Roşculeţ V. (2004b) Composite structures with thermosensitive materials, *Proceedings of 7th European Adhesion Conference - EURADH 2004*, 5-9 September 2004, Freiburg im Breisgau, Germany.

Zanoaga M., Harnagea F. (2005) Aspecte privind extinderea chimizarii în procesul de confectionare a incaltamintei, *Proceedings of Sesiunea anuală de comunicări ştiinţifice, Facultatea de Textile şi Pielărie,* 26-27 mai 2005, Oradea, Romania.

Zanoaga M. (2006) Structuri compozite cu materiale termosensibile, *Proceedings of A XVIII-a Conferinţă Internaţională de Inventică "Cercetări şi Tehnologii Inovative Performante",* 5-9 iulie 2006, Iaşi, Romania.

Zanoaga M. (2007) Investigations related to a copolyamide for fusible linings. *Buletinul Institutului Politehnic Iasi, Textile. Pielarie,* Vol. LIII (LVII), No 5, pp. 163-168.

Zanoaga M., Melinte V. (2008a), A modified polyamide — a hot melt adhesive for thermally bonded interliners. *Annals of the University of Oradea,* Vol. IX, pp. 163-167.

Zanoaga M., Harnagea F. (*2008b)* Bulky nonwoven composites based on copolyamidic polymer and textile fibers. *Annals of the University of Oradea,* Vol. IX, pp. 155-162.

Zanoaga M., Tanasa F. **(**2010a) Effect of different additives on the adhesive properties of a copolyamide 6/6.6, *Proceedings of The Annual International Symposium in Knitting and Apparel – ISKA-2010,* 19-20 November 2010, Iasi, Romania.

Zanoaga M., Tanasa F. (2010b) Multi-layer nonwoven technical materials obtained by thermal bonding, *Proceedings of The Annual International Symposium in Knitting and Apparel – ISKA-2010,* 19-20 November 2010, Iasi, Romania.

Zimmerman J. (1989) Polyamides, In: *Encyclopedia of polymer science and engineering,* Vol. 11, Mark H. F., Bikales N. M., Overberger C. G. and Menges G. (Eds.), Wiley-Interscience, New York, USA, p. 315.

Zydowicz N., Chaumont P., Soto-Portas M. L. (2001) Formation of aqueous core polyamide microcapsules obtained via interfacial polycondensation. Optimization of the membrane formation through pH control. *J. Membr. Sci.*, Vol. 189, No 1, pp. 41-58.

Chapter 3

Block Copolymers and Composite Polymeric Materials on Their Base

Volodymyr GRISHCHENKO[1]*, Nataliya BUSKO*[1]*,*
Antonina BARANTSOVA[1]*, Volodymyr MYSHAK*[1]*,*
Madalina ZANOAGA[2]*, Fulga TANASA*[2]*.*

[1]Institute of Macromolecular Chemistry of National Academy of Sciences of Ukraine, Kyiv
[2]Institute of Macromolecular Chemistry "Petru Poni" of Romania Academy, Iasi

¶

Summary

A series of novel thermoplastic diene-styrene and diene-acrylate block copolymers (BCPs) based on an aliphatic copolyamide and an oligodiene having isocyanate end groups was prepared. The synthesis and properties of BCPs obtained by photoinitiated radical polymerization using oligomeric azo- and polyazoinitiators have been investigated. The distributions of molecular weight and viscosity of the BCPs were determined. The morphology, thermal and dynamic - mechanical behavior were investigated by IR spectroscopy, differential scanning calorimetry, dynamic mechanical analysis and small angle X-ray scattering. New polymeric blends based on BCPs and polyethylene waste were obtained and subsequently characterized.

Notations and acronyms

AGN-CH	azo-bis-isobutyrohydrazone of cyclohexanone
BCP	block copolymer
coPA	aliphatic statistic copolyamide
DR	diene rubber
MAI	macroazoinitiator
MDIR	macrodiisocyanate dienic rubber
MDIBIR	macrodiisocyanate of butadiene-isoprene rubber
OAI	oligomeric azoinitiator
ODH	oligodiene with end hydroxil groups
OSDG	oligostyrenedihydrazide
OSt	oligostyrene
PAI	polyazoinitiator
PE	polyethylene
PP	polypropylene
PS	polystyrene
s-PE	secondary high density polyethylene
RC	rubber crumb
2,4-TDI	toluilendiisocyanate
TEP	thermoelastoplasts
DMA	dynamic mechanical analysis
DSC	differential scanning calorimetry
SAXS	small-angle X-ray scattering
T_g	glass transition temperature, K
$\sigma_{rupture}$	tensile strength, MPa
ε	relative elongation, %
C_p	heat capacity, J/(g·K)
K_f	effective constant of a photolysis, s^{-1}

1. Introduction

Block copolymers represent the specific class of the polymers whose main chains consist of two or higher number of sections – blocks, each of them constructed by the correct alternation of certain units *[Noshey and McGrath, 1980]*. Block copolymers (BCPs) are excellent materials that can form a variety of self-assembled structures. They are polymer chains consisting of blocks with different chemical composition *[Columbia Encyclopedia, 2001-2005]*. Their preference to phase-separation on nanometric scale can lead to distinct physical and chemical properties. A wise choice of components and method of synthesis offers the possibility to tailor the properties of the final block copolymers. Due to their improved characteristics compared to the initial co-monomers, these materials can potentially be less costly substitutes for already existing materials.

Regular block copolymers belong to the family of thermoelastoplastics, in which the phase morphology (and hence, the mechanical properties) depend on the relative contents of the constitutive thermodynamically incompatible chain blocks *[Hamley, 1999; Meier, 1983]*. Thermoelastoplasts (TEP) is a perspective class of polymeric materials whose properties are close to those of normal rubbers, but they are processed just like plastics and can bu submitted to repeated processing *[Abdelhadi et al, 2004; Akchyrin et al., 2004; Jushik et al., 2004; Kyokoet al., 2004; Perevosnik et al., 2004; Schmalz et al., 2003; Yuichi and Akira, 2004]*. Among the important TEP there are the diene-styrene blockcopolymers with rigid polystyrene blocks and elastic polydiene blocks which are divided into phases with properties of corresponding homopolymers *[Judin et al., 1975]*. Thus, polydiene blocks form the continuous elastic phase and connect polystyrene blocks in a single space grid. The temperature interval where block copolymers exhibit high elastic properties depends on the compatibility of blocks and degree of association of rigid blocks *[Estes et al., 1970]*. Due to the phase separation, BCPs are characterized by two glass transition temperatures (T_g) which correspond to glass transition temperatures of the corresponding homopolymers. With the increase of the amount of blocks in a macromolecule of BCPs, the microphase separation becomes complicated, while for an increase of molecular mass and an approximately equal volume fractions of blocks in a macromolecule, the microphase separation increases. The higher the difference between solubility parameters of blocks, the more effective microphase separation *[Schmalz et al., 2003]*. Properties of BCPs are appreciably defined by type of supramolecular structures which are formed therein *[Moiseev, 1985]*. The introduction of polar groups has considerable influence on the formation of supermolecular structures, so studies of synthesis of BCPs based on functionalized oligomers rouse considerable scientific and practical interest.

Currently, block copolymers are used in a wide variety of applications, ranging from compatibilizer for polymeric blends *[Choi et al., 1998; El-Sabbagh, 2003; Lin et al., 2009; Pospiech 2008; Sperling, 1997; Tsitsilianis and Voulgaris, 1997]* to biocompatible and biodegradable materials *[Caillol et al., 2003; Chen and Wang, 2006; Noro et al., 2005; Xiong et al., 2003]*, from nanoporous drug release vehicles *[Cleary, 1993; Kim, 1996; Lavik et al., 2005]* to hi-tech and engineering polymers *[Adhikari et al., 2005; Bratton et al., 2006; Ignatious et al., 1995; Popa et al., 1998; Verdonck et al., 2003; Zhuang et al., 1997]*, templating materials *[Fraser et al., 2000; Thurn-Albrecht et al., 2000; Yokozawa et al., 2002]*, etc. Various polymerization methods are employed to obtain block copolymers: cationic *[Faust and Kennedy, 1987; Takeuchi and Aida, 2000]* and anionic *[Ioanid et al., 2003; Park et al., 2002]* polymerization, chain transfer reaction *[Han et al., 2002]*, ‘‘living’’ radical polymerization *[Gaynor and Matyjaszewski, 1997; Narrainen et al., 2002]*, (mini)emulsion polymerization *[Keoshkerian et al., 2001]*, ATRP *[Lu et al., 2002]*, redox polymerization *[Ozturk and Cakmak, 2007]*, polycondensation *[Kotliar, 1981]* etc.

Development of investigations aiming to create prospective technologies for using and conversion of polymer waste, waste tires and rubber-technical products into new materials is a very important goal from economic, ecological as well as scientific point of view. Carrying out research in the field of development of composite materials based on secondary raw materials opens wide possibilities in the design of technological processes to obtain new materials, for example thermoelastoplasts, highly filled thermoplastic composites and others, using methods of reactive forming, methods of grafting on the surface of matrix components of different functional groups which will provide their characteristics. The earlier investigations showed that commodities made of thermoplastic polymers PE, PP, PS underwent structural-chemical changes under the action of different factors that are tied with processes of thermooxidation *[Gul, 1986; Kirilova and Shulgina, 1988; Mamunya et al., 1990]*. Waste tires represent vulcanized rubber with three dimensional structure. Different methods (physical, chemical) of crushing rubbers until finelly dispersed crumbs gives the chance to utilize waste of rubber technical goods, including tires *[Drozdovskiy, 1992, Mamunya et al., 2005, Shalyganov et al., 2005, Volkov, 2004]*. Thus, characteristics of rubber crumbs essentially differ and depend on the method of crushing and, therefore, influence characteristics of composite materials on their base *[Goncharuk, 1998, Kowalska and Wielgosz, 1996; Kuznetsova et al., 2004, Trofimova et al., 2000]*.

Volume growth of production and consumption of polymeric and elastometric materials causes constant increase and accumulation of their waste resulting during production and process of their conversion, however 85% of polymer waste results during their use *[Bledzki and Sperber, 2003; Myshak and*

Lebedev, 2006]. As regards the rubber products waste, auto tires represent up to 80 % of specific weight compound waste which creates significant problems (ecological, as well as in production aspects) that have not been yet solved. That is why development of scientific investigations on the design of prospective technologies of using and conversion of waste tires into new materials is very important. Today, the main directions of tires waste conversion are obtaining of reclaim and crumb. The perspective method of conversion of waste tires and rubber waste products is their dividing with obtaining disperse vulcanizate (crumbs), which can be used as filler for composite materials which could be applied for production of different goods of technical designation, sport grounds coverings, transport stations, roofing civil buildings.

One important direction to use polymer and rubber waste is the design of composite materials (CM) on their base – thermoplastic elastometric materials *[Myshak et al., 2002, Vol'fson, 2000, Trofimova et al., 2003]*. They represent by themselves thermoplastic matrices in which rubber particles with different dispersion can be included up to 80%. Rubberplasts, by their structural constitution and characteristics, refer to disperse-filled polymer composites and can be processed by methods typical for conversion of thermoplastic polymers *[Myshak et al., 2004]*.

2. Synthesis and properties block copolymers and composite polymeric materials

2.1 Synthesis and properties of block copolymers on the base of oligomeric azo- and polyazoinitiators

Until now, the largest by far part of block copolymers (BCPs) has been produced by living polymerization of anionically reactive monomers which enabled a narrow molar mass distribution *[Maeda, 2009]*. The alternative method of BCPs synthesis by chain-radical polymerization using oligomeric thermo- or photoinitiators has not been considered feasible in the view of its low selectivity (hence, lower probability of block structure formation). However, a possible remedy to this deficiency may be the use of an oligomeric compound (macroazoinitiator MAI*) [Alli et al., 2006; Eroglu et al., 1998; Furukawa et al., 1967; Hazer, 1995; Nagamune et al., 1996; Simionescu et al., 1997; Ueda et al., 1989, 1992, 1996; Ueda and Nagai, 1994; Walz et al., 1977; Walz and Heitz, 1978; Yagci and Denizligil, 1991; Yildiz and Cape, 2000; Yildiz and Hazer, 2003]*. This method seems more versatile, in so far as not only a well-characterized MAI block is directly incorporated into the BCP chain, but the companion blocks can be prepared by different routes (i.e., either polymerization or polycondensation). Moreover, this would offer an opportunity to realize in full all the attractive features of a radical polymerization e.g. (i) a considerably lower sensitivity to reaction conditions, (ii) a possibility of synthesis in aqueous media and (iii) much wider choice of monomers, including those which can produce macroradicals only under the action of free radicals, such as vinyl chloride and/or vinyl acetate, etc. A polyazoinitiator (PAI) can be defined as a polymer or an oligomer with reactive azo-groups attached to the chain, which can easily split thermally to produce radicals for polymerization initiation of a monomer to form another block of a block copolymers. In our previous papers *[Busko et al., 1993, 1996a, 1996b; Busko, 2001]*, oligomeric PAI synthesized from a macro-diisocyanate (oligomer) and azo-compounds with end functional groups were used for both thermal- and photo-initiation of vinyl monomers polymerization. The latter method of reaction initiation turned out to be preferable due to the easier control of both the initiation rate (by changing the light intensity) and the growth rate and chain length of the second block (by changing the temperature). This contribution is devoted to the investigation of synthesis and characterization of block copolymers obtained on the base of oligomeric azo- and polyazoinitiators by photo- and thermoinitiated radical polymerization.

2.1.1 Synthesis of oligomeric azo- and polyazoinitiators

Oligomeric azo- and polyazoinitiators were synthesized from the macrodiisocyanate of butadiene-isoprene rubber (MDIBIR; mass ratio:80/20; molar mass: 4500±200; NCO content: 1.9%, and azo-bis-isobutyrohydrazone of cyclohexanone (AGN-CH) (melting point 116-118°C, 7.2% of azo-nitrogen, gas number 57.4 ml/g) *[Gritsenko et al., 1990]* at different molar ratio, as previously described *[Busko et al., 1993, 1996a]*.

At the molar ratio MDIBIR/AGN-CH = 1/2, the structure of oligomeric azoinitiators (OAI) can be represented as RXR and at molar ratio MDIBIR/AGN-CH = 1/1 the structure of oligomeric polyazoinitiators (PAI) can be represented as – $(RX)_nR$, where R is a butadiene-isoprene rubber block, and X is the initiator block shown below:

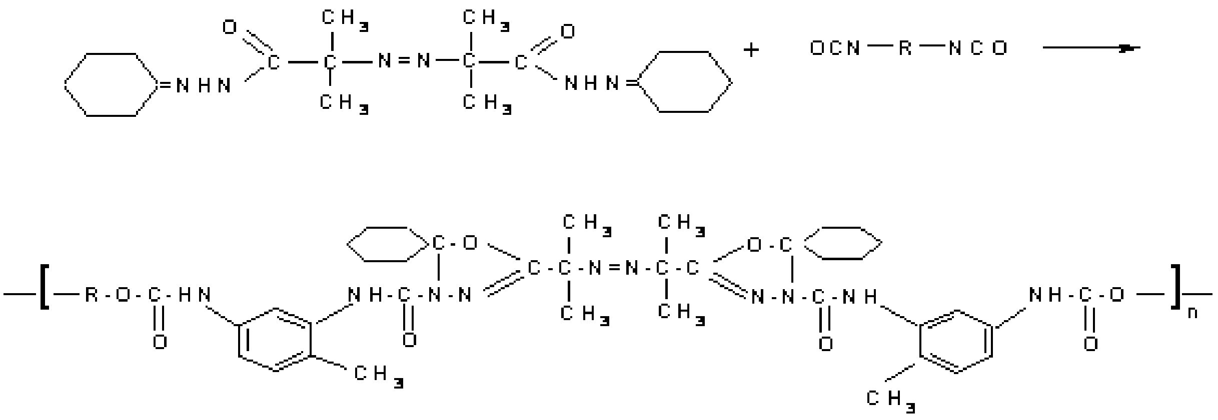

where R is a butadiene-isoprene rubber block

The oxadiazolinilcarbamate cycles are obtained by the interaction of acylhydrazone groups with isocyanate groups *[Kochetov et al., 1991]*. Their structures were confirmed by UV-spectra (Figure 1)·and IR-spectra (Figure 2). Infrared spectra (IR) were obtained from TENSOR-37 spectrophotometer (Bruker Optics) at room temperature using the KBr pellet technique. Molecular weight of olygomeric initiators was determined by the method of measurement of heat effects of condensation (MHEC) *[Bechly et al., l976]*

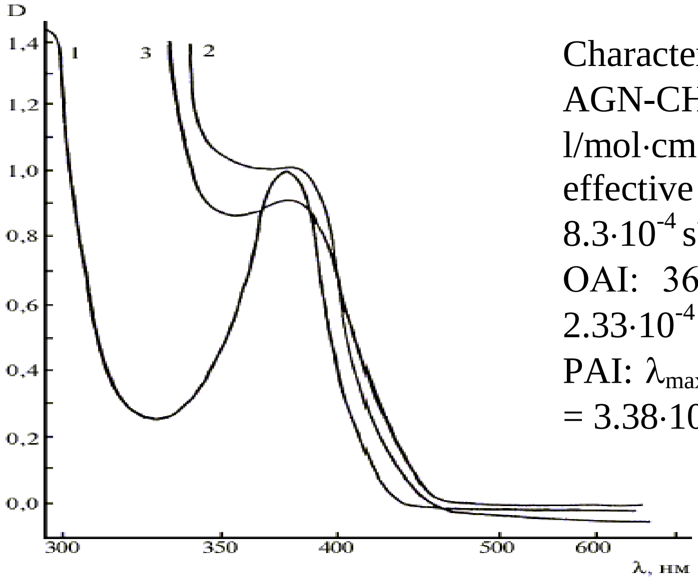

Characteristics of potoinitiators:

AGN-CH: λ_{max} = 371 nm, ε= 51 l/mol·cm;

effective constant of a photolysis (K_f) = $8.3{\cdot}10^{-4}$ s^{-1}

OAI: 369 nm, ε= 14 l/mol·cm; K_f = $2.33{\cdot}10^{-4}$ s^{-1}

PAI: λ_{max} = 370 nm, ε = 16 l/mol·cm, K_f = $3.38{\cdot}10^{-4}$ s^{-1}

Figure 1. UV-spectra of AGN-CH (1), PAI (2), OAI (3)

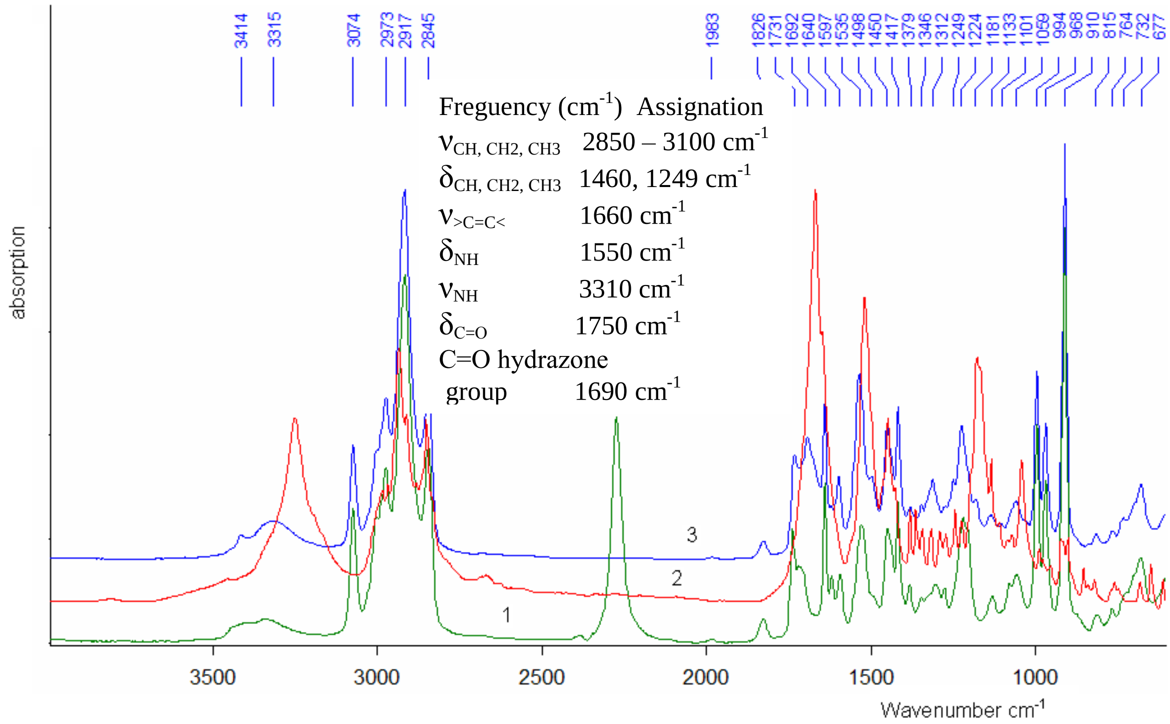

Freguency (cm^{-1})	Assignation
$\nu_{CH, CH2, CH3}$	2850 – 3100 cm^{-1}
$\delta_{CH, CH2, CH3}$	1460, 1249 cm^{-1}
$\nu_{>C=C<}$	1660 cm^{-1}
δ_{NH}	1550 cm^{-1}
ν_{NH}	3310 cm^{-1}
$\delta_{C=O}$	1750 cm^{-1}
C=O hydrazone group	1690 cm^{-1}

Figure 2. IR spectra of MDIBIR (1), AGN-CH (2), PAI (3)

The high pressure mercury lamp DRT-1000 has been used for the investigation of initiator photolysis under the following conditions: 298 K, distance h = 0.2 m, cell width l = 0.01 m.

2.1.2 Synthesis and properties of block copolymers on the base of oligomeric azoinitiators

Based on the synthesized oligomeric azoinitiator OAI and styrene block copolymers of the type ABA (A – butadiene-isoprene rubber block, B – oligostyrene block) with the constant oligodiene block length and various oligostyrene (OSt) one have been synthesized by photo- and thermoinitiated radical polymerization. The BCPs were obtained at molar ratio OAI/St = 1/143, 1/200, 1/400 under the following conditions: 298 K, distance h = 0.2 m, cell width l = 0.01 m. The high pressure mercury lamp DRT-1000 that has been used for the synthesis of block copolymers has a linear emission spectrum and the band of emission spectrum of 365 nm coincides with maximum absorbance of initiator. For comparison, one sample was also synthesized by thermally-initiated radical polymerization at molar ratio PAI/BMA = 1/400. The synthesis was performed in a metallic reactor at 95^0C for 12 h. The synthesized BCPs were precipitated in methanol, then filtered and dried under vacuum.

In accordance with the general scheme of styrene polymerization:

$$I \rightarrow N_2 + 2fR\bullet + (1\text{-}f)RR\ ,$$

$$R + nM \rightarrow R\text{-}M_n\bullet,$$

$$R\text{-}M_n\bullet + R\text{-}M_m\bullet \rightarrow R\text{-}M_{n+m}\text{-}R$$

BCP of ABA type has to be obtained, where A – isoprene-butadiene block, B – block of oligostyrene, because styrene is breaking by recombination, while breakage by disproportioning is practically absent in its case. However, at the initiation stage, the probability of exiting primary radicals from "cell" and initiation of styrene polymerization by them is f<1. For the majority of azoinitiators this value is 0.7 *[Bagdasaryan, 1966]*, hence, about 30% of the initiator should be consumed in the formation of a type AA product, not containing styrene block.

In order to determine the weight ratio of oligostyrene and oligodiene blocks in block copolymers, spectra have been analyzed of accurately described oligostyrene (m. m. 8000), oligomer azoinitiator, model block copolymer, on the basis of butadiene-isoprene rubber and oligomer styrene, and the compound of same homopolymers. In result, as analytical, two absorption bands have been selected: 1500 cm^{-1} (oscillation of monosubstituted benzene ring), related to oligostyrene, and 1550 cm^{-1} (deformation oscillation of bond NH), related to oligomer initiators. As it has been established that spectra of model block copolymer and compound of homopolymers are identical, calibration dependency between the relation of intensity of bands of 1500 cm^{-1} and 1550

cm^{-1} and given concentration of macroinitiator and oligostyrene has been constructed. By means of the calibration graph, weight ratios of oligostyrene and oligodiene blocks in block copolymers (Table 1) were defined.

Research of molecular-mass characteristics of the obtained BCPs (Table 1) by the method of exclusion chromatography (DuPont 8000, eluent: chloroform) has shown that in the course of polymerization three products are formed: block copolymer ABA, recombination product of oligomer rubber (AA) and oligomer of styrene. Peaks of rubber and oligostyrene were identified on the time of exit of individual substances. For obtaining of the calibration curve of dependency of time of keeping from molecular mass at determination of MMP of synthesized block copolymers model three-block copolymer of ABA structure has been synthesized. Macrodiisocyanate on the basis of butadiene-isoprene rubber (MM = 4500 ± 200) and oligostyrenedihydrazide (OSDG, MM = 8000 ± 200) have been used for synthesis. The solution of oligostyrene (OSt) was added to macrodiisocyanate BIR under careful mixing at molar ratio OSt:MDIBUR=1:2. At the expense of reaction between isocyanate groups BIR and end hydrazone groups of oligostyrene, a three-block copolymer with accurately described blocks was formed.

Table 1. Molar mass characteristics of BCPs[#] of the type ABA

OAI/styrene (molar ratio)	**$\langle M_n \rangle$**	**$\langle M_w \rangle$**	**$\langle M_z \rangle$**	**$\langle M_z \rangle / \langle M_n \rangle$**	**$\langle M_z \rangle / \langle M_w \rangle$**	**A*/B** ratio**
Photopolymerization						
1/143	8716	14441	22377	1.6568	1.5496	45/23
1/200	11168	24349	41471	2.1801	1.7032	45/61
1/400	12042	29102	63414	2.4165	2.1790	45/170
1/400***	62522	101266	109909	1.0945	1.0853	
Thermopolymerization						
1/400	16560	35846	58524	2.4235	1.7261	45/240
1/400***	76560	104735	147363	1.3680	1.4070	

[#] $\langle M_n \rangle$, $\langle M_w \rangle$ and $\langle M_z \rangle$ are the number average, weight average, and Z-average molar masses

*rubber; ** - oligostyrene; *** values in parenthesis were obtained from the integral areas under the first peaks on the chromatograms

The measurement of molecular-mass characteristics of new products by method of exclusive chromatography has shown that in the course of polymerization block copolymers ABA were formed with admixture of recombination product of oligomer rubber (AA) and oligomer of styrene.

Relaxation transitions in the soft (rubber) and hard (oligostyrene) blocks of new synthesized block-copolymers were investigated by the DSC method.

The specific heat capacity (C_p) of the samples in the temperature range of 133-433 K were measured by a differential calorimeter with diathermic shells (DSC-d) *[Godovsky, 1977; Privalko et al., 2000]* at a heating rate of 2 K/min after sudden quenching of the samples in liquid nitrogen. Experimental data for heat capacity are summarized in Table 2, and thermograms corresponding to block copolymers of the type ABA model BCPs are presented in Figure 3. For comparing relaxation transitions, the original butadiene-isoprene rubber with isocyanate end groups blocked by methanol to prevent side reactions (BIRUR), oligostyrene (OSt) with hydrazide end groups (molecular weight 8000) and model three-block copolymer were investigated.

Table 2. Thermodynamic characteristics of block copolymers of the type ABA

Samples	**$T_{g,1}$ K**	**$\Delta C_{p,1}$ J/(g·K)**	**$T_{g,2}$ K**	**$\Delta C_{p,2}$ J/(g·K)**
OSt	-	-	332	0.27
BIRUR	193	0.43	-	-
mechanical mixture (2BIRUR + OSt)	194	0.34	345	0.08
model BCP	191	0.38	347	0.17
BCPs: OAI/styrene (molar ratio)				
Photopolymerization				
1/143*	191	0.45	-	-
1/200	197	0.28	351	0.15
1/400	200	0.14	353	0.12
Thermopolymerization				
1/400*	193	0.19	343	0.13
*Additional jumps of heat capacity are observed: 1/143 - ΔC_p = 0.5 J/(g·K) at T_g = 228 K; 1/400 (thermo) - ΔC_p = 0.06 J/(g·K) at T_g = 243 K				

The curve of dependency of heat capacity from temperature for original BIRUR shows jump of $\Delta C_{p,1}$ = 0.43 J/(g·K) with glass transition at $T_{g,1}$ = 193 K and small peak of endothermic transition at the region $T_{m,1}$ = 280 K, then the speed of linear growth of C_p with temperature decreases (Fig. 3) Magnitude of $T_{g,1}$ for BIRUR reaches to assumed before value for copolymer cis-polybutadiene (ΔC_p = 0.61 J/(g·K), T_g = 165 K *[Privalko, 1984]*, cis-isoprene (ΔC_p = 0.46 J/(g·K), T_g = 196 *K* *[Dainton et al., 1962; Wunderlich and Jones, 1969]*; in the meantime, magnitude of ΔC_p slightly decrease that could be explained by the presence of a network of hydrogen bonds with participation of urethane end groups.

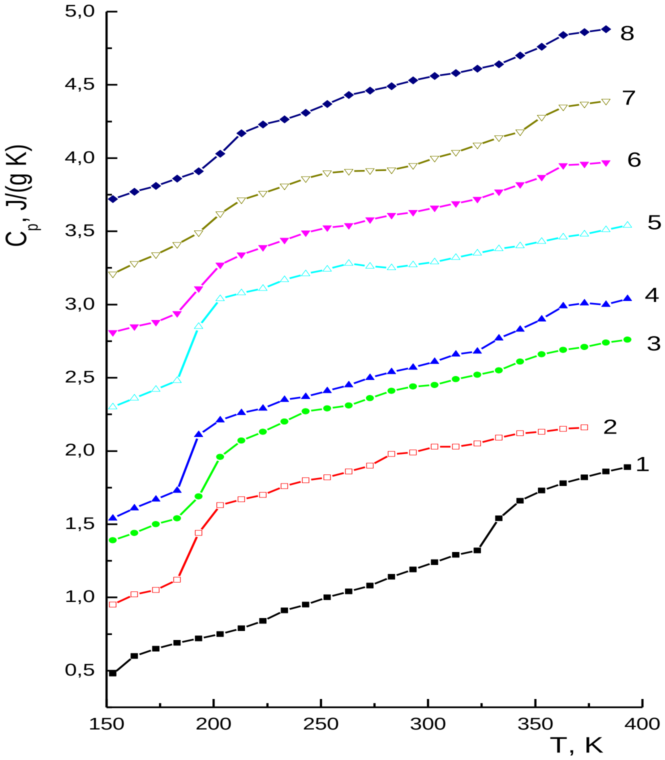

Figure 3. Temperature dependences of heat capacity OSt (1), BIRUR (2), mixture (2BIRUR + OSt) (3), model BCP (4), BCP ABA at molar ratio OAI/St = 1/143 (5), 1/200 (6), 1/400 (7), 1/400 thermo (8). Beginning at curve 3, all the subsequent ones are displaced relative to the ordinate axe 0.5

The endothermic transition that has been found in our experiments could be explained by melting of microregions of local quasi-crystalline order of butadiene blocks BIRUR chain, taking into consideration that crystalline part of cis-1,4-polybutadiene melts at T_m = 280 K *[Fedors, 1979]*.

The curve of heat capacity of olygostyrene (molecular weight 8000) (Fig. 3) has a slight break at 200 r and jump $\Delta C_{p,2}$ = 0.27 J/(g·K) at glass transition $T_{g,1}$ = 332 K. The decrease of $T_{g,2}$ for OSt comparatively with assumed one (T_g= 350 K *[Privalko, 1984]*) could be due to the excess porosity of molecular packing (in other words, due to the presence of excess free volume) of bulk end groups of the chain.

As it has been considered, the heat capacity curve of mixture BIRUR/OSt/BIRUR showed jumps of heat capacity at glass temperature of BIRUR ($T_{g,1}$ = 194 K) and OSt ($T_{g,2}$ = 345 K) and weak break near 280 K. “Partial” magnitudes of $\Delta C_{p,1}$ and $\Delta C_{p,2}$ respect approximately the components composition in the mixture, however if $T_{g,1}$ for mixture is the same as for T_g for individual BIRUR, then $T_{g,2}$ for mixture increases by 15 K comparatively with the individual one for OSt.

Curves of heat capacity for mixture (2BIRUR + OSt) and for model BCP ABA with the same composition are qualitatively the same. However, for the last one T_m = 280 K, and jump $\Delta C_{p,2}$ is twice. These data mean that long central block of styrene in BCP restricts formation of microregions based on butadiene fragments of BIR.

The above discussed experimental data could be analyzed as follows. Presence of two jumps of heat capacity for glass transitions of BIRUR and OSt in the mixture and the model BCP ABA is a feature of the thermodynamic incompatibility. Invariance of glass transition of BIRUR's parameters versus composition is the native result of fact that BIRUR presented in the all samples as the continuous phase with undisturbed structure. Additionally, an increase of glass transition temperature of oligostyrene in the mixture and in model BCP ABA, where OSt is assumable present as isolated impurities ("domains"), until "normal" value of $T_{g,2}$ = 350 K could be explained due to the disappearance of excess free volume as a result of either physical (in the mixture) or chemical (in the copolymer) interactions between end groups of OSt and functional groups of BIRUR.

Temperature curve of heat capacity of BCP 1/143 has jumps of $\Delta C_{p,1}$ = 0.45 J/(g·K) at $T_{g,1}$ = 191 K and $\Delta C_{p,2}$ = 0.05 J/(g·K) at $T_{g,2}$ = 228 K, plateau with C_p=const in the range of 250 – 280 K with following rise of heat capacity. Due to low value of $T_{g,2}$ and $\Delta C_{p,2}$ in the discussed BCP, the presence of styrene blocks is not significant; in other words, the short central sequences of styrene blocks serve as chain extenders for BIR fragments in BCP.

Decrease of $\Delta C_{p,1}$ with simultaneous increase of $T_{g,1}$, as well as an increase of glass transition of styrene blocks till $T_{g,2}$ = 351 K, as well as an increase of corresponding jumps of $\Delta C_{p,2}$ for BCP 1/200, 1/400, reflects a relative increase of concentration (i.e. actually molecular weight) of central styrene blocks in the chain.

It should be noted that in the temperature range between $T_{g,1}$ and $T_{g,2}$ all BCPs present the changing of the character of C_p dependence, namely either there is some break in the range of 240 – 250 K (for BCP 1/200) or dependence reaches the plateau in the range of 250 – 280 K (for BCP 1/143 and BCP 1/400). Considering the qualitative of heat capacity curves for BCP and original BIRUR in the above mentioned temperature range, it is possible to assume that the anomaly could be connected with thermal dissociation of ordered microregions of butadiene blocks from BCP chain. Due to absence of the above anomaly in the model BCP ABA, the molecular weight of styrene blocks in the BCP is not big enough (at least, less then 8000) to suppress the butadiene blocks ability to get ordered.

Finally, it should be noted that the complete identity of heat capacity curves for samples BCP 1/400 that have been obtained by both photo- and thermal polymerization, in the whole investigated range of temperatures with the exception of interval 250 – 280 K.

Thus, the possibility of synthesis of oligomeric azoinitiator based on azo-bis-isobutyrohydrazone of cyclohexanone and butadiene-isoprene rubber, using an initiator to form BCPs by photoinitiated radical polymerization, has been shown. The obtained BCPs have two distinct glass transitions in the whole range of compositions, that evidences the incompatibility of blocks and their separation into microregions.

To increase the output of block copolymers and decrease the quantity of admixture of recombination product of oligomer rubber, in the future for the synthesis of block copolymers by method of photoinitiated radical polymerization, a polyazoinitiator PAI has been used.

2.1.3 Synthesis and properties of block copolymers on the base of oligomeric polyazoinitiators

In so far, as PAI formation through the reaction between the isocyanate groups of BIR and the hydrazone groups of AGN-CH proceeds independently of the photo-initiated polymerization of styrene *[Busko et al., 1996a, 1996b]*, it was possible to prepare two series of polyblock BCPs of type $(AB)_n$ (where A is PAI, and B is the styrene block). The sequential one (series A) was obtained by the synthesis of PAI in the first step, and by subsequent radical polymerization of styrene photo-initiated by PAI, while both reactions were carried out in a single step to prepare the simultaneous one (series B). For comparison, one sample of series B was also synthesized by thermally-initiated radical polymerization.

As proved by exclusion chromatography (DuPont 8000, eluent: chloroform), for both BCP series, the major part of the reaction products was $(AB)_n$, with traces of the recombination product of oligomeric rubber and styrene oligomer. The molar masses of $(AB)_n$ (Table 3) were calculated from the chromatograms using for calibration the model BCP prepared from macro-diisocyanate of BIR and oligostyrene dihydrazide (OSDH; molar mass: 8000 ± 200). The mass ratio A/B of constituent blocks in the BCPs was estimated by IR spectroscopy *[Busko, 2001]* (maximum error of the order of 10%). For calibration, the IR spectra of 5.5 % carbon tetrachloride solutions of the PAI, of the OSDH and of their mixtures were recorded, and the intensity ratios of absorption bands at 1500 cm^{-1} (stretching vibrations of a monosubstituted benzene ring) and at 1550 cm^{-1} (bending vibrations of the NH bond) were plotted as a function of the PAI/OSDH ratio.

In view of the high initiating activity of AGN-CH, it could be expected that the initiation rates of OSt polymerization would be higher (hence, the molar masses of OSt blocks would be lower) in samples of series B; however, the molar mass characteristics of the BCP of both series turned out to be little affected by the method of synthesis (Table 3). In a striking contrast to other samples of series B, the thermally-polymerized sample 5 of series B consisted, predominantly, of uninterrupted OSt blocks (Table 3).

Table 3. Molar mass characteristics of BCPs*# of the type $(AB)_n$

No	**PAI/St (molar ratio)**	$\langle M_n \rangle$	$\langle M_w \rangle$	$\langle M_z \rangle$	$\langle M_z \rangle / \langle M_n \rangle$	$\langle M_z \rangle / \langle M_w \rangle$	**A/B ratio**
Series A							
1	1/143	12050 (23700)	24700 (37650)	38040 (41430)	2.05 (1.11)	1.54 (1.10)	45/41
2	1/200	12600 (27100)	21900 (29700)	30840 (32410)	1.74 (1,10)	1.41 (1.10)	45/49
3	1/400	10000 (31660)	27330 (35790)	38060 (39760)	2.73 (1.13)	1.39 (1.11)	45/82
Series B							
1	1/143	14120 (26020)	26130 (28730)	46270 (31465)	1.85 (1.10)	1.77 (1,09)	45/42
2	1/200	15870 (27630)	43280 (42610)	89820 (82480)	2.73 (1.54)	2.08 (1.09)	45/49
3	1/300	16095 (37600)	45490 (46010)	78490 (80630)	2.56 (1.22)	1.58 (1.20)	45/58
4	1/400	12845 (36910)	30360 (73690)	80980 (138300)	2.36 (2.01)	2.67 (1.67)	45/88
5	1/400 (thermo)	16380 (119400)	41590 (164900)	149185 (208500)	2.54 (1.38)	3.58 (1.26)	45/498

* values in parenthesis were obtained from the integral areas under the first peaks on the chromatograms

[#] $\langle M_n \rangle$, $\langle M_w \rangle$ and $\langle M_z \rangle$ are the number average, weight average, and Z-average molar masses

Because the molar mass characteristics of the styrene-diene BCPs *[Busko et al., 2004, 2010]* of the type $(AB)_n$ of both series turned out to be little affected by the method of synthesis the acrylate-diene BCPs have been synthesized in the first step. Based on the synthesized polyazoinitiator and butylmethacrylate block copolymers of the type $(AB)_n$ (A – butadiene-isoprene rubber block, B – oligobutylmethacrylate block) with the constant oligodiene block length and divers oligobutylmethacrylate (OBMA) one have been synthesized by thermo- and photoinitiated radical polymerization. The structure of the BCPs are shown below:

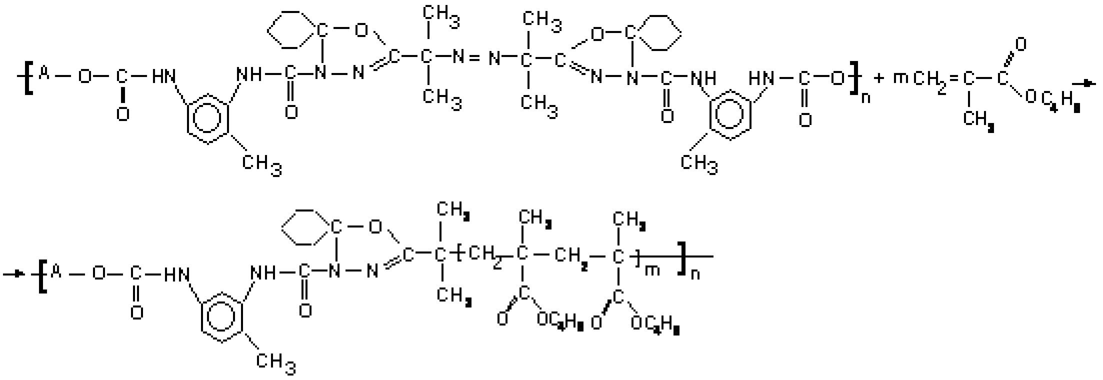

where A is a butadiene-isoprene rubber block.

The BCP was obtained by the synthesis of PAI in the first step, and by subsequent radical polymerization of butylmethacrylate photo-initiated by PAI at molar ratio PAI/BMA = 1/143, 1/200, 1/300, 1/400 at room temperature during 3 h. The high pressure mercury lamp DRT-1000 has been used for the synthesis of block copolymers under the following conditions: 298 K, distance h = 0.2 m, cell width l = 0.01 m. For comparison, one sample was also synthesized by thermally-initiated radical polymerization at molar ratio PAI/BMA = 1/400. The synthesis was performed in a metallic reactor at 95°C during 12 h. The synthesized BCPs were precipitated in methanol, then filtered and dried under vacuum.

The structure of the new block copolymers was investigated by the means of IR- spectroscopy. Typical diene rubber bands are identified in the range 900–1000 cm^{-1} as follows: absorption peak at 998 cm^{-1} corresponds to off-frequency vibrations of CH in CH=CH groups, band at 967 cm^{-1} is due to off-frequency vibrations of CH in trans-CH=CH– moieties, band at 910 cm^{-1} is determined by off-frequency vibrations of CH_2 in $–CH_2=CH–$ groups. The deformation vibration for $=CH_2$, which usually appears under 1465 cm^{-1}, is displaced at 1450 cm^{-1} due to the influence of the double bond. The band at 1410 cm^{-1} concerns groups $=CH_2$. The bands in the interval 2800–2950 cm^{-1} can be attributed to asymmetric and symmetric $–CH_2$ groups. The group $–CH_3$ shows two bands: one at 1375 cm^{-1} due to symmetrical deformation vibration of $–CH_3$ groups and another at 1460 cm^{-1} determined by asymmetric deformation vibrations of $–CH_3$ groups. The intensities of band at 1390 cm^{-1} concerns deformation vibration of butyl radical, which relates to OBMA. The deformation vibration for urethane NH groups are a little displaced due to the presence of urethane NH in the range 3090–3300 cm^{-1}. The stretching vibration of NH-bond is exhibit at 1550 cm^{-1}. At 1680– 1760 cm^{-1} both block copolymers exhibit stretching vibrations of C=O groups. Bands at 1000–1200 cm^{-1} can be attributed to stretching vibrations of C–O–C moieties *[Kuptsov and Zhizhin, 2001; Silverstein et al., 1974; Vera et al., 2004]*.

For determination of the weight ratio of rubber and oligobutylmethacrylate blocks and investigation on the thermal behavior of the acrylate-diene BCPs, block copolymers OBMA with hydrazone end groups and model BCPs have been synthesized. Oligomer BMA (OBMA) with hydrazone end groups (OBMADH) was prepared by method of the thermoinitiated radical polymerization in the presence of the initiator an azo-*bis*- isobutyrohydrazone of cyclohexanone at 95°C during 8 h. Its molecular weight determined by size exclusion chromatography (DuPont 8000, eluent: chloroform) was equal to 41100 g/mol. Model BCPs were synthesized by the reaction of OBMA with hydrazone end groups and macro-diisocyanate butadiene-isoprene rubber (MDIR) at molar ratio OBMA/rubber = 1/2, respectively.

The weight ratio of rubber block and oligobutylmethacrylate blocks was calculated from IR-spectroscopy data on preliminary built calibration relationship between the relation on intensities of bands 1390 cm^{-1} (deformation vibration of butyl radical), which relates to OBMA, and 1550 cm^{-1} (stretching vibration of NH-bond), which connects with the oligomeric azoinitiator and given concentration of macroinitiator and OBMA (Table 4).

For synthesized BCP and modeling BCP the resulted viscosity has been calculated for what relative viscosities have been defined at use of Ubbelohde type viscosimeter at temperature 25°C (Table 4).

The specific viscosities were calculated for synthesized and model BCPs which entirely correlate with the data on the weight ratio of blocks in BCP, which was drawn from IR- spectroscopy. This is the evidence of regular OBMA block increasing at increasing quantity of butylmethacrylate under BCP synthesis (Table 4).

Table 4. The specific viscosities and weight relation between rubber and OBMA blocks of BCPs and model BCPs

BCP: PAI/OBMA (molar ratio)	**specific viscosity [η]**	**weight relation rubber/OBMA (IR-spectroscopy)**
1/143	0.70	45/344
1/200	0.76	45/363
1/300	0.91	45/450
1/400	1.19	45/570
1/400 (thermo)	1.43	45/980
OBMADH	0.28	-
model BCPs	0.87	45/410

Thermal behaviour of the new block copolymers was evaluated by differential scanning calorimetry (DSC), with respect to relaxation transitions in the soft (rubber) and the hard (OBMA or OSt) blocks of the type $(AB)_n$. Experimental data for heat capacity and glass transition temperatures are summarized in Table 5, 6 and thermograms corresponding to block copolymers $(AB)_n$ model BCPs are presented in Figure 4, 5.

Table 5. Thermodynamic characteristics of styrene-diene BCP of the type $(AB)_n$

BCP: PAI/styrene (molar ratio)	**$T_{g,1}$, K**	**$\Delta C_{p,1}$, J/(g·K)**	**$T_{g,2}$, K**	**$\Delta C_{p,2}$, J/(g·K)**
Series A				
1/143*	205	0.21	299	0.04
1/200	201	0.17	313	0.04
1/400	207	0.10	340	0.10
Series B				
1/143	207	0.30	305	0.10
1/200	208	0.29	317	0.07
1/300	191	0.27	355	0.09
1/400	193	0.13	357	0.17
1/400 (thermo)	179	0.08	327	0.22
Additional jumps of heat capacity are observed *-ΔC_p=0.04 J/(g·K) at T_g = 247 K				

The glass transition temperature of the rubber component ($T_{g,1}$) (Table 5, 6) and the amorphous phase of the OBMA and OSt ($T_{g,2}$) were determined from the half-height of the corresponding heat capacity jump.

Research of relaxational transitions in styrene-diene BCP of type $(AB)_n$ by method of DSK has shown that the general for thermal capacity curves of both series samples (Figure 4) is presence of jumps of a thermal capacity at glass temperatures of oligodiene and oligostyrene quasiphases (accordingly $T_{g,1}$ and $T_{g,2}$) that is a characteristic sign of phase separation in polymer-polymeric systems.

The major distinctive feature of samples of series A in comparison with samples of series B is some reduction of $T_{g,1}$, and also essentially lower values (by the order of 30-40 %) of the corresponding jump of thermal capacity $\Delta C_{p,1}$, and this effect amplifies as a measure of growth of relation PAI/OSt (Table 5). It is possible to assume that noted features are connected with the raised maintenance in samples of B series recombination products of diene fragments.

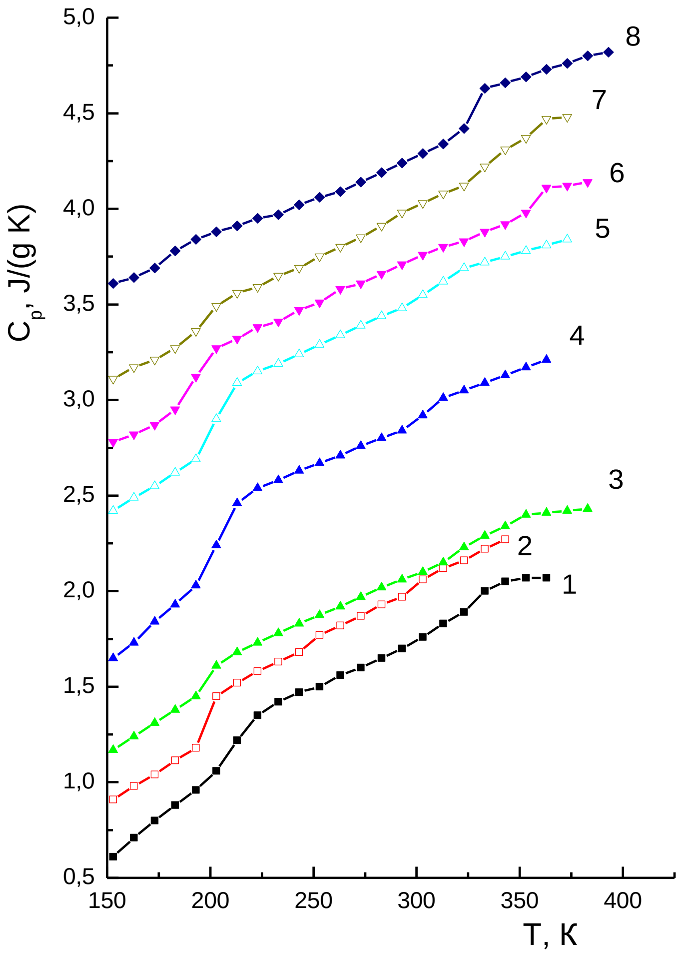

Figure 4. Temperature dependences of heat capacity styrene-diene BCP of the type $(AB)_n$ series A at molar ratio PAI/styrene: 1/143 (1), 1/200 (2), 1/400 (3) and series B of the type at molar ratio PAI/styrene: 1/143 (4), 1/200 (5), 1/300 (6), 1/400 (7), 1/400 thermo (8). Beginning a curve 3, all the subsequent ones are displaced relative to the ordinate axe 0.5

Table 6. Thermodynamic characteristics of acrylate-diene BCP of the type $(AB)_n$

BCP: PAI/ OBMA (molar ratio)	**$T_{g,1}$, K**	**$\Delta C_{p,1}$, J/(g·K)**	**$T_{g,2}$, K**	**$\Delta C_{p,2}$, J/(g·K)**
1/143	213	0.11	308	0.15
1/200	212	0.09	308	0.17
1/300	213	0.08	306	0.18
1/400	211	0.07	303	0.20
1/400 (thermo)	242	0.12	300	0.19
model BCPs	255	0.11	307	0.13
BIRUR	193	0.43	-	-

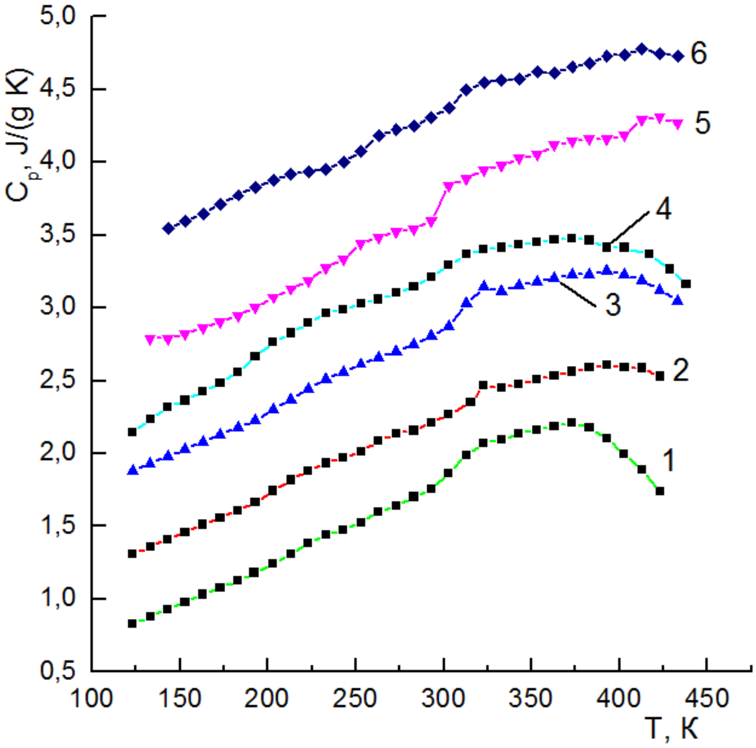

Figure 5. Temperature dependences of heat capacity acrylate-diene BCP of the type $(AB)_n$ at molar ratio PAI/BMA: 1/143 (1), 1/200 (2), 1/300 (3), 1/400 (4), 1/400 (thermo) (5) and model BCPs (6)

The research of relaxation transitions in type block copolymers (AB)n has shown that the heat capacity curves commonly reveal two heat capacity steps (Figure 5) at the glass transition of oligodiene and oligobutylmethacrylate microphases (accordingly $T_{g,1}$ and $T_{g,2}$) which is characteristic of the phase separation in polymer blends.

Insignificant reduction of $\Delta C_{p,1}$ at almost invariable $T_{g,1}$, and also increase of jumps of thermal capacity $\Delta C_{p,2}$ of butylmethacrylate blocks testify about increase in the relative maintenance of butylmethacrylate blocks in the chain.

Acrylate-diene BCPs of the type $(AB)_n$ were studied by the method dynamic mechanical analysis (DMA) using a relaxometer with forced sinusoidal oscillations at a frequency of 100 Hz. Both, the dynamic elastic modulus E′ and the loss modulus E″ were measured in the temperature range from 170 to 350 K, and at heating rate of 2 K/min *[Rosovitsky and Shifrin, 1981; Privalko et al., 1993]*. The glass transition temperature (T_g) was determined as the position of the maximum of log E″ (Table 7, 8). The block copolymers obtained are twophase polymer systems for all compositions, as it is indicated by the existence of two relaxation maxima (Figure 6). This result is due to the blocks immiscibility and their phase separation into micro-domains.

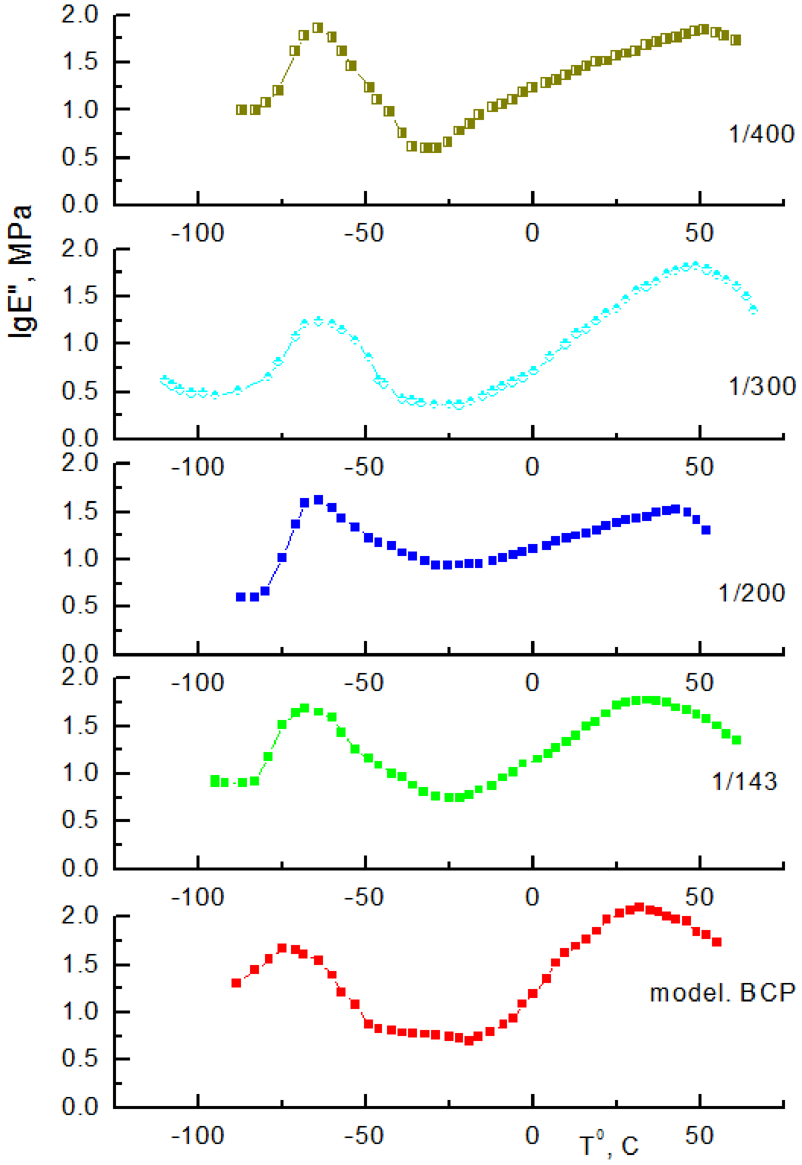

Figure 6. Temperature dependence of the loss modulus E'' for acrylate-diene BCPs of the type $(AB)_n$

Table 7. Compositions and viscoelastic parametrs for acrylate-diene BCPs of the type $(AB)_n$

BCP: PAI/OBMA (molar ratio)	**$T_{g,1}$, by lg E'', K**	**$T_{g,2}$, by lg E'', K**	**max lgE''_1, MPa**	**max lgE''_2, MPa**	**lgE', MPa by 188К**
1/143	205	307	1.68	1.77	3.08
1/200	209	316	1.62	1.76	3.06
1/300	205	322	1.69	1.81	3.13
1/400	205	324	1.86	1.85	3.45
model BCPs	198	305	1.67	1.95	3.42

As it can been seen in Table 7, the glass transition temperature of the oligodiene component ($T_{g,1}$) practically does not change, but for poly(butyl methacrylate) component both the $T_{g,2}$ and the corresponding value of log E''_{max} increases when the molar concentration of BMA increases in formed block copolymer. At the same time, the value of elastic modulus in glassy state (at 188 K) is increased as well and tends to E' value for model system (Table 7). It is an indication of enhanced intermolecular interaction in the system that can be caused by an increase of the amount of OBMA block *[Busko, 2010]*.

Styrene-diene BCPs of the type $(AB)_n$ of both series were studied by the method DMA and Small-angle X-ray scattering (SAXS). SAXS data were obtained with the Kratky camera (KRM-type diffractometer). The primary beam intensity was controlled with a monitoring channel in the scattering angle range 3-5 deg (2θ). Copper K_α radiation and nickel filtering of the primary beam were used. Recording of the scattering radiation with a scintillation counter and digital conversion were performed using the step-by-step scanning regime. The geometrical parameters of the X-ray beam in the specimen plane and the detector position (30 mm for the length of the homogeneous portion of the X-ray beam, and 290 mm for the specimen-detector distance) were chosen so as to satisfy the conditions of an "infinite" slit collimation *[Lipatov et al., 1982]*.

A common feature of the SAXS patterns for both the BCP series (except the thermally-polymerized sample 1/400 of series B) is the relatively high scattering intensity in the range of the scattering vectors $0.3 < q < 2.0$ nm^{-1} (Figure 7) which is characteristic of heterogeneous, microphase-separated systems. Reasonably sharp SAXS peaks around $q = 0.8$ nm^{-1} for samples of series B (Figure 7b) may be regarded as experimental evidence for a well-ordered, three-dimensional lattice of isolated oligostyrene domains within a continuous rubber matrix. In contrast, the absence of well-defined SAXS peaks in the same range of scattering vectors for samples of series A (Figure 7a) suggests a broad distribution of microheterogeneities by size, which may be tentatively attributed to the existence of two co-continuous, randomly interpenetrated microphases of oligostyrene and rubber blocks. The complete absence of SAXS heterogeneity for sample 1/400 thermo of series B (Figure 7b) can be regarded as evidence of a continuous macroscopic phase of uninterrupted oligostyrene blocks with a few very small, randomly distributed inclusions of rubber blocks *[Busko, 2001]*.

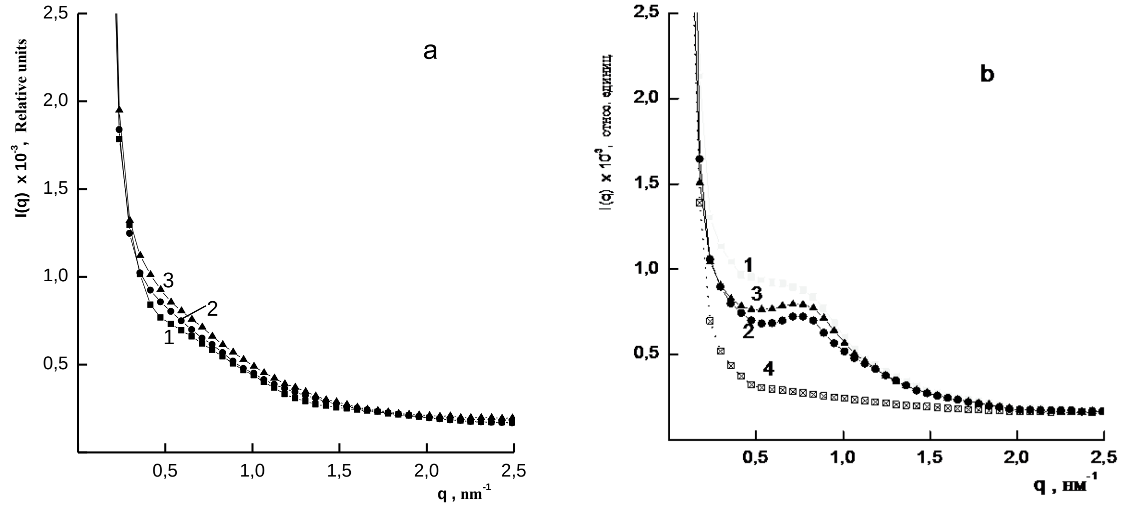

Figure 7. SAXS curves for samples of series A (a) and series B (b). Numbers correspond to the entries in Table 3: 1/143 (1), 1/200 (2), 1/400 (3) in (a), and 1/143 (1), 1/200 (2), 1/400 (3), 1/400 (thermo) (4) in (b)

Similar conclusions can be reached from the analysis of log E' vs. T plots (Figure 8). In fact, the occurrence of distinct E' falls concomitant to the glass-rubber transitions for microphases of each chain component (in the temperature intervals $T_{g,1}$ = –60 (± 15)°C and $T_{g,2}$ = 60 (± 15)°C for rubber and oligostyrene microphases, respectively) for both BCP series is characteristic for microphase-separated systems. Moreover, the precipitous fall in E' by two orders of magnitude around $T_{g,1}$ for samples 1/143 and 1/200 of series B (Figure 8b) is exactly what one would have expected for a continuous soft rubber medium with isolated stiff oligostyrene inclusions. In contrast, a nearly two-fold smaller log E′ drop at $T_{g,1}$ for samples of series A (Figure 8a) is clear evidence of the reinforcement of the continuous rubber microphase by the co-continuous oligostyrene microphase. This conclusion (i.e., absence of, or presence of a co-continuity of both microphases for samples 1/143 and 1/200 of series B, or for all samples of series A, respectively) is consistent with the widely different magnitudes of log E' falls around $T_{g,2}$ (Figure 8).

Apparently, similar morphological implications can be also invoked to explain both the SAXS patterns (Figure 7b) and the log E′ vs. T plots (Figure 8b) for the remaining samples of series B. In particular, the persistence of high values of log E' over the broad temperature interval up to $T_{g,2}$ (with only a small inflection at $T_{g,1}$) for sample 1/400 thermo is consistent with the above morphological evidence for a continuous macroscopic phase of uninterrupted oligostyrene blocks with a few very small, randomly distributed inclusions of rubber blocks.

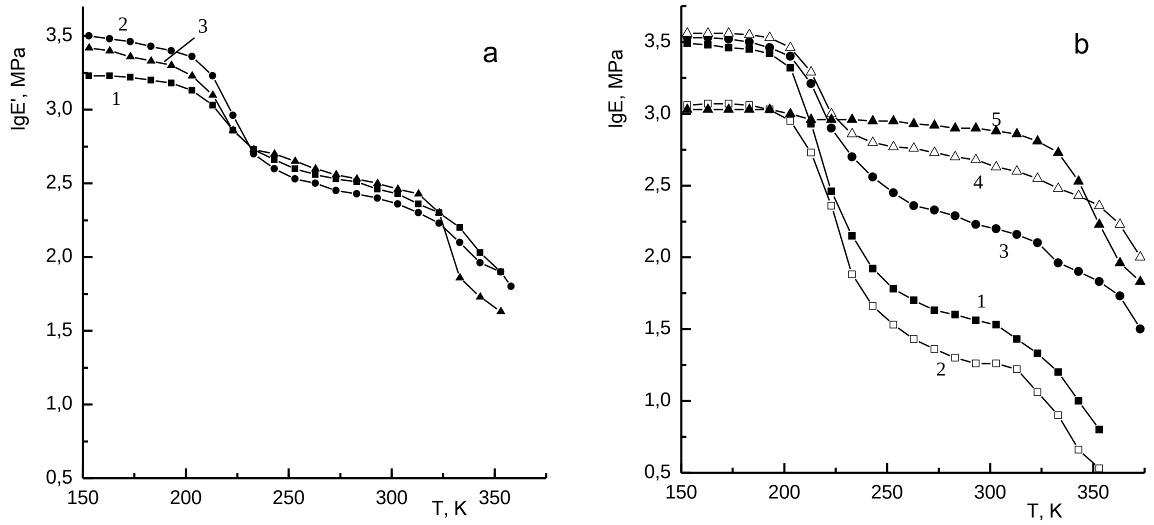

Figure 8. log E' vs. T plots for samples of series A (a) and series B (b). Numbers correspond to the entries in Table 3: 1/143 (1), 1/200 (2), 1/400 (3) in (a), and 1/143 (1), 1/200 (2), 1/300 (3), 1/400 (4), 1/400 (thermo) (5) in (b)

In summary the molar mass characteristics of two BCP series of the (AB)$_n$ type (where A is the oligomeric azo-initiator and B is the styrene block) turned out to be little affected by the method of photo-initiated synthesis (sequential and simultaneous for series A and B, respectively), whereas their morphologies and mechanical behavior in the bulk state were widely different. Reasonably sharp SAXS peaks and distinct log E' falls concomitant to the glass-rubber transitions for microphases of each chain component for samples of series B were regarded as evidence for a well-ordered, three-dimensional lattice of isolated oligostyrene domains within a continuous rubber matrix. In contrast, the absence of well-defined SAXS peaks in the same range of scattering vectors combined with nearly two-fold smaller log E' falls at T$_{g,1}$ for samples of series A suggested the existence of two co-continuous randomly interpenetrated microphases of oligostyrene and rubber blocks, with a broad distribution of microheterogeneities by size.

2.2 Synthesis and properties of block copolymers of polycondensation type

Block copolymers, the last stage of which includes the reaction of polycondensation, are related to so called block copolymers of polycondensation type *[Valetsky and Storojuk, 1979]*.

Practically, any homopolymer of polymerization or polycondensation type can be seen in the view of appropriate oligomer with functional end groups and used in reactions of polycondensation, yielding in block copolymers. Receiving oligomers with condensation able functional end groups by polymerization is much easier and more technologically accessible than by polycondensation of oligomers with polymerization able end groups. Hence, synthesis of the first type oligomers opens wide, practically implementable possibilities of synthesis of block copolymers, containing simultaneously polymer blocks of polymerization and polycondensation type.

Block copolymers of polycondensation type, as well as block copolymers received on the basis of PAI, unlike block copolymers of polymerization type, can contain blocks of very different nature: aliphatic and aromatic, soft and rigid, hydrophilic and hydrophobic, unsaturated and saturated, organic and inorganic, and others.

Majority of block copolymers of polycondensation type represent polyblock BCPs with controllable length of blocks, whereas block copolymers of polymerization type are basically two- and three-block copolymers. Transition to the polyblock structure for the block copolymers in which microphase separation was realized is accompanied by the creation of more perfect and strong physical network at the expenses of formation of larger number of domains, consisting of high-melting blocks, their uniform distribution in volume of copolymer and participation of the same macromolecule in their construction.

Among the various types of block copolymers, polyamide–diene rubber ones are of increasing technical and scientific interest due to their specific properties and wide range of applications *[Hadjichristidis et al., 2002; Hu et al., 2002]*.

For the synthesis of the polyamide–diene BCPs, two different polymers were employed, on the basis of their specific properties *[Busko et al., 2008]*.

2.2.1 Study of polyamide–diene BCPs properties

One of them is an aliphatic copolyamide (coPA) which is a statistic polyamide (type 6/6.6/6.10) with molecular weight M_n=2600±200, low melting point and hot-melt adhesive properties *[Crusos et al., 1983, 1995; Crusos and Zanoaga, 1989; Zanoaga, 2001]*. The other polymer employed in the synthesis of these new block copolymers is a diene rubber with hydroxylic terminal groups having molecular mass M_n =3200±200, OH groups content of 1.0–1.13% and dynamic viscosity of 3.0 Pa·s (measured at 25°C). The main chain of diene rubber is a statistic copolymer consisting of butadiene isomers in various proportions: 1,4-cis (10–15% wt.), 1,4-trans (20–25% wt.) and 1,2-(vinyl) macrodiisocyanate diene rubber (MDIR).

The copolyamide coPA was also characterized by the means of spectroscopy. The IR and 1H NMR spectra are presented in Figures 9 and 10, followed by the corresponding assignation of the signals.

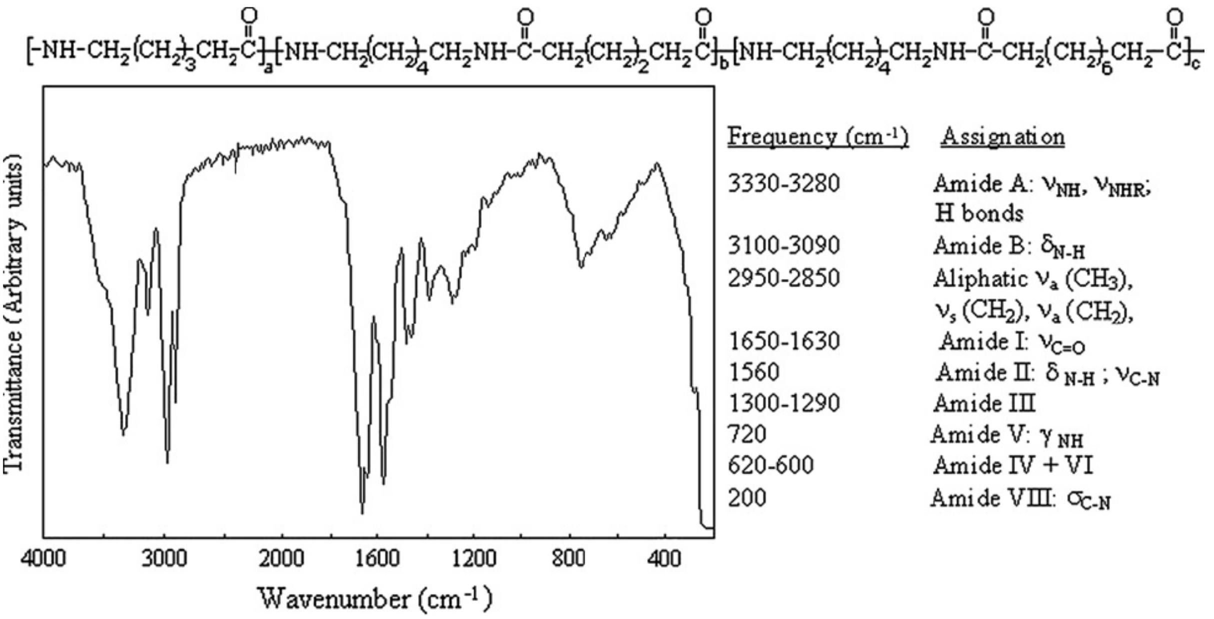

Figure 9. IR spectrum of coPA

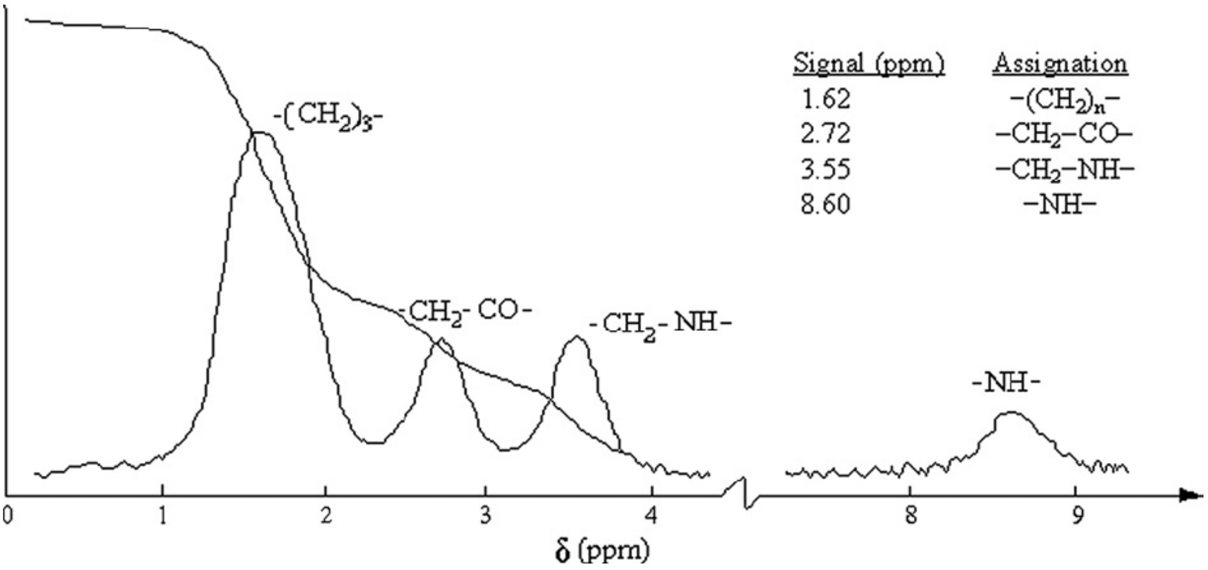

Figure 10. ^{1}H NMR spectrum of coPA

The macrodiisocyanate dienic rubber (MDIR) was obtained by the condensation of a diene rubber having hydroxylic terminal groups with 2,4-toluene diisocyanate (TDI) in a molar ratio rubber:TDI=1:2 *[Saunders and Frisch, 1962]*. The final product, MDIR, has a dynamic viscosity of 14 Pa·s (measured at 70°C) and the concentration of NCO groups in block copolymers is 2.15–2.4%. After purification, the product was characterized through FTIR spectroscopy (Figure 11).

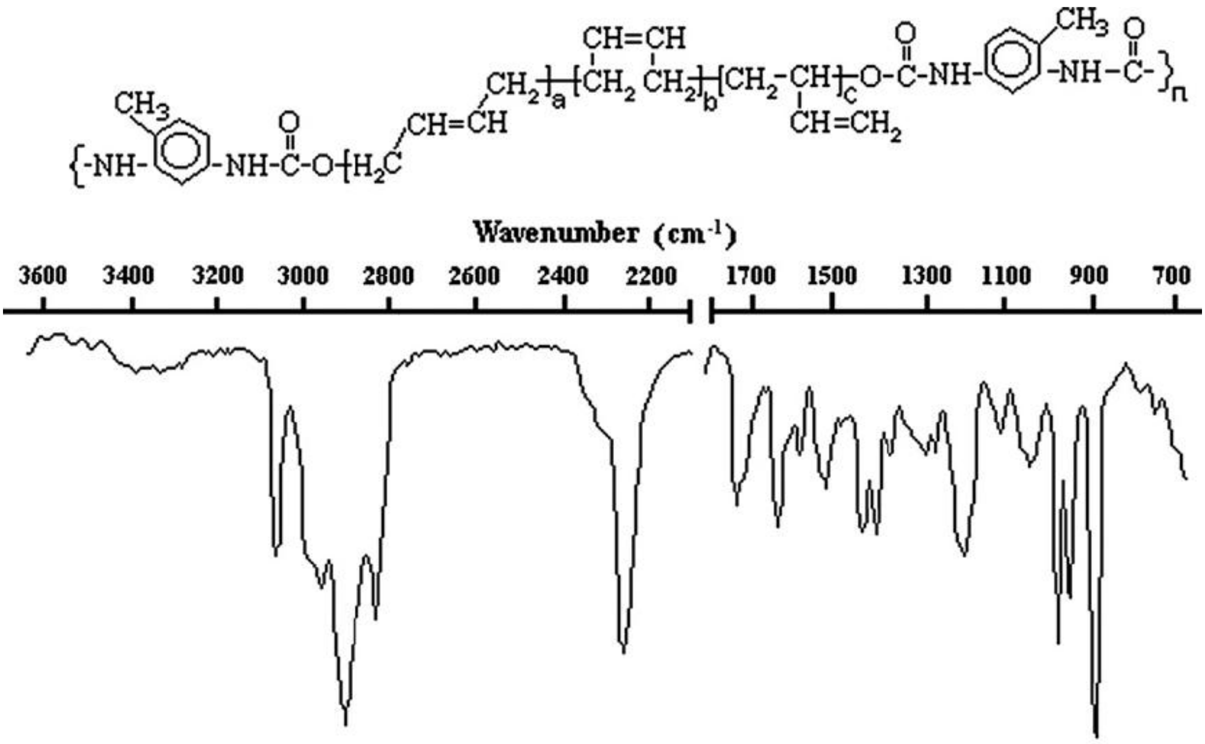

Frequency (cm^{-1})	Assignation
998	CH in CH=CH
967	CH in CH=CH *trans*
910	CH_2 in $CH=CH_2$
2260	-NCO
750-800	aromatic disubstituted

Figure 11. IR spectrum of MDIR

Two types of block copolymers were obtained by using MDIR and coPA in different molar ratios *[Barantsova et al., 2005; Busko et al., 2005, 2008]* as follows:

– when molar ratio MDIR:coPA = 1:1, block copolymers of $(AB)_n$ type were obtained;

– for a molar ratio MDIR:coPA = 1:2, block copolymers of ABA type resulted (A – coPA block, B – rubber block).

Based on their characteristics, blocks A form rigid (hard) segments, while blocks B are the soft ones.

2.2.2 Structural study of polyamide–diene BCPs

The structure of the new block copolymers (Schema 3) was investigated by the means of IR (Figure 12) and ^{1}H NMR (Figures 13 and 14) spectroscopy.

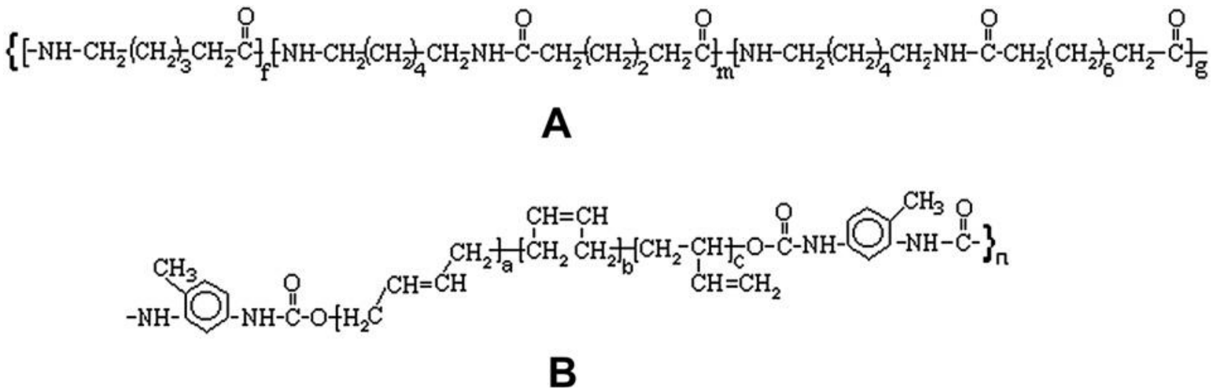

Structure of block copolymers of the type $(AB)_n$: A – copolyamide blocks; B – rubber blocks.

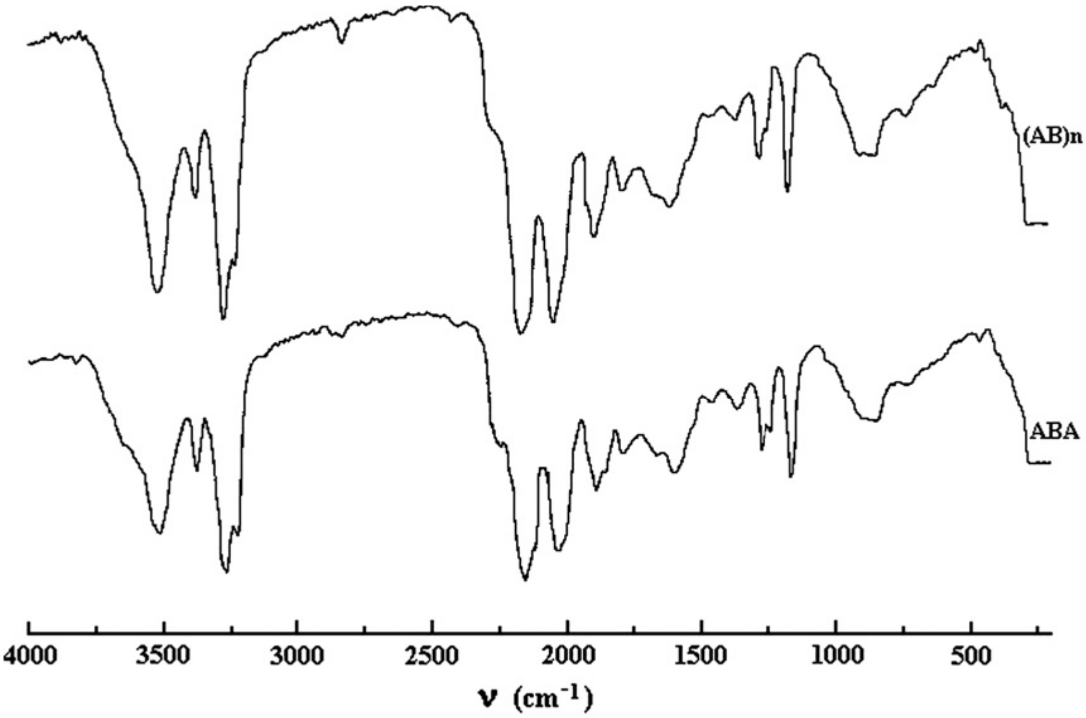

Figure 12. IR spectrum of block copolymers $(AB)_n$ and ABA

Typical amide bands can be observed in the IR spectrum (SPECORD M-80 (Carl Zeiss, Jena) instrument, using 1% w/w polymer/KBr pellets) of block copolymers. Stretching vibrations of NH groups are a little displaced due to the presence of urethanic NH in the range 3090–3300 cm^{-1}. Bands amide I (1630–1650 cm^{-1}) and amide II (1560 cm^{-1}) are not modified, while band amide III (1290–1300 cm^{-1}) shows a redistribution of intensities. Bands amide IV–VI have a lower intensity. Urethane bands are overlapped by amide bands. At 1680–1700 cm^{-1} both block copolymers exhibit stretching vibrations of C=O groups, but with different intensities (peak for $(AB)_n$, small shoulder for ABA). Bands at

1000– 1200 cm^{-1} can be attributed to stretching vibrations of C–O–C moieties *[Kuptsov and Zhizhin, 2001; Silverstein et al., 1974]*.

Typical diene rubber bands are easy to identify in the range 900–1000 cm^{-1} as follows: absorption peak at 998 cm^{-1} corresponds to off-frequency vibrations of CH in CH=CH groups, band at 967 cm^{-1} is due to off-frequency vibrations of CH in trans-CH=CH– moieties, band at 910 cm^{-1} is determined by off-frequency vibrations of CH_2 in $–CH_2=CH–$ groups. The deformation vibration for $=CH_2$, which usually appears under 1465 cm^{-1}, is displaced at 1450 cm^{-1} due to the influence of the double bond. The band at 1410 cm^{-1} concerns groups $=CH_2$. The bands in the interval 2800–2950 cm^{-1} can be attributed to asymmetric and symmetric $–CH_2$ groups. The group $–CH_3$ shows two bands: one at 1375 cm^{-1} due to symmetrical deformation vibration of $–CH_3$ groups and another at 1460 cm^{-1} determined by asymmetric deformation vibrations of $–CH_3$ groups.

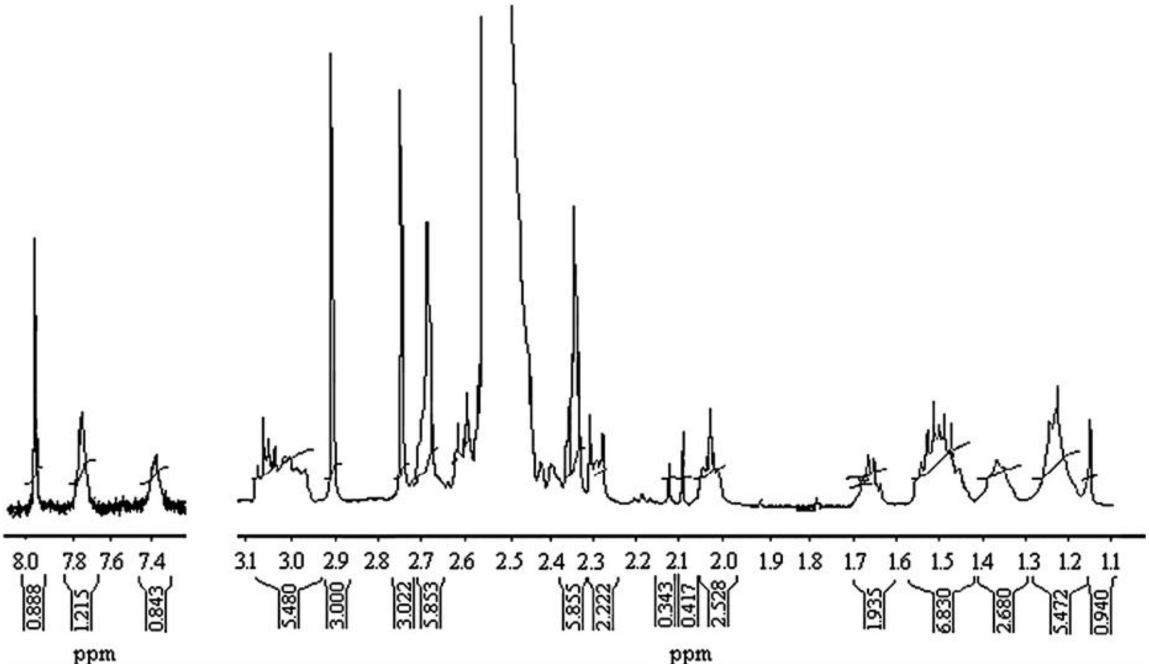

Figure 13. ^{1}H NMR spectrum of block copolymer $(AB)_n$

^{1}H NMR spectroscopy (Bruker AvanceDRX400 instrument (400 MHz), in DMSO) data confirm the results obtained from IR spectrum, for both copolymers (Figures 13 and 14). As presented, typical signals for the dienic rubber and copolyamide coPA were identified in ^{1}H NMR spectra of block copolymers, as follows. For the rubber component: the multiplet at 1.5 ppm corresponds to $–CH_2–$ groups in the vicinity of C–CH– moieties; the triplet at 2.03 ppm belongs to CH_2 groups located near the double bond C=C linked in trans position; in the interval 2.27–2.36 ppm, signals specific for –CH groups next to double bond C=C as pendant *[Slonim and Urman, 1982]*.

As for the signals typical for coPA, in the field 1.15–1.24 there are signals corresponding to $-CH_2$ protons for groups surrounded by other $-CH_2$ moieties, while the triplet at 3.04 ppm belongs to protons from $-CH_2$ groups near –NH moieties.

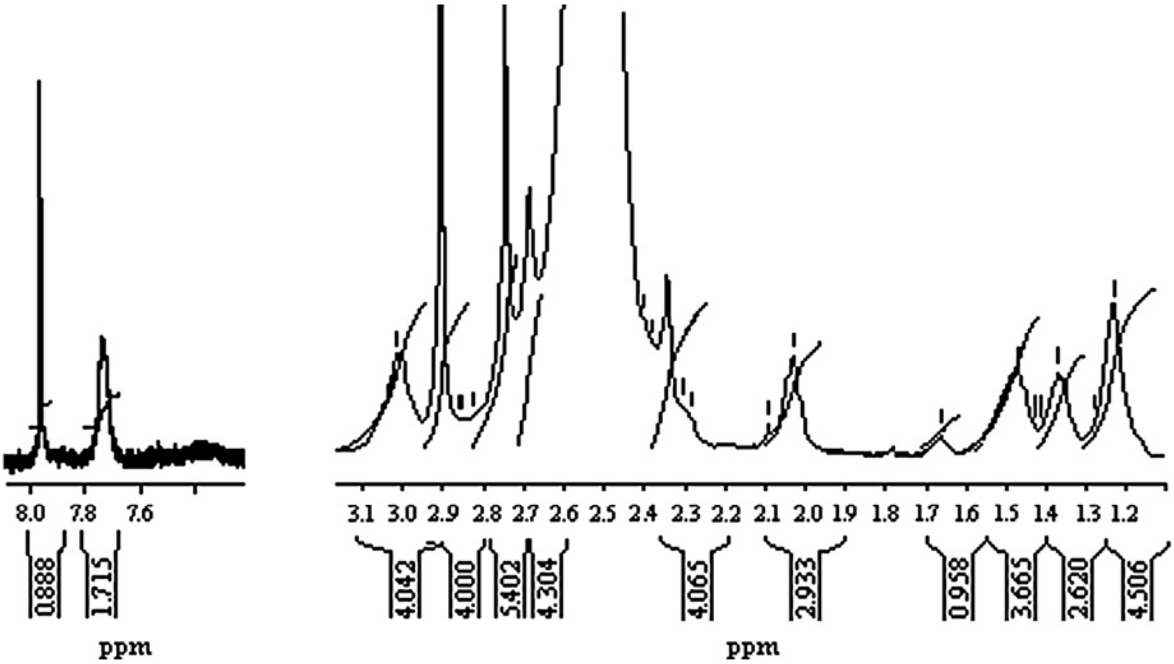

Figure 14. ^{1}H NMR spectrum of block copolymer ABA

It is notable that chemical shifts of protons bonded to oxygen or nitrogen atoms are less characteristic, due to their ability to form inter- and intramolecular hydrogen bonds. The interval 7.0–8.0 ppm is relevant as it shows the influence of the chemical conversion on the integral intensities of labile protons from reactive groups, having correspondence to significant chemical shifts, as follows: 7.9 ppm CH in C_6H_6, 7.7 ppm (NH) and 7.5 ppm (NH_2) *[Slonim and Urman, 1984; Vera et al., 2004]*.

The values of the integral intensities correspond to the amount of different groups in the block copolymers. Considering the amount of NH groups, it can be observed that the integral intensity for block copolymer ABA is 1.5 times higher than for the copolymer $(AB)_n$. Signals assigned to NH_2 groups are present in the ^{1}H NMR spectrum of block copolymer ABA and are practically absent for copolymer $(AB)_n$, which confirms the formation of three-block and polyblock copolymers.

In both ^{1}H NMR spectra, signals at approximately 2.5 ppm and 3.3 ppm correspond to undeuterated solvent (DMSO) and water present in the solvent, respectively.

2.2.3 Thermal behavior of polyamide–diene BCPs

Thermal behavior of the new block copolymers was evaluated by differential scanning calorimetry (DSC), with respect to relaxation transitions in soft (rubber) and hard (copolyamide) blocks The thermal characteristics were determined using a METTLER TA Instrument DSC 12E calorimeter (Atkinson, USA). shells (DSC-d), as specified in literature *[Godovsky, 1977; Privalko et al., 2000; Titov, 1980]*, at a heating rate of 2 K/min after quenching the samples in liquid nitrogen. The melting point and melting heat were determined from the endothermal peaks' area.

Experimental data for heat capacity and glass transition temperatures are summarized in Table 8, and thermograms corresponding to block copolymers $(AB)_n$ and ABA are presented in Figure 15.

Table 8. Thermodynamic characteristics of the polyamide–diene BCPs

Samples	**$T_{g,1}$, K**	**$\Delta C_{p,1}$, J/(g·K)**	**$T_{g,2}$, K**	**$\Delta C_{p,2}$, J/(g·K)**	**T_m, K**	**ΔH, J/g**
coPA			294	0.24	406	29.67
MDIR	240	0.46				
$(AB)_n$	228	0.17	296	0.08	405	5.38
ABA	232	0.21			408	41.30

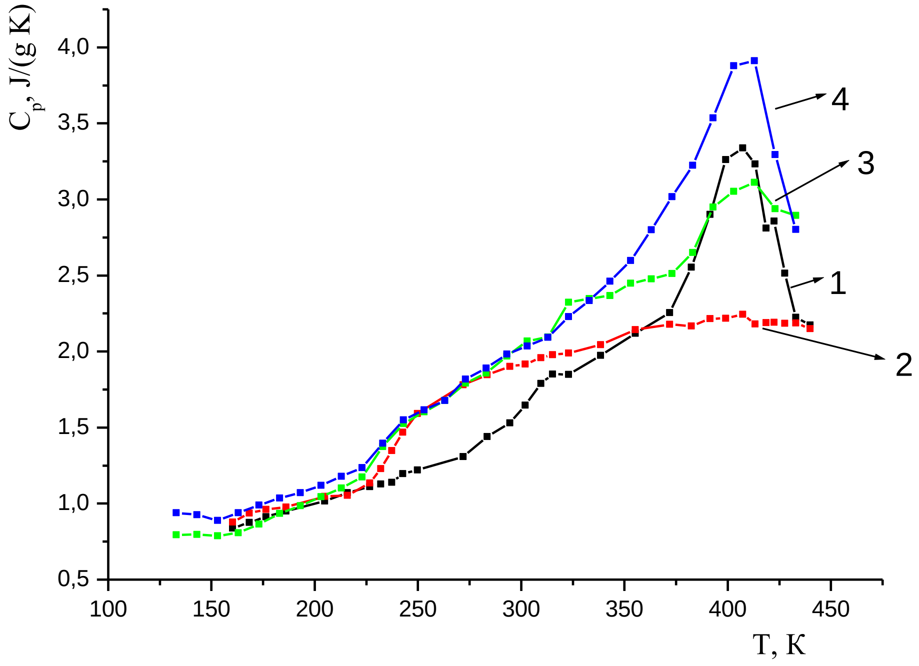

Figure 15. Temperature dependences of heat capacity of: coPA (1), MDIR (2), block copolymers ABA (3) and $(AB)_n$ (4)

The glass temperature of the rubber component (T_{g1}) (Table 8) and the amorphous phase of the copolyamide (T_{g2}) were determined by the half-height of the corresponding heat capacity jump; the crystalline phase melting temperature (T_m) was measured at the maximum position on the heat capacity–temperature dependence (Figure 15). A jump ΔC_{p1} = 0.46 J/(g·K) at the glass temperature T_{g1} = 240 K (Table 2, Figure 8) was observed on the heat capacity – temperature graph for MDIR. The value of T_{g1} for rubber is overstated, whereas the ΔC_p value is understated compared with known data for cis-polybutadiene (ΔC_p = 0.61 J/(g·K), T_g = 165 K *[Privalko, 1984]*), which can be explained by the presence of hydrogen bonds with the participation of urethane groups distributed along the polymer chain. The jump on the heat capacity curve of copolyamide (ΔC_{p2} = 0.24 J/(g·K) at T_{g2} = 294 K), which is a semicrystalline material, concerns the relaxation transition of the amorphous phase of coPA, while the melting peak with maximum at T_m = 406 K is connected to the phase transition of the crystalline phase of coPA.

This study showed that the common feature for heat capacity curves of triblock- and polyblock copolymers (Figure 15 curves 3, 4) is the presence of a heat capacity jump at the glass temperatures of oligodiene and copolyamide microphases (for $(AB)_n$ block copolymer) and a melting endothermic peak of polyamide microphase, which is characteristic of the phase separation in polymeric systems. The low glass temperatures (T_{g1} = 228 K for $(AB)_n$ and T_{g1} = 232 K for ABA) of flexible oligodiene blocks compared to homopolymer is observed on the heat capacity curves. This may be correlated with the alteration of segment packing in the oligodiene microphase due to the introduction of the coPA hard blocks, and withdrawing polar urethane groups into the copolyamide microphase that structure the homopolymer. The ΔC_{p1} decrease for BCPs (ΔC_{p1} = 0.17 J/(g·K) for $(AB)_n$ and ΔC_{p1} = 0.21 J/(g·K) for ABA) may be connected to the mobility suppression in the oligodiene microphase due to the decreased mobility at low temperatures of hard blocks *[Bershtein and Egorov, 1990]*.

As can be seen from Figure 15, heat capacity anomalies occur in coPA hard blocks. If for $(AB)_n$ the heat capacity jump is the same at the glass temperatures of copolyamide microphase (ΔC_{p2} = 0.08 J/(g·K) at T_{g2} = 296 K), for ABA it is absent. At this temperature, ΔH_m for $(AB)_n$ is quite low while for ABA it is quite high and has a very broad range of melting points compared to neat coPA. This behavior might be explained by the vicinity of rubber blocks with high mobility at increased temperatures, as well as by the influence of intermolecular interactions in BCPs. In the case of $(AB)_n$ the quantity of rubber is considerably lower than in ABA. Therefore, the presence of two coexisting randomly interpenetrating microphases (copolyamide and dienic blocks), with a broad distribution of dimensions, is possible. The $(AB)_n$ has a copolyamide block content 1.5 times higher and, accordingly, more polar group connecting blocks. The intermolecular interactions in hard blocks are more intense, which may lead to the suppression of the coPA amorphous phase and to an increase of the ΔH_m.

2.2.4 Mechanical properties of polyamide–diene BCPs

Mechanical tests were performed in order to evaluate tensile strength and elongation of the novel block copolymers. Taking into consideration the initial characteristics of the rubber (soft blocks) and coPA (hard blocks), as well as their molar ratios in the BCPs formulation, it was expected that mechanical properties of BCPs to be different from the raw oligomers. A comparative study is presented in Table 9.

Table 9. Mechanical characteristics of polyamide–diene BCPs

Block copolymers	**Tensile strength $\sigma_{rupture}$ MPa**	**Relative elongation ε, %**
PA	20.0	300
$(AB)_n$	14.6	700
ABA	15.4	400
ABA after annealing	16.9	450

Tensile strength and elongation measurements in general accordance with ISO 527 were performed on a mechanical tensile machine FU-1000 (Rauenstein, Germany) and a testing machine PM-400 (Ivanovo, Russia), at room temperature. The crossheads' speeds were 20 mm/min and 50 mm/min, respectively. Samples were dumbbell shaped with length 150 mm, width of testing part 10 mm and thickness 4 mm and were pressed in a special mould. At least five samples were tested in each case.

The mechanical properties of the copolymers were compared to coPA. It is easy to notice that for the polyblock copolymer $(AB)_n$ the tensile strength is lower than that of coPA, but the elasticity is significantly increased in comparison with the copolyamide, more than 2 times higher. In the case of the three-block copolymer ABA, the higher content of coPA results in increased elongation, while the tensile strength is slightly increased compared to $(AB)_n$. An interesting behavior is shown by copolymer ABA after annealing: the tensile strength increases, close to the value for coPA, while the elasticity is comparable to that of ABA before annealing. This behavior might be explained by a rearrangement of the chains, finally a higher ordered structure being obtained.

In conclusion, the introduction of soft blocks increases the elasticity of block copolymers, but when hard blocks are preponderant, the tensile strength is higher. Therefore, it is possible to tailor the mechanical properties of BCPs according to the final application.

2.2.5 Morphology of polyamide–diene BCPs

An electron microscope type BS 340 TESLA (Brno, Czech Republic) was used to study the morphology of the BCPs and blends. The surface of samples were prepared by successive treatments of abrasion (from coarse to fine) and finally by polishing with a special paste. A replication method was used to obtain the image. Optical observation of the morphology was performed with an optical microscope IOR type MC1 (IOR Bucharest, Romania).

The microphotographs obtained for coPA and copolymers $(AB)_n$ and ABA, which were frozen in liquid nitrogen and then fractured, are presented in Figure 16.

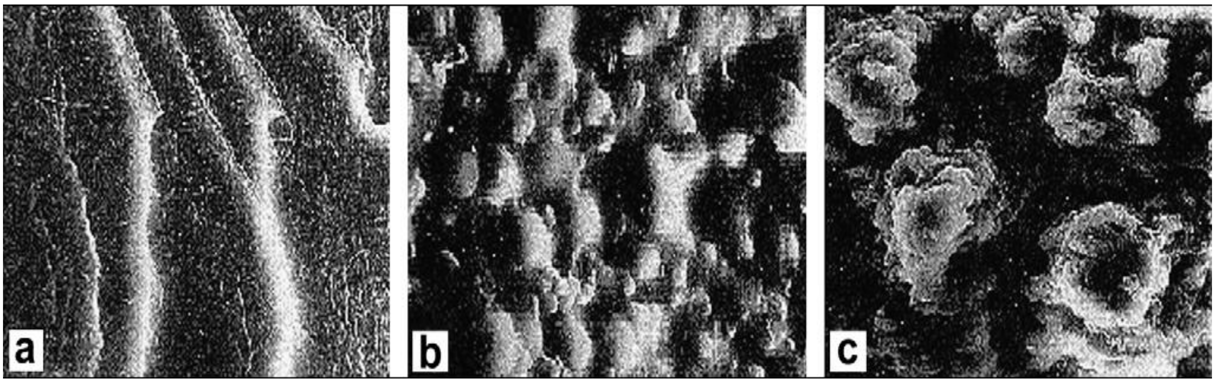

Figure 16. SEM microphotographs for copolyamide coPA and of polyamide–diene BCPs: a – coPA; b – $(AB)_n$; c – ABA

This study reveals that the sample of coPA has behavior typical of fragile polymers, while samples of block copolymers show an increased elasticity due to the introduction of soft rubber blocks. The block copolymer $(AB)_n$ is characterized by the presence of two interpenetrating microphases consisting of copolyamide and rubber blocks, which is in good concordance with its thermal behavior. In the case of the block copolymer ABA, the increased coPA content leads to agglomeration and a neat microphase separation.

2.3 Study of composite polymeric materials

2.3.1 Properties of composite polymeric materials on the based secondary polyethylene and polyamide–diene BCPs

To obtain composites, different ratios of secondary high density polyethylene (s-PE), coPA and polyamide–diene block copolymers $(AB)_n$ and ABA were used *[Busko et al., 2004b, 2008]*. Composites were obtained by melt extrusion, using a laboratory single screw extruder with three different temperature zones (135°C, 145°C and 165°C) and the following parameters: diameter 25 mm, length to diameter ratio of the screw L/D = 15. The extrudates were processed to obtain powders and then molded at 140°C and 1 MPa for 5 min. Characteristics of s-PE/BCPs compositions were comparatively studied with s-PE/coPA blends due to the fact that coPA is the hard component of BCPs.

IR spectrometry was employed to confirm the composition of the new materials. Spectra of s-PE and compositions s-PE/$(AB)_n$ at ratios of 90/10, 80/20 and 70/30 are presented in Figure 17. The spectral study was performed by the method of multiple attenuated total internal reflection. Specific bands for polyethylene (upper scale) are easy to identify, as follows: CH_2 (symmetric and asymmetric) valence vibration is located in the interval 2850–2950 cm^{-1}, deformation vibration of CH_2 groups are at 1440–1460 cm^{-1}. In the case of blends, amide specific bands can be identified (lower scale): band amide I at 1630– 1650 cm^{-1} – vibration of carbonyl groups; band amide II (low intensity) at 1560 cm^{-1} – valence vibration of NH moieties for secondary amides; bands under 3300 cm^{-1} and 3100 cm^{-1} can be attributed to NH groups bonded by intermolecular and intramolecular linkages, respectively.

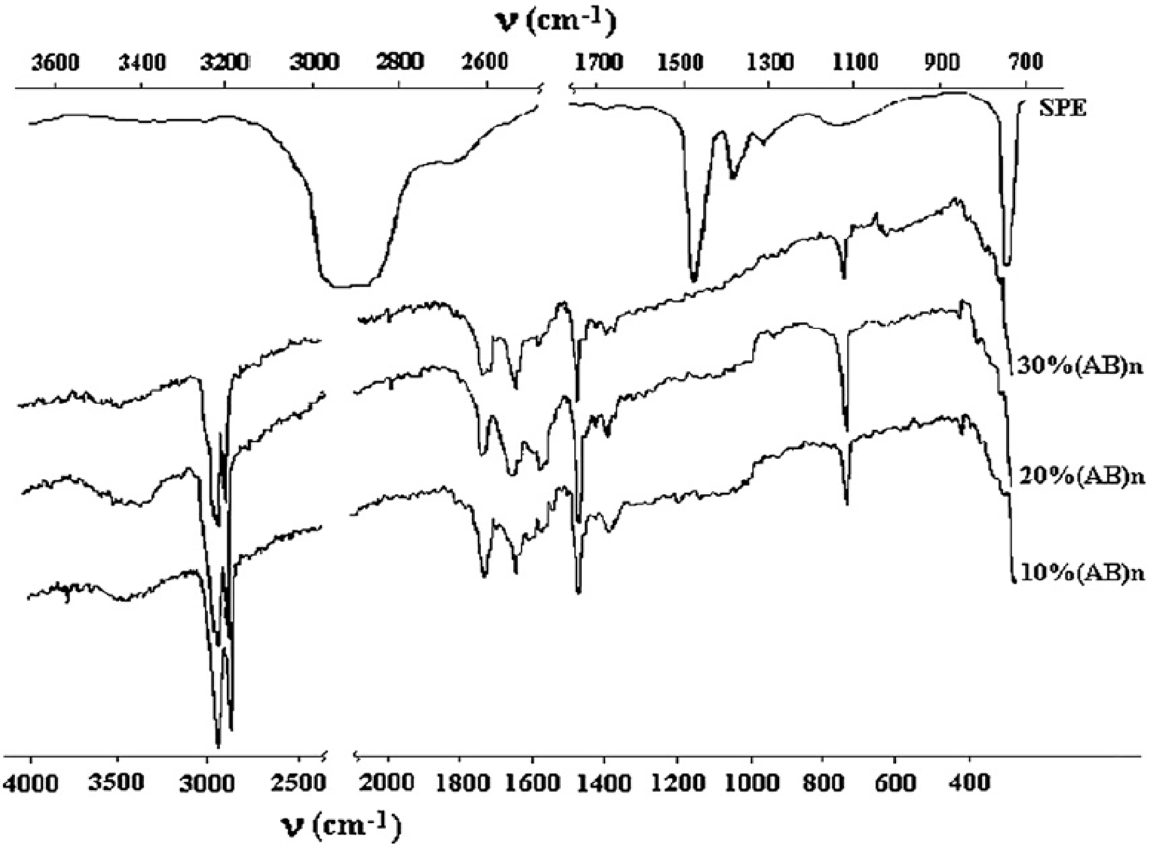

Figure 17. IR spectrum of s-PE and compositions s-PE/$(AB)_n$ containing 10%, 20% and 30% $(AB)_n$, respectively

Mechanical characteristics of these compositions were comparatively evaluated in order to estimate if copolymers $(AB)_n$ and ABA can be used for this application on a large scale. Experimental data obtained for composites s-PE/coPA are presented in Table 10 and Figure 18. A comparison between SPE and coPA with respect to tensile strength and elongation at break shows that the copolyamidic component has a higher strength (curve 1) and an increased elasticity (curve 2). Blending s-PE and coPA yielded in materials with a slightly improved tensile strength compared to s-PE, but their elasticity decreased with the coPA content (up to 30%).

Table 10. Mechanical characteristics of compositions s-PE/coPA related to coPA content

Composition s-PE/PA, %	**Tensile strength $\sigma_{rupture}$ MPa**	**Relative elongation ε, %**
100/0	10.55	96.93
95/5	11.10	73.40
90/10	12.10	65.30
80/20	12.90	49.80
70/30	13.00	16.40
50/50	15.70	19.8
0/100	23.30	375

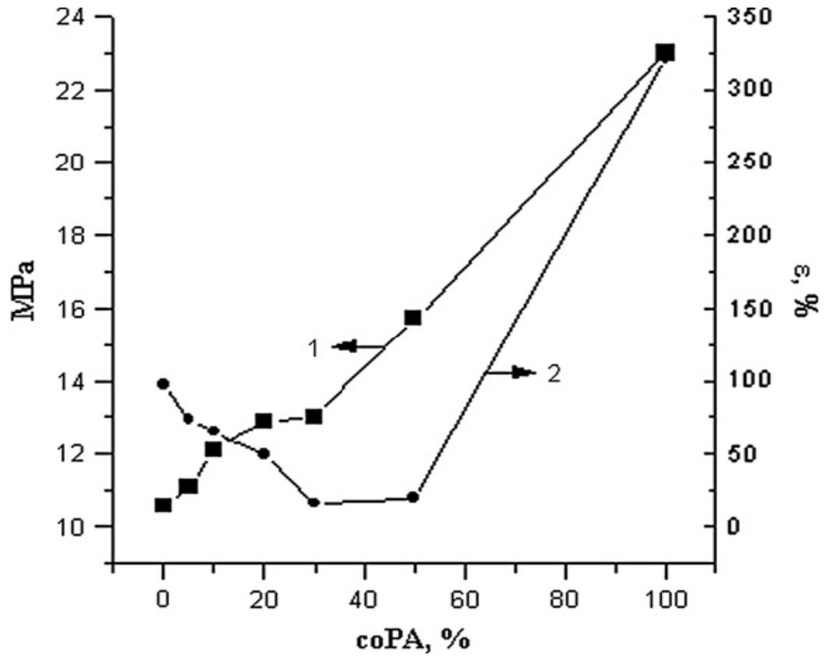

Figure 18. Dependency of mechanical properties of composites on coPA content

Table 11. Mechanical characteristics of compositions s-PE/$(AB)_n$

Composition s-PE/$(AB)_n$, %	**Tensile strength $\sigma_{rupture}$ MPa**	**Elongation at rupture ε, %**
100/0	10,55	96.93
90/10	9.10	320
80/20	8.30	400
70/30	8.50	250

Table 12. Mechanical characteristics of compositions s-PE/ABA

Composition s-PE/$(AB)_n$, %	**Tensile strength $\sigma_{rupture}$ MPa**	**Elongation at rupture ε, %**
100/0	10.55	96.93
90/10	10.60	400
80/20	11.50	550
70/30	15.30	520

A similar evaluation was performed on composites made of s-PE/$(AB)_n$ and s-PE/ABA in various ratios, experimental data being summarized in Tables 11 and 12 and Figure 19.

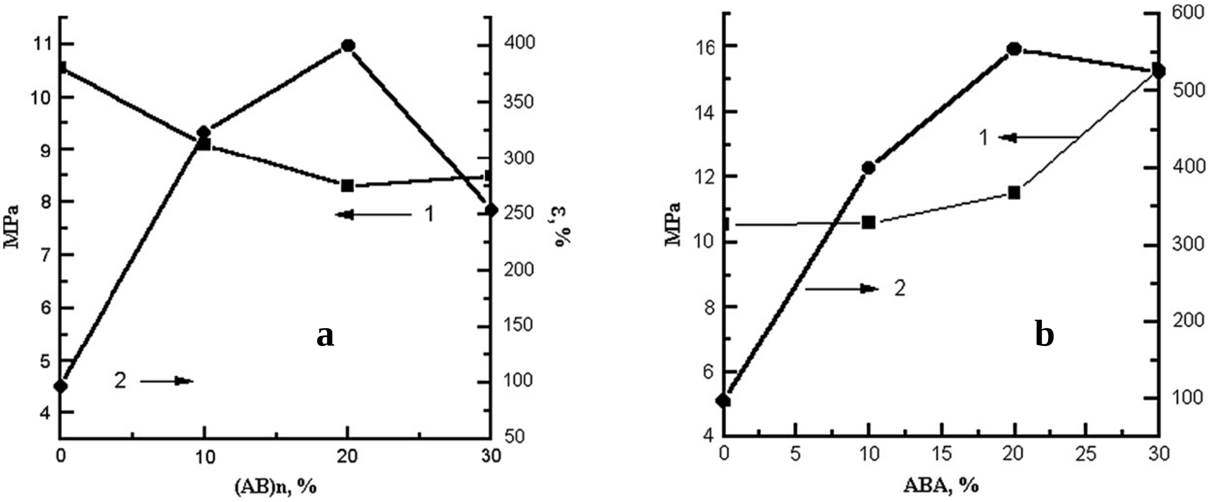

Figure 19. Dependency mechanical properties of compositions: s-PE/$(AB)_n$ (a) and s-PE/ABA (b)

Analyzing data obtained for blends s-PE/$(AB)_n$, it was noticed that tensile strength values (curve 1) slightly decreased with increasing block copolymer content, while the elongation curve (curve 2) showed that elasticity strongly increased for up to 20% of $(AB)_n$, but decreased at a higher content. It can be stated that the optimal composition for these blends is s-PE/$(AB)_n$ = 80/20 (% wt), when maximal elongation and relatively small decrease of tensile strength are reached.

When block copolymer ABA was used to obtain composites with s-PE, materials with improved elasticity and tensile strength resulted. This is due to the higher amount of coPA in the structure of ABA block copolymer. The values of tensile strength (curve 1) are increasing continuously with the ABA content. Maximum elongation is reached at 20% ABA, but for higher amounts it decreases. In this case, we consider the optimum composition for a ratio s-

PE/ABA = 80/20 (% wt), although the tensile strength is still increasing for higher ABA content.

A morphology study was also performed on the compositions and microphotographs are presented in Figure 20.

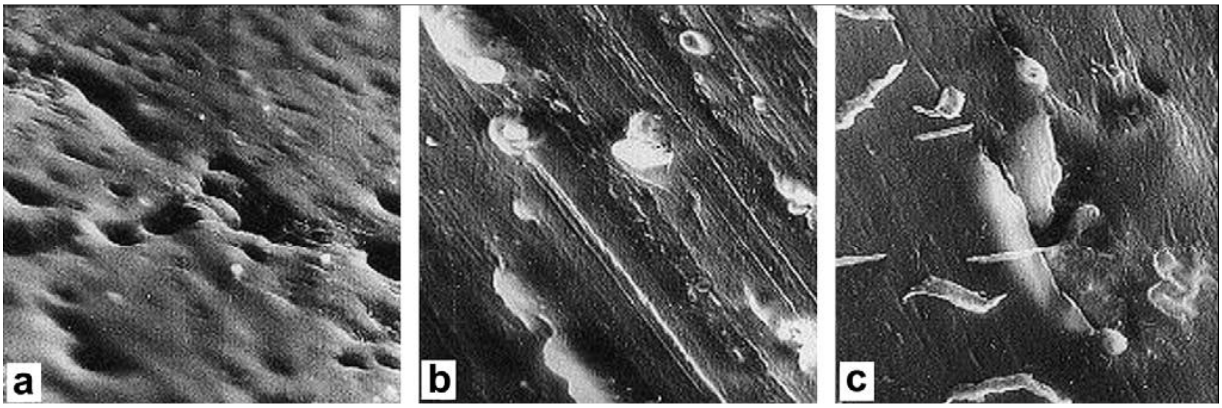

Figure 20. SEM microphotographs of s-PE/(AB)n blends: a – 90/10(% wt); b – 80/20(% wt); c – 80/30(% wt) *[after Busko et al., 2008]*

The microphotographs corresponding to composites with ratios s-PE/(AB)$_n$ = 90/10 and 80/20 show irregular inclusions of block copolymer cast in the entire mass of s-PE, which is a characteristic feature for blends made of incompatible polymers. In spite of this situation, results obtained for mechanical tests substantiate that these blends have good characteristics for some applications.

2.3.2 Polymeric composites on the base of thermoplastics, disperse rubber crumbs and modifiers

For creation of rubber filled composites, rubber crumbs obtained from waste tires on worm-rotary disperser-plodder „Deckcher” by method of high-temperature shift crushing have been used. Compositions were prepared by mechanical mixing of polymer and disperse rubber crumbs with subsequent homogenization of mixture in the plodder under appropriate deformation and temperature regimes *[Bledzki and Sperber, 2003; Mishak et al., 2002; Serenko et al., 1998; Wolfson, 2000]*. Mass fraction of crumbs in compositions has been changed from 5 to 80% mass. As modifiers, diisocyanates and hidden macrodiisocyanates have been used; they were obtained on the base of liquid rubber of molecular weight 3000, with hydroxyl groups, content of hydroxyl groups – 1.13 %, viscosity at 25°C – 3.0 Pa·s *[Myshak and Lebedev, 2006]*.

Polymer compositions have being prepared with the ratio of secondary polyethylene to rubber crumbs 50:50 mass %, accordingly, with the introduction of different quantity of macrodiisocyanate or hidden macrodiisocyanate (3-20%) as modifiers.

Structure of rubber crumbs (RC) has being studied by method of spectral analysis (Figure 21).

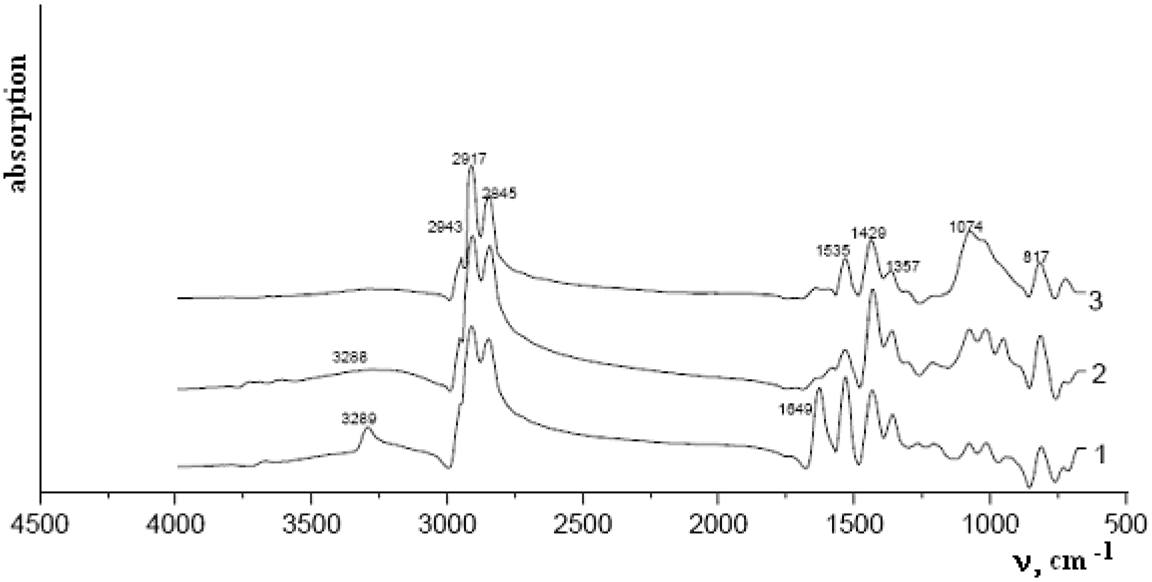

Figure 21. IR spectra: of the rubber crumb received: 1 – a method of high-temperature shift crushing; 2 – a method of cryogenic crushing; 3 – a method high-speed slicing *[after Myshak and Lebedev, 2006]*

IR spectra of rubber crumbs have valence vibrations of CH, CH_2 , =CH groups, deformation vibrations of CH, CH_2 , =CH groups, vibrations of CH, CH_2 groups of carbon chain. It is known *[Kuznetsova et al., 2004; Shalyganov et al., 2005]* that rubber crumb, depending on the obtaining method, could have different active groups on its surface; however, the processes of destruction with devulcanization and oxidation occur during crushing. As it could be seen from IR-spectra of rubbers, obtained: by method of high temperature crushing (spectra 1); by method of cryogenic crushing (spectra 2); by method of high-speed slicing (Figure 3), the surface of the crumb has a number of characteristic bands that show the presence of polar NH, OH, C=O, ester R-(C=O)-O- and other functional groups, that were created as a result of chemical processes of oxidation of rubbers, which could enter into chemical and intermolecular interactions with functional groups of polymer of matrix- s-PE. All three types of crumb have a set of valence vibrations of linked OH-groups, which are characterized by wide band in the region of 3100-3500 cm^{-1} and characteristic bands of absorption of -CH=, $-CH_2$ groups in different regions of the spectrum ($\nu_{\text{-CH=}}$ - 2950-2970 cm^{-1} , $\delta_{\text{-CH=}}$ - 968-972 cm^{-1}), valence vibrations of C=C – groups in the region of 1640 cm^{-1}. It can be also mentioned, that crumb obtained by method of high temperature crushing has remains of amide cord, proven by absorption bands of valence vibrations – in the region of 3300 cm^{-1} and deformation vibrations of NH-groups in region of 1530 cm^{-1}, valence vibrations C=O (amide II) *[Kuptsov and Zhizhin, 2001; Nakanisi, 1965]*. For crumbs obtained by methods of cryogenic crushing (spectra 2) and high-speed slicing (spectra 3), the bands in the interval 1050- 1200 cm^{-1} can be attributed to ether and ester groups in different ratio.

The structure of polyethylene matrix is confirmed also by method of IR-spectroscopy (Figure 22).

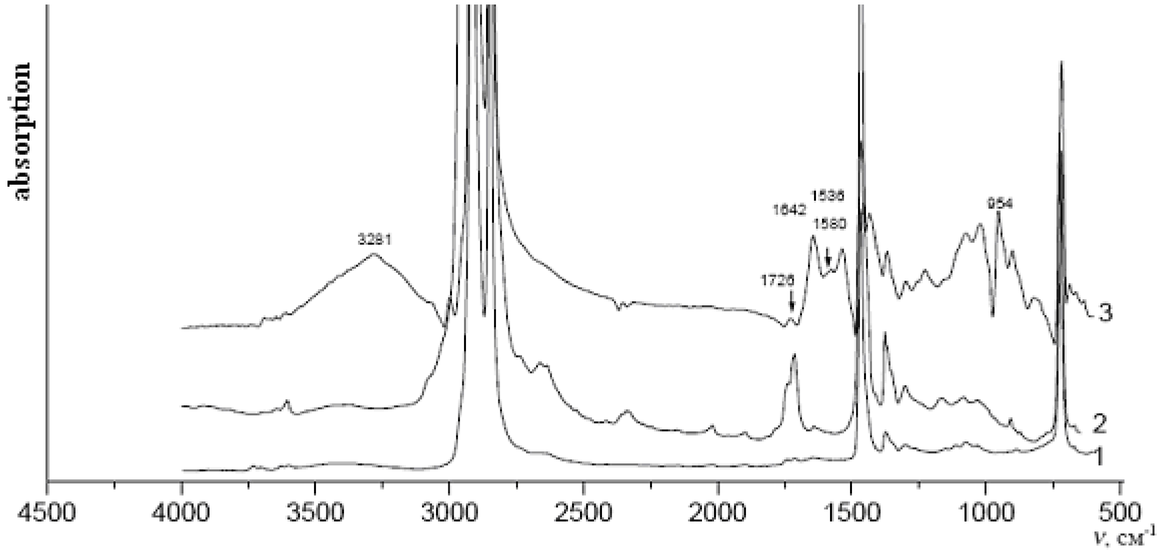

Figure 22. IR- spectra: 1 – PE, 2 – s-PE, 3 – s-PE : RC (50:50 mas.%) *[after Myshak and Lebedev, 2006]*

As we can see from Figure 22 (curves 1, 2, 3), IR-spectra have typical absorption bands for polyethylene. Together with this, comparison of primary and secondary polyethylene shows their essential difference. The most typical changes in chemical structure of s-PE are expressed by the appearance of characteristic absorption bands in spectrum which are absent in spectrum of primary PE. Thus, increase of optical density of band 907 cm^{-1} indicates an increase of quantity of unsaturated bonds of vinyl type R-CH=CH$_2$ *[Kuptsov and Zhizhin, 2001; Mamunya et al., 1990; Nakanisi, 1965]*. Presence in spectrum characteristic band 1715-1720 cm^{-1} related to appearance in s-PE carbonate groups C=O in ketones, presence of rather intensive bands 1050, 1260 cm^{-1} show the creation of ether groups C-O-C in the polymer chain, and some broadening from high frequency side bands 1720 and 1170 cm^{-1} testifies about the rise of certain quantity of ester groups R-(C=O)-O in macromolecules of s-PE. It is known that in the process of ageing, polymer materials are subjected to essential chemical and physical changes. As a result, increases in materials of oxygen-containing groups – carbonyl, hydroxyl, carboxyl, ether and destruction of polymer chains take place. It leads to magnification of the content of gel-fraction and, respectively, considerable decay of physical-mechanical, rheological characteristics, reduction of molecular weight, broadening molecular weight distribution. At the same time, the presence of functional groups on the surface of rubber crumb and polymer matrix can assist in rise of intermolecular interactions between them and has an influence on the structure and characteristics of rubberplast. The presence of intermolecular interactions between polymer matrix and rubber filler can be evaluated by position changes of characteristic bands in spectrum of polymer-rubber composition. Band of stretching vibrations of linked OH groups at 3350 cm^{-1} of polyethylene matrix at introduction of rubber crumbs becomes more intensive, changes its profile with maximum 3281 cm^{-1} at the expenses of the NH groups of rubber crumbs. Bands of stretching vibrations of carbonyl groups (1726 cm^{-1}) appear in spectrum as well, band of deformation vibrations of NH groups in region of 1580 cm^{-1}, their appearance could be connected to interactions of functional groups of s-PE and RC (Figure 25, curve 3). Earlier, this kind of interactions have being established between s-PE and wood *[Mamunya et al., 1994]*, that were bringing improvements of physical-mechanical and operational characteristics of composite materials.

From the presented diagrams (Figure 23) it can be seen that filling of polyethylene by disperse particles of vulcanized rubber, leads to change of its behaviour under tension.

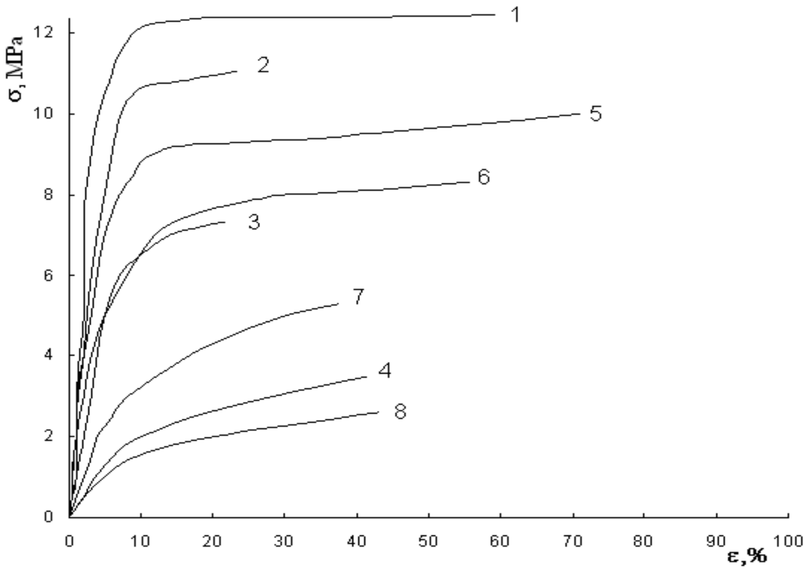

Figure 23. Tension diagrams of rubberplasts base on s-PE (curves 1-4) and primary PE (curves 5-8). The crumb content in compositions: curves 1, 5 - 5; curves 2, 6 - 20; curves 3, 7 – 50; curves 4, 8 – 80 mas. %

Distinction between the compositions base on primary and secondary PE is made of different values of strength and deformation under tension of samples with different filling content *[Gul and Kuleznev, 1979; Nilsen, 1978]*. It could be seen that increase of rubber crumbs content from 5 to 50 mass % changes the stress-strain curve appearance. Curves 1, 5 (Figure 23, crumbs content -5%) show that in compositions on the base of primary and secondary PE, after elastic deformation, significant plastic deformation develops, but the material does not strengthen. Further increase of crumbs content in compositions leads to lowering of fluidity and deformation of composites.

From the diagram of dependency of strength vs. deformation it can be seen that location of curvesfor compositions on the base of s-PE (1-4) is higher in comparison with curves for compositions on the base of primary PE (5-8). This testifies that reactionary-capable groups, which are in s-PE and on the surface of the rubber crumbs, contribute to the increase of strength and elasticity of composites in comparison with the same kind of composites on the base of primary PE.

The investigations have shown ratio between polymer matrix and disperse rubber filler have determinant influence on the characteristics of compositions – σ_r decreases from 12.4 to 2.7 MPa at increase of crumb in compositions from 5 to 80%, thus observed sharp reduction of σ_r already at 5-10 % of crumb content relative to σ_r not filled PE and s-PE, accordingly (Figure 24).

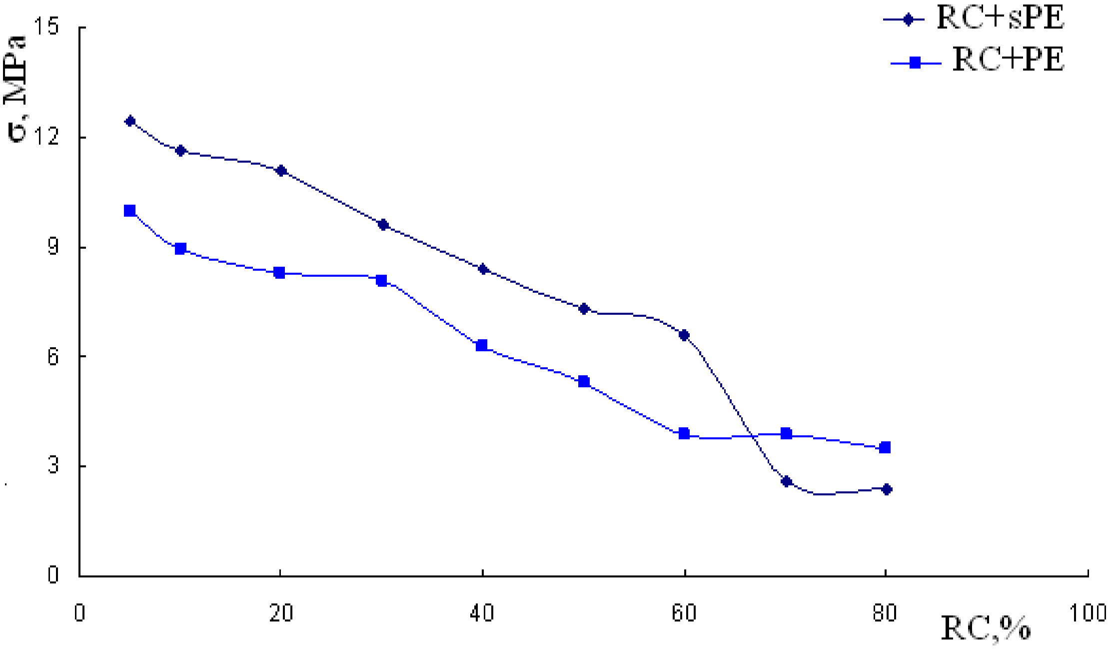

Figure 24. Dependence of a breaking point at a stretching rubber layers on the content of a rubber crumb

Thus, the important fact is compositions on the base of s-PE have higher strength for a large interval of concentrations of rubber filler (10-60 mass %), in comparison with composites on the base of primary PE, which substatiates on the influence of the above mentioned factors on the strength of material *[Pasko et al., 2006]*.

For the dependency of relative elongation (Δε) on the content of filler (Figure 25), the sharp reduction of Δε in the range of values of rubber content in the composite material until 10% it is characteristic, in the range of medium concentrations Δε almost does not depend on the filler content, and for concentrations over 50% of rubber the increase of Δε is observed, which could be linked to structural effects in composite materials *[Kirilova and Shulgina, 1988].*

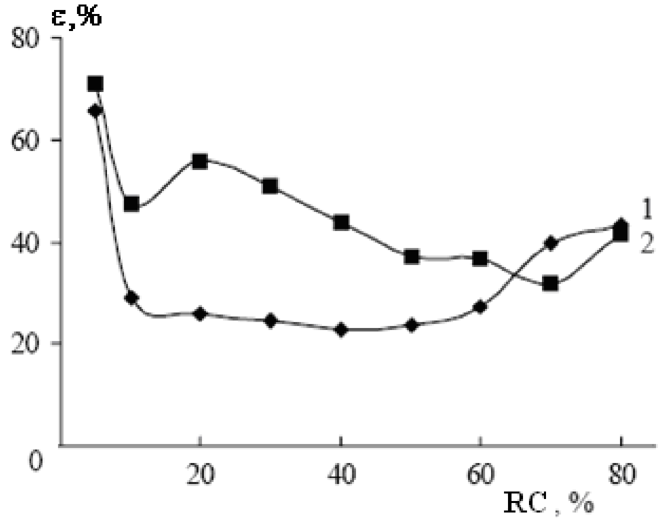

Figure 25. Dependency of the relative elongation of rubberplats on the rubber crumb content

2.3.3 Modification of rubberplasts by low-molecular rubber with functional groups

The adhesion and interaction at the polyethylene-rubber interphase in composites that contain disperse fillers are factors of considerable importance, which influence on physical-mechanical characteristics of materials. As known, adhesion between components of matrix and their interactions depend on relationship of components and their ability to combine and are defined by their chemical structure, presence of functional and reactive groups on the surface *[Lipatov, 1980]*. In the case of obtaining rubberplasts, modifiers play significant role, which also fulfill the role of plasticizers, compatibilisers, and also can create additional chemical or physical bonds with functional groups of components of composite materials *[Guo et al., 2004; Trofimova et al., 2003]*. When working with rubber waste, the perspective is the use of liqud rubber with functional groups, which has the carbon chain structure similar to rubbers and has to provide compatibility for these components.

Macrodiisocyanates and hidden macrodiisocyanates have been used for modification of rubberplasts, which have been synthesized on the base of liquid rubbers.

Macrodiisocyanate have been obtained by the reaction of oligodiene with final hydroxil groups (ODH) and 2,4-toluilendiisocyanate (2,4-TDI) according to the scheme:

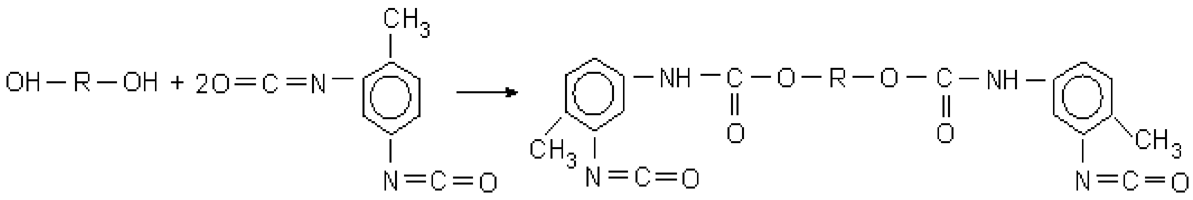

where R - [$–CH_2–CH=CH–CH_2–]_n$.

The structure of the obtained macrodiisocyanate has been confirmed by IR-spectroscopy: reduction by two times of intensity of absorbtion band of isocyanate groups 2270 cm^{-1} by comparison of spectra of reaction product with outgoing mixture of substances, and also the disappearance of absorption band of hydroxil group ~3450 cm^{-1}, appearance of absorption bands of hydrogen-linked ν_{NH} 3320-3330 cm^{-1} , $\nu_{C=O}$ 1700-1720 cm^{-1}, δ_{NH} 1530-1540 cm^{-1} urethane groups.

Obtained oligodiendiisocyanates were introduced into a mixture of 50% of rubber crumb and 50% of s-PE. The results of physical-mechanical investigations of resulted materials are shown in Figure 26 and 27.

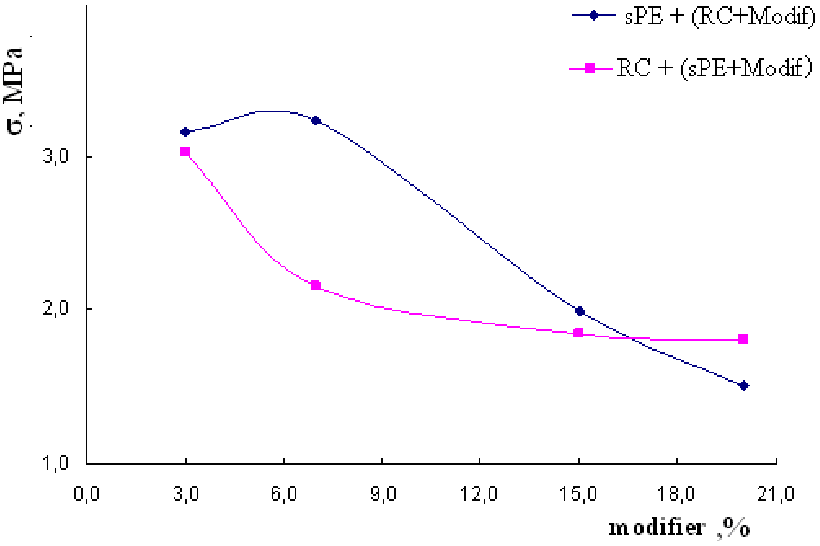

Figure 26. Dependency of the tensile strength of rubberplasts on the content of macrodiisocyanate

As it can be seen from presented data, physical-mechanical characteristics (σ_r, $\Delta\varepsilon$) are not high, that could be explained by interactions of isocyanate groups with the moisture from the air, but not with the functional groups of rubber and s-PE, because the first reaction goes at room temperature, while second – at high temperature. Physical-mechanical characteristics also

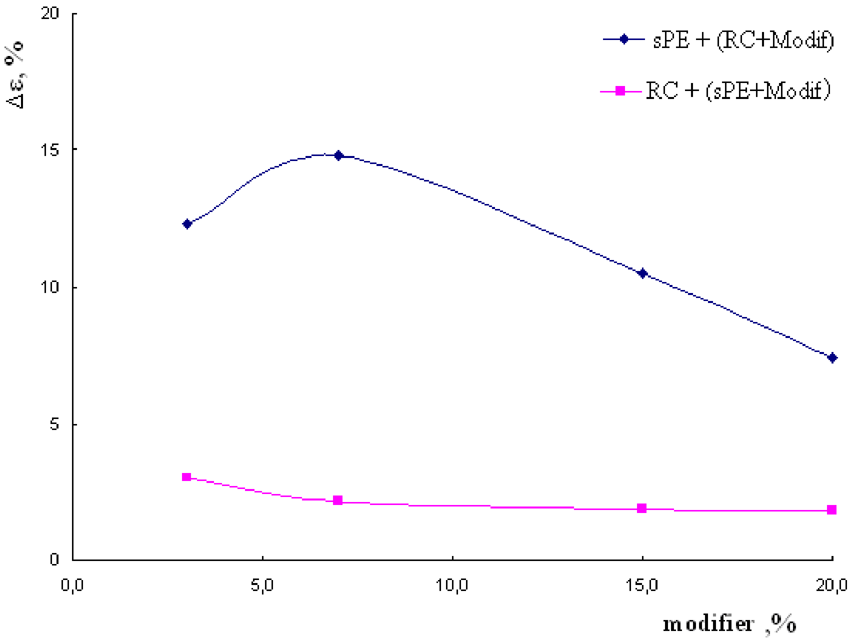

Figure 27. Dependency of the relative elongation of rubberplasts on the content of macrodiisocyanate

depend on the order of mixing of modifier with components of rubber-plastic composition. Thus, when mixing of modifier with rubber crumbs, σ_r and $\Delta\varepsilon$ are higher then for mixing with secondary polyethylene, that could be explained by similar nature of liquid rubber and rubber crumbs and, correspondingly, by better compatibility of modifier with rubber crumbs and the ability to chemical interactions between them.

Taking into consideration the obtained result, in order to hamper the interaction of modifier with the moisture from air during the preparation of rubber-plastic composition, hidden macrodiisocyanates were synthesized on the base of oligodienediisocyanate and n-quinonedioxime according to the scheme:

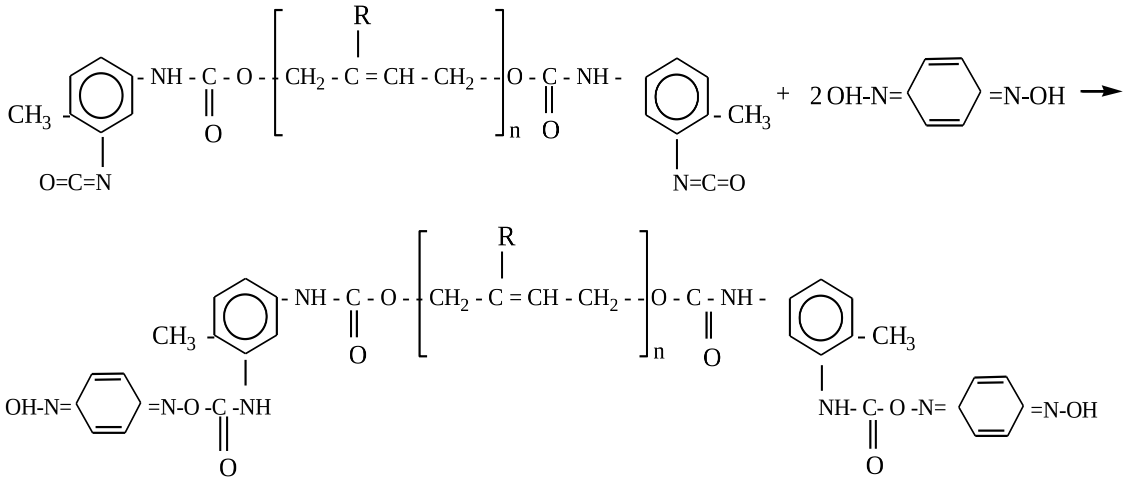

R – H, CH$_3$

Kinetic laws of interaction of oligodienediisocyanate and n-quinonedioxime have been studied through IR-spectroscopy (Figure 28) by the decrease of intensity of absorption band of NCO-groups (2274 cm^{-1}) relative to the absorption band of CH-groups (2930 cm^{-1}), intensity of which does not change during the reaction (Figure 29). As can be seen (Figure 28), at 20°C the reaction practically does not take place, but at 80°C the reaction terminates in 10-11 hours.

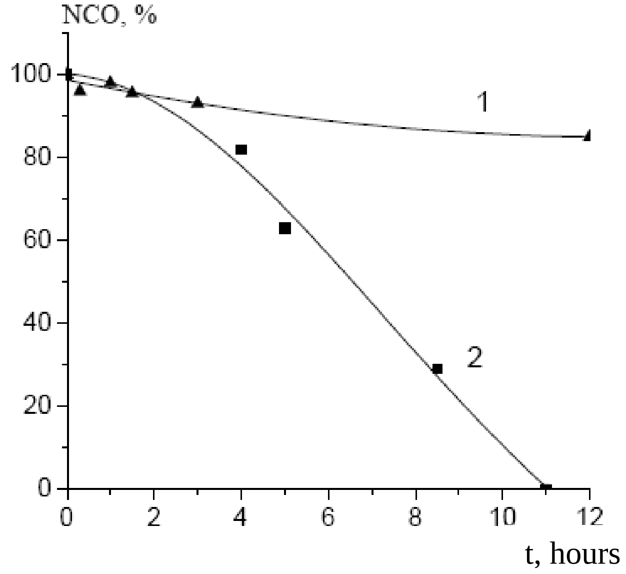

Figure 28. Reaction kinetics of oligodienediisocyanate with n-quinonedioxime; 1- temperature 20°C, 2 - temperature 80°C

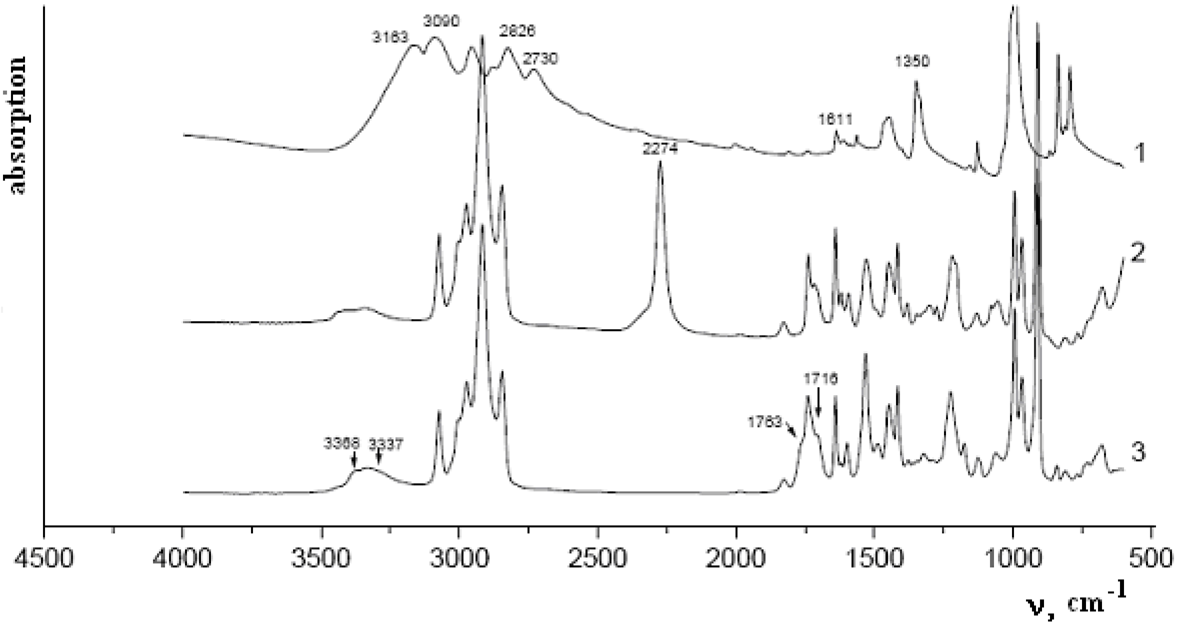

Figure 29. IR spectra: 1- n-quinonedioxime; 2- macrodiisocyanate base on the liquid rubber; 3 – capped hidden macrodiisocyanate base on the 1 and 2

From the presented IR spectra of n-quinonedioxime (curve 1), macrodienediisocyanate (curve 2) and product of their interaction (curve3) it can be seen that spectrum of n-quinonedioxime is characterized by a complex set of peaks in the range 3160-2730 cm^{-1} with enhanced background, that indicates strong hydrogenous bonds inside molecules. The band at 3163 cm^{-1} could refer to stretching vibrations of hydroxyl groups connected by hydrogenous bonds, band at 2731 cm^{-1} - to stretching vibrations of hydroxyl groups connected into complexes. The bands at 1742 cm^{-1} prove the presence of stretching vibrations C=O, 1809 cm^{-1} – of stretching vibrations N=O, and 1350 cm^{-1} – of stretching vibrations C=N-O groups. These data confirm the presence n-dinitrozobenzene in this material, beside n-quinonedioxime. In the spectrum of macrodienediisocyanate there are absorption band of stretching vibrations -3343 cm^{-1}, absorption peak - 1529 cm^{-1} vibrations of NH groups, stretching vibrations -1738 cm^{-1} C=O groups, stretching vibrations -1640 cm^{-1} C=C groups, vibrations -N=C=O groups - 2274 cm^{-1}. There are also absorption bands of hydrocarbon chain of stretching vibrations -2974, 2918, 2846 cm^{-1} of CH and CH_2 groups, deformational vibrations - 1440-1460 cm^{-1} of CH and CH_2 groups, and absorption vibrations of CH groups of hydrocarbon chain - 994, 968, 910 cm^{-1} *[Kuptsov and Zhizhin, 2001]*.

By comparing spectra of n-quinonedioxime (curve1), macrodiisocyanate (curve 2) and product of their interaction (curve3), the disappearance of absorption bands of isocyanate group (2274 cm^{-1}), appearance of strip of stretching vibrations NH (3368 cm^{-1}) and C=O (1763cm^{-1}) of urethane group, redistribution of intensity of deformational vibrations of NH groups in the range 1500-1531cm^{-1}, decrease of intensity of absorption C= N - (1620 cm^{-1}) were observed, that prove the reaction product – oligodienediurethanoxime.

At temperature of 120°C, the unblocking of oligodienediuretanoxime takes place, therefore macrodiendiisocyanate n-quinonedioxime is formed. The macrodiediisocyanate further reacts with functional groups that are present in secondary rubber crumbs and polyethylene, therefore additional chemical bonds are formed, which contribute to the building-up of the rubberplast. In turn, n-quinonedioxime is oxidized to n-dinitrozobenzene, which reacts with hydrocarbone chain of rubber crumbs or polyethylene, according to the scheme *[Blokh, 1972]*:

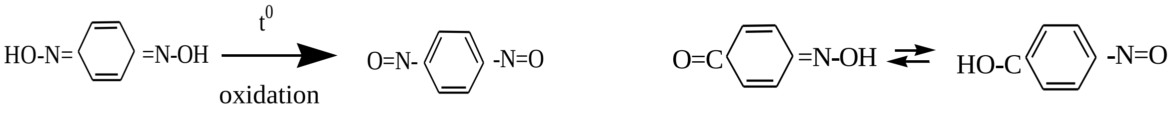

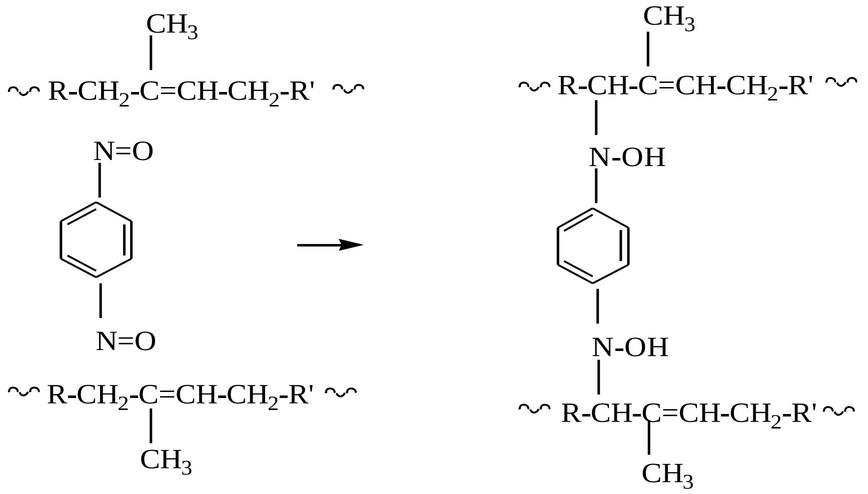

The occurrence of these reactions is confirmed by IR-spectroscopy (Figure 30).

By comparison of IR-spectra of mixture of hidden macrodiisocyanate and liquid rubber with hydroxyl end groups and products of their interaction, it is possible to line out the disappearance of absorption band of stretching vibrations of hydroxyl group and appearance of a more complicated band of stretching vibrations of NH urethane groups. Appropriate changes take place in the range of stretching vibrations C=O (1710-1762 cm^{-1}) and deformational vibrations of NH- groups (1710-1750 cm^{-1}). Variations in the range of valence vibration 2800-3010 cm^{-1}, deformation vibration at 1400-1450 cm^{-1} and band at 920-1050 cm^{-1} vibrations of CH and $CH_{2.}$- groups substantiate the changes that took place during the reaction.

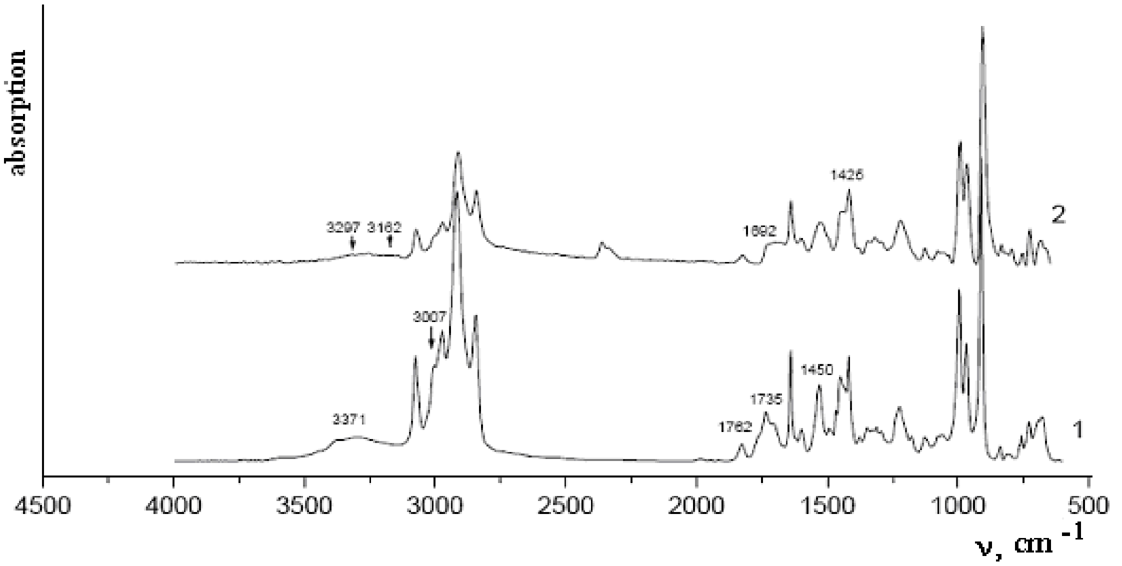

Figure 30. IR spectra: 1 - polymer composition based on capped n-quinonedioxime macrodiisocyanate and oligodienediol; 2 - cured polymer based on capped n-quinonedioxime macrodiisocyanate and oligodienediol (100^{0}C, 18 h)

Introduction of capped macrodiisocyanates into the mixture of 50% rubber crumbs and 50% s-PE has resulted in the enhancement of tensile strength (σ_r) and relative elongation ($\Delta\varepsilon$) by 2 – 2.5 times, that confirmes the use of capped macrodiisocyanates as modifiers of rubber-plastic composite materials as a prospective application.

This research proved that it is possible to design and obtain thermoplastic composites with high mechanical properties based on s-PE and disperse rubber crumbs. Mechanical characteristics of the newly developed rubberplasts depend on the type of polymer matrix, degree of filling of the composites and chemical nature of the rubber crumbs modifier.

3. Conclusions

The synthesis of block copolymers obtained on the base of oligomeric polyazoinitiators by photoinitiated radical polymerization, as well as their properties, have been studied. Oligomeric azo- and polyazoinitiators for radical polymerization, on the base of azo-bis-isobutyrohydrazone of cyclohexanone and butadiene-isoprene rubber, have been synthesized. Threeblock and polyblock copolymers with constant oligodiene block length and various oligostyrene or oligobutylmethacrylate block lengths have been obtained. Their structures were confirmed by means of FTIR spectroscopy. The molar mass characteristics and viscosity of BCPs was determined. Thermal behaviour of these new compounds was studied by DSC, DMA and SAXS. It was shown that studied BCPs are typical two-phase polymeric systems with two glass temperatures and an interphase domain. In was presented that sequential synthesis yields two randomly interpenetrated microphases, which consist of styrene (butylmethacrylate) and butadiene blocks whereas one-stage synthesis of block copolymers gives a well-ordered, three-dimensional lattice of isolated styrene domains within a continuous diene matrix. The photoinitiated radical polymerization method using polyazoinitiators may be applied to obtain block copolymers in the one-stage synthesis to simplify the experimental protocol.

Novel thermoplastic block copolymers based on an aliphatic copolyamide coPA and a diene rubber with isocyanate end groups (MDIR) were obtained. Their structures were confirmed by means of FTIR and ^{1}HNMR spectroscopy. Thermal behaviour of these new compounds was studied by DSC and the conclusion was that their heat capacities depend on the coPA/MDIR ratio due to the differences of crystallinity and polarity. Microphase separation was revealed for both copolymers during the morphology study performed by SEM. As for their mechanical properties, the investigation concluded that the introduction of soft blocks (rubber) increases the elasticity of block copolymers, but when hard blocks (copolyamide) are preponderant, the tensile strength is higher. This study demonstrated that, depending on the application, BCPs with tailored properties can be obtained.

New composites based on these BCPs and s-PE were prepared and studied. The results indicated that s-PE/BCPs compositions have improved mechanical properties in terms of elasticity in both cases, and tensile strength in the case of s-PE/ABA compositions, which make them fit for various applications (interior design, light furniture, packaging, etc.).

Based on these conclusions, we can state that it is possible to use these novel BCPs in composites with secondary polymeric materials. This is a convenient alternate method for waste recovery and recycling. Also, the possibility of using these block copolymers as compatibilizing agents for polyamide–polydiene blends will be further studied.

Rubberplasts on the base of secondary low density polyethylene, disperse rubber crumbs and rubber modifiers based on liquid rubbers with functional groups have been studied. It has been shown that mechanical characteristics of the newly developed rubberplasts depend on the type of polymer matrix, degree of filling of composites and chemical nature of rubber modifier.

4. References

Abdelhadi S., Finerman T. M., Sunny J. (2004) Thermoplastics elastomers having foaming and physical properties. US Patent 6787607.

Adhikari R., Buschnakowski M., Lebek W., Godehardt R., Michler G.H., Baltar Calleja F. J., Knoll K. (2005) Asymmetric PS-block-(PS-coPB)-block-PS block copolymers: morphology and deformation behavior of star block copolymer/PS blends. *Polym. Adv. Technol.*, Vol. 16, No 2–3, pp. 175-182.

Akchyrin R., Chanuschev R., Gilim‘ianov F. (2004) Thermoplastic elastomers composition. Russia Patent 2003118634/04.

Alli A., Hazer B., Baysal B. M. (2006) Determination of solubility parameters of cross-linked macromonomeric initiators based on polypropylene glycol. *Eur. Polym. J.,* Vol. 42, No. 11, pp. 3024–3031.

Bagdasaryan Ch. S. (1966), *Theory of radical polymerization*, Nayka, Moscow, USSR.

Barantsova A., Zanoaga M., Busko N., Tanasa F., Grishchenko V. (2005) New block copolymers based on an aliphatic copolyamidic and dienic rubber. I. Synthesis, *Proceedings of International Conference on Materials Science and Engineering BRAMAT*, 24-26 February 2005, Brasov, Romania, pp. 259-263.

Bechly Y. U., Novikov D. D., Entelis S. G. (l976) Thermoelectric method of molecular weight on value of a temperature maximum. *Vysokomol. Soed.*, Ser. A, Vol. 9, No 12, pp. 2754-2763.

Bershtein V. A., Egorov V. M. (1990) *Differential scanning calorimetry in the physicochemistry of polymers*, Khimiya, Leningrad, USSR.

Bledzki A. K., Sperber V. E. (2003) Recycling of plastic materials – Development, advantage, future, *Proceedings of 2 Mid-European Conference "Plastics Recycling Science – Industry"*, Torun, Poland.

Blokh G. A. (1972), *Organic accelerators of vulcanization of rubber,* Khimiya, Moscow, USSR.

Bratton D., Yang D., Dai J., Ober C. K. (2006) Recent progress in high resolution lithography. *Polym. Adv. Technol.*, Vol. 17, No 2, pp. 94-103.

Bryson N., Meyrueix R. (2003) Synthesis and characterization of AB-type copolymers. *Macromolecules*, Vol. 36, No 4, pp. 1118-1124.

Busko N. A., Grishchenko V. K., Kochetov D. P. (1993) Photoinitiated radical polymerization of urethane-containing copolymer. *Teor. Eksper. Khim.*, Vol. 29, pp. 539-543.

Busko N. A., Grishchenko V. K., Kochetov D. P. (1996a) Block copolymers on the base reactive oligomers. *Ukr. Chem. J.*, Vol. 62, No 1, pp. 65-69.

Busko N. A., Grishchenko V. K., Privalko V. P., Kochetov D. P. (1996b) Properties of triblock copolymers from reactive oligomers. *Komposits. Polimer. Mater.*, No. 57, pp.150-156.

Busko N. A. (2001) Block copolymers on the base of vinil monomers and oligomeric initiators (synthesis, stracture and properties), *PhD Thesis*, Institute of Macromolecular Chemistry, Kyiv, National Academy of Sciences of Ukraine.

Busko N. A., Grishchenko V. K., Shtompel V. I., Babkina N. V., Rosovitski V. F., Privalko V. P. (2001) Phase morphology and dynamic mechanical properties of model polyblock copolymers prepared from reactive. *Polymers & Polymer Composites,* Vol. 9, No 8, pp. 509-513.

Busko N. A., Barantsova A., Babkina N. V., Privalko E. P., Grishchenko V. K. (2004a) Synthesis and properties of block copolymers on the base of oligomeric polyazoinitiators and butylmethacrylate, *Polymer Journal,* Vol. XXVI, No 2, pp. 78-82.

Busko N., Barantsova A., Grishchenko V., Myshak V., Zanoaga M., Tanasa F. (2004b) Composite polymeric materials based on polyamide-diene copolymers and secondary raw materials, *Proceedings of 3-th Central-Evropean Conference "Plastics Recycling. Science-Industry"*, Krynica, Poland, pp. 23-24.

Busko N., Barantsova A., Grishchenko V., Zanoaga M., Tanasa F., Myshak V. (2005) Synthesis and properties of block copolymers on the base of copolyamide and diene rubber. *Polymer Journal,* Vol. 27, No 3, pp. 194-201.

Busko N., Tanasa F., Barantsova A., Zanoaga M., Grishchenko V. (2008) Study of properties of some new thermoplastic block copolymers and their corresponding blends with secondary polyethylene. *Polymer Testing*, No 27, pp. 807-817.

Busko N. A., Grishchenko V. K., Barantsova A. V., Babkina N. V., Silchenko Yu. (2010) Physico-chemical properties of block copolymers based on polyazoinitiator and butylmethacrylate. *Kautshuk Gummi Kunstoffe,* No. 1-2, pp. 36-39.

Caillol S., Lecommandoux S., Mingotaud A. F., Schappacher M., Soum A., Bryson N., Meyrueix R. (2003) Synthesis and self-assembly properties of peptide-polylactide block copolymers. *Macromolecules,* Vol. 36, No 4, pp. 1118-1124.

Chao H., Murphy J., Pytela J., Tian N. (2003) New development of hydroxyl-terminated polybutadienes, *Proceedings of Conference Proceeding – Polyurethane Expo,* 1-3 October 2003, Orlando, United States, pp. 539–548.

Chen D. P., Wang J. (2006), Synthesis and characterization of block copolymer of polyphosphoester and poly(ε-caprolactone). *Macromolecules,* Vol. 39, No 2, pp. 473-475.

Choi Y. K., Bae Y. H., Kim S. W. (1998) Block copolymers: Synthesis, characterization, and their physical properties, *Macromolecules*, Vol. 31, No 25, pp. 8766-8774.

Cleary G. W. (1993) Transdermal delivery systems: a medical rationale, In: *Topical Drug Bioavailability, Bioequivalence and Penetration,* Shah V. P., Maibach H. I. (Eds.), Plenum, New York, USA, pp. 17–68.

Columbia Encyclopedia, (2001-2005) Sixth ed. Columbia University Press, New York, USA.

Crusos A., Ungureanu C., Rez T., Murariu G., Zanoaga M. (1983) Procedeu de obţinere a unor termoadezivi de tip copoliamidic. Romania Patent 82985.

Crusos A., Zanoaga M. (1989) Procedeu de obtinere a unor pulberi adezive pe baza de polimer copoliamidic. Romania Patent 97989.

Crusos A., Crusos G., Zanoaga M., Tataru D., Bordei A., Dobinda V. (1995) Metoda de macinare criogenica pentru transformarea diferitelor produse din granule in pulberi fine si foarte fine. Romania Patent 112252.

Dainton F. S., Evans D. M., Hoare F. E., Melia T. P. (1962) Thermodynamic functions of linear high polymers. Part 5. Cis- and trans-1,4- polybutadiene. *Polymer,* Vol. 3, No 2, pp. 297-309.

Drozdovskiy V.F. (1992) Status and prospects of processing and use of waste tires abroad. *Kauchuk and rezina*, No 4, pp.23-29.

El-Sabbagh S. H. (2003) Compatibility study of natural rubber and ethylene-propylene diene rubber blends. *Polymer Test.,* Vol. 22, No 1, pp. 93-100.

Eroglu M. S., Hazer B., Baysal B. M. (1998) Synthesis and thermal characterization of macromonomeric azo initiator containing poly(ε-caprolactone): styrene and methyl methacrylate copolymerization. *J. Appl. Polym. Sci.,* Vol. 68, No 7, pp. 1149-1157.

Estes G. M., Cooper S. L., Tobolsky A. V. (1970) Block polymers and related heterophase elastomers. *J. Macromol. Sci.* Vol. 4, No 2, pp. 313-366.

Faust R., Kennedy J. P. (1987) Living carbocationic polymerization. IV. Living polymerization of isobutylene. *J. Polym. Sci., Part A: Polym. Chem.,* Vol. 25, No 7, pp. 1847-1869.

Fedors R.F. (1979)**,** Glass transition temperature and molecular weight, *Polymer,* Vol. 20, No 9, pp. 1055-1056.)

Fraser C. L., Smith A. P., Wu X. (2000) Metal template-assisted block copolymer synthesis. Use of solvent polarity to control chain conformation and reactivity at the metal core. *J. Am. Chem. Soc.*, Vol. 122, No 37, pp. 9026-9027.

Furukawa J., Takamori S., Yamashita S. (1967) Preparation of block copolymers with a macro-azonitrile as an initiator. *Angew. Makromol. Chem.*, Vol. 1, No 1, pp. 92-104.

Gaynor S. G., Matyjaszewski K. (1997) Step-growth polymers as macroinitators for "living" radical polymerization. Synthesis of ABA block copolymers. *Macromolecules*, Vol. 30, No 14, pp. 4241-4249.

Godovsky Yu. K. (1977) *Differential scanning calorimetry in physico-chemical polymers,* Khimiya, Moscow, USSR.

Goncharuk G.P., Knunyants M.I., Kryuchkov A.N., Obolonkova E.S. (1998) Effect of the specific surface area and shape of rubber crumb on the mechanical properties of Rubber-modified plastics. *Vysokomol. soed. Ser. B,* Vol. 40, No 5, pp.873-877

Gritsenko F. R., Falchenko Z. V., Busko N. A., Grishchenko V. K. (1990) New initiators for radical polymerization. *Vysokomol. Soed.,* Ser. B, Vol. 32, pp. 728-734.

Gul V. E., Kuleznev V. N. (1979) *Structure and mechanical properties of polymers,* Chemistry, Moscow, USSR.

Gul V. E. (1986) More efficient use of secondary materials. *Plast. Masses,* No 6, pp.8-10.

Guo B., Cao Y., Jia D., Qiu Q. (2004) Thermoplastic elastomers derived from scrap rubber powder/LLDPE blend with LLDPE-graft-(epoxidized natural rubber) dual compatibilized. *Macromol. Mater. Eng.,* Vol. 289, No 4, pp.360-367.

Han C. J., Lee M. S., Byun D. J., Kim S. Y. (2002) Synthesis of hydroxy-terminated polyethylene via controlled chain transfer reaction and poly(ethylene-b-caprolactone) block copolymer. *Macromolecules,* Vol. 35, No 24, pp. 8923-8925.

Hadjichristidis N., Pispas S., Floudas G. (2002) *Block copolymers: synthetic strategies, physical properties and applications,* John Wiley & Sons, Inc., Hoboken, USA.

Hamley I.W. (1999) *Block Copolymers,* Oxford University Press, Oxford, England.

Hazer B. (1995) Synthesis of macroazoinitiators and their use in vinyl polymerization. *Macromol. Rep.,* Vol. A32, (suppls. 5&6), pp. 889-895.

Hu G.-H., Li H., Feng L.-F. (2002) A two-step reactive extrusion process for the synthesis of graft copolymers with polyamides as grafts. *Macromolecules,* Vol. 35, No 22, pp. 8247-8254.

Ignatious F., Lu C., Kim J., Kantor S. W., Lenz R. W. (1995) Liquid crystalline block copolymers containing rigid units and flexible ethylene terephthalate segments. *J. Polym. Sci., Part A: Polym. Chem.,* Vol. 33, No 8, pp. 1329-1335.

Ioanid A., David G., Simionescu B. C. (2003) Morphological study of poly[(N-acetylimino) ethylene]/polystyrene block and graft copolymers, *Rev. Roum. Chim.,* Vol. 48, No 11, pp. 873-879.

Judin V., Shatalov V., Nesterova S. (1975) *Synthesis, properties and application an isoprene-styrene and butadiene-styrene,* CNIITEchim, Moscow, USSR.

Jushik Y., Raman P., Darnel W. (2004) High performance TPVs for long term high temperature applications. *Rubber World*, Vol. 231, No 1, pp. 52-58.

Keoshkerian B., MacLeod P. J., Georges M. K. (2001) Block copolymer synthesis by a miniemulsion stable free radical polymerization process. *Macromolecules,* Vol. 34, No 11, pp. 3594-3599.

Kim S. W. (1996) Temperature sensitive polymers for delivery of macromolecular drugs, In: *Advanced biomaterials in biomedical engineering and drug delivery systems,* Ogata N., Kim S. W., Feijen J. (Eds.), Springer, Tokyo, Japan, pp. 126–133.

Kirilova E. I., Shulgina E. S. (1988) *Aging and stabilization of thermoplastics*, Khimiya, Moscow, USSR.

Kochetov D. P., Barantsova A. V., Grishchenko V. K, Trachevskiy V. V., Yatsimirskaya T. S. (1991) Structure of products by interaction acylhydrazones with isocyanate. *Ukr. Chim. J.,* Vol. 57, No 2, pp. 215-218.

Kotliar A. M., (1981) Interchange reactions involving condensation polymers. *J. Polym. Sci.: Macromol. Rev.,* Vol. 16, No 1, pp. 367-395.

Kowalska E., Wielgosz Z. (1996) Scrap rubber reused – a new process produces porous pipes from worn-out tyres. *Polymer Recycling,* Vol. 2, No 3, pp. 213-219.

Kuptsov A. K., Zhizhin G. N. (2001) *Fourier-CD and Fourier-IR Spectra of Polymers,* FIZMATLIT, Moscow, USSR.

Kuznetsova O. P., Zhorina L. A, Prut E. V. (2004) Blends based on ground tire rubber. *Vysokomol. soed. Ser. A.,* Vol. 46, No 2, pp. 275-284.

Kyoko K., Yuichi I., Takayuki O. (2004) Thermoplastic olefin elastomer composition. US Patent 6803418.

Lavik E. B., Klassen H., Warfvinge K., Langer R., Young M. J. (2005) Fabrication of degradable polymer scaffolds to direct the integration and differentiation of retinal progenitors. *Biomaterials,* Vol. 26, No 16, pp. 3187-3196.

Lin Y., Yakovleva V., Chen H., Hiltner A., Baer E. (2009) Comparison of olefin copolymers as compatibilizers for polypropylene and high-density polyethylene. *J. Appl. Polym. Sci.*, Vol. 113, pp. 1945-1952.

Lipatov Y.S. (1980) *Interfacial phenomena in polymers*. Naukova Dumka, Kyiv, Ukraine.

Lipatov Yu. S., Shilov V. V., Gomza Yu. P., Kruglyak N. E. (1982) *X-ray methods of characterization of polymer systems,* Naukova Dumka, Kyiv, Ukraine.

Lu S., Fan Q. L., Liu S. Y., Chua S. J., Huang W. (2002) Synthesis of conjugated-acidic block copolymers by atom transfer radical polymerization. *Macromolecules*, Vol. 35, No 27, pp. 9875-9881.

Maeda R., Hayakawa T., Tokita M., Kikuchi R., Kouki J., Kakimoto M., Urushibata H. (2009) Double liquid crystalline side-chain type block copolymers for hierarchically ordered nanostructures: Synthesis and morphologies in the bulk and thin film. *Reactive and Functional Polymers*, Vol. 69, No 7, pp. 519-529.

Mamunya Eu. P., Myshak V. D., Semenovich G. M., Lebedev E. V. (1990) The influence of polymer blends based on secondary thermoplastics on their structure and properties. *Plast. masses.*, No 9, pp. 48-54.

Mamunya E. P., Myshak V. D., Semenovich G.M., Lebedev E.V. (1994) Influence of interaction between the components on the properties of polymer-wood composites based on recycled thermoplastics. *Vysokomol. Soed. Ser. A*, Vol. 36, No 7, pp.1358-1361.

Mamunya Ye. P, Bey I.N, Tolstov A.L, Fainleib A.M., Gladkiy E.P. (2005) Thermal and Physical-mechanical properties of thermoplastic elastomers based on secondury polyethylene and rubber powder. *Polymer Journal*, No 2, pp.117-122.

Meier D. J. (Ed.) (1983), *Block copolymers science and technology*, Hardwood Academic, New York, USA.

Myshak V. D., Lebedev E. V., Gristchenko V. K., Mamunya E. P. (2002) Rubber-plastic composites based on thermoplastic polymers, *Proceedings of II-Ukrainian-Polish Conference "Polymers for special purposes"*, Dnepropetrovsk, Ukraine.

Myshak V.D., Lebedev E.V., Semynog V.V. (2004) Filled with rubber thermoplastics is the way to recycling of thermoplastic and elastomeric polymer. The III Int. scientific-technical. conf. "Composite materials", Kyiv, NTU "KPI", Ukraine, p.106.

Myshak V. D., Lebedev E. V. (2006). The problems of recycling of polymeric materials in Ukraine, *Proceedings of III Intern. conf. "Cooperation for Waste Issues"*, Kharkov, Ukraine, pp.176-178.

Moiseev V.V. (1985) *Thermoelastoplastics*, "Chimiyi", Moscow, USSR.

Nagamune T., Nagai S., Ueda A. (1996) Synthesis of (AB)n–type block copolymers employing surface-active macro-azo initiators. *J. Appl. Polym. Sci.*, Vol. 62, No 2, pp. 359-365.

Nakanasi K. (1965) *Infrared spectra and structure of organic compounds*, Mir, Moscow, USSR.

Narrainen A. P., Pascual S., Haddleton D. M. (2002) Amphiphilic diblock, triblock, polyblock copolymers. Synthesis and aggregation behavior. *J. Polym. Sci., Part A: Polym. Chem.*, Vol. 40, No 4, pp. 439-454.

Nielsen L. E. (1978) *Mechanical properties of polymers and composites.* Chimiyi, Moscow, USSR.

Noro A., Nagata Y., Tsukamoto M., Hayakawa Y., Takano A., Matsushita Y. (2005) Novel synthesis and characterization of bioconjugate block copolymers having oligonucleotides. *Biomacromolecules*, Vol. 6, No 4, pp. 2328-2333.

Noshey A., McGrath J. (1980) *Block copolymers,* Mir, Moscow, USSR.

Ozturk T., Cakmak I. (2007) Synthesis of block copolymers via redox polymerization process: A critical review. *Iranian Polymer Journal,* Vol. 16, No 8, pp. 561-581.

Pasko N.I., Boiko T.A., Drebezova L.P., Savelyeva N.V. (2006) Technology and equipment for the recycling of mechanical rubber waste, *Proceedings of the Third Int. Conf. "Cooperation for Waste Issues"*, Kharkov, Ukraine.

Park S., Cho D., Ryu J., Kwon K., Lee W., Chang T. (2002) Fractionation of block copolymers prepared by anionic polymerization into fractions exhibiting three different morphologies. *Macromolecules,* Vol. 35, No 15, pp. 5974-5979.

Perevosnik K. A., Jacob S., Stevenson W. G. (2004) Thermoplastic elastomers having improved adhesive properties. US Patent 6790911.

Popa M., Abadie M. J., Bulacovschi V., Arnautu Z. (1998) Systèmes multiphasiques à base des polymères thermoplastiques et élastomères. 2. Polymérisation d'une solution de polyisoprène en styrène. *Rev. Roum. Chim.,* Vol. 43, No 11, pp. 1069-1078.

Pospiech D. (2008) Influencing the interface in polymer blends by compatibilization with block copolymers. In: *Polymer surfaces and interfaces,* Etamm M (Ed.), Springer, Dresden, Germany, pp. 275-298.

Privalko V. P., In: Lipatov Yu.S. (Ed.) (1984) *The properties of polymers in block state. Handbook on polymer physical chemistry,* Naukova Dumka, Kiev, USSR.

Privalko V. P., Kramarenko V. Yu., Maslak Yu. V., Rosovitsky V. F. (1993) Mechanical properties of heterocyclic polymer networks. *Colloid & Polymer Science,* Vol. 271, No 4, pp. 322-331.

Privalko V., Mudrak C., Karpova I., Korskanov V., Shapoval R., Usenko A. (2000) Solution behavior of copoly(amide imide)s. *Designed monomers and polymers,* Vol. 3, No 3, pp. 363-367.

Rosovitsky V. F., Shifrin V.V. (1981) Simple method of dynamic mechanical analysis of polymers, In: *Physical methods of polymer characterization* (Ed. Privalko V. P.), Naukova Dumka, Kyiv, USSR, pp. 85 (in Russian).

Saunders J. H, Frisch K. C. (1962), Polyurethanes Chemistry and Technolgy, Part 1. Chemistry, In: *High polymers,* vol. XVI, Interscience Publishers, New York, USA, pp. 64-65, 72–75.

Schmalz H., Abetz V., Lange R. (2003) Thermoplastic elastomers based on semicrystalline block copolymers. *Compos. Sci. and Technol.,* Vol. 63, No 8, pp. 1179-1186.

Serenko O. A., Goncharuk G. P., Knunyants M. I., Kryuchkov A. N. (1998) Flow of highly filled thermoplastic-dispersed elastic filler compositions. *Vysokomol. Soed. Ser. A.,* Vol. 40, No 7, pp. 1186-1190.

Shalyganov E. F., Anisimov P. V., Borisov E. M. (2005) Resource-saving and environmentally friendly technology of recycling waste tires. *Kauchuk and rezina,* No 1, pp. 16-18.

Simionescu C. I., David G., Simionescu B. C., Paraschiv V. (1997) Photochemical polymerization of methacrylic acid in the presence of poly(N-acetyliminoethylene) macroinitiators. *Eur. Polym. J.,* Vol. 33, No 8, pp. 1251-1254.

Silverstein R. M., Bassler G. C., Morril T. C. (1974) *Spectrometric identification of organic compounds,* John Wiley & Sons, New York, USA.

Slonim I. Ya., Urman Ya.G. (1982) *NMR-Spectroscopy of heterochain polymers*, Khimiya, Moscow, USSR.

Sperling L.H. (Ed.) (1997) *Polymeric multicomponent materials. An introduction,* John Wiley & Sons, New York, USA.

Takeuchi D., Aida T. (2000) Sequential cationic and anionic polymerizations by titanium triflate complexes with bulky bisphenolate ligands. controlled one–pot synthesis of polyoxetane–poly(e-caprolactone) block copolymers. *Macromolecules,* Vol. 33, No 13, pp. 4607-4609.

Thurn-Albrecht T., Schotter J., Kastle C. A., Emley N., Shibauchi T., Krusin-Elbaum L., Guarini K., Black C. T., Tuominen M. T., Russell T.P. (2000) Ultrahigh-density nanowire arrays grown in self-assembled diblock copolymer templates. *Science,* Vol. 290(5499), pp. 2126-2129.

Titov G.V., Khmelenko G.I., Privalko V.P., in: Privalko V.P. (Ed.) (1980) *Physical Methods of Polymer Characterization*, Naukova Dumka, Kiev (in Russian).

Trofimova G. M., Novikov D. D., Kompaniets L. V. (2003) The modification of rubber crumb. *Vysokomol. Soed, Ser. A,* Vol. 45, No 6, pp. 912-920.

Tsitsilianis C., Voulgaris D. (1997) Poly(2-vinylpyridine)-based star-shaped polymers. Synthesis of heteroarm star (AnBn) and star-block (AB)n copolymers. *Macromol. Chem. Phys.,* Vol. 198, pp. 997-1007.

Ueda A., Agari Y., Nagai S., Minamii N. (1989) Synthesis of new macro-azo-initiators for block copolymerization. *Chem. Express,* Vol. 4, No 3, pp. 193-196.

Ueda A., Agari Y., Nagai S., Minamii N. (1990) Synthesis of macro-azo-initiators from azo-diols and the block copolymerization. *Kobunshi Ronbunshu,* Vol. 47, No 4, pp. 321-329.

Ueda A., Agari Y, Kosai K., Nishioka N. (1992) Synthesis of polyvinylpyrrolidone-polystyrene block copolymer by the use of a macro-azoinitiator. *Chem. Express,* Vol. 7, No 9, pp. 725-728.

Ueda A., Nagai S. (1994) Macroinitiators including syntheses and applications of block copolymers derived therefrom. *Macromolecular Design: Concept and Practice.*, (M. K. Mishra, ed.), Polymer Frontiers, Int. Inc., New York, pp. 265-312.

Ueda A., Shimada M., Agari Y., Nishitsuzi H., Nishioka N. (1996) Synthesis of polystyrene-polyperfluoroacrylate block copolymers by the use of macro-azo-initiator and surface properties of molded plate of the block copolymer/polystyrene blends. *Nippon Setchaku Gakkaishi,* Vol. 32, No 2, pp. 44-50.

Valetsky P. M., Storojuk E. P. (1979) Block copolymers of polycondensation type. *Successes of Chemistry,* Vol. 48, No 1, pp. 75-114

Vera M., Franco L., Puiggali J. (2004) Synthesis of Poly(ester amide)s with lateral groups from a bulk polycondensation reaction with formation of sodium chloride salts. *Macromol. Chem. Phys*., Vol. 205, pp. 1782-1792.

Verdonck B., Goethals E. J., Du Prez F. E. (2003) Block copolymers of methyl vinyl ether and isobutyl vinyl ether with thermo-adjustable amphiphilic properties. *Macromol. Chem. Phys.,* Vol. 204, No 17, pp.2090-2098.

Wol'fson S.A. Recycling of polymers (2000) *Vysokomol. soed. Ser. S,* Vol. 42, No 11, pp. 2000-2014.

Volkov V.P., Zelenetsky A.N., Fedoseev M.S. (2004) Mechanochemical modification of polyethylene vinyltrialkoksisilanes. *Plast. masses.*, No 10, pp. 33-38.

Walz R., Bomer B., Heitz W. (1977) Monomeric and polymeric azoinitiators, *Makromol. Chem.,* Vol. 178, pp. 2527-2534.

Walz R., Heitz W. (1978), Preparation of (AB)n-type block copolymers by use of polyazoesters. *J. Polym. Sci., Polym. Chem. End*., Vol. 16, No 8, pp. 1807-1814.

Wolfson S.A. (2000) Recycling of polymers, *Vysokomol. Soed. Ser. S.,* Vol .42, No 11, pp. 2000-2014.

Wunderlich B, Jones L. D. (1969) Heat capacities of solid polymers. *J. Macromol. Sci. Ser. B,* Vol. 3, No 1, pp. 67-79.

Xiong X. Y., Tam K. C., Gan L. H. (2003) Synthesis and aggregation behavior of pluronic f127/poly(lactic acid) block copolymers in aqueous solutions. *Macromolecules*, Vol. 36, No 26, pp. 9979-9985.

Yagci Y., Denizligil S. (1991) Functional polyamides. 2. The use of multifunctional polyazoamide for the synthesis of block copolymers. *Eur. Polym. J.*, Vol. 27, No 12, pp. 1401-1404.

Yildiz U., Cape I. (2003) Microemulsion polymerization of styrene in the presence of macroinimer. *Polymer*, Vol. 44, pp. 2193–2200.

Yildiz U., Hazer B. (2000) Dispersion redox copolymerization of methyl methacrylate with macromonomeric azoinitiator as a macrocrosslinker, *Polymer*, Vol. 41, No 2, pp. 539-544.

Yokozawa T., Ogawa M., Sekino A., Sugi R., Yokoyama A. (2002) Chain-growth polycondensation for well-defined aramide. Synthesis of unprecedented block copolymer containing aramid with low polydispersity. *J. Am. Chem. Soc.*, Vol. 124, pp.15158-151589.

Yuichi I., Akira U. (2004) Thermoplastic elastomer composition with high resistance to thermal deterioration. US Patent 6720376.

Zanoaga M. (2001) Novel thermoplastic copolyamides based on caprolactam, 1,6-hexane diamine. Synthesis and study of properties, *Proceedings of 12th Romanian International Conference on Chemistry and Chemical Engineering - RICCCE*, 13-15 September 2001, Bucureşti, Romania.

Zhuang, J., Engel A., Pages J-M., Bolla J. M. (1997) The Campylobacter jejuni porin trimers pack into different lattice types when reconstituted in the presence of lipid. *Eur. J. Biochem.*, Vol. 244, No 2, pp. 575-579.

Chapter 4

Polymeric Materials on the Base of Oligomers with Terminal Functional Groups

Volodymyr GRISHCHENKO, Antonina BARANTSOVA, Vitaliy BOIKO, Nataliya BUSKO

Institute of Macromolecular Chemistry of National Academy of Sciences of Ukraine, Kyiv

---

Summary

A progressive method of polymer synthesis without solvents, through a stage of an isocyanate prepolymer (liquid rubber), was developed. On this base, a range of polymeric composites with controlled characteristics and required physical-mechanical properties can be developed. It is a result of using carbochain oligomers with different end groups which can be obtained with the help of specially synthesized initiators for radical polymerization. Using the liquid rubbers with different functional end groups, polymeric materials with properties ranging from sticky adhesives, mild elastic adhesives to strong abrasive-resistance materials resistant over a wide temperature interval, were prepared.

Notations and acronyms

AIBA	2,2'-azo-bis-izobutiroamide
AIBN	2,2'-azo-bis-izobutironitrile
AIH	2,2'-azo-bis-izobutirohydrazide
AIHN-A	2,2'-azo-bis-izobutirohydrazone acetone
AIHN-M	2,2'-azo-bis-izobutirohydrazone methyl-ethyl-ketona
AIHN-D	2,2'-azo-bis-izobutirohydrazone dipropilketona
AIHN-CH	2,2'-azo-bis-izobutirohydrazone cyclohexanona
AIHN-B	2,2'-azo-bis-izobutirohydrazone diisobytylketona
β-AIOEA	2,2'-azo-bis-izobutiro-β-oxiethylamide
DMA	dimethacrylate
EG	epoxy group
FD	functionality distribution
HTPD	hydroxyl-terminated polydienes
HTPB	hydroxyl-terminated polybutadiene
HTPI	hydroxyl-terminated polyisoprene
HP	hydrogen peroxide
ODH	oligodienedihydrazide
ODHN	oligodienedihydrazone
ODUI	oligodieneurethanediisocyanate
OIH	oligoisoprendihydrazide
OIHN-A	oligoisoprendihydrazone acetone
OIHN-M	oligoisoprendihydrazone methylethylketone
OIODC	oligoisoprenoksadiazolinilcarbomatdiisocyanate
ORD	oligomer radical dienic
PDODC	poly(diene oxadiazolinyl carbamate acrylates)
PDUA	poly(dien urethane acrylates)
PEUA	poly(ester urethane acrylates)
PDUE	polybutadieneurethaneepoxide
PE	polyethylene
PIODC	polyisoprenoksadiazolinilcarbomate
PP	polypropylene
PU	polyurethane
2,4-TDI	2,4-toluenediisocyanate
DSC	differential scanning calorimetry
C_p	heat capacity, J/(g·K)
$\Delta_f H^0$	standard enthalpy of reaction
M_n	molar mass, kg mol^{-1}
T	temperature, K
T_c	glass temperature

1. Introduction

Liquid oligomer systems are characterized by a certain type of the intermolecular organization which influences laws of formation and polymer properties *[Grishchenko1985; Maslyuk1989; Mejikovskiy, 2005, 2008]*. One of the important factors defining supramolecular structure of polymer is the presence of polar functional groups able to form molecular associates of different types. The influences of functional end groups oligomers of different chemical nature on laws of synthesis and properties of the new obtained polymeric materials have been studied.

The liquid rubbers are synthetic oligomers, that yield in rubbery materials at curing (vulcanizations) *[Mogilevich, 1983; Petrov,* 1983*]*. By their nature and basic chain microstructure, diene liquid rubbers (oligodienes) are analogous to synthetic or natural rubber (so-called without functional liquid rubbers), and can contain functional groups (OH, COOH, NH_2, epoxide or other) located statistically along the chain or only at the ends. Liquid rubbers are viscous liquids with MM 500-10000 (usually 1000-4000). They can be modified at the double bonds of the main chain (hydrogenation, malleinization, epoxidation, halogenation or other) and at functional groups, in particular the pendant functional groups.

At present, oligodienes with functional end groups gain a great importance not only as sealants, filling materials, insulants, but also as polymer modifiers, first of all rubbers and epoxy resins, as compatibilizers in polymeric composites, particularly in rubberplasts *[Grishchenko and Boiko, 2004; Gusev et al., 2009]* etc. Efficiency of their use in these applicatios is determined by the wide range of possibilities of adjusting their properties by varying the nature and content of functional groups, molecular weights, microstructure, viscosity etc. that enables the decision concerning the diverse technical tasks. The distribution by functionality (FD) is the factor of outmost importance for functionalized oligomers because it determines the uniformity of chemical network and, consequently, properties of material. Azoinitiators are the best initiators. They cleave with the formation of radicals with low activity in the chain transfer reactions, and their decomposition constants slightly depend on solvent *[Boiko, 2004]*. Peroxide initiators – peroxides and hydroperoxides – give much wider FD, first of all, due to the high activity of oxyl radicals. As the cost of azoinitiators exceeds manifold the one of peroxide`s, the formers are used mainly in those areas where very high quality materials and wares are required, while the latters are used in mass-production and customary performance applications.

It is known that the best properties of polymers based on liquid hydrocarbon rubbers (LHR) are obtained in the case of reactions at terminal groups *[Grishchenko, 1992, 2000]*. In this respect, the researches on systems which are cured by polyaddition attract considerable theoretic and practical interest due to the advantages of polymer materials based on rubbers. They are highly resistance in aqueous medium, show frost resistance, elastic properties, and good dielectric characteristics. Investigations on new oligomeric curing systems give the possibility not only to enlarge the present variety of materials, but also to obtain new materials possessing properties which are not accessible in known systems using hydrocarbon rubbers as components.

At the Institute Macromolecular Chemistry of NAN of Ukraine, research on synthesis of oligodienes with terminal functional groups and polymeric materials based on them has been conducted for many years. Oligodienes with hydroxyl *[Grishchenko, 1992]*, amine *[Gritsenko, 1972a]*, hydrazide, acylhydrazone *[Grishchenko, 2000]*, hydroxyethylamide *[Grishchenko, 1986]*, isocyanate *[Barantsova, 2002]* and other end groups have been synthesized. They have molecular weight 500-6000, viscosity 15-90 Pa·s and functionality close to 2.

2. Initiators for reactive oligomers

2.1 Hydrogen peroxide

Hydrogen peroxide (HP) is the first member of the homologous series of peroxides and hydroperoxides. They are mainly obtained with HP as a source of active oxygen *[Antonovskyi, 1972]*. Although HP is known for long time as initiator of radical polymerization, it did not have a wide range of industrial applications in this quality. An exception is oligobutadiene with hydroxyl terminal groups (HTPB). This oligomer is produced at industrial scale only in a few countries *[Boiko and Grishchenko, 2011]*.

The low cost and ecological friendly character are the main advantages of HP: it decomposes with releasing water and oxygen. However, due to its high bond strength (HO-OH bond strength is 214.2 kJ/mol) additions of activators is required for its homolytic decomposition; activators lower the activation energy of decomposition. Other deficiency of this initiator is the high non-selective activity of hydroxyl radical. High chemical activity of HP, dependency of decomposition speed and mechanism on medium (both solvent and monomer), complexity of the decomposition mechanism itself make hitherto the wide application of HP in radical polymerization even more difficult *[Grishchenko, 2000]*. Taking into account the fact that HP is a source of active oxygen for obtaining more expensive and dangerous (hydro)peroxides, the research of HP decomposition mechanisms is very actual considering its use in polymerization processes instead of (hydro)peroxides, thus eliminating the labor-consuming synthesis of these HP derivatives. Once more, the limiting factor is HP immiscibility with non-polar substances. However, this problem is decided in industry by choosing common solvents for HP and monomer or by using emulsion polymerization method *[Mogilevich et al., 1983]*. Thus, the comprehensive research of HP as initiator of radical polymerization corresponds to the modern trends in technologic development by economic and ecological criteria.

2.2 Azoinitiators

One of advantages of azoinitiators, in comparison with initiators from other classes of organic substances, is the fact that decomposition takes place by a reaction of the first order and the rate of decomposition depends only on temperature and not on medium *[Pronin, 1977]*. Initiators of this type are not sensitive to inductive influences; don't participate in reaction of the chain transfer. Introduction of functional groups into the azoinitiators structure doesn't render special influence on their ability to initiate, caused by remoteness of functional groups from the reactive center *[Costa 2010; Drach, 1977; Dumitri, 1983; Hepuzer, 2004; Yoshida 2004]*. Bis-structure azoinitiators allows bifunctional oligomers. One of the most extended azoinitiators is 2,2'-azo-bis-izobutyronitrile (AIBN) used in polymerization *[Burkhart, 1969; Costa 2010; Van Hook, 1958; Yiğitoğlu, 2007]*. AIBN is a toxic compound, which decomposes by the absorption of thermal or photochemical energy into two free radicals and nitrogen:

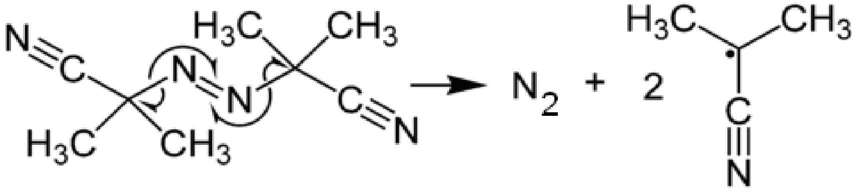

These radicals can be used to initiate free radical polymerization and other radical reactions. The rate of free radical formation can be controlled by the temperature. The presence of additives does not affect its rate of decomposition. AIBN does not cause oxidative degradation and discoloration, generally associated with peroxides. This enables transparent polymers able to maintain their physical properties.

Introduction of reactive end groups into the azoinitiator structure allows to regulate their physical and chemical properties (solubility, melting and decomposition temperatures etc.) and also to obtain bifunctional oligomers *[Busko, 2000; Kochetov, 2001; Zil'berman, 1972]*.

Azoinitiators with various reactive functional groups: 2,2'-azo-bis-izobutirohydrazide (AIH) *[Gritsenko, 1972b]*, 2,2'-azo-bis-izobutirohydrazone acetona (AIHN-A), 2,2'-azo-bis-izobutirohydrazone methyl-ethyl-ketona (AIHN-M), 2,2'-azo-bis-izobutirohydrazone cyclohexanona (AIHN-CH) *[Gritsenko, 1990]*, 2,2'-azo-bis-izobutiroamide (AIBA) *[Gudzenko, 2010]*, 2,2'-azo-bis-izobutiro-β-oxiethylamide (β-AIOEA) *[Grishchenko, 1986]* described by a general formula:

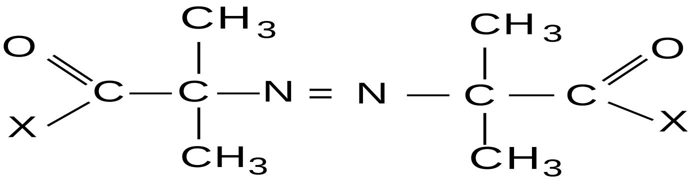

$$\mathrm{X(O{=})C-C(CH_3)_2-N=N-C(CH_3)_2-C({=}O)X}$$

where: X = $NHNH_2$, NH_2, $NHCH_2CH_2OH$, NH-NH=C(R_1R_2), (R_1, R_2 – alkyl, aryl, cycloalkyl, etc.) have been synthesized.

The azoinitiators have differed solubility in polar and nonpolar mediums and decomposition rate constant (Table 1). The possibility of introduction of various terminal functional groups into oligomers, which may interact with a broad range of reagents, permits to develop oligomeric formulations with controlled conditions of curing and cured polymers with required properties.

Table 1. Properties azoinitiators with functional groups

Initiator	Conversion	MM	Functional groups, %	T_{melt}, K	Gas number, mg/g
AIH	87	230	40.7	433-435	103
AHN-A	89	265	26.5	427-429	-
AHN-M	90	338	32.5	367-369	-
AHN-CH	86	390	41.5	395-397	-
β- AIOEA	95	288	29.86	412-413	78
AIBA	60	200	41.3	404.5-405	112

Introduction of polar functional groups into azoinitiators allows increasing their solubility in various solvents and monomers that allows the oligomerization without solvent (Table 2). Solubility of AIH makes it fit for polymerization of water-soluble monomers.

Using the synthesized azoinitiators by thermo- and photo-initiated polymerization under mild conditions, in solution and in bulk, reactive oligomers with functional groups have been obtained. Incorporation of groups of various chemical natures into an azoinitiator makes possible the adjustment in a broad range of properties of oligomers obtained on their base.

Table 2. Solubility of azoinitiators with functional groups and kinetic parameters of initiation of isoprene polymerization in methanol

Initiator	**Solubility, mol/l**			**$\lambda\cdot10^{-4}$,s^{-1} (T=368K)**	**f**	**E_{act}, kJ/mol**
	water	**methanol**	**benzene**			
AIH	0.7	0.025	-	0.47	0.72	127.3
AHN-A	-	0.90	0.04	0.30	0.44	149.2
AHN-M	-	1.80	0.05	0.37	0.50	144.6
AHN-CH	-	2.5	0.22	0.37	0.77	108.7

2.3 Synthesis of hydroxy-containing oligodienes with hydrogen peroxide

Polymerization of dienes under the action of HP begun in the middle of the past century – the first patents appeared in 1945. The first academic research *[Baxendale et al., 1946]* was performed using methylmethacrylate as monomer and the Fenton reagent as initiator. The Fenton reagent is an oxidative-reducing system consisting of a mixture of HP and ferrous sulphate (II) in acid medium *[Sychev and Duka, 2002]*, in which hydroxyl radicals are actively generated already at room temperature. Authors *[Baxendale et al., 1946]* also revealed the fact of including hydroxyl terminal groups into polymers. Since then, many works were conducted on the polymerization initiated with the Fenton reagent. This method appeared especially effective for polymerization of water soluble monomers, such as (meth)acrylic acid and their salts, vinylpyrrolidone etc. *[Kirsh, 1999]*.

Emulsion polymerization and copolymerization of butadiene and styrene under the action of HP and ferrous sulphate were studied *[Marvel et al., 1948]*. The ferric sulphate showed approximately the same efficiency and, in the presence of sodium pyrophosphate, both salts showed a synergistic effect increasing the yield in copolymer approximately twice. Ferripyrophosphate also was an activator of HP decomposition, providing high yields for some polymers (Table 3).

In spite of these quite good results, the production of typical rubbers by polymerization initiated HP did not gain further development. This method achieved a commercial application for manufacturing low-molecular oligomeric dienes containing hydroxyl end groups, otherwise named liquid rubbers *[Mogilevich et al., 1983; Grishchenko and Boiko, 2004; Gusev et al., 2009; Boiko and Grishchenko, 2011]*.

Table 3. Polymerization of some monomers in the system HP–ferripyrophosphate *[after Boiko and Grishchenko, 2011]*

Monomer	Conversion, %
Butadiene	69
Styrene	95
Butadiene + styrene 3:1 (wt.)	80
Acrylonitrile	5
Vinylacetate	0
Methylacrylate	99

Oligodienes with hydroxyl end groups (HTPD: HTPB with butadiene and HTPI with isoprene) are basic classes of liquid rubbers - low-molecular forms of ordinary high-molecular rubbers. Due to their liquid consistency, they are processed by the technology of the reactive injection molding, having large advantages over traditional technology of rubber. HTPD are the hydrocarbon analogues of polyethers and polyesters and as well as those used for the production of PUs. They find application for the fabrication of waterproof, frost-resistant and anti-abrasion elastomers and insulants *[Schnecko et al., 1978; Zachariasiewicz, 1986; Boutevin et al., 2007]* due to their high hydrophobicity, flexibility of chain, and capacity towards easy modification at both hydroxyl groups and double bonds in the main chain, availability for filling with fillers of various types. The technology of making PU casting tires has been worked out from HTPB, which reduces production time by 1.5-2 times, energy output and working areas by 2-3 times against traditional technology, promotes their property of being environmentally friendly at the simultaneous considerable improvement of quality and operating properties *[Veselov et al., 2008]*. Lately *[Barcia et al., 2004; Raju et al., 2008]*, HTPB and products of its modification are intensively studied as modifiers of epoxy resins for increasing their toughness and bending strength. It can be assumed that in the near future epoxy resins free from traditional shortcomings through additions of oligodienes will go out to the wide market. All the above mentioned testifies that HTPD have good prospects and the demand will grow up to a considerable volume.

The hydroxy-containing oligodienes are manufactured in industry since the sixties of the past century. The typical synthesis of HTPD is carryed out under the action of HP in solutions of alcohols which are common solvents for the non-polar phase of diene and HP water solution *[Grishchenko and Boiko, 2004]*. It is appeared, however, that alcohols are not only solvents in the process but they are also activators for HP decomposition, and the hydroxy-containing fragments of alcohols enter the composition of oligomers *[Grishchenko et al., 1992]*.

The inclusion of alcohol fragments into oligomers is supported by data on functionality of oligomers in solutions of labeled ^{14}C primary methyl, ethyl and secondary isopropyl (IPA) alcohols (Table 4).

Table 4. Functionalities of oligoisoprenes synthesized in labeled alcohol solutions *[after Valuev et al., 1982]*

Alcohol	**Monomer conversion (%)**	**Molecular weight (M_n)**	**Average functionality**	
			By acetylation results f_n^{ac}	By label f_n^*
Methyl	25	1850	2.03	0.46
	-	2100	2.06	0.45
	50	1700	2.04	0.47
	54	1850	2.07	0.60
	72	1900	1.96	0.74
Ethyl	25	2150	1.94	0.38
	40	2310	1.95	0.35
	45	2400	1.94	0.35
	74	2950	2.01	0.45
Isopropyl	38	4600	1.47	0.43
	40	1700	1.59	0.51
	-	2250	1.52	0.51
	60	4700	-	0.47
	74	4050	1.67	0.44
	80	2250	1.77	0.52

It can be seen that functionality in primary alcohols is close to 2, whereas in IPA it close to 1.5 (at a conversion of 60 %). Taking into account a label (which incorporates into oligomer primary hydroxyl groups from methanol, secondary from ethanol and tertiary from IPA), functionality was calculated in oligomer obtained in IPA (Table 5).

Table 5. FD oligoisoprenes synthesized in labeled isopropyl alcohols *[after Valuev et al., 1982]*

Sample	$\bar{M}_n$	**FD, mol. % by primary OH-groups**			$\bar{f}_n$ **(by acetylation)**	**FD, mol. % by primary and tertiary OH-groups**			$\bar{f}_n$ **(by FD)**	$\Sigma f_i m_i$ **(acetylation + label)**
		1	2	3		1	2	3		
1	1700	41	59	-	1.59	8	87	5	1.97	2.03
2	1400	45	55	-	1.55	5	81	14	2.09	2.12

It appeared that at the account of label, that is tertiary hydroxyl groups, the number-average functionality calculated based on the results of chemical analysis of hydroxyl groups is close to 2, as in other alcohols.

Thus, the obtained data allow to conclude that during polymerization of dienes initiated by HP in alcohol solutions, the alcohol fragments containing hydroxyl groups are included into oligomers as end-capping fragments. Functionality by these groups is close to 0.5, namely, every fourth end group presents an alcoholic fragment, regardless the alcohol employed in the reaction. Such situation can take place when initiation of polymeric chains fulfills by hydroxyl radicals and alcohol radicals, containing hydroxyl groups, in equal amounts. Termination of chains is realized only by hydroxyl radicals or through the chain transfer by macroradical onto HP *[Grishchenko et al, 1992]*. The original scheme of the polymerization reactions sequence is presented (for simplicity, only 1,4-structure and butadiene used as monomer were indicated everywhere):

1. Generation of primary initiating radicals by decomposition of complex HP-IPA

$$[H_2O_2 \ldots (CH_3)_2CHOH] \rightarrow HO\bullet + (CH_3)_2C\bullet OH + H_2O$$

2. Initiation:
   i) by hydroxyl radical

$$HO\bullet + CH_2{=}CHCH{=}CH_2 \rightarrow HOCH_2CH{=}CHCH_2\bullet$$

   ii) by alcoholic radical

$$(CH_3)_2C\bullet OH + CH_2{=}CHCH{=}CH_2 \rightarrow HOC(CH_3)_2CH_2CH{=}CHCH_2\bullet$$

3. Chain propagation:

$$HOCH_2CH{=}CHCH_2\bullet + (n-1)\ CH_2CH{=}CHCH_2 \rightarrow HO(CH_2CH{=}CHCH_2)_n\bullet$$

$$HOC(CH_3)_2CH_2CH{=}CHCH_2\bullet + (n-1)\ CH_2CH{=}CHCH_2 \rightarrow$$

$$\rightarrow HOC(CH_3)_2(CH_2CH{=}CHCH_2)_n\bullet$$

4. Termination:

$$HO(CH_2CH{=}CHCH_2)_n\bullet + H_2O_2 \rightarrow HO(CH_2CH{=}CHCH_2)_nOH + \bullet OH$$

$$HOC(CH_3)_2(CH_2CH{=}CHCH_2)_n\bullet \; + H_2O_2 \rightarrow$$

$$\rightarrow HOC(CH_3)_2(CH_2CH{=}CHCH_2)_nOH \; + \; \bullet OH$$

The analysis according literature data *[Deb, 1975]* shows that in this system termination by primary hydroxyl radicals is less probable than transfer onto HP.

This scheme explains all experimental facts we found, namely:

- possibility of generating radicals from HP already at the temperature of oligomerization 363 K
- incorporation of hydroxy-containing alcoholic radicals into molecules of oligomers
- lower effective functionality of oligomers obtained in solution of IPA due to the presence of tertiary hydroxyl groups
- order on monomer higher than 1.5 in IPA

It was afterwards discovered that HP does not decompose to radicals in the presence of IPA at the temperature of polymerization 363-373 K, so the stage 1 of the scheme must be specified. Orders of polymerization reactions by monomer and initiator were measured out *[Boiko, 2008]* in order to complete the scheme with corresponding specifications. The average values of orders for five series of experiments (at a confidence level of 95%) are:

- order by monomer $a = 1.69 \pm 0.05$
- order by initiator $b = 0.75 \pm 0.04$.

It was noted that an order by monomer (isoprene) considerably exceeds value 1.0 and by initiator (HP) has a value 0.5, characteristic for ideal radical polymerization. Because the polymerization of isoprene in IPA is accompanied by the separation of oligomer as thin emulsion, polymerization of isoprene was conducted in ethyl acetate, in which both monomer and oligomer are soluble *[Boiko, 2010]*. In this case, the values were: $a = 1.49 \pm 0.03$ and $b = 0.46 \pm 0.05$. The first value is close to 1.5 and indicates the interaction between initiator and monomer in the process of initiation; the second one fits the ideal value of an order by initiator. These results unambiguously pointed that monomer takes part in the process of initiation. However, we cannot exclude solvent from this process, because the fragments of alcohols are incorporated into oligomer. Therefore, we postulated the formation of the triple complex isoprene - IPA - HP, which spontaneously decomposes to two primary radicals, with the release of one molecule of water:

$$H_2O_2 + CH_2{=}CHCH{=}CH_2 + (CH_3)_2CHOH \rightarrow HOCH_2CH{=}CHCH_2\bullet \; +$$

$$+ (CH_3)_2C\bullet OH \; + H_2O$$

To confirm this assumption, thermochemical calculations of the HP reactions with monomer and solvent and in a triple complex were performed. From the possible reactions of HP with IPA *[Boiko and Dyakova, 2010]*, the most advantageous is the following reaction:

$$H_2O_2 + (CH_3)_2CHOH \rightarrow (CH_3)_2C\bullet OH + \bullet OH + H_2O,$$

for which standard enthalpy is $\Delta_f H^0 = 99.2$ kJ/mol. Standard enthalpy of a reaction of HP with butadiene is $\Delta_f H^0 = 46.0$ kJ/mol. Only the reaction of decomposition of triple complex has negative value $\Delta_f H^0 = -69.0$ kJ/mol, because it can proceed spontaneously.

The simplest interaction mechanism of the components and decomposition of the triple complex (A) supposes the simultaneous forming of hydroxyl and alcoholic hydroxy-containing radicals *[Boiko and Grishchenko, 2009]*:

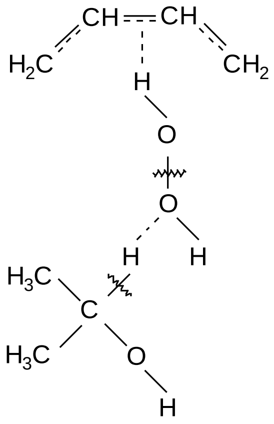

A

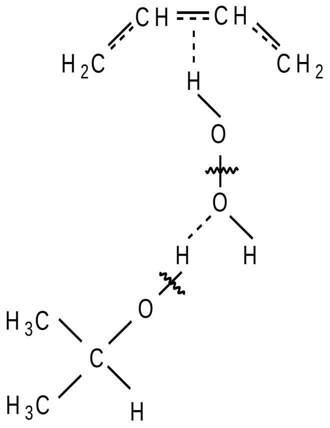

B

However, the quantum-chemical calculations showed *[Solovyev et al., 2011]* that the complex decomposition can not evolve in this manner. The complex is formed by the participation of hydrogen from alcoholic hydroxyl groups (B), but not α-hydrogen of methine groups, the weakest hydrogen bond to an atom of carbon. The molecule of IPA is coordinated by HP with hydrogen from hydroxyl group (Scheme II). At decomposition of this complex, an alkoxyl radical $(CH_3)_2CHO\bullet$ is formed, not a radical with a center on the α-atom of carbon of alcohol $(CH_3)_2C\bullet OH$, this is an alcohol radical which does not save a hydroxyl group. However, it is known *[Burchill and Ginns, 1970]* that an alkoxyl radical underwent a rapid isomerization into hydroxy-containing one:

$$(CH_3)_2CHO\bullet \rightarrow (CH_3)_2C\bullet OH$$

The latter initiates the polymerization at the interaction with the monomer molecule, including thus a tertiary hydroxyl group into the oligomer, fact which was discovered experimentally *[Grishchenko et al., 1992]*.

Therefore, complex research on the reaction of initiation of dienes polymerization under the action of HP with chemical, radiochemical, quantum-chemical, kinetic methods allowed the plausible mechanism of generation of radicals from HP. This mechanism includes the formation of a supramolecule diene-alcohol-HP through hydrogen bonds, whose decomposition to radicals is thermochemically advantageous. The scheme presented herein is consistent with data on FD and the results of chemical analysis of hydroxyl groups, and it can be useful (taking into account specific features) in other polymerization systems under the action of HP.

2.4 Properties of hydroxy-containing oligodienes

The properties of commercial marks HTPB (trade mark Poly-bd) of Sartomer Co. (USA) are shown in Table 6.

Table 6. The properties of commercial products of Sartomer *[after Sartomer, 2002]*

Product	Functionality	Vinyl group content, %	Mol. weight M_n	Hydroxyl number, mol_{eq}/g	Viscosity Pa s, 30 °C	Notes
R-45HTLO	2.50	20	2800	0.84	5.0	standard product
R-20LM	2.50	20	1350	1.70	1.4	with lowed viscosity
LF1	2.35	31	2291	0.87	5.0	with lowed functionality and lowed content of vinyl groups
LF2	2.20	42	2029	0.89	5.3	with lowed functionality and medium content of vinyl groups
LF3	2.05	53	2474	0.90	5.8	with lowed functionality and high content of vinyl groups
600E	2.50	20	1350	1.70	7.0	epoxized, eqv. on EG 460
605E	2.50	20	1450	1.74	22.0	epoxized, eqv. on EG 300

HTPB of Liquiflex brand produced by the company Petrochem (Brazil) has similar characteristics *[Pennachi et al., 1988]*. A difference between them consists in that Sartomer produces liquid rubbers with the use of isopropyl alcohol, while Petrochem use ethanol. Properties of rubbers and PUs made from both oligodienes are close.

These products have number-average functionality higher than 2 which causes difficulties for obtaining macrodiisocyanates – forepolymers with isocyanate terminal groups. On the other hand, branching agent assisting formation of network during obtaining elastic materials is not required at their curing. However, a bifunctional product is preferable. It can be obtained under polymerization at lower temperatures – no higher than 363 K. The characteristics of the typical sample obtained under such condition (ORD – oligomer radical dienic) is shown in Table 7.

It is known that, practically, any functional group may be introduced in polymers (oligomers) with hydroxyl terminal groups through macrodiisocyanate. It is easily formed from HTPD even at room temperature, because the reactivity of hydroxyl groups in oligodienes is much higher than in oligoethers *[Boiko et al., 2010]:*

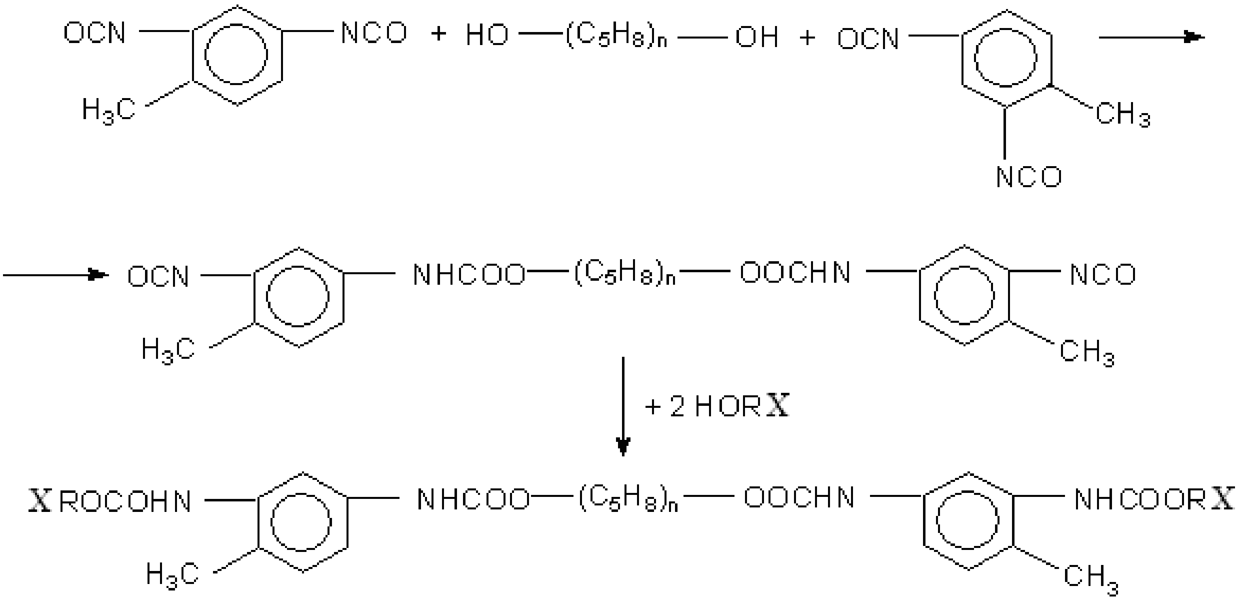

where X is a requested functional group.

Thus, HTPD are base products for obtaining oligomers with different functional end groups. This is the way we synthesized oligodienes with carboxyl, epoxy, tertiary amine, amide and other functional end groups *[Boiko and Grishchenko, 2011]*.

Dienes are easily copolymerized with a wide range of monomers. Co-oligomers of isoprene with acrylonitrile were also obtained under the action of HP.

Table 7. The properties of oligobutadiene ORD, synthesized in methyl and butyl alcohols at 363 K *[after Spirin and Grishchenko, 1969]*

Product	**Functionality**	**Vinyl group content, %**	**Mol. weight M_n**	**Content of hydroxyl groups, %**	**Viscosity Pa s, 30 °C**
ORD-M	2.0-2.1	20	2000	1.8	7
ORD-B	2.02	24	1600	2.14	9

Further treatment of this product with HP results in simultaneous appearance of amide and epoxy groups due to the reaction of HP with nitrile groups and double bonds of oligomer (the Radziszewski-Payne reaction) *([Boiko and Grishchenko, 2011])*. Co-oligomers of isoprene with allyl alcohol *[Boiko et al., 2011]* and co-oligomers of butadiene (in the composition of the C_4 fraction from oil refining) with other monomers *[Grishchenko et al., 1996]* have been prepared.

2.5 Synthesis of oligodienes with functional groups based on azoinitiators

In free-radical polymerization, the mode of bimolecular termination is very important: this affects the degree of polymerization and the molecular weight distribution of the resulting polymer *[Bessière, 1993]*. Bis-structure azoinitiators allows bifunctional oligomers with different terminal groups.

Using synthesized azoinitiators, the reactive oligomers, described by the common formula:

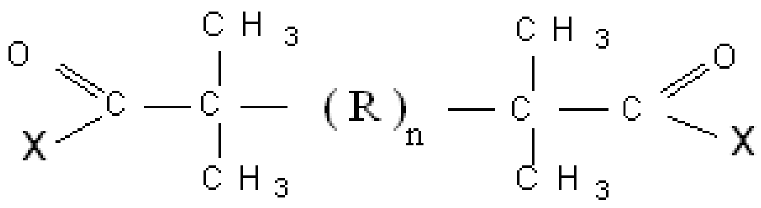

$$X-\overset{\overset{O}{\|}}{C}-\underset{CH_3}{\overset{CH_3}{C}}-(R)_n-\underset{CH_3}{\overset{CH_3}{C}}-\overset{\overset{O}{\|}}{C}-X$$

where: R – oligodiene, oligoisoprene, oligostyrene, ets., n= 40-65, X = $-NHNH_2$, $-NH_2$, $-NHCH_2CH_2OH$, $-NH-NH=C(R_1R_2)$, (R_1, R_2 – alkyl, aryl, cycloalkyl, etc.) with different molecular weight from diene and vinyl monomers have been obtained by thermo- and photo-initiated polymerization under mild conditions in solution and in bulk (Table 8) *[Kochetov, 2001]*.

Incorporation of groups of various chemical natures into an azoinitiator permits to adjust in a broad range the properties of oligomers obtained on their base. The possibility of incorporation of various terminal functional groups into oligomers, which may interact with a broad range of reagents, permits to develop oligomeric compositions with controlled conditions and properties.

Table 8. Thermo*- and photoinitiated polymerization of diene and vinyl monomers

Monomer	**Monomer c, mol/l**	**Initiator**	**Initiator c, mol/l**	**Solvent**	**T, K**	**Time**	**M_n**
Isoprene*	5.00	AIH	0.05	Methanol	368	12	4500
Isoprene	5.00	AIH	0.10	Methanol	298	4	500
Isoprene	5.00	AIH-CH	0.10	Methanol	298	9	850
Styrene*	3.5	AIH	0.14	Butanol	388	2.5	3700
Styrene	5.2	AIH	0.10	Methanol	298	2	4700
Styrene	5.2	AIH-CH	0.08	Methanol	298	2	4300
Styrene	8.6	AIH-CH	0.12	Without solvent	298	2	4350
Acrylamide	5.20	AIH	0.10	Water	298	0.25	$7.5 \cdot 10^5$

The structure of oligoisoprenes with functional groups was confirmed by IR-spectra (Figure 1).

IR-spectra oligoisoprendihydrazide (OIH), oligoisoprendihydrazone acetone (OIHN-A) oligoisoprendihydrazone methylethylketone (OIHN-M) are characterized by similar bands in different regions. Negligible distinctions are present in the range of valence vibrations C=O (1664 cm^{-1} for OIH, 1655 cm^{-1} for OIHN-A, 1655 cm^{-1} for OIHN-M) and NH (extensive bands with maximums 3316 cm^{-1} for OIH, 3305 cm^{-1} for OIHN-A and 3288 cm^{-1}, 3211for OIHN-M), as well as deformation vibrations NH_2 (1644 cm^{-1} for OIH) hydrazide groups.

The reactive oligoisoprenes: OIG, OIG-M, macrodiisocyanates based on HTPD (MHTPD), HTPD and oligoisoprene with amidoxime groups(OIAO) were investigated by differential scanning calorimetry (DSC) (Figure 2) and thermogravimetric analysis (TGA). Experimental data for heat capacity and glass transition temperatures are summarized in Table 9. As can be seen from Table 9, oligoisoprenes with functional end groups have low glass temperatures T_{g1} = 212 K for OIG-M and OIA and T_{g1} = 215 K for OIG. The insignificant reduction of $\Delta C_{p,1}$ at almost invariable $T_{g,1}$ and the reduction of decomposition temperatures also testify about the increase in the relative polarity of functional groups of oligoisoprenes.

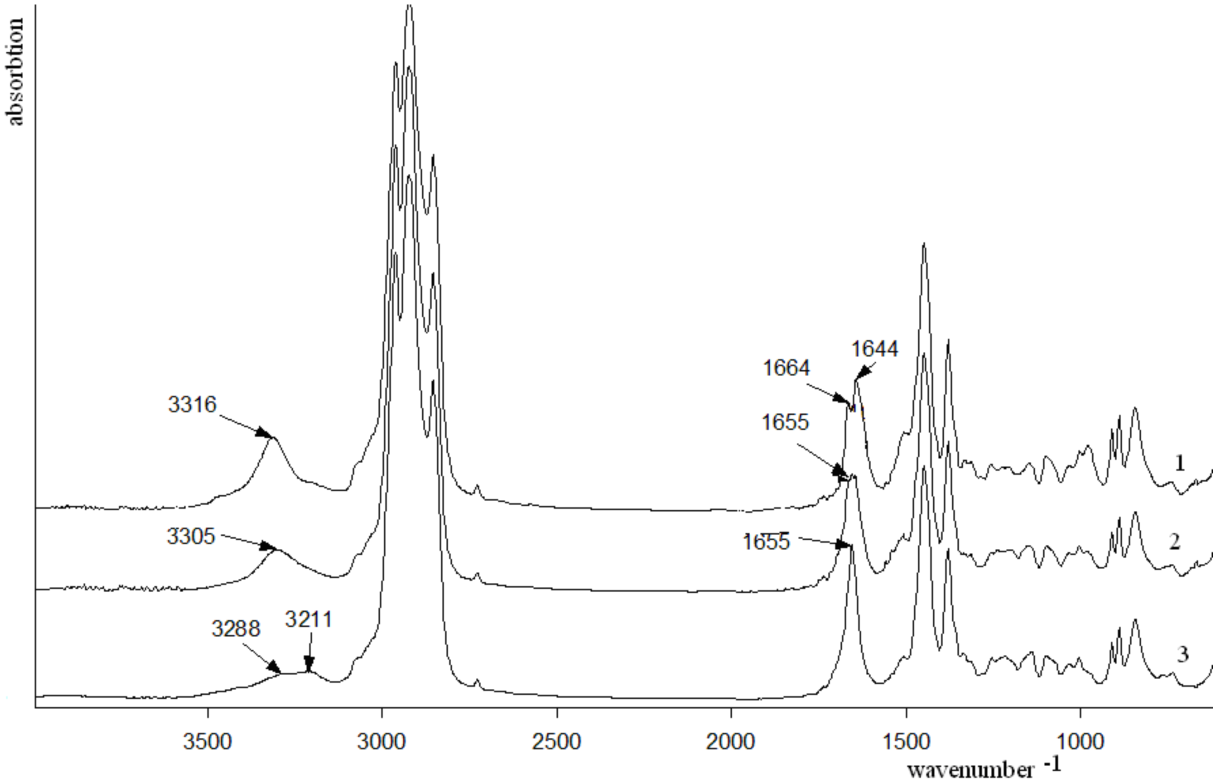

Figure 1. IR-spectra of oligoisoprendihydrazide (1), oligoisoprendihydrazone acetone (2), oligoisoprendihydrazone methylethylketone (3)

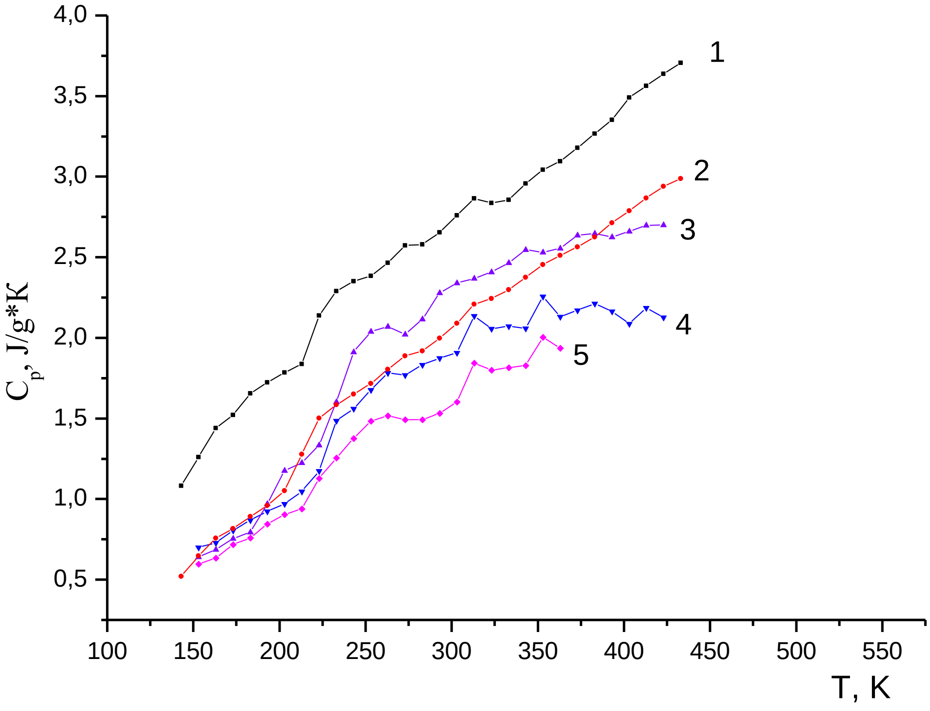

Figure 2. Temperature dependencies of the thermal capacity for OIG (1), OIG-M (2), MHTPD (3), HTPD (4), OIAO (5)

It was noted that thermal characteristics of oligoisoprenes slightly depend on the of nature functional end groups of reactive oligomers. The distinctive features of oligoisoprenes samples are some reduction of $T_{g,1}$ and lower values of the corresponding jump of thermal capacity $\Delta C_{p,1}$.

Table 9. Thermodynamic characteristics of the oligodienes

Samples	**$T_{g,1}$, K**	**$\Delta C_{p,1}$, J/(g·K)**	**$T_{decomposition}$, K**
OIG	215	0.55	380
OIG-M	212	0.50	360
OIA	212	0.43	365

This may be correlated with the alteration of segment packing in the oligoisoprene microphase due to the introduction of polar groups into the microphase that structures the oligoisoprenes.

Viscosity research of OIHN ketones has shown that the higher the level of hydrogen bonds in initial oligoisoprenes, the higher the viscosity in all interval of temperatures. Rise in the temperature range 55-65 ^{0}C leads to the change of viscous current as the destruction of intermolecular hydrogen bonds is possible. The course of dependency of viscosity for oligoisoprenes with partially and completely formed hydrogen bonds is different. At curing until gel formation rate of increase of viscosity also depends on quantity of hydrogen bonds. For ODHN-A hydrogen bonds are formed already in the course of polymer formation, but for ODH diisobutylketone saturation of hydrogen bonds practically is not reached.

Between the highest Newtonian viscosity and weight-average values of molecular weight the interrelation is defined by the equation:

$$\eta = \kappa \cdot M_{\omega}^{\alpha},$$

where α is close to 1 in the area of undercritical values of M_{ω} or to 3.4 – at $M_{\omega} > M_{\omega cr}$. For all investigated systems, the absence of rectilinear dependence is observed. Value of index α in all cases is within limits $1<\alpha<3.4$. Thus, the slope accentuated at increase in the contribution of intermolecular interactions (with increase of part of connected by hydrogen bond groups NH – CO at transition from ODHN of diisobutylketone to ODHN of acetone).

Thus, compiling of hydrogen bonds leads to the formation of microphase structure in which associations of rigid blocks play the role of the cross-link node. Properties (structural, viscous and physical-mechanical characteristics) of polymeric materials based on liquid rubbers with acylhydrazone end groups are defined by minimum change in the chemical structure of oligomers.

Macrodiisocyanates on the base of oligodienediacylhydrazones of aliphatic ketones and diisocyanates obtained at the molar ratio of 1:2.1, accordingly, in the solution of a ester, at 393-403 K, during 0.25-1 hours. Procedure reaction was carried out by the IR-spectroscopy (Figure 3). It was established that during reagents interaction there is the reaction of cyclization of acylhydrazone groups with the formation of oligoisoprenoksadiazolinilcarbomat diisocyanates (OIODC), containing 1,3,4-oxadiazoline cycles, with the following structure *[Fedorenko., 1988]:*

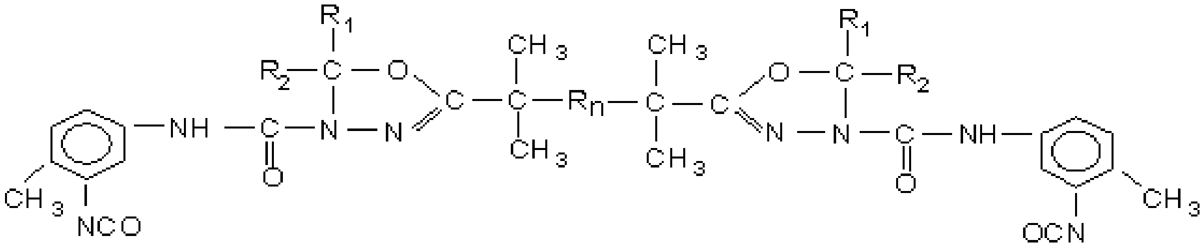

where: -C_4H_6-, - C_5H_8-; $R_{1,2}$: -Alk; n = 50-60.

Interaction of oligodienediacylhydrazones with diisocyanate has been finished at reduction on 50 % of the intensity of absorption band in the IR-spectrum, characteristic for N=C=O groups, in the range of 2240–2270 cm^{-1}.

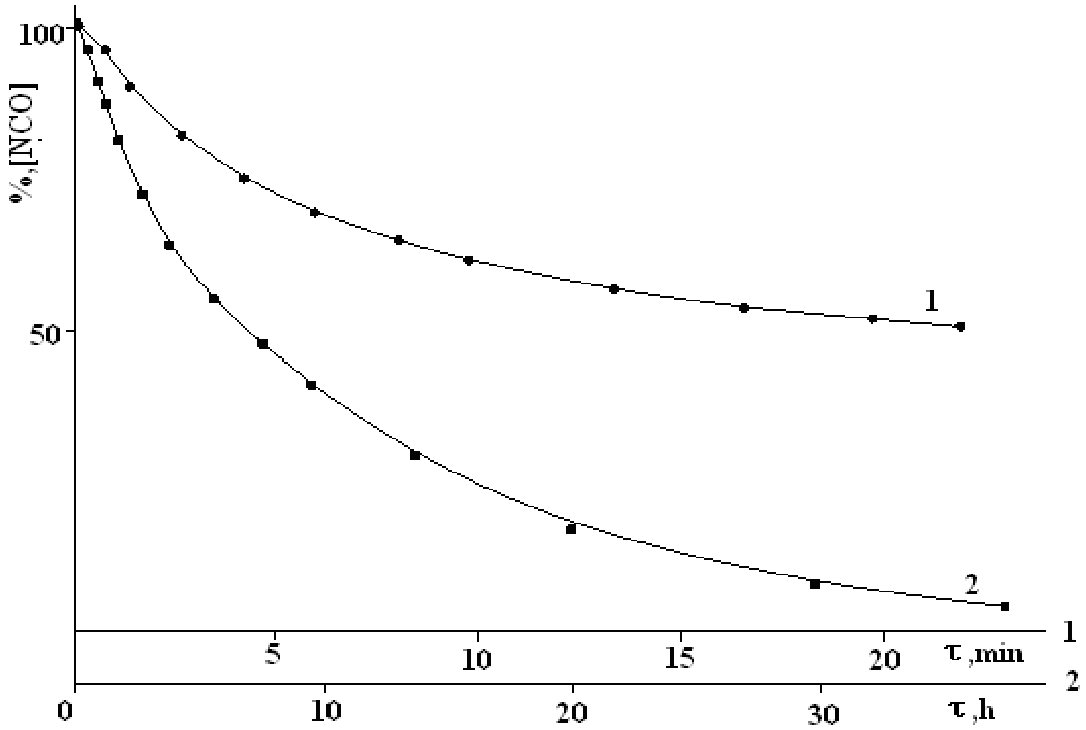

Figure 3. Kinetic laws of formation of OIODC (1) and polyisoprenoksadiazolinil-carbomate (PIODC) (2)

Carbonyl absorption happens, as the result of disappearing of groups C=O and C=N of acylhydrazone, and appearing of C=N groups of oxadiasoline cycle of C=O carbamatic group, which are formed as a result of reaction. Disappearing 3200 cm^{-1} - NH acylhydrazone group and appearing of acylhydrazone group and bands at 3300 cm^{-1}, 3440 cm^{-1} NH – free and hydrogen-bonded carbamate groups.

It is found at that the cyclization of acylhydrazone groups under action of diisocyanate takes place with forming oligomers containing 1,3,4-oxadiazoline cycles *[Kochetov, 1991, Barantsova, 2002]:*

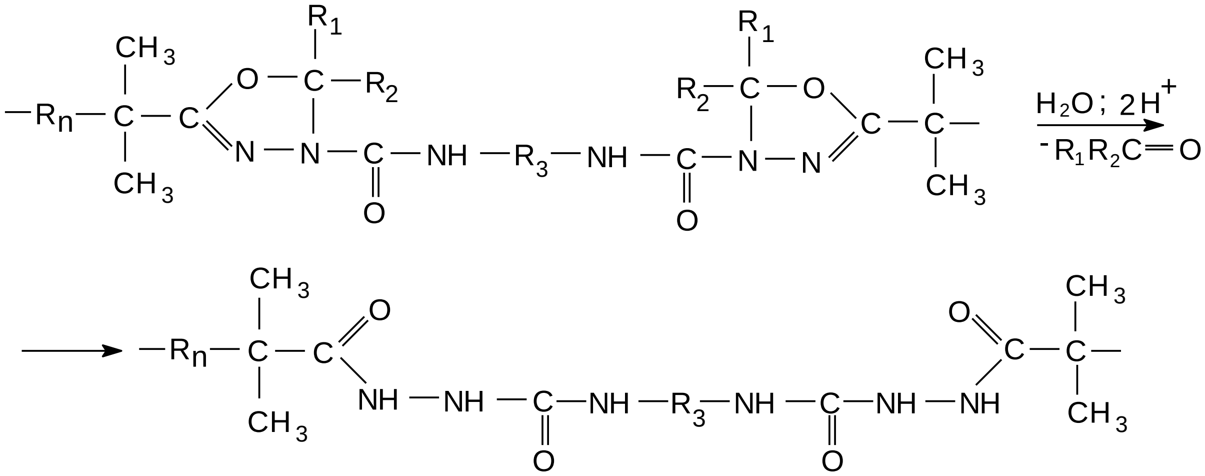

R: $-C_4H_6-$, $-C_5H_8-$; $R_{1,2}$: -Alk, R_3: Alk, Ar; n=30-83.

The possibility of incorporation of various functional end groups into oligomers, which may interact with a broad range of reagents, permits to develop oligomeric compositions with controlled conditions of curing and cured polymers with tailored properties.

This rection is confirmed by the IR- and UV- spectroscopy methods. It was shown from the comparison of UV-spectra of products of the model substances interaction (butylisocyanate with benzhydrazide and benzhydrazone of methylethylketone) that they are different. At addition of sulfuric acid during 15-20 min, their UV-spectra become identical which substantiates the transformation of oxadiazolinylcarbamate groups into acylsemicarbazides. In IR-spectra of the polymers with oxadiazolinylcarbamate groups, the changes are observed after treating with hot water or acid solutions which indicates the transformation of oxadiazolinylcarbamate group into acylsemicarbazide. The absorbance bands at 1350 cm^{-1} and 1670 cm^{-1} which are typical for an urea and C=O group in acylhydrazide moieties respectively appeared, as well as the intensity redistribution in the region 1500-1600 cm^{-1} of NH group deformation vibrations.

2.6 Microstructure of functional oligomers

Microstructure, that is a fraction and distribution along a chain of units of a different structure, defines at a great extent properties of high-molecular rubbers. It is also true for liquid rubbers. The different ratio of units in oligobutadienes of radical (Poly-bd) and anionic polymerization (Krasol) strongly influences many properties of these rubbers, firstly low-temperature ones.

Oligobutadiene consists of units of three configurations : 1,4-cis, 1,4-trans and 1,2- (vinyl). In the radical polymerization, their ratio is approximately 20:60:20% molar. Units are statistically situated in a chain.

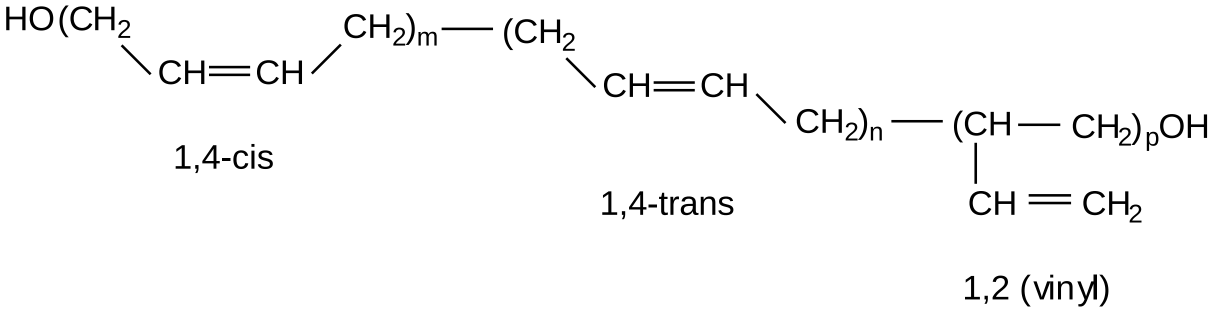

The analysis of FTIR- and NMR-spectra confirmed the structure and mechanism of formation of HTPI. The spectra of oligodienes that we synthesized does not, generally, differ from spectra presented in other works.

Infrared spectroscopy is widely used for assignment of units with different configuration (microstructure) in polydienes *[Zbinden, 1966]*. The stretching vibrations of C=C groups are located at 1640-1680 cm^{-1} and have low intensity. The band of out-of-plane deformation vibrations of CH groups (Table 10) is usually used for analytic purposes. The extinction coefficients of CH groups in different units were taken from literature *[Zbinden, 1966]*.

Table 10. Wavenumbers of analytical bands of polydienes double bonds *[after Zbinden, 1966]*

Unit	**Wavenumber, cm^{-1}**	
	polybutadiene	**polyisoprene**
1,4-cis-	680	835
1,4-trans	967	842
1,2- (vinyl)	911	909
3,4-	-	888

The first work on infrared spectroscopy of HTPB *[Tompa, 1972]* showed that the microstructure of radical HTPBs did not substantially differ from that of high molecular analogues.

The typical ratio of 1,4-trans:1,4- cis:1,2- units in the chain of butadiene obtained by radical polymerization gives 60:15-20:20-25% mol *[Schnecko et al., 1978]* and insignificantly differs from the oligomers prepared with different initiators and in different solvents. The ratio for units 1,4-, 1,2-, and 3,4- in radical oligoisoprene is approximately 88:6:6. The units distribution in a chain is statistical, as showed by Sato *[Sato et al., 1977]*.

The determination of content of 1,2- and 3,4-units in HTPI is not difficult (Figure 4). The content of units of different microstructure is (mol. %) *[Svistova et al., 1987]* as follows: 1,4 (trans and cis) – 87.5 (88), 1,2- 6.9 (5), 3,4- 5.6 (7). Data cited in brackets were also obtained by IR-spectroscopy *[Daury, 1977]*.

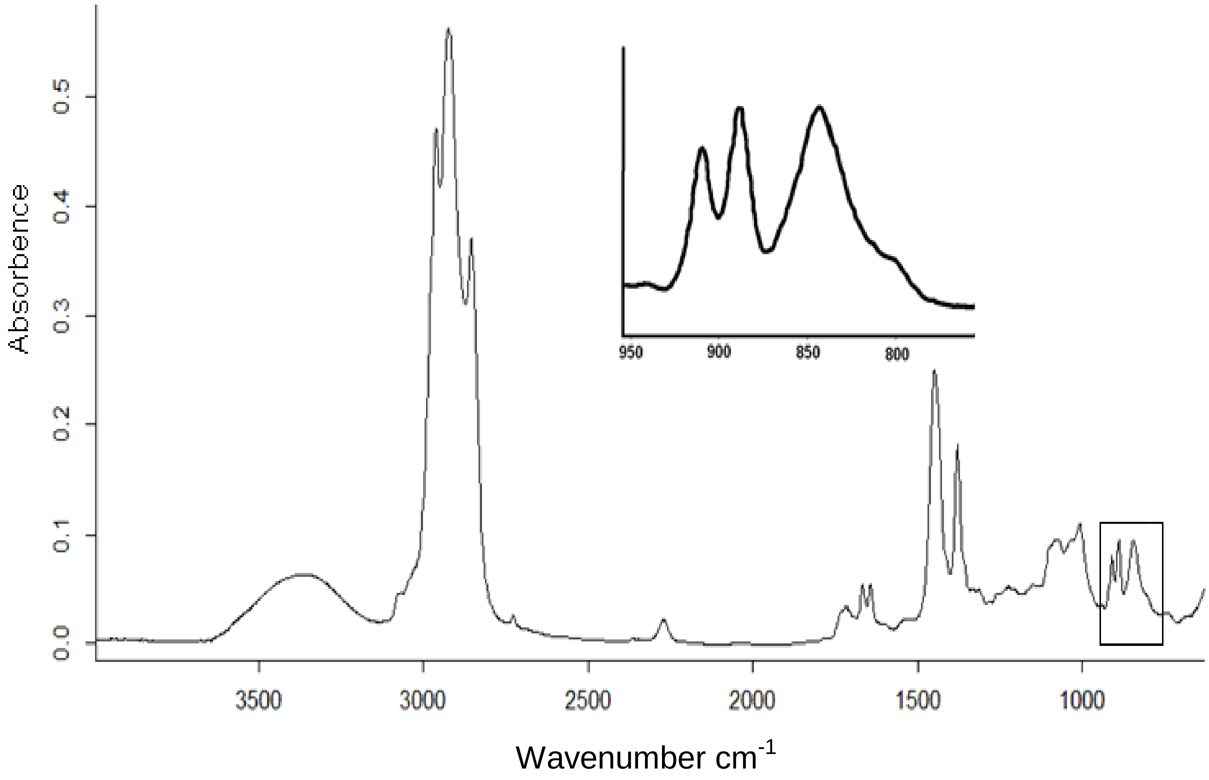

Figure 4. FTIR spectrum of HTPI, synthesized in an IPA solution (700-1000 cm^{-1} region of bending vibration CH-group)

The separate determination of 1,4-cis and 1,4-trans units in a polyisoprene by the IR method is possible only at the complete absence of 1,2-units, therefore, a NMR method was employed for the decision. This method is more comfortable and less labour intensive. It does not require calibration and knowledge of extinction coefficients as the IR method (Figure 5).

The main peaks necessary for determination of microstructure in oligodienes are presented in Table 11.

The relative content of the structures is determined through peak areas, which are responsible for signals pointed protons in different units. The ratio of 1,4-cis and 1,4-trans structures was found by height of peaks at 1.68 and 1.60 ppm *[Burel et al., 2000]*. The calculated formulas are taken from literature *[Burel et al., 2000; Burel et al., 2011]*.

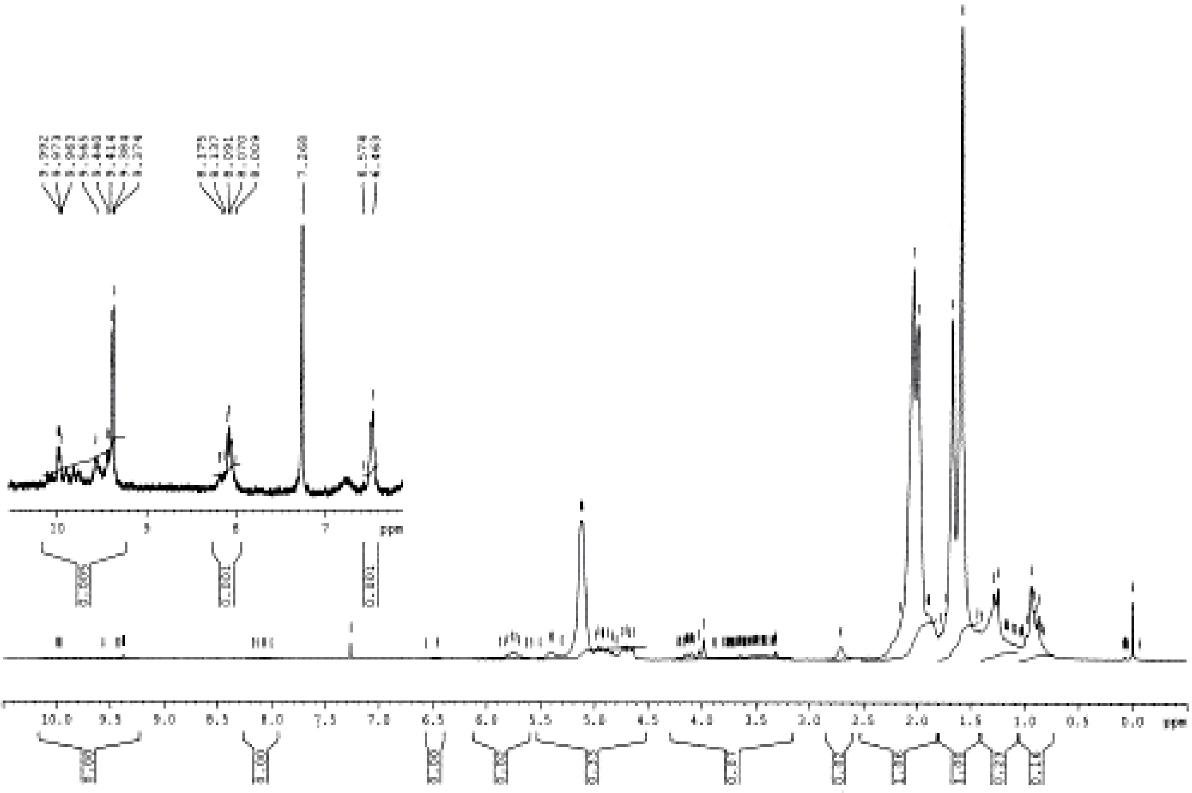

Figure 5. ^{1}H NMR spectrum of oligoisoprene obtained in IPA solution

The obtained results for various solvents and initiators are presented in Table 12. They show that in all cases microstructure is close to that cited earlier for oligodienes of radical polymerisation.

At the same time, it was proven that a chain microstructure in HTPI *[Svistova et al., 1987]*, as well as in HTPB *[Sadeghi et al., 2006]*, can depend on solvent and deviates from the value indicated in Table 12.

This problem requires further examination. We will also note that the determination of microstructure by the NMR method gives more exact results than method of IR - spectroscopy *[Frankland et al., 1991; Sadeghi et al., 2006]*. In a number of cases, the distribution of unsaturation obtained by the IR spectroscopy is incorrect because of its method limitations; therefore, the the NMR method must be preferred as less labor-consuming, more exact and universal valide.

Table 12. Microsrtuctures of oligoisoprenes of radical polymerization after ^{1}H NMR data

Solvent	**Initiator**	**Units 1,4-T:1,4-C:1,2-: 3,4-**	**Reference**
Ethanol	HP	85^a :7 : 8	*Daury, 1977*
IPA	HP	87.4^a :6.9 :5 :6	*Svistova et al., 1987*
IPA	HP	56 :32 :6 :6	*Burel et al., 2000*
n-Butanol	HP	57.5: 29.9: 6.7: 5.9	*This work*
Ethanol	Azo-bis(isobutyroamide)	60.5: 27.9: 6.0: 5.6	*This work*
Ethanol	Azo-bis (isobutyroamidoxime)	60.5: 28.7: 5.5: 5.3	*Burel et al., 2011*

^{a}1,4-cis and -trans

2.7 Synthesis of Polymers based on oligomers with functional groups

PUs obtained on the basis of liquid rubbers have considerably lower characteristics, than those based on polyethers. The comparative analysis of maximal level of properties of PUs are referred in *[Speckhard and Cooper, 1986]*: it is possible to obtain engineering strength and elongation at break on polyesters (polytetramethyleneadipinate), polyethers (polypropylenoxide), and polybutadiene 41-48, 34, 21 MPa and 500, 300 and 300 % accordingly, and the maximal elongation in last case can reach 1600 %. The lower properties of PUs based on oligodienes are explained by their non-polar nature with less energy of cohesion between hydrocarbon chains and the absence of oxygen atom from the chain because they are active parts in formation of intermolecular hydrogen bonds in polyethers (polyesters) *[Speckhard and Cooper, 1986]*.

The best properties of PUs are obtained on oligobutadienediols synthesized with azoinitiators. For example, strength and relative elongation of PUs obtained by this process have values of 8-12 MPa and 400-600 % *[Time, 1992]*. The composites of liquid rubbers filled with carbon-black reached the level of physico-mechanical properties of rubbers on the basis of high molecular rubbers of general appointment, acceptable for producing tyre rubbers (20 MPa). Such results can be attained using oligodienes with a high degree of bifunctionality. The PU properties on the Poly-bd oligobutadienes are not that good, although in the filling systems tensile strength was 15.44 MPa and elongation 315% *[Moore, 1969]* and tensile strength 17.5 MPa *[Daury, 1977]*.

In compositions intended for sealing, pouring and other applications, where high strength and elastic properties are not required, breaking strength usually equals 0.2-5 MPa, elongation – 100-500 %. In example, we present typical results of oligoisoprene ORD, obtained in solution of IPA: strength 1.19 MPa, elongation (ε) 245%. The component ratio in the composition wasn't optimized, filler was absent in the system.

It is known that high physico-mechanical properties of polyurethanes are due to the presence in their molecules of amide and carboxylic groups which are able to associate *[Minoura, 1978; Keercha, 1990]*. Increasing the concentration of such groups at the transition to polymers with urea groups leads to increasing physico-mechanical properties which attracts interest towards such polymers. So, we consider that the use of oligodienes with hydrazide and acylhydrazone groups for the development of materials stable to hydroabrasive wear in corrosive mediums is prospective *[Barantsova, 2009]*.

The synthesis of oligodienes with terminal functional groups was realized by radical polymerization of diene monomers in the presence of azoinitiators with various functional groups, as well as by modification of functional end groups of reactive oligomers *[Gritsenko, 1989]*.

The oligodienes with terminal hydrazide groups are liquid rubbers which react easily with various nucleophilic reagents – diisocyanates, polyepoxides, diimides – and at 20-100^{0}C change into linear polymers or networks. The properties of some polymers are shown in Table 13.

ODH may be cured with polyepoxide compounds. They are compatible with PDUE of the same type chain at any temperatures and ratios. At 20^{0}C curing is finished in 7 days, at 100^{0}C it is completed in 10 h. To cure with epoxy resins, an increased (80 – 100^{0}C) temperature is required. The viscosity of compounds may be regulated by epoxy oligomers of low viscosity as additives. The cured epoxy components are frost-resistant and elastic.

The measurement of physico-chemical properties of epoxy compounds on the base of PDUE and ODH shown that the compound is elastic even at the temperature of –70^{0}C (Table 14). The compound is stable at 200 – 220^{0}C. Decomposition (by 10 %) is observed at temperatures over 220^{0}C.

Table 13. The properties of polymers obtained on the base of oligoisoprene-dihydrazide with various curing agents *[after Grishchenko, 2000]*

Oligomer molecular weight	**Coagent**	**Physico-mechanical polymer properties**			
		linear		**network**	
		σ, MPa	**ε, %**	**σ, MPa**	**ε, %**
1700	2,4-Toluenediisocyanate (2,4-TDI)	8.0	600	-	-
1700	Polybutadieneurethaneepoxide (PDUE)	-	-	3.0	560
1700	Epoxy resin	-	-	7.0	130
1000	Meta- phenylen-bis-maleimide (MPhBM)	15.0	300	-	-

Table 14. The change of physico-mechanical characteristics of epoxy sealant based on PDE and ODH at low temperatures *[after Grishchenko, 2000]*

T, ^{0}C	**20**	**0**	**-10**	**-40**	**-60**	**-70**
σ, MPa	1.0	2.7	3.5	7.5	11.0	17.0
ε, %	270	330	350	390	380	180

Epoxy sealants are used in applications where moisture resistance is required. The hydrophobic nature of an PDUE and of an curing agent (ODH) ensures good sealant water-resistant properties. The compound has good dielectric properties: tangent of angle of dielectric loss at frequency 10^3 Hz and 20^0C – 0.007; dielectric constant at frequency 10^3 Hz and 20^0C - 2.4 electrical strength, - 25.3 кV/mm. The new obtained sealant is recommended for applications in electrical engineering and radio-electronic industry.

Polymers obtained on the base of ODH and MPhBM – polyimidehydrazides *[Grishchenko, 1983]* as follow:

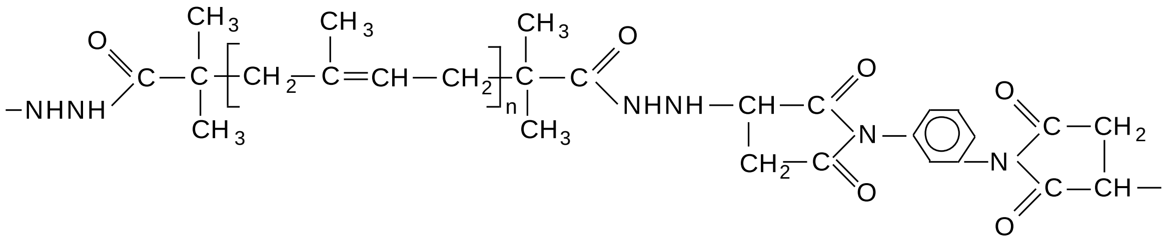

are linear polymers, whose properties (Table 13) are analogues to polyurethane networks, but show higher heat resistance and resistance to oxidation. The last appears to be explained by retaining in polymer structure of substituted hydrazide fragments – an antioxidant, built in a polymer chain. Polyimidehydrazides are characterized over a wide range of working temperatures: from -60 °C to +360 °C. The essential advantage of synthesis of these polymers, as compared with synthesis of polyimides by cyclization of polyamidoacids, consists in one-stage process proceeding without release of by-products.

The use of up-to-date methods a small-angle X-ray measurements for investigation of polyimidehydrazides showed that they are polyblock polymers with alternating “soft” (diene) and “rigid” (imide) blocks. Polyimidehydrazides are characterized by a high level of phase separation which is responsible for their high strength characteristics. The presence of hydrocarbon chain in the polymer ensures their good dielectric properties and hydrolytical stability. Polyimidehydrazides are of practical value as frost-resistance coatings and adhesives.

The reaction of ODH with isocyanates procceds instantly with a large exothermic effect, giving in result polyacylsemicarbazides as follow:

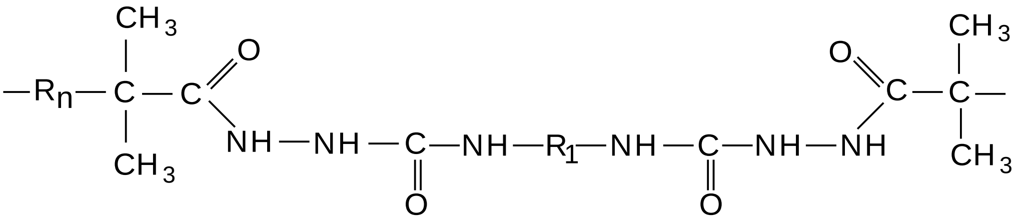

R: $C_4H_{6,}$ -C_5H_8-; R_1=Alk, Ar, n=35 - 52

characterized by high physico-mechanical properties, but the high rate of reagent interaction does not permit to carry out the synthesis of polyacylsemicarbazides without a solvent. A change of hydrazide group to acylhydrazone decreases the rate of the reaction with isocyanates.

The reaction of ODHN and diisocyanate yields in polydieneoxadiazolinylcarbamates (PDODC) of common formula:

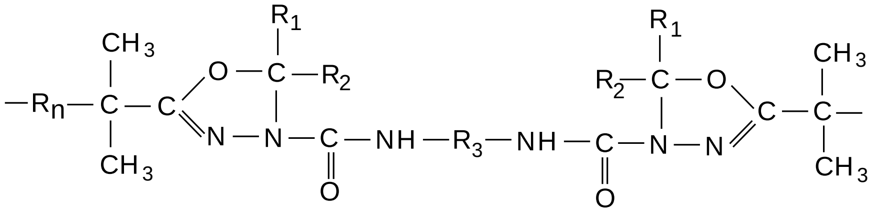

where R: -C_4H_6-; -C_5H_8-; $R_{1,2}$: -Alk; R_3: -Alk, -Ar.

It is confirmed by IR-spectroscopy data: a process interaction is characterized by disappearing of the absorbance band in the range of 2240–2270 cm^{-1}, typical for N=C=O groups, appearance of a band at 1310 cm^{-1} assigned to C-O-C-group valence vibrations; redistribution of intensities in the range of carbonyl absorbance, for which C=O and C=N groups of initial acylhydrazone are responsible, as well as C=O of a carbamate group, formed in the reaction and an C=N group, which is in an oxadiazoline cycle; the disappearance of the band at 3200 cm^{-1} of - NH acylhydrazone group and appearance of a band at 3300 cm^{-1} of NH – hydrogen-bonded carbamate group, as well as the band at 3410 – 3440 cm^{-1} which, depending on a chosen diisocyanate, belongs to an NH hydrogen-unbonded carbamate group.

The rate of the interaction between ODHN and diisocyanates is determined by the structure of the acylhydrazone group, mainly, steric factors *[Barantsova, 1990]*

The compositions on the base of ODHN and diisocyanates with regulated pot life are of interest as sealants and protective coatings. Mechanical properties of PDODK, depending on the nature of carbonyl groups of acylhydrazone fragment, are shown in Table 15*[Barantsova, 2009]*.

Table 15. Mecanical properties of linear PDODC obtained on the base of ODHN and diisocyanates (ratio 1:1)

Oligodienedihydreazone	**Diisocyanate**	**σ, MPa**	**ε, %**	**ε, %**
acetone	2,4-TDI	5.1	1400	5
methylethylketone	2,4-TDI	4.5	1300	10
dipropylketone	2,4-TDI	1.8	850	7

As a result of IR-spectroscopic studies of polymers (Figure 6) based on ODHN-A (Figure 6a), ODHN-M (Figure 6b) and ODHN-D (Figure 6c) and 2,4-TDI, it has been established that the amount of hydrogen bonded groups in freshly prepared polymers differs. And, the longer the radical ketone in ODHN-D, the more remains of free CO and NH groups (curve 1, 2 c). After storage of samples for a long time (1 year), almost full saturation of hydrogen bounds occurs.

According to the amount of hydrogen bonded groups in a solution of polymer, there are associative processes that expresses in the viscosity increase of a polymer solution in nonpolar solvents. The difference in time of growth of a macromolecule and the formation of hydrogen bonds between them affects the supramolecular structure of the polymer. Study by small-angle X-ray spectrometry has shown that hydrogen bonds are the basic driving force of association, hence, segregation of blocks of the various natures of the segmented polymers.

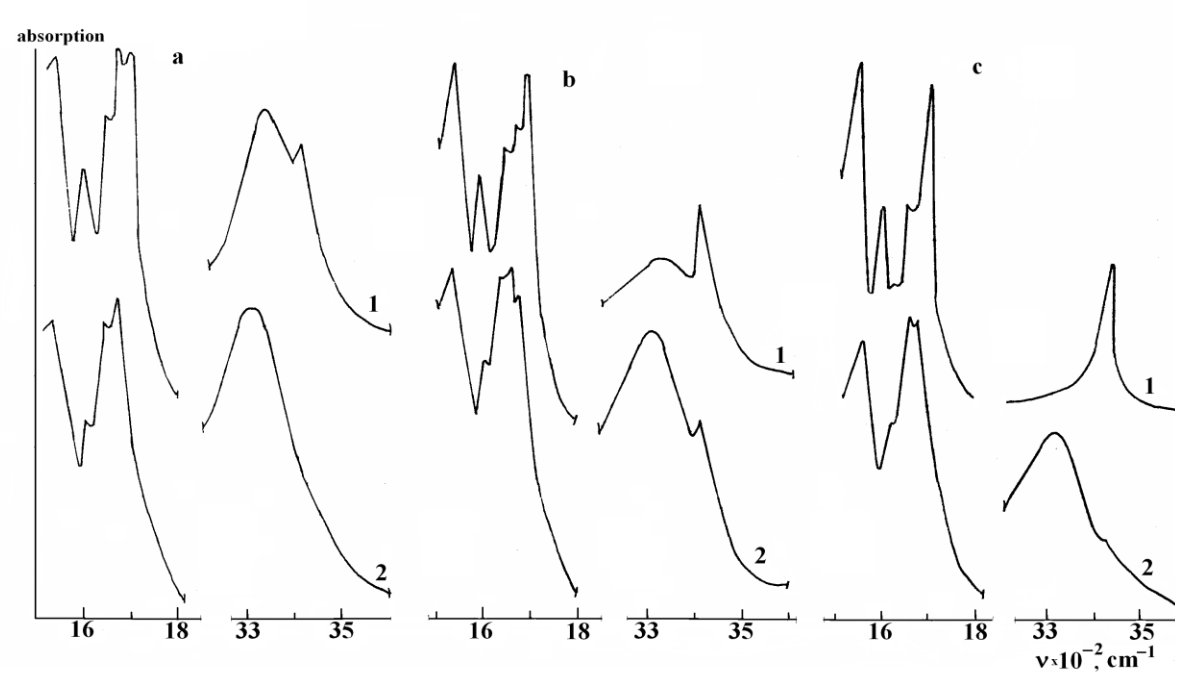

Figure 6. IR-spectra initials (1) and films sustained during 0.5 year (2) a base on acetone (a), methyl ethyl ketone (b), diisobutyl ketone (c) *[after Fedorenko, 1988]*

From Table 16 it can be seen that levels of dispersion and degree of segregation of blocks naturally decrease when transition from OHDN acetone to ODHN diisobutylketone occurs, that correlates with the degree of hydrogen bond association inside these oligomers *[Kochetov, 1989]*.

Table 16. Structural properties PDODC base on ODHN and 2,4-TDI

ODHN	**α, nm**	**$\Delta\rho^2\cdot10^3$**	**$\Delta\eta^2\cdot10^3$**	**α_p**	**α_{IR}**
acetone	5.22	1.585	0.602	0.380	0.600
methylethylketone	5.30	0.900	0.253	0.281	0.280
diisobutylketone	5.34	0.889	0.130	0.146	0.125

For protection of the technological equipment working in aggressive environments, use of liquid rubbers with functional end groups which properties are defined by the ability to form strong chemical and physical bonds is prospective, allowing polymeric materials with properties that can not be achieved by nonfunctional rubbers. The optimal way of obtaining rubber component is synthesis of isocyanate forepolymers based on aliphatic ketones ODHN, since a high rate of reaction between hydrazide and isocyanate groups (a reaction completes in 2-5 min) does not allow isocyanate forepolymers. The substitution of a ketone component in an initial ODHN permits to regulate its interaction rate with diisocyanates.

The isocyanate-containing forepolymers were cured with di- and polyfunctional agents with active hydrogen atoms. The compositions were prepared directly before using. The gel time was determined by the nature of a curing agent and changed from 15-60 min to 8-30 h. The study of the forepolymer curing showed that the best technological and mechanical characteristics of polymeric materials are achieved using aromatic diamines as chain extenders *[Barantsova, 2002]*. So, by curing an isocyanate-containing forepolymer prepared from liquid rubber and 3,3-dichloro-4,4-diaminediphenylmethane in organic solvent, which does not have in its structure active hydrogen atoms, e. g. methylethylketone, a series of polymeric materials were obtained and they are characterized by high physico-chemical properties, depending on the ratio of soft (forming on the base of diene chain) and hard (forming on the base of diisocyanate and a chain extender) blocks. Decreasing an elastic block length of these polymers leads to increasing their hardness and strength. In Table 17 the properties of linear polymers on the base of oligodienedihydrazones of various molecular weights and 50% solution of 3,3-dichloro-4,4-diaminediphenylmethane in methylethylketone are presented *[Barantsova, 2002]*.

Table 17. The properties of polymers on the base of oligodienedihydrazides of various molecular weight

Molecular weight	Shore A hardness	Tensile strength, MPa	Tensile elongation, %	Residual elongation, %
1350-2000	85-95	20-25	200-400	0-4
2350-3000	69-85	12-20	300-400	0-8
3350-4480	52-69	6-12	350-500	2-10

The hydrophobicity of diene blocks in a polymer chain explains the fact that elastomers obtained have swelling as low as 10-100 times compared with urethane elastomers based on polyethers.

The resistance to hydroabrasive wear was estimated by the weight loss (the loss coefficient was determined as the ratio of wear of stainless steel to that of an elastomer). It was shown that the obtained elastomers, depending on the oligodienedihydrazide molecular weight, exceed in hydroabrasive wear stainless steel as much as 4-20 times (Table 18).

The resistance of elastomers to the influence of acid and alkali solutions of different concentrations was determined by the comparison of physico-mechanical properties (tensile strength and tensile elongation) of the obtained polymers before and after their submission to the corrosive environment The investigation was carried out at the temperature 22±2^{0}C for 1000 h.

Table 18. The relative hydroabrasive wear of stainless steel and polymers based on ODHN ketones

Polymer based on	Molecular weight	Wear coefficient
oligodienedihydrazone	2000	18.9
oligodienedihydrazone	2800	15.3
oligodienedihydrazone	3550	9.7
oligodienedihydrazone	4400	3.8
steel 12X18H10T	-	1.0

The specimens were considered to be stable if they saved up to 80% of mentioned properties. The results of the polydieneoxadiazolinylcarbamates resistance to the influence of corrosive media are shown in Table 19.

The changes of the stability coefficient are connected with changing of the oxadiazolinylcarbamate group (formed by the interaction of acylhydrazones with isocyanates) to acylsemicarbazide under the influence of liquid corrosive media *[Barantsova, 2003]*.

Table 19. Resistance of the polymers based on oligodienedihydrazone, 2,4-TDI and 3,3-dichloro-4,4-diaminodiphenylmethane (reagent ratio 1:2:1) to the influence of corrosive mediums

Test medium	Concentration, %	Swelling degree, %
H_2O	-	0.07
HNO_3	30	2.99
H_2SO_4	50	-0.39
H_3PO_4	50	-1.40
HCl	10	-0.32
HF	30	2.22

For determination of application fields experimental-industrial tests of the given polymers have been conducted on the station of water purification of sewage of the galvanic manufacturing. The media of this manufacture represented the difficulties caused by multicomponent systems including several dozens of various chemical compounds. As could be seen from the presented in the table data, polymeric samples on the basis of liquid functional rubbers are stable in the present mediums (Table 20).

Table 20. Stability of polymers based on liquid functional rubbers to the influence of liquid aggressive media of the station of water purification of the galvanic manufactures (time of tests 1000 h)

Medium	Loss of mass of the sample, %
Solution on the stage of cleansing sewage	1.7
Solution on the stage of the cationite regeneration H_2SO_4	2.0
Solution on the stage of anionite regeneration NaOH	2.1

On the base of the liquid rubbers with reactive end groups and curing agents, a series of polymeric materials which may use as sealants (Figure 7a), cold-curing adhesive (Figure 7b), non-case capsulation (Figure 7c), chemical resistant protective coatings and construction materials (Figure 7d), abrasive-resistant materials (Figure 7e), had been synthesized.

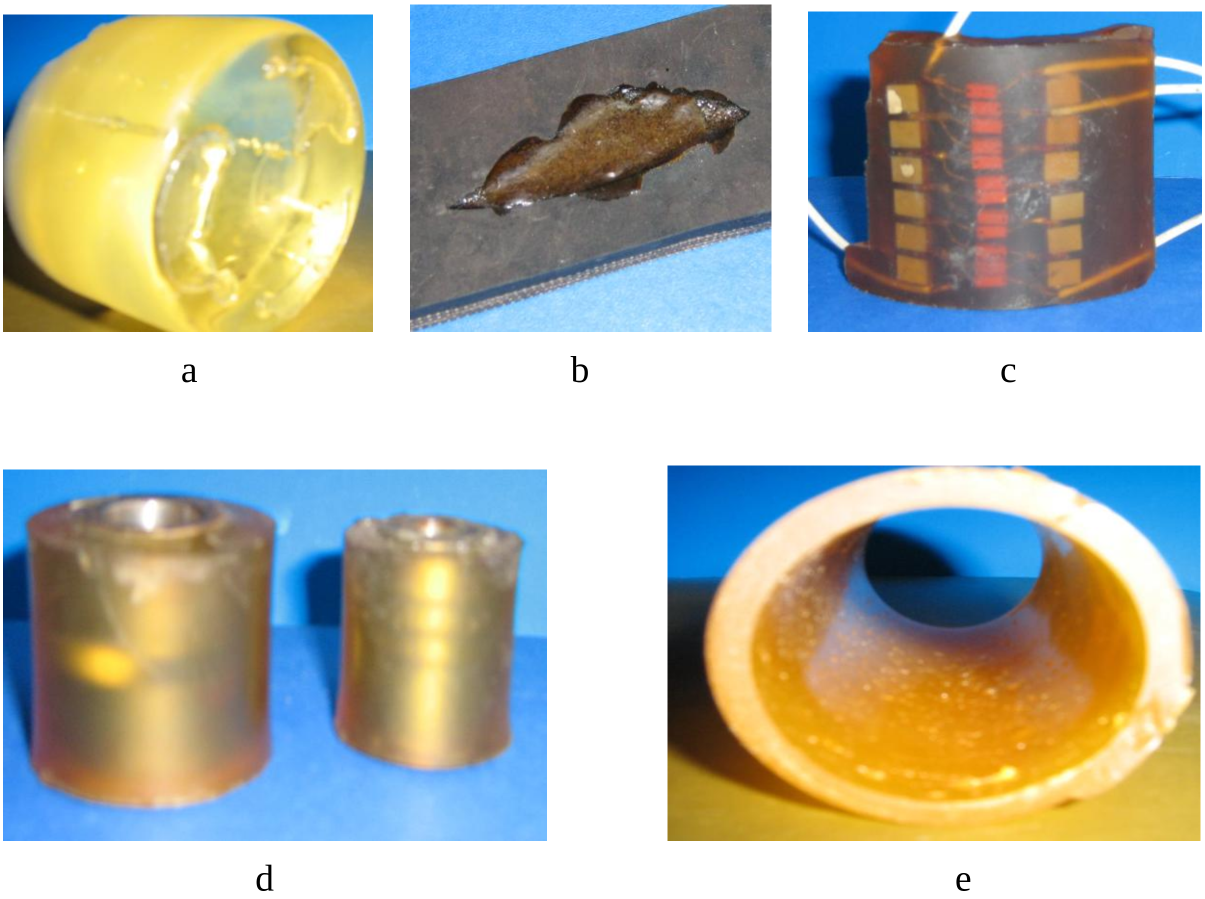

Figure 7. Samples of the polymeric products obtained on the basis of developed oligomers with functional end groups

2.7 Poly(ester urethane acrylates) and holographic properties of formulations on their basis

It is of interest to examine block copolymers in which unsaturated bonds occur in hard blocks (containing urethane, urea, phenyl, semicarbazide, and other polar groups) alternating with soft blocks (containing polyester, poydiene groups). The incompatibility of soft and hard blocks with different chemical compositions gives rise to a stable microphase separation; as a result, domains consisting of hard blocks are formed in the soft matrix. These domains serve as junctions of the three-dimensional physical network of the copoly(urethane) block largely via hydrogen bonds that are tens of times less strong than chemical bonds *[Berlin, 1967]*. Therefore, a certain mobility is preserved in stiff blocks. This situation makes it possible to form additional chemical bonds under certain conditions upon heating or irradiation of block copoly(urethanes) *[Maslyuk, 1989]*.

Synthesis of photocured elastomeric materials was carried out in two stages: by interaction of functional end groups of the initial oligomers with spacers containing nonsaturated groups, and then photopolymerization of these groups. In this way, the soft elastic material is formed in the first stage, it can be molded in certain forms and sizes, and then increase of durability properties during the photocuring stage.

On the basis of oligodienes (or oligoethers) with hydroxyl end groups (ODHL or OEHL) and 2,4-TDI, at a ratio 1:2, oligodieneurethane diisocyanates (ODUI) or oligoetherurethane diisocyanates (OEUI) were obtained, according the following scheme:

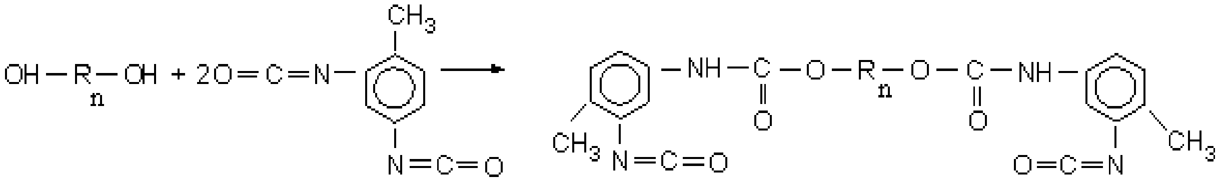

R: $-CH_2CH_2O$, $-C_4H_6$, $-C_5H_8$; n = 45-60.

For the synthesis of macrodiisocyanate half of the isocyanate groups is consumed, that was confirmed by IR spectroscopy. The structure of the synthesized macrodiisocyanate was confirmed by comparison of IR-spectra of initial substances and products of their interaction. Disappearance of bands of absorption in the area of valence oscillations of hydrogen-bonded hydroxyl groups ~3440-3450 cm^{-1}, two times reduction of the intensity of the absorption band of isocyanate groups of 2274 cm^{-1} in comparison with the initial mixture; formation of absorption bands of valence oscillations of hydrogen-bonded amide groups of 3320-3330 cm^{-1} and deformation oscillations of amide groups -1530-1540 cm^{-1}; valence oscillations of carbonyl groups in the area of 1700-1720cm^{-1}, all these testify that there is the reaction yielding in urethane groups.

ODH of aliphatic ketones incorporate more polar acylhydrazone groups, therefore it was natural to expect higher physical-mechanical characteristics of polymers on their basis in comparison with ODHL.

The formation of dimethacrylate (DMA) of the following formula:

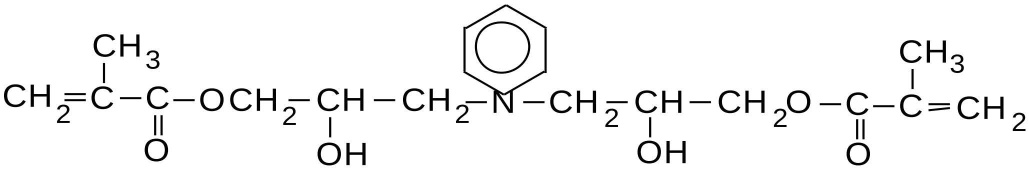

was confirmed by IR spectroscopy. In the spectrum corresponding to the product resulted from the reaction of aniline with 2,3-epoxypropyl methacrylate, absorption bands due to the NH2 group of aniline (in the region of bending vibrations at 1650 cm^{-1} and of stretching vibrations at 3300–3400 cm^{-1}) and the absorption band due to the epoxy group (at 920 cm^{-1}) disappeared. On the other hand, a complex band corresponding to the stretching vibrations of free and hydrogen-bonded hydroxyl groups at 3550–3400 cm^{-1}, the stretching vibrations of carbonyl groups 1720 cm^{-1}, and bending vibrations of acrylate bonds 1637 cm^{-1} appeared.

The interaction of DMA with OEUI or ODUI yields in poly(ester urethane diacrylate)s (PEUA) or poly(diene urethane diacrylate)s (PDUA) with the following structure:

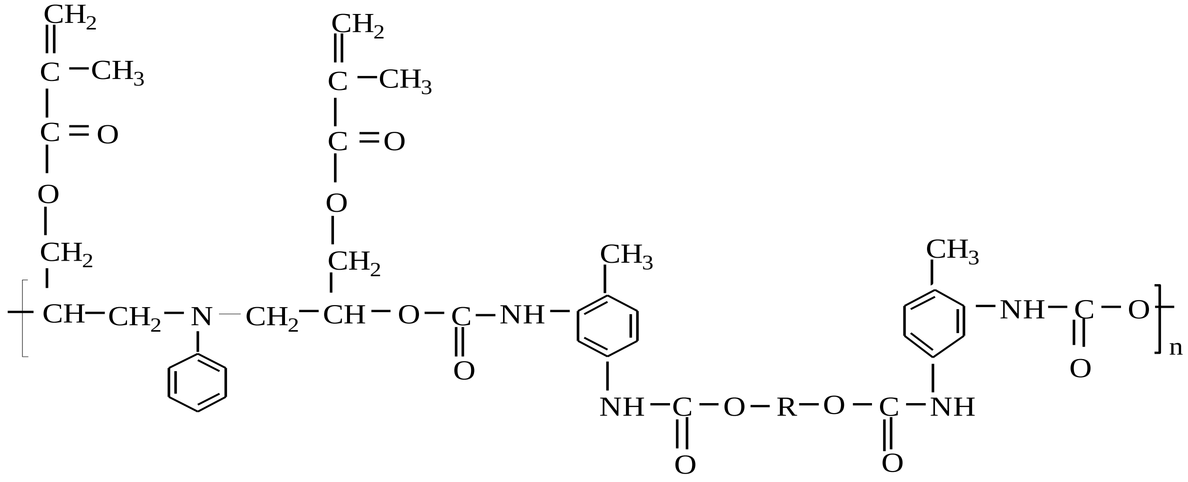

R: -CH_2CH_2O, -C_4H_6, - C_5H_8;   n = 45-60.

The end of the reaction was estimated by IR spectroscopy (Figure 8) from the disappearance of the absorption band at 2240–2260 cm^{-1} attributed to NCO groups. Upon removal of the solvent, the polymer samples were exposed to UV light. The photoinitiated interaction of methacrylate groups was monitored by the disappearance of the absorption band due to C=C bonds at 820 and 1637 cm^{-1}. The structure of the polymer is confirmed by the presence of the absorption bands due to the stretching vibrations ν NH (3338 cm^{-1}), the doublet ν C=O (1658–1656 cm^{-1}), the doublet of the bending vibrations δ NH (1533–1530 cm^{-1}), and vibrations of urethane groups C–O–C (1223 cm^{-1}) and of C–O–C ester groups $\nu_{C=C}$ (1719 and 1059 cm^{-1}).

The Table 18 shows the properties of the initial PEUA film, the film exposed to UV light (with benzoin isobutyl ester as initiator) and the film that was initially uniaxially stretched and then irradiated.

Characteristics of films differ appreciably, as presented. The irradiated films exhibit a higher onset temperature of degradation, better strength, and, accordingly, lower elongation. This effect is associated with the formation of chemical bonds that appear in the hard block of the polymer upon UV irradiation. The properties of uniaxially stretched and not stretched irradiated films are also different.

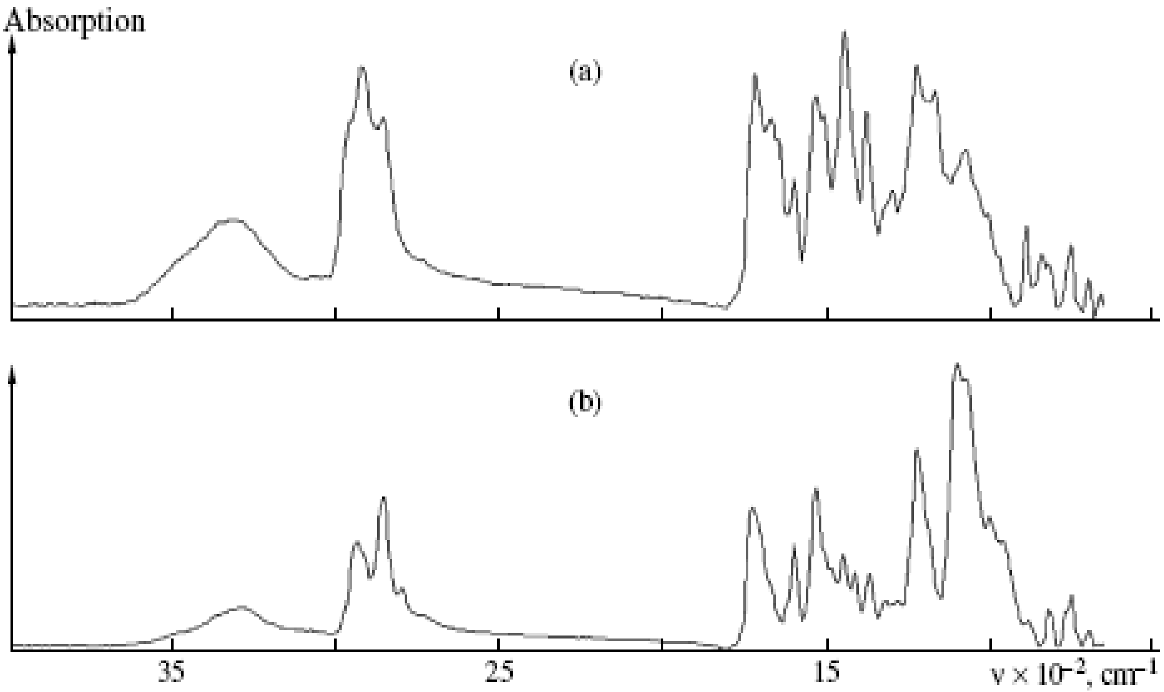

Figure 8. IR spectra of (a) the starting and (b) UV irradiated poly(ester urethane diacrylate) samples

Table 21. Properties poly(ester urethane diacrylate) before and after photoirradiation *[after Barantsova, 2007]*

Film	**Solubility in DMF**	**Onset temperature of degradation,^{0}C**	**Tensile strength, MPa**	**Elongation at break, %**
Starting	Soluble	200	2-5	500-700
Irradiated	Insoluble	230	8-12	200-250
Stretched by 100% and then irradiated	Insoluble	260	15-20	80-100

This situation may be explained by the orientation of functional groups in the hard block. As a result, additional physical bonds develop in the polymer and its supramolecular structure changes under mechanical stress (stretching) and irradiation. Thus, the molecular organization of rigid blocks that act as junctions in the three-dimensional structure of the block copolymer significantly depends on the formation of chemical and physical bonds in these blocks. Curves of elongation of not irradiated (curve 1) and UV-irradiated (curve 2) samples of poly(dien urethane metacrylate) are shown on Figure 9, accordingly, not irradiated (curve 1) and UV-irradiated (curve 2) samples of poly(dien oxadiasolinil carbamat metacrylate) are shown on Figure 10.

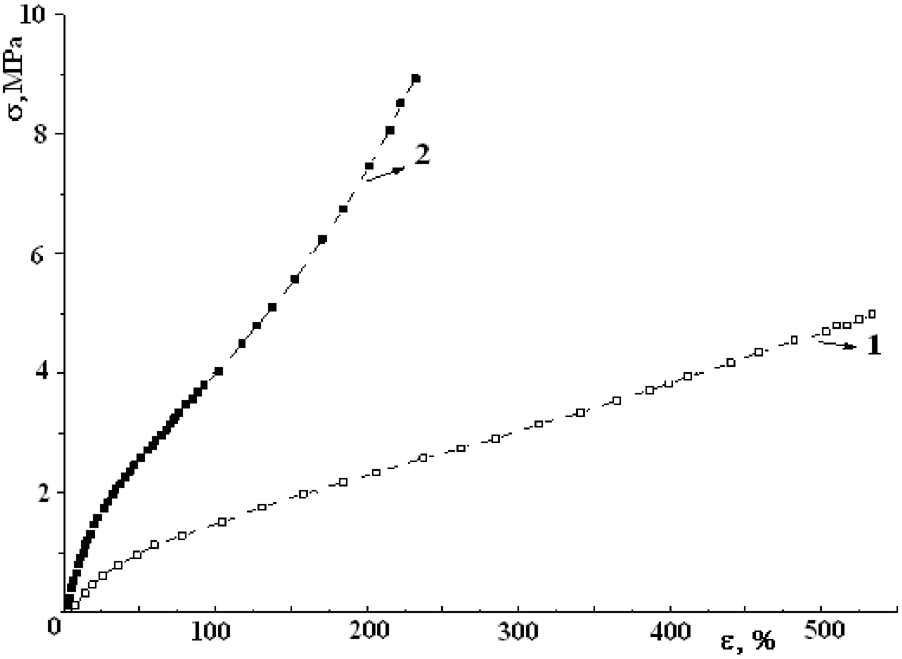

Figure 9. Elongation curves of not irradiated (1) and UF-irradiated (2) samples poly(dien urethane metacrylates)

Physical and chemical properties of initial and UV-irradiated PDODC and PDUA have been investigated. Thermal behaviour of PDODC and PDUA was evaluated by DSC, with respect to relaxation transitions in soft (diene) and hard (oxadiasoline carbamate urethane metacrylates and urethane metacrylates) blocks.

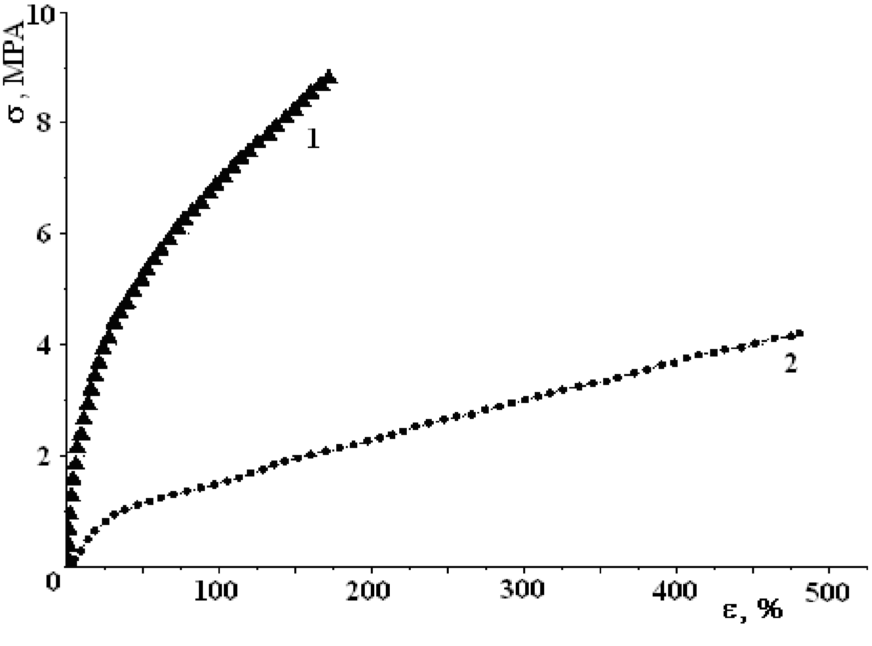

Figure 10. Elongation curves of not irradiated (1) and UV-irradiated (2) samples poly(dien oxadiasoline carbamate urethane metacrylates)

The thermograms of these polymers are presented in Figure 11. The glass temperatures of flexible oligodiene blocks (T_{g1} = 231 K for PDODC and T_{g1} = 235 K for PDUA) are rather distinctive from glass temperatures of oligoisoprenes (T_{g1} = 212-215 K) (Table 22).

Table 22. Thermodynamic characteristics of the PDUA and PDODC

Samples	**$T_{g,1}$ K**	**$\Delta C_{p,1}$ J/(g·K)**	**$T_{g,2}$ K**	**$\Delta C_{p,2}$ J/(g·K)**
PDUA	235	0.22	340	0.50
UV-irradiated PDUA	235	0.20	327	0.41
PDODC	231	0.25	338	0.39
UV-irradiated PDODC	231	0.23	328	0.59

The increase of glass temperatures of oligoisoprene blocks of PDUA and of PDODC against oligoisoprenes is observed on the heat capacity graphs. This may be correlated with the alteration of segment packing in the oligoisoprene microphase due to the introduction in PDUA and PDODC hard blocks, and transition of polar urethane metacrylates groups or oxadiasoline carbamate urethane metacrylates groups into the microphase structure of the polyisoprene.

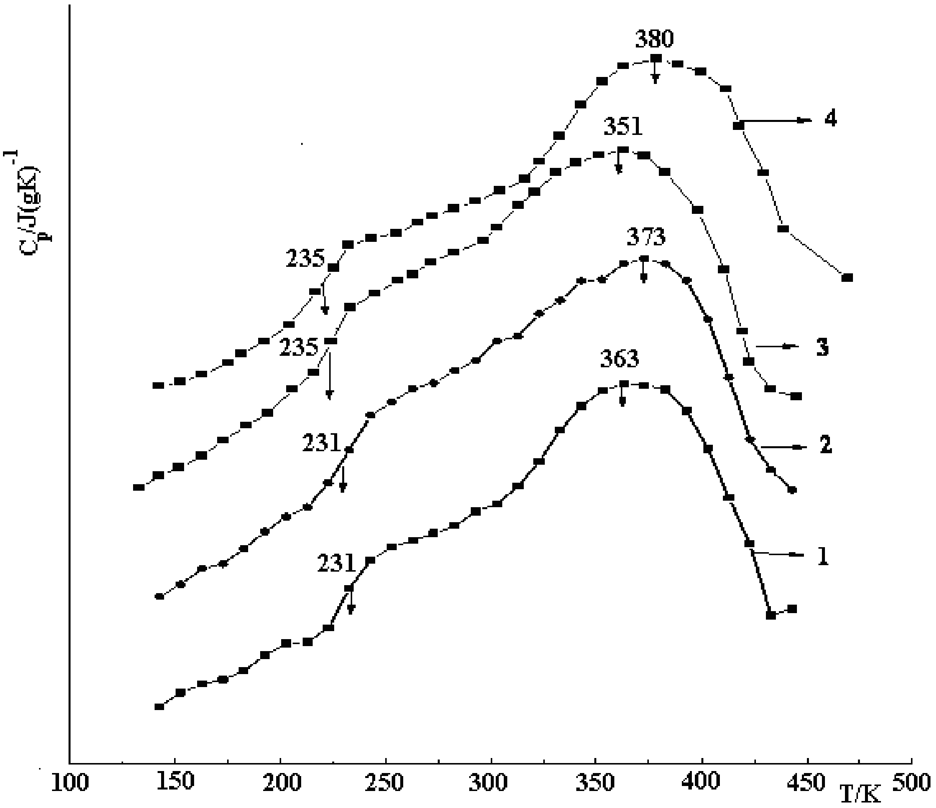

Figure 11. Temperature dependencies of the thermal capacity before and after photostructuring poly(diene oxadiasoline carbamate urethane metacrylates) (1,2) and poly(diene urethane metacrylates)(3,4)

Magnitude of $T_{g,2}$ for PDUA slightly decrease against $T_{g,2}$ PDODC but magnitude of $T_{g,2}$ for UV-irradiated PDUA increase against $T_{g,2}$ UV-irradiated PDODC which could be explained by the presence of different network of hydrogen bonds with participation of urethane metacrylates groups and oxadiazoline carbamate urethane metacrylates groups. As level of hydrogen bondings in PDODC is higher than in PDUA, restricted mobility in the hard blocks in the first case is more considerable that proves to be true lower degree of transformation metacrylates tied in the hard block. Accordingly, it leads to difference in properties of these polymers before and after photostructuring

Poly(ester urethane acrylates) (PEUA) with unsaturated bonds in rigid blocks in which chemical bonds could be realized under photoirradiation were synthesized; based on these block copolymers, new materials were obtained and their holographic characteristics were studied. At the first stage, recording layers of certain size and thickness are formed via the polyaddition reaction, while at the second stage holographic recording proceeds via the space-modulated photoinduced postcure. The obtained photostructured poly(ester urethane diacrylate) are used for holograms.

The kinetic curves of hologram recording are shown in Figure 12. The kinetics of recording on layers formed between glass supports is characterized by a low rate (Fig. 12, curve 1). The maximal diffraction efficiency is achieved within 800 s. When open layers were used, the rate of recording and the diffraction efficiency increased markedly. Figure 12 (curves 2, 3) shows the kinetic curves for recording on open layers with *dL* = 215 μm that were prepared with solvent (curve 3) and without any solvent (curve 2).

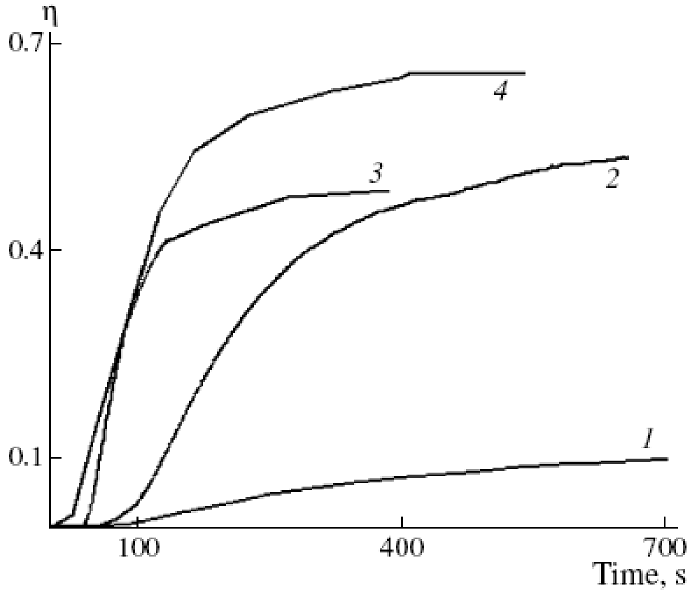

Figure 12. Kinetic curves of recording on (1) closed and (2–4) open layers with the following parameters: (1) $d_L = d_{\text{eff}} = 35$ μm with toluene as a solvent; (2) $d_L = 220$ μm without any solvent; (3) $d_L = 212$ μm with benzene as a solvent; and (4) $d_L = 202$ μm, contains 12 wt % α-bromonaphthalene

A comparison of curves 1, 2, and 3 shows that the time it takes to attain the maximal diffraction efficiency on the open layer decreased for the layer lacking the residual solvent and for the layer containing the residual solvent; the induction period also decreased. An increase in the rate of recording on the layer containing the solvent compared to the layer lacking the solvent may be associated with the diffusion limitation on the rate of polymerization with an increase in the polymer viscosity (the layer without the residual solvent). A small difference in the maximal diffraction efficiency of the gratings on the above layers is related to their different thicknesses (see, figure captions). For the photoinitiation system (camphorquinone and Michler's ketone) that provides the holograms formation, the polymerization of the monomers was inhibited by atmospheric oxygen *[Smirnova, 2000]*. The ability of the light-sensitive formulation based on the above described poly(ester urethane acrylates) for holographic recording on open layers may be attributed to the involvement of catalysts of the chemical reactions of their formation (tertiary amines) in photochemical transformations of the tested photoinitiation system. Atmospheric oxygen and acrylate blocks of polymer chains may also take part in the formation of transient donor–acceptor complexes, thus hampering the inhibiting effect of oxygen on the photopolymerization process *[Granchak, 2005]*. For hologram fixation, the selection of the initial concentrations of initiation system components is of crucial significance. Our studies showed that the optimal concentration of camphorquinone in the mixture is 3 wt %. This value ensures an acceptable rate of recording and the fixation of holograms under heat treatment. In order to record holograms with a stable diffraction efficiency, they should be stored at a temperature of 60°C for 1 h. Further UV irradiation stabilizes the hologram owing to the complete phototransformation of active groups. In this case, the diffraction efficiency of the gratings decreases by 5–7%. The enhancement and fixation of holograms was also investigated via addition of a neutral diffusant into the starting formulation. α-Bromonaphthalene with a higher refractive index compared to the polymer n =1.66 was used as a diffusant. In the course of recording, the neutral diffusant gets dispersed from regions of the crosslinked polymer network at maxima of the interference field to its minima, thus increasing the amplitude of the refractive index modulation and stabilizes the grating *[Sakhno, 2008]*. The kinetic curve of recording is shown in Fig. 11 (curve 4). Upon introduction of the neutral diffusant, the induction period shortens, while the rate of recording and its diffraction efficiency increase. The gratings thus obtained do not need fixation. Further heating (time and temperature are shown above) causes an increase in the diffraction efficiency from 65 to 73%, and this value remains invariable upon cooling to room temperature. It appears that the heating of the grating facilitates the diffusion separation of the polymer and the neutral diffusant. As a result, the value of n_1 and, accordingly, the diffraction efficiency of the grating increase.

Poly(ester urethane acrylates) with unsaturated bonds in hard blocks were synthesized using oligo(ester acrylates) containing functional groups. The mechanical characteristics of these polymers turned out to be appreciably improved upon UV irradiation. On the basis of these poly(ester urethane acrylates), light-sensitive formulations suitable for holographic recording have been developed (Figure 13). These formulations are characterized by the acceptable energy sensitivity (~400 mJ/cm^2) and provide formation of stable holographic gratings with a diffraction efficiency of 65–75% in the case of formulations containing the neutral diffusant. For formulations without this component, the diffraction efficiency is 35–40%. The holograms do not require further chemical treatment. For the formulation containing the neutral diffusant, the grating is fixed during recording. In the absence of the neutral diffusant, fixation is achieved via heating the grating to 60°C. This study showed that the oligo(ester acrylates) developed during our research are promising materials as photostructuring media for holography.

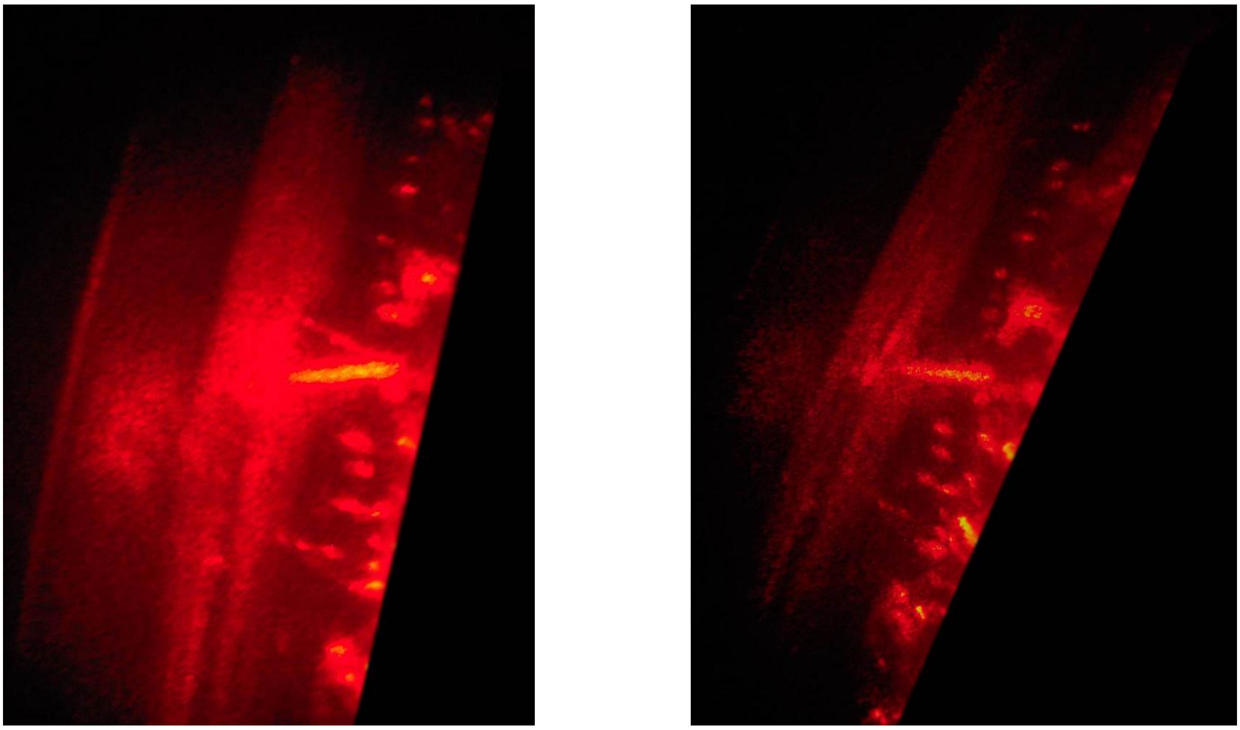

a b

Figure 13. Reading of a grating from an open surface (a) and from a support side (b)

The propagation of the beams in the layer was photographed with a digital camera. When the grating was red on the open surface side, refracted and diffracted beams were observed in the layer upstream the support. If the reading beam was directed on the grating from the support side, the diffracted beam was absent in the layer. The above picture shows that the grating is situated near the open surface. It is pertinent to note that samples with an increased heterogeneity were selected for visualization of trajectories of beam propagation in the layer.

Our results show that the oligo(ester acrylates) are promising as photostructuring media for holography.

3. Conclusion

The reactive diene oligomers (liquid rubbers) are subject of an increasing demand not only as casting elastomers of liquid moulding, sealants, filling compositions but also as modifiers for rubbers and epoxy resins, compatibilizers for rubberplasts etc. At present, industry produces oligodienes with hydroxyl end groups which allow a wide range of oligomers, containing practically any type of functional group, through the reaction of macrodiisocyanate synthesis. The effective methods of adjusting properties of the reactive oligodienes and their comprehensive characterization have been carried out. The use of HP deserves attention as a cheap and environmentally friendly initiator for the synthesis of HTPD. The mechanism of initiation in diene radical polymerization with HP was studied and this will allow scientists to extend its applications and methods of adjusting properties of oligomers.

Thus, a series of polymer materials was developed on the base of the reactive liquid rubbers. The investigations we performed permit to simplify the technology of synthesis of polymeric materials on the base of reactive oligodienes. We succeeded to conduct the reaction by a progressive method without solvents through a stage of isocyanate forepolymer synthesis. The physico-mechanical properties and abrasive-corrosive resistance of these polymeric materials may be improved, if necessary, during the process of exploitation in corrosive media.

4. References

Antonovskiy V. L. (1972) *Organic peroxide initiators*, Khimiya, Moscow, USSR.

Barantsova A.V. (1990), PhD Thesis, Institute of Macromolecular Chemistry, National Academy of Sciences of Ukraine

Barantsova A.V., Grishchenko V.K., Bus’ko N.A (2002) Polymeric materials based on oligodienediacilhydrazones for corrosive stable coating the Physical and chemical mechanics of the materials. Special release. No 3. *Problems of corrosion and anticorrosive protection of materials*, Lviv, Ukraine, pp. 593-596.

Barantsova A.V., Grishchenko V.K., Bus’ko N.A., Fal’chenko Z.V., Kochetova J.V. (2003) Oligodienediacilhydrazones and hidroabrasive-resistance polymers on their base, *Kompositsionnie. Polimernie. Materiali*. Vol. 25, No 1, pp. 24-27.

Barantsova A. V., Grishchenko V. K., Fal'chenko Z. V., Bus'ko N. A., Smirnova T. N., Ezhov P. V., and. Bondarenko O. F. (2007) Poly(ester urethane acrylates) and Holographic Properties of Formulations on Their Basis, *Vysokomolekulyarnye Soedineniya*, Ser. A, Vol. 49, No 8, pp. 1524–1531.

Barantsova A.V., Grishchenko V.K., Bus'ko N.A (2009) Characterization of polymeric materials base on liquid rubbers with terminal functional groups, *Kautshuk Gummi Kunstoffe*, No10, pp. 525-528.

Barcia F. L., Soares B. G., Sampaio I. (2004) Adhesive properties of epoxy resin modified by end-functionalised liquid polybutadienes, *J. Appl. Polym. Sci*., Vol. 93, No 5. pp. 2370-2378.

Baxendale J. H., Evans M. G., Park G. S. (1946) The mechanism and kinetics of the initiation of polymerization by systems containing hydrogen peroxide, *Trans. Faraday Soc.*, Vol. 42, No 3-4, pp. 155-169.

Berlin A. A., Kefeli T. Ya., and Korolev G. V. (1967) Poly(esteracrylates), Nauka, Moscow.

Bessière J.-M., Boutevin B., and Loubet O. (1993) Synthesis of a perfluorinated azo initiator, *Polymer Bulletin*, Vol. 31, No. 6, pp.673-677.

Boiko V. P. (2004) Transfer reactions and molecular parameters of oligodienes obtained under the action of hydrogen peroxide, *Institute of Macromolecular Chemistry of NAN of Ukraine*, *Dep. in State Science and Technology Library of Ukraine*, Kyiv.

Boiko V.P. (2008) The determination of the orders of isoprene polymerization initiated with hydrogen peroxide in the isopropyl alcohol solution, *Dopovidi NAN of Ukraine*, No 2, pp. 140-144.

Boiko V. P., Grishchenko V. K. (2009) The Influence of Solvent on the Isoprene Polymerization Initiated with Hydrogen Peroxide, *Kautschuk Gummi Kunst*., N 12, pp. 546-549.

Boiko V. P., Dyakova A. N. (2010) The thermochemistry of initiation of diene polymerization in alcoholic solution under the action of hydrogen peroxide, *Vopr. chim. i chim. tekhnol*., No 1, pp. 39-46.

Boiko V. P. (2010) Polymerization of isoprene in ethylacetate in the presence of hydrogen peroxide, *Chem. Chem. Technol.*, Vol. 4, No 1, pp. 57-60.

Boiko V. P., Grishchenko V. K., Gruzevich A. B., Kozlova G. A. (2010) The kinetics of acetylation of hydroxyl groups of oligodienes, *Polym. J*., Vol. 32, No 2, pp. 171-177.

Boiko V. P., Grishchenko V. K., Fedoseev M. S. (2011) Synthesis and characterization of oligoisoprene obtained in allyl alcohol solution in the presence of hydrogen peroxide, *Chem. Chem. Technol*., Vol. 5, No 2, pp. 173-180.

Boiko V. P., Grishchenko V. K. (2011) Hydrogen peroxide in the rubber chemistry, *Khim. Prom. Ukraine*, No 4, pp. 65-79.

Boutevin B., David G., Boyer C. (2007) Oligomers and Macromonomers by Radical Polymerization, *Adv. Polym. Sci*., Vol. 206, pp. 31-135.

Burchill C. E., Ginns I. S. (1970) The radiation-induced oxidation of ethanol and methanol by hydrogen peroxide in aqueous solution, *Canad. J. Chem*., Vol. 48, No 16, pp. 2628-2632.

Burel F., Oulyadi H., Bunel C. (2000) Microstructural characterization of hydrogen peroxide initiated hydroxy-telechelic polyisoprene, *Int. J. Polym. Anal. Charact*., Vol. 6, No 1-2, pp.193-212.

Burel F., Oulyadi H., Bunel C., Grishchenko V., Busko N., Barantsova A., Boiko V. (2011) Synthesis and structural characterization of a liquid polyisoprene bearing amidoxime end groups, *J. Polym. Res*., on line 15.07.2011.

Burkhart Richard D. (1969) Photo- and thermal initiator efficiency of 2,2'-azobisisobutyronitrile at 25.deg, *J. Phys. Chem.*, Vol. 73 No 8, pp 2699–2703.

Bus'ko N.A, Barantsova A.V., Grishchenko V.K., Falchenko Z.V. (2000) Azoinitiators, hydrocarbon oligomers with tail functional groups and polymers on their basis, *Kompositsionnie. Polimernie Materiali*, Vol. 22, No.1, pp.194-201

Chao H., Murphy J., Pytela J., Tian Nan (2003) New development of hydroxyl-terminated polybutadienes, *Conference Proceeding, Polyurethane Expo*, Oct. 1-3, 2003, Orlando, FL, United States, pp. 539-548.

Costa C. V. Santos H. S., H. Araujo P. H., Sayer C., Santos A. F., Dariva C., Fortuny M. (2010) Rapid decomposition of a cationic azo-initiator under microwave irradiation, *Journal of Applied Polymer Science*, Vol. 118, No. 3**,** pp. 1421–1429.

Daury J. D. (1977) Synthese et etude d'un polyisoprene hydroxytelechelique liquide, *Rev. gen. caoutch. et plast.*, Vol. 54, pp. 85-87.

Deb P. C. (1975) Non-ideal polymerization. Treatment of non-ideality due to primary radical termination and degradative chain transfer, *Eur. Polym. J*., Vol. 11, No 1, pp. 31-36.

Drach V. A, Barantsevich E.N. (1977) Polymerization diene hydrocarbons at presence azonitrile initiators containing carboxyl and hydroxyl groups. *Vysokomolekulyarnye Soedineniya*, Ser. A, Vol. 19, No. 6, pp. 1226-1229.

Dumitri J.S., Shaikh A. S., Comanita E.and Simionescu Cr. (1983) Bifunctional initiators, *European Polymer Journal*, Vol. 19, No 3, pp.263 – 266.

Fal'kova O. S., Slyakhter R. A., Valuev V. I., Avanesova Kh. M., Korol'kova M. D., Spirin Yu. L. (1974) The application of the functionality distribution for studying radical polymerization of butadiene-1,3 initiated with hydrogen peroxide, *Vysokomol. Soedin., Ser. A*, Vol. 16, No 10, pp. 2230-2232.

Fedorenko O.M., Kochetov D.P., Barantsova A.V., Khranovskii V.A., Grishchenko (1988) Intermolecular interactions in polymers on a basis oligodienediacilhydrazones. Vysokomolekulyarnye Soedineniya, Ser. B, Vol. 30, No 8, pp. 606–610.

Frankland J. A., Edwards H. G. M., Johnson A. F., Lewis I. R., Poshyachinda S. (1991) Critical assessment of vibrational and NMR spectroscopy technique for the microstructure determination of polybutadienes, *Spectrochim. Acta. Part A.*, Vol. 47A, No 11, pp. 1511-1524.

Granchak V. M. (2005) Extended Abstract of Doctoral Dissertation in Chemistry, Kiev.

Grishchenko V. K., Gritsenko F. R., Manzhula S.A. (1983) The method of obtaining elastic polyimidohydrazides, Cert. 923142, USSR.

Grishchenko V. K., Maslyuk A. F., and Gudzera S. S. (1985), Liquid Photopolymerizable Compositions, *Naukova Dumka*, Kiev.

Grishchenko V. K., But N.M., Gritsenko F. R. (1986) β-oxiethilamid azo-bis-izomasjanoj acid as the initiator of radical polymerization diene and vinil monomers, Cert.1211998, USSR

Grishchenko V. K., Boiko V. P., Svistova E. I., Yatsimirskaya T. S., Valuev V. I., Dmitrieva T. S. (1992) Hydrogen-Peroxide-Initiated Polymerization of Isoprene in Alcohol Solutions, *J. Appl. Polym. Sci*., Vol. 46, No 12, pp. 2081-2087.

Grishchenko V. K., Boiko V. P. , Kondratyuk A. Z., Dyshlova T. I. (1996) Synthesis of low-molecular liquid rubbers by radical polymerization of the fraction C_4 of oil products pyrolysis, *Dopovidi NAN of Ukrainian SSR*, No 10, pp. 123-126.

Grishchenko V. K. (2000) The processes of decomposition of hydrogen peroxide in reactions of diene polymerization, *Kompos. polim. mater*., Vol. 22, No 2, pp. 93-100.

Grishchenko V.K., Bus'ko N.A., Barantsova A.V., Fal'chenko Z.V. (2000) Azoinitiators and hydrocarbon oligomers with reactive terminal functional groups and polymers based on them, *Compos. Polym. Mater*., Vol. 22, No1, pp. 22-25.

Grishchenko V.K., Barantsova A.V.,. Bus'ko N.A. (2002) Polymeric coverings based on reactive liquid rubbers, *Voprosi chimii i chimicheskoy texnologii*, No 3, pp. 175-177.

Grishchenko V. K., Boiko V. P. (2004) Liquid rubbers – actuality, prospects of production, *Khim. Prom. Ukraine*, No 4, pp. 11-16.

Gritsenko F.R., Spirin Yu.L, Grishchenko V.K., Kochetova G.I. (1972 a) Oligodiene-diamine monomers and polymers, *Polymer Science U.S.S.R***.,** Vol. 14, No 6, pp. 1423-1429.

Gritsenko F.R., Spirin Yu.L, Grishchenko V.K., Pinchuk A. M. (1972 b) Method obtaining hydrazide of azo-bis-izobutyric acid, Cert. 389082, USSR.

Gritsenko F.R., Fal'chenko Z.V., Busko N.A., Grishchenko V.K. (1990) New initiators radical polymerization, *Vysokomolekulyarnye Soedineniya*, Ser. B, Vol.32, No 10, pp. 728–731

Gudzenko N.V., Grishchenko V.K., Barantsova A.V.,. Bus'ko N.A. (2010) Synthesis of amide of 2,2-azo-bis-isobutyric acid as an initiator of radical polymerization of diene and vinyl monomers , *Polymerniy journal*, Vol.32, No 2, pp.. 153-157

Gusev Yu. K., Glukhovskoy Yu. K., Yudin V. S., Shvetsova E. A. (2009) Low-molecular polydienes. Synthesis, properties, modification, application, *Kauchuk i Rezina*, No 2, pp. 15-17.

Hepuzer Yesim, Guvener Ufuk, Yagci Yusuf (2004) A New Azo Initiator for the Synthesis of Polymers with Pyrene Terminal Groups, *Polymer Bulletin*, Vol.52 No1, pp.17-23

Kercha Yu.Yu,.Oleinik S.P,.Shelkovnikova L.A,. Dashevskii L.I, Bogdanovic V.A.. (1990) Special features of the structure and properties of segmented oligodiene polyurethane elastomers with rigid segments of different structure, *Polymer Science U.S.S.R*, Vol. 32, No 5, pp. 955-960.

Kirsh Yu. E. (1998) *Polyvinylpyrrolidones and other poly-N-vinylamines*, Nauka, Moscow, URSS.

Kochetov D.P., Gomza Yu. P., Fedorenko O.M., Barantsova A.V., Khranovskii V.A., Grishchenko (1989) Interrelation of intermolecular interactions in carbamate polymers with their microphase structure *Vysokomolekulyarnye Soedineniya*, Ser. A, Vol. 31, No 5, pp.1-8.

Kochetov D. P., Barantsova A. V., Grishchenko V. K., Kotov V. D., Kostrichkin A. V., Kokorev V. A (1992), Oligodieneoxadiazolinylcarbamatediisocyanates and the method of their preparation. Cert. 1772106 USSR.

Kochetov D. P, Barantsova A. V., Grishchenko V. K, Trachevskiy V.V., Yatsimirskaya T.S.(1991) Structure of products of interaction acylhydrazone with isocyanates, *Ukr. Chim. J.*, Vol. 57, No2, pp 215-218.

Kochetov D.P., Bus'ko N.A., Barantsova A.V., Khranovskii V.A., Grishchenko V.K. (2001) Study of kinetic of azoinitiators photolysis, *Ukr. Chim. J.*, Vol. 67, No12, pp. 113-116.

Kogelnik H. (1969) Coupled wave theory for thick hologram gratinds, *Bell Syst. Tech. J.* Vol. 48. No. 9 P. 2909.

Marvel C.S., Deanin R., Claus C.J., Wyld M.B. (1948) Hydrogen Peroxide as Catalyst for Emulsion Polymerization of Butadiene and Styrene, *J. Polym. Sci.*, Vol. 3, No 3, pp. 350-353.

Maslyuk A. F. and Khranovskii V. A. (1989) *Photochemistry of Polymerizable Oligomers*, Naukova Dumka, Kiev.

Mogilevich M. M., Turov B. S., Morosov Yu. L, Ustavshchikov B. F. (1983) *Liquid hydrocarbon rubbers*, Khimiya, Moscow, USSR.

Mezhikovskiy S.M., Arinshtein A. E., Deberdeev R. Ya. (2005) The oligomeric state of substance, Nauka, Moscow, Russia.

Mejikovskiy S.M., Irjak V.I. (2008) *Chemical Physics curing of Oligomers Nauka*, Moscow, Russia, P. 269.

Minoura Yuji, Yamashita Shinzo, Okamoto Hiroshi, Matsuo Tadao, Izawa Michiaki, Kohmoto Shun-Ich (1978) Crosslinking and mechanical property of liquid rubber. I. Curative effect of aliphatic diols, *Journal of Applied Polymer Science,* Vol. 22, No 7, pp. 1817–1844.

Moore R.A., Kuncl K.L., Gower B.G. (1969) Liquid castable elastomers from hydroxyl-terminated polybutadienes, *Rubber World*, Vol. 159, No 5, pp. 55-58.

Myshak V.D., Lebedev E.V., Seminog V.S., Grishchenko V.K., Barantsova A.V., Bus'ko N.A.. (2006), Properties of polymeric composites on the base thermoplastic and the crushed rubber. Plastics in machine design, *Proceedings of 9rd Scientific conference*., 25-28 September 2006, Krakow, Poland, pp.373-376.

Pennachi V. A., Vilar V. D., Cardoso L. G. C., Mignez de Mello L. A. (1988) Liquiflex II – liquid hydroxyl terminated polybutadienes, *Eur. Adhes. and Sealants*, Vol. 2, Part 1, No 2, pp. 20-21, 24; Part 2, No 4, pp. 14-15, 18.

Petrov G.N., Kalaus A.E., Belov I.B. (1983) Liquid hydrocarbon rubbers, In book Synthetic rubber 2 publ., Chemia, Leningrad, pp. 377-411.

Pronin B.N., Barantsevich E.N., Shumniy L.V., Ivanchev S.S. (1977) Some kinetic features of radical polymerization butadiene-1,3 in a solution, initiated azodinitrile and peroxide the initiators containing atoms of halogens, *Vysokomolekulyarnye Soedineniya, Ser. A,* Vol. 19, No 7, pp. 1615-1619.

Raju T., Ding Yumei, He Yuelong, Yang Le, Paula M., Yang Weimin, Tibor C., Sabu T. (2008) Miscibility, morphology, thermal, and mechanical properties of a DGEBA based epoxy resin toughened with a liquid rubbers, *Polymer*, Vol. 49, No 2, pp. 278-294.

Sadeghi G. M. M., Morshedian J., Barikani M. (2006) The effect of solvent on the microstructure, nature of hydroxyl end groups and kinetics of polymerization reaction in synthesis of hydroxyl terminated polybutadienes, *React. & Funct. Polym,* Vol. 66, pp. 255-266.

Sakhno O.V., Smirnova T.N.,. Goldenberg L.M (2008) Holographic patterning of luminescent photopolymer nanocomposites, *Materials Science and Engineering,* Vol. 28, No 1, pp. 28-35.

Sartomer *(2002) Product bulletin Poly-bd® resins*.

Sato H., Ono A., Tanaka Y. (1977) Distribution of isomeric structures in polyisoprenes, *Polymer*, Vol. 18, No 6, pp. 580-586.

Schnecko H., Degler G., Dongowski H., Caspary R., Angerer G., Ng T.S. (1978) Synthesis and Characterization of Functional Diene Oligomers in View of their Practical Applications, *Angew. Makromol. Chem*., Vol. 70, No 1, pp. 9-30.

Smirnova T. N., Sakhno O. V. (2000) PPC: self-developing photopolymers for holographic recording, *Proc. SPIE* Holography., Vol. 4149, p. 106-112,

Solovyev M. E., Lyubimov D. V., Boiko V. P., Grishchenko V. K. (2011) Computer Modeling of Radical Polymerization in the System Butadiene – Hydrogen Peroxide – Isopropyl Alcohol, *Teor. Exper. Khim.*, Vol. 47, No 3, pp. 152-155.

Speckhard T.A., Cooper S.L. (1986) Ultimate tensile properties of segmented polyurethane elaastomers: factors leading to reduced properties for polyurethanes based on nonpolar soft segments, *Rubb. Chem. Technol.,* Vol. 59, No 3, pp. 405-431.

Spirin Yu. L., Grishchenko V. K. (1969) Carbochain polymers with terminal functional groups, *Institute of Macromolecular Chemistry of AN of Ukrainian SSR. Information letter No 13*, Naukova dumka, Kiev, Ukrainian SSR.

Svistova E. I., Khramova T. S., Boiko V. P., Grishchenko V. K. (1987) Reactivity of hydroxyl groups in oligoisoprene, obtained in the presence of hydrogen peroxide, *Ukr. Khim. J.*, Vol. 53, No 11, pp. 1213-1216.

Sychev A. Ya., Duka G. G. (2002) *Fundamental and applied aspects of homogeneous catalysis with metal complexes. Oxide and peroxide systems. In 2 parts,* Izd. center of Kishinev university, Kishinev, Moldova.

Time T. A., Moukhina K. M., Sidorovich E. A., Dmitrieva T. C (1992) The influence of the nature of a diol-extender on polyurethane structure and properties, *Kauchuk and rubber*, No 4, pp. 15-19.

Tompa A. S. (1972) Infrared Determination of Carboxyl and Hydroxyl Contents of Functionally Terminated Polybutadienes, *Anal. Chem*., Vol. 44, No 3, pp. 628-630.

Valuev V.I., Dmitrieva T.S., Schlyakhter R.A., Yatsimirskaya T.S., Boiko V.P., Grishchenko V.K. (1982) Polymerization of dienes under the action of hydrogen peroxide. *Vysokomol. Soedin. Ser. A,* Vol. 24, No. 6, pp. 1168-1173.

Van Hook J. P., Tobolsky A. V. (1958) The initiator efficiency of 2, 2′-azobisisobutyronitrile in the polymerization of styrene and methyl methacrylate, and dicumyl peroxide as a polymerization initiator, *Journal of Polymer Science,* Vol. 33, No 126, pp. 429–445.

Veselov I. V., Lyubartovich C. A. (2008) Moulding technologies in tire industry, *Kauchuk i Rezina*, No 5, pp. 27-35.

Yiğitoğlu Mustafa, Işıklan Nuran, Özmen Rukiye (2007) Graft copolymerization of *N*-vinyl-2-pyrrolidone onto sodium carboxymethylcellulose with azobisisobutyronitrile as the initiator, *Journal of Applied Polymer Science*, Vol. 104, No 2, pp. 936–943.

Yoshida Y, Itoh N, Saito Y, Hayakawa M, Niki E. (2004) Application of water-soluble radical initiator, 2,2'-azobis[2-(2-imidazolin-2-yl)propane] dihydrochloride, to a study of oxidative stress. *Free Radic Res*. Apr, Vol. 38, No 4, pp. 375-84

Zachariasiewicz M. (1986) The poly bd urethane challenge, *Plast. Rubber Int*., Vol. 11, No 5, pp. 36, 38-39.

Zbinden R. (1966) *Infrared Spectroscopy of High Polymers*, Mir, Moscow, URSS.

Zil'berman E. (1972) *Reactions nitrile,* Moscow::Khimiya.

Chapter 5

Polyurethanes and Their Derivatives

Cristina PRISACARIU, Elena SCORTANU,
Bogdan AGAPIE

Institute of Macromolecular Chemistry “Petru Poni” of Romania Academy, Iasi

---

Summary

This chapter presents new ideas in the fundamentals of conventional and novel PUs and PUUs which can be tailored, by both chemistry and processing, to yield products in a wide variety of forms and which allow the processor to control the nature and the properties of the end product. This review summarizes a series of researches made in the last years on the synthesis, and properties of PUs and PUUs and their sensitivity to molecular structure.

The dibenzyl system represents the simplest biaromatic system able for rotational isomerism which allows multiple spatial arrangements, with different reciprocal influences of the functional groups situated in the two rings. The possibility of introducing this system to a macromolecular chain and its influence on some properties of the polymer obtained was studied of the cases of polyurethanes, polyureas, poly(parabanic acids) and polyimides. Some practical applications of polymers with dibenzyl structures are presented.

Notations and acronyms

PPA	poly(parabanic acid)s
PU	polyureas
PUs	polyurethanes
SMPUs	shape memory polyurethanes
PUUs	polyurethane-ureas
BG	1,4-butanediol
DAB	4,4’-diamino-dibenzyl
DAPO	2,5-bis-(4-amino-phenylene)-1,3,4-oxadiazole
DAPY	2,6-diaminopyridine
DBDI	4,4’-dibenzyl diisocyanate
DEG	diethylene glycol
DMA	dynamic mechanical analysis
DSC	differential scanning calorimetry
EG	ethylene glycol
GPS	gel permeation chromatography
HDI	hexamethylene diisocyanate
HS	hard segment
IR	infrared spectroscopy
MDI	4,4’-methylene-bis-(phenyl isocyanate)
MDA	4,4’-methylene-dianiline
Mw	molar mass, kg mol^{-1}
$(COCl)_2$	oxalyl chloride
PEA	poly(ethylene adipate)
PTHF	polytetrahydrofuran
SAXS	small-angle X-ray scattering
SS	soft segment
TDI	2,4-and 2,6- toluene diisocyanate
TGA	thermogravimetric analysis
T	temperature, K
WAXS	wide-angle X-ray scattering
ε	strain, %
σ	stress, MPa

1. Polyurethanes and polyurethane-ureas

1.1 Introduction

Polyurethane (PUs) polymers form a class of materials with unique versatility. They are all characterized by presence of the urethane link –NH–CO–O– in the macromolecular backbone, and formed by reaction between isocyanates and polyols *[Krol, 2007]*, but materials with wide variations in physical properties are possible *[Chattopadhyay and Raju, 2007]*, by varying the choice of these ingredients *[Hepburn, 1982; Oertel, 1985]*. An important sub-group is the polyurethane elastomers, where at least one ingredient has a glass transition below room temperature *[Rogulska et al, 2007; Yilgor et al, 2006]*. In the segmented copolyurethane elastomers studied in the present work, molecules consist of alternating flexible (soft) and relatively rigid and/or mobile (hard) segments *[Dieterich and Uhlig, 2001]*. Phase segregation occurs during and following polymerization, to produce an elastomeric matrix of the soft segments, containing rigid inclusions (of size scale 10-100 nm) formed by association of the hard segments. The structure is therefore that of a polymer matrix microcomposite *[Petrovic, 2004]*. PUs are produced from three components: hard diisocyanate segments, soft macrodiol segments, and a low molecular mass diol acting as chain extender; or a diamine chain extender in the case of polyurethane-ureas (PUUs).

The present work is a review of a wider study of the effects on mechanical response of systematically varying the key structural variables: hard segment *[Kim et al, 1998]*, soft segment *[Ahn et al, 1994; Kim et al, 1998]*, crosslinking *[Sekkar et al, 2003]*, as well as the processing conditions *[Pompe et al, 1998]*. Such variations in composition lead to significant changes in the key mechanical properties of the elastomer, such as stiffness, strain recovery and strain energy recovery. In the present review, in particular, two hard segments were compared, based on the diisocyanates: 4,4'-methylene bis(phenyl isocyanate) (MDI) and 4,4'-dibenzyl diisocyanate (DBDI). Rotation around the central –CH_2–CH_2– bridge in DBDI allows alignment of aromatic rings and hence crystallization within the hard phase, which is not available with MDI in melt-cast polyurethanes (Figure 1).

As reported by ourselves *[Buckley et al, 2002, 2003; Prisacariu et al, 2003, 2005; Prisacariu and Scortanu, 2006; Scortanu et al, 2004]* and Lyman *[Gowerr et al, 1994]*, the MDI molecule introduces the rigid –Ph–CH_2–Ph– moiety in the elastomeric PU hard segments. In contrast when using DBDI, the specific –Ph–CH_2–CH_2–Ph– moiety introduces a variable geometry into the hard segments due to the possibility of internal rotation of this isocyanate around the –CH_2–CH_2– ethylene bridge *[Caraculacu and Coseri, 2001; Caraculacu and Caraculacu, 1985]*. This leads to the appearance of both “syn” and “anti” rotational conformations, which coexist in the DBDI based PU macromolecules. As a result, in this latter case the PU macromolecules can adopt a more compact packing which enhances significantly the ability to order in crystalline structures involving predominantly the “anti” form *[Prisacariu et al, 2003, 2005]*.

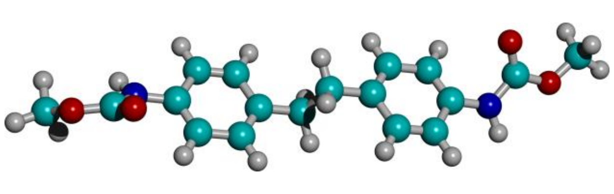

(a) (b)

Figure 1. Schematic of 4,4’-dibenzyl diisocyanate (DBDI) in “anti” configuration (a) and “syn” configuration (b)

Thus, new polymers were achieved, with a controlled ordering of copolymer hard segment blocks on the macromolecular chain. A systematic investigation was made of the effects of varying hard and soft segment chemistry, crosslinking and preparation procedures, on the mechanical response of polyurethane elastomers as shown in Figures 2 and 3. Structural investigation of the as-moulded polymers revealed the presence of crystallinity in some cases, in the DBDI-based PU materials (Figure 4) *[Prisacariu and Scortanu, 2007]*.

A major structural feature which was explored was the relationship between the nature of the hard segment (crystallizing or not) *[Brunnette et al, 1982]* and that of the soft segments.

1.2 Mechanical response of dibenzyl-based polyurethanes with diol or triol chain extension

The conventional isocyanate MDI and the novel diisocyanate DBDI, a diol, or a triol chain extender (1,1,1-trimethylol propane (TMP)) were included as well as more widely-used components, in order to widen the range of structures achievable beyond those normally available.

A systematic investigation was made of the effects of varying the chemistry of hard and soft segment and chain extender, and the preparation procedures employed, on mechanical response of the PUs. Since their structures could be varied systematically, they were used to probe the sensitivity of elastic and inelastic responses to structural detail, more comprehensively than has been possible previously *[Buckley et al, 2005, 2007; Prisacariu et al, 2006;*

Prisacariu and Buckley, 2007]. The results are compared with many known articles dealing with studies on shape memory behavior of different PUs based on MDI, TDI, HDI *[Hu et al, 2005; Jeong et al, 2000; Kim et al, 2000; Lin and Chen, 1998a, 1998b]*. Structures had been characterized by SAXS and WAXS as described elsewhere *[Prisacariu et al, 2003, 2005]*. Mechanical responses studied were small strain linear viscoelasticity (by tensile creep *[Buckley et al, 2007; Prisacariu et al, 2006]* and tensile DMA tests) and large strain, constant strain-rate and cyclic strain responses, including interrupted tests. In polymers with diol chain extenders there were tendencies to phase separation, with a characteristic length of ca 20nm, and, when DBDI was employed with certain chain extenders, to crystallization of the hard phase. In polymers prepared with the triol TMP as chain extender a crosslinked system was obtained, preventing phase separation.

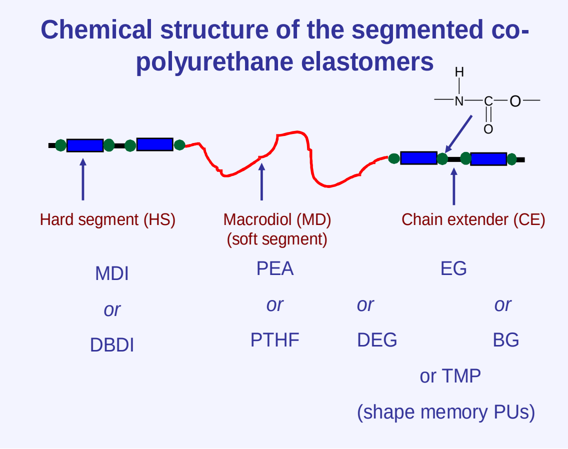

Figure 2. Structure of PUs. MDI – 4,4’ diphenyl methane diisocyanate; DBDI – 4,4’ dibenzyl diisocianate; PEA – poly(ethylene adipate); PTHF – polytetrahydrofurane; EG – ethylene glycol; DEG – diethylene glycol; BG – butanediol; TMP -1,1,1- trimethylol propane

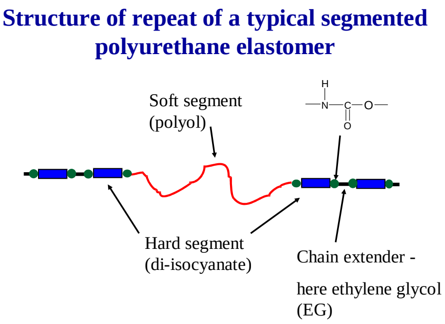

Figure 3. The PUs structure.

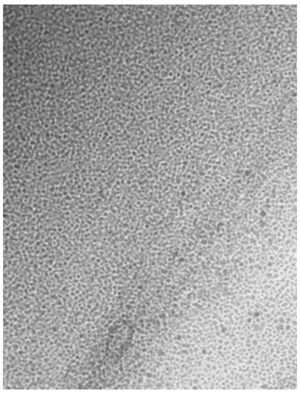

Figure 4. The two –phase microstructure of a PU based on DBDI; TEM micrograph

Measurements of the mechanical responses revealed clear evidence for a change in relaxation spectrum with phase separation, showing a bimodal distribution of molecular mobility of the soft segments: a mobile fraction remote from the hard phase and a constrained fraction at junctions with the hard phase. Moreover the relative mobilities of the constrained fractions could be seen to reflect those of the corresponding hard segments (DBDI being more flexible than the more usual MDI) to which they were joined. Even in the crosslinked systems a similar effect was observed, with the isocyanate-capped crosslink junctions playing the role of a hard phase. In large deformation cyclic experiments at room temperature, the degree of hysteresis and stress relaxation were found to be greatly enhanced by hard-phase crystallinity, through its effect on the flow stress *[Prisacariu et al, 2005]*. The extent of the Mullins effect showed a complex behaviour, dependent on both the degree of phase separation and the hysteresis *[Buckley et al, 2005; Prisacariu et al, 2005; Prisacariu and Buckley, 2007]*. These results provided new insight into the role played by nm-scale structures in determining the mechanical properties of PUs.

1.3 PUs stress-strain data and tensile strength properties

The characterization of different PU block copolymers consisting of different chemical, physical and consequently mechanical properties was made by means of uniaxial tensile experiments. Mechanical responses studied were large strain, constant strain-rate and cyclic strain responses.

Three PUs materials are compared between the PU stress-strain data of three PUs at nominal strain-rate = 0.0042/s; polytetrahydrofuran (PTHF) was used as a soft phase; A = PU based on MDI; B = PU based on DBDI; C = PU based on mixtures of MDI/DBDI, as well as for Pus for materials with poly(ethylene adipate (PEA) as soft phase. PUs materials labeled A, B, C, have hard segment compositions as follows (%MDI/%DBDI): A 100/0; B 0/100; C 50/50. In the case of copolymer C, the MDI and DBDI were pre-mixed before reaction with the soft segments, followed by chain extension. In all three cases the soft segment macrodiol was polytetrahydrofuran (PTHF) of molar mass 2000±50. The chain extender was ethylene glycol (EG). Molar proportions were diisocyanate DII:PTHF:EG = 4:1:2.64. With these proportions, the macrodiol accounted for 62-63% by mass and provided the continuous phase, and the 10% excess of isocyanate groups provided crosslinks at an average rate of 8 per 10 repeats of the DII-PTHF prepolymer, between hard segments. The experimental procedure was detailed elsewhere *[Prisacariu et al, 2003, 2005]*.

Stress-strain curves for the three types of PUs with PTHF or PEA are compared. Polymer B representing a PU based on DBDI has a higher flow stress than PU type A based on MDI and PU type C based on mixtures of MDI and DBDI. Yet PU derived from DBDI shows less pronounced strain stiffening. Polymer C shows more pronounced strain-stiffening than PU type A. A, B and C are polymers with PTHF as soft segment and ethylene glycol (EG) as a chain extender. The same behavior was observed in polymers where the adopted macrodiol (MD) was polyethylene adipate (PEA). The molar proportions used in the syntheses for these tests were diisocyanate D:MD:EG = 4:1:2.64.

1.4 PUs tensile load/unload cycles. Cyclic strain response

It has been shown that these chemical changes, and variation of thermal history, lead to varying degrees of phase segregation and crystallization in the hard segment *[Buckley et al, 2005; Prisacariu et al, 2003, 2005]*. In a recent preliminary collaborative study funded by a NATO Collaborative Project Grant, we have studied a series of these PUs elastomers under cyclic straining. We found trends in the cyclic stress-strain response, including a systematic variation in the degree of Mullins effect shown *[Buckley et al, 2005]*, with varying chemical structure. We have shown that the origin of these effects is intimately related to the nano-scale structure of the elastomers: the degree of phase segregation and the size and perfection of the hard domains. The presence of DBDI hard segments instead of MDI led systematically to increases in: the input strain energy to a given elongation, hysteresis and residual strain under cyclic loading, and stress relaxation.

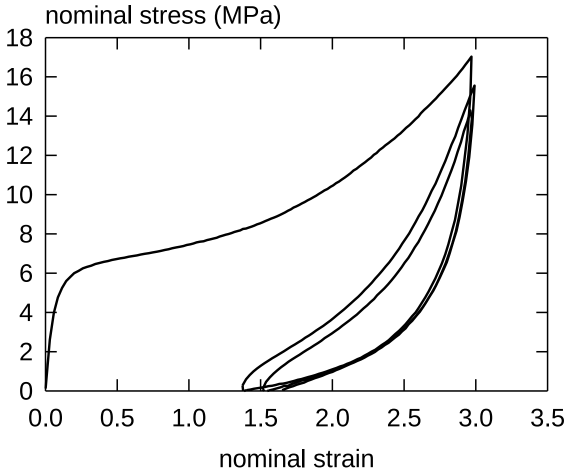

Figure 5. Tensile load/unload cycles for material A based on MDI: (EG-PEA-MDI,I=100), at strain rate 0.03 s^{-1} *[Prisacariu et al, 2005]*. Reprinted from *[Prisacariu and Scortanu, 2009]* from IJPAC, Copyright 2009

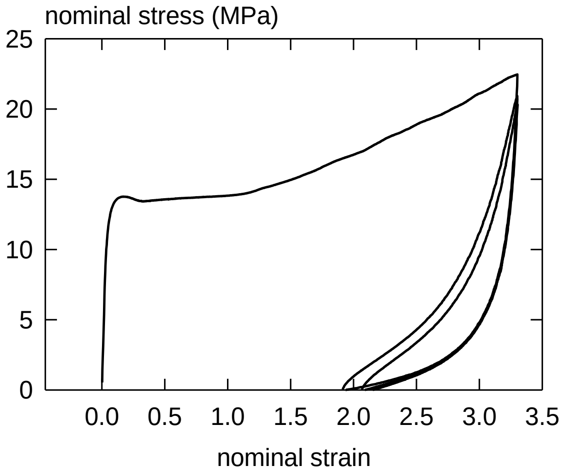

Figure 6. Tensile load/unload cycles for material B based on DBDI: (EG-PEA-DBDI,I=100), at strain rate 0.03 s^{-1} *[Prisacariu et al, 2005]*. Reprinted from *[Prisacariu and Scortanu, 2009]* from IJPAC, Copyright 2009

Typical results for uniaxial tensile load/unload cycles are shown in Figures 5 and 6 for polymers PU type A with MDI, and PU type B with DBDI C and a nominal strain-rate 4.2×10^{-3} s^{-1}. Each curve applies to a new specimen. Polymers based on DBDI hard segments, display higher stiffness and strength than the conventional MDI based PUs. The dominant feature is a hysteresis loop with a width that varies between the three polymers. Polymer with MDI hard segments gave the lowest stresses and least hysteresis, whereas polymer with DBDI hard segments gave the highest stresses and most hysteresis. Such features of the response were attributed to differences in hard phase plastic flow stress, resulting from crystallinity in the DBDI phase. Lower strain recovery and strain energy recovery on cycling (hysteresis) are observed in the case of PU derived from dibenzyl structures. Polymers with the structure EG-PEA-DBDI, displays higher Young Modulus values and higher residual elongation than does the conventional MDI based PUs.

Inelasticity (residual strain, hysteresis) increases with hard-phase crystallinity. Inelasticity reduces with better phase segregation and is greater for DBDI hard segments than for MDI. The stress-strain curves have the characteristic shape for elastomers containing reinforcing particles. There is a rate-dependent flow stress associated with stress-activated segmental diffusion at the surface or interior of reinforcing particles, superimposed on the strain-stiffening hyperelastic stress response of the elastomeric matrix. The most extreme difference between the effects of MDI and DBDI hard segments was seen in the cases where the chain extender–diisocyanate couple is EG-DBDI or BG-DBDI, where the hard segments were observed to crystallize. In such materials the stiffness, hysteresis, residual elongation and stress relaxation were all increased relative to the corresponding MDI based PU. When the couple was DEG-DBDI the same trend was observed, although the differences were less pronounced because DEG inhibits crystallization of the hard segments *[Prisacariu et al, 2005]*. These differences between DBDI and MDI could be attributed to the greater flexibility of DBDI allowing a higher tendency to self-associate by hydrogen bonding. The results were interpreted in terms of a physically-based constitutive model framework previously proposed *[Buckley et al, 2003; Buckley and Jones, 1995; Prisacariu et al, 2005; Sarva et al, 2007; Qi and Boyce, 2005]*. This revealed that the observed effects of varying hard segment could all be explained by the hard domains having a higher flow stress in the presence of DBDI relative to MDI, associated with increased hydrogen bonding in DBDI-based polymers, which is enhanced in some cases by hard segment crystallinity.

The performance of these materials as elastomers was shown to vary greatly depending on the composition. In large deformation cyclic experiments at room temperature, the degree of hysteresis and stress relaxation were found to be greatly enhanced by hard-phase crystallinity, through its effect of increasing the flow stress *[Buckley et al, 2003, 2005; Prisacariu et al, 2005]*.

1.5 Mechanical response of dibenzyl-based polyurethanes with diamine chain extension

1.5.1 PUUs stress-strain data and tensile strength properties

A series of polyurethane-ureas (PUUs) was synthesized by solution polyaddition reaction by using the polyetherdiol PTMO or polyesterdiol PEA and an aromatic diisocyanate, DBDI or MDI. As chain extenders were used 2,5-bis-(4-amino-phenylene)-1,3,4-oxadiazole (DAPO) or 2,6-diaminopyridine (DAPy), as well as two aromatic diamines: 4,4'-methylene dianiline (MDA) and 4,4'- diamino-dibenzyl (DAB), as shown in Figure **7** from below:

Synthesis of polyurethane and polyurethane-ureas.

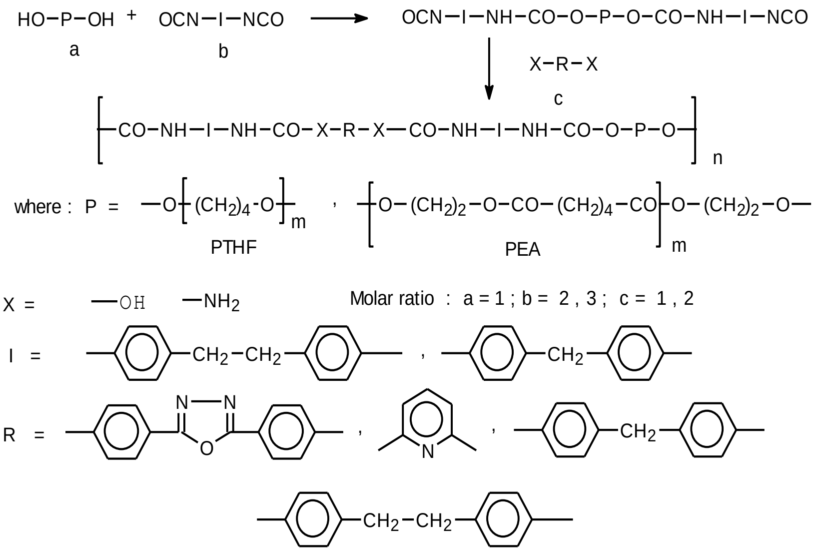

Figure 7. Synthesis of PUUs and PUs. The structures of adopted diamine chain extenders

Table 1. Composition of polyurethane-ureas. Molar ratio P/DI/DA 1:2:1

PU	Composition	Hard segment (%)	η_{inh} (dL/g)
PUOX$_1$	PEA/DBDI/DAPO	27.82	0.6
PUOX$_2$	PEA/MDI/DAPO	26.30	0.9
PUOX$_3$	PTMO/DBDI/DAPO	28.08	0.6
PUOX$_4$	PTMO/DBDI/DAPO	39.37	0.5
PUPY$_1$	PTMO/MDI/DAPy	24.69	0.6
PUPY$_2$	PTMO/DBDI/DAPy	24.93	0.4
PUPY$_3$	PTMO/DBDI/DAPy	34.47	0.5
PUPY$_4$	PEA/MDI/DAPy	23.18	0.4
PUDB	PTMO/DBDI/DAB	27.43	0.9
PUMD	PTMO/MDI/MDA	25.89	1

Investigation of PUUs mechanical behaviour was made by means of uniaxial tensile experiments. Mechanical responses studied were large strain, constant strain-rate and cyclic strain responses as shown in Figure 8 and 9 from below.

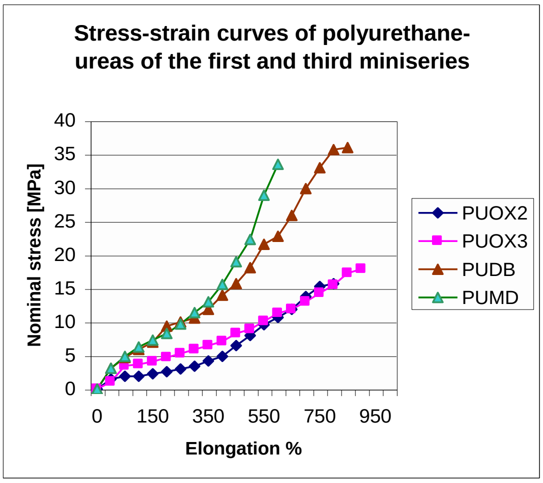

Figure 8. Stress-strain curves of selected PUUs extended with diamines DAPO, DAB and MDA

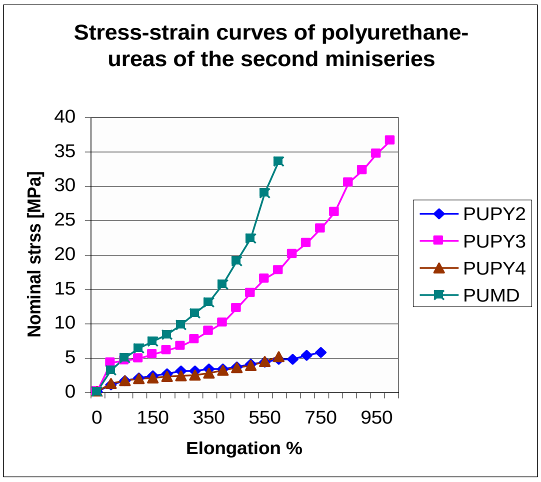

Figure 9. Stress-strain curves of selected PUUs extended with diamines DAPy. DAB and MDA

Mechanical properties of PU depend on their molecular weights (expressed as viscosity) and chemical structure of macromolecular chains *[Prisacariu et al, 2011a, 2011b; Scortanu et al, 2006a, 2006b]* (Table 1). Higher values of the stress-strain data were observed in the case of the PUUs sub-set chain extended with DAPO, for materials PUOX$_2$ and PUOX$_{3,}$ (Figure 8). For the series chain extended with DAPy, (Figure 9) higher values of the stress-strain data (strength stress value (36 MPa)), were found for polymers PUDB, PUMD and PUPY$_3$ (with 34.47% hard segment). The strength stress value increase with increasing the hard segment block content.

A comparison between the stress-strain curves of PUUs selected from Table 1 and a sub-set (Table 2) of two polyurethanes (PUs) chain extended with the diol ethylene glycol (EG), PUEG$_1$ and PUEG$_2$, was made as shown in Figure 10.

Table 2. Composition of diol-extended polyurethanes

PU	Structure	Molar ratio	Hard segment (%)
PUEG$_1$	EG-PEA-DBDI	2 / 1 / 2	37.5
PUEG$_2$	EG-PEA-MDI	2 / 1 / 2	38.6

The best mechanical properties are for polymers PUEG$_{1,2}$ with the longest hard segments as built during the synthesis, followed by polymers PUDB and PUMD, and lastly, PUUs containing heterocycles.

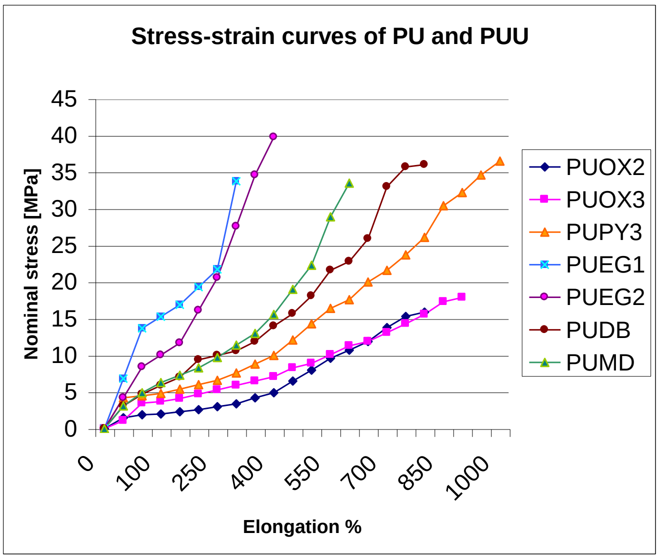

Figure 10. Stress-strain curves of polyurethane-ureas chain extended with DAPO (PUOX$_{2,3}$), DAPy (PUPY$_3$) DAB (PUDB), MDA (PUMD) as compared to polyurethanes chain extended with ethylene glycol (EG), PUEG$_1$ and PUEG$_2$

The best mechanical properties are for polymers PUEG$_{1,2}$ with the longest hard segments as built during the synthesis, followed by polymers PUDB and PUMD, and lastly, PUUS containing heterocycles.

The study of the relationships between structure and properties reveals the influence of the nature of starting materials, macrodiols, diisocyanates and chain extenders on the mechanical properties of the polymers. The great number of hydrogen bonding that formed between urea and urethane groups of polyurethane-ureas and the presence of oxadiazole or pyridine rings in the polymer chain induced an improved thermal stability in these polymers *[Prisacariu et al, 2011a, 2011b; Prisacariu and Scortanu, 2010; Sarva et al, 2007; Scortanu et al, 2006a, 2006b; Qi and Boyce, 2005]*.

1.5.2 PUUs tensile load/unload cycles

Typical results for uniaxial tensile load/unload cycles are shown in Figure 11 for a DBDI-based polyurethane-urea elastomer (PUDB) and in Figure 12 for a similar polymer but with MDI (PUMD). The structure of the two polymers is shown in Table 1 from above. Each curve applies to a new specimen. Polymers based on DBDI hard segments, display higher stiffness and strength than the conventional MDI based PUs. Polymer with MDI hard segments gave the lower stresses and least hysteresis, whereas polymer with

DBDI hard segments gave higher stresses and most hysteresis. Same conclusion could be drawn as in the case of polyurethanes chain extended with diol EG detailed in previous section 1.2: such features of the response can be attributed to differences in hard phase plastic flow stress, resulting from crystallinity in the DBDI phase.

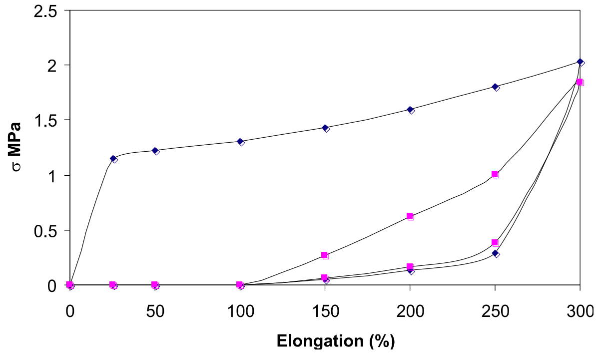

Figure 11. Tensile load/unload cycles for polyurethane-urea based on DBDI: PUDB (PTHF/DBDI/DAB)

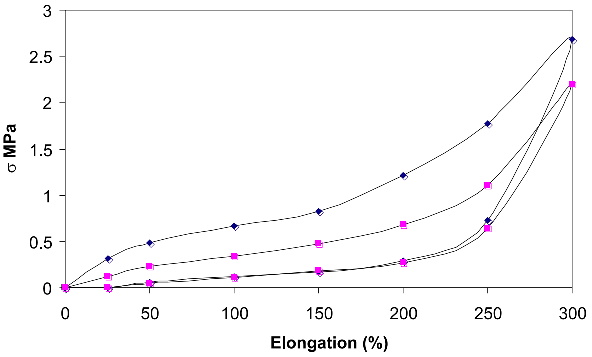

Figure 12. Tensile load/unload cycles for polyurethane-urea based on MDI: PUMD (PTHF/MDI/MDA)

1.6 Structural studies

1.6.1 WAXS Measurements

X-ray diffraction patterns showed significant crystallisability for the PUs materials based on DBDI hard segments. The three PUs materials detailed at section 1.1. are shown in Figures 13 a-c - labeled A,B,C, with hard segment compositions as follows (%MDI/%DBDI): A 100/0; B 0/100; C 50/50. In the case of copolymer C, the MDI and DBDI were pre-mixed before reaction with the soft segments, followed by chain extension. There was evidence of the appearance of more or less complete phase separation associated with the formation of discrete crystalline hard domains *[Prisacariu et al, 2003, 2005; Scortanu et al, 2004]*. However, when the mixture MDI/DBDI was used for hard segments (polymer B), the crystallinity was considerably reduced. As seen in Figure 13 b from below, the crystallinity index decreased from χ=0.14 (case for polymer B with DBDI) to χ=0.03 (case for polymer C with mixed MDI/DBDI) to χ=0 in the case of polymer A with single MDI. As mentioned elsewhere *[Prisacariu et al, 2005]*, in the case of polymer B with DBDI, the degree of crystallinity can be reduced also by employing a more flexible chain extender. However, the crystallinity of the DBDI based PUs is sensitive to the choice of chain extender. Chain extenders BG and EG lead to distinct diffraction peaks, but DEG gives an amorphous polymer *[Prisacariu et al, 2005]*. It is also noteworthy that the sample preparation technique also influences PU crystallization. It should be mentioned that the crystallinity of PUs with DBDI is more pronounced when the polymer is obtained as a sheet cast directly as a melt following synthesis than when the same PU has been obtained by evaporation from 10% solution of DMF. The crystallinity also changed completely if the solution-cast PU film was stretched to 300% elongation and released *[Prisacariu et al, 2005]*.

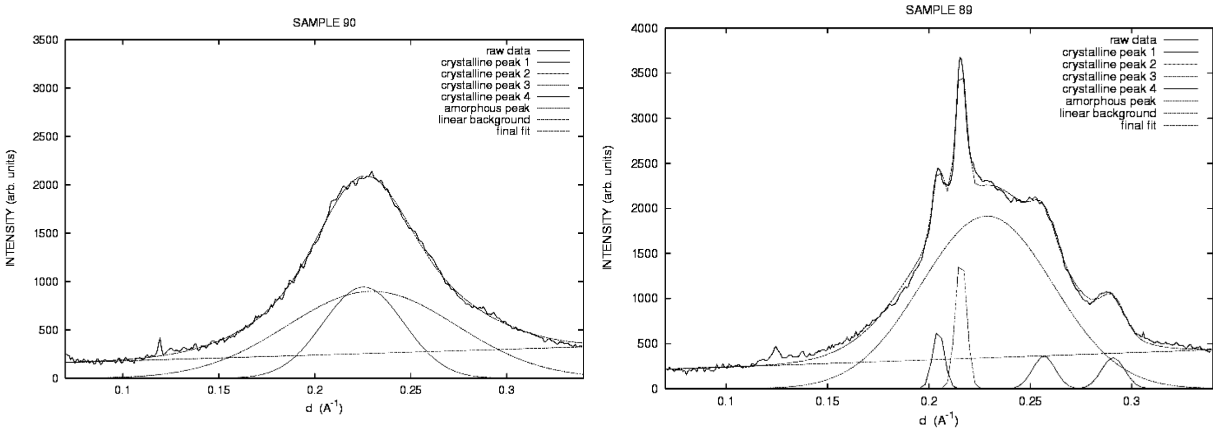

(a) Polymer A Hard segments = MDI
χ=0

(b) Polymer B: (Hard segments = DBDI
χ=0.14

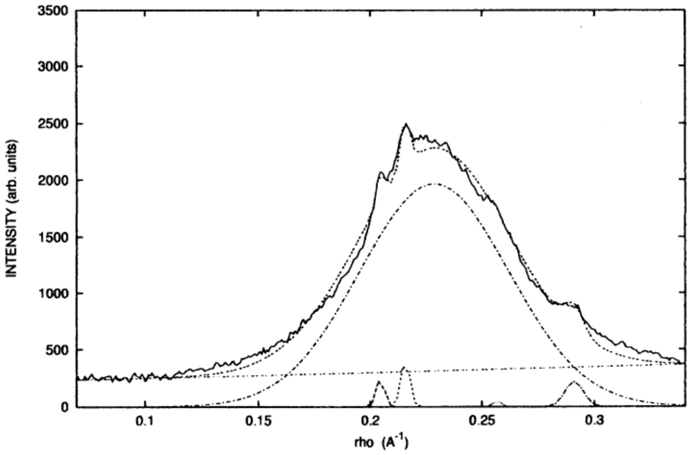

(c) Polymer C: Hard segments = MDI/DBDI χ=0.03

Figure 13 a-c. Crystallinity. WAXS profiles of PUs with hard segment compositions (%MDI/%DBDI): (a) 100/0; (b) 50/50 ; (c) 0/100

1.6.2 DMA and DSC results

PUs based on the chain extender EG and on DBDI or MDI alone were compared. The changes in crystallinity occurring in PUs were followed by means of dynamic mechanical analysis (DMA). The tests started at –140°C and the complex modulus E*, storage modulus E’, loss modulus E” and the loss factor tan δ were measured as functions of temperature at a heating rate of 1

K/min (Figures 14 and 15). The instrument was operated with controlled sinusoidal force with a frequency of 1 Hz. Depending on the type of synthesis and PUs structure, significant differences of the storage modulus (E'), and consequently differences in softening were found. The glass transition temperature depends on the mobility of the macromolecular chain. PU based on DBDI displayed a higher tendency to crystallize. The DMA results are presented in Figure 14 and 15. The storage modulus in the temperature range above the glass transition region is the highest for PU with DBDI and is controlled primarily by the crystalline content of hard segments. The DMA measurements have shown that the E' in the temperature range above the glass transition region is the highest for the DBDI based material. This is because of the higher content of DBDI based hard segments with a coplanar packing. For the series of elastomers the glass transition temperatures as defined by the maximum of the loss factor at f=1Hz was found to range from –11°C to –27ºC, the lowest T_g value corresponding to PU with DBDI and PEA, which displays a variable geometry. The glass transition temperatures are shown in Table 3.

Table 3. DMA measurements: values of Tg (from tan δ) and peak tan δ

PUs	$PU_{1\ (with\ DBDI)}$	$PU_{2\ (with\ MDI)}$
T_g, °C	-27	-19
Tan δ	0.176	0.34

The decrease of the modulus at about 150°C is due to the PU softening and melting.

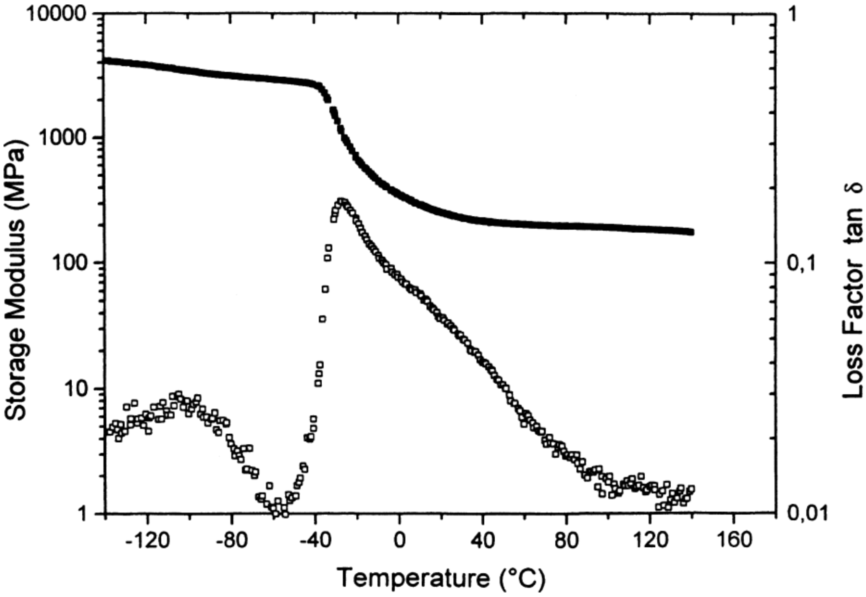

Figure 14. Storage modulus and Loss Factor as a function of temperature for PU1 (EG :PEA:DBDI)

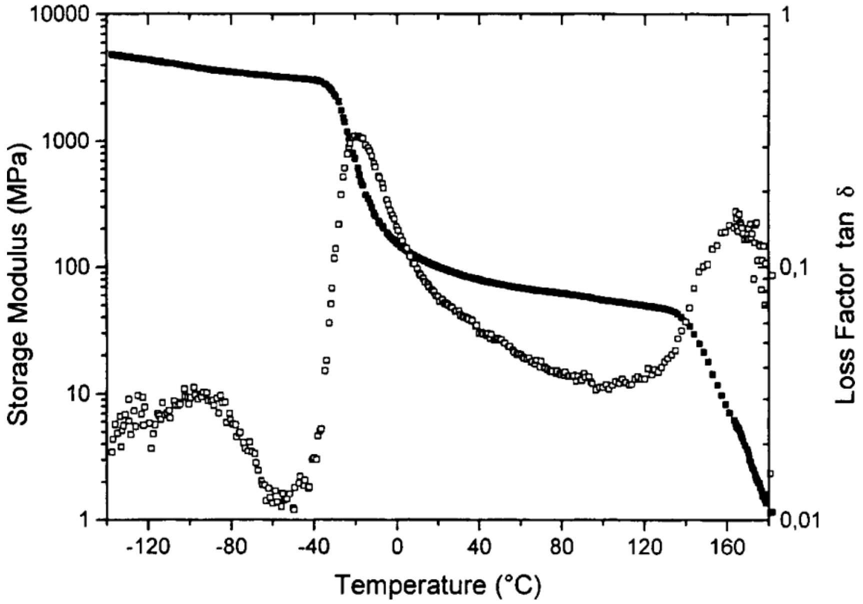

Figure 15. Storage modulus and Loss Factor as a function of temperature for PU2 (EG:PEA:MDI)

As shown elsewhere, a general improvement in PUs properties is obtained after polymer annealing at 160ºC for 30 minutes *[Prisacariu et al, 2003]* when two diisocyanates (MDI+DBDI) are employed in the PU synthesis (polymer C in sections 1.1 and 3.1 respectively).

The above results are in agreement with the results from WAXS *[Prisacariu et al, 2003; Prisacariu and Scortanu, 2007]*. PU with DBDI which displays a 50% degree of crystallinity has the lowest value of loss factor at Tg and the highest modulus above Tg, and degraded at a temperature above 250°C in DSC.

As seen in Figure 16 PU based on DBDI alone, displays the highest thermal stability with two pronounced endotherm maxima occurring at 310º–315ºC. In the case of material based on mixtures of MDI/DBDI (polymer C), a decrease in the polymer stability is apparent: two large maxima are found situated at temperatures below 300ºC, e.g. at 290º and 295ºC respectively. This is due to the substitution of DBDI by MDI. Previous work has also shown a tendency for the polymer network ordination and crystallinity to decrease *[Buckley et al, 2005; Prisacariu et al, 2003, 2005; Prisacariu and Scortanu, 2007; Scortanu et al, 2004]*. In the case of polymer C with mixtures of MDI/DBDI, with decreased crystallinity and intermolecular interactions, there is even a tendency of soft segments to crystallize. This is evidenced by the appearance of an endotherm maximum during heating, at approximately 50ºC. It should be also mentioned that in the case of PU_D there appear mesophase structures *[Prisacariu et al, 2003]* which are evidenced by a small endotherm maximum at about 220ºC.

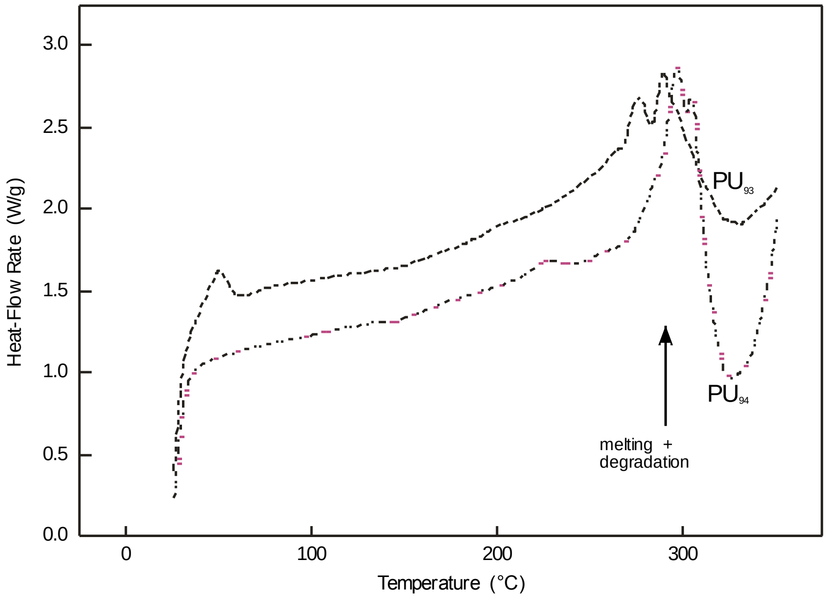

Figure 16. DSC curves for a polymer with DBDI alone (PU94 = B) and for a polymer with mixtures of MDI/DBDI (PU 93 = C), for a heating-rate of 20 K/min: high temperature region. Reprinted from Prisacariu et al. from Polymer Journal, copyright 2011

1.7 Conclusions

A range of novel segmented copolyurethane polymers was synthesized, in which the hard segment consisted of the flexible isocyanate 4,4'-dibenzyl diisocyanate (DBDI), the conventional rigid isocyanate MDI, or mixtures of these two isocyanates. Polyurethane elastomers derived from DBDI are based on hard segments of variable geometry. This induces increased degrees of crystallinity in the polymer, arising from rotation around the central $–CH_2–CH_2–$ bond in DBDI. This allows alignment of successive aromatic rings thus favoring a tendency to crystallization of the DBDI hard phase. In such polymers there is a remarkable tendency of the EG-DBDI couple to crystallize by self-association.

The conformational mobility of 4,4'-dibenzyl diisocyanate (DBDI) causes an unusually wide range of mechanical, physical and chemical properties, associated with the possibility of pronounced phase separation into a domain-matrix morphology, and with a higher tendency to crystallization and self-association by hydrogen bonding

New insight has been gained into structure-property relations in polyurethane elastomers by preparing them using mixtures of isocyanates. In large deformation cyclic experiments at room temperature, the degree of hysteresis and stress relaxation were found to be greatly enhanced by hard-phase crystallinity, through its effect of increasing the flow stress. Hard segments in polyurethanic materials based on DBDI and EG crystallize readily, but crystallinity is strongly reduced when the hard segment is a mixture of DBDI and MDI. Improvement in elastomeric properties, by reducing the crystallinity in PUs based on DBDI, was obtained when both diisocyanates were included and reacted together. The presence of the flexible DBDI hard segments instead of other conventional rigid isocyanates led systematically to increases in: the input strain energy to a given elongation, hysteresis and residual strain under cyclic loading, and stress relaxation. They were found to be greatly enhanced by hard-phase crystallinity.

The results of the stress-strain and hysteresis measurements effected on PUs and PUUs show that the polymers based on DBDI, display higher stiffness and strength than the conventional MDI based materials irrespective of the used chain extender (diols or diamines), with lower strain recovery and strain energy recovery on cycling - a primary consideration for elastomers.

PUs and PUUs properties depend strongly on the structure of the hard segment involved in the materials. With regard to the different types of hard segments derived from DBDI and usual diol or diamine chain extenders, in all of the cases their phase separation tendency is greater then that of similar hard segments based on MDI. In all cases the more mobile DBDI structure leads to hard segments with a higher tendency to self associate evidenced by higher melting points and crystallization tendency which is visible even when such structures are included in the polyurethane soft segment matrix.

2. Parabanic polymers and copolymers

2.1 Introduction

The researches about parabanic polymers started in our country as earlier as 1980, when a research group of “Petru Poni” Institute from Iassy was studied the novel methods of preparation of polymers and to diversify the parabanic copolymers types. The paper presents an overview on the knowledge in the poly(parabanic acid) domain by highlighting the Romanian research role in the promoting new methods of preparation and characterization of parabanic polymers and copolymers.

The polymers containing 1,3-imidazolidine-2,4,5-trione rings on the macromolecular backbone are known as poly(parabanic acid)s. There are known a few methods to obtain this kind of polymers starting from diisocyanates: by polyaddition reaction of diisocyanates with hydrogen cyanide followed by hydrolysis *[Patton, 1971]*, by polyaddition-polycondensation reaction between diisocyanates and bisesteroxalamides *[Reese and Kraft, 1970]*, the cycloaddition of oxalyl chloride at carbodiimide groups polycarbodiimides followed by the hydrolysis with water, as reported by Imashiro Y. and coworkers *[Imashiro et al, 1989, 1990]* and also syntheses of parabanic copolymers by using as comonomers, beside diisocyanates and hydrogen cyanide, some difunctional compounds like dicarboxylic acids, aromatic tetracarboxylic bis-anhydrides etc *[Chen and Onder, 1980]*. It is known that the air oxidation of polyhydantoines can produce polymers containing parabanic rings *[Koton et al, 1978]*.

2.2 New methods of parabanic polymer synthesis developed by Romanian researchers

Caraculacu and his coworkers have reported an original synthetic method to obtain poly(parabanic acids) by a cyclocondensation reaction with oxalyl chloride on polyureas (Scheme 1) *[Caraculacu et al, 1983; Scortanu, 1996; Scortanu et al, 1993, 1998a, 1998b, 1998c, 1998d, 2000, 2001a]*.

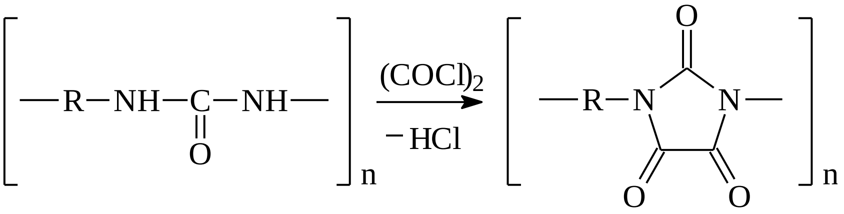

Scheme 1

The reaction way between polyureas and oxalyl chloride depends on the nature of substituents bound to the urea groups. In the case of urea groups incorporated into the polymer chain, the parabanic ring formation takes place quantitatively only if one of two radicals has an aliphatic or a non-symmetrical aromatic structure. For polyureas *[Scortanu et al, 2000]* containing only p-substituted aromatic radicals, the cyclocondensation reaction between polyureas and oxalyl chloride takes place partially as observed from IR absorption spectra. Based on the absorbances data, we calculated the transformation degree using an earlier reported method *[Caraculacu et al, 1983; Scortanu et al, 1993]*. All polymers show a good thermal stability T_d = 285-360°C (TGA) and T_g = 137-255°C (DSC), solubility, inherent viscosity values: 0.18-0.53 dl/g; by testing of electrical conductivity (0.38-4.0 x 10^{-16} ohm^{-1}.cm^{-1}) the polymers were found as being good electrical insulators *[Scortanu, 1996; Scortanu et al, 1998a]*. They were characterized also by X-ray diffraction measurements and it was observed that unlike polyureas, only two polyparabanates shown a semicrystalline behaviour: poly(hexamethylene-1,3-imidazolidinetrione), and poly(hexamethylene-1,3-imidazolidinetrione-p, p'-dibenzyl-diyl-1,3-imidazolidinetrione) with the degree of crystallinity of 72% and, respective, 45%. The molecular weight determined by GPC presented values of molar masses between 10,000 and 100,000 and polydispersities between 1.310-2.460. The products were characterized by IR spectra, elemental analysis, TGA and

DSC, GPC, solubility, inherent viscosity and by transformation degree values *[Scortanu et al, 1998b, 1998c, 1998d, 2001a, 2001b]*.

Recently new polymers like polyureas with 2,6-pyridyl structure *[Scortanu et al, 2003]* or poly-bis-ureylenes were subjected to cyclocondensation reaction with oxalyl chloride *[Scortanu et al, 2002; Scortanu and Caraculacu, 2001; Scortanu and Prisacariu, 2009]*. The products were characterized by IR spectra, elemental analysis, TGA and DSC, GPS, solubility, inherent viscosity and by transformation degree values.

2.2.1 Parabanic copolymers based on monomers with preformed parabanic rings

A series of monomers with parabanic rings (Scheme 2) was prepared and used for a variety of polyaddition or polycondensation reactions by some researchers groups *[Caraculacu et al, 1983]*. Caraculacu and coworkers *[Caraculacu and Caraculacu, 1984; Caraculacu et al, 1983, 1988, 1989, 1993, 1995, 1999, 1999b, 2001; Lungu et al, 1989; Scortanu et al, 1989]* have synthesized a part of the following monomers. Polyurethanes *[Caraculacu and Caraculacu, 1984]* with parabanic structure were synthesized by a two-step method. Some diisocyanates with urea structure were obtained by the addition reaction between different diamines and diisocyanate.

They were subjected to cyclocondensation reaction with oxalyl chloride and diisocyanates containing at least two parabanic rings were obtained. These monomers were reacted with diverse polyether and polyester diols leading to the corresponding polyurethanes *[Caraculacu and Caraculacu, 1984]*. Polymers presented melting points between 150-190°C and thermal stability up to 280°C. Their structure was confirmed by IR and NMR spectra and elemental analysis also.

2.2.2 Copolymers obtained from 1,3-bis(3-isocyanato-4-tolyl) parabanic acid (DITP)

Heterocyclic copolyureas *[Scortanu et al, 1989]* were prepared by polyaddition reaction between DITP and some heterocyclic diamines containing oxadiazole or benzothiazole rings. These polyureas presented viscosity values of 0.2-0.6 dL/g, melting points between 300-400°C and good solubility in amidic solvents. Polyquinazolinediones *[Caraculacu et al, 1989]* were obtained by polyaddition reaction of DITP and bis-anthranilic acid. The polyurea with pendant carboxylic groups was then heated to polyquinazoline-diones by cyclodehydration and transposition reaction at 220-230°C. All products structure was confirmed by TGA, IR and NMR spectra and elemental analyses.

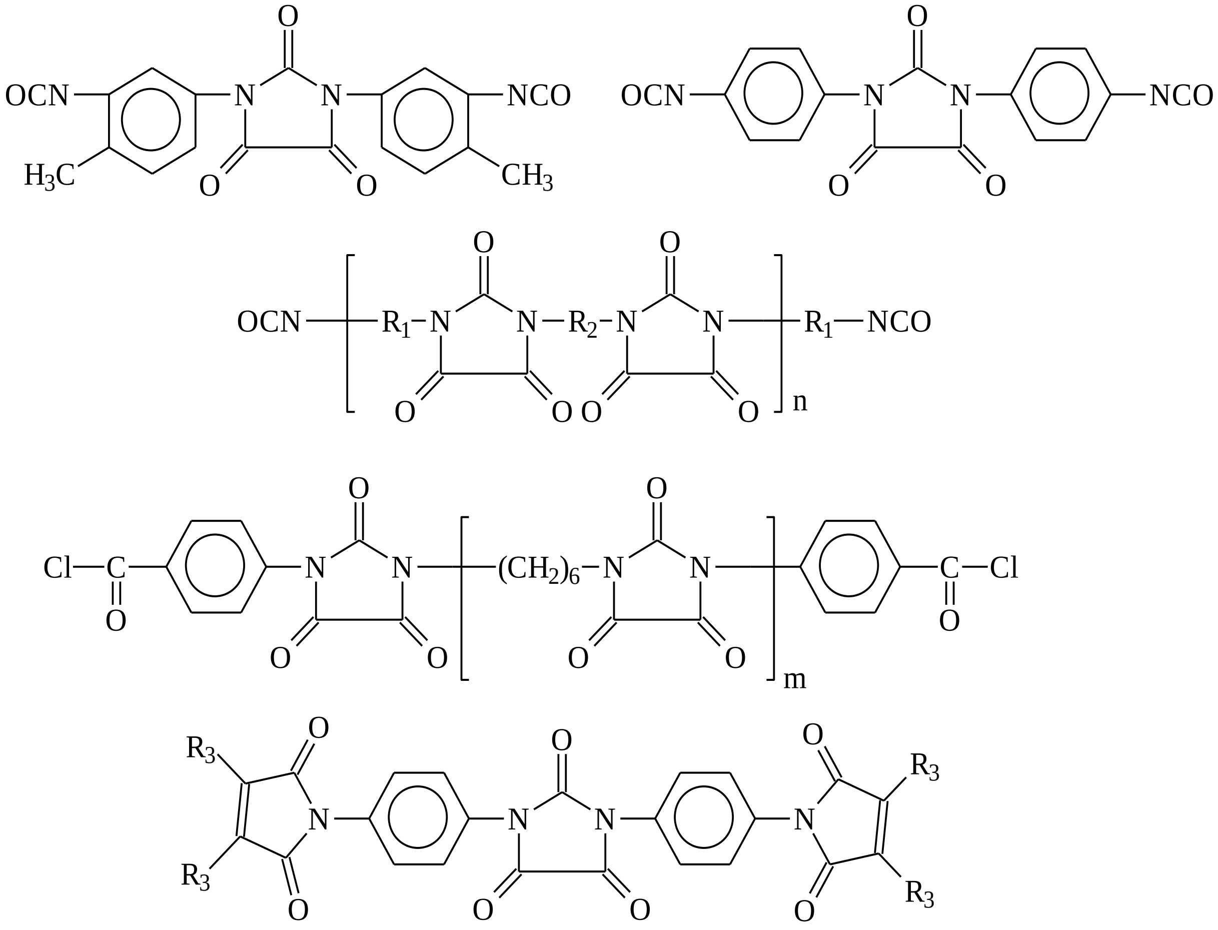

where : R_1 , R_2 are aliphatic or aromatic radicals
R_3 = H , Cl .
n = 1 - 6
m = 0 , 1

Scheme 2

This kind of polymer is thermally stable above 400°C. Polyamides, polyamid-imides and polyimides *[Caraculacu et al, 1993, 1995, 1999]* with parabanic structure were synthesized by polycondensation reaction between DITP and isophthalic acid, trimellitic anhydride, pyromellitic anhydride and benzophenontetracarboxylic dianhydride. The reactions took place in amidic solvents at 90-130°C with carbon dioxide evolving. These polymers exhibited decomposition temperatures between 330-400°C and good solubility in aprotic solvents also.

Parabanic polybarbiturate *[Scortanu et al, 1989]* was obtained by a two steps reaction of DITP and n-butyl-cyano-acetate, followed by cyclocondensation with the alcohol elimination. This polymer decomposed about 430°C *[Scortanu et al, 1989]*.

2.2.3 Copolymers obtained from 1,3-bis(4-chloroformyl-phenylene) parabanic acid (DCPP)

This monomer was prepared by Caraculacu and coworkers *[Caraculacu et al, 1988]* for the first time and used for polyamide preparation. All parabanic polyamides formed flexible films from solution that presented a tensile strength around 850 kg/cm^2 and good electro-insulator properties *[Lungu et al, 1989]*. Parabanic polyhydrazides were prepared by polycondensation reaction of dihydrazides *[Caraculacu et al, 1993, 1995, 1999, 1999b]* or aromatic dihydrazines *[Caraculacu et al, 2001]* and DCPP. Polyhydrazides based on dihydrazides can be thermal or chemical cyclodehydrated to polyoxadiazoles; they can be also transformed in polychelates with metal salts producing diverse colored precipitates.

2.2.4 Copolymers based on 1,3-bis (4-isocyanato-phenylene) parabanic acid (DIPP)

This monomer was prepared from DCPP by a Curtius rearrangement reaction of corresponding azide derivative *[Caraculacu et al, 1995]*. Copolyureas with Mg^{2+} salt on macromolecular chain were obtained from DIPP and diamines, one of them being a diamine containing Mg^{2+}. Diluted polyurea solutions exhibited electrical conductivity while in the solid state (pellets) polymers presented electrical conductivities ranging of 1-7x10^{-10} ohm^{-1}.cm^{-1}.

2.2.5 Parabanic compouds obtained by a dipolar 1,3 cycloaddition

Diisocyanates can react with benzaldazines by forming new type of heterocyclic polymers *[Caraculacu et al, 1999]*. Starting from the two parabanic diisocyanates (DITP and DIPP) we obtained α, ω-diisocyanate telechelics containing 1,3,5,7-tetraaza-bicyclo[3,3,0]-octane-2,6-dione. These compounds can be reacted further with macrodiols or diamines to form block-copolymers.

Based on parabanic monomer DCPP, Surpateanu and coworkers have obtained polymers with ylide structures by reacting DCPP with dipyridylium dicarbethoxymethylide *[Surpateanu et al, 1999]*. A new monomer containing two parabanic rings and two acyl chloride groups (BCPP) was prepared by Gaina and coworkers *[Gaina et al, 2001]*. Parabanic polyesters were obtained from BCPP and bis-phenols. They exhibited good solubility, thermal stability, and even a liquid crystalline behavior.

2.2.6 Parabanic polybismaleimides

Gaina and coworkers *[Gaina et al, 1997a, 1997b]* have synthesized other new monomers that contain a parabanic ring and two maleimide (or dichloro-maleimide) functional groups. Based on these monomers the authors have prepared two series of parabanic polymers: polyamino-bismaleimides and polyether-bismaleimides. Their structures were confirmed by analytical and IR and NMR spectral measurements.

3. Thermoplastic polymers containing parabanic structure and some potential applications

A few decades ago Patton and coworkers have initiated the researches concerning parabanic polymers by publishing the first data about the synthesis and characteristics of this kind of polymers. Their excellent thermal stability and solubility have recommended these polymers for a variety of applications in diverse domains by using as films, coatings, adhesives, semi-permeable membranes, etc. This work deals with some aspects concerning the potential applications as shown in the literature.

3.1 Parabanic polymers properties

Their properties devolved to the chemical structure of macromolecular chains, the parabanic rings presence, as well as from their linear nature. These polymers join the class of amorphous thermoplastic polymers and combine the solubility and heat molding with other properties belonging to heterocyclic polymers like as mechanical and thermal strength as shown by Russo *[Russo, 1973]* (Table 4 and 5). Mechanical properties of PPA-M and PPA-E (containing diphenylmethane and diphenylether structure) were studied as comparing to those of polyethyleneterephthalate (PET) and polyimides (Table 4). Dielectric properties are similarly to those of polyimides. The electrical properties are less sensible to heating as compared to those of PET being very alike to those of polyimides (Table 5).

Table 4. Comparation of properties of PPA and other polymers

Properties	**PPA - M**	**PPA - E**	**PET oriented**	**Polyimides**
Tensile strength at 23°C, kg/cm^2	984	1055	844	703-984
Tensile strength at 200°C	316	316	<70.5	422
Elongation retention %, 23°C	8-9	8-9	4	3-4
Elongation at break %, 23°C	8-50	15-60	100	35-70
Modulus kg/cm^2 at 23°C	23200	26175	38665	30230
Bending fatigue resistance (cycles) (MIT) at 23°C	10,000	<200,000	<200,000	10,000
Tear strength (initial) kg/cm^2 at 22°C	>63.3	70.3	70.3-211	77.3
Tear strength (propagation) g/25μm at 23°C	>8	10	15	8
Explosion test kg/cm^2, 23°C	1.4-2.1	2.1-2.8	2.1-5.6	5.27

3.2 Applications of parabanic polymers

PPAs are known as attractive thermoplastic materials due to a complex of different factor such as: accessible raw materials, rather simple methods of synthesis, the favorable balance of properties. They can be used mostly for the production of electrical and electronic devices because of their dielectric properties *[Kamioka et al, 1990]*, the flexibility or mechanical and thermal stability also. Some applications can be noted for printed circuit boards production as insulator layers applied on Cu or Al foils. Parabanic polymers can be casted from its DMF solution *[Kato et al, 1990]*, or can be bonded as films with an adhesive containing PPA also *[Ichikawa, et al, 1990]*. They were included also into photoresist compositions: either positive *[Sakaguchi, et al 1990]*, either negative resist *[Sakaguchi et al, 1990]* that was developed with alkaline solutions after UV irradiation. *[Matsuda et al, 1992]*.

Parabanic polymers can be used as insulator layers for flat microcoil elements of integrated circuit *[Toshiba Co, 1982]* or as casted polymers on vapor deposited Al coated polyester for capacitors production *[Ichikawa et al, 1992; Yamauchi et al, 1992]*. PPAs are used for their exceptional electrical resistivity *[Kamioka et al, 1987-1990]* like the breakdown voltage of about 50 kV/mm. They can be used simple or mixed by forming compositions for insulating coatings applied on Cu wire *[Fujisawa et al, 1992]*, as insulators useful for dry-type transformers, motors, generators *[Sakota et al, 1989]*, or by mixing with mica and producing some mica-tape insulators useful for high-voltage electrical apparatus *[Okunoyama et al, 1986]*.

Table 5. Thermal and electrical properties of PPA films

Properties	**PPA-M**	**PPA-E**
Heat distorsion temperature (2% elongation), °C	271	282
Linear thermal expansion coefficient 10^{-5} °C	5.7	3.3
Flamability (125 µm)	Self-extinction	Self-extinction
Dielectric constante 10^3 cps	3.82	3.60
Dissipation factor, 10^3 cps	0,0040	0,0027
air	6000	6000
oil	6700	6000
Volume resistivity Ω·cm	$>10^{17}$	$>10^{17}$
Surface resistivity Ω·cm	$>10^{16}$	$>10^{16}$
Electrical arc resistivity (second)	125	125

Composites based on PPA can be blended with electro-conductive powders *[Yamamoto et al, 1992]* like Ag powder, metal sulfides etc, leading to conductive adhesives or coatings exhibiting good shielding of electromagnetic waves property *[Iida et al, 1989]*. Thin PPA films coating Al foils were used for obtaining thermo-insulating composites that can be bonded under vacuum and formed insulating bags with applications in food industry *[Kaneko et al, 1988]*.

One can make also cryogenic containers that resist at the liquid nitrogen temperature *[Kaneko et al, 1982-1988]*, useful for blood or physiological fluids preservation. Blends of PPA and Teflon (PTFE) were found more resistant (improved pencil hardness and wear resistance) than the fluorinated polymer; thus such blends were used as container coatings including cooking utensils *[Kaneko et al, 1988]*.

Oriented PPA films were used as liquid crystal (LC) orientation control films that can blended with polyanilines or polypyrroles, useful as coatings of electrodes in LC display devices *[Watanabe et al, 1993]* PPA films for LC orientation *[Hayashi et al, 1992]* show a high alignment of macromolecules that determined a constant and uniform orientation of the stable phase leading to a substantial improvement of the image contrast *[Watanabe et al, 1984- 1993]*.

PPA films were successfully used for manufacturing of semipermeable membranes useful in reverse osmosis apparatus *[Knickel et al, 1976]*. These materials had a good thermal stability, selectivity and permeation rate as well as a high resistance in acid and alkaline media; they have a smaller density than those of polyimides. Because of their features, parabanic polymers can be used as selective separation membranes with salt removal of 99.9% for the sea water at working pressure of 130 atms. Liquid-liquid mixtures (such as acetic acid – water) can be separated by pervaporation through parabanic membranes with 80% yield *[Maeda et al, 1991]*. Because of their chemical and thermal stability, PPA membranes were prepared showing tenacity, porosity and permeability to CO_2, H_2, H_2O etc *[Maeda et al, 1991]*.

PPA having low heat distortion temperatures can be used for the preparation of thin thermally stable tubes (Φ 25μm) useful in precision apparatus as endless belts *[Tomita et al, 1976-1992]*.

4. Conclusion

This chapter presents only a part of parabanic polymers possible applications. There are other applications also, this kind of polymers being very attractive because of their lower costs as compared to other materials like polyimides. Compared to the cheaper polyesters, parabanic polymers were frequently preferred due to their higher thermal stability. In conclusion, these new polymers can be considered as very promising materials for different applications which represent enough reasons for justify our option to research the parabanic polymers domain.

5. Acknowledgements

The authors are grateful to Professor Paul C. Buckley, Department of Engineering Science, University of Oxford UK and to Professor Adrian

Caraculacu, Institute of Macromolecular Chemistry "Petru Poni", Iasi, Romania for helpful assistance in the polymer synthesis and characterization.

The authors are grateful to NATO for support via a CLg grant.

6. References

Ahn, T. O., Jung, S.-U., Jeong, H. M., and Lee, S. W. (1994), The properties of polyurethanes with mixed chain extenders and mixed soft segments. *Journal of Applied Polymer Science*, 51, 43-49. doi: 10.1002/app.1994.070510105

Brunette, C. M., Hsu, S. L., and MacKnight, W. J. (1982), Hydrogen-bonding properties of hard-segment model compounds in polyurethane block copolymers, *Macromolecules*, 15, 1, 71–77.

Buckley, C. P., Prisacariu, C., and Caraculacu A. (2003), 12th International Conference on Deformation, Yield and Fracture of Polymers, Cambridge, April, p. 349.

Buckley, C. P., Prisacariu, C., and Caraculacu, A. (2002), *Euromech Colloquium and Workshop*, Vienna, July; 96.

Buckley, C. P., Prisacariu, C., and Caraculacu, A. (2007), Novel triol-crosslinked polyurethanes and their thermorheological characterization as shape-memory materials, *Polymer* 48(5), pp. 1388-1396.

Buckley, C. P., Prisacariu, C., Caraculacu, A., and Martin, C. M. (2005), Inelasticity of hard-phase reinforced elastomers: A study of copolyurethanes with varying hard and soft segments, in *Constitutive Models for Rubber IV*, P.-E. Austrell, L. Hari. (Eds.), Taylor and Francis, p. 465.

Buckley, C. P., and Jones, D. C. (1995), Glass-rubber constitutive model for amorphous polymers near the glass transition, *Polymer* 36(17), pp. 3301–3312.

Caraculacu, A. A., and Caraculacu, G. (1985), Dibenzyl Structures in Macromolecular Chains, *Journal of Macromolecular Science: Part A - Chemistry* 22(5-7), pp. 631–652.

Caraculacu, A. A., and Coseri, S. (2001), Isocyanates in polyaddition processes. Structure and reaction mechanisms, *Progress in Polymer Science* 26(5), pp. 799–851.

Caraculacu, A. A., and Caraculacu, G. (1984), Poly(urethane-parabanic acid)s, *Die Makromolekulare Chemie*, 185, pp. 1079–1093. doi: 10.1002/macp.1984.021850602

Caraculacu, A. A., Lungu, N. C., and Caraculacu, G. (1988), Aromatic polyamide with parabanic structure, *European Polymer Journal* 24(12), pp. 1207–1209.

Caraculacu, A. A., Scortanu, E., and Caraculacu, G. (1999), New Parabanate Products by 1, 3-Dipolar Cycloaddition Reaction ('Criss-Cross' Cycloaddition), *High Performance Polymers* 11(4), pp. 477–482.

Caraculacu, A. A., Scortanu, E., and Hitruc, E. G. (2001), Polyhydrazides based upon aromatic dihydrazines, *European Polymer Journal* 37(12), pp. 2491–2497.

Caraculacu, G., Gaina, C., Caraculacu, A. A., and Stoica, G. (1995), Synthesis of metal containing polyureas with a parabanic structure, *European Polymer Journal* 31(10), pp. 987–991.

Caraculacu, G., Gaina, C., Gaina, V., Caraculacu, A. A., and Diaconu, I. (1993), Polyhydrazides and poly(1,3,4-oxadiazole)s with parabanic structures, *European Polymer Journal* 29(8), pp. 1143–1147.

Caraculacu, G., Scortanu, E., Agherghinei, I., Caraculacu, A. (1989), *Mater. Plast.*, 26, 18-20.

Caraculacu, G., Scortanu, E., and Caraculacu, A. A. (1983), Copolymer of poly(parabanic acid) and polyimide, *Journal of Polymer Science: Polymer Letters Edition* 21(4), pp. 277–280.

Caraculacu, G., Scortanu, E., Caraculacu, A. (1999), *Roum. Chem. Quart. Rev.*, 7, 251–268.

Caraculacu, G., Scortanu, E., and Caraculacu, A. A. (1983), The heterocyclization of several reactive polymers Poly(parabanic acids), *European Polymer Journal* 19(2), pp. 143–146.

Chattopadhyay, D. K., and Raju, K. V. S. N. (2007), Structural engineering of polyurethane coatings for high performance applications, *Progress in Polymer Science* 32(3), pp. 352–418.

Chen, A. T., Onder, K. B. (1980), *Polymer Preprints*, 21, pp. 136-137.

Dieterich, D., and Uhlig, K., (2001), *Polyurethanes, Ind. Polym. Handbook, Products, Processes, Apllications*, E. S. Wilks (Ed.) Wiley-VCH, Verlag GmbH, D-69-469, Weinheim (Germany) Vol I, pp. 445.

Fujisawa, K., et al, Composition for producing flexible heat-resistant insulation sheet or film and flexible heat-resistant insulation sheet or film JP. 04,314,754/1992, CA:**119**:10114e.

Gaina, C., Gaina, V., and Cozan, V. (2001): Synthesis and characterization of new polyesters containing imidazolidine-2,4,5-trione rings, *European Polymer Journal* 37(1), pp. 79–84.

Gaina, V., Gaina, C., Sava, M., Stoleriu, A., and Rusu, M. (1997), Bismaleimide Resins Containing Urethanic Moieties, *Journal of Macromolecular Science, Part A* 34(12), pp. 2435–2449.

Gaina, C., Gaina, V., Stoleriu, A., Sava, M., Chiriac, C., and Cozan, V. (1997), Heterocyclic Poly(bismaleimide)s. I. Synthesis and Characterization of New Poly(amino-bismaleimide)s Containing Parabanic Rings, *Journal of Macromolecular Science, Part A* 34(1), pp. 191–200.

Gower, L. A, Wang, T. L. D, Lyman, D. J. (1994), Morphology of block copolyurethanes: V. The effect of $–CH_2CH_2–$ vs $–CH_2–$ spacers between aromatic rings, *J. Biomater. Sci. Polymer Edn.*;6, 761.

Hayashi, O., et al, PPA copper laminated useful for electrical anisotropy conductivity; Ger. Offen DE, 4, 128,261/1992, CA: 117: 132504m.

Hepburn, C., *Polyurethane elastomers* (1982), Applied Science Publishers (London and New York).

Hu, J., Yang, Z., Yeung, L., Ji, F., Liu, Y. (2005), Crosslinked polyurethanes with shape memory properties, *Polymer International* 54(5), John Wiley&Sons, Ltd., pp. 854–859.

Ichikawa, R., et al, ; Heat-resistant laminated sheet JP. 02,120,037/1990, CA:113:133793j.

Ichikawa, R., et al, Manufacture of resin film having metal thin film layer JP. 04,339,647/1992, CA:119:29520f.

Imashiro, Y., and colab., US. 4,939,210, (1990), Imashiro Y. and colab., Eur. Pat. Appl. EP. 330,400, (Chem. Abstr. 1989, 112:99556e).

Jeong, H. M.; Lee, S. Y.; Kim, B. K. (2000), Shape memory polyurethane containing amorphous reversible phase, *Journal of Materials Science* 35, volume 35, Springer Netherlands, pp. 1579–1583, doi: 10.1023/A:1004761206709.

Kamioka, I. et al, Insulated wire JP. 02,304,809/1990, CA:115:210331c.

Kaneko, Y., et al Composition of PPA+PES+PTFE useful as cryogenic containers that resist at the liquid nitrogen temperature, including cooking ustensils JP. 82,100,057/1982, CA:97:199238q; JP.63,39,258/1988, CA:109:212200j.JP. 63,265,969/1988, CA:110:137169w.

Kato, M., et al, Thermally curable varnish, JP. 02,269,783/1990, CA:114:166497g;

Kim, B. K., Shin, Y. J., Cho, S. M., Jeong, H. M. (2000) Shape-memory behavior of segmented polyurethanes with an amorphous reversible phase: The effect of block length and content, *Journal of Polymer Science Part B: Polymer Physics* 38(20), John Wiley&Sons, pp. 2652–2657.

Kim, H. D., Huh, J. H., Kim, E. Y., Park, C. C. (1998), Comparison of properties of thermoplastic polyurethane elastomers with two different soft segments, *Journal of Applied Polymer Science* 69(7), John Wiley&Sons, pp. 1349–1355.

Knickel, B., et al, Semipermeable membranes; Ger. Offen. 2.431.071/1974, CA:84:123056q.

Koton, M. M., Kiseleva, T. M. et al. (1976), Vysokomol. Soedin, Ser. A; 18, 2092-2096; (1978) Vysokomol. Soedin, Ser.B., 20 , 803-805

Król, P. (2007), Synthesis methods, chemical structures and phase structures of linear polyurethanes. Properties and applications of linear polyurethanes in polyurethane elastomers, copolymers and ionomers, *Progress in Materials Science* 52(6), pp. 915–1015.

Lin, J. R., Chen, L. W. (1998), Study on shape-memory behavior of polyether-based polyurethanes. I. Influence of the hard-segment content, *Journal of Applied Polymer Science* 69(8), John Wiley&Sons, pp. 1563–1574.

Lin, J. R., Chen, L. W. (1998) Study on shape-memory behavior of polyether-based polyurethanes. II. Influence of soft-segment molecular weight, *Journal of Applied Polymer Science* 69(8), John Wiley&Sons, pp. 1575–1586.

Lungu, N., Caraculacu, G., Caraculacu, A. (1989), *Mat. Plast.* 26, pp. 193-195.

Maeda, Y. et al., in proceedings Int. Conf. Pervaporation Processes Chem. Ind., 5-th, 1991, 31-44; CA:118:23315a; Maeda, Y., PCT. Int. Appl. WO91,05,602/1991, CA:115:184913x.

Maeda, Y. et al., JP. 63, 91,123/1988, CA:109:111791x; JP. 65,91,124/1988, CA:109:111790w.

Matsuda, I. et al, Heat resistant adhesive composition; JP. 04,122,784/1992, CA:117:214127e.

Matsuda, I. et al, Heat-resistant adhesive composition; JP. 04,122,716/1992, CA:117:214126d;

Oertel, G. (1985), *Polyurethane Handbook*, Munich: Hanser Publishers, pp. 570.

Okunoyama T. et al, Heat-resistant and electroconductive adhesive; JP. 61, 21,172/1986, CA:105:44315x.

Patton, T. L. (1971), *Polymer Preprints*, 12, pp. 163-168, Patton, T. L. (1979), *Polymer Preprints*, 20, 183-196.

Petrovic, Z. S. (2004), *Polyurethanes, Handbook of Polymer Synthesis, Sec. Ed.*, Kricheldorf, H. R., Nuyken, O., and Swift, G. (Eds.) CRC Press, pp. 503.

Pompe, G., Pohlers, A., Pötschke, P., Pionteck, J. (1998) Influence of processing conditions on the multiphase structure of segmented polyurethane, Polymer 39(21), pp. 5147–5153.

Prisacariu, C., Buckley, C. P., Caraculacu, A. A. (2005): Mechanical response of dibenzyl-based polyurethanes with diol chain extension, *Polymer* 46(11), pp. 3884–3894.

Prisacariu, C., Scortanu, E. (2006), in Proc. 13th Intern. Conf. on Deformation, Yield and Fracture of Polymers, Rolduc, 9-13.04. 433.

Prisacariu, C., Scortanu, E. (2007) Crystallization and Properties of Novel Polyurethanes Based on the Chain Extender Ethylene Glycol and Aromatic Diisocyanates of

Variable Flexibility, *Macromolecular Symposia* 254(1), Wiley-VCH Verlag, pp. 153–159.

Prisacariu, C., Scortanu, E. (2009), Hard Segment Inelastic Effects on the Stress-Strain Response of Polyurethane Elastomers Based on Hard Segments of Variable Geometry, *International Journal of Polymer Analysis and Characterization (I.J.P.A.C)*, 14, pp. 527–539.

Prisacariu, C., Buckley, C. P. (2007), Synthesis and Characterization of Some Novel Polyurethanes Based on Rigid or Flexible Aromatic Diisocyanates and Mixtures of Them, *Annual Technical Conference "ANTEC 2007"* Cincinnati, OH, SUA, 6-11 May 2007, pp. 992.

Prisacariu, C., Buckley, C. P., Caraculacu, A. A. (2006), Synthesis and characterisation of novel shape memory polyurethanes derived from 4,4'-dibenzyl diisocyanates, *PU Deutsche Magazin*, 4, pp. 253.

Prisacariu, C., Olley, R. H., Caraculacu, A. A., Bassett, D. C., Martin, C. (2003), The effect of hard segment ordering in copolyurethane elastomers obtained by using simultaneously two types of diisocyanates, *Polymer* 44(18), pp. 5407–5421.

Prisacariu, C., Scortanu, E., Agapie, B. (2011), From highly crystaline to amorphous thermoplastic polyurethanes: sensitivity of the mechanical response to physical and chemical structure, PPS-27, *27th World Congress of the Polymer Processing Society*, May 10-14, Marrakech, Morocco.

Prisacariu, C., Scortanu, E., Agapie, B. (2011), New Developments in hard-phase reinforced elastomers: a study of copolyurethanes derived from mixtures of diisocyanates, PPS-27, *27th World Congress of the Polymer Processing Society*, May 10-14, Marrakech, Morocco.

Prisacariu, C., Scortanu, E., *Structural studies and the correlation with the stress-strain response in polyurethanes* (2010), Encyclopedia of Analytical Chemistry, ISBN: 978-04-7002-731-8, ap.150,1-24 R.A. Meyers (Ed.), John Wiley& Sons P+d.

Prisacariu, C., Scortanu, E., Stoica, I., Agapie, B., Barboiu, V. (2011), Morphological features and thermal and mechanical response in segmented polyurethane elastomers based on mixtures of isocyanates, *Polymer Journal*, 43, pp. 613–620 (2011).

Qi, H. J., Boyce, M. C. (2005), Stress–strain behavior of thermoplastic polyurethanes, *Mechanics of Materials* 37(8), pp. 817–839.

Reese, J., Kraft, K., Ger. Offen 1,920,845, (Chem. Abstr. 1970, 74: 23719h); Fr. 2,042,761, (Chem. Abstr. 1971, 78: 44448s).

Rogulska, M., Kultys, A., Podkościelny, W. (2007), Studies on thermoplastic polyurethanes based on new diphenylethane-derivative diols. II. Synthesis and characterization of segmented polyurethanes from HDI and MDI, *European Polymer Journal* 43(4), pp. 1402–1414.

Russo, M. (1973), *Mater. Plast. Elastomeri*, 39(3), pp. 218.

Sakaguchi, S. et al., Substrate for flexible printed circuit JP. 02,278,890/1990, CA:114:187179c.

Sakota K., et al., Electrically conductive adhesive JP. 01,135,885/1989, CA:111:246074 c;

Sarva, S. S., Deschanel, S., Boyce, M. C., Chen, W. (2007), Stress-strain behavior of a polyurea and a polyurethane from low to high strain rates, *Polymer* 48(8), 2208–2213.

Scortanu, E., Prisacariu, C., Caraculacu, A. A., Bruma, M., Sulitanu, N. (2006), New Heterocyclic Polyurethane-ureas based on 4,4′-dibenzyl diisocyanate, Part 1: Influence of Oxadiazole Structure on Mechanical Properties, *High Performance Polymers* 18(2), pp. 127–143.

Scortanu, E., Priscariu, C., Caraculacu, A. A. (2004) Study of the Mechanical Properties of Dibenzyl-Based Polyurethane Containing a Molecularly Dispersed UV Absorber, *High Performance Polymers* 16(1), pp. 113–121.

Scortanu, E., Prisacariu, C., Hitruc, E. G., Caraculacu, A. A. (2006), New Heterocyclic Polyurethane-ureas Based on 4,4'-dibenzyl diisocyanate. 2. Influence of Pyridine Units on the Mechanical Properties, *High Performance Polymers* 18(6), pp. 877–891.

Scortanu, E., (2009) Polymers and copolymers with 1,3-imidazolidine-2,4,5-trione structure, In: *Recent research trends in polymer science*, publisher: Transworld Research Network, Trivandrum-695 023, Kerala, India.

Scortanu, E., Prisacariu, C. (2009), New heterocyclic polymers with vicinal parabanic structure, *Rev. Roum. Chim.*, 54 (11-12), pp. 969-974.

Scortanu, E., Caraculacu, A., 12th International Conference of Chemistry and Chemical Engineering RICCCE 12, Bucuresti, 13-15 Sept. 2001, p. 101-106.

Scortanu, E., Caraculacu, A. A., Caraculacu, G., Agherghinei, I. (1993), Dibenzyl structure on the macromolecular chain – IV. Polyureas and poly(parabanic acid)s, *European Polymer Journal* 29(7), pp. 999–1001.

Scortanu, E., Caraculacu, A., Taranu, A., *Academy days of Iassy*, 3-5 Oct. 2002.

Scortanu, E., Caraculacu, G., Caraculacu, A., Ioan, C. (1998), *Synthetic Polymer Journal*, 5, pp. 148-157 .

Scortanu, E., Caraculacu, G., Caraculacu, A. A. (1998), Dibenzyl Structure on the Macromolecular Chains (VII): Heterocyclic Polymers from 2,2(,4,4(-Dibenzyl Tetramine, *Iranian Polymer Journal* 7(4), pp. 243–254.

Scortanu, E., Caraculacu, G., Caraculacu, A. (1989), *Mater. Plast.*, 26, pp. 74-78.

Scortanu, E., Caraculacu, G., Caraculacu, A. (1998), *Rev. Roum. Chim.*, 43, pp. 875-883.

Scortanu, E., Hitruc, E. G., Caraculacu, A. A. (2003), Parabanic polymers obtained by the cyclocondensation reaction of polyureas containing 2,6-pyridyl structure, *European Polymer Journal* 39(5), pp. 1051–1061.

Scortanu, E., Hitruc, E. G., Caraculacu, A. A. (2001), Chemical. Bulletin of "POLITEHNICA" Univ. (Timisoara), vol.46 (60), Fascicola 1-2, ISBN 1224-6018, Ed. Politehnica.

Scortanu, E., Nicolaescu, I., Caraculacu, A. A, Caraculacu, G. (2000), Dibenzyl structure on the macromolecular chain. XII. Polyureas: structure-property relatonships, *Polymer International* 49(8), John Wiley&Sons, pp. 881–887.

Scortanu, E., Nicolaescu, I., Caraculacu, G., Diaconu, I., Caraculacu, A. A. (1998), Poly(parabanic acid)s. New aspects of structure–properties relationships, *European Polymer Journal* 34(9), pp. 1265–1272.

Scortanu, E., *Parabanic Polymers and copolymers*, Ph. D. Diss., Inst. P. Poni, 1996.

Scortanu, E., Stoleriu, A., Caraculacu, A. A., Caraculacu, G. (2001), Structure-thermal properties relationships of poly(parabanic acid)s, *Iranian Polymer Journal,* 10, pp. 207-216.

Sekkar, V., Gopalakrishnan, S., Devi, K. A. (2003), Studies on allophanate–urethane networks based on hydroxyl terminated polybutadiene: effect of isocyanate type on the network characteristics, *European Polymer Journal* 39(6), pp. 1281–1290.

Surpateanu, G., Depature, L., Fourmentin-Lamotte, S. (1999), Polycycloimmonium salt and ylidic polymers. Polycondensation between N,N′-dipyridylium dicarbethoxymethylide and 1,3-bis(p-chloroformylphenyl)parabanic acid, *European Polymer Journal* 35(4), pp. 663–667.

Suzuki, S. et al., Photocurable polyparabanic acid resin composition; JP. 02, 64,156/1990, CA:113:98783j.

Suzuki, S. et al., Photosensitive polyparabanic acid resin composition; JP. 02 64155/1990

Tomita I. et al., PPA for preparation of thin thermally stable tubes useful in precision apparatus as endless belts, Japan Kokai 76, 50,378/1976, CA:85:79283f; JP.02,252,734/1990, CA:115:30767r; JP.04,197,622/1992, CA:118:8048x.

Toshiba C. O.; *Neth. Appl.* NL 81, 84,176/1982, CA:97:65104j.

Watanabe, T. et al., PPA films for LC orientation useful in LC display devices, JP. 80, 12,911/1982, CA:92:207161y; JP. 56,176,725/1984, CA:102:103740v; JP.01,88,425/1989, CA:111:173756p.JP. 05, 19,264/1993, CA:119:282370v; JP.05,34,698/1993, CA:120:42060w.

Yamamoto, T., Kubota, E., Taniguchi, A., Dev, S., Tanaka, K., Osakada, K., Sumita, M. (1992), Electrically conductive metal sulfide-polymer composites prepared by using organosols of metal sulfides, *Chemistry of Materials* 4(3), pp. 570–576.

Yamauchi, Y. et al., Heat resistant film capacitor JP.04,111,305/1992, CA:117:122982b.

Yilgor, I., Yilgor, E., Guler, I. G., Ward, T. C., Wilkes, G. L. (May 2006), FTIR investigation of the influence of diisocyanate symmetry on the morphology development in model segmented polyurethanes, *Polymer* 47(11), pp. 4105–4114.

Chapter 6

Recent Developments in Generation of Porous Polymer Materials

Kristina GUSAKOVA[1], *Olga GRIGORYEVA*[1],
Olga STAROSTENKO[1], *Alexander FAINLEIB*[1],
Daniel GRANDE[2]

[1] Institute of Macromolecular Chemistry, National Academy of Sciences of Ukraine, 48, Kharkivske shose, 02160 Kyiv, Ukraine
[2] Equipe "Systèmes Polymères Complexes", Institut de Chimie et des Matériaux Paris-Est, UMR 7182 CNRS – Université Paris – Est Créteil – Val-de-Marne, 2, rue Henri Dunant, 94320 Thiais, France

Summary

The present review summarises the main ways and up-to-date advances on generation of porous materials based on thermostable polymers. The main attention has been paid to basic principles and recent developments of pore generation techniques mainly for film-forming polymer materials suitable for application as membranes, absorbents, filters, etc. Effect of pore generation methods on chemical structure and morphological peculiarities as well as on physical-chemical properties of porous polymers produced have been analysed and summarized.

Notations and acronyms

iPP	isopolypropylene
PC	polycyanurate
PCL	poly-ε-caprolactone
PCNs	polycyanurate networks
PE	polyepoxide
PEA	polyetheramide
PEG	polyethylene glycol
PET	polyethylene terephthalate
PI	polyimide
PMMA	polymethylmethacrylate
PPO	polypropyleneoxide
PVME	polyvinylmethyl ether
AAm	acrylamide
DBP	dibutyl phthalate
DCBE	dicyanate ester of bisphenol E
DMP	dimethyl phthalate
DMPU	1,3-dimethyl-3,4,5,6-tetrahydro-2(1H)- pyrimidinone
DMSO	dimethyl sulfoxide
DVB	divinylbenzene
HEA	2-hydroxyethyl acrylate
MBAAm	*N*,*N*-methylene bisacrylamide
DMTA	dynamic mechanical thermal analysis
DSC	differential scanning calorimetry
FTIR	Fourier transform infrared spectroscopy
SAXS	small-angle X-ray scattering
SEM	scanning electron microscopy
TEM	transmission electron microscopy
HIPE	highly internal phase emulsion
HLB	hydrophilic-lipophilic balance
LIPE	low internal phase emulsion
MIPE	medium internal phase emulsion
MIP	molecularly imprinting polymers
o/w	oil-in-water
polyHIPE	polymer developed from HIPE
w/o	water-in-oil
d_{eff}	effective pore diameter
T_b	boiling temperature, ^{o}C
T_g	glass transition temperature, ^{o}C

1. Introduction

Porous materials, especially based on different polymers, are widely used in various industries (chemistry, engineering, biotechnology, microelectronics, etc.) as highly efficient membranes, porous substrates, selective adsorbents and filters, porous electrodes for fuel cells, sensors or insulators. Over the last 30 years intensive progress in synthesis and characterization techniques of porous polymer materials was noticed, appearing in advances in molecular and micellar imprinting, sol-gel techniques, radiation technologies and others stipulated by growing requirements of the up-to-date technologies *[Bryk, 2005, 2006; Ensinger et al., 2010; Hentze and Antoinetti, 2002; Minamisawa et al., 2009; Mulder, 1999; Reddy and Takahara, 2009; Waheed et al., 2009]*.

As it is known, the first porous polymer material was obtained by Staudinger and Husemann *[Staudinger and Husemann, 1935]* in 1935 by free radical copolymerization of styrene with divinylbenzene (DVB) in the presence of toluene (as a porogen) followed by removal of the later. As a result, the pore structure with pore size about 3-50 nm, was formed.

Last literature search through only Science Direct database (www.sciencedirect.com) has shown more than 222 500 references on synthesis and investigation of structure and properties of different porous materials, including about 65 500 papers, describing characterization of porous media based on polymers and mixtures thereof. Moreover, an impressive list of books (about ~30 500 results) was found by Google Books search (www.books.google.com), including ones on membrane and membrane technology and more than 26 100 publications, directly relating to porous materials and media appeared in the last 10 years.

Many scientific works are focused on generation of porous polymer materials with predicted porous structure (means a certain pore geometry, pore size, pore distribution, etc.) and desired complex of physical and chemical properties, such as high thermal, chemical or biological stability, permeability and mechanical strength, etc. *[Alexander et al., 2006; Hentze and Antoinetti, 2002; Hou et al., 2009; Ishizaki et al., 1998; Yang et al., 2006]*. However, due regard to creation and characterization of porous thermosetting polymers should be given.

In this chapter the main and most widely used methods of creation of porous polymers with both the controlled porosity and the desirable characteristics have been reviewed and the effect of pore generation methods on chemical structure and morphological peculiarities as well as on physical-chemical properties of porous polymer materials have been analyzed and summarized. The chapter is expected to be a guide on the preparation of porous thermosets based on thermally and chemically stable polycyanurates.

2. Basic classification of synthetic porous materials

Generally, the term “pores” indicates local three-dimensional hollow formations (voids) in the volume of solid phase, characterized by a certain shape, size and orientation relatively to the surface of the material *[Bryk, 2006; Zefirov and Kulov, 1995]*.

Pores could be open or closed, through or blind, interconnected or isolated, linear or branched, uni- or multidirectional (relatively to the surface of the material etc.) *[Oláh et al., 2007; Knunyanc, 1990; Matsuyama et al., 2002; Reinger and Huneault, 2006; Zefirov and Kulov, 1995]*.

According to the recommendations of the International Union of Pure and Applied Chemistry (IUPAC) *[Sing et al., 1985]*, pores are classified on macropores (with pore diameter exceeding 50 nm), mesopores (pore size ranging from 2 nm to 50 nm) and micropores (with pore diameter less than 2 nm) (cf. Fig. 1).

Further significant development of nanotechnologies stipulated the necessity of single standard on terminology in “nanoscience”. Therefore, based on the recommendations presented on the 7th International Conference on nanotechnologies in Wiesbaden, 2004, the technical committee E56 of the ASTM International formerly known as the American Society for Testing and Materials (ASTM) developed new international standard E2456-06, offering new classification in nanomaterials and nanotechnologies, where the materials with pore structure sizing from 1 to 100 nm were defined as nanomaterials *[ASTM, 2006; Maynard, 2006]*. However, such ranking is not widespread in scientific community.

Depending on matrix nature, all porous materials are divided into ***natural*** (biological: protein, lipid, etc.) and ***synthetic*** (based on polymers such as perfluorine polymers, organosilicon polymers, polyamides, polysulfones, etc.) *[Bryk, 2005, 2006; Ishizaki et al., 1998; Hentze and Antoinetti, 2002]*.

For synthetic porous materials such characterization features, as method of producing, chemical nature, type of porous structure, pore size, dimensional shape of the samples and others (cf. Fig. 1), are commonly used.

3. Basic principles of pore formation

Properties of porous polymer materials as well as application area of the latters are defined by porous structure developed. In turn, pore geometry as well as pore surface (smoothed or embossed) strongly depend on the approach applied, namely on synthesis conditions of polymer matrix, type and content of porogen used, etc. The number of typical porogen-containing methods of pore creation in polymer materials is shown in Fig. 2, and the main techniques to produce porous polymer materials without any porogen are summarized in

Fig. 3. The pore formation process can be divided into two main steps: 1) *in-situ* synthesis of polymer in the presence of porogen; 2) porogen removal (by extraction, heating, pressure change, etc.). An obligatory condition for pore generation in polymer sample, being synthesized in the presence of porogen, is that the latter still has to be inside the sample even after completion of polymer matrix formation.

Gases, solvents, supercritical fluids, macromolecules of different sizes, etc. are typical porogens allowing generation of well-defined porous structure. As a result foams and membranes based on thermoplastic or thermosetting polymers, as well as sponge rubbers can be successfully produced (cf. Fig. 2) *[Bryk, 2005, 2006; Ishizaki et al., 1998; Hentze and Antoinetti, 2002; Mulder, 1999; Russel and Hedrick, 2001]*.

There are some non-porogen methods of creation of porous polymer materials (mainly as film materials or hollow fibers), such as mechanical stretching, electrospinning, powder sintering or track etching (cf. Fig. 3). Characteristic feature of these methods is that porous structure occurs as a result of additional physical or physical-chemical treatment rather than selective degradation or extraction of one of the compounds.

The most common methods of generation of pore structure in polymer materials are discussed below in more details.

4. Foaming technique of pore-generation

Generally, foaming approach consists of gas saturation during polymer synthesis followed by the removal of gaseous product (e.g. by temperature or pressure changes, etc.) after formation of porous structure *[Bibin et al., 2007; Ferrero-Heredia et al., 1996; Kim et al., 2006; Klempner et al. 2004; Lips et al., 2005; Nam et al., 2000; Shutov, 1991]*. However, gas can be also formed as a result of chemical interaction between the components of the reaction mixture.

Lips et al. *[Lips et al., 2005]* has obtained porous polymer material by foaming of polyetheramide, comprising 25 mol.% and 50 mol.% of bisamide segment content, with CO_2 under 50 bar. SEM and microcomputer tomography results showed that the pores generated were predominantly closed, sizing from 2.5 to 100 μm, maximum porosity of the samples was 90%. It was found that pore characteristics of the samples obtained extremely depends on foaming temperature, namely the higher bisamide to ester ratio, the smaller pores revealed.

The authors have also established that lowering of CO_2 saturation pressure led to the decreasing of porosity of the foams prepared along with increasing of pore sizes. The investigations have also shown that at temperatures up to 80 °C the porous materials obtained have suitable mechanical properties and dimensional stability *[Lips et al., 2005]*.

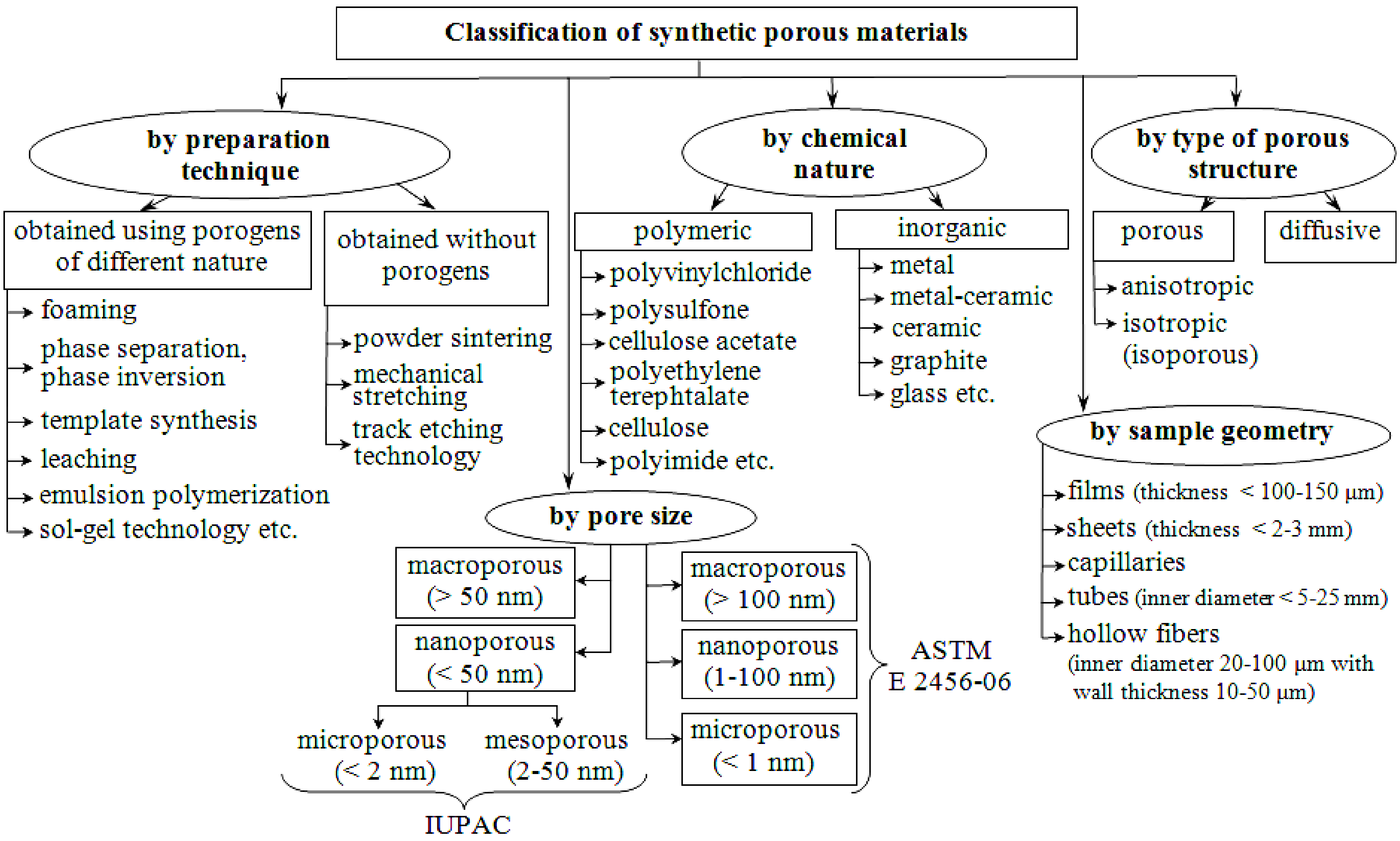

Figure 1. Classification of synthetic porous materials

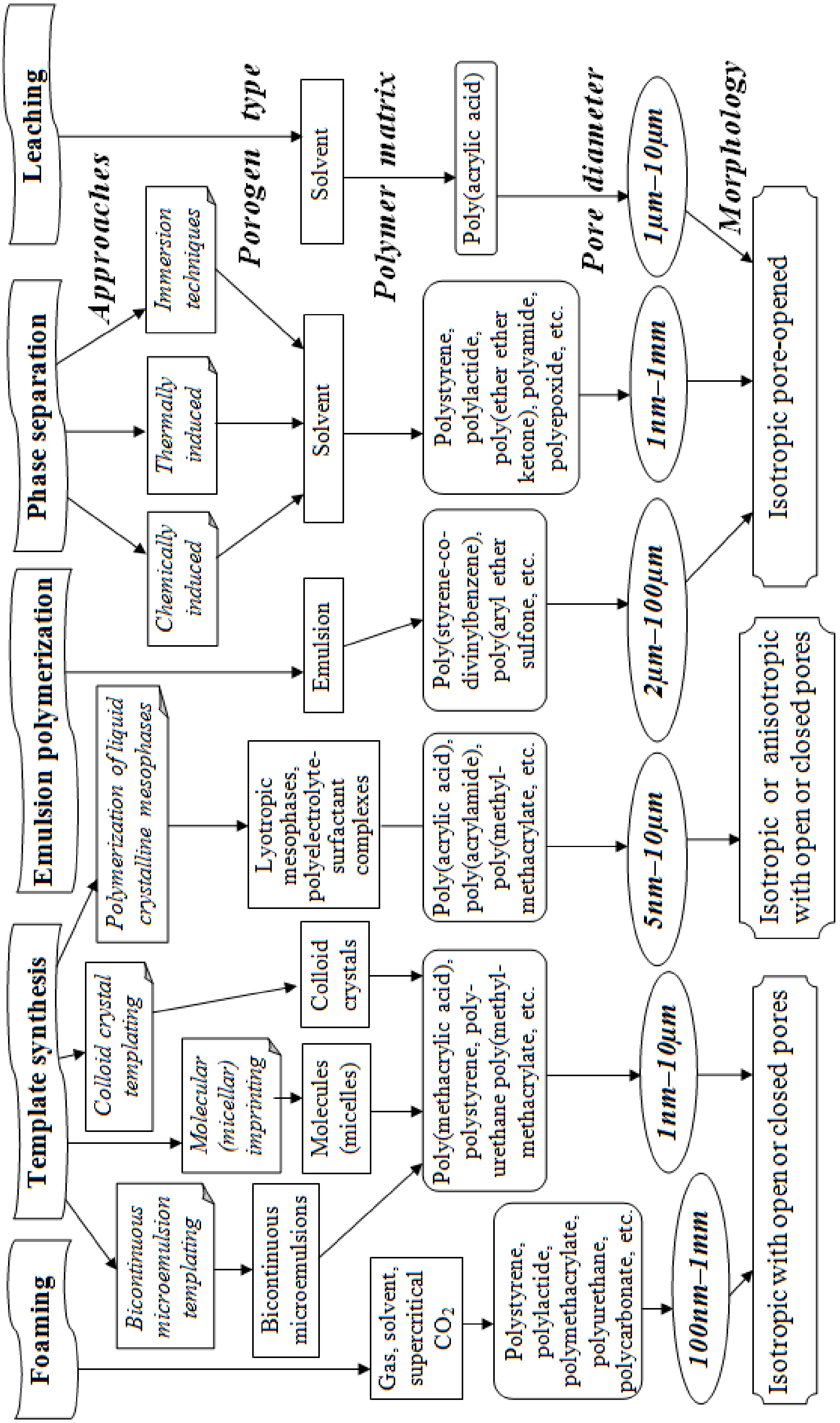

Figure 2. Some porogen-containing methods of pore creation in polymer materials *[after Hentze and Antoinetti M., 2002]*

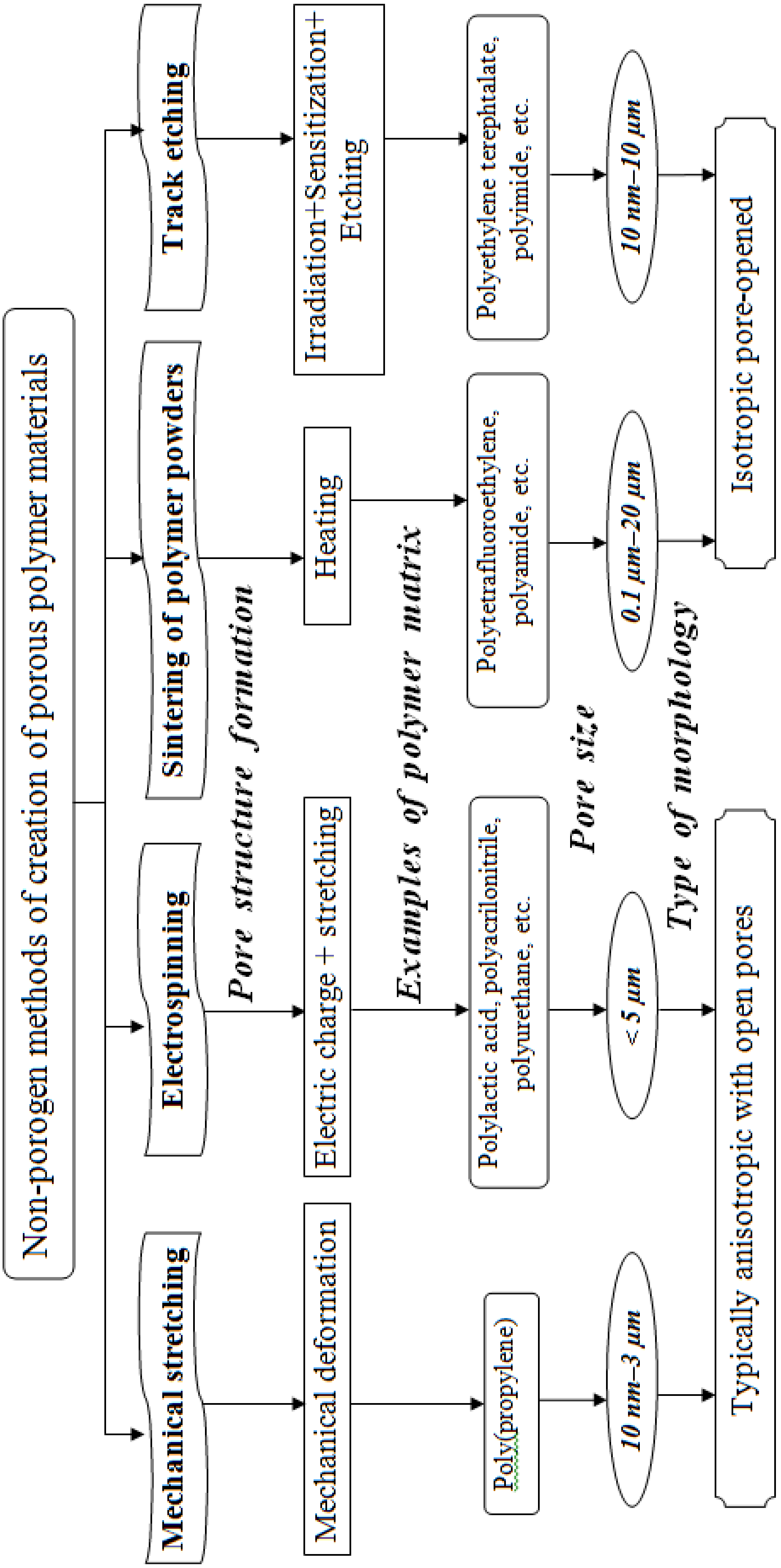

Figure 3. Main techniques to produce porous polymers without porogens *[after Hentze and Antoinetti M., 2002; Silverstein et al., 2011]*

5. Creation of porous structure in polymer materials using phase separation or phase inversion methods

To produce porous polymer materials as blocks, thin films, or powders with isotropic predominantly pore-opened structure, having an average diameter ranging from 1 nm to 1mm, the so-called "phase separation" (or phase inversion) technique can be used *[Kiefer et al., 1999; Loera et al., 2002; Yang et al., 2006; Zorin et al., 2010]*. Nevertheless, the phase separation method is mostly applied for development of macroporous polymer materials. Different low molecular mass solvents as well as oligomeric and polymeric compounds of different nature and molecular mass are used as porogens.

Phase separation occurs during polymerization and polymer crosslinking due to several reasons:

1) thermally induced phase separation: heating or cooling changes a solubility of polymer in the solvent (non-solvent) *[Luo et al., 2008; Matsuyama et al., 1999; Mulder, 1999; Ramaswamy et al., 2002; Russel and Hedrick, 2001; Yang et al., 2006];*

2) physically induced phase separation: addition of non-solvent for polymer to the resulting mixture, comprising polymer and solvent (immersion techniques) *[Bibin et al., 2007; Duarte et al., 2009; Loera et al., 2002; Mulder, 1999; Russel and Hedrick, 2001]*;

3) chemically induced phase separation: a) if in the reaction mixture of monomer/solvent the polymer formed does not dissolve in the solvent (i.e. solvent for a monomer is a non-solvent for a polymer) *[Kiefer et al., 1996a; Kiefer et al., 1999; Li et al., 2009; Mulder, 1999; Russel and Hedrick, 2001];* b) if synthesis is done from a miscible mixture of monomers, oligomers (or monomer and polymer) and the resulting mixture is not miscible.

Generally, thermally induced phase separation is utilized to fabricate porous membranes or microcellular foams *[Silverstein et al., 2011]*.

In 2002, Loera et al. *[Loera et al., 2002]* obtained macroporous polyepoxides (PE) by polymerization-induced phase separation process (the kind of chemically induced ones). The phase separation of the components occurred at synthesis of semi-interpenetrating polymer networks of PE network and thermoplastic polyvinylmethyl ether (PVME). A porous structure was formed at oxidative thermal degradation of the PVME phase during high-temperature treatment of the synthesized PE/PVME interpenetrating polymer networks above 200 °C. It was found that depending on PVME content, phase separation degree varied, and, consequently, different porous structures with submicrometer-sized voids (dispersed closed cells, i.e. spheres or open cells, or bicontinuous percolating canals) were generated. Quantitative analysis fulfilled using transmission electron microscopy (TEM) has shown that maximum pore size was nearly 200 nm. Whereas at high PVME content (20-25 wt.%) porous structure was represented by continuous percolation channels (i.e. by open interconnected pores), the systems with PVME content lower than 20 wt.% were characterized by mainly single closed pores.

The applicability of the thermally induced phase separation process to the production of thermally and chemically stable anisotropic microporous isopolypropylene (iPP) membranes was investigated in details in *[Matsuyama et al., 1999]*. However, rather dangerous diphenyl ether as a porogen was used. Therefore, later Luo et al. *[Luo et al., 2008]* have applied more safety co-diluent comprising dibutyl phthalate (30 wt.%) and soybean oil (70 wt.%) in fabrication of porous isopropylene film materials (thickness was around 0.25 mm). Porous structure was formed by evaporation of the porogen mixture from the top surface of the membrane at 160 °C, while temperature at the membrane bottom was kept between 160 and 195 °C. The scanning electron microscopy (SEM) studies in combination with "Sigmascan" software have shown that average pore diameter in the samples was varied from 0.88 to 1.44 μm. It was established that the higher temperature at the bottom of the membrane and the higher evaporation time, the lower pore size and the higher difference in pore diameters between the top and the bottom surfaces of the membrane synthesized. Depending on the conditions of synthesis, the porosity of the membranes (assessed by saturation degree in isobutanol for 24 hours) was varied from 48 to 66%.

A number of porous membranes based on cellulose acetate *[Reverchon and Cardea, 2004]*, polysulfone *[Reverchon and Cardea, 2005]* and polymethylmetacrylate *[Reverchon et al., 2006]* were obtained by Reverchon and co-authors via phase inversion process. Generation of porous capsules, having around 2.5 cm in diameter and nearly 300 μm in height, based on biocompatible polymethylmethacrylate (PMMA) as well as creation of porous PMMA capsules filled with antibiotic (amoxicillin) for controlled drug removal in pharmaceutics were studied in *[Reverchon et al., 2006]*. PMMA was dissolved first either in dimethyl sulfoxide (DMSO, 10-25 wt.%) or in acetone (10-40 wt.%). To produce film sample, the solution obtained was then injected into a steel capsule-like mold (capsule volume was ~ 80 ml), where solution was distributed over the walls of the capsule. After that, the preheated capsule (at T = 35- 65 °C) was fed by supercritical CO_2 under high pressure (p = 150-250 bar). As a result, porous capsule-like PMMA film was formed. Porous PMMA capsules filled with antibiotics were produced in a similar way, the antibiotic component (10 or 30 wt.%) was preliminarily added either to PMMA/DMSO or PMMA/acetone solution. It was found that during structure forming process, the diffusion rate of supercritical CO_2 in PMMA/acetone mixture was higher than in PMMA/DMSO, resulting in faster phase separation in the first case. Therefore, the porous PMMA capsules obtained from acetone were characterized by highly porous interconnected structure with pore sizes of 2-12 mm (according to SEM data), while in the porous samples obtained from DMSO the isolated pores with a diameter of 12-32 mm were found. The authors studied also an influence of synthesis conditions on size and shape of the resulting pores. It is established that individual amoxicillin dissolved completely in physiological solution, having pH equal to 7.2, in 10 min, while removal of antibiotic from porous PMMA capsules was prolonged to 20 hours and depended on the peculiarities of the porous structure formed.

Based on the existing literature data on producing of porous polymer materials, one can conclude that phase separation techniques, namely chemically induced approaches, are essential and the mostly used ones for generation of porous materials based on thermostable and thermosetting polymers. In Fig. 4 the main stages of preparation of porous thermosets by chemically induced phase separation technique are presented schematically. Since phase separation is induced during polymerization, then the removal of the solvent or porogen at the end of polymerization leaves behind cavities, generating pores in the polymers *[Silverstein et al., 2011]*.

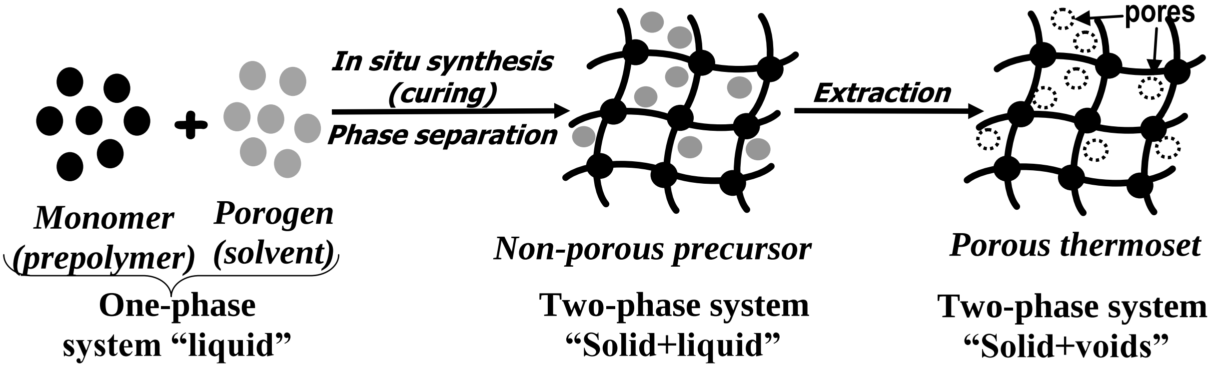

Figure 4. Scheme of preparation of porous thermosets by chemically induced phase separation

As known *[Connor et al., 2008; Jayakody et al., 2006; Kerres et al., 2004; You et al., 2006]*, polyarylenes (polyphenylene oxides, polyetherketones, thermotropic aromatic polyethers, polysulfones, aromatic polyamides) and polyheteroarylenes (such as thermoplastic polyimides, polyamideimides, etc.) as well as their derivatives are perspective polymers for creation of porous thermostable materials of low permittivity and refractive index in combination with good physical and mechanical properties. First attempts in synthesis of nanoporous polyarylene-containing film materials with a pore size of 7-10 nm were patented in 2006-2008 *[Connor et al., 2008; You et al., 2006]*. Polystyrene particles as porogen component were used. Formation of porous structure was carried out by depolymerization of the particles at high temperatures (250-450 °C) under ionizing radiation. Pore size was specified by the size of polystyrene particles.

6. Applicability of chemically or thermally induced phase separation to creation of thermostable porous polycyanurates

Polycyanurate networks (PCNs), possessing high dimensional stability in combination with unique complex of physical-chemical properties, including high thermal stability and glass transition temperatures ($T_g > 250\ ^oC$), low dielectric constants (2.5-3.2), flame retardation and chemical resistance, excellent adhesion to different conducting materials and composites, attract much attention as perspective thermosetting porous films, membranes or filters working in severe environment (at high temperatures, in corrosive media) *[Fang and Shimp, 1995; Hamerton, 1994; Nair et al., 2001]*. Single-step reaction of PCNs formation, the absence of disengagement of by-products or any necessity in solvents or other auxiliary chemicals make PCNs more technologically advanced and promising polymers as compared to other thermosets.

First cyanate esters appeared in the middle of 1960's, but only in 1984 dicyanate esters of a number of bisphenols with the desired high purity (> 99%) were produced and commercial production started. At the present time, PCNs are used as adhesives for different metals, carbon and glass fiber, various composite materials, etc. A great number of films, substrates, circuit boards, coatings and other products on PCNs basis for electronics, aerospace and other industries were produced.

In 1990's Hedrick, Kiefer et al. have extended chemically and thermally induced phase separation approaches as a route to porous PCNs *[Hedrick et al., 1996, 1998; Kiefer et al., 1996b, 1996c, 1999]*. For example, in *[Kiefer et al. 1996b, 1996c]* Kiefer and coworkers described synthesis of PCN foams using cyclohexane preliminarily dissolved in cyanate monomer. To prevent premature phase separation in cyanate/cyclohexane mixture prior to PCN formation, the porogen content was limited to 20 wt.%. Inopportune evaporation of cyclohexane was excluded by decreasing of curing temperature to 80 °C with simultaneous addition of 100 ppm of cobalt acetylacetonate (as a catalyst of polycyclotrimerization) and by carrying out the synthesis in a sealed ampules. The Fourier transform infrared spectroscopy (FTIR spectroscopy) data confirmed the formation of partially cured PCN network containing a considerable amount of reactive cyanate groups remained. Appearance of melting point of cyclohexane at ~ 8 °C on DSC curves of a number of samples was interpreted by authors as an occurrence of phase separation of the components in the systems investigated. Foam creation as well as full network curing was accomplished by heating to 280 °C in vacuum. It was established that formation of porous structure in the fully cured PCNs led to disappearance of the cyanate monomer doublet on the corresponding FTIR spectra, increasing the T_gs and decreasing density of the PCN samples by ~ 0.86-7.21 % (depending on the initial content of cyclohexane). Moreover, dielectric constant values for porous PCNs as low as 2.5 were measured. The SEM micrographs confirmed the presence of interconnected porous structure with round pores having diameter from 10 to 20 μm. The dependences of pore morphology, their interconnectivity and sizes on porogen concentration as well as temperature conditions of synthesis were defined.

The first nanoporous PCN-containing material was obtained by Hedrick et al. *[Hedrick et al., 1996]* via *in situ* polycyclotrimerization of 4,4'-hexaflourinepropylidene dicyanate in the presence of reactive polypropyleneoxide (PPO) or PPO-based polyurethane as thermally labile porogens. Synthesis of the samples was carried out in 3 stages: 1) heating to 120 °C under vacuum for 2-4 h; 2) post curing at 150 °C for 1 h and at 220 °C for 2 h; 3) final curing under nitrogen to 250 °C, 270 °C and either 300 °C or 325 °C for 1 h at each temperature step.

It was found that during PCN synthesis the aforementioned PPO or polyurethane used were fully incorporated into PCN structure, resulting in formation of hybrid PCNs. Using dynamic mechanical thermal analysis (DMTA) microphase structure of the samples investigated was studied and it was established that the samples obtained were characterized by two-phase structure: T_g of thermally labile component was around -60−-50 °C, and PCN fragments of hybrid networks devitrified at ~ 265 °C.

Using SAXS method, the average size of the domains of microphase enriched in PPO was found to be equal to ~ 70 Å (with initial content of the latter in the composition equal to 15 vol.%). Pore structure was generated during subsequent step-by-step heating at T ~ 200 °C, 225 °C or 240 °C for 4-6 h in oxygen atmosphere when degradation of thermally labile fragments of the networks occurred.

However, the authors *[Hedrick et al., 1996]* have found that porous structure formed during curing was destroyed, pores collapsed, and structural order was broken due to significant increase of the mobility of PCN fragments while PPO degradation took place, resulting in partial pore collapse.

The authors considered that the pore collapse was caused by two manifestation reasons: the narrow difference between the decomposition temperature and the T_g of PCN and the mobility of the network nearly the T_g. In addition, the stress of isolated spherical particles was inversely proportional to the radius and therefore, smaller voids inherently tended to collapse *[Hedrick et al., 1996]*.

We have successfully used the methods of chemically induced phase separation for creation of nanoporous polymer thin films based on PCNs *[Fainleib et al., 2009, 2010a; Grande et al., 2008; Grigoryeva et al., 2011b; Gusakova, 2009]*. Precursors to porous thermosets were synthesized by *in situ* polycyclotrimerization of dicyanate ester of bisphenol E (DCBE) in the presence of linear reactive and hydrolytically labile poly-ε-caprolactone (PCL) or in the presence of high-boiling dimethyl phthalate (DMP), or dibutyl phthalate (DBP). Pore structure was developed by partial (in a case of PCN/PCL compositions) or full (in case of phthalate-containing PCNs) extraction of porogen, selective hydrolysis or thermal decomposition of PCL-component followed by removal of degradation products. In our previous work *[Fainleib et al., 2007]* partial incorporation of PCL component into network structure during synthesis of hybrid PCL-containing PCN was confirmed (reaction scheme is presented in Fig. 5).

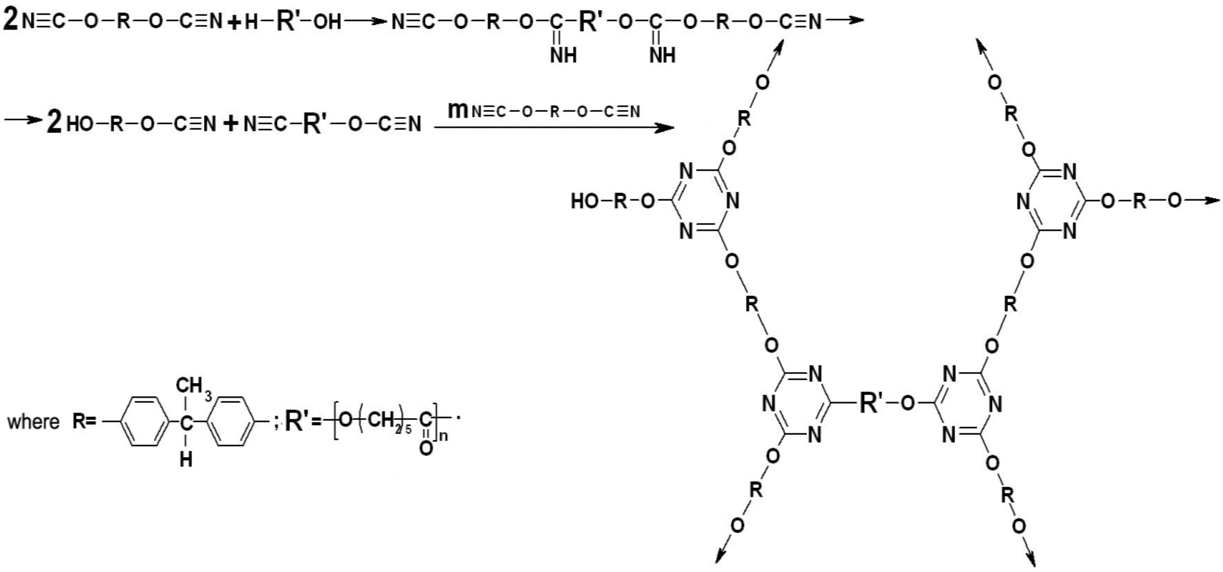

Figure 5. Scheme of PCN/PCL hybrid network formation

FTIR spectroscopy data, gel fraction content determination and the results of density measurements showed the presence of PCL component in all porous PCN/PCL compositions. Using DSC technique it was established that formation of PCN prevented crystallization of PCL macromolecules (both chemically incorporated and non-embedded) and initial and porous hybrid PCN/PCL networks were fully amorphous. For instance, T_g of the PCN/PCL porous sample, containing 14.6 wt.% of PCL, is by 75 °C lower as compared to the glass transition of the individual PCN that is associated with decreasing density of the hybrid network due to the presence of ~14.6% of the chemically embedded PCL, lower T_g of the PCL component as well as with an appearance of pores.

SEM and DSC-thermoporometry measurements confirmed the occurrence of nanoporous structure in PCN/PCL samples after extraction, hydrolysis or thermal degradation (cf. Fig. 6) of the labile PCL component, and the calculations performed have shown (calculation procedure was described in detail in *[Gusakova, 2009]*) the maximum pore size less than 150 nm, and average diameter of the predominant pore majority of ~ 25-45 nm (Table 1). It was also found that resistance to thermal and thermal-oxidative degradation of porous hybrid PCN/PCL networks was higher as compared with the initial (non-porous) samples of a similar composition.

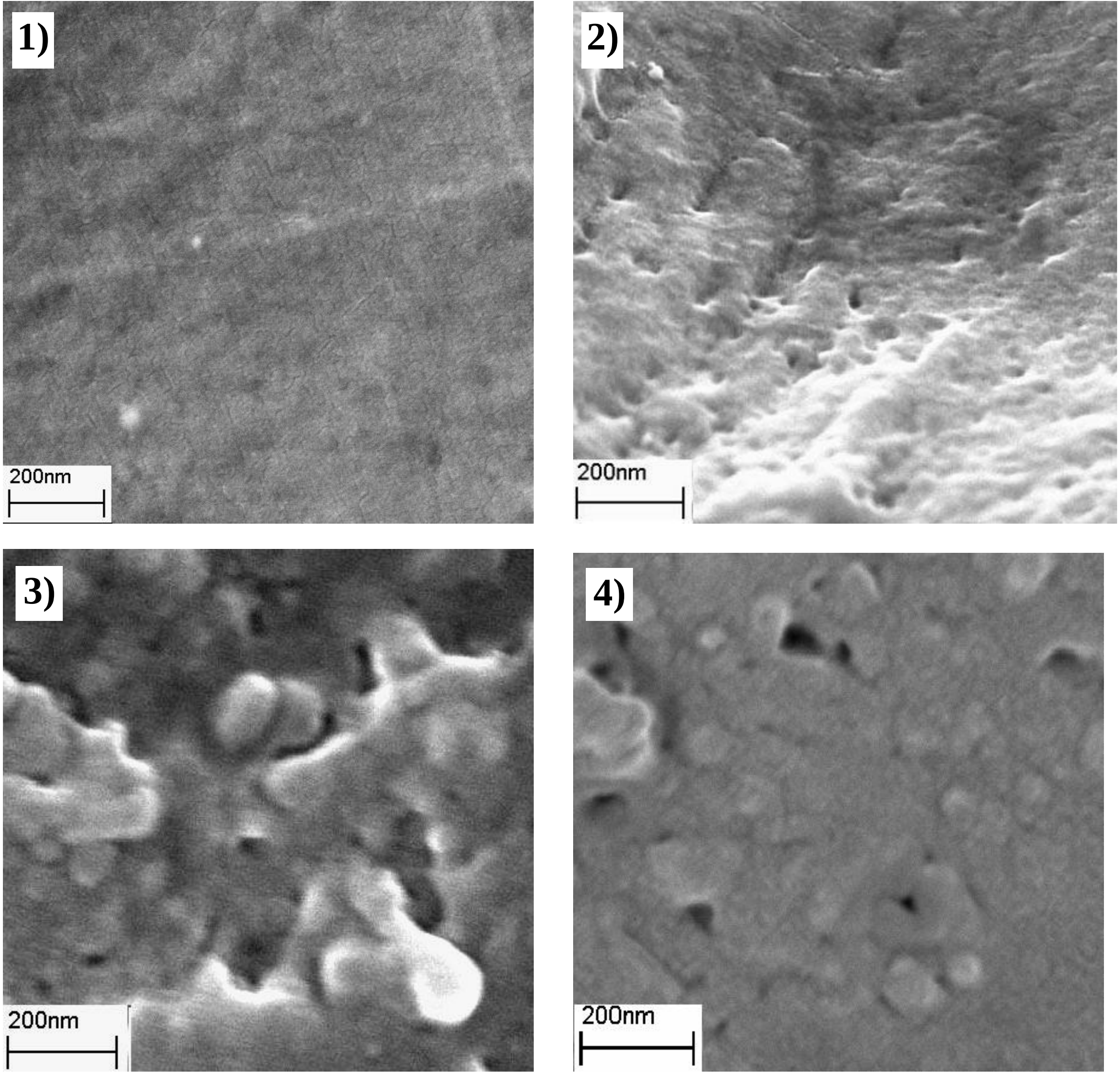

Figure 6. SEM micrographs of the hybrid PCN/PCL samples: (1) initial (reference) sample PCN/PCL=60/40 (wt.%); porous samples obtained after (2) extraction, (3) hydrolysis or (4) thermal degradation of labile PCL component

Table 1. Characterization of porous structure in the PCN/PCL samples

Sample	**Composition (wt.%)**	**Average pore diameter (nm)**	
		DSC-thermoporometry	**SEM**
PCN/PCL (initial)	60/40	–	–
PCN/PCL after:			
– extraction	73/27	25	30
– hydrolysis	77/23	45	45
– thermal degradation	80/20	30	30

In a case of *in situ* synthesis of PCN in the presence of inert high boiling temperature porogens, such as DMP or DBP, no chemical interaction of cyanate monomer with porogen occurred, and the presence of the porogen in the PCN network after high-temperature synthesis was confirmed by the presence of the characteristic absorption bands for individual DMP or DBP (valence vibrations of C=O-groups at $\nu \approx 1721\text{-}1726$ cm^{-1}). After porogen extraction by acetone and following drying of the samples up to the constant weight, the characteristic absorption bands of DMP or DBP in the FTIR spectra of the samples produced completely disappeared, confirming complete removal of the porogens from the PCN networks.

Full extraction of DMP or DBP out of the PCN/DMP or PCN/DBP compositions, respectively, was also confirmed by gel fraction content data (cf. Fig. 7). Moreover, it was found that during extraction of the porogen from PCN/DBP=70/30 (wt.%) sample, not only DBP was extracted. Gel fraction content was determined to be ~ 50% that is lower compared to the expected 70%. It can be explained by formation of more defective polycyanurate network in the presence of 30 wt.% of DBP. As a result, a certain part of the branched cyanurate fragments was not embedded into the resulting PCN structure and was further removed during extraction.

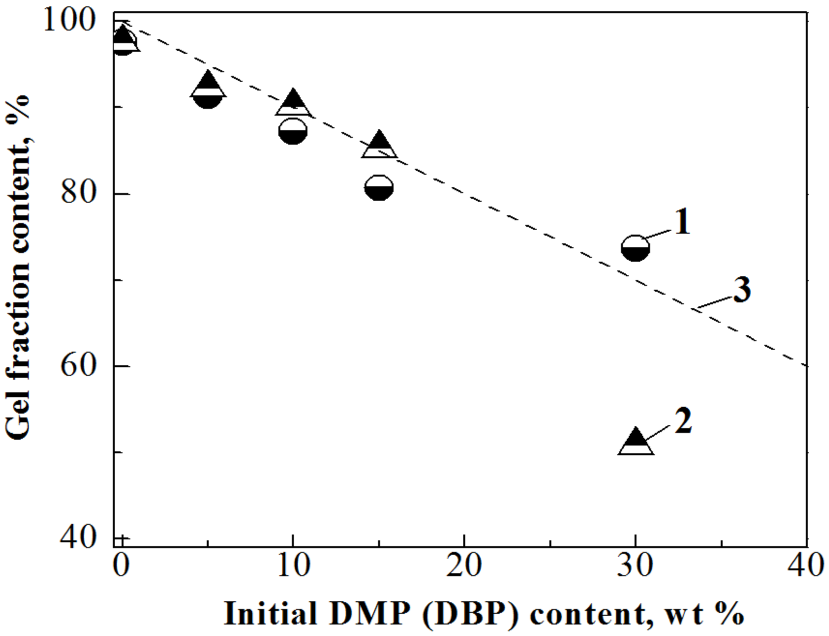

Figure 7. Dependence of gel fraction content on (1) DMP or (2) DBP content in initial mixture with DCBE; (3) corresponding additive data

Generation of the porous structure in the PCN films after removal of DMP or DBP was confirmed by SEM and DSC-thermoporometry methods. It is established that pore diameter in the porous PCN was ranged from ~15 to

~140 nm, and an average pore diameter was about 30-50 nm (depending on composition) (cf. Table 2), i.e. the PCN samples produced can be classified as nanoporous polymer material (cf. Fig. 1).

Table 2. Characteristics of nanoporous PCN samples (DSC-thermoporometry data)

Initial porogen content in PCN (wt.%)	Average pore size (nm)	Pore size distribution (nm)	Total pore volume ($cm^3 \cdot g^{-1}$)
DMP = 5	33	16–150	0.04
DMP = 15	37	15–148	0.06
DMP = 30	50	18–146	0.06
DBP = 5	29	24–144	0.03
DBP = 15	42	15–147	0.07
DBP = 30	45	14–148	0.09

Thus, the conclusion on the possibility of synthesis of nanoporous materials with controlled porosity by varying the sample composition was made. DSC studies showed that DMP and DBP in the synthesized PCN/DMP or PCN/DBP samples acted as plasticizers and during further extraction manifested themselves as porogens that could be easily and completely removed from the samples, resulting in formation of well-developed porous structure. It was established that thermal properties of the porous PCN samples obtained close to the characteristics for the individual crosslinked PCN, synthesized without any porogen.

7. Formation of porous polymer materials by template technique

Template synthesis based on self-assembly is preferable approach when porous structure of the material obtained does not meet the desired pattern. Templating methods include using ordered arrays of colloidal crystals, molecules, micelles, microphase separated block copolymers, polymers with rod coil architecture etc. that forms honeycomb structures and templating using emulsions etc. (cf. Fig. 8) *[Hoa et al., 2006; Balaji et al., 2004]*. Such techniques allow producing, for instance, of porous composite polymer membranes with improved thermal and chemical stability as well as excellent mechanical properties in combination with high selectivity etc. *[Bryk, 2005, 2006; Hoa et al., 2006; Mulder, 1999]*.

The process consists in formation of cross-linked polymers with high crosslink degree around the so-called template molecules (cf. Fig. 8). Polymer synthesis takes place due to copolymerization of functional and crosslink monomers in the presence of matrix molecule. Extraction of the latter after network formation results in generation of the cavities, complementary by size

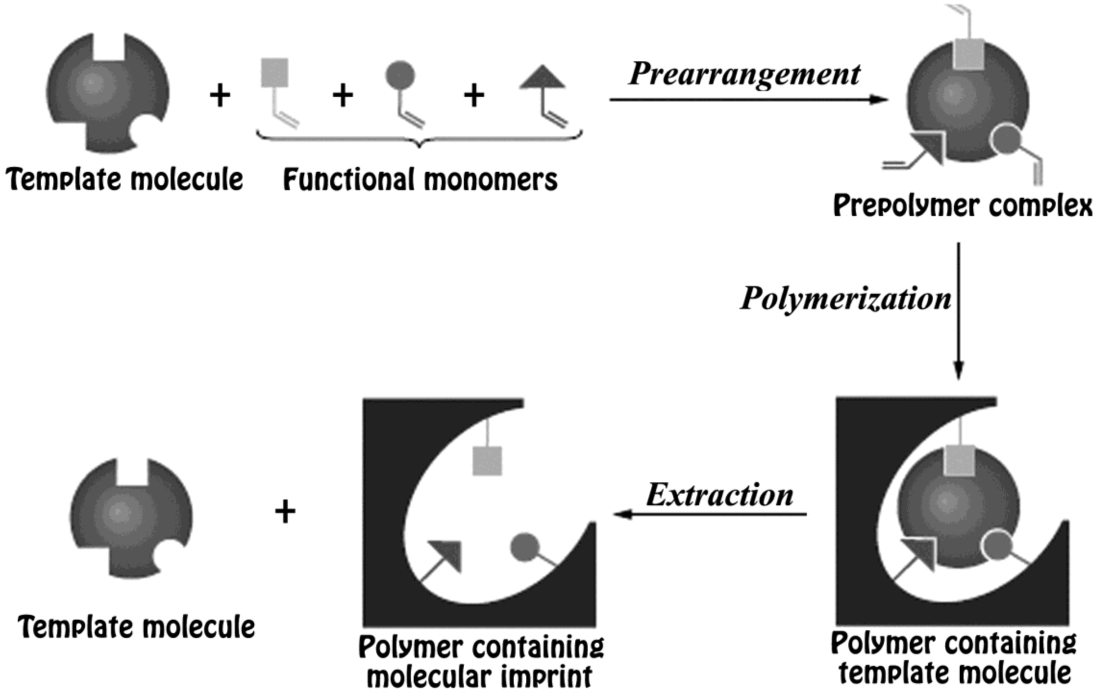

Figure 8. Schematic representation of the molecular imprinting method *[after Balaji et al., 2004; Blagutina, 2011]*

and configuration of functional groups *[Sergeyeva et al., 2009]*. Therefore, depending on chemical structure of the template applied one can obtain polymer materials with isotropic or anisotropic pore structure, open or closed pores sizing from nanometer to several microns.

Hoa et al. *[Hoa et al., 2006]* in the review analyzed the recent advances in production of porous materials, including polymers, by various techniques and using inorganic or organic substrates (templates) as well as the ways of pore size control, and advantages and disadvantages of different methods of pore generation and possible areas of applications for porous materials obtained. So, here and below in the present review we will not linger round the so well-studied subject.

Methods of creation of porous morphology in polymer materials called molecular or micellar imprinting are of a considerable practical interest *[Alexander et al., 2006; Gendrikson et al., 2006; Haginaka, 2008; Pauling, 1940; Takeda and Kobayashi, 2006]*, the process of pore generation by these techniques is similar to one shown in Fig. 8.

Rapid scientific and technological progress in preparation and characterization of molecularly imprinted polymers (MIP) was noticed in the 1990’s, however Linus Pauling proposed the concept of imprinting of biomolecules as early as 1940, when discussion of the structure and formation process of antibodies took place *[Pauling, 1940]*. Pauling affirmed that "introducing of animal antigen into the organism resulted in trapping and retaining of some of its molecules in zone of antibody formation. Antibody to that antigen was a molecule with complementary configuration of the molecule to the antigen." He also postulated the reversibility of the formation of "antigen-antibody" complexes, as well as that "the antigen molecule might serve as a pattern in creation of other antibody molecules".

The MIP technology involves formation of polymer composite with high crosslink degree around molecules-matrices. Subsequent extraction of molecules-matrices out of the synthesized polymer material leads to the formation of pore structure in the latter with pore sizes, configuration and the volume occupied completely corresponding to the molecules-matrices. Moreover, even spatial location of the functional groups is fixed.

Porous polymer materials obtained by this method are capable to repeatable selective re-binding of matrix molecules, i.e. they can serve as sensors for determination, for example, various toxic substances. Based on more than 2 000 papers and reviews on MIP, Gendrikson et al in a recent review *[Gendrikson et al., 2006]* pointed out that molecular imprinting is a prime subject of investigations of more than 100 academic and industrial research groups around the world, moreover, many developments were patented. Extraordinary attraction of the imprinted polymers for practical applications is caused by such properties as extremely high stability, simplicity of synthesis, the ability to recognize and bind a variety of target molecules with high specificity, etc.

8. Interparticle crosslinking method of creation of porous polymers

Mähr and coworkers *[Mähr et al., 2000]* have synthesized macroporous polymer membranes with average pore diameter of about 3.5 μm using interparticle crosslinking technique. The gel of 3D structure was obtained by the interaction between the particles of the suspension of polyacrylic acid with crosslink agent – diglycidylhexanediol ether. The gel obtained was poured on a substrate and kept at 90 °C for 24 h, and then the pre-frozen gel was finally dried in a vacuum. Using mercury porosimetry the porosity of the membrane obtained equal to 89-95%, and specific pore volume to about 9.8-17.2 cm^3/g were determined. It was shown that the increase of the amount of diglycidyl hexanediol ether from 20 to 50 mol.% allowed generating more compact structure (density increases from 0.058 to 0.102 cm^3/g) with improved mechanical strength and an increase in initial concentration of polyacrylic acid led to the decrease in gas permeability of the membranes obtained.

9. Porous polymeric materials created by emulsion polymerization technique

Preparation of porous polymeric materials by emulsion polymerization is well-known technique for producing of polymer foams, possessing a unique “honeycomb” cell structure with cell diameter ranging from 2 to 100 μm (cf. Fig. 2). The types of materials synthesized include copolymers, interpenetrating polymer networks, biodegradable materials, organic-inorganic hybrids, etc. *[Junkar et al., 2007; Menner et al., 2006; Normatov and Silverstein, 2007, Silverstein et al., 2011]*. Generally, an emulsion is a heterogeneous system consisting of two liquids, referred to as phases, which are immiscible or possess limited miscibility. In an emulsion, one phase (the internal phase) is dispersed as droplets within the other phase (the continuous phase). Usually, one phase comprises water or an aqueous solution and the other phase comprises oil, although non-aqueous emulsions comprising two immiscible organic phases can be produced. Emulsions can be classified as oil-in-water emulsions (o/w) in which oil constitutes the internal phase or water-in-oil emulsions (w/o) in which water (or an aqueous solution) constitutes the internal phase *[Bismark et al., 2010]*.

General procedure of synthesis of polymer foams through o/w emulsion schematically is presented on Figure 9. The preparatory stage consists in separate preparation of internal (discrete) and continuous phases. To produce polymer foam, the continuous phase consists of the monomers, forming a rigid polymer skeleton with cell structure during polymerization, and crosslinkers (or initiators). In the first stage dribble introduction of internal phase into continuous one under constant intensive mixing results in formation of stable emulsion. Then polymerization and/or curing of components of continuous phase takes place. Afterwards, drops, corresponding to the discrete phase (as well as unreacted components) have to be removed (by heating, rinsing, filtration or evacuation) leaving empty cells (voids) in place of the internal phase

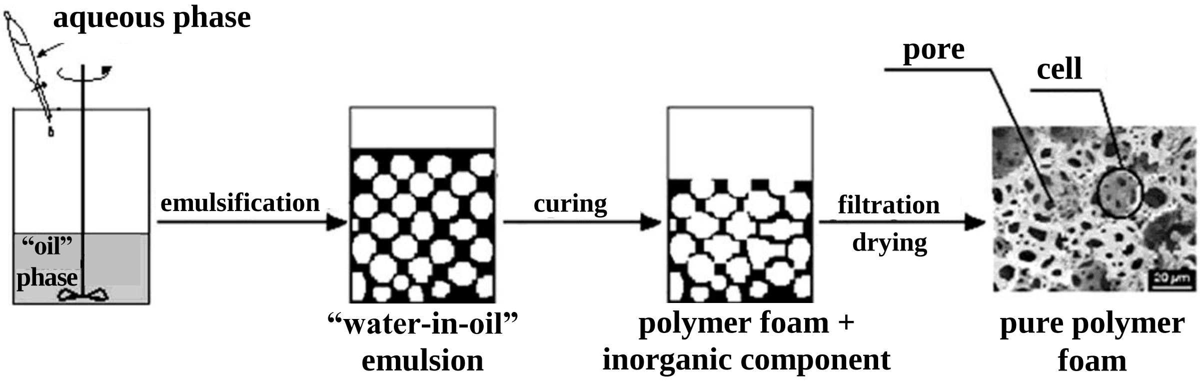

Figure 9. The main stages of preparation of porous polymer materials via o/w emulsion polymerization technique

droplets and thus providing porous foam structure. Therefore, the drops of the internal phase act as a porogen pattern (template) and, consequently, the method is also called emulsion templating *[Bismark et al., 2010]*.

The porosity and permeability parameters as well as physical-mechanical properties of polymer material strongly depend on the internal phase content in the reaction mixture. Thus, one can single out low internal phase emulsion (LIPE, the discrete phase volume under 30%), medium internal phase emulsion (MIPE, with internal phase contents from 30 to 74%) or highly internal phase emulsion (HIPE, the discrete phase volume more than 74%). Noteworthily, that the porous polymer monoliths developed from HIPE (the so-called, polyHIPE) are characterized by unique properties with the highest porosity and degree of pore interconnectivity, presence of highly open porous structure, etc. These porous polymers, usually synthesized through free radical polymerization, include both hydrophobic polymers synthesized within w/o emulsions and hydrophilic polymers synthesized within o/w emulsions. PolyHIPEs may also be produced from non-aqueous templates.

The key parameter in producing of polyHIPE foams having favorable properties is obtaining of stable emulsion. Usually different molecular surfactants as emulsifiers are used. To choose the best stabilizer, one has to take into consideration hydrophilic-lipophilic balance (HLB) of a surfactant. Thus, high HLB surfactants that are more soluble in water than in oil has to be used in o/w emulsions and, consequently, low HLB surfactants will be more suitable in w/o emulsions. Moreover, much attention has to be paid to matching to the Bancroft rule, stating that "the phase in which an emulsifier is more soluble constitutes the continuous phase" *[Wikipedia, 2011a]*.

However, most polyHIPEs exhibit a rather chalky and brittle nature *[Moghbeli and Shahabi, 2011]*. Traditionally, to solve the problem, elastomeric components as comonomers are introduced, however, this usually decreases the degree of pore interconnectivity and reduces the T_g values.

Menner et al. *[Menner et al., 2006]* increased significantly the strength properties of porous samples based on a copolymer of styrene with methacryloxytrimethoxysilane and divinylbenzene, DVB, (the continuous phase volume was 40 vol.%), synthesized by the same procedure, using silica particles (up to 30 wt.% of a monomer) as reinforcing additive and emulsifier simultaneously. SEM data confirmed the presence of cellular (honeycomb) structure consisting of interconnected open pores (pore diameter of 3-50 μm). Depending on the composition and synthesis conditions, porosity of the samples was varied from 63 to 77%. The increasing Young's modulus and the crush strength by 3.6 times and by 3.0 times, respectively, for the samples obtained in the presence of silicate particles was registered.

Over the last years to improve mechanical and thermal properties along with stabilizing emulsions several attempts were made using carbon nanotubes, silica particles or organoclays, such as natural and organically modified montmorillonites, etc. *[Menner et al., 2007; Moghbeli and Shahabi, 2011]*. Thus, it was established that the addition of carbon nanotubes not only eliminated the need for traditional non-ionic surfactants but also increased the mechanical and electrical properties of polyHIPE foams prepared. Recent investigations in reinforcement of elastomeric foams based on 2-ethylhexylacrylate, styrene and DVB using organoclays (Cloisite® 15A and Cloisite® 30B) have shown a decrease in the mean size of the voids and intercellular pores for the nanocomposite copolymer foams as compared with the copolymer foam without any reinforcement. It was also found that incorporating organoclays lowered the foam emulsion viscosity to some extent. Therefore, the authors concluded that the organoclay acted as a co-surfactant in weakening the water/monomer interfacial interactions and consequently in lowering the viscosity of foam emulsion.

In 2010, authors *[Bismark et al., 2010]* have patented the utilization of functionalized nanoparticles comprised titanium (TiO_2) or silica (SiO_2) dioxides instead of molecular surfactants as emulsion stabilizers in preparation of the o/w HIPEs to produce polymeric foams based on styrene and DVB. It was established that the functionalization of hydrophilic particle comprising a core by coating, for example by imparting a hydrophilic core with some hydrophobic character, changes the particle wettability. Thus, the use of the particles with appropriate wetting behaviour provides stabilization of an emulsion.

Silverstein et al. reported *[Silverstein et al., 2011]* that supercritical carbon dioxide ($scCO_2$) can be used as the dispersed phase within an aqueous phase for the formation of a $scCO_2$-in-water (c/w) HIPEs, and polyHIPEs had also been synthesized through these c/w HIPE emulsions. The aqueous phase in such c/w HIPEs consisted of a solution of acrylamide (AAm) or 2-hydroxyethyl acrylate (HEA) with *N*,*N*-methylene bisacrylamide (MBAAm) as a crosslinking comonomer. The porous materials resulting from polymerization in the c/w HIPE exhibited typical polyHIPE structures. Block copolymer surfactants were used to enhance the internal phase content of the HIPEs. Emulsion templated porous polymers were also produced using an aqueous polymer solution instead of a monomer solution in c/w HIPEs *[Silverstein et al., 2011]*.

10. Non-porogen created porous polymer materials by sintering technique or mechanical stretching

Methods of creation of porous polymer materials without using porogen are more often used for synthesis of thermally, chemically and dimensionally stable porous polymers. Therefore, this section is focused on polymers with high thermal characteristics and chemical resistance.

Sintering of polymer powders, mechanical stretching, electrospinning, as well as track etching techniques are the most important non-porogen approaches for preparation of porous polymers *[Mulder, 1999]*.

Sintering of polymer powders is simple and consists in pressing with simultaneous sintering (heating at the elevated temperatures) of polymer powders (polyethylene, polytetrafluoroethylene, polypropylene, etc.), containing particles of a certain size. The sintering temperature depends on the nature of the material used. During sintering a surface between the contacting particles disappears and porous structure is formed (cf. Fig. 10). The pore size range of the final material depends on size of powder particles, their distribution and sintering conditions (pressure, temperature, etc.) *[Bryk, 2005, 2006; Mulder, 1999]*. Additionally alteration of rheological and thermal properties of the powder compositions as well as enhancing of strength and permeability characteristics of the porous material produced can be attained by modification of polymer powder with solvents, plasticizers, or porogens *[Bryk, 2005, 2006]*.

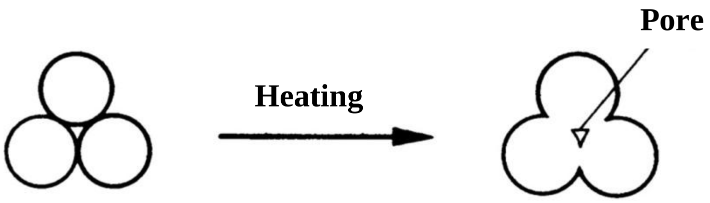

Figure 10. Scheme of sintering technique *[Mulder M., 1999]*

Mechanical stretching method is based on distension of an extruded film of semi-crystalline polymer (polytetrafluoroethylene, polypropylene, polyethylene, etc.) perpendicularly to the direction of extrusion. As a result the crystalline regions are oriented parallel to the direction of extrusion. During mechanical deformation small cracks appears and porous structure with pore sizes in the range of 10 nm-3 μm *[Bryk, 2005, 2006; Mulder, 1999]* is formed.

11. Track etching technique in producing of porous polymeric films

Fleischer et al. *[Fleischer et al., 1964]* were one of the pioneers in the field of generation of porous polymer materials (thin films) applying nuclear technologies. The method consists in irradiating of thin polymer films with high-energy particles such as heavy ions, formed by the decay of heavy atomic nuclei (Ar, Kr, Xe, U), protons, α-particles, etc. As a result the radiation destruction of macromolecules in bulk occurs and tracks (channels with fragments of polymer macromolecules) are formed (cf. Fig. 11) *[Apel P., 2001; Gomez Alvarez-*

Arenas et al., 2009; Ilić et al., 2003]. During subsequent etching of the irradiated films by alkalis, acids, oxidizers or other chemicals the fragments of macromolecules are leached out from the tracks leading to formation of pore structure (cf. Fig. 11). This method provides the formation of interconnected pores of regular geometry and nearly the same diameter. Applicability of nuclear technologies in producing of porous polymers is limited mainly by the film thickness (generally not exceeding 50-60 μm) and by the rate of particle flux, while size and shape (cylindrical, conical, bottle-like etc.) of the pores formed strongly depend on a choice of the type of particles used, the etching composition and conditions (temperature, pressure, duration of etching etc.) *[Apel P., 2001; Gomez Alvarez-Arenas et al., 2009; Ilić et al., 2003]*. Noteworthy that along with track leaching during etching procedure, the bulk material is also damaged, but etching rate inside the tracks is significantly higher. Kravets et al. in *[Kravets et al., 2000a]* have pointed out that in order to produce high-performance membranes with cylindrical pores, the ratio between longitudinal rate of track etching (longitudinal rate) and etching rate of initial (non-irradiated) sample (radial rate), called selectivity of track etching, usually has to exceed 300. The authors mentioned also the main characteristics of an efficiency of etching solution: selectivity of track etching, track etching rate (defining time of formation of through pores), full process duration, availability and recyclability of etching composition *[Kravets et al., 2000a]*. It should be noted that etching rate can be increased by bringing into service, the so-called, sensitization stage (exposure to ultraviolet irradiation or using of additional heat treatment etc.) resulting in increasing imperfection of macromolecular structure inside the tracks and, consequently, enhancing the track etching rate tenfold. Generally, after sensitization, pores become more regularly-shaped, pore size distribution narrows and permeability of membranes produced increases *[Apel P., 2001]*.

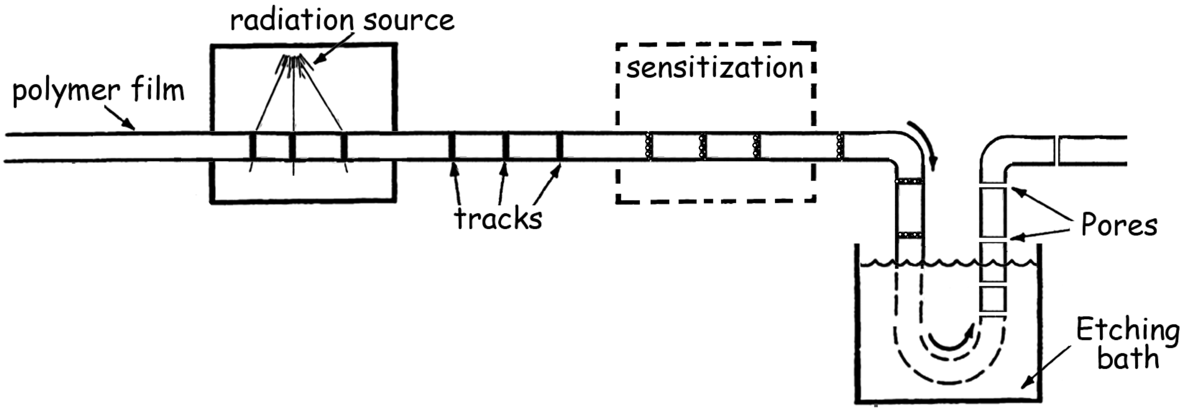

Figure 11. General scheme of obtaining of polymer porous films using nuclear technologies followed by track etching *[after Porter, 1990]*

Thus, track-etched porous polymer materials have distinct advantages over conventionally synthesized porous polymers due to their precisely determined structure with controllable pore size, shape and density and meet the required transport and retention characteristics *[Apel P., 2001]*. Moreover, the surface of the porous materials produced can be relatively easily modified (by graft polymerization, adsorption of low molecular weight, oligomeric and polymer surfactants, etc.), and one can obtain the charged membranes, membranes with special properties, composite micro-, ultra- and nano-filtration membranes, etc. *[Clough, 2001; Ilić et al., 2003]*.

It is known *[Apel, 2001; Clough, 2001; Gomez Alvarez-Arenas et al., 2009; Ilić et al., 2003]* that the maximal path of high-energy particles in polymer materials does not exceed 20 μm. Therefore, until recently the essential lack in producing of porous polymer materials using nuclear technologies was explained by limiting film thickness (less than 30 μm). However, Apel et al. in *[Apel et al., 1988]* concluded that the higher energy of charged particles, the higher thickness of porous films can be passed by them. To confirm the statement, the polyethylene terephthalate (PET) films having about 50 μm in thickness were prepared. Then the samples were irradiated by argon ions with the energy of 5.6 MeV/nucleon and etched by a solution of sodium hydroxide. The etching duration was matched and, finally, the through channels in the films with diameter ranging from 6 to 10 μm (confirmed by SEM) were obtained.

Some progress in producing of high-performance track membranes with strictly cylindrical pores for purification of chemically aggressive media was made by Kravets et al. *[Kravets et al., 2000a, 2000b]*. Commercially available polypropylene-based films "Torayfan"® produced by "Toray" (Japan) with a nominal thickness of 10.0 and 10.2 μm were taken as test subject. Irradiation was accomplished in vacuum by ^{54}Xe and ^{36}Kr ion beams with energies 1 and 3 MeV/nucleon, respectively, using cyclotron U-300 and U-400. The stream was varied between 10^6-10^9 ions/cm^2. Based on previously established relationship *[Apel et al., 1990]* between nuclear charge and selectivity of etching (the greater etching selectivity in PP films irradiated by ^{54}Xe ions in comparison with the samples irradiated by ^{36}Kr ions), most experiments in *[Kravets et al., 2000a, 2000b]* were performed on Kr-irradiated samples. It was revealed that two-step processing of the samples in aqueous solution, comprising CrO_3 (c = 1000-1100 g/l) were the most effective for etching of the irradiated PP films.

In the first stage, during the short-term (for 4 min) etching procedure at T ~ 80 °C, formation of open channels of 0.1 μm in diameter occurred. Afterwards, etching at 20 °C, followed by rinsing in distilled water, allowed achieving the given pore size (0.3 μm). It was found that in order to remove the adsorbed chromium-containing compounds from the membrane surface, subsequent treatment in aqueous or aqueous-alcoholic alkaline solutions (the concentration of alkali metal hydroxide was varied from 0.5 to 20 wt.%) at

T ~ 40-70 ºC for 5-30 min has to be carried out. The membranes had high tensile strength and resistance to oxidation. The SEM micrographs confirmed the presence of well-defined cylindrical-shaped pore structure with diameter of 0.1-3.0 µm suitable for microfiltration.

To produce PP membranes for ultrafiltration using the technology described above Kravets et al. *[Kravets et al., 2000b]* have developed interesting sensitization method consisting in treatment of the irradiated PP films by chemicals, which are solvents for radiolysis products in track area (i.e. low-molecular homologues of the polymer used), but non-solvents for polymer matrix. It was found that treatment of pre-irradiated (with ^{54}Xe ion beam) PP films by organic solvents (namely, in benzene, heptane, *m*-xylene, carbon tetrachloride, butyl alcohol, kerosene, mineral spirits, trichloroethylene, etc.) for 3-10 min resulted in track sensitization and in significant increasing of free volume in track area due to elution of degradation products appeared at radiolysis. Removal of the solvents from polymer matrix was performed in two stage heat treatment: at *T* ~ 20-40 ºC for 5-10 min for removal of the solvent from the tracks occurred and at *T* ~ 85-105 ºC for 10-15 min for evacuation of solvent from polymer matrix. It was established depending on time and temperature of sensitization one can vary the final pore shape in the PP films studied from conical to cylindrical sizing from 0.85-1.10 to 0.34-0.38 µm (depending on solvent used) *[Kravets et al., 2000b]*.

Nowadays methods of producing of commercially available track membranes based on polyethylene terephthalate, PET, (irradiation and etching conditions, selection of etching agents, etc.) are well studied *[Albrecht et al., 2006; Apel, 2001; Apel et al., 1998, 2001, 2006; Apel and Dmitriev, 2004; Bomko et al., 2006; Dmitriev et al., 1998; Gomez Alvarez-Arenas et al., 2009; Gopalani et al., 2000; Lazea et al., 2005; Pahomov et al., 2001, 2005; Vilensky et al., 1992]*. Typically, PET films with thickness of 3-12 µm are irradiated by ions of Xe, Au, U, Kr, or Ar with varying intensity followed by physical-chemical treatment (etching) giving track membranes possessing through pores with a diameter of 0.02-5.0 µm.

Apel et al. *[Apel et al., 1998]* have studied the changes in track and, consequently, pore geometry after irradiation of PET films with thickness of 3-10 µm by ions of different energies (from 1 to 11.6 MeV/nucleon) and intensity from 1 to 10^7 ions/cm^2 followed by etching in 0.1N NaOH at 80 ºC. It was found that the higher the atomic number of the accelerated ions the easier creation of cylindrical pores of a minimum diameter under constant etching conditions. It was shown that for the samples irradiated under the same conditions the longer etching time the larger pores appeared. Later, Apel et al. *[Apel et al., 2001]* confirmed the above mentioned relationships and evaluated the effect of etching composition on pore geometry. It was established that an addition of small amounts of organic surfactants, such as nonylphenyl polyethylene glycol, sodium dodecyl diphenyloxide sulfonate or polyvinylpyrrolidone to the etching bath led to the increase in effective pore diameter simultaneously with improving in its cylindricity. This fact was explained by adsorption of the surfactant on the surface of polymer film, namely by arranging of the surfactant molecules around narrow spout of the etched channel formed. The etching composition with the surfactant penetrated into channel through the spout formed and ratio between the inner and the outer diameters of the pore was tend to 1.

Gopalani et al. *[Gopalani et al., 2000]* irradiated PET films (with thickness of 15-25 μm) by ^{28}Si ions with subsequent etching of the irradiated films in aqueous solution, comprising NaOH at $T \sim 50\text{-}60$ °C for 2 hours. To increase etching rate additional sensitization was carried out by using IR-, UV-, γ- or laser irradiation, etc. SEM studies performed have confirmed the presence of through pores ranging from 0.4 to 1.4 μm depending on the method of sensitization applied. The porous films obtained were used as filters for water purification and their capacity was evaluated by filtration of aqueous solutions containing the bacteria called *Escherichia coli*. Strong dependence of the efficiency of the bacteria removal at filtration on pore sizes was found, namely changing in pore size from 1.4 to 0.4 μm led to the increasing of the amount of removed bacteria from 72.7 to 94.0%, respectively. Authors have also shown the reusability of these filters after ultrasonic cleaning in 5N NaOH solution at room temperature for 15 min.

Track polyimide (PI) film materials having high thermal stability were obtained and investigated in several studies *[Apel, 2001; Apel et al., 1998; Gomez Alvarez-Arenas et al., 2009; Koshikawa et al., 2009; Mitrofanov et al., 2006; Vilensky et al., 1994a, 1994b, 1994c, 1994d, 1997]*. For example, Vilensky et al. *[Vilensky et al., 1994a, 1994b, 1994c, 1994d]* studied in detail all the steps of pore formation in track PI films and they found that exposure to high-energy ions (with energies above 0.3 MeV/nucleon) led to degradation of imide cycles with the formation of amide groups and intermolecular crosslinks. Tracks geometry was identified and the location of sites with the polymer of modified chemical structure possessing intermolecular crosslinks was found. The authors have developed techniques for the preparation of porous PI films with cylindrical or conical pores (cf. Table 3). Such materials are suitable as membranes for micro- and ultrafiltration, in reverse osmosis or gas separation processes.

Apel et al. *[Apel et al., 1987]* have found the effect of pores collapsing ("healing") occurred at drying the microporous PET track membranes after etching. It was shown that the above mentioned phenomenon was caused by capillary contraction, i.e. by volume deformation and pore compression under capillary forces. Using conductometric and gas-dynamic methods the effective pore diameter d_{eff} was defined. It was established that capillary contraction

Table 3. Effect of the type of irradiation ion and etching time on pore shape of PI track membranes *[after Vilensky et al., 1994d]*

Etching time (h)	Irradiation ion	Thickness (μm)	Pore diameter on the surfaces of both sides of membrane (μm)
5 10	Ar	10	0.1/0.15 0.29/0.41
5 10	Kr	10	0.15/0.30 0.46/0.53
5 10	Kr	20	0.35/0.40 0.65/0.65

* etching was carried out in H_2O_2 at 90°C.

occurred when the $d_{\text{eff}} < 15$ nm and contraction essentially depended on tensile characteristics of the material.

In spite of the existence of a large number of studies on complex investigation of structure-property relationships for porous film materials based on different thermosetting, there are some limitations of their industrial application. Thus, for example, PET based membranes possess poor chemical resistance at elevated temperatures. The main drawback of porous polymer materials based on PI and polyarylenes is the method of synthesis of reference polymers, which consists of several stages as well as necessity of using of a solvent or removing of low molecular weight reaction products. Moreover, toxicity of the initial chemicals for synthesis of these polymers has to be taken into account.

Contrariwise, synthesis of polycyanurate networks (PCN) excludes the aforementioned disadvantages and leads to formation of the material possessing the aforementioned attractive features of the polymer used. We have developed the novel technology in producing of porous PCN-containing nanoporous film materials using irradiation followed by track etching *[Fainleib et al., 2009, 2010b; Gusakova, 2009]*. Film samples (with thickness of ~ 30-50 μm) from PCN modified by PCL or polyoxytetramethylene glycol (PTMG) were synthesized by *in situ* polycyclotrimerization of dicyanate ester of bisphenol A in the presence of 30 wt.% of PCL or PTMG through step-by-step heating from 150 to 180 °C for 9 h. Irradiation by α-particles with energy of 27.2 MeV for 0.5-3.0 min was carried out using cyclotron U-120 at the Institute of Nuclear Research of the National Academy of Sciences of Ukraine (Kyiv, Ukraine). Track etching procedure was performed in 5% KOH alcoholic solution at 70 °C. Nanoporous structure in the PCN-based samples with a rather narrow pore size distribution and geometrically regular pore shape was confirmed by SEM and DSC-thermoporometry studies (cf. Fig. 12, Table 4). The average pore diameter was 30-40 nm and their maximum size was not higher than 80 nm.

12. Electrospinning approach in producing of hollow polymer fibers

The first patents on electrospinning appeared in 1900 and 1902, however only in the early 1990's along with the development of nanotechnologies the process became more popular. Nowadays electrospinning is represented as relatively novel processing technique for production of fibers with diameters in the range of a few nanometers to tens of micrometers using electrostatic force. Generally, electrospinning process consists of an elongation of thin fibers from liquid medium under electrostatic forces *[Borgaonkar et al., 2007]*.

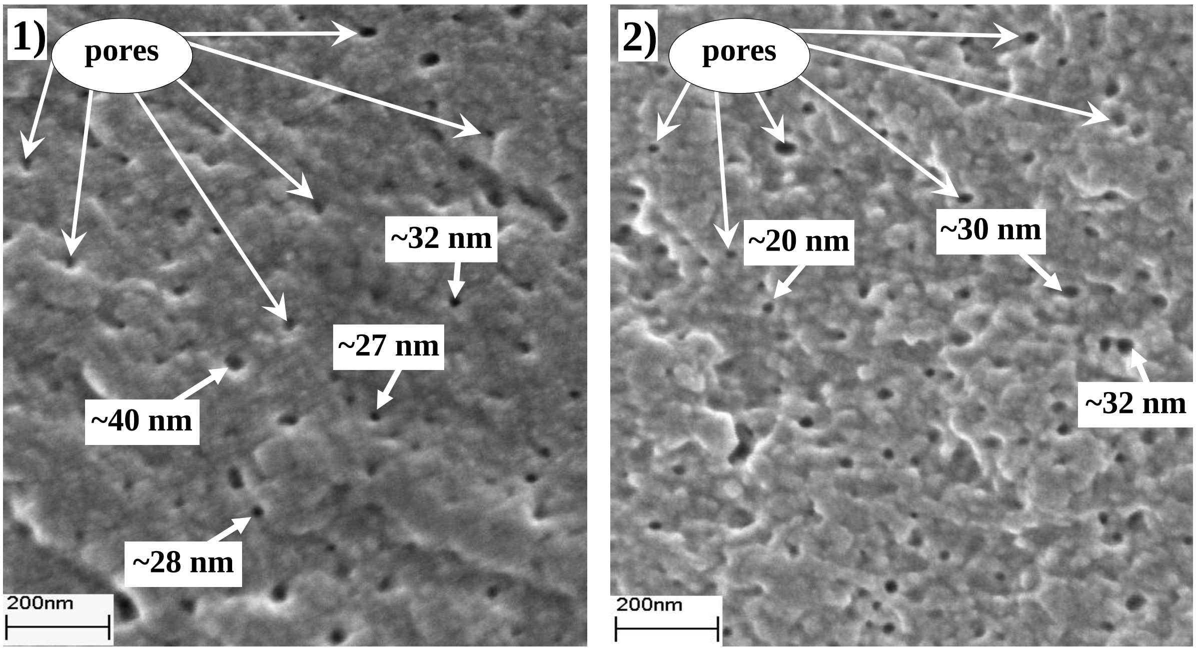

Figure 12. SEM micrographs of surfaces of porous PCN-based hybrid networks obtained using track etching technique: 1) PCN/PCL; 2) PCN/PTMG, containing 70 wt.% of PCN-component in the initial composition

Table 4. Porosity characteristics of PCN-based hybrid networks after irradiation and subsequent etching procedure

Initial composition (wt.%)	Average pore diameter, $D_{p(av)}$ (nm)	Total pores volume, V_p (cm^3·g^{-1})	Total porosity, *P* (%)
PCN/PCL (70/30)	34-38	0.084	9.0
PCN/PTMG (70/30)	30-32	0.154	11.0

Among the unquestionable advantages of electrospinning there are the process simplicity and uselessness of cogulation chemistry or high temperatures to produce solid threads from solution. Many polymers, both synthetic and natural, have been successfully electrospun into nanofibers, for example, PET, polystyrene, poly(vinyl chloride), polyamide. Introduction of various solvents and additives to the polymer solution during fiber formation can reduce fiber diameter (to 50 nm), change fiber shape and add surface roughness *[Hsieh et al., 2005]*. On the orher hand, to avoid the presence of solvent molecules in the polymer product, some precursors are often used. Noteworthily that electrospinning allows also preparing of porous three-dimension polymer matrixes with high porosity, large surface area, suitable as scaffolds for tissue engineering, in drug delivery and in composite materials, for example, as reinforcing additives etc. The pores vary from densely packed, well-formed nanopores with diameters in the range of 20-350 nm to larger flat pores of about several microns. These features can be realized in different polymeric fibers increasing their range of application significantly *[Megelski et al., 2002; Wikipedia, 2011b]*.

However, lack of pore interconnectivity of electrospun fiber scaffolds is a major drawback of the technique, since the scaffolds are very dense allowing only poor cell infiltration and tissue in growths *[Milleret et al., 2011]*. Analysis of the literature data has shown the possibility of pore generation using porogen-containing polymer scaffolds formed by electrospinning, i.e. the nessesity of combining of electrospinning with the other well-known techniques (thermally-, vapor- or nonsolvent-induced phase separation, templating etc.), aiming at porogen removal after completion of fiber formation *[Lenning, 2009; Moon et al., 2007, Nayani et al.]*. For instance, Moon et al. *[Moon et al., 2007]* have coupled the concept of phase separation with electrospinning to create nanoporous fibers by electrospinning of the mixture of polyacrylonitrile and polystyrene followed by removal of the phase-separated polystyrene domains via solvent extraction. To compose the scaffold the polymer was spun in the mixture with a water-soluble template polymer, which was then removed from the scaffold obtained by extensive rinsing with water *[Baker et al., 2008; Lenning, 2009; Milleret et al., 2011]*. The removed co-spun polymer leaved behind voids throughout the scaffold that provided improved porosity and interfiber spacing.

In other work, the effect of the way of electrospinning (either from a common polymer solution or adjacent of fluid jets of PCL and poly(ethylene oxide), PEO, onto a common target) on porous structure of polymeric material obtained was described *[Lenning, 2009]*. To create pores the water-soluble PEO was selectively washed out after electospinning completion. It was established that electrospinning from a common solution led to a significant (up to 80%) decrease of the pore diameter with increasing PEO removal that was explained by PCL chain rearrangement and contraction of the polymer fibers. Implementation of dual jet electrospinning technique allowed increasing or decreasing of the effective pore diameters depending on processing conditions used *[Lenning, 2009]*.

To create electrospun of the nonwoven fabrics with pore size distribution controlled independently of fiber diameter, the similar strategy consisting in intimately blending two nanofibers of dissimilar polymers (Nylon-6 and PEO) during the independent electrospinning was employed in *[Frey and Li, 2007]*. Electrospinning voltage, feed rate, needle size and needle-to-collector distance were optimized for each polymer solution. Electospun fibers were mixed in grounded collector, rotated not rapidly enough to impart anisotropy or alignment in the resulting fabric. To increase the void volume and associated pore size, PEO component (23 wt.% of the electrospun fabrics) was then selectively dissolved during subsequent washing and pore sizing from 400 nm to 1 μm was revealed. It was also established that removal of PEO changed the pore size distribution in the fabric from a narrow distribution of pores less than 200 nm in diameter to a broad distribution with pore sizes ranging from 100 nm to 1μm in diameter *[Frey and Li, 2007]*.

13. Combination of several methods for preparing of porous materials with original structure and properties

Nowadays, porous materials with original properties are produced using several approaches simultaneously *[Oláh et al., 2007, Reinger and Huneault, 2006, Matsuyama et al., 2002]*. For example, Matsuyama et al. *[Matsuyama et al., 2002]* obtained macroporous asymmetric membranes based on PMMA with large pores on the top side and small-sized pores on the bottom of the membrane produced using both the thermally induced phase separation, allowing formation of porous material with isotropic cell structure, and the immersion precipitation technique.

To change pore size and geometry, to increase hydrophilicity, selectivity and productivity of track membranes, some physical, chemical and physical-chemical methods of surface modification are widely used *[Dmitriev et al., 1998, Lazea et al., 2005, Albrecht et al., 2006, Qiu et al., 2008]*. All these techniques can be divided into two groups, namely into the methods, changing the physical-chemical properties of thin surface layer of polymer membrane and into procedures, implying a coating of membrane surface by low- or high-molecular weight compounds, forming a layer with the desired properties. Thus, to decrease surface activity of track PET membranes to different adsorbates, Sergeev et al. *[Sergeev et al., 2004]* chemically modified the membranes with water-soluble polymers, such as poly-N-vinyl amide, comprising terminal hydroxyl groups, heparin, polyvinyl alcohol and polyethylene glycol (PEG). It was established that the modification made led to the reduction of surface adsorption activity of the PET membranes to biphilic sensitive ionic components, namely to proteins and dyes by 0.7-2.3 times and by 2-5 times, respectively. Decreasing in protein and dye adsorption observed for the modified membranes was explained by shielding effect of adsorptionally-active centers of electrostatic and hydrophobic nature with modifiers molecules on the surface of PET membranes.

Lee et al. and Jiang et al. *[Jiang et al., 2006; Lee et al., 2005]* have studied the possibility of producing of nanoporous PI films with low dielectric constant using silica nanoparticles. Pore structure was generated by removing of SiO_2 particles from hybrid PI/SiO_2 films via chemical treatment with hydrofluoric acid. TEM studies confirmed the formation of isolated pores geometrically corresponding to size and shape of the removed SiO_2 particles while PI matrix was not destroyed or deformed. Hybrid PI/SiO_2 compositions were more thermally stable as compared to the individual PI due to high thermal stability of the SiO_2 particles. However, thermal stability of the porous PI samples (after extraction of SiO_2 particles) was approximately the same as that for the individual (nonporous) PI. It was found that T_g values of the porous samples were slightly lower as compared to the T_g of the individual PI and the authors explained this fact by development of nanoporous structure resulted in expansion of polymer free volume and consequently in increasing of segmental mobility of PI macromolecules. It was shown that the dielectric constant ε' (measured at 1 MHz) for porous samples was lower than that for the initial references, namely: for non-porous PI $\varepsilon' = 3.26$; for the hybrid PI/SiO_2 (80/20 wt.%) the value of $\varepsilon' = 3.4$; for the porous PI $\varepsilon' = 1.84$. This very low value for porous PI film obtained by removal of SiO_2 from $PI/SiO_2 = 80/20$ sample seems to be at least strange.

Bosak et al. *[Bosak et al., 2007]* have described preparation of polysulfone membranes modified by oligomeric surfactants of branched structure with terminated anion or cation active groups. Formation of membranes was performed as follows: first polysulfone UDEL-3500® was mixed with porogen (PEG) in the specified ratio in N,N-dimethylacetamide, than the mixture was filtered under vacuum followed by addition of 0.1-3.0 wt.% of oligomeric surfactants and subsequent stirring until a homogeneous clear solution was formed. The resulting composition was poured onto a glass substrate and kept in air at $T = 60 \pm 5$ °C (for the partial evaporation of the solvent). The substrate with a polymer film was then immersed into coagulation bath at $T \sim 22 \pm 2$ °C where polysulfone precipitation along with formation of membrane occurred. It was established that applying surfactants significantly resulted in increase of hydrophilicity of the membrane surface, appearing in significantly decreasing wetting angles values of membrane surface (cf. Fig. 13) and changed their transport properties. It was also found that the modified membranes were characterized by narrower pore size distribution in comparison with similar non-modified analogues.

14. Conclusions

Thus, the chapter summarizes and systematizes the data published on the existing methods of producing of porous polymer materials. A detailed analysis of the effect of pore formation method, the chemical nature of polymer matrix and porogen used (for example, inert or reactive, low molecular weight or polymeric nature, etc.), as well as its amount on the pore size and shape, pore size distribution and other porosity characteristics of the resulted materials is presented. The influence of the above mentioned parameters on thermal, thermal-physical and other properties of final membranes, which determine the area of their possible application, is defined. The basic works describing the creation of porous structure in film materials by irradiation with high-energy particles followed by etching of tracks obtained were observed. The possibility of changing pore geometry by variation of different parameters, namely of irradiation intensity and etching composition and conditions, etc. is described. In conclusion, it should be noted that despite the variety of the existing methods for producing of porous polymers, to create porous polymer materials with additional and/or improved mechanical, thermal characteristics, water permeability or else, many scientists combine a number of ways of pore generation, perform surface modification, etc.

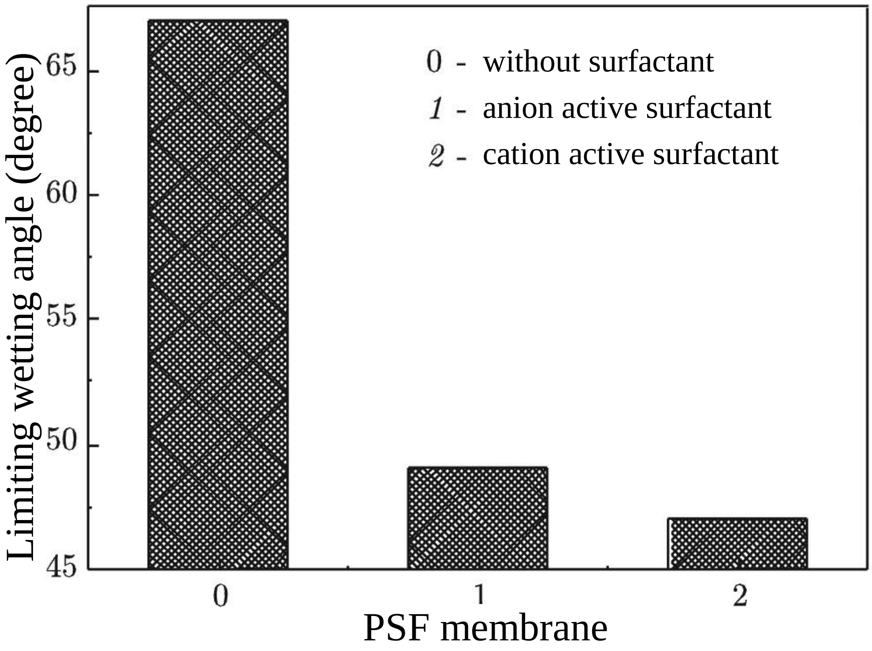

Figure 13. Limiting wetting angles of the surface (measured in water) for PSF membranes *[after Bosak et al., 2007]*

15. Acknowledgments

The National Academy of Sciences of Ukraine (NASU) and the "Centre National de la Recherche Scientifique" (CNRS) are gratefully acknowledged for partial financial support through Ukraine-France cooperation projects (bilateral grant No 21294 and PICS No 5700).

16. References

Albrecht W., Schauer J., Weigrl Th., Richau K., Groth Th., Lendlein A. (2006) Preparation of novel composite membranes: Reactive coating on microporous poly(ether imide) support membranes, *J. Membrane Sci.*, Vol. 269, pp. 49-59.

Alexander C., Andersson H. S., Andersson L. I., Ansell R. J., Kirsch N., Nicholls I. A., O'Mahony J., Whitcombe M. J. (2006) Molecular imprinting science and technology: a survey of the literature for the years up to and including 2003, *J. Molecular Recogn.*, Vol. 19, No 2, pp. 106–180.

Apel P. (2001) Track etching technique in membrane technology, *Rad. Meas.*, Vol. 34, No 1-6, pp. 559-566.

Apel P.Yu., Blonskaya I.V., Didyk A.Yu., Dmitriev S.N., Orelovitch O.L., Root D., Samoilova L.I., Vutsadakis V.A. (2001) Surfactant-enhanced control of track-etch pore morphology, *Nucl. Instrum. Meth. in Phys. Res.: B*, Vol. 179, No 1, pp. 55-62.

Apel P.Yu., Blonskaya I.V., Dmitriev S.N., Orelovitch O.L., Sartowska B. (2006) Structure of polycarbonate track-etch membranes: Origin of the "paradoxical" pore shape, *J. Membr. Sci.*, Vol. 282, No 1-2, pp. 393-400.

Apel P.Yu., Didyk A.Yu., Kuznetsov V.I. (1988) Procedure of preparing of single tracks of heavy ions in polymer samples, *Pribory i technika eksperimenta*, No 6, pp.48–49.

Apel P.Yu., Dmitriev S.N. (2004) Optimization of track membranes pore shape, *Membranes. Critical Technologies* (in Russian), Vol. 23, No 3, pp. 32-37.

Apel P.Yu., Kuznetcov V.I., Ovcinnikov V.V. (1987) A capillary contraction of pores in polymer nuclear membranes, *Kolloidnyi Zhurnal*, Vol. 49, No 3, pp. 537-538

Apel P.Yu., Schulz A., Spohr R., Trautmann C., Vutsadakis V. (1998) Tracks of very heavy ions in polymers, *Nucl. Instrum. Meth. Phys. Res.: B*, Vol. 146, No 1-4, pp. 468-474.

Apel P.Yu., Shyrkova V.V., Soboleva T.I., Kuznetsov V.I., Shestakov V.D. (1990) Polypropylene nuclear membranes – a new type of membranes for cleaning and analysis of aggressive mediums, *Vysokochistue Veschestva*, No 2, pp. 105-107.

ASTM E2456-06. Standard terminology relating to nanotechnology (2006) retrieved from http://www.astm.org/Standards/E2456.htm.

Baker B.M., Gee A.O., Metter R.B., Nathan A.S., Marklein R.A., Burdick J.A., Mauck R.L. (2008) The potential to improve cell infiltration in composite fiber-aligned electrospun scaffolds by the selective removal of acrificial fibers, *Biomaterials*, Vol. 29, pp. 2348-2358.

Balaji R., Boileau S., Guérin Ph., Grande D. (2004) Design of Porous Polymeric Materials from Miscellaneous Macromolecular Architectures: An Overview, *Polymer News*, Vol. 29, No 7, pp. 205-212.

Bibin J., Nair C.P.R., Devi K.A., Ninan K.N. (2007) Effect of low-density filler on mechanical properties of syntactic foams of cyanate ester, *J. Mat. Sci.*, Vol. 42, No 14, pp.5398-5405.

Bismarck A., Menner A., Ikem V.O. (2010) High Internal Phase Emulsions. USA Patent Application 20100261803, retrieved from http://www.freepatentsonline.com/y2010/0261803.html

Blagutina V. (2011) Imprints of Molecules, In: *Himiya i Zhyzn'*, No. 3, retrieved from http://elementy.ru/lib/431359?page_design=print

Bomko V.O., Bryk M.T., Vorob'yova I.V., D'yachenko O.F., Egorov O.M., Zhuravlyova V.G., Zabotin O.V., Zaytsev B.V., Kravchenko A.I., Korobec A.P., Lesnyh M.S., Reshetnikov V.M. (2006) Accelerated ion beam irradiation of polyethylene terephthalate films for track membranes obtaining, *Naukovi Zapysky, Himiya i Himichna technologia*, Vol. 55, pp. 37-41.

Borgaonkar P., Sharma S., Chen M., Bhowmick S., Schmidt D.F. (2007) A flexible approach to the preparation of polymer scaffolds for tissue engineering *Macromol. Biosci.*, Vol. **7**, pp. 201-207.

Bosak V. Z., Vakuluk P. V., Burban A. F., Isaev S.D., Vortman M. Ya., Klimenko N.S., Shevchenko V.V. (2007) Charged polysulfone ultrafiltration membranes formed at presence oligomeric surfactants, Reports of the NAS of Ukraine (in Ukrainian), No 11, pp. 130-134.

Bryk M.T. (2005) *The encyclopedia of membranes in two volumes.* Vol. 1, Kyiv-Mohyla Academy, Kyiv, Ukraine.

Bryk M.T. (2006) *The encyclopedia of membranes in two volumes.* Vol. 2, Kyiv-Mohyla Academy, Kyiv, Ukraine.

Chang J.-Y., Hong J.-L. (2001) Polycyanurates modified with hydroxyl-terminated or cyanated poly(ether sulfone), *Polymer*, Vol. 42, No 4, pp. 1525-1532

Clough R. L. (2001) High-energy radiation and polymers: A review of commercial processes and emerging applications, *Nucl. Instrum. Meth. in Phys. Res.: B*, Vol. 185, No 1-4, pp. 8-33

Connor E., Godschalx J.P., Hawker C.J., Hedrick J.L., Lee V.Y.-W., Magbitang T.P., Miller R.D., Niu J.Q., Volksen W. (2008) Porous composition of matter, and method of making same. US Patent 7368483.

Dmitriev S.N., Kravets L.I., Sleptsov V.V. (1998) Modification of track membrane structure by plasma etching, *Nucl. Instr. Meth. Phys. Res.: B*, Vol. 142, No 1, pp. 43-49.

Duarte A.R.C., Mano J.F., Reis R.L. (2009) Preparation of starch-based scaffolds for tissue engineering by supercritical immersion precipitation, *J. of Supercritical fluids*, Vol. 49, pp. 279-285.

Ensinger W., Sudowe R., Brandt R., Neumann R. (2010) Gas separation in nanoporous membranes formed by etching ion irradiated polymer foils, *Rad. Phys. Chem.*, Vol. 79, pp. 204-207.

Fainleib A., Garda M. R., Saiter J. M., Lauprêtre F., Lorthioir C., Grande D. (2007) Synthesis and characterization of polycyanurate networks modified by oligo(ε-caprolactone) as precursors of porous thermosets, *J. Appl. Polym. Sci.*, Vol.106, No 6, pp. 3929-3938.

Fainleib O.M., Grigoryeva O.P., Gusakova K.G., Sakhno V.I., Zelinsky A.G., Grande D. (2009) Novel nanoporous thermostable polycyanurates for track membranes, *Fizyka i himiya tverdogo tila*, Vol. 10, No 3, pp. 692-696.

Fainleib O.M., Grigoryeva O.P., Gusakova K.G., Grande D. (2009) Method of preparing of polycyanurate. Ukrainian Patent 39202.

Fainleib O.M., Grigoryeva O.P., Gusakova K.G., Starostenko O.M., Grande D. (2010a) Method of preparing of polycyanurate. Ukrainian Patent 50501.

Fainleib O.M., Grigoryeva O. P., Gusakova K. G., Danilenko I.Yu., Sahno V.I., Zelinsky A.G., Grande D. (2010b) Method of preparing of polycyanurate. Ukrainian Patent 50519.

Fang T., Shimp D.A. (1995) Polycyanurate esters: science and application, *Prog. Polym. Sci.*, Vol. 20, No 1, pp. 61-118.

Ferrero-Heredia M.A., Day J., Gaines G.L. (1996) Method of preparing polyurethane foam of low thermal conductivity. US Patent 5530035.

Fleischer R.L., Price P. B., Symes E.M. (1964) Novel filter for hiological materials, *Science*, Vol. 143, pp. 249-250.

Frey M.W., Li L. (2007) Electrospinning and porosity measurements of Nylon-6/poly(ethylene oxide) blended nonwovens, *J. Engineered Fibers &Fabrics*, Vol. 2, Iss.1., pp.31-37.

Gendrikson O.D., Jerdeev A.V., Dzantiev B.B. (2006) Molecular imprinted polymers and their application in a biochemical analysis, *Uspehi biologicheskoy himii*, Vol. 46, pp. 149-192.

Gomez Alvarez-Arenas T. E., Apel P. Yu., Orelovitch O. L., Munoz M. (2009) New ultrasonic technique for the study of the pore shape of track-etched pores in polymer films, *Rad. Meas.*, Vol. 44, No 9-10, pp. 1114-1118.

Gopalani D., Kumar S., Jodha A. S., Singh R., Khatri P. K., Gopal R. (2000) A novel method for production of polyester films-based nuclear track microfilters, *J. Membr. Sci.*, Vol. 178, No 1-2, pp. 93-98.

Grande D., Grigoryeva O., Fainleib A., Gusakova K., Lorthioir C. (2008) Porous thermosets via hydrolytic degradation of poly(ε-caprolactone) fragments in cyanurate-based hybrid networks, *Eur. Polym. J.*, Vol. 44, No 11, pp. 3588–3598.

Grigoryeva O., Gusakova K, Fainleib A., Grande D. (2011b) Nanopore generation in hybrid polycyanurate/poly(ε-caprolactone) thermostable networks, *Eur. Polym. J.*, Vol. 47, No 9, pp. 1736-1745.

Grigoryeva O.P., Gusakova K.G., Starostenko O.M., Fainleib O.M. (2011a) About state-of-the-art classifications and methods of investigation of porous structure of polymer materials (Review), *Polymernyi Zhurnal*, Vol. 33, No 1, pp. 6-23.

Gusakova K.G. (2009) Synthesis, structure and properties of porous cross-linking film-forming polycyanurates, *Manuscript. Thesis for a Candidate of Chemical Sciences Degree*, Kyiv, Ukraine.

Haginaka J. (2008) Monodispersed, molecularly imprinted polymers as affinity-based chromatography media, *J. Chromatography: B.*, Vol. 866, pp. 3-13

Hamerton I. (Ed.) (1994) Chemistry and technology of cyanate ester resins, Chapman & Hall, Glasgow, UK.

Hedrick J.L., Russell T.P., Hedrick J.C., Hilborn J.G. (1996) Microporous polycyanurate networks, *J. Polym. Sci., Polym. Chem.*, Vol. 34, No 14, pp. 2879-2888.

Hedrick J., Shih J., Yuan D. (1998) Electronic devices comprising dielectric foamed polymers, US Patent 5756021.

Hentze H.-P., Antoinetti M. (2002) Porous polymers and resins for biological and biomedical application, *Rev. Molec. Biotech.*, Vol. 90, pp. 27-53.

Hsieh Y.-L., Warner S.B., Schreuder-Gibson H. (2005) Nano- Porous Ultra-High Specific Surface Fibers. NTC Project: C04-CD06s // National Textile Center Research Briefs– Chemistry Competence retrived from <http://trc.ucdavis.edu/textiles/ntc%20projects/C03.CD01s.12.html >

Hoa M. L. K., Lu M., Zhang Y. (2006) Preparation of Porous Materials with Ordered Hole Structure, *Adv. Colloid Interface Sci.*, Vol. 121, pp. 9-23.

Jayakody J.R.P., Khalfan A., Mananga E.S., Greenbaum S.G., Dang T.D., Mantz R. (2006) NMR investigation of water and methanol transport in sulfonated polyareylenethioethersulfones for fuel cell applications, *J. Power Sources*, Vol. 156, No 2, pp. 195-199.

Jiang L., Liu J., Wu D. Li H., Jin R. (2006) A methodology for the preparation of nanoporous polyimide films with low dielectric constants, *Thin Solid Films*, Vol. 510, No 1-2, pp. 241-246.

Junkar I., Koloini T., Krajnc P., Nemec D., Podgornik A., Štrancar A. (2007), Pressure drop characteristics of poly(high internal phase emulsion) monoliths *J. Chromatography: A*, Vol. 1144, No 1, pp. 48-54.

Ilić R., Skvarč J., Golovchenko A.N. (2003) Nuclear tracks: present and future perspectives, *Rad. Meas.*, Vol. 36, No 1-6, pp. 83-88.

Ishizaki K., Komarneni S., Nanko M. (1998) *Porous Materials: process technology and applications,* Kluwer Academic Publishers, Dordrecht, The Netherlands.

Kerres J., Ulrich A., Hein M., Gogel V., Friedrich K. A., Jörissen L. (2004) Cross-linked polyaryl blend membranes for polymer electrolyte fuel cells, *Fuel cells,* Vol. 4, No 1-2, pp. 105-112.

Kiefer J., Hilborn J.G., Hedrick J.C. (1996a) Chemically induced phase separation: a new technique for the synthesis of macroporous epoxy networks, *Polymer,* Vol. 37, No 25, pp. 5715-5725.

Kiefer J., Hilborn J.G., Hedrick J.L., Cha H.J., Yoon D.Y., Hedrick J.C. (1996b) Microporous cyanurate networks via chemically induced phase separation, *Macromolecules*, Vol. 29, No 26, pp. 8546-8548.

Kiefer J., Hedrick J.L., Hilborn J.G. (1999) Macroporous thermosets by chemically induced phase separation, *Adv. Polym. Sci.*, Vol. 147, pp. 161-247.

Kiefer J., Porouchani R., Mendels D. Ferrer J.B., Fond C., Hedrick J.L., Kausch H.H., Hilborn J.G. (1996c) Macroporous thermosets via chemically induced phase separation, *MRS symposium proceedings series,* 8-11 April, San Francisco, USA.

Kim T.K., Yoon J.J., Lee D.S., Park T.G. (2006) Gas foamed open porous biodegradable polymeric microspheres, *Biomaterials*, Vol. 27, pp. 152-159.

Klempner D., Sendijarevic V., Aseeva R.M. (2004) *Handbook of polymeric foams and foam technology,* Carl Hanser Verlag, München.

Knunyanc I.L. (Ed.) (1990) *Chemical encyclopedia in five volumes.* Vol. 2, Bolshaya Rossiiskaya encyclopedia, Moscow, Russia.

Koshikawa H., Usui H., Maekawa Y. (2009) Thermally stable and anisotropically conducting membranes consisting of sub-micron copper wires in polyimide ion track membranes, *J. Membr. Sci.*, Vol. 327, No 1-2, pp. 182-187.

Kravets L.I., Dmitriev S.N., Apel P.Yu. (2000a) Polypropylene track membranes for micro- and ultrafiltration of chemically aggressive mediums. I. Heavy ions tracks etching in propylene, *Membranes. Supercritical Mediums* (in Russian) No 7, retrieved from http://www.chem.msu.su/rus/journals/membranes/7/st_73/krav_tx1.htm

Kravets L.I., Dmitriev S.N., Apel P.Yu. (2000b) Polypropylene track membranes for micro- and ultrafiltration of chemically aggressive mediums. II. Sensitization of tracks of heavy ions in propylene, *Membranes. Supercritical Mediums* (in Russian), No 8, retrieved from
http://www.chem.msu.su/rus/journals/membranes/8/st_83/krve_tx1.htm

Lazea A., Kravets L. I., Albu B., Ghica C., Dinescu G. (2005) Modification of polyester track membranes by plasma treatments, *Surf. Coat. Techn*., Vol. 200, No 1-4, pp. 529-533.

Lee Y. J., Huang J.-M., Kuo S.-W., Chang F. C. (2005) Low-dielectric, nanoporous polyimide films prepared from PEO–POSS nanoparticles, Polymer, Vol. 46, No 23, pp. 10056-10065.

Lenning L.J. (2009) Characterization and modification of porosity in electrospun polymeric materials for tissue engineering application, Abstract on Ph. D. Thesis, Massachusetts, USA.

Li J., Du Z., Li H., Zhang C. (2009) Porous epoxy monolith prepared via chemically induced phase separation, *Polymer*, Vol. 50, No 6, pp. 1526-1532.

Lips P.A.M., Velthoen I.W., Dijkstra P.J., Wessling M., Feijen J. (2005) Gas foaming of segmented poly(ester amide) films, *Polymer*, Vol. 46, No 22, pp. 9396–9403.

Loera A.G., Cara F., Dumon M., Pascault J.P. (2002) Porous epoxy thermosets obtained by a polymerization-induced phase separation process of a degradable thermoplastic polymer, *Macromolecules*, Vol. 35, No 16, pp. 6291-6297.

Luo B., Li Z., Zhang J., Wang X. (2008) Formation of anisotropic microporous isotactic polypropylene (iPP) membrane via thermally induced phase separation, *Desalination*, Vol. 233, No 1-3, pp. 19-31.

Mähr U., Purnama H., Kempin E., Schomäcker R., Reichert K.-H. (2000) Synthesis and characterization of porous polymer membranes produced by interparticle crosslinking *J. Membr. Sci.*, Vol. 171, No 2, pp. 285-291.

Matsuyama H., Berghmans S., Lloyd D.R. (1999) Formation of anisotropic membranes via thermally induced phase separation, *Polymer*, Vol. 40, pp. 2289-2301.

Matsuyama H., Takida Y., Maki T., Teramoto M. (2002) Preparation of porous membrane by combined use of thermally induced phase separation and immersion precipitation, *Polymer*, Vol. 43, pp. 5243-5248.

Maynard A.D. (2006) Nanotechnology: assessing the risks, *Nanotoday*, Vol. 1, No 2, pp. 22-33.

Megelski S., Stephens J.S., Chase D.B., Rabolt J.F. (2002) Micro- and nanostructured surface morphology on electrospun polymer fibers, *Macromolecules*, Vol. 35, pp. 8456-8466.

Menner A., Haibach K., Powell R., Bismarck A. (2006) Tough reinforced open porous polymer foams via concentrated emulsion templating, *Polymer*, Vol. 47, No 22, pp. 7628-7635.

Menner A., Verdejo R., Shaffer M., Bismarck A. (2007) Particle-stabilized surfactant-free medium internal phase emulsions as templates for porous nanocomposite materials: poly-pickering-foams, *Langmuir*, Vol. 23, pp. 2398-2403.

Milleret V., Simona B., Neuenschwander P., Hall H. (2011) Tunning electrospinning parameters for production of 3D-fiber fleeces with increased porosity for soft tissue engineering applications, *European Cells & Materials*, Vol. 21, pp. 286-303

Minamisawa R.A., Zimmerman R.L., Ila D. (2009) Characterization of nanopores in PFA thin films, *Surf. Coat. Technol*., Vol. 203, pp. 2493-2496.

Mitrofanov A. V., Apel P. Yu., Blonskaya I. V., Orelovitch O. L. (2006) Diffraction filters based on polyimide and poly(ethylene naphthalate) track membranes, *Techn. Phys*.,Vol. 51, No 9, pp. 1229-1234.

Moghbeli M. R., Shahabi M. (2011) Morphology and Mechanical Properties of an Elastomeric Poly(HIPE) Nanocomposite Foam Prepared via an Emulsion Template, *Iranian Polymer Journal*, Vol. 20, No 5, pp. 343-355, retrieved from http://www.sid.ir/en/VEWSSID/J_pdf/813201113101.pdf

Moon S.C., Choi J.K., Farris R.J. (2007) Highly porous polyacrylonitrile/polystyrene nanofibers by electrospinning, *Fibers& Polymers*, Vol. 9., No. 3, pp. 276-280.

Mulder M., (transl. Alentiev A.Yu., Yampolskaya G.P.) (1999). *Introduction to membrane technology: tutorial,* Mir, Moscow, Russia.

Nair C.P.R., Mathew D., Ninan K.N. (2001) Cyanate ester resins, recent developments, *Adv. Polym. Sci.*, Vol. 155, No 1, pp. 1-99.

Nam Y.S., Yoon J.J., Park T.G. (2000) A novel fabrication method of macroporous biodegradable polymer scaffolds using gas foaming salt as a porogen additive, *J. Biomed. Mat. Res.*, Vol. 53, pp. 1-7.

Nayani K., Katepalli H., Sharma C.S., Sharma A., Patil S., Venkataraghavan R. Electrospinning combined with nonsolvent-induced phase separation to fabricate highly porous and hollow submicrometer polymer fibers, *Industrial & Engineering Chemistry Research, Nigam Issue*, ACS Publications – *in print*.

Normatov J., Silverstein M. S. (2007) Porous interpenetrating network hybrids synthesized within high internal phase emulsions, *Polymer,* Vol. 48, No 22, pp. 6648-6655.

Oláh L., Filipczak K., Czvikovszky T., Czigány T., Borbás L. (2007) Changes of porous poly(ε-caprolactone) bone rafts resulted from e-beam sterilization process, *Rad. Phys. Chem.*, Vol. 76, pp.1430-1434.

Pahomov P.M., Malanin M.N., Hizhnyak S.D. (2005) IR-method for determination of porosity of polymers, *Vysokomolek. Soedineniya*, Vol. B47, No 6, pp. 1066-1072.

Pahomov P.M., Malanin M.N., Kruglova E.V., Hizhnyak S.D. (2001) Track membranes from polyethylene terephthalate, *Vysokomolek. Soedineniya*, Vol. B43, No 4, pp. 764-768.

Pauling L.A. (1940) A theory of the structure and process of formation of antibodies, *J. Amer. Chem. Soc.*, Vol. 62, pp. 2643-2657.

Porter M.C. (Ed.) (1990) *Handbook of industrial membrane technology*, Noyes Publications, New Jersey, USA.

Qiu G.-M. , Zhu L.-P., Zhu B.-K. Xu Y. Y. (2008) Grafting of styrene/maleic anhydride copolymer onto PVDF membrane by supercritical carbon dioxide: Preparation, characterization and biocompatibility, *J. Supercritical Fluids*, Vol. 45, No 3, pp. 374-383.

Ramaswamy S., Greenberg A.R., Krantz W.B. (2002) Fabrication of poly (ECTFE) membranes via thermally induced phase separation, *J. Membr. Sci*., Vol. 210, pp. 175-180.

Reddy T.T., Takahara A. (2009) Simultaneous and sequential micro-porous semi-interpenetrating polymer network hydrogel films for drug delivery and wound dressing applications, *Polymer*, Vol. 50, pp. 3537-3546.

Reinger J., Huneault M.A. (2006) Preparation of interconnected poly (ε-caprolacone) porous scaffolds by a combination of polymer and salt particulate leaching, *Polymer*, Vol. 13, No 13, pp. 4703-4717.

Reverchon E., Cardea S. (2004) Formation of cellulose acetate membranes using a supercritical fluid assisted process, *J. Membr. Sci*. Vol. 240, No 1-2, pp. 187-195.

Reverchon E., Cardea S. (2005) Formation of polysulfone membranes by super-critical CO_2, *J. Supercritical Fluids*, Vol. 35, No 2, pp. 140-146.

Reverchon E., Cardea S., Rappo E.S. (2006) Production of loaded PMMA structures using the supercritical CO_2 phase inversion process, *J. Membr. Sci.*, Vol. 273, No 1-2, pp. 97-105.

Russel T.P., Hedrick J.L. (2001) Block copolymers as precursors to porous materials, In: *Encyclopedia of materials: Science and technology*, Elsevier Science Ltd.

Sergeev A. V., Nechaev A. N., Pervov N. V., Vlasov S. V., Mchedishvili B. V. (2004) Track membranes as element of template synthesis of nanostructures. I. Modified track membranes, *Membranes. Critical Technology* (in Russian), Vol. 21, No 1, pp. 19-28.

Silverstein M.S., Cameron N.R., Hillmyer M.A. (Eds.) (2011) *Porous Polymers*, John Wiley & Sons, New York, USA.

Sing K.S.W., Everett D.H., Haul R.A.W., Moscou L., Pierotti R.A., Rouquerol J., Siemieniewska T. (1985) Reporting physisorption data for gas/solid systems with special reference to the determination of surface area and porosity, *Pure Appl. Chem*., Vol. 57, No 4, pp. 603–619.

Sergeyeva T.A., Sergeeva L.M., Brovko O.O. (2009) Molecularly-imprinted polymers for the development of new analytical methods. Molecularly-imprinted polymer membranes, *Polimernyi Zhurnal,* Vol. 31, No 3, pp. 199-206.

Shutov F.A. (1991) Blowing agents for polymer foams, In: *Handbook of polymeric foams and technology,* Hanser Publisher, Munich, Germany.

Staudinger H., Husemann E. (1935) Über hochmolekulare Verbindungen. 116. Mitt. Über das begrenzt quellbare Poly-styrol, *Chemische berichte,* p.1618.

Takeda K., Kobayashi T. (2006) Hybrid molecularly imprinted membranes for targeted bisphenol derivatives, *J. Membr. Sci.,* Vol. 275, No 1-2, pp. 61-69.

Vilensky A.I., Markov N.G., Oleynikov V.A., Kupcova I.V., Kushyn V.V., Zagorskiy D.L., Doncova E.P., Mchedishvili B.V., Nesterov N.A., Plotnikov S.V. (1994a) Tracks of high-energy ions in polyimide. II Tracks etching. Producing of track membranes from polyimide, *Himiya Vykokih Energiy,* Vol. 28, No 5, pp. 409-412.

Vilensky A.I., Markov N.G., Oleynikov V.A., Zagorskiy D.L., Mchedishvili B.V. (1994b) Tracks of high-energy ions in polyimide. III Investigation of etching procedure, track's structure and pores shape in polyimide track membranes, *Himiya Vykokih Energiy,* Vol. 28, No 6, pp. 507-511.

Vilensky A.I., Mchedishvili B.V., Kluev V.A., Toporov Yu.P. (1997) Thickness of the broken layer along the track created by a high-energy ion in polyimide, *Letters to the Journal of Technical Physics* (in Russian), Vol. 23, No 23, pp. 68-71.

Vilensky A.I., Oleynikov V.A., Kupcova I.V., Markov N.G., Mchedishvili B.V., Gusinskiy G.M. (1994c) Tracks of high-energy ions in polyimide. I Properties of high-energy ion-beam irradiated polyimide, *Himiya Vykokih Energiy,* Vol. 28, No 4, pp. 326-329.

Vilensky A.I., Oleinikov V.A., Markov N.G., Mchedishvili B.V., Doncova E.P. (1994d) Polyimide track membranes for ultra- and microfiltration, *Vysokomolec. Soedineniya,* Vol. A36, No 3, pp. 475-485.

Vilensky A.I., Oleinikov V.A., Mchedishvili B.V. (1992) Investigation of Xe ions tracks structure in polyethylene terephthalate, *Himia vusokih energii,* Vol. 26, No 4, pp. 300-303.

Waheed A., Forsyth D., Watts A., Saad A.F., Mitchell G.R., Farmer M., Harris P.J.F. (2009) The track nanotechnology, *Rad. Meas.,* Vol. 44, pp. 1109-1113.

Wikipedia (2011a) Bancroft rule, In: *Wikipedia, the free encyclopedia,* retrieved from <http://en.wikipedia.org/wiki/Bancroft_rule>.

Wikipedia (2011b) Electrospinning, In: *Wikipedia, the free encyclopedia,* retrieved from <http://en.wikipedia.org/wiki/Electrospinning>.

Yang Z., Li P., Xie L., Wang Z., Wang S.-C. (2006) Preparation of iPP hollow-fiber microporous membranes via thermally induced phase separation with co-solvents of DBP and DOP, *Desalination,* Vol. 192, No 1-3, pp. 168-181.

You Y., Annan N., Gallagher M.K., Gore R.H. (2006) Porous materials. US Patent 6998148.

Zaręba-Grodź I., Miśta W., Sikora A. Gotszalk T., Stręk W., Hermanowicz K., Maruszewski K. (2005) Textural properties of silica-based organic-inorganic polymer hybrid xerogels, *Mat. Sci. (*Poland), Vol. 23, No 1, pp. 147-153.

Zefirov N.S., Kulov N.N. (Eds.) (1995) *Chemical encyclopedia in five volumes.* Vol. 4, Bolshaya Rossiiskaya encyclopedia, Moscow, Russia.

Zorin I.M., Zorina N.A., Bilibin A.Yu. (2010) Phase separation in mixture of two polymers and selective degradation as a method of formation of porous structure, *Vysokomolek. Soedineniya, A,* Vol. 52, No 2, pp. 235-245.

Hybrid Polymer Materials

Chapter 7

Modern Trends in Progress of Hybrid Organic-Inorganic Polymer Systems

Maksym IURZHENKO[1,2]*, Yevgen MAMUNYA*[1]*,*
Gisele BOITEUX[2]*, Eugene LEBEDEV*[1]

[1] Institute of Macromolecular Chemistry of National Academy of Sciences of Ukraine, Kharkivske shossee 48, Kyiv 02160, Ukraine
[2] Universite de Lyon, F-69361, Lyon, France; CNRS, UMR 5223, Ingenierie des Materiaux Polymeres, F-69622, Villeurbanne, France; Universite Claude Bernard Lyon 1, F-69622, Villeurbanne, France

Summary

Hybrid organic-inorganic systems (HOIS) are a new class of polymer materials, high interest to which appeared in recent years. It is explained by their peculiar structure, which includes organic and inorganic units, and, accordingly, possesses their common properties. Such combination provides the opportunity to obtain materials with predefined properties, which are regulated by variation of chemical composition of organic and inorganic components. Considering onrush of up-to-date technology, that require new materials with specific properties, their application area is constantly expanding. Overall, it is often that new hybrid organic-inorganic polymer systems show characteristics, which far exceed the corresponding characteristics of the existing analogs.

Notations and acronyms

BOPP	biaxially oriented polypropylene
HOIS	hybrid organic-inorganic system
PA	polyamide
PAA	polyamine acid
PANI	polyaniline
PDMS	polydimethylsiloxane
PEEK	polyetheretherkitone
PEG	polyethylene glycol
PEGMA	polyethyleneglycol methylethermethacrylate
PEO	polyethyleneoxide
PET	polyethyleneterephthalate
PI	polyimide
PMMA	polymethylmetacrylate
PP	polypropylene
PPy	polypyrrole
PU	polyurethane
PVC	polyvinylchloride
SOSI	sulfonated polyetheretherketone
SPAEK-6F	pre-sulfonated polyaryletherketone
SPEEK	post-sulfonated polyetheretherketone
HEMA	2-hydroxyethyl methacrylate
MAA	methacrylic acid
MMT	montmorillonite
OMMT	organically modified montmorillonite
POSS	polyhedraoligomeric silsesquioxane (polyhedral silsesquioxane)
SiO_2	silicate in various forms
SSQ	silsesquioxane
TEOS	tetraethoxysilane
TMOS	tetramethylortosilicate
DC	direct current
DMTA	dynamic mechanical thermal analysis
HIPE	high internal phase emulsions
E'	elasticity modulus, MPa
ε'	dielectric permittivity
σ	conductivity, S/cm
$\tan \delta$	loss tangent

1. Classification and synthesis of hybrid organic-inorganic polymeric materials

1.1 Classification of hybrid organic-inorganic polymer systems

Nowadays the term “hybrid materials” is used for many different systems, thus covering a wide range of polymeric materials such as polymer composites, materials with or without interaction between the organic and inorganic components. The broadest definition of hybrid material has the form *[Kickelbick, 2007]*:

hybrid material is a material, which structure includes two parts that are mixed at the molecular level.

Basing on this definition of hybrid material it is possible to offer a generalized definition of hybrid organic-inorganic system:

hybrid organic-inorganic system (HOIS) is a system, which structure includes both organic and inorganic units that interact with each other. In this case possible compositions and structures of hybrid materials can be characterized as follows:

- *Matrix* (crystalline or amorphous, organic or inorganic);
- *Building blocks* (molecules, macromolecules, particles etc);
- *Interactions between components* (strong or weak).

The hybrid organic-inorganic systems can be conditionally divided into two classes using interaction between organic and inorganic blocks as the classification *[Kickelbick, 2007]*. Structural model of different types of HOIS is shown in Figure 1. Class 1 of hybrid systems are characterized by weak interactions between the two phases, such as van der Waals, hydrogen bonding or weak electrostatic interactions (Figure 2). When the strong chemical interaction between organic and inorganic blocks is absent, the blend is formed (Figure 1,a). An example of such hybrid systems can be cross-linked polymer matrix with the inclusions of inorganic clusters or particles that have only physical interactions with the polymer *[Serap and Sariciftci, 2008; Zhang Z. et al., 2004]*. In the case, when the organic and inorganic networks interpenetrate each other, without forming strong chemical interactions, the structure of such system has the form of interpenetrating networks (Figure 1,b). Both cases belong to the class 1 of hybrid systems. For class 2 of hybrid systems the strong chemical interaction between organic and inorganic blocks is inherent, when inorganic structural units, clusters or particles covalently bonded to an organic matrix (Figure 1,c) or inorganic and organic polymers covalently connected with each other (Figure 1,d). This classification is also adopted for other types of polymer materials in Chapter 8.

The last „characteristic“ of the hybrid materials that is left without passing attention is building blocks (Figure 3). It is well known that each component and/or structural block of a system is responsible for some specific function,

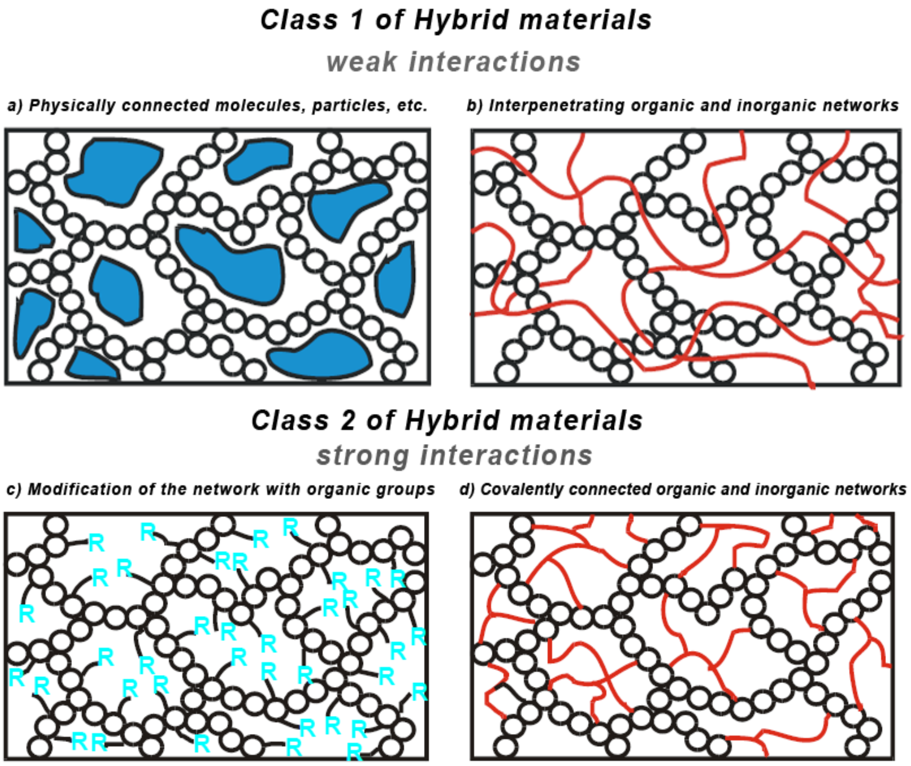

Figure 1. The different types of hybrid materials *[after http://www.chimica.unipd.it/offerte/pubblica/dottorato/hybridmaterials.pdf]*

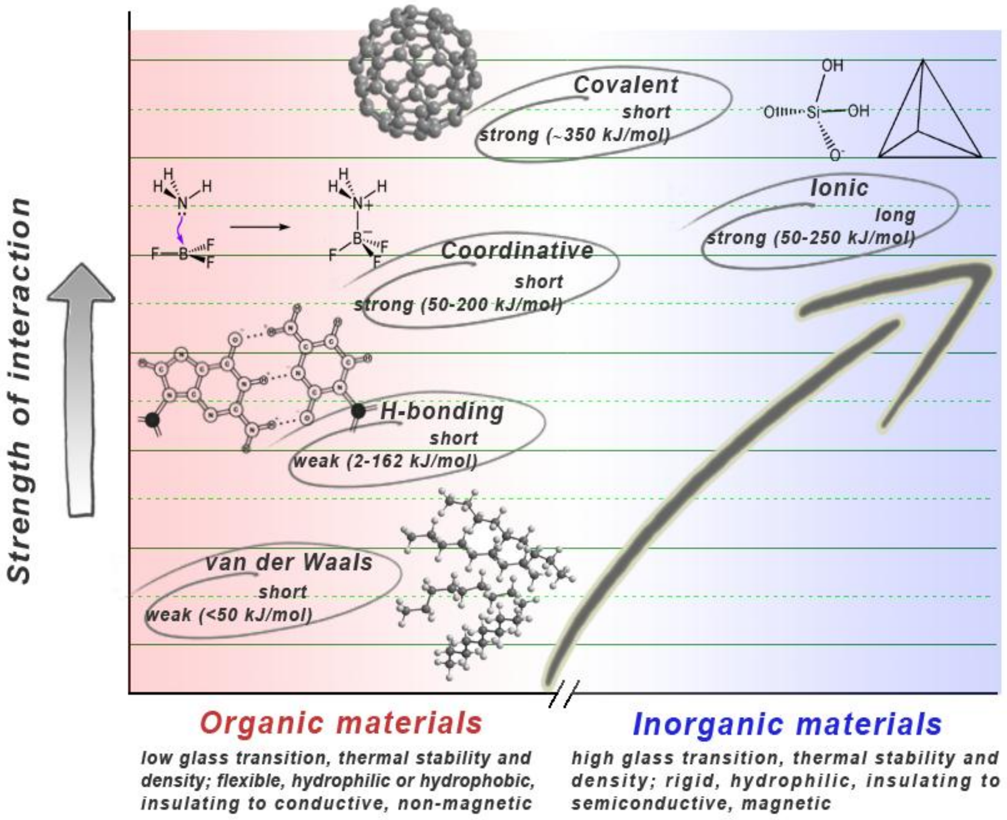

Figure 2. Dependence of the interactions usually existed in hybrid materials on their relative strength *[after Kickelbick, 2007]*

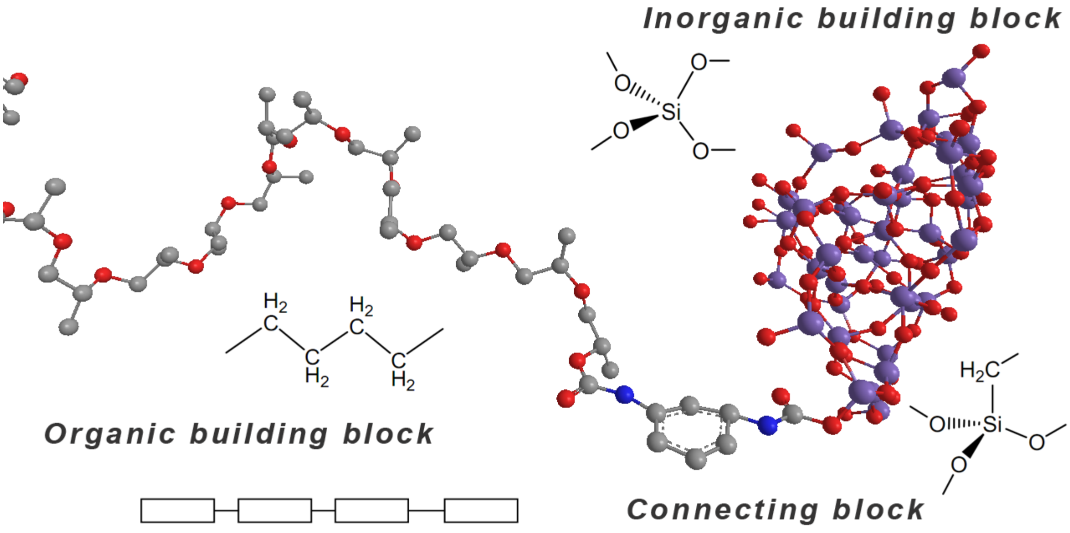

Figure 3. Building blocks of a hybrid system *[after http://www.chimica.unipd.it/offerte/pubblica/dottorato/hybridmaterials.pdf]*

thereby in regard to hybrid materials three types of their building blocks allow to possess the unique properties of a total system. Thus, *inorganic building blocks* can improve thermal, mechanical, optical, electrical and magnetic properties of a hybrid system, whereas the main goals of *organic building blocks* are crosslinking and polymerizability with the aim to obtain flexible, elastic and processable matrix of a hybrid system *[http://www.chimica.unipd.it/offerte/pubblica/dottorato/hybridmaterials.pdf]*. Finally, it is impossible to imagine a hybrid system (firstly *Class 2* of hybrid systems that includes modified network or covalently connected organic and inorganic networks) without *connecting blocks*, which are the crucial point for reduction of the crosslinking density and coupling sites between inorganic/organic components.

1.2 Synthesis of hybrid organic-inorganic polymer systems

Analysis of literature data *[Kickelbick, 2007]* gives the opportunity to highlight three main ways of synthesis of organic-inorganic hybrid systems (Figure 4): using sol-gel process, using pre-formed inorganic structural blocks and polymerization with simultaneous formation of both components. Sol-gel process *[Adachi et al., 2005; Armon et al., 2000; Bronstein et al., 2001; Cardoen and Coughlin, 2004; Dahmouche et al., 1997, 1998; Girardi et al., 2008; Haoying et al., 2001; Honma et al., 1999a, 1999b; Nishi et al., 2000; Sanchez et al., 2000; Schmidt et al., 2000; Shilova and Shilov, 2003; Sugimoto et al., 2004; Qiu et al., 2005]* (Figure 5) is chemically related to the polycondensation reactions of organic molecules in which small molecules form a polymeric structure due to the loss of substituents. At the first stage, during gelation, when the sol (colloidal dispersion of solid nanoparticles in liquid)

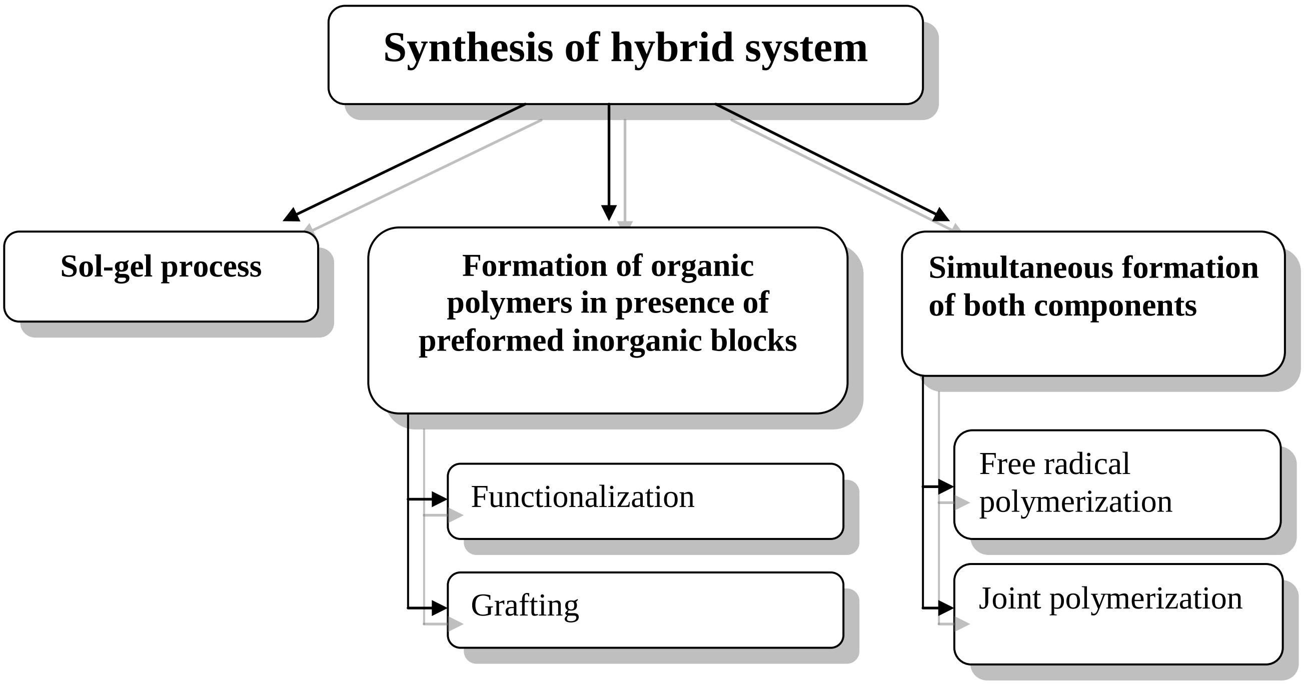

Figure 4. Ways and methods of synthesis of hybrid systems

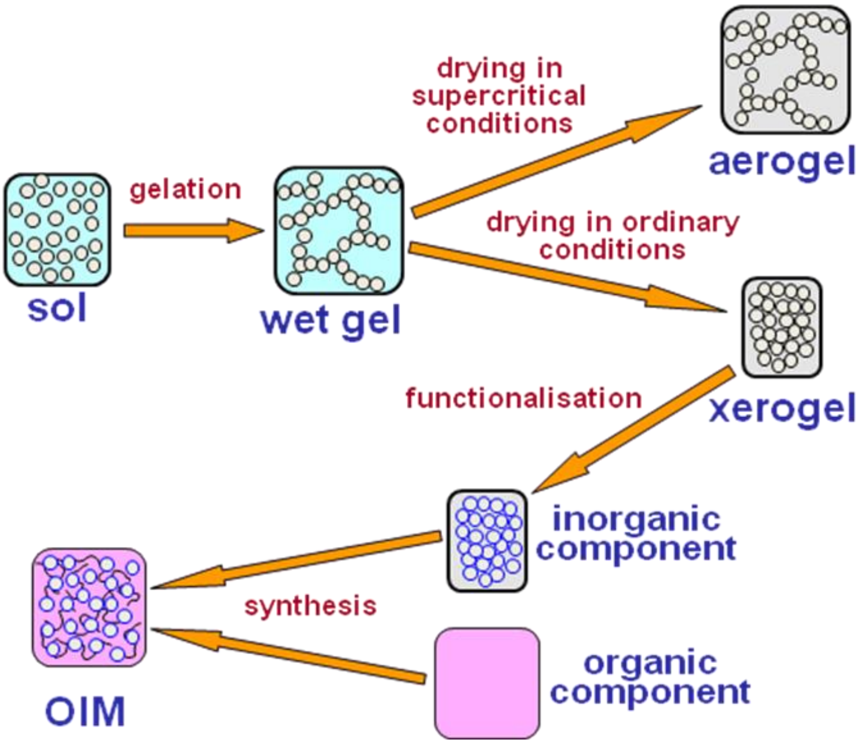

Figure 5. Schematic diagram of one of the routes of sol-gel technology for obtaining HOIS

passes into the wet gel (gel, which contains continuous solid and liquid phases), nanoparticles are grouped and form inorganic skeleton. Thereafter, depending on drying conditions, two different structures of dry gel - aerogel or xerogel are formed. Dry gel can be functionalized to join the reactive groups on the surface of the gel. The hybrid system is formed in the reactions of organic gel and the corresponding component. Usually sol-gel process leads to the formation of three-dimensional cross-linked network *[Kickelbick, 2007]*. Using small molecules as precursor for the formation of cross-linked structure implies several advantages, such as high control of the purity and composition of final products, the use of a solvent based chemistry which offers many advantages for the processing of the material formed.

The silicon based sol-gel process is the most studied, therefore the fundamental principles of reactions are usually described using the process as a model system *[Kickelbick, 2007]*. $R_{4-n}SiX_n$ compounds (n = 1-4, X = OR') used as molecular precursors, in which the Si-X bonds is labile to hydrolysis reactions and forms unstable silanols (Si-OH) that condensate leading to Si-O-Si bonds. In the first steps of this reaction oligomers and polymers as well as the cycles are formed subsequently resulting in colloids that determine the sol. Solid particles in the sol afterwards undergo cross-linking reactions and form the gel.

The second way of synthesis of hybrid systems is conditioned on the presence of pre-formed inorganic structural blocks *[Kickelbick, 2007]*. This way consists two methods of the preliminary surface modification of inorganic structural blocks *[Boven et al., 1990; Huang X. and Wirth, 1997; Prucker and Rime, 1998; Tsubokawa et al., 1990; Werne and Patten, 1999]*: *functionalization [Angiolini et al., 1997; Kickelbick et al., 1999; Kickelbick and Schubert, 1997, 1998, 1999; Mayer et al., 2000; Ribot et al., 1997]* (increasing the number of functional groups on the surface of inorganic block) and *grafting [Annenkov et al., 2003; Kickelbick and Schubert, 2001; Laible and Hamann, 1975; Pankow and Schmidt-Naake, 2004; Takai et al., 2007; Tsubokawa et al., 1990; Tsubokawa and Ishida, 1992]* (grafting end functionalized polymer to the surface of inorganic block). Surface *functionalization* can be done *in situ*, i.e. during formation, and *post-synthetic*, when the inorganic blocks have been already formed, while the *grafting* applies to post-synthetic process only. Using the example of polyhedral silsesquioxane (POSS) $R_8Si_8O_{12}$ *[Mather et al., 2000; Pyun et al., 1999; Pyun and Matyjaszewski, 2000]*, which received widespread use due to the possibility of modifications of Si-O clusters by different types of functional groups. Depending on the number of reactive functional groups the hybrid systems with different structures can be obtained.

Depending on the placement of organic functional groups on the surface of inorganic structural block the hybrid organic-inorganic systems with different types of structures are formed during the polymerization *[Kickelbick and Schubert, 2001]* (Figure 6). The presence of one organic functional group on the surface of inorganic structural block leads to the formation of hybrid systems with linear structure. Formation of the cross-linked hybrid system is a

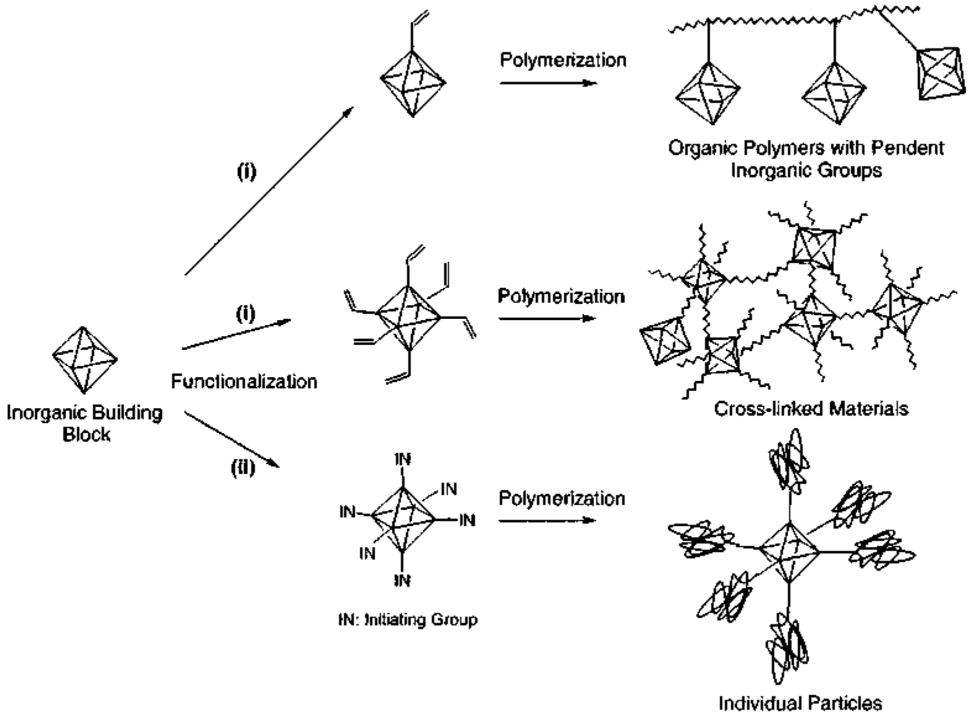

Figure 6. Possible structures of hybrid systems synthesized using pre-formed inorganic structural blocks *[after Kickelbick and Schubert, 2001; reprinted under permission of Springer-Verlag Wien. Copyright 2001]*

consequence of the use of inorganic structural block with multiple organic functional groups. When the inorganic building block plays the role of initiator for the polymerization reactions, hybrid system will be in the form of organic phase grafted to inorganic core.

If the surface of inorganic block is not modified, it may contain nonreactive organic groups (e.g. alkyl chains) attached to its surface *[Kickelbick, 2007]*. In this case, inorganic material can be dissolved in a monomer which is subsequently polymerized. The resulting product after organic polymerization is a blend, the inorganic component has only very weak or no interactions with organic polymer, other words class 1 of hybrid systems is formed. The strongest interactions occur if class 2 of hybrid systems is formed, provided the formation of covalent bonds.

The third major way of synthesis of hybrid systems is a process with the simultaneous formation of both components *[Kickelbick, 2007]*, i.e. organic and inorganic polymers that is revealed in obtaining the most homogeneous types of interpenetrating networks. Typically, for example, for sol-gel process precursors are mixed with organic monomers for organic polymerization and both processes take place simultaneously with or without solvent. Thus, three processes are competing with each other: hydrolysis and condensation forming the inorganic phase, polymerization of organic phase and thermodynamics of the phase separation between the two phases. This way includes two methods (see

Fig.4): free radical polymerization *[Haddad and Lichtenhan, 1996; Prucker and Rime, 1998]* (including atom transfer radical polymerization *[Matyjaszewski et al., 1996; Patten and Matyaszewski, 1998]*, which was reviewed earlier) and the joint polymerization. The mechanism of free radical polymerization is very intense and leads to very homogeneous materials *[Kickelbick, 2007]*, but only selected monomers can be used for this process.

Formation of hybrid organic-inorganic systems by joint polymerization of organic and inorganic components can be attributed to processes with simultaneous formation of both components. Joint polymerization was developed in the Institute of Macromolecular Chemistry of NAS of Ukraine. The distinguishing feature of this method is the simultaneous polymerization of organic and inorganic components in their reactive mixture due to the presence of reactive groups in both organic and inorganic components, without their prior modification *[Ishchenko et al., 1998; Kang et al., 2004; Mamunya et al., 2004a 2004b]*. The main reactions between organic and inorganic component can be written as follows *[Bergaya et al., 2006; Leventis N. et al., 2004]*:

$$RNCO + Na\text{-}O\text{-}Si\equiv \rightarrow R\text{-}NNa\text{-}COOSi\equiv$$

or

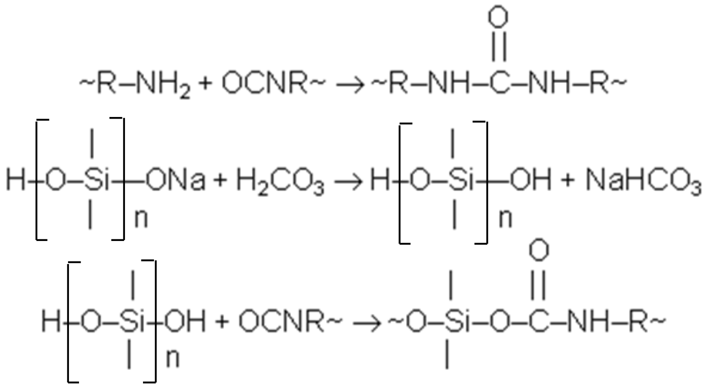

$$\sim R-NH_2 + OCNR\sim \rightarrow \sim R-NH-\overset{O}{\overset{\|}{C}}-NH-R\sim$$

$$H\left[O-\underset{|}{\overset{|}{Si}}\right]_n ONa + H_2CO_3 \rightarrow H\left[O-\underset{|}{\overset{|}{Si}}\right]_n OH + NaHCO_3$$

$$H\left[O-\underset{|}{\overset{|}{Si}}\right]_n OH + OCNR\sim \rightarrow \sim O-\underset{|}{\overset{|}{Si}}-O-\overset{O}{\overset{\|}{C}}-NH-R\sim$$

The reactive mixture obtained took part in the hydrolysis reactions:

$$R\text{-}NNa\text{-}COOSi\equiv + H_2O \rightarrow R\text{-}NH\text{-}COOSi\equiv + NaOH$$

$$R\text{-}NH\text{-}COOSi\equiv + H_2O \rightarrow R\text{-}NH\text{-}COOH + HO\text{-}Si\equiv \rightarrow R\text{-}NH_2 + CO_2$$

Hydrolysis reactions, in which carbon dioxide CO_2 plays the role of initiator for inorganic component polycondensation with it subsequent separation in dispersed phase, can be given of the next general form:

$$Na_2Si_2O_5 + 2H_2O \rightarrow H_2Si_2O_5 + 2NaOH$$

$$NaOH + CO_2 \rightarrow NaHCO_3$$

$$Na_2O\cdot nSiO_2 + CO_2 + mH_2O = Na_2CO_3 + nSiO_2\cdot mH_2O$$

$$H_2CO_3 + NaOH \rightarrow Na_2CO_3 + H_2O$$

The formation of inorganic phase occurs in polycondensation reactions:

$$\equiv SiOH + OH^- \rightarrow SiO^- + H2O\equiv$$

$$\equiv SiO^- + HO\text{-}Si\equiv \rightarrow \equiv Si\text{-}O\text{-}Si\equiv + OH^-$$

Besides the major reviewed methods of formation and modification of hybrid systems less extended methods exist. Some of them are described in *[Akle, 2005; Akle et al., 2007; Di Noto et al., 2007, 2008; Gizdavic-Nikolaidis et al., 2008; Kalapos et al., 2007; Kim S. et al., 2007; Licoccia and Traversa, 2006; Liu G.et al., 2007; Liu X. et al., 2008; Phillips and Moore, 2006; Rosa-Fox et al., 2007; Satterfield et al., 2006; Somani et al., 2008; Timonov, 2000; Wang et al., 2007; Zhou T.H. et al., 2007; Zhu et al., 2008]*.

2. Thermomechanical properties of organic-inorganic polymer systems

The term "*thermomechanical*" is significant and contains all the mechanical properties of materials in a wide range of temperatures, pressures, frequencies etc., and includes static thermomechanical, dynamic thermomechanical, mechanical etc. investigations which, in turn, are common methods of studying the structure and behavior of materials under various conditions. Information of material characteristics such as hardness or elasticity *[Koch et al., 2007; Xi and Tang, 2004]*, the ability to elongation and compression *[Aburatani et al., 2003; Koch et al., 2007; Xi and Tang, 2004]*, the relaxation and creep *[Adalja and Otaigbe, 2002; Xia et al., 2007]*, dynamic and complex viscosity *[Adalja and Otaigbe, 2002]*, presence of structural modifications and transitions depending on temperature and composition *[Aburatani et al., 2003; Koch et al., 2007]*, strain energy *[Lyulin and Michels, 2007]* and, in some cases, existence of specific structural formations in the material, acceleration and ability of mechanical degradation *[Peschanskaya and Hristova, 2006a; Wiggins et al., 2003]* can be obtained using these methods. In *[Aniskevich et al., 2000; Beake, 2006; Bronnikov, 1999; Colak, 2005; Hartmann et al., 1996; Huang G. and Lu, 2006; Kontou, 1998; Matsuo et al., 2006; Oyen, 2007; Raghavan and Meshii, 1997; Rzehak and Zimmermann, 2003; Vinogradov and Schumacher, 2001; Yang et al., 2004]* authors considered the existing theoretical models of mechanical deformation, creep and relaxation of elastic, viscoelastic materials and polymers, and methods of their investigation. Some changes to the well-known models, equations and methods of investigation were suggested. New models were presented and their theoretical justifications were provided.

In the paper *[Xi and Tang, 2004]* the properties of organic-inorganic polymer composites obtained by dispersion and doping methods of filler in polymer matrix, which was polyethyleneoxide PEO with the dispersed lithium salts $LiClO_4$, were studied. The silicate SiO_2, mesoporous silicate SBA-15 and mesoporous silicate P123@SBA-15 were used as the filler. Mechanical investigations of the synthesized HOIS were performed at elongation and showed that the increasing the content of filler SBA-15 leads to reduction of relative elongation of the material with simultaneous increasing its strength. Similar work is *[Kim Y.M. et al., 2004]*. However, unlike *[Xi and Tang, 2004]*, the hybrid systems have been synthesized by sol-gel method and sulfonated fluorinated polymer SDF-F based on decafluorobiphenyl and 4,4 (hexafluoroisopropylidene)dephenol was used as the matrix. The results of mechanical investigations showed the strength decreasing with the increasing the content of inorganic component SiO_2 in the volume of organic SDF-F matrix. At the same time, SDF-F and SDF-F containing 4% SiO_2 showed improved strength characteristics comparing with known solid electrolyte Nafion. The investigation of mechanical properties of hybrid systems, which contain modified inorganic component, were carried out in *[Bae et al., 2008; Ohtsuki et al., 2007; Qiao et al., 2007]*. In *[Bae et al., 2008]* the organic-inorganic system in the form of thin films, which were synthesized based on tetraethoxysilane TEOS, which was previously modified, were studied. New method of mechanical tests – nanoindentation was used by authors for determination the rigidity and Young modulus of the material obtained. This method was developed for studying the mechanical properties of thin films, because the use of classical methods of mechanical investigations was found impossible due to very small thickness of working area of the material (10-1000 nm). The main concepts of nanoindentation are the use of minimal loading and penetration of indentor (within nanometers) and high sensitivity of electronic mechanical analyzer. It was shown that the mechanical characteristics of samples tended to decrease, due to increasing the porosity of the materials obtained with the decreasing number of connections C-H and C-C and the increasing number of Si-O connections in the structure of thin films that was achieved by decreasing the temperature of annealing during formation of the material. Authors of *[Ohtsuki et al., 2007]* investigated bioactive organic-inorganic system synthesized by sol-gel method, based on methacryloxypropyltrimethoxysilane MPS and 2-hydroxyethylmethacrylate HEMA, which were modificated by simulated body fluid SBF (Kokubo solution). The investigation of mechanical properties of obtained systems showed the possibility of synthesis of materials with different levels of strength, which, in most cases, have higher values compared with similar biomaterials, depending on the composition of organic-inorganic systems and content of various types of SBF. Authors of *[Qiao et al., 2007]* studied the organic-inorganic systems based on polyamide PA-6 that were obtained by the original one-step method. Cement-based precursor montmorillonite MMT and ε-caprolactam were used as inorganic component. Results showed that organic-inorganic systems with nanointerphases were synthesized by proposed method. Nanohybrids with high mechanical properties were obtained by further modification of the synthesized systems, and the necessary content of nanointerphases for such characteristics was not less than 15%.

The hybrid organic-inorganic materials, which were synthesized in reactive mixture of organic and inorganic oligomers, were studied in *[Zois et al., 2004]*. Urethane oligomers with different molecular masses were used as the organic components. Sodium silicate, which exists in the form of oligomer in aqueous solution, was taken as inorganic component. Parameters obtained from the mechanical investigations, which were carried out by dynamic mechanical thermal analysis, authors used for comparison with the parameters identified by other investigation methods. It was given the values of different glass transition temperatures of the compositions that were determined using dielectric and calorimetric investigations. It was shown that increasing the molecular weight of organic component and content of inorganic phase in HOIS volume leads to significant reduction of the glass transition temperature values.

The main purpose of *[Di Vona et al., 2007]* was to study the properties of materials that may be promising as solid electrolytes for fuel cells. In this paper, hybrid organic-inorganic membranes were obtained from commercial product polyetheretherkitone PEEK that was previously modified and further mixed with Si-containing component. The research results of sulfonated polyetheretherketone SOSI-PEEK authors compared with the characteristics of known electrolyte Nafion. Mechanical studies showed that the synthesized material SOSI-PEEK has higher strength and much lower values of deformation at elongation compared with Nafion.

The hybrid systems based on epoxy resins and modified nano-SiO_2 precursor synthesized by sol-gel method and doped with carbon filler were studied in *[Zhang C.H. et al., 2007]*. Mechanical investigations showed that with increasing the filler content and the change of nanoparticle dimensions strength of the systems grew in parallel with the increasing the matrix packaging value. Similar studies were carried out in *[Zhou H. et al., 2008]*, but unlike *[Zhang C.H. et al., 2007]*, the thermosensitive polyurethane was used as a polymer matrix here. Mechanical properties of the synthesized systems were studied at elongation. Authors showed that with increasing the content of SiO_2 nanoparticles in the bulk of compositions strength and their elongation at break grew rapidly due to connections Si-C and Si-O-C and acquired their maximums at 5% mass parts.

In *[Zhou T.H. et al., 2007]* the industrial polypropylene PP, polybutylacrylate PBA and their mixtures were used as the polymer matrix. The nanoscale particles SiO_2 (aerosil) as well as in the previous papers and previously modified particles SiO_2 were inorganic component. Hybrid organic-inorganic systems were obtained by mixing the polymeric and inorganic components. Previous modification enabled authors to obtain the systems with chemically bonded components. Mechanical studies showed that creep of the systems, which were filled with nanoscale particles SiO_2, decreased in comparison with pure polymer, while the systems with chemically bonded components showed even lower values of creep, i.e. the rigidity of the systems increased.

The broad studies of thermomechanical properties of different hybrid organic-inorganic systems have been carried in *[Bonilla et al., 2006; Huang J. et al., 2005; Mominul Alam et al., 2007; Ni et al., 2004; Normatov and Silverstein, 2007; Peschanskaya and Hristova, 2006b; Robertson et al., 2003; Silverstein et al., 2005; Zhang Z. et al., 2007]*. Authors used various methods of thermomechanical investigations. Among the most popular dynamic mechanical thermal analysis (DMTA) can be highlighted. In *[Bonilla et al., 2006]* hybrid organic-inorganic materials based on polyurethane, polymethylmetacrylate PMMA and tetraethoxysilane TEOS synthesized by sol-gel method were investigated. Mechanical studies were carried using DMTA, which allowed authors to explore the properties of the synthesized materials in broad temperature and frequency ranges. Studying the properties of systems depending on their composition passed in two ways. In the first case the influence of content of organic component, which consisted of two products (polyurethane and PMMA) and gradually changed, on the properties of the material was explored, while correlation between the organic and inorganic components remained constant. In the second case, authors investigated the influence of inorganic component on the properties of the synthesized systems, while the ratio between organic and inorganic components was sequentially varied. In the first part, it was shown that the increase the content of PMMA in organic component of hybrid systems leads to the rapid growing of the stiffness. The results of mechanical studies of the second part of the work allowed saying that the rigidity decreased with the increase of inorganic phase in the volume of such systems.

Authors of *[Mominul Alam et al., 2007]* studied organic-inorganic systems based on polyimide PI prepared from pyromellitic dianhydride PMDA and 4,4-oxydianiline ODA, organically modified montmorillonite OMMT and polydimethylsiloxane PDMS, which were synthesized *in situ* by sol-gel method. Mechanical and dynamic mechanical studies showed the improved mechanical properties of hybrid systems in comparison with the results of separately made components. Thus, hybrid systems have higher values of elasticity, strength and elongation at break. The reduction of glass transition temperatures with increasing the structural heterogeneity was found for hybrid systems.

In *[Huang J. et al., 2005; Ni et al., 2004; Zhang Z. et al., 2007]* the hybrid organic-inorganic polymer systems synthesized on polyhedraoligomeric silsesquioxane POSS were investigated by DMTA methods. In *[Ni et al., 2004]* authors studied the hybrid system based on epoxy resins and modified POSS. During the investigations the concentration dependences of mechanical parameters such as the mechanical loss tangent tan δ, elasticity modulus E′ etc. on temperature were constructed. Results showed that values of glass transition temperatures decreased with the injection of modified POSS into polymer matrix. Authors explain this phenomenon by the rise of free volume with increasing POSS content in the material. Paper *[Zhang Z. et al., 2007]* is similar to previous work. Just as in *[Ni et al., 2004]* authors investigated hybrid organic-inorganic systems, which included the epoxy resin and POSS. Mechanical properties of hybrid systems were studied by dynamic and static methods. As in the previous paper, authors constructed the concentration dependences of mechanical characteristics. It is interesting that unlike *[Ni et al., 2004]*, glass transition temperatures of these systems increased with the injection of POSS. This inconsistency of the results may be explained by differences in the properties of modified and unmodified POSS, and their impact on the general properties of the systems. However, in *[Ni et al., 2004]* conclusions were made for the general case, detailed effects of POSS on the properties of hybrid system was not considered. Later, in the paper *[Zhang Z. et al., 2007]*, authors examined the influence of POSS on the glass transition temperatures shift of hybrid systems and their mechanical properties. It was shown that the values of the glass transition temperatures increased with the rise of POSS concentrations, while the values of mechanical parameters increased only within the small concentrations of POSS (<10%) and rapidly decreased exceeding 10% of the mass part. In the paper *[Huang J. et al., 2005]* polyamine acid PAA was used as the polymer matrix of hybrid systems. Results of mechanical and thermomechanical studies showed that, as in the previous works, the rise of systems heterogeneity (increasing the content of POSS) led to deterioration of mechanical and thermomechanical properties of materials.

Another type of hybrid organic-inorganic polymer systems was studied by authors of *[Normatov and Silverstein, 2007; Silverstein et al., 2005]*. In these works porous polymers (polyHIPEs) were synthesized by polymerization of monomers and crosslinking co-monomers in the continuous phase of high internal phase emulsions (HIPE). Such hybrid systems are a new type of polymers, and, therefore, interesting to study. In the paper *[Normatov and Silverstein, 2007]* monomer 2-ethylhexyl acrylate EHA and crosslinking co-monomer divinyl benzene DVB, tetraethylorthosilicate TEOS and sorbitan monooleate SMO were used as the components for synthesis of hybrid systems. Mechanical investigations showed that the formation of hybrid polymer-inorganic interpenetrating networks leads to increasing the temperature and intensity of maximum of mechanical loss tangent tan δ. It is also shown that the elasticity modulus and plateau of highly elastic strain increased with the increasing of TEOS content in the compositions. Similar work is *[Silverstein et al., 2005]*, in which authors studied polyHIPE systems that combined silsesquioxane SSQ and organic conductive polymeric (polypyrrole PPy, polyaniline PANI) networks. As a result, similar to the previous work, the interpenetrating organic and inorganic networks have been obtained. DMTA investigations showed that the mechanical properties of hybrid systems at high temperatures (> 250 ^{o}C) strongly depended on the content of SSQ, while at room temperature (≈ 30 ^{o}C) mechanical properties were independent on the content of mineral phase subject to the presence of organic rigid network. When such network was absent in the systems, mechanical parameters were dependent on the content of SSQ.

Among the variety of thermomechanical investigations nanoindentation method deserves special attention *[Peschanskaya and Hristova, 2006b; Robertson et al., 2003]*, which has already been mentioned *[Bae et al., 2008; Peschanskaya and Hristova, 2006a]*. Nanoindentation is new and very promising method, as it allows to study the behavior of materials at the lowest load and deformation and, in some cases, to detect and investigate nanostructural formations in its volume. In *[Peschanskaya and Hristova, 2006a, 2006b]* the hopping creep was studied using this method, which reflects the heterogeneity of the structure at meso-and nanolevels of amorphous polymer systems. Epoxy resin D-450 and PVC were used as the polymer matrix, and diabase particles were used as nanoscale inclusions. Using laser interferometer authors registered the speed of creep at submicron transformations during compression. It was found that periodic fluctuations of speed depending on time or deformation correspond to the discontinuous nature of deformation. Thus, it was experimentally shown that diabase particles resulted in appearance of jumps in creep with the same scale, while jumps of deformation at nanolevel related to the globule sizes. Authors showed that the study of jump deformations gives the opportunity not only to assess the formation of micro-and nanolevels in amorphous polymers, but to make conclusions about the connections between ordered structures.

In the paper *[Robertson et al., 2003]* the investigations of properties of hybrid organic-inorganic coatings based on tetraethoxysilanes TEOS, glycidoxypropyltrimethoxysilanes GPTMS and diethylenetriamine DETA, which were synthesized by sol-gel method, were carried out. Mechanical properties of materials obtained were studied using nanoindentation method. Results of experiments showed that the coatings, which were obtained with the ratio TEOS/GPTMS equal to 80/20, had considerable rigidity and fragility. Values of mechanical characteristics of these systems increased with increasing the curing temperature up to 350 ^{o}C. Data obtained from the investigations of coatings, which were synthesized based on GPTMS and DETA, showed less rigidity and flexibility than previous. The rise of DETA content in compositions resulted in increasing the number of connections in organic network and values of mechanical parameters. It was found that presence of many connections in organic network inhibited thermal degradation that, in all cases, started at 250 ^{o}C.

3. Electrical and dielectric properties of organic-inorganic polymer systems

Fundamental studies of electric and dielectric properties make it possible to expand the range of information about materials and to obtain the information about molecular mobility, relaxation processes and ways of charge transport in materials etc. Among the leading sources, which reveal the fundamental principles and basic aspects of dielectric and electrical behavior of polymeric materials *[Bottcher and Bordewijk, 1978; Hedvig, 2006; Jonscher, 1983; Kremer and Schonhals, 2003; Ku and Liepins, 1987; McCrum et al., 1967; Riande and Saiz, 1998; Seanor, 1982]*, can be distinguished. Authors of *[Mijovic and Fitz, 1998; Williams and Thomas, 1998]* reviewed in detail the theories and models of dielectric relaxation, molecular mobility and conductivity. Using of models and theories for description the real results of studies of electric and dielectric properties of polymeric materials is given in *[Kapoor et al., 2002; Pissis and Polizos, 2005]*.

Recently the ion (proton) conductivity of polymer materials acquired great popularity. Such a significant interest to this field of polymer physics can be explained by the possibility of obtaining the solid electrolytes and fuel cells based on ion- and proton conducting polymer systems and the perspectives of their implementation in industry and energetics as alternative ecological sources of energy *[Licoccia and Traversa, 2006; Timonov, 2000]*. In the cited works the commercial hybrid material Nafion and its modifications were considered. The popularity of this material may be explained by the high ionic conductivity, which is uncharacteristic for pure polymers in general, and ionselectivity and cation-exchange properties that allow its use as the solid electrolyte as well as the fuel cell. Not less interesting to study the hybrid polymer systems that contain silicates SiO_2, ions of lithium, sodium, aluminum, etc. So in *[Honma et al., 1999a, 1999b]* the properties of high-conducting polymer membranes with proton conductivity, which may be promising for use in electrochemical equipment, were studied. Organic-inorganic nanocomposite membranes based on silicate SiO / polyethyleneoxide PEO, which were synthesized by sol-gel method, are known to be generally related to the family of isotropic, elastic, amorphous polymers. Hybrid membranes doped with protons and various ions are characterized by high conductivity at elevated temperatures (> 100 ^{o}C).

Conductive membranes are generally stable at high temperatures due to the presence of inorganic component SiO in their structure. The conductive membranes synthesized in these works showed high proton conductivity ($\sigma \approx 10^{-4}$ S/cm at 160 °C) that allows to attribute them to the family of solid polymer electrolytes with proton conductivity, which can be implemented into the manufacturing process and used in high-temperature electrochemical devices such as fuel cells, displays, chemical sensors and others.

Mamunya et al. *[Mamunya et al., 2007]* synthesized and investigated dielectric and thermal-mechanical properties of hybrid organic-inorganic polymer systems, which were obtained in reactions of the organic oligomer (macrodiisocyanate + poly(isocyanate) (MDI+PIC)) which have free NCO-groups with inorganic oligomer - sodium silicate (SS). The structure of HOIS was formed as two interpenetrated networks: an elastic network as a result of reactions MDI-SS and a rigid network PIC-SS resulting respectively from the reaction of MDI with SS and PIC with SS. Depending on NCO-groups content, one of the networks features is prevailing as attested by dielectric, electrical and thermal-mechanical experiments. As it is shown (Figure 7), the elastic network MDI-SS possesses high values of dielectric parameters ε', tan δ and conductivity σ whereas for the rigid network PIC-SS the values of these characteristics are much lower and are typical for usual thermosets.

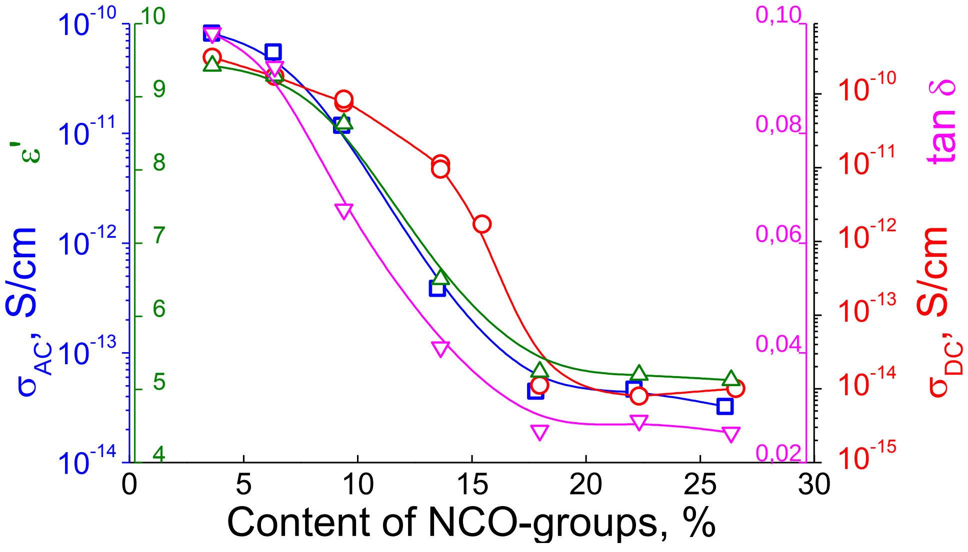

Figure 7. Concentration dependencies of permittivity, loss factor and conductivity of HOIS

Authors of *[Zhang J. et al., 2005]* studied the dielectric properties of hybrid organic-inorganic systems based on polyimide PI and silicate SiO_2, which were obtained in sol-gel reactions and thermally stabled. Results showed that the permittivity of the synthesized hybrid materials is in the range from 3.4 to 6.0. With increasing the content of inorganic component the permittivity of the systems grew rapidly. Thus, the possibility to control the dielectric properties and thermostability of the materials by variation of SiO_2 content that is perspective for the use of such hybrid polymer systems in dielectric equipment has been shown. The results were well described using Maxwell-Garnett model *[Maxwell-Garnett, 1982]*.

Di Noto et al. *[Lavina et al., 2007a]* studied the hybrid organic-inorganic films based on polymethylmethacrylate PMMA and polyvinylchloride PVC as the polymer matrix and SiO_2 as inorganic component. Electrical and dielectric properties of the synthesized films were studied using dielectric spectroscopy. It was shown that the permittivity ε' of the obtained materials was less 3.5 and the dielectric loss tangent tan δ was less 0.05 in the frequency range 40 Hz-10 MHz and temperature range 0-130 ^oC. Dielectric spectroscopy gave the opportunity to build the dependences of molecular relaxation in composites $[(PMMA)_x(PVC)_y]/(SiO_2)_z$ on the temperature and compositions of the systems. In fact, the the permittivity ε' of hybrid films with $20<z<35$ mass percents was less compared with pure inorganic component SiO_2 ($\varepsilon'=3.9$, $\tan\delta<0.05$). These results enabled authors to speak about the perspectives of implementation this material in microelectronic equipment.

Authors of *[Xi and Tang, 2004]* investigated hybrid organic-inorganic polymer composites based on polyethyleneoxide PEO, mesoporous silicate and lithium ions as the filler. Number of lithium ions that conduct were determined by impedance spectroscopy combined with stabilized current technique, which was proposed by Bruce and Vincent *[Bruce and Vincent, 1987; Riley et al., 2002]*. Results showed the possibility of increasing the ionic conductivity by increasing the number of lithium ions that conduct and creation a new way of lithium ions transport. This made it possible to consider this hybrid material as a promising electrolytic material for lithium polymer batteries.

In *[Qi and Dong, 2007]* authors investigated hybrid organic-inorganic polymer electrolytes based on polyethylene oxide PEO, SiO_2 and lithium salts $LiClO_4$ synthesized by sol-gel method. Electrochemical studies were carried out using impedance spectroscopy. Results showed that the obtained membranes doped with lithium salts have the significant electrical conductivity ($\sigma \approx 10^{-6}$ S/cm at room temperature) and with the elasticity and thermal stability can potentially be applied in the production of high-temperature electrochemical devices (displays, chemical sensors, fuel cells etc.).

In *[Nagasubramanian et al., 2006]* the electrical properties of hybrid polymer materials based on polyethyleneoxide PEO and lithium salts synthesized by sol-gel method were studied. These hybrid organic-inorganic systems showed the improved values of dielectric characteristics in comparison with similar nonhybrid materials. It was found the possibility to charge/discharge hybrid systems at lower temperatures and higher values of current, whereas higher temperature and lower values of current were required for analogs. On the basis of lithium salts the ion conducting organic-inorganic polymer systems were also synthesized in *[Barbosa et al., 2008; Kao et al., 2006]*. In *[Kao et al., 2006]* the hybrid systems that contain tetraethoxysilane TEOS, (3-glydicyloxypropyl)trimethoxysilane GLYMO, lithium salts $LiClO_4$ and poly(propylene glycol)-block-poly(ethylene glycol)-block-poly(propylene glycol) bis(2-aminopropyl ether) D2000 were synthesized using sol-gel method. Changes of dielectric properties were studied. The hybrid materials with very high ionic conductivity even at room temperature ($\sigma \approx 10^{-2}$ S/cm) were obtained. Authors of *[Barbosa et al., 2008]* investigated hybrid solvent free organic-inorganic solid polymer electrolytes, which were synthesized by sol-gel method. The commercial product d-U(900) based on oxyethylene oligomers was used as polymer matrix, which was filled with lithium bis(trifluoromethanesulfonyl) imide LiTFSI. Electrical properties of electrolytes were determined by the level of ionic conductivity using voltage-current characteristics. It was shown that the obtained solid polymer electrolytes are completely amorphous and can be used in electronic devices due to its high ionic conductivity at room temperature ($\sigma \approx 10^{-4}$-10^{-1} S/cm) and electrochemical stability.

Authors of *[Nishi et al., 2000]* studied organic-inorganic polymer systems based on polyethylene glycol 200 PEG_{200}, tetramethylortosilicate TMOS and lithium salts $LiClO_4$ obtained by sol-gel method. The possibility of using the synthesized systems as high density electrolytes on the basis of lithium salts was investigated. Ionic conductivity of the obtained systems was determined by complex impedance spectroscopy. The results showed that with increasing PEG_{200} content ionic conductivity increased, while in the hybrids without lithium salts the ionic conductivity was absent. Materials with the conductivity $\sigma \approx 10^{-5}$ S/cm at room temperature were obtained.

In the paper *[Dahmouche et al., 1998]* the organic-inorganic polymeric materials based on tetraethoxysilane TEOS, polyethylene glycol PPG with and without covalent organic-inorganic chemical bonds doped with lithium salts $LiClO_4$, with general name ORMOLYTES (organically modified electrolytes), were synthesized by sol-gel method. Results of electrical studies showed that the authors obtained ion conducting ORMOLYTES with high ionic conductivity ($\sigma \approx 10^{-6}$ S/cm), that, together with optical and mechanical properties, makes it possible to use these materials in electrochemical devices. The rise of ionic conductivity with increasing silicate content in the bulk of polymer matrix was also found.

Similar paper is *[Dahmouche et al., 1997]*, in which authors also studied the family of Li^+ ion conducting hybrid organic-inorganic polymer systems called ORMOLYTES, which included tetraethoxysilane TEOS and polyethylene glycol PEG, obtained by sol-gel method. Using method of complex impedance spectroscopy the ionic conductivity of materials obtained as a function of polymer chain length and concentration was defined. It was revealed that the ionic conductivity decreased with increasing the polymer chain length, but increased with increasing the concentration of organic component. The highest conductivity ($\sigma \approx 10^{-2}$ S/cm) at room temperature were found for the sample with PEG/TEOS = 40% mass parts.

In the paper *[Qiu et al., 2005]* somewhat different family of hybrid organic-inorganic materials entitled ORMOCERS (organically modified ceramics as polymer electrolyte) based on organically modified polysiloxane monomer, which were obtained under the action of ultraviolet radiation in the presence of liquid electrolyte, were considered. Electrochemical properties of hybrid organic-inorganic polymer electrolytes were investigated by impedance spectroscopy and cyclic voltage-current measurements. It was found that ionic conductivity strongly increased with increasing the amount of liquid electrolyte. So at 80% mass parts of liquid electrolyte conductivity equaled to $3.3 \cdot 10^{-3}$ S/cm at 21 ^{o}C and $8 \cdot 10^{-4}$ S/cm at -23 ^{o}C. Hybrid organic-inorganic polymer electrolytes also showed the extraordinary electrochemical and surface stability. Surface stability of the materials increased with time and achieved the best performance after 2 days. Stability of surface to oxidation was higher in contrast to lithium and steel electrodes.

Polyurethanes can also be used as polymer matrix for hybrid organic-inorganic polymer systems with ionic conductivity. Actually, systems based on polyurethanes are very interesting to study because they can be used as a model for investigation the formation of networks and processes of charge transport, mobility of chains and groups etc. For example, in *[Tsonos et al., 2001]* authors studied dielectric and electrical behavior of films with ionic conductivity based on polyurethanes by dielectric relaxation spectroscopy and conductivity on DC. It was shown that films with ionic conductivity were characterized by the presence of microphase separation on elastic and rigid microareas. To explain the results two mechanisms of conductivity were considered. It was suggested that the short relaxation times related to the elastic microareas and longer relaxation processes referred to hard microareas. It was shown that the fast relaxation mechanism of conductivity of elastic microareas accelerated the mechanism of conductivity relaxation of hard microareas.

To explain the properties of polyurethanes authors of *[Baillif et al., 2000]* studied the evolution of the α-relaxation process during their polymerization by dielectric spectroscopy methods. It was determined that the form and temperature dependences of relaxation times were similar for pure triols, and their evolution during polymerization of polyurethane systems depended on the molecular weight of triols. This fact was explained by the transformation of active dipoles as the result of reactions and appearance of new dynamic connections between new active dipoles.

In the paper *[Zois et al., 2004]* authors investigated the relationships between microstructure, dielectric properties and molecular mobility of hybrid organic-inorganic polymer composites, which were obtained in the reactive mixture of polyurethane and sodium silicate. It was shown that the molecular mobility was higher in the composites compared with pure polyurethane matrix and electrical conductivity increased with increasing the content of inorganic phase or molecular weight of polyurethane.

Due to the different methods of formation of hybrid organic-inorganic polymer systems that were previously considered, it is possible to obtain hybrid materials with different organic and inorganic components, which have different structures and, therefore, properties *[Benavente et al., 2004; Galal et al., 2007; Gross et al., 2003; Khan and Inamuddin, 2006; Kudo et al., 2008; Lavina et al., 2007b; Li et al., 2006; Yakuphanoglu, 2008]*. In the paper *[Bronstein et al., 2004]* new hybrid solid polymer electrolytes, which included polyethylene oxide PEO, microphases of lithium salts LiTf and organically modified aluminosilicate OM-AlSi were studied. Impedance spectroscopy was used to study the conductivity and permittivity of obtained films. Results of experiments showed that the modification of aluminosilicates significantly affected on the conductivity of hybrid systems. Isolation of inorganic phase by reducing the dimensions of OM-AlSi domains increased interfacial area between OM-AlSi and PEO+LiTf. The presence of CN groups on the surface of OM-AlSi/PEO + LiTf increased the permittivity of interfacial layer and conductivity. At the same time temperature dependences of conductivity showed no change in the mechanism of conductivity of synthesized modified solid polymer electrolytes.

Obviously, due to wide range of characteristics and suitability of synthesis of hybrid organic-inorganic polymer materials with desired properties and prospects of their use in industry, new fundamental works, which examined the structure and conductivity mechanisms, are carried out, new models of ion and proton conductivity, and their theoretical basis are proposed, new ways and means of their introduction in industry are searched *[Akle, 2005; Guimard et al., 2007; Nasser and Thomas, 2004]*. Nowadays, some developed organic-inorganic hybrid systems are already patented and used in industry, despite the novelty of this field of polymer science *[Hong et al., 2006; Pinto and Aliev, 2007; Ulrich et al., 2002]*.

4. Sorption and sensory properties of hybrid organic-inorganic polymer systems

Unlike the thermomechanical, thermal, electrical and dielectric studies, which are primarily used to study the structure and ways of charge transport in materials, investigations of sorption and sensory properties mainly cause a practical interest. Among the main areas of practical application of hybrid materials *[Nikolaeva, 2002]* with the specific sensory and sorption properties can be defined as follows:

- solid polymeric electrolytes for use in power sources *[Satterfield et al., 2006; Timonov, 2000]*, which showed the effectiveness in comparison with salt and alkaline analogs;

- fuel cells, which are ecological alternative energy sources *[Silva et al., 2005a, 2005b]*;

- chemical and gas sensors *[Albert et al., 2000; Holthoff and Bright, 2007; Lange et al., 2008]*;

- medications. This area can be conventionally divided into two trends: 1) the introduction of hybrid polymer materials for direct use in medical purposes *[Armon et al., 2000; Guimard et al., 2007; Holthoff and Bright, 2007]* (the struggle with some viruses, the insertion in living tissues as implants, artificial bones, cartilages etc.); 2) the use of hybrid systems for transporting the drugs into the body («drug delivery»);

- construction and industry. In these spheres of human life the hybrid polymeric materials can be used as coatings, adhesives and others due to the presence of properties required for various needs that can be purposefully regulate. Among the most important heat resistance, fire resistance, chemical and radiation resistance, high adhesion to many materials etc. are emitted *[Arafa et al., 2004; Ishchenko and Lebedev, 2001; B. Singh et al., 2007]*.

The major tenors of researches of properties of hybrid polymer systems are:

- sorption properties (sorption of water and various types of solvents *[Bae et al., 2008; Di Noto et al., 2007; Di Vona et al., 2007; Fu et al., 2008; Kim Y.M. et al., 2004; Ng and Mintova, 2008; Siddiqui et al., 2007]*, swelling *[Martinez et al., 2004; Ruffmann et al., 2003]*) and their influence on the conductivity (proton and ion) *[Di Vona et al., 2006; Kalapos et al., 2007; Lee et al., 2007; Phillips and Moore, 2006; Silva et al., 2005a, 2005b]*;

- sensitivity to different gases and vapors of various substances *[Itoh et al., 2008; Mika et al., 2007; Silverstein et al., 2005]*;

- permeability of hybrid polymer materials *[Amberg-Schwab et al., 2000; Cong et al., 2007; Paulussen et al., 2005; Seo et al., 2007]*;

In the paper *[Mamunya et al., 2003]* authors studied hybrid organic-inorganic polymer systems based on urethane oligomers and aqueous solution of sodium silicate, synthesized in the reactive mixture of organic and inorganic components. The aim of this work was to study sorption and electrical properties of the synthesized hybrid materials. It was shown that hybrid systems are characterized by high sorption capacity (up to 2000%) due to the presence of inorganic phase in polymer matrix. Cyclic sorption/desorption experiments showed good reproducibility and changing of the conductivity up to several orders of magnitude because of ionic conductivity due to the presence of inorganic phase and the adsorbed water. Also, authors showed that sorption and electrical properties depended on molecular weight of organic component.

Conductivity of hybrid systems increased with increasing the molecular weight, while the values of sorption characteristics contrary decreased.

Mamunya et al. *[Mamunya et al., 2008]* studied soprtion properties of hybrid organic-inorganic systems based on urethane oligomers woth different molecular weight and sodium silicate. Comparing of the diffusion parameters of HOIS (Figure 8,a) and respective polyurethanes (Figure 8,b) shows that water-absorbing properties of HOIS are determined by the presence of hydrophilic inorganic phase, where stabilization of the incoming sorbate (water) takes place. Organic polymer matrix of HOIS does not limit the water-incoming rate and diffusion constant value depends on conditions of water stabilization in the inorganic phase. HOIS-2102 posses the highest sorption capacity due to the high molecular weight of respective oligooxypropyleneglycole and its linear structure that provides the maximal elasticity.

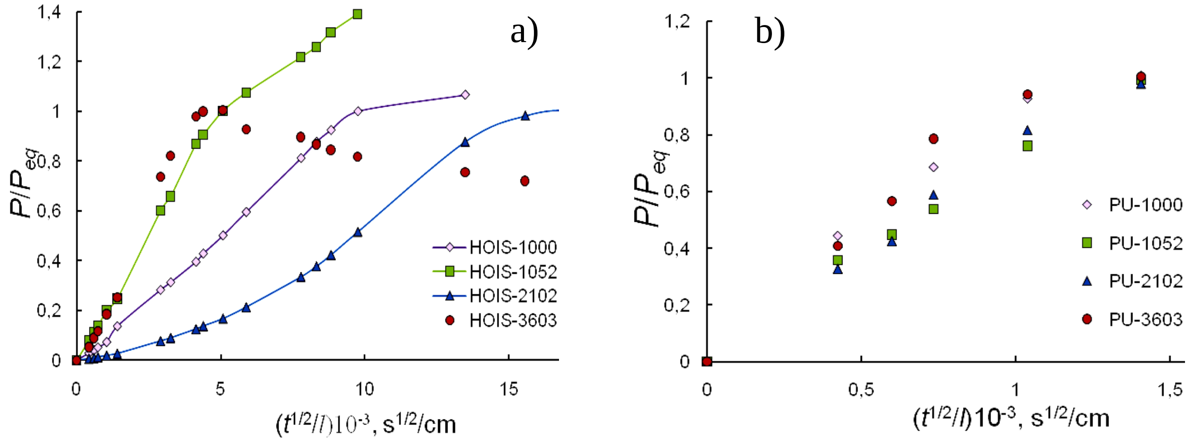

Figure 8. Kinetic curves of water sorption for HOIS (a) and PU (b) based on differnet urethane oligomers treated by Fickian equation

In *[Nguyen et al., 2005]* scientists investigated hybrid polymer coatings based on acrylate/TiO_2 synthesized by sol-gel method. Sorption properties of the obtained systems were studied by methods of thermogravimetry and impedance spectroscopy. For description the obtained results authors used Fickian and Berens-Hopfenberg models *[Crank, 1975]*, and Brasher-Kingsbury equation *[Brasher and Kingsbury, 1954]*. Comparison of the Fickian and Berens-Hopfenberg models gave to authors the opportunity to conclude that linear capacity increased at longer times of immersion that was explained by the slow relaxation of polymer chains during the process of water sorption. The change of water condition during immersion (increase of water clusters) was noted by authors as the another important factor that influenced on the long-term immersion.

In the paper *[Park et al., 2008]* the hybrid organic-inorganic composite membranes based on two different polymer matrices: post-sulfonated poly(ether ether ketone) (SPEEK) and pre-sulfonated poly(aryl ether ketone) (SPAEK-6F) were studied. Nanoscale particles of boron phosphate (BPO_4) were used as an inorganic filler. Both systems were synthesized by sol-gel method. It was shown that the hybrid membranes based on SPEEK/BPO_4 had higher proton conductivity in comparison with the systems based on SPAEK-6F/BPO_4 at the same level of water sorption. This was explained by different particles sizes of inorganic phase BPO_4, which had a few micrometers in diameter in SPEEK compositions, while for SPAEK-6F size did not exceed a few hundred nanometers. Results showed very high proton conductivity at the level of known solid polymer electrolytes such as Nafion.

Similar work is *[Nunes et al., 2002]*, in which SPEEK and SPEK were used as the polymer matrix, but the inorganic components were SiO_2, TiO_2 and ZrO_2. It was shown that extraordinary reduction of permeability of methanol and water was achieved due to the insertion of inorganic component into the polymer matrix. The best balance between high conductivity and low permeability of methanol and water was obtained due to the decreasing the content of ZrO_2 and zirconium phosphate.

In *[Di Vona et al., 2005]* hybrid systems were synthesized based on poly(ether ether ketone) (SPEEK) sulfonated up to 90% and mixed with $SiCl_4$. The investigations of the structure using nuclear magnetic resonance and infrared spectroscopy methods showed the presence of covalent bonds between organic and inorganic components. Authors noted that the formation of such hybrid materials made it possible to obtain membranes with high thermostability, unusual sorption properties and high electrical characteristics.

In the paper *[Gaowen and Zhentao, 2005]* the hybrid organic-inorganic materials based on SPEEK and organically modified montmorillonite (OMMT) were synthesized. Results of experiments showed that the obtained membranes are characterized by low swelling at high temperatures due to the separation of OMMT, high conductivity ($\sigma \approx 10^{-2}$ S/cm) at high temperatures and very low methanol permeability. Authors emphasized that the proposed membrane easy to produce, they are economically efficient, unlike the popular commercial analogs and can be qualified as composite membranes for fuel cells as an alternative to Nafion membranes due to high proton conductivity and low methanol permeability.

In regard to Nafion, in *[Satterfield et al., 2006]* its properties and properties of materials with its modifications (Nafion doped with TiO_2) were directly studied. It was found that modified membranes had higher conductivity compared to Nafion in vapor of water and gave the best performance in fuel cells. Water sorption was the balance between the energy of sulfation of sulfonate groups and energy for the swelling of membranes. Sorption of modified membranes based on Nafion increased with temperature rise, the membrane obtained sorbed water faster and more in comparison with extruded Nafion. Water sorption in Nafion membranes was revealed in increasing the swelling pressure. Thus, the swelling pressure of samples of Nafion 115 at 100%

humidity and 80 °C equaled to 0.55 MPa, while it was almost insensitive to temperature changes.

In *[Xiang et al., 2006]* the hybrid organic-inorganic nanocomposites based on 2-hydroxyethyl methacrylate (HEMA), poly(ethylene glycol) methylethermethacrylate (PEGMA) and methacrylic acid (MAA) synthesized by free radical polymerization with the insertion the fibrillar attapulgite in the polymer matrix were studied. It was found that the way of water transport in nanoscale hydrogel had abnormal non-Fickian character of diffusion. Nanoscale hydrogels showed much higher value of sustainable swelling compared with the correspondent cross-linked hydrogel. Content of inorganic phase also had an impact on the swelling. With increasing the content of inorganic component the swelling of the hybrid materials decreased.

Authors of *[Nagai and Chiba, 2005]* studied organic-inorganic composites with proton conductivity based on 3-glycidoxypropyltrimethoxysilane as organic component and SiO_2, Al_2O_3 as inorganic components. Synthesized hybrid system showed high values of swelling in methanol and water. It was found that materials obtained from the mixture of both inorganic components can be promising as membrane for use in fuel cells.

Authors of *[Kim J.Y. et al., 2006]* studied the organic-inorganic membranes based on poly(styrene–NaSS–UAN) random copolymer (PSSU) consisting of a sulfonated monomer (NaSS) and a non-sulfonated monomer (styrene) and urethane acrylate non-ionomer (UAN). As a result of the synthesis membranes containing hydrophilic domains with 5-10 nanometers in diameter dispersed in nanodimensional hydrophobic polymer matrix were obtained. The hybrid membranes showed two-phase behavior of swelling during sorption of water and toluene due to such heterogeneous structure. It was found that with increasing the content of sulfonated monomer content the level of swelling, proton conductivity and permeability of materials increased.

In *[Honma et al., 2003]* the proton conducting organic-inorganic nanohybrids based on bridged polysilsesquioxanes doped with acidic moieties such as 12-phosphotungstic acid (PWA) synthesized by sol-gel method, were considered as the promising material, which has high proton conductivity ($\sigma \approx 10^{-2}$ S/cm) at high temperatures (up to 160 °C), for use as solid electrolytes. For the obtained membranes it was found that the conductive of material essentially depended on its humidity within temperature range from 120 to 160 °C, when conductivity decreased exponentially with the pressure of water vapors. Conductivity reached value $2 \cdot 10^{-3}$ S/cm even at 20% humidity and temperature 120 °C. Proton conductivity was stable above 100 °C with low dependence on humidity. Thus, organic-inorganic hybrids in this work showed the presence of constant channel of conductivity even in the structure of elastic macromolecules.

In the paper *[Amberg-Schwab et al., 1998]* scientists investigated the permeability of water vapors, oxygen in the organic-inorganic polymer coatings based on tetramethoxysilane, zirconium propoxide, aluminum-sec-butylate, 3-glycidoxyproyl-trimethoxysilane and 3-aminopropyltriethoxysilane, applied on biaxially oriented polypropylene (BOPP) films and coated with a thin layer of SiO_2- PET (polyethyleneterephthalate). The results showed the presence of a barrier to flavors (one layer) and water vapors and oxygen (two layers in combination with SiO_2) in synthesized hybrid organic-inorganic polymer films. Such materials can be used as coatings as well as highbarrier laminating agents in multilayered structures. It was shown that even after high mechanical and thermal stress and storage in humidity the composite film revealed excellent oxygen barrier properties.

Researchers in *[Singla et al., 2007]* studied the sensory properties of hybrid organic-inorganic materials based on polyaniline/Mn_3O_4 doped with organic-inorganic acids. It was found that the systems with imposed acids showed the rise of resistance with increasing the relative humidity, while the sensitivity depended on the type of doped anions. It was shown that the response of each composition was almost linear with respect to the level of humidity, but the compositions doped with organic acids were more sensitive compared to systems with inorganic dopants. However, polyaniline doped with the same acids in the same conditions showed the opposite behavior. The resistance decreased with increasing the relative humidity, but, in this case, the sensitivity was much lower. This anomalous behavior was explained by the presence of proton conductivity in polymer matrix with increasing the humidity. Thus, due to the linear dependence of resistance on humidity of composites doped with organic acids, such materials can be used as humidity sensors.

Apparently, the investigations of sorption and sensory properties, in terms of possible of using the hybrid organic-inorganic polymers as solid polymer electrolytes, which are characterized by improved characteristics in comparison with salt and alkaline analogs, as membranes for fuel cells, which attract a significant interest as alternative energy sources, as coatings for use in ordinary and extreme conditions (in space, under the effect of high radiation, temperature, active environments etc.), and as sensors.

In addition to studying the necessary properties of hybrid organic-inorganic systems, theories and methods of their applications are actively developed. For example, in *[Moore and Koros, 2005]* authors proposed to use the hybrid systems as gas barriers (coatings) and methods of calculation the level of permeability of oxygen, nitrogen and some gases in such systems. In terms of significant interest to the sensory properties of organic-inorganic systems, some theories, methods of application and techniques of analysis of reactions to environment change were proposed in *[Briglin et al., 2002; Kim S.H. et al., 2005; Pearce and Sanchez-Montanes, 2002; Severin and Lewis, 2000; Severin et al., 2000; Sotzing et al., 2000; Vaid et al., 2001; Zhou H. et al., 2008]*. Even software for conversion of received signals into digital data was developed in *[Burl et al., 2001]*. Finally, the hybrid materials find their applications in industry and various types of equipment *[Akle et al., 2006; Giannelis and Mehrota, 1991]*.

The analysis of literature showed the presence of significant interest to hybrid organic-inorganic polymer systems, in terms of prospects of their use in various spheres of human life and the possibility of implementation in industry due to their unique properties, which are inherent to both organic and inorganic components, and simplicity of regulating these properties.

5. Acknowledgement

Dr. Maksym Iurzhenko would like to acknowledge French Government, Ministère des Affaires étrangères et européennes and Egide for the Bourse Eiffel Doctorant grant for the financial support, and to gratitude the staff of the Laboratory of Polymer Materials and Biomaterials (CNRS, UMR 5223, Ingenierie des Materiaux Polymeres, Universite Claude Bernard, Universite de Lyon), especially Prof. Gerard Seytre, Prof. Philippe Cassagnau, Prof. Eliane Espuche for the comprehensive help.

6. References

Aburatani Y., Tsuru K., Hayakawa S., Osaka A. (2003) Mechanical property and microstructure of bioactive organic-inorganic hybrids containing colloidal silica particles. *Journal of the ceramic society of Japan*, Vol. 111, pp. 247-251.

Adachi K., Iwamura T., Chujo Y. (2005) Microwave assisted synthesis of organic-inorganic polymer hybrids. *Polymer Bulletin*, Vol. 55, pp. 309-315.

Adalja S., Otaigbe J. (2002) Creep and recovery behavior of novel organic-inorganic polymer hybrids. *Polym. Comp.*, Vol. 23, pp. 171-181.

Akle B.J. (2005) *Characterization and modeling of the ionomer-conductor interface in ionic polymer transducers*, Thesis, Blacksburg, USA.

Akle B., Leo D., Bennett M., Wiles K., Mcgrath J.E. (2006) Direct assembly process for fabrication of ionomeric polymer devices. United States Patent US2006/0266642 A1.

Akle B., Nawshin S., Leo D. (2007) Reliability of high strain ionomeric polymer transducers fabricated using the direct assembly process. *Smart Mater. Struct.*, Vol. 16, pp. 256-261.

Albert K.J., Lewis N.S., Schauer C.L., Sotzing G.A., Stitzel S.E., Vaid T.P., Walt D.R. (2000) Cross-reactive chemical sensor arrays. *Chem. Rev.*, Vol. 100, pp. 2595-2626.

Amberg-Schwab S., Hoffmann M., Bader H., Gessler M. (1998) Inorganic-organic polymers with barrier properties forwater vapor, oxygen and flavors. *J. of Sol-Gel Sci. and Tech.*, № 1, pp. 141-146.

Amberg-Schwab S., Katschorek H., Weber U., Hoffmann M., Burger A. (2000) Barrier properties of inorganic-organic polymers: influence of starting compounds, curing conditions and storage -scaling-up to industrial application. *J. of Sol-Gel Sci. and Tech.*, Vol. 19, pp. 125-129.

Angiolini L., Caretti D., Vito R.D., Niesel F.T., Salatelli E., Carlini C., Ribot F., Sanchez C. (1997) Hybrid organic-inorganic copolymers from oxohydroxoorganotin dimethacrylate and methyl methacrylate. *J. Inorg. Organomet. Polym.,* Vol. 7, pp. 151-162.

Aniskevich K., Khristova J., Jansons J. (2000) Creep of polymer concrete in the nonlinear region. *Mech. of Comp. Mat.,* Vol. 36, pp. 85-96.

Annenkov V.V., Filina E.A., Danilovtseva E.N., Zinchenko S.V., Mikhaleva A.I. (2003) Aluminum complexes with a donor polymer: new route to organic/inorganic polymer hybrids. *J. of Sol-Gel Sci. and Tech.,* Vol. 27, pp. 163-166.

Arafa I.M., Fares M.M., Barham A.S. (2004) Sol–gel preparation and properties of interpenetrating, encapsulating and blend silica-based urea-formaldehyde hybrid composite materials. *Europ. Polym. J.,* Vol. 40, pp. 1477-1487.

Armon R., Starosvetzky J., Saad I. (2000) Sol-gel as reaction matrix for bacterial enzymatic activity. *J. of Sol-Gel Sci. and Tech.,* Vol. 19, pp. 289-292.

Bae I.-S., Cho S.-J., Choi W.-S., Hong B.-Y., Kim Y.-J., Kim Y.-M., Boo J.-H. (2008) Electrical, mechanical, and optical properties of the organic-inorganic hybrid-polymer thin films deposited by PECVD. *Thin Solid Films,* Vol. 516, pp. 3577-3581.

Baillif P., Tabellout M., Emery J.R. (2000) Dielectric study of the a-relaxation process evolution during polyurethane networks formation. *Polymer,* Vol. 41, pp. 5305-5314.

Barbosa P.C., Rodrigues L.C., Silva M.M., Smith M.J. (2008) Preparation of hybrid organic–inorganic materials based on a di-ureasil matrix doped with lithium bis(trifluoromethanesulfonyl)imide. *J. of Power Sources,* Vol. 180, pp. 607-611.

Beake B. (2006) Modelling indentation creep of polymers: a phenomenological approach. *J. Phys. D: Appl. Phys.,* Vol. 39, pp. 4478-4485.

Benavente E., Santa Ana M. A., González G. (2004) Electrical conductivity of MoS2 based organic–inorganic nanocomposites. *Phys. Stat. Sol. (B),* Vol. 241, pp. 2444-2447.

Bergaya F., Theng B.K.G., Lagaly G., (Ed(s).) (2006) *Handbook of clay science,* Elsevier Ltd., Amsterdam, Holland.

Bonilla G., Martinez M., Mendoza A.M., Widmaier J.-M. (2006) Ternary interpenetrating networks of polyurethane-poly(methyl methacrylate)-silica: Preparation by the sol–gel process and characterization of films. *Eur. Polym. J.,* Vol. 42, pp. 2977-2986.

Bottcher C.J.F., Bordewijk P. (1978) *Theory of electric polarization*, Elsevier, Amsterdam, Holland.

Boven G., Oosterling M., Chella G., Schouten A.J. (1990) Grafting kinetics of poly(methyl methacrylate) on to microparticulate silica. *Polymer,* Vol. 31, pp. 2377-2383.

Brasher D.M., Kingsbury A.H. (1954) Electrical measurements in the study of immersed paint coatings on metal. I. Comparison between capacitance and gravimetric methods of estimating water-uptake. *J. Appl. Chem.,* Vol. 4, pp. 62-72.

Briglin S.M., Freund M.S., Tokumaru P., Lewis N.S. (2002) Exploitation of spatiotemporal information and geometric optimization of signal/noise performance using arrays of carbon black-polymer composite vapor detectors. *Sensors and Actuators B,* Vol. 82, pp. 54-74.

Bronnikov S.V., Vettegren V.I. (1999) Temperature and time relaxation of complex Young’s modulus of isotropic and oriented polymers. *Mechanics of composite materials,* Vol. 35, pp. 63-70.

Bronstein L.M., Joo C., Karlinsey R., Ryder A., Zwanziger J.W. (2001) Nanostructured inorganic–organic composites as a basis for solid polymer electrolytes with enhanced properties. *Chem. Mater.,* Vol. 13, pp. 3678-3684.

Bronstein L.M., Karlinsey R.L., Ritter K., Joo C.G., Stein B., Zwanziger J.W. (2004) Design of organic–inorganic solid polymer electrolytes: synthesis, structure, and properties. *J. Mater. Chem.*, Vol. 14, pp. 1812-1820.

Bruce P.G., Vincent C.A. (1987) Steady state current flow in solid binary electrolyte cells. *J. Electroanal. Chem.*, Vol. 225, pp. 1-17.

Burl M.C., Doleman B.J., Schaffer A., Lewis N.S. (2001) Assessing the ability to predict human percepts of odor quality from the detector responses of a conducting polymer composite-based electronic nose. *Sensors and Actuators B*, Vol. 72, pp. 149-159.

Cardoen G., Coughlin E.B. (2004) Hemi-telechelic polystyrene-POSS copolymers as model systems for the study of well-defined inorganic/organic hybrid materials. *Macromolecules*, Vol. 37, pp. 5123-5126.

Colak O.U. (2005) Modeling deformation behavior of polymers with viscoplasticity theory based on overstress. *International journal of plasticity*, Vol. 21, pp. 145-160.

Cong H., Radosz M., Towler B.F., Shen Y. (2007) Polymer–inorganic nanocomposite membranes for gas separation. *Separation and Purification Techn.*, Vol. 55, pp. 281-291.

Crank J. (1975) *The mathematics of diffusion*, Clarendon Press, Oxford, UK.

Dahmouche K., Atik M., Mello N.C., Bonagamba T.J., Paneppucci H., Aegerter M.A., Judeinstein P. (1997) Investigation of new ion-conducting ormolytes: structure and properties. *J. of Sol-Gel Sci. and Tech.*, Vol. 8, pp. 711-715.

Dahmouche K., De Souza P.H., Bonagamba T.J., Paneppucci H., Judeinstein P., Pulcinelli S.H., Santilli C.V. (1998) Investigation of new ion conducting ormolytes silica-polypropyleneglycol. *J. of Sol-Gel Sci. and Tech.*, Vol. 13, pp. 909-913.

Di Noto V., Gliubizzi R., Negro E., Vittadello M., Pace G. (2007) Hybrid inorganic–organic proton conducting membranes based on Nafion and 5 wt.% of MxOy (M = Ti, Zr, Hf, Ta and W) Part I. Synthesis, properties and vibrational studies. *Electrochimica Acta*, Vol. 53, pp. 1618-1627.

Di Noto V., Piga M., Piga L., Polizzi S., Negro E. (2008) New inorganic–organic proton conducting membranes based on Nafion ® and [(ZrO2) ·(SiO2)0.67] nanoparticles: Synthesis vibrational studies and conductivity. *J. of Power Sources*, Vol. 178, pp. 561-574.

Di Vona M.L., Marani D., D'Epifanio A., Traversa E., Trombetta M., Licoccia S. (2005) A covalent organic/inorganic hybrid proton exchange polymeric membrane: synthesis and characterization. *Polymer*, Vol. 46, pp. 1754-1758.

Di Vona M.L., D'Epifanio A., Marani D., Trombetta M., Traversa E., Licoccia S. (2006) SPEEK/PPSU-based organic–inorganic membranes: proton conducting electrolytes in anhydrous and wet environments. *J. of Membrane Science*, Vol. 279, pp. 186-191.

Di Vona M.L., Marani D., D'Epifanio A., Licoccia S., Beurroies I., Denoyel R., Knauth P. (2007) Hybrid materials for polymer electrolyte membrane fuel cells: Water uptake, mechanical and transport properties. *J. of Membrane Sci.*, Vol. 304, pp. 76-81.

Fu R.Q., Woo J.J., Seo S.J., Lee J.S., Moon S.H. (2008) Covalent organic/inorganic hybrid proton-conductive membrane with semi-interpenetrating polymer network: Preparation and characterizations. *J. of Power Sources*, Vol. 179, pp. 458-466.

Galal A., Darwish S.A., Ahmed R.A. (2007) Hybrid organic/inorganic films of conducting polymers modified with phthalocyanines. I—Film preparation and voltammetric studies. *J. Solid State Electrochem.*, Vol. 11, pp. 521-530.

Gaowen Z., Zhentao Z. (2005) Organic/inorganic composite membranes for application in DMFC. *J. of Membrane Sci.*, Vol. 261, pp. 107-113.

Giannelis E.P., Mehrota V. (1991) Organic-inorganic composites. United States Patent US5032547.

Girardi F., Graziola F., Aldighieri P., Fedrizzi L., Gross S., Di Maggio R. (2008) Inorganic-organic hybrid materials with zirconium oxoclusters as protective coatings on aluminium alloys. *Prog. Org. Coat.*, Vol. 62, pp. 376-381.

Gizdavic-Nikolaidis M.R., Edmonds N.R., Bolt C.J., Easteal A.J. (2008) Structure and properties of GPTMS/DETA and GPTMS/EDA hybrid polymers. *Current Applied Physics,* Vol. 8, pp. 300-303.

Gross S., Di Noto V., Schubert U. (2003) Dielectric investigation of inorganic–organic hybrid film based on zirconium oxocluster-crosslinked PMMA. *J. of Non-Cryst. Solids*, Vol. 322, pp. 154-159.

Guimard N.K., Gomez N., Schmidt C.E. (2007) Conducting polymers in biomedical engineering. *Prog. Polym. Sci.*, Vol. 32, pp. 876-921.

Haddad T.S., Lichtenhan J.D. (1996) Hybrid organic-inorganic thermoplastics: styryl-based polyhedral oligomeric silsesquioxane polymers. *Macromolecules*, Vol. 29, pp. 7302-7304.

Haoying L., Yunfa C., Chengxiang R., Weimin G., Yusheng X. (2001) Preparation of organic–inorganic multifunctional nanocomposite coating via sol-gel routes. *J. of Nanoparticle Research*, Vol. 3, pp. 157-160.

Hartmann B., Lee G.F., Lee J.D., Fedderly J.J., Berger A.E. (1996) Calculation of relaxation time in polyurethanes using additive group contributions. *J. of App. Polym. Sci.*, Vol. 60, pp. 1985-1993.

Hedvig P. (2006) *Dielectric spectroscopy of polymers*, Adam Hilger, Bristol, UK.

Holthoff E.L., Bright F.V. (2007) Molecularly templated materials in chemical sensing. *Analytica Chimica Acta*, Vol. 594, pp. 147-161.

Hong W., Stucky G.D., Tasaki K. (2006) Hydrophilic polymer-oxide-phosphoric acid compositions for proton conducting membranes. United States Patent US007118821 B2.

Honma I., Takeda Y., Bae J.M. (1999a) Protonic conducting properties of sol-gel derived organic/inorganic nanocomposite membranes doped with acidic functional molecules. *Solid State Ionics*, Vol. 120, pp. 255-264.

Honma I., Hirakawa S., Yamada K., Bae J.M. (1999b) Synthesis of organic / inorganic nanocomposites protonic conducting membrane through sol-gel processes. *Solid State Ionics*, № 118, pp. 29-36.

Honma I., Nakajima H., Nishikawa O., Sugimoto T., Nomura S. (2003) Organic/inorganic nano-composites for high temperature proton conducting polymer electrolytes. *Solid State Ionics*, Vol. 162, pp. 237-245.

Huang G., Lu H. (2006) Measurement of Young's relaxation modulus using nanoindentation Mech Time-Depend Mater. 10 (2006) 229

Huang J., He C., Liu X., Xu J., Tay C.S.S., Chow S.Y. (2005) Organic–inorganic nanocomposites from cubic silsesquioxane epoxides:direct characterization of interphase, and thermomechanical properties. *Polymer*, Vol. 46, pp. 7018-7027.

Huang X., Wirth M.J. (1997) Surface-initiated radical polymerization on porous silica. *Anal. Chem.,* Vol. 69, pp. 4577–4580.

Ishchenko S.S., Lebedev E.V. (2001) Chemical, atmospheric and radiation stability of organic-mineral polymer composites. *Ukr. Chem. J.*, Vol. 67, pp. 116-119.

Ishchenko S.S., Rosovickiy V.F., Pridatko A.B., Babkina N.V., Lebedev E.V. (1998) The influence of organic modifiers on formation of organic-silicate polymer composites. *Rus. J. Pract. Chem.,* Vol. 11, pp. 1929-1933.

Itoh T., Matsubara I., Shin W., Izu N., Nishibori M. (2008) Preparation of layered organic–inorganic nanohybrid thin films of molybdenum trioxide with polyaniline derivatives for aldehyde gases sensors of several tens ppb level. *Sensors and Actuators B*, Vol. 128, pp. 512-520.

Jonscher A.K. (1983) *Dielectric relaxation in solids*, Chelsea Dielectric Press, London, UK.

Kalapos T.L., Decker B., Every H.A., Ghassemi H., Zawodzinski T.A.Jr. (2007) Thermal studies of the state of water in proton conducting fuel cell membranes. *J. of Power Sources,* Vol. 172, pp. 14-19.

Kang H.U., Park J.K., Kim S.H. (2004) Material and rheological properties of (glycidoxypropyl) trimethoxysilane modified colloidal silica coatings. *Korea-Australia rheology journal*, Vol. 16, pp. 175-182.

Kao H.-M., Chang P.-C., Chao S.-W., Lee C.-H. (2006) Li NMR, ionic conductivity and self-diffusion coefficients of lithium ion and solvent of plasticized organic–inorganic hybrid electrolyte based on PPG-PEG-PPG diamine and alkoxysilanes. *Electrochimica Acta*, Vol. 52, pp. 1015-1027.

Kapoor A.K., Jain S.C., Poortmans J., Kumar V., Mertens R. (2002) Temperature dependence of carrier transport in conducting polymers: Similarity to amorphous inorganic semiconductors. *J. Appl. Phys.*, Vol. 92, pp. 3835-3838.

Khan A.A., Inamuddin (2006) Preparation, physico-chemical characterization, analytical applications and electrical conductivity measurement studies of an ‘organic–inorganic’ composite cation-exchanger: Polyaniline Sn(IV) phosphate. *React. & Funct. Polym.*, Vol. 66, pp. 1649-1663.

Kickelbick G., Schubert U. (1997) Oxozirconium methacrylate clusters $Zr_6(OH)_4O_4(OMc)_{12}$ and $Zr_4O_2(OMc)_{12}$ (OMc = methacrylate). *Chem. Ber.*, Vol. 130, pp. 473-477.

Kickelbick G., Schubert U. (1998) An unusual ring structure of an oligomeric oxotitanium alkoxide carboxylate. *Eur. J. Inorg. Chem.,* Vol. 159, pp. 159-161.

Kickelbick G., Wiede P., Schubert U. (1999) Variations in capping the $Zr_6O_4(OH)_4$ cluster core: X-ray structure analyses of $[Zr_6(OH)_4O_4(OOCCH{=}CH_2)_{10}]_2(\mu\text{-}OOCCH{=}CH_2)_4$ and $Zr_6(OH)_4O_4(OOCR)_{12}(^nPrOH)$ (R = Ph, CMe=CH_2). *Inorg. Chim. Acta*, № 284, pp. 1-7.

Kickelbick G., Schubert U. (1999) Hydroxy carboxylate substituted oxozirconium clusters. *Journal of chemistry society Dalton,* Vol. 130, pp. 1301–1305.

Kickelbick G., Schubert U. (2001) Inorganic clusters in organic polymers and the use of polyfunctional inorganic compounds as polymerization initiators. *Monatshefte fur Chemie*, № 132, pp. 13-30.

Kickelbick G. (2007) *Hybrid materials. Synthesis, characterization and applications*, Wiley-VCH Verlag GmbH&Co, Weinheim.

Kim J.Y., Mulmi S., Lee C.H., Park H.B., Chung Y.S., Lee Y.M. (2006) Preparation of organic–inorganic nanocomposite membrane using a reactive polymeric dispersant and compatibilizer: Proton and methanol transport with respect to nano-phase separated structure. *J. of Membrane Sci.*, Vol. 283, pp. 172-181.

Kim S.H., Engel J., Liu C., Jones D.L. (2005) Texture classification using a polymer-based MEMS tactile sensor. *Journal of micromechanics and microengineering,* Vol. 15, pp. 912-920.

Kim S., Kim Y., Kal Y., Kim S.J. (2007) A new organic .inorganic hybrid framework containing octahedral hexarhenium cluster and its transformation by ligand exchange. *Inorg. Chimica Acta*, Vol. 360, pp. 1870-1874.

Kim Y.M., Choi S.H., Lee H.C., Hong M.Z., Kim K., Lee H.-I. (2004) Organic–inorganic composite membranes as addition of SiO_2 for high temperature-operation in polymer electrolyte membrane fuel cells (PEMFCs). *Electrochimica Acta*, Vol. 49, pp. 4787-4796.

Koch T., Kogler F., Schubert U., Seidler S. (2007) Mechanical properties of organic-inorganic hybrid materials determined by indentation techniques. *Monatshefte fur Chemie,* Vol. 138, pp. 293-299.

Kontou E. (1998) Relaxation time spectra of linear and crosslinked polymers. *J. of App.Polym. Sci.*, Vol. 67, pp. 679-684.

Kremer F., Schonhals A. (2003) *Broadband dielectric spectroscopy*, Springer, Berlin, Germany.

Ku C.C., Liepins R. (1987) *Electrical properties of polymers*, Hanser, Munich, Germany.

Kudo N., Shimazaki Y., Ohkita H., Ohoka M., Ito S. (2007) Organic–inorganic hybrid solar cells based on conducting polymer and SnO2 nanoparticles chemically modified with a fullerene derivative. *Solar Energy Materials & Solar Cells,* Vol. 91, pp. 1243-1247.

Laible R., Hamann K. (1980) Formation of chemically bound polymer layers on oxide surfaces and their role in colloidal stability. *Advances in colloid and interface science*, Vol. 13, pp. 65–99.

Lange U., Roznyatovskaya N.V., Mirsky V.M. (2008) Conducting polymers in chemical sensors and arrays. *Analytica Chimica Acta*, Vol. 614, pp. 1-26.

Lavina S., Negro E., Pace G., Gross S., Depaoli G., Vidali M., Di Noto V. (2007a) Dielectric low-k composite films based on PMMA, PVC and methylsiloxane-silica: Synthesis, characterization and electrical properties. *J. of Non-Cryst. Solids,* Vol. 353, pp. 2878-2888.

Lavina S., Negro E., Gliubizzi R., Depaoli G., Pace G., Di Noto V. (2007b) New hybrid inorganic–organic complexes based on poly(3-butylthiophene)and titanium tetrachloride: Synthesis, structure and conductivity. *Electrochimica Acta,* Vol. 52, pp. 5062-5070.

Lee C.H., Min K.A., Park H.B., Hong Y.T., Jung B.O., Lee Y.M. (2007) Sulfonated poly(arylene ether sulfone)–silica nanocomposite membrane for direct methanol fuel cell (DMFC). *J. of Membrane Science*, Vol. 303, pp. 258-266.

Leventis N., Fabrizio E.F., Meador M., Johnston C. (2004) Mechanically strong aerogels formed by templated growth of polymer crosslinkers on inorganic nanoparticles. *Research and Technology,* NASA/TM-2004-212729, pp. 29-30.

Li S., Zhou Z., Liu M., Li W., Ukai J., Hase K., Nakanishi M. (2006) Synthesis and properties of imidazole-grafted hybrid inorganic–organic polymer membranes. *Electrochimica Acta,* Vol. 51, pp. 1351-1358.

Licoccia S., Traversa E. (2006) Increasing the operation temperature of polymer electrolyte membranes for fuel cells: From nanocomposites to hybrids. *J. of Power Sources,* Vol. 159, pp. 12-20.

Liu G., Zhang H., Yang X., Wang Y. (2007) Facile synthesis of silica/polymer hybrid microspheres and hollow polymer microspheres. *Polymer*, Vol. 48, pp. 5896-5904.

Liu X., Peng Y., Ji S. (2008) A new method to prepare organic–inorganic hybrid membranes. *Desalination,* Vol. 221, pp. 376-382.

Lyulin A.V., Michels M.A.J. (2007) Time scales and mechanisms of relaxation in the energy landscape of polymer glass under deformation: direct atomistic modeling. *Physical review letters*, № 99, pp. 085504-1-085504-4.

Mamunya Ye., Kanapitsas A., Pissis P., Boiteux G., Lebedev E. (2003) Water sorption and electrical/dielectric properties of organic-inorganic polymer blends. *Macromol. Symp.*, Vol. 198, pp. 449-459.

Mamunya Ye.P., Shtompel V.I., Lebedev E.V., Pissis P., Kanapitsas A., Boiteux G. (2004a) Structure and water sorption of polyurethane nanocomposites based on organic and inorganic components. *Europ. Polym. J.*, Vol. 40, pp. 2323-2331.

Mamunya Ye.P., Myshak V.D., Lebedev E.V. (2004b) Synthesis and electrical properties of polymer composites based on urethane oligomers and inorganic OH-groups-containing component. *Ukr. Polym. J.*, Vol. 26, pp. 40-45.

Mamunya Ye.P., Iurzhenko M.V., Lebedev E.V., Ishchenko S.S., Boiteux G., Seytre G. (2007) Dielectric and thermal-mechanical properties of hybrid organic-inorganic polymer systems based on isocyanate-containing oligomers. *J. Non-Cryst. Sol.*, Vol. 353, pp. 4288-4292.

Mamunya Ye.P., Iurzhenko M.V., Lebedev E.V., Ishchenko S.S., Parashchenko I.M. (2008) Sorption properties of hybrid organic-inorganic systems based on urethane oligomers and sodium silicate. *Ukr. Polym. J.*, Vol. 30, pp. 37-42.

Martinez Y., Retuert J., Yazdani-Pedram M., Colfen H. (2004) Hybrid ternary organic–inorganic films based on interpolymer complexes and silica. *Polymer*, Vol. 45, pp. 3257-3265.

Mather P.T., Chun S.B., Pyun J., Matyjaszewski K., Jeon H.G. (2000) Synthesis and microstructural characterization of poss-based triblock copolymers prepared using atom transfer radical polymerization. *Polym. Prep. (Am. Chem. Soc. Polym. Div.),* Vol. 41, pp. 582.

Matsuo M., Yamada T., Ito N. (2006) Stress relaxation behavior of knitted fabrics under uniaxial and strip biaxial excitation as estimated by corresponding principle between elastic and visco-elastic bodies. *Textile Research J.*, Vol. 76, pp. 465-477.

Mayer C.R., Thouvenot R., Lalot T. (2000) New hybrid covalent networks based on polyoxometalates. Hybrid networks based on poly(ethyl methacrylate) chains covelently cross-linked by heteropolyanions : synthesis and swelling properties. *Chem. Mater.*, Vol. 12, pp. 257-260.

Matyjaszewski K., Patten T.E., Xia J., Abernathy T. (1996) Polymers with very low polydispersities from atom transfer radical polymerization. Invention Science, № 272, pp. 866-870.

Maxwell-Garnett J.C. (1904) Colours in metal glasses and in metallic films. *Philosophical transactions of the royal society A: mathematical, physical and engineering sciences*, № 203, pp. 385-420.

Mijovic J., Fitz B. D. (1998) *Application note dielectrics 2: Dielectric spectroscopy of reactive polymers*, Novocontrol GmbH, Germany.

Mika M., Paidar M., Klapste B., Masinova M., Bouzek K., Vondrak J. (2007) Hybrid inorganic–organic proton conducting membranes for fuel cells and gas sensors. *J. of Phys. and Chem. of Solids*, Vol. 68, pp. 775-779.

McCrum N.G., Read B., Williams G. (1967) *Anelastic and dielectric effects in polymer solids*, Wiley, NY, USA.

Mominul Alam S.M., Agag T., Kawauchi T., Takeichi T. (2007) Organic–inorganic hybrids containing polyimide, organically modified clay and in situ formed polydimethylsiloxane. *React. & Funct. Polym.*, Vol. 67, pp. 1218-1224.

Moore T.T., Koros W.J. (2005) Non-ideal effects in organic–inorganic materials for gas separation membranes. *J. of Molecular Structure*, Vol. 739, pp. 87-98.

N/A (2006) Inorganic-organic hybrid materials, In: *N/A presentation*, retrieved from http://www.chimica.unipd.it/offerte/pubblica/dottorato/hybridmaterials.pdf.

Nagai M., Chiba Y. (2005) Fabrication and evaluation of inorganic–organic composite protonic conductors using inorganic sols as a dispersoid. *Solid State Ionics*, Vol. 176, pp. 2991-2995.

Nagasubramanian G., Bronstein L., Carini J. (2006) mproved performance of Li hybrid solid polymer electrolyte cells. *J. of Power Sources*, Vol. 162, pp. 847-850.

Nasser S.N., Thomas C.W. (2004) Chapter 6: Ionomeric Polymer-Metal Composites, In: *Electroactive polymer actuators as artificial muscules – reality, potential and challenges. Second Edition*, SPIE-press.

Ng E.-P., Mintova S. (2008) Nanoporous materials with enhanced hydrophilicity and high water sorption capacity. *Microporous and Mesoporous Mat.*, Vol. 114, pp. 1-26.

Nguyen V.N., Perrin F.X., Vernet J.L. (2005) Water permeability of organic/inorganic hybrid coatings prepared by sol–gel method: a comparison between gravimetric and capacitance measurements and evaluation of non-Fickian sorption models. *Corrosion Science*, Vol. 47, pp. 397-412.

Ni Y., Zheng S., Nie K. (2004) Morphology and thermal properties of inorganic–organic hybrids involving epoxy resin and polyhedral oligomeric silsesquioxanes. *Polymer*, Vol. 45, pp. 5557-5568.

Nikolaeva E. (2002) Current is conducted by polymers here. *Rus. Chem. J.*, № 12, pp. 28-31.

Nishi K., Okubo K., Watanabe Y., Tsuchiya T. (2000) Structural analysis and properties of organic-inorganic hybrid ionic conductor prepared by sol-gel process. *J. of Sol-Gel Sci. and Tech.*, Vol. 19, pp. 187-191.

Normatov J., Silverstein M.S. (2007) Porous interpenetrating network hybrids synthesized within high internal phase emulsions. *Polymer*, Vol. 48, pp. 6648-6655.

Nunes S.P., Ruffmann B., Rikowski E., Vetter S., Richau K. (2002) Inorganic modification of proton conductive polymer membranes for direct methanol fuel cells. *J. of Membrane Sci.*, Vol. 203, pp. 215-225.

Ohtsuki C., Miyazaki T., Kamitakahara M., Tanihara M. (2007) Design of novel bioactive materials through organic modification of calcium silicate. *Journal of the European ceramic society*, Vol. 27, pp. 1527-1533.

Oyen M.L. (2007) Sensitivity of polymer nanoindentation creep measurements to experimental variables. *Acta Materialia*, Vol. 55, pp. 3633-3639.

Pankow O., Schmidt-Naake G. (2004) Preparation and characterization of organic/inorganic polymer composites based on Mg-Silicates. *Macromol. Mater. Eng.*, Vol. 289, pp. 990-996.

Park S.-H., Park J.-S., Yim S.-D., Park S.-H., Lee Y.-M., Kim C.-S. (2008) Preparation of organic/inorganic composite membranes using two types of polymer matrix via a sol–gel process. *J. of Power Sources*, Vol. 181, pp. 259-266.

Patten T.E., Matyaszewski K. (1998) Atom transfer radical polymerization. *Adv. Mater.*, Vol. 10, pp. 901-905.

Paulussen S., Rego R., Goossens O., Vangeneugden D., Rose K. (2005) Plasma polymerization of hybrid organic–inorganic monomers in an atmospheric pressure dielectric barrier discharge. *Surface & Coatings Tech.*, Vol. 200, pp. 672-675.

Pearce T.M., Sanchez-Montanes M.A. (2002) Chapter 14. Chemical sensor array optimization: geometric and information theoretic approaches, In: *Handbook of machine olfaction: electronic nose technology*, Wiley-VCH, Weinheim, Germany.

Peschanskaya N.N., Hristova Y. (2006a) Step deformation of polymer composites at micron and submicron levels of structure. *Rus. J. Phys. Sol. State*, Vol. 48, pp. 1786-1790.

Peschanskaya N.N., Hristova J. (2006b) Jumplike deformation of polymer materials on the micrometer and submicrometer structural levels. *Phys. of the Solid State*, Vol. 48, pp. 1896-1901.

Phillips A.K., Moore R.B. (2006) Mechanical and transport property modifications of perfluorosulfonate ionomer membranes prepared with mixed organic and inorganic counterions. *J. of Polym. Sci. :Part B: Polym. Phys.*, Vol. 44, pp. 2267-2277.

Pinto N.J, Aliev F.M. (2007) Conducting polymer. United States Patent US007160575 B1.

Pissis P., Polizos G. (2005) Molecular dynamics and ionic conductivity studies in polyurethane thermoplastic elastomers, In: n/a, Wiley, n/a.

Prucker O., Rime J. (1998) Mechanism of radical chain polymerization initiated by azo compounds covalntly bound to the surface of spherical particles. *Macromolecules*, Vol. 31, pp. 602-613.

Pyun J., Miller P.J., Kickelbick G., Matyjaszewski K., Schwab J., Lichtenhan J. (1999) The synthesis of multifunctional star and hyperbranched polymers using atomtransfer radical polymerization and atom transfer radical addition. *Polym. Prep. (Am. Chem. Soc. Polym. Div.),* Vol. 40, pp. 452-454.

Pyun J., Matyjaszewski K. (2000) Synthesis of hybrid polymers using atom transfer radical polymerization: homopolymers and block copolymers from polyhedral oligomeric silsesquioxane monomers. *Macromolecules, Vol.* 33, pp. 217-220.

Qi L., Dong S.J. (2007) Organic/inorganic nanocomposite polymer electrolyte. *Chinese Chem. Let.*, № 18, pp. 185-188.

Qiao Y., Chen J., Han A., Deliwala J.K. (2007) A simplified processing technique of organic–inorganic intercalation/exfoliation nanohybrid. *Mat. Research Bulletin,* Vol. 42, pp. 1332-1336.

Qiu W.L., Ma X.H., Yang Q.H., Fu Y.B., Zong X.F. (2005) UV-cured hybrid inorganic-organic polymer electrolyte based on organically modified polysiloxane. *J. of Mat. Sci.: Mat. in electronics,* Vol. 16, pp. 89-95.

Raghavan J., Meshii M. (1997) Creep of polymer composites. *Comp. Sci. and Tech.,* Vol. 57, pp. 1673-1688.

Riande E., Saiz E. (1992) *Dipole moments and birefringence of polymers,* Prentice Hall, NY, USA.

Ribot F., Banse F., Sanchez C., Lahcini M., Jousseaume B. (1997) Hybrid organic-inorganic copolymers based on oxo-hydroxo organotin nanobuilding blocks. *J. Sol-Gel Sci. Tech.,* Vol. 8, pp. 529-533.

Riley M., Fedkiw P.S., Khan S.A. (2002) Transport properties of lithium hectorite-based composite electrolytes. *J. Electrochem. Soc.,* Vol. 149, pp. A667–A670.

Robertson M.A., Rudkin R.A., Parsonage D., Atkinson A. (2003) Mechanical and thermal properties of organic/inorganic hybrid coatings. *J. of Sol-Gel Sci. and Tech.,* Vol. 26, pp. 291-295.

Rosa-Fox N., Morales-Florez V., Toledo-Fernandez J.A., Pinero M., Mendoza-Serna R., Esquivias L. (2007) Nanoindentation on hybrid organic/inorganic silica aerogels. *Journal of the European ceramic society*, Vol. 27, pp. 3311-3316.

Ruffmann B., Silva H., Schulte B., Nunes S.P. (2003) Organic/inorganic composite membranes for application in DMFC. *Solid State Ionics*, Vol. 162, pp. 269-275.

Rzehak R., Zimmermann W. (2003) Static dynamics approach to relaxation modes and times for deformed polymers. *Physical review letters,* №. 68, pp. 021804-1-021804-14.

Sanchez C., Lebeau B., Ribot F., In M. (2000) Molecular design of sol-gel derived hybrid organic-inorganic nanocomposites. *J. of Sol-Gel Sci. and Tech.*, Vol. 19, pp. 31-38.

Satterfield M.B., Majsztrik P.W., Ota H., Benziger J.B., Bocarsly A.B. (2006) Mechanical properties of Nafion and Titania/Nafion composite membranes for polymer electrolyte membrane fuel cells. *J. of Polym. Sci. :Part B: Polym. Phys.*, Vol. 44, pp. 2327-2345.

Schmidt H., Jonschker G., Goedicke S., Mennig M. (2000) The sol-gel process as a basic technology for nanoparticle-dispersed inorganic-organic composites. *J. of Sol-Gel Sci. and Tech.*, Vol. 19, pp. 39-51.

Seanor D.A. (1982) *Electrical properties of polymers*, Academic press, NY, USA.

Seo Y., Kim S., Hong S.U. (2006) Highly selective polymeric membranes for gas separation. *Polymer*, Vol. 47, pp. 4501-4504.

Serap G., Sariciftci N.C. (2008) Hybrid solar cells. *Inorganica Chimica Acta*, Vol. 361, pp. 581-588.

Severin E.J., Lewis N.S. (2000) Relationships among resonant frequency changes on a coated quartz crystal microbalance, thickness changes, and resistance responses of polymer-carbon black composite chemiresistors. *Anal. Chem.*, Vol. 72, pp. 2008-2015.

Severin E.J., Doleman B.J., Lewis N.S. (2000) An investigation of the concentration dependence and response to analyte mixtures of carbon black/insulating organic polymer composite vapor detectors. *Anal. Chem.*, Vol. 72, pp. 658-668.

Shilova O.A., Shilov V.V. (2003) Nanosystems, nanomaterials, nanotechnology, In: *Scientific materials* № 1, Academpereodica, Moscow, pp. 9-83.

Siddiqui W.A., Khan S.A., Inamuddin (2007) Synthesis, characterization and ion-exchange properties of a new and novel ‘organic–inorganic’ hybrid cation-exchanger:Poly(methyl methacrylate) Zr(IV) phosphate. *Colloids and Surfaces A: Physicochem. Eng. Aspects*, Vol. 295, pp. 193-199.

Silva V.S., Ruffmann B., Silva H., Gallego Y.A., Mendes A., Madeira L.M., Nunes S.P. (2005a) Proton electrolyte membrane properties and direct methanol fuel cell performance I. Characterization of hybrid sulfonated poly(ether ether ketone)/zirconium oxide membranes. *J. of Power Sources*, Vol. 140, pp. 34-40.

Silva V.S., Schirmer J., Reissner R., Ruffmann B., Silva H., Mendes A., Madeira L.M., Nunes S.P. (2005b) Proton electrolyte membrane properties and direct methanol fuel cell performance II. Fuel cell performance and membrane properties effects. *J. of Power Sources*, Vol. 140, pp. 41-49.

Silverstein M.S., Tai H., Sergienko A., Lumelsky Y., Pavlovsky S. (2005) PolyHIPE: IPNs, hybrids, nanoscale porosity, silica monoliths and ICP-based sensors. *Polymer*, Vol. 46, pp. 6682-6694.

Singh B., Bouchet J., Rochat G., Leterrier Y., Manson J.-A. E., Fayet P. (2007) Ultra-thin hybrid organic/inorganic gas barrier coatings on polymers. *Surface & Coatings Tech.*, Vol. 201, pp. 7107-7114.

Singla M.L., Awasthi S., Srivastava A. (2007) Humidity sensing; using polyaniline/Mn_3O_4 composite doped with organic/inorganic acids. *Sensors and Actuators B*, Vol. 127, pp. 580-585.

Somani S.P., Somani P.R., Umeno M. (2008) Carbon nanotube incorporation: a new route to improve the performance of organic-inorganic heterojunction solar cells. *Diamond & Related Materials*, Vol. 17, pp. 585-588.

Sotzing G.A., Briglin S.M., Grubbs R.H., Lewis N.S. (2000) Preparation and properties of vapor detector arrays formed from poly(3,4-ethylenedioxy)thiophene-poly(styrene sulfonate)/insulating polymer composites. *Anal. Chem.*, Vol. 72, pp. 3181-3190.

Sugimoto H., Nakanishi E., Yamauchi K., Daimatsu K., Yasumura T., Inomata K. (2004) Preparation and properties of organic-inorganic hybrid materials from sodium silicate. *Polymer Bulletin*, Vol. 52, 209-218.

Takai C., Fuji M., Takahashi M. (2007) A novel surface designed technique to disperse silica nano particle into polymer. *Colloids and Surfaces A: Physicochem. Eng. Aspects., Vol.* 292, pp. 79-82.

Timonov A.M. (2000) Solid polymer electrolytes. *Rus. Soros Edu. J.,* № 8, pp. 69-75.

Tsonos C., Apekis L., Viras K., Stepanenko L., Karabanova L., Sergeeva L. (2001) Electrical and dielectric behavior in blends of polyurethane-based ionomers. *Solid State Ionics,* Vol. 143, pp. 229-249.

Tsubokawa N., Kogure A., Sone Y. (1990) Surface grafting of polymers onto inorganic ultrafine particles: reaction of functional polymers with acid anhydride groups introduced onto inorganic ultrafine particles. *J. Polym. Sci. Part A: Polym. Chem.*, Vol. 28, pp. 697–702.

Tsubokawa N., Ishida H. (1992) Graft polymerization of methyl methacrylate from silica initiated by peroxide groups introduced onto the surface. *J. Polym. Sci. Part A: Polym. Chem.,* Vol. 30, pp. 2241-2246.

Ulrich R., Zwanziger J.W., De Paul S., Spiess H.W., Wiesner U. (2002) Solid hybrid polymer electrolytes. United States Patent US006472104 B1.

Vaid T.P., Burl M.C., Lewis N.S. (2001) Comparison of the performance of different discriminant algorithms in analyte discrimination tasks using an array of carbon black-polymer composite vapor detectors. *Anal. Chem.*, Vol. 73, pp. 321-331.

Vinogradov A.M., Schumacher S. (2001) Cyclic creep of polymers and polymer matrix composites. *Mech. of Comp. Mat.*, Vol. 37, pp. 29-34.

Von Werne T., Patten T.E. (1999) Preparation of structurally well-defined polymer-nanoparticle hybrids with controlled/living radical polymerizations. *J. Am. Chem. Soc.,* № 121, pp. 7409-7410.

Wang J.P., Du X.D., Niu J.Y. (2007) A one-dimensional organic .inorganic hybrid based on the bimolecular$\{[Cu(en)_2]_2[Cu_2\ Si_2\ W_{22}\ O_{78}\ ]\}_8$ polyoxometalate. *J. of Solid State Chem.,* Vol. 180, pp. 1347-1352.

Wiggins M.J., Anderson J.M., Hiltner A. (2003) Effect of strain and strain rate on fatigue-accelerated biodegradation of polyurethane. *Wiley Periodicals,* Vol. 66, pp. 463-475.

Williams G., Thomas D.K. (1998) *Application note dielectrics 3: Phenomenological and molecular theories of dielectric and electrical relaxation of materials*, Novocontrol GmbH, Germany.

Xi J., Tang X. (2004) Enhanced lithium ion transference number and ionic conductivity of composite polymer electrolyte doped with organic-inorganic hybrid P123@SBA-15. *Chem. Phys. Let.*, № 400, pp. 68-73.

Xia H., Song M., Zhang Z., Richardson M. (2007) Microphase separation, stress relaxation, and creep behavior of polyurethane nanocomposites. *J. of App. Polym. Sci.*, Vol. 103, pp. 2992-3002.

Xiang Y., Peng Z., Chen D. (2006) A new polymer/clay nano-composite hydrogel with improved response rate and tensile mechanical properties. *Eur. Polym. J.*, Vol. 42, pp. 2125-2132.

Yakuphanoglu F. (2008) Photovoltaic properties of the organic–inorganic photodiode based on polymer and fullerene blend for optical sensors. *Sensors and Actuators A*, Vol. 141, pp. 383-389.

Yang S., Zhang Y.-W., Zeng K. (2004) Analysis of nanoindentation creep for polymeric materials. *J. Appl. Phys.*, Vol. 95, pp. 3655-3666.

Zhang C.H., Zhang Z.Q., Cao H.L. (2007) Effects of epoxy/SiO2 hybrid sizing on the mechanical properties of carbon fiber composites. *Solid State Phenomena*, Vol. 121, pp. 1253-1256.

Zhang J., Zhu B.-K., Xu Y.-Y. (2005) Characterization and dielectric property of polyimide-silica composite films prepared via sol–gel and thermal imidization process. *J. of Mat. Sci.,* Vol. 40, pp. 2623-2625.

Zhang Z., Yang J.L., Friedrich K. (2004) Creep resistant polymeric nanocomposites. *Polymer*, Vol. 45, pp. 3481-3485.

Zhang Z., Liang G., Wang J., Ren P. (2007) Epoxy/POSS organic–inorganic hybrids: viscoelastic, mechanical properties and micromorphologies. *Polym. Comp.*, Vol. 28, pp. 175-179.

Zhou H., Chen Y., Fan H., Shi H., Luo Z., Shi B. (2008) The polyurethane/SiO2 nano-hybrid membrane with temperature sensitivity for water vapor permeation. *J. of Membrane Sci.*, Vol. 318, pp. 71-78.

Zhou T.H., Ruan W.H., Yang J.L., Rong M.Z., Zhang M.Q., Zhang Z. (2007) A novel route for improving creep resistance of polymers using nanoparticles. *Comp. Sci. and Tech.*, Vol. 67, pp. 2297-2302.

Zhu Y., Huang X., Li W., Fu J., Tang X. (2008) Preparation of novel hybrid inorganic-organic microspheres with active hydroxyl groups using ultrasonic irradiation via one-step precipitation polymerization. *Materials letters*, Vol. 62, pp. 1389-1392.

Zois H., Kanapitsas A., Pissis P., Apekis L., Lebedev E., Mamunya Ye.P. (2004) Dielectric properties and molecular mobility of organic/inorganic polymer composites. *Macromol. Symp.*, Vol. 205, pp. 263-270.

Chapter 8

(Bis)Maleimides for Organic-Inorganic Hybrid Materials

Viorica GAINA, Oana URSACHE, Constantin GAINA

"Petru Poni" Institute of Macromolecular Chemistry, Iasi, Romania

---

Summary

Remarkably, strategies of hybridization apply to all families of materials: not only to polymers but also to cements and materials for electronics or medical uses. Hybridization intensifies the need for multidisciplinary cooperation: molecular biologists, chemists, chemical engineers, mechanical engineers, electronic engineers and physicists have to collaborate. Thus hybrid materials constitute a composite field of research requiring the knowledge and the know-how of various disciplines. Organic-inorganic hybrid materials offer the opportunity to combine the desirable properties of organic polymers, such as, for example, processability, toughness, and impact strength, with the desirable properties of inorganic materials, such as, for example, high temperature stability, durability, and high modulus.

Since microsynthesis has been successful applied in making computer components, materials scientists have aimed to go beyond the microscale and to build up materials atom by atom (that is at the nanoscale: less than 100 nanometers) in order to make complex materials that can function as devices or micromachines. Again biological systems provided the model.

Notations and acronyms

APTES	3-aminopropyltriethoxysilane
APTMS	3-aminopropyltrimethoxysilane
BMI	bismaleimide
DA	Diels-Alder
LPS	Ladder-like polysilsesquioxanes
MMT	montmorillonite
OAPS	octa(aminophenyl)silsesquioxane
OMPS	octa(maleimidophenyl)silsesquioxane
POSS	polyhedral oligomeric silsesquioxane
POSS-NH_2	octa(aminopropylsilsesquioxane)
PPSQ	polyphenylsilsesquioxane
TEOS	tetraethoxysilane or tetraethylorthosilicate
DMA	dynamic mechanical analysis
DSC	differential scanning calorimetry
E'	dynamic storage modulus (tensile)
FT-IR	Fourier transform infrared spectra
SEM	scanning electron microscopy
$\tan \delta$	loss tangent from DMA; equal to E''/E'. δ is the phase angle between the imposed sinusoidal strain function and the responding stress function. δ=0° implies a perfectly elastic solid, δ=90° implies a purely viscous liquid
TEM	transmission electron microscopy
T_g	the glass transition temperature
XRD	X-ray diffraction

1. Introduction

Recent technological breakthroughs and the desire for new functions generate an enormous demand for novel materials. Composites are formed by the incorporation of a basic structural material into a second substance (the matrix*)*, and are regularly used for lightweight materials with advanced mechanical properties (for example in the construction of vehicles of all types or sports equipment). The structural building blocks in these materials which are incorporated into the matrix are predominantly inorganic in nature and show a size range from the lower micrometer to the millimetre range and therefore their heterogeneous composition is quite often visible to the eye. Soon it became evident that decreasing the size of the inorganic units to the same level as the organic building blocks could lead to more homogeneous materials that allow a further fine tuning of material properties on the molecular and nanoscale level, generating novel materials that either show characteristics in between the two original phases or even new properties.

Although we do not know the original birth of hybrid materials exactly it is clear that the mixing of organic and inorganic components was carried out in ancient world. At that time the production of bright and colourful paints was the driving force to consistently try novel mixtures of dyes or inorganic pigments and other inorganic and organic components to form paints that were used thousands of years ago. Therefore, hybrid materials or even nanotechnology is not an invention of the last decade but was developed a long time ago. An incredible amount of research investigations have appeared the last 10 years in the field of hybrid materials indicating the growing interest of chemists, physicists and materials researchers to fully exploit this technical opportunity for creating materials and devices with benefits of the best of the two worlds namely inorganic and organic. The combination of different analytical techniques gives rise to novel insights into hybrid materials and makes it clear that bottom-up strategies from the molecular level towards materials' design will lead to novel properties in this class of materials.

The "hybrid material" term is used for many different systems spanning a wide area of different materials, such as crystalline highly ordered coordination polymers, amorphous sol–gel compounds, materials with and without interactions between the inorganic and organic units.

When it comes to formal classifications hybrid materials tend to resist rigid categorizing. Their variety is too large – and growing – to allow for a systematic grouping criterion. Figure 1 tries to convey this variety by showing examples of general types of hybrids spreading on a field of organic and inorganic dimensions of their organic and inorganic components. The limited space prevents an exhaustive list of materials and only several representative types are shown. Yet, this visual arrangement provides a first general overview of the area, spanning from molecular to extended organic-inorganic combinations. In this respect, the graph also shows the greater richness of the field in the twilight region of supramolecular and nanostructured materials, forming a broad continuum between molecular and solid state chemistry.

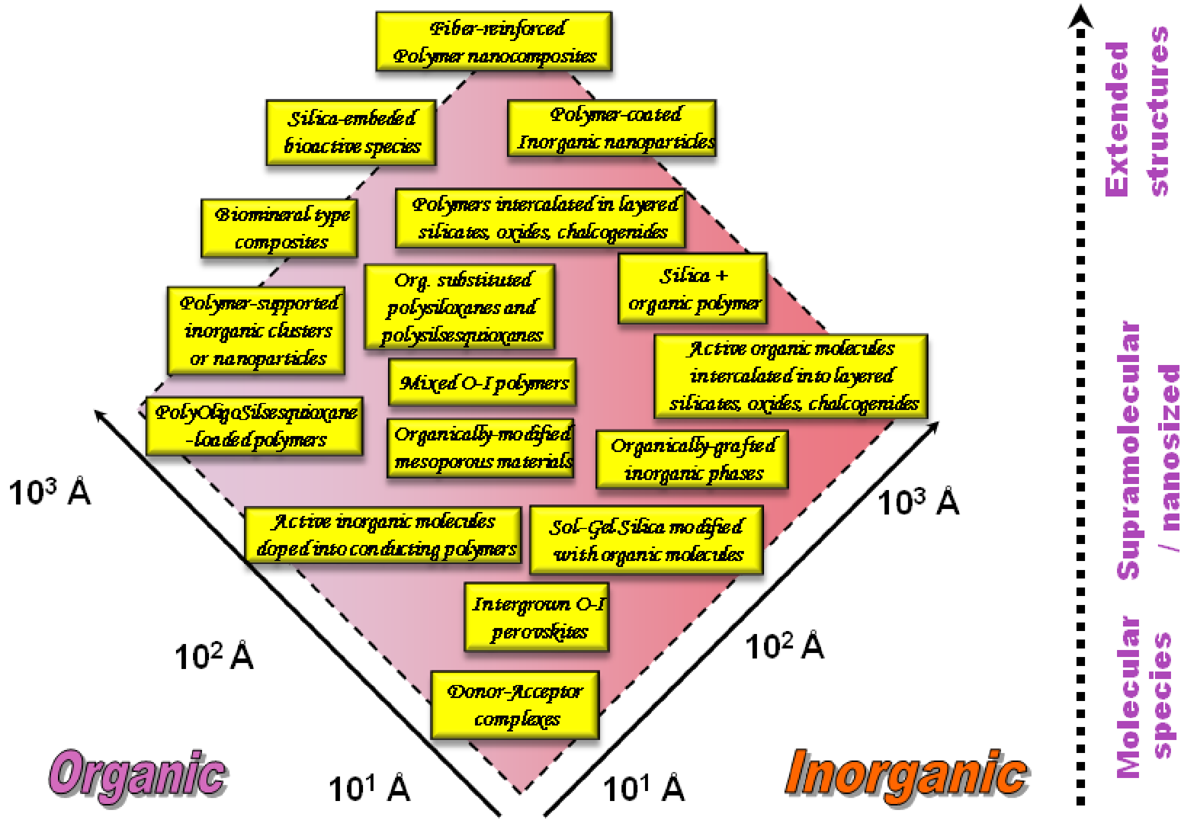

Figure 1. The field of hybrid organic-inorganic materials *[Reprinted with permission from Hybrid Materials, Functional Applications. An Introduction © 2005 John Wiley and Sons]*

The bidimensionality of this graph could suggest some type of classification according to the nature of the predominant phase in the hybrid, i.e. organic-inorganic vs. inorganic-organic materials depending on whether the extended, host or matrix phase were organic or inorganic, respectively. Such classification has been conveniently used to categorize a particular type of polymer-based hybrid although it could be difficult to generalize due to the abundance of intermediate cases and to the indistinct use of both terms in the literature, where the label organic-inorganic is most commonly used in a generic way.

Gómez-Romero and Sanchez *[Gómez-Romero and Sanchez, 2004]* defined hybrid materials as organic-inorganic hybrid materials or inorganic-biomaterials. They also mentioned that the characteristic scale of hybrid materials was less than 103 nm. They did not provide a strict definition of hybrid materials, and did not mention the formation of new electron orbitals or chemical bonds. In the Gomez-Romero & Sanchez definition, mixtures of materials were focused at the viewpoint of the characteristic scale and materials category. Their definitions of "hybrid materials" required an atomic or nanometer-level mixture of materials. Figure 2 shows a classification of materials by different scale levels, as proposed by the Materials Science Society of Japan *[Materials Science Society of Japan, 1993]*.

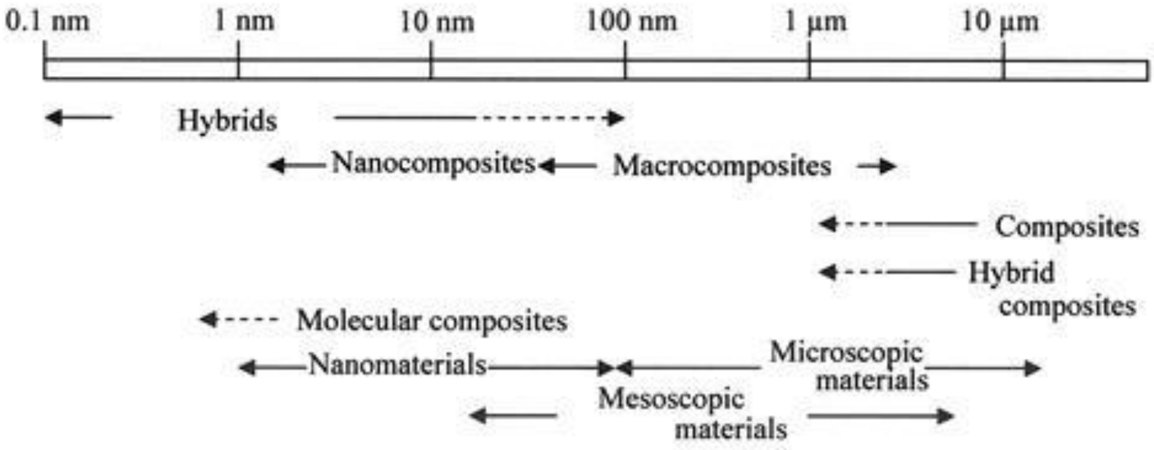

Figure 2. Classification of materials at different scale levels

On the other hand, Judenstein et al. have proposed a classification based on the bonding chemical nature between the organic-inorganic interphase *[Judenstein et al., 1999]*. This classification consists of two major groups: *Class I* where organic and inorganic components are embedded and only weak bounds (Van der Waals, hydrogen bonding, ionic bonds) give the cohesion to the whole structure; and in *Class II* the two components are linked together through strong chemical bonds (covalent, iono-covalent or coordination bonds) (Figure 3).

Blends are formed if no strong chemical interactions exist between the inorganic and organic building blocks. One example for such a material is the combination of inorganic clusters or particles with organic polymers lacking a strong (e.g. covalent) interaction between the components (Figure 4a).

If an inorganic and an organic network interpenetrate each other without strong chemical interactions, so called interpenetrating networks (IPNs) are formed (Figure 4b), which is for example the case when a sol–gel material is formed in the presence of an organic polymer or vice versa. Both described materials belong to class I hybrids. Class II hybrids are formed when the discrete inorganic building blocks, e.g. clusters, are covalently bonded to the organic polymers (Figure 4c) or inorganic and organic polymers are covalently connected with each other (Figure 4d).

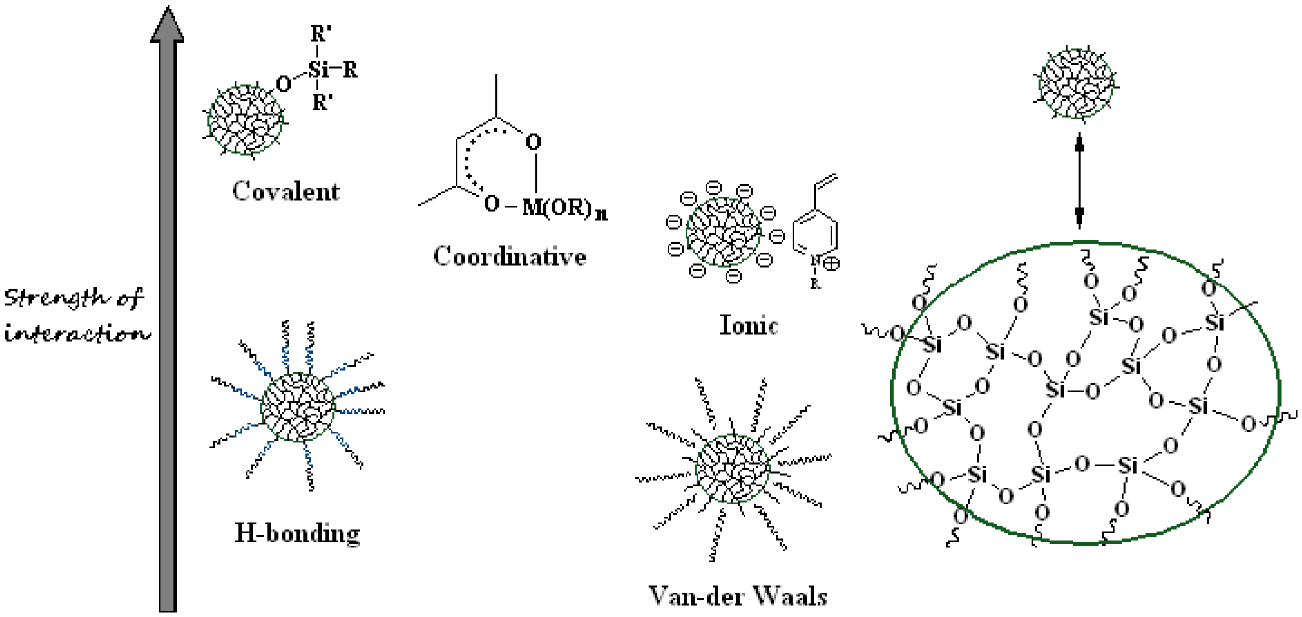

Figure 3. Selected interactions typically applied in hybrid materials and their relative strength

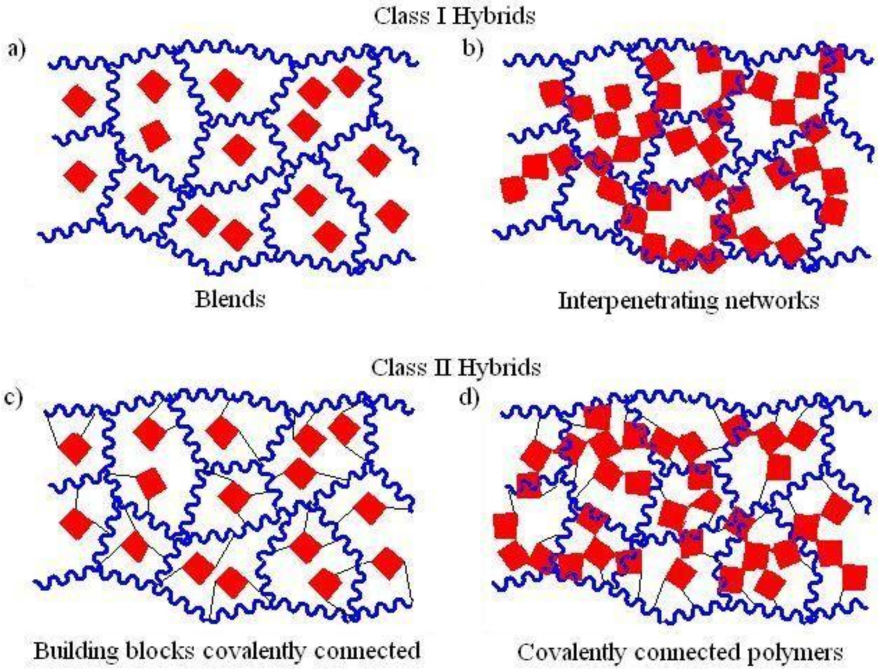

Figure 4. The different types of hybrid materials

In this review, structures, preparation, and properties of the maleimides based organic-inorganic hybrid materials, in general, are critically reviewed. We have classified these materials according to the inorganic component used for their preparation, as organic-inorganic hybrid materials including:

- silsesquioxanes
- nanoparticles unmodified or modified with coupling agents
- functionalized organotrialkoxysylane.

2. Organic-inorganic hybrid materials with silsesquioxanes

Hydrolytic condensation of the organotrialkoxysilanes, $RSi(OR'_3)$, performed in the presence of water and an acid or base as catalysts, leads to oligomeric or polymeric products that are generically called silsesquioxanes. These polymers have acquired increasing importance for the synthesis of functionalized organic–inorganic hybrid materials. The study of organic-inorganic hybrid materials focused on the following points: exploration of new preparative methodology for hybrid materials, new combinations between different materials, functionalization of hybrid materials, and modification of hybrids for industrial applications.

Species present in a silsesquioxane may vary from perfect polyhedra of formula $(RSiO_{1.5})_n$ or T_n which denotes a cage structure with the number of the $SiO_{3/2}$ groups of *n*, where n is an even number ($n \geq 6$), and R is hydrogen or any alkyl, alkylene, aryl, arylene, or organofunctional derivatives of alkyl, alkylene, aryl, arylene groups, denoted as polyhedral oligomeric silsesquioxanes (POSS), to partially condensed (but completely hydrolyzed) products of generic formula $T_n(OH)_m$, where $T = RSiO_{1.5\_m/2n}$ *[dell'Erba et al., 2003; Fasce et al., 1999]*. The structures of silsesquioxanes have been reported as random structure, ladder structure, cage structures, and partial cage structure (Figure 5).

Brown et al. first reported the synthesis of ladder-like PPSQ by the equilibration method in 1960 *[Brown et al., 1960]*. They possess superior heat, radiation, water, and fire resistance, high laser threshold values, and outstanding electrical properties. High-strength films of such materials make them suitable for applications in coatings and electronic and optical devices. The equilibration method can be summarized as follows: (1) hydrolysis of phenyltrichlorosilane in a solvent with excess water to give a hydrolyzate with a molecular weight of $\sim 10^3$, (2) equilibration of the hydrolyzate with potassium hydroxide at a relatively low concentration (~50%) and a low temperature (~100°C) to give a prepolymer with a molecular weight of $\sim 10^4$, and (3) equilibration of the prepolymer at a high concentration (80-90%) and a high temperature (~250°C) to give the polymer with a molecular weight of over 10^5.

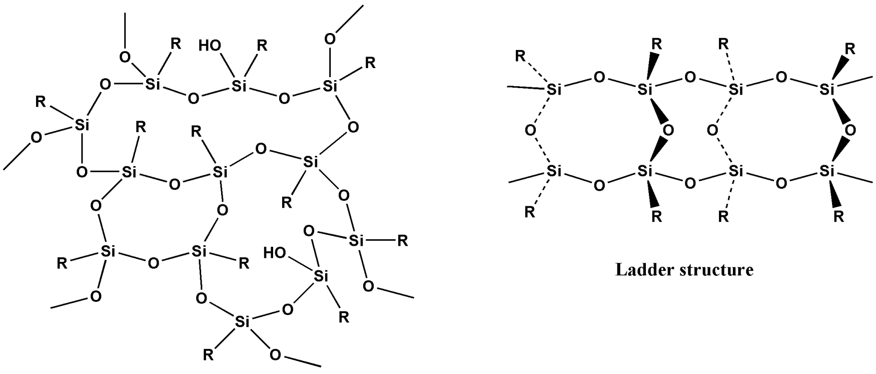

Random structure

Ladder structure

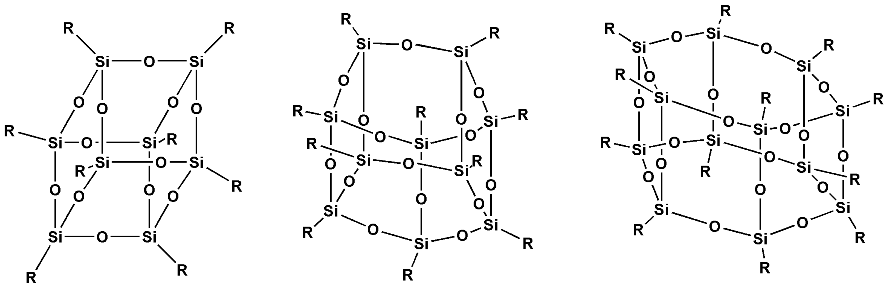

(T$_8$)

(T$_{10}$)

(T$_{12}$)

Cage structures

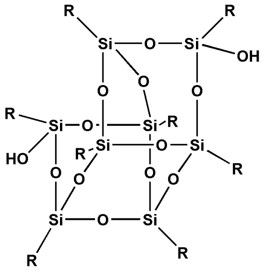

Partial cage structure

Figure 5. Structures of silsesquioxanes

Due to the harsh reaction conditions (250°C in the presence of KOH) used by Brown, his method cannot be used to synthesize reactive LPS. In the late 1980s, a new polymerization method called *stepwise coupling polymerization* was reported to synthesize reactive LPS *[Xie et al., 1989]*. It involves pre-aminolysis of trichlorosilanes, followed by hydrolysis and polycondensation. Based on this method, two ladder-like polysilsesquioxanes (LPS) containing side-chain maleimide groups have been synthesized successfully by reacting *N*-(4-hydroxyphenyl) maleimide with LPS containing 100 mol % of chloropropyl groups (Ladder A) and 50 mol % of each methyl and chloropropyl group (Ladder B), followed by the curing reaction of maleimide groups (Scheme 1) *[Krishnan et al., 2004]*. Characterization data indicated that these polymers had ordered ladder-like structures with possible defects. Activation energy determined for the curing of Ladders A' and B', indicated that the presence of a ladder-like structure in the main chain influenced the curing behavior of the maleimide group.

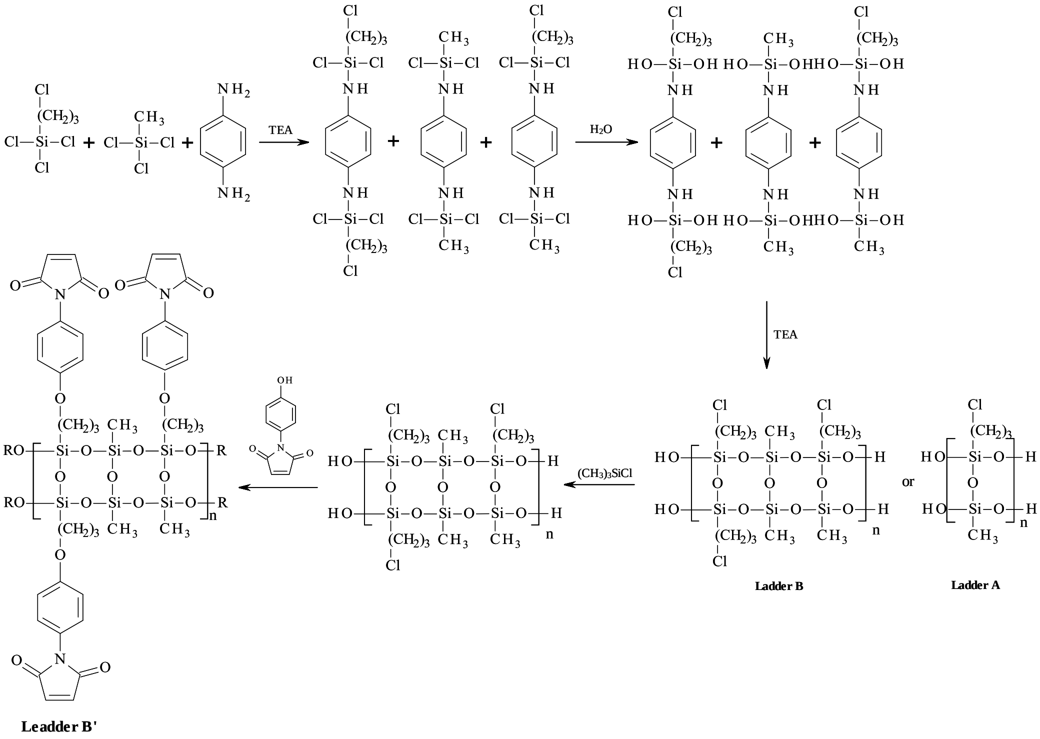

Scheme 1. Synthetic route for preparation of LPS containing side-chain maleimide groups (Ladder B')

Polyhedral oligomeric silsesquioxanes (POSSs) with their nanosized cage structures are widely regarded as some of the most promising and rapidly emerging nanocomposite materials. POSS is a substance with an inner inorganic framework, made up of silicon and oxygen atoms in the ratio of 1:1.5 $(SiO_{1.5})_n$, and organic functional groups capped. POSS materials have excellent thermal stability due to their inorganic structures, which contributes to their high glass transition and decomposition temperatures. Similarly to conventional polymers, POSS monomers can be copolymerized with other monomers. POSS monomers with one or more covalently bonded reactive groups are suitable for polymerization, grafting, surface bonding, blending in molecular level.

By nitration of octa(phenyl)silsesquioxane in fuming nitric acid to form octa(nitrophenyl)silsesquioxane, followed by mild reduction with Pd/C as a catalyst, OAPS was prepared. Modification of a bismaleimide resin with OAPS and dipropargyl ether of bisphenol A leads to a hybrid resin with good processability and thermal stability (Scheme 2) *[Huang et al., 2008]*.

Considering the importance of OAPS in developing high-performance nanocomposites, it was reported a novel and facile way for the preparation of OAPS by using the stable, inexpensive, and readily available hydrazine hydrate as the reducing agent, offering a low cost alternative to the Pd/C catalyst *[Zhang et al., 2007]*.

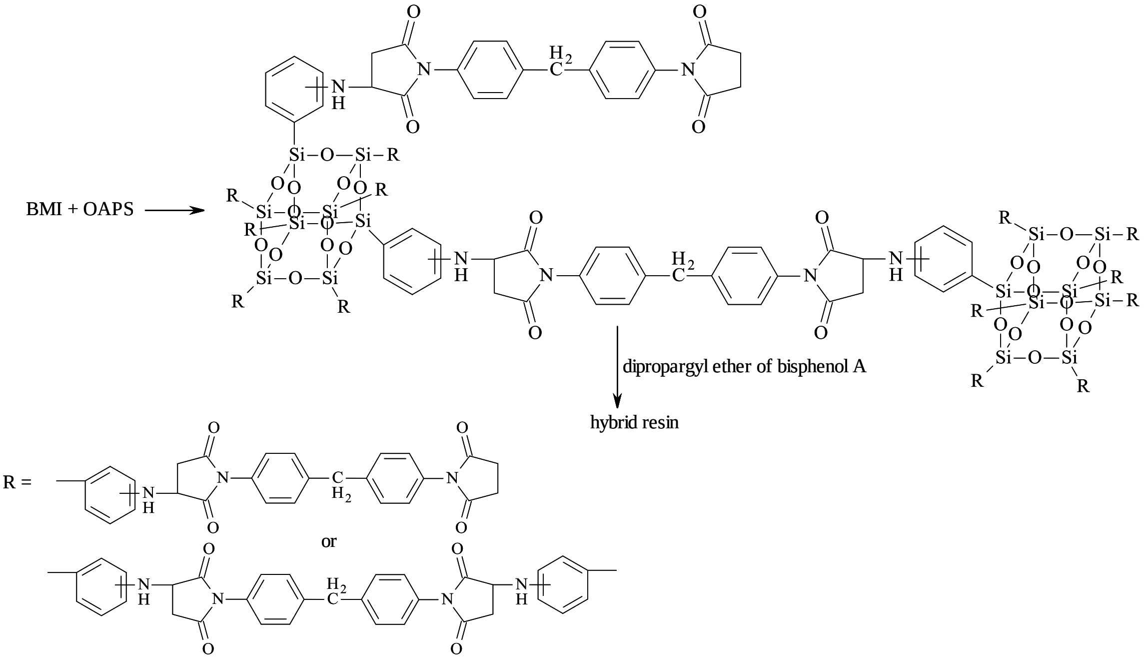

Scheme 2. Preparation of OAPS/BMI/dipropargyl ether of bisphenol A hybrid resin

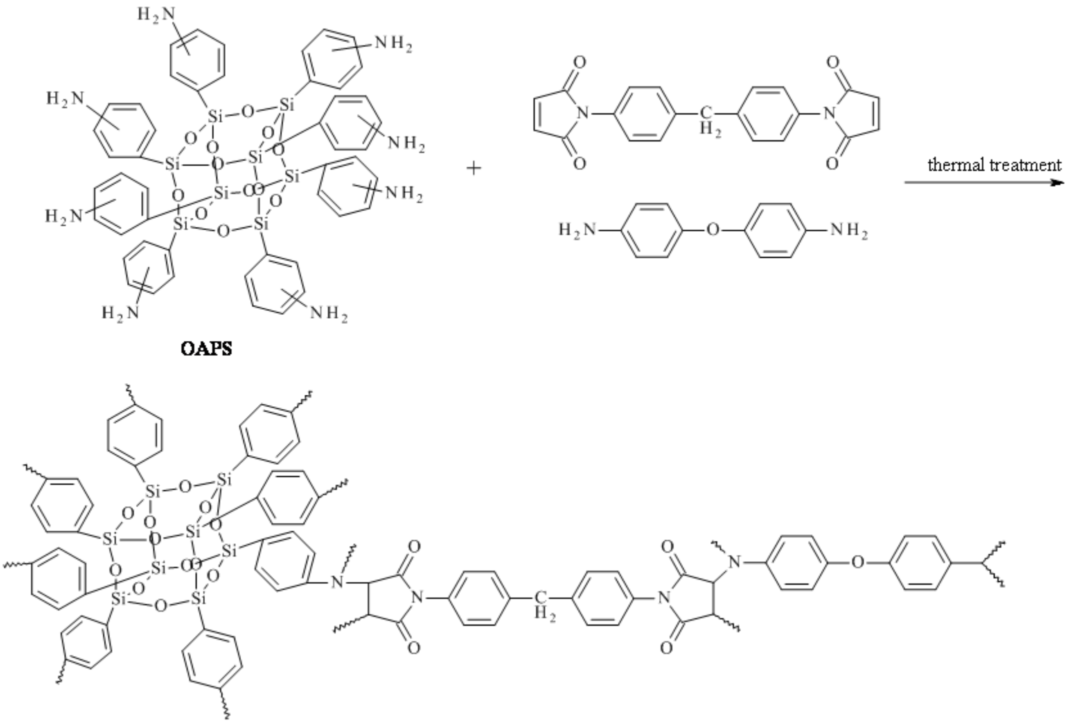

Scheme 3. Synthesis of BMI-diamine/OAPS nanocomposite

In addition, polyimide nanocomposites by Michael addition reaction of OAPS and 4,4'-diaminodiphenyl ether with *N*,*N*'-bismaleimido-4,4'-diphenylmethane were prepared (Scheme 3). The DSC data showed that the glass transition temperature of nanocomposite was enhanced by 36°C with a content of OAPS around 15 wt %. As the feed amount of OAPS increased further, the decrease in *Tg*'s could be observed. Introduction of OAPS into bismaleimide-diamine resin may improve the thermomechanical stabilities of the resulting product.

Mainly two reactions occurred in BMI-diamine system at high temperature: BMI–BMI double-bond polymerization and BMI-diamine Michael addition reaction. The Michael addition of BMI and diamine leads to the formation of a secondary amine, which may react with another BMI molecule at higher temperature resulting in a crosslinked network. The commonly held view is that the Michael addition reaction predominates at lower temperature (<180°C), and at higher temperature the homopolymerization reaction of BMI occurs at a comparable rate.

The functionalization of POSS with maleimide groups leads to OMPS by the reaction between OAPS and anhydride maleic followed by the imidization reaction of amic acid intermediary either with triethyl amine and acetic anhydride or *p*-toluenesulfonic acid. OMPS was used as a nanocrosslinker in the copolymerization reaction with BMI and urethane methacrylate *[Krishnan et al., 2005]* (Scheme 4A), BMI and allylated novolac *[Li et al., 2007]* (Scheme 4B) and BMI-triazine resins *[Cao et al., 2008]* (Scheme 4C), or in the Michael addition reaction with diglycidylether of bisphenol-A and 4,4'-diaminodiphenylmethane *[Jothibasu et al., 2008]* (Scheme 4D). In general, the thermal stability and the glass transition temperature of hybrid materials were enhanced by the incorporation of OMPS in the case of the copolymerization reaction.

In the BT resins/OMPS hybrid materials based on BMI and 2,2'-bis(4-cyanatophenyl)propane it was found that OMPS accelerated the curing reaction of 2,2'-bis(4-cyanatophenyl)propane, and the onset temperature of the cyclotrimerization was reduced up to 95.5°C (by DSC) *[Cao et al., 2008]* (Scheme 4C). As demonstrated by DSC and FTIR measurements, there was no evidence that indicated the coreaction between maleimide and cyanate ester. Scheme 5 depicts the possible reaction path for the polymerization of cyanate ester catalyzed by H_2O and hydrogen donors. When the hydrogen donor is a phenolic compound, the imidocarbonate *viz*. cumyl imidoether is formed for the first step in the reaction. 2,2'-diallyl bisphenol A and diglycidyl ether of bisphenol A (E-51) were also used to enhance the toughness of BT resin. The thermal properties of the obtained resins incorporated with 1 wt % of OMPS exhibit enhanced thermal properties in comparison with their pristine resins respectively, while more contents of OMPS may impair the thermal

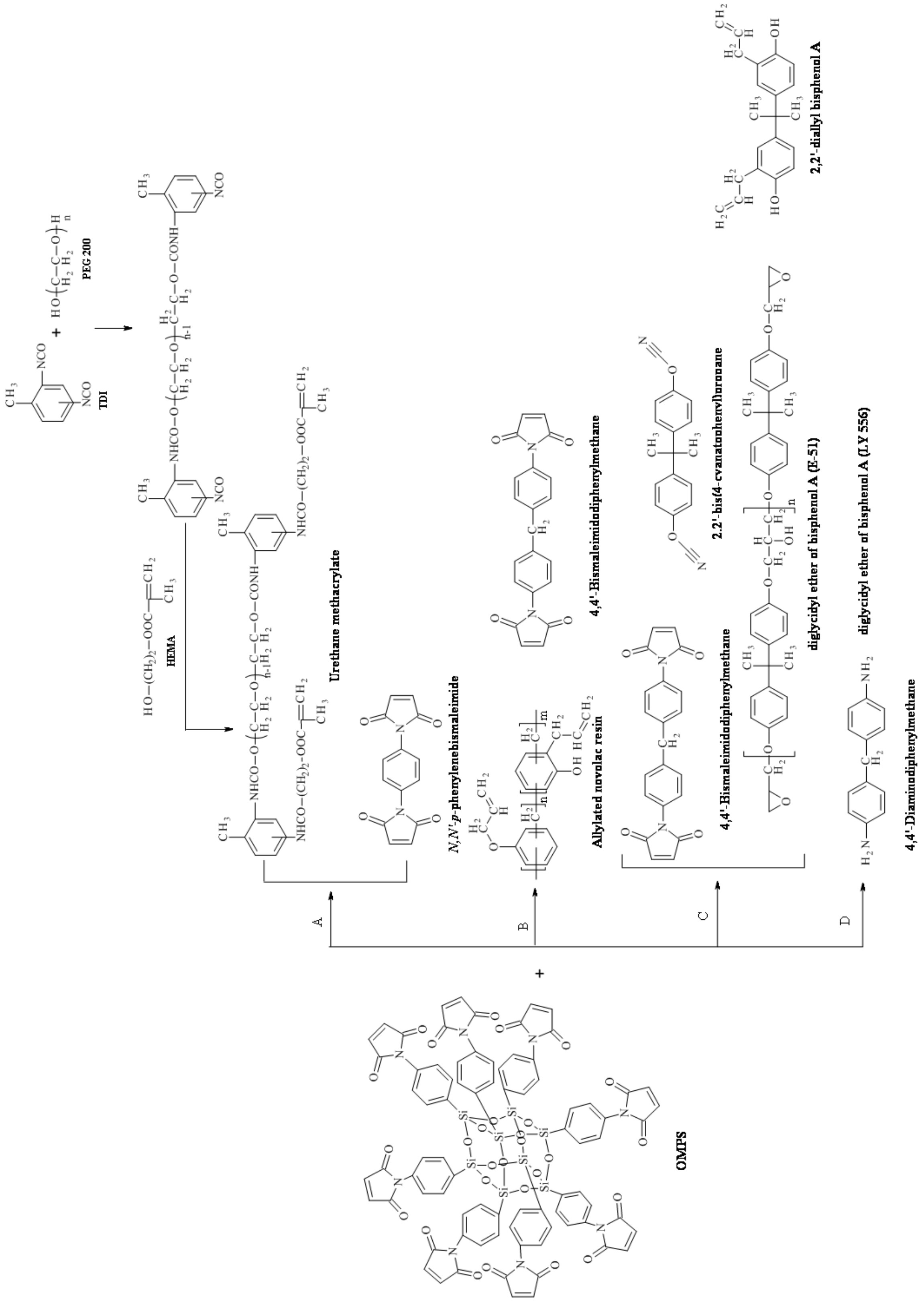

Scheme 4. Synthetic route for the preparation new hybrid materials

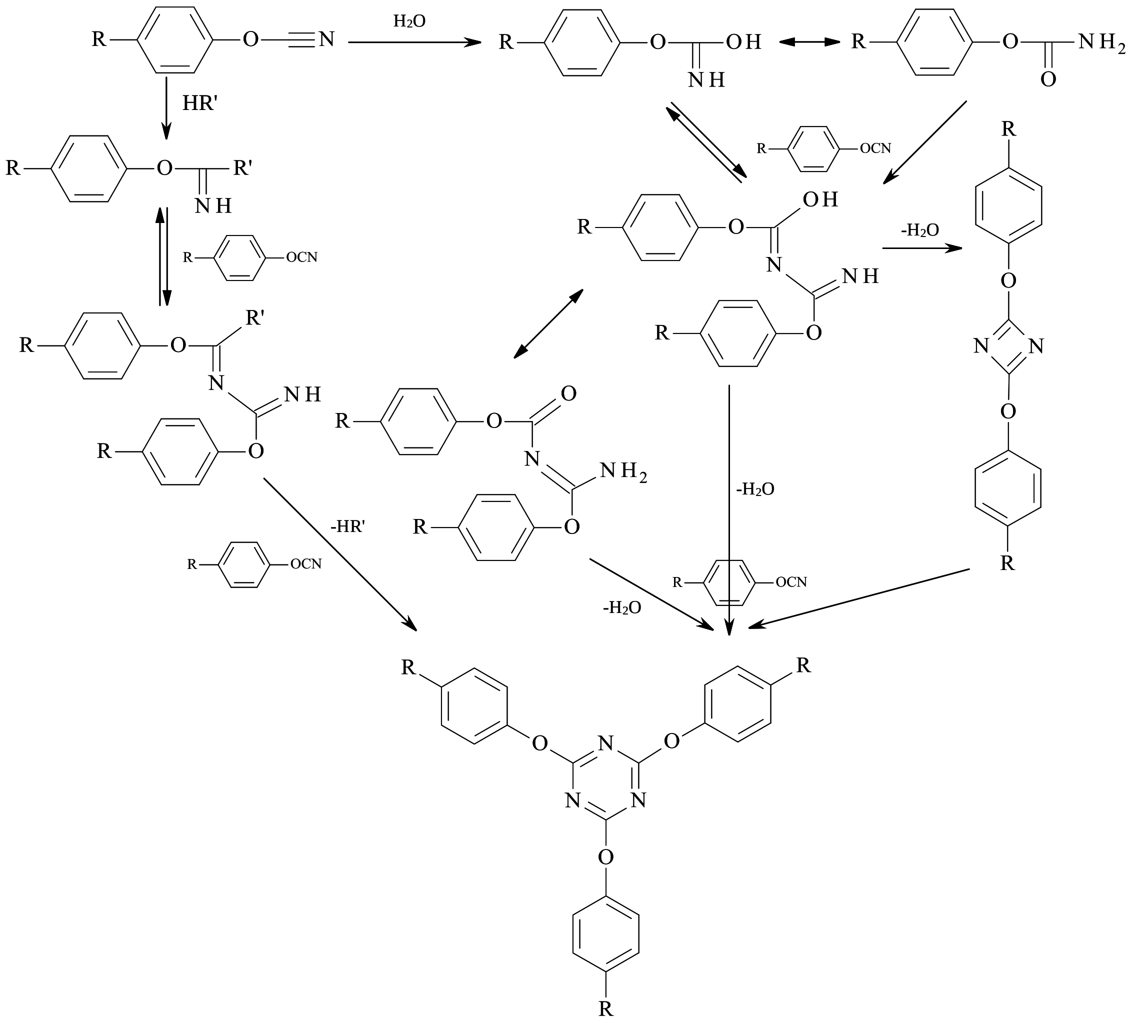

Scheme 5. Reaction mechanism for polymerization of cyanate ester catalyzed by hydrogen donors and H_2O

properties of the polymer matrix, though the effect of OMPS was slight. Finally, the dielectric constant of these hybrid materials were detected, and their dielectric constant were distinctly reduced by the incorporation of OMPS (2-4 wt %), while overmuch contents of OMPS (up to 8 wt %) were disadvantageous for dielectric constant because of the aggregation of OMPS.

Jothibasu et al. reported the preparation of epoxy POSS-based hybrid nanocomposites by *in situ* polymerization of a homogeneous blend of the diglycidylether of bisphenol-A and 4,4'-diaminodiphenylmethane in the presence of OMPS *[Jothibasu et al., 2008]* (Scheme 4D). The FTIR studies confirm that the formation of hybrid POSS-maleimide-modified epoxy system proceeds through the following routes: (i) the reaction between amino groups of 4,4'-diaminodiphenylmethane and the oxirane ring of the epoxy resin (scheme 6a) and (ii) the reaction between the amino groups of 4,4'-diaminodiphenylmethane and the maleimide double bonds through Michael addition (Scheme 6c). According to DSC study the curing reaction between the epoxy and 4,4'-diaminodiphenylmethane commences at 120°C and reaches its peak maximum temperature at 164°C. The large exotherm obtained during the cure reaction of epoxy–diamine may be attributed to a combination of (i) the oxirane ring-opening reaction with active amino hydrogens of 4,4'-diaminodiphenylmethane and (ii) the autocatalytic reaction of the oxirane ring with pendent hydroxyl groups of epoxy resin and hydroxyl groups formed during cure reactions (Scheme 6b).

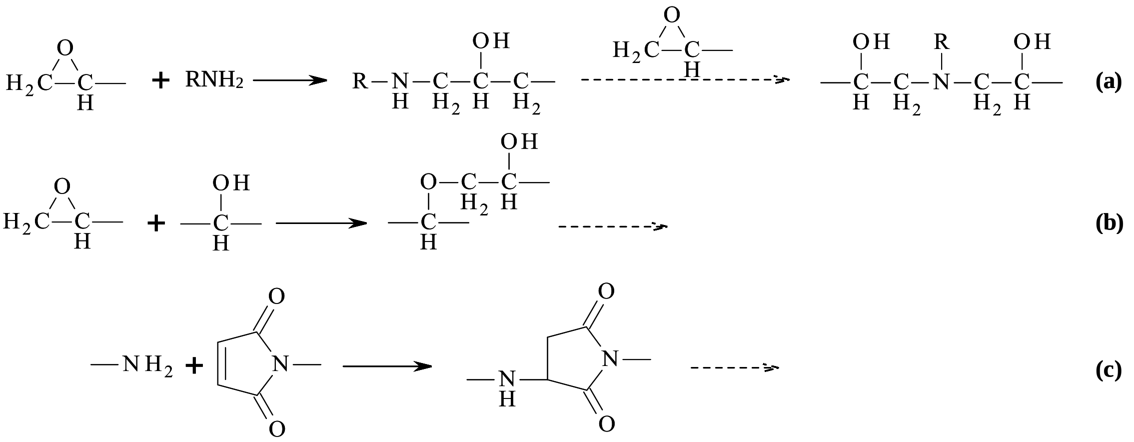

Scheme 6. Simplified reactions involved during curing

Dynamic mechanical analysis studies indicated that the crosslinked structures of the nanocomposite networks were predominantly formed between the terminal maleimide double bonds and the amino groups of 4,4'-diaminodiphenylmethane through a Michael addition reaction. The values of the glass transition temperatures (*T*g) decreased with increasing POSS-maleimide content and this was likely to be due to the inclusion of POSS cages into the system and the consequent increase in free volume. The dynamic thermal stability of the cured polymers was increased by increasing the POSS content in the hybrid epoxy matrices as evidenced from thermogravimetric analysis data.

Recently, Shibata and co-workers reported new hybrid materials, partially crosslinked and insoluble to general organic solvents, by the thermo-reversible DA reaction between maleimide/phenyl-substituted oligomeric silsesquioxane and bio-based furfuryl ester-terminated butylene succinate oligomer (FBSO) in DMF at 60°C for 48 h *[Shibata et al., 2011]* (Scheme 7). The ^{1}H-NMR study on this reaction revealed that the conversion of the DA reaction is low (ca 10 %). The flexural strength and modulus of the P(MPOSS21-FBSO) prepared by the solution casting method were higher than that of the P(MPOSS21-FBSO) prepared by the melt mixing (15.5 MPa) and was comparable to that of FBSO.

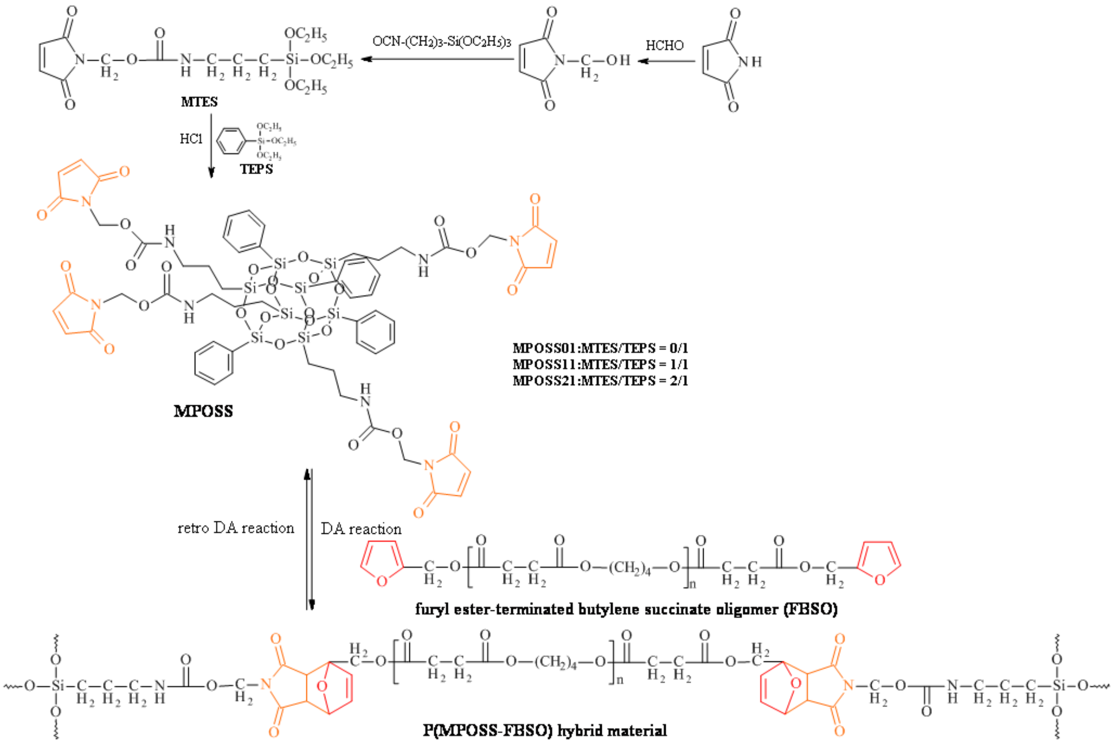

Scheme 7. Scheme of hybrid material preparation; MTES-maleimidomethyl 3-(triethoxysilyl)propyl-carbamate; TPES-triethoxyphenylsilane; MPOSS-maleimide/phenyl-substituted oligomeric silsesquioxane

Along with the LPS, OAPS and OMPS, the literature reported the preparation of organic-inorganic hybrid materials based on octa(aminopropylsilsesquioxane) (POSS-NH_2) *[Hu et al., 2011; Liu and Lee, 2006]* and hydrogen silsesquioxane (HSQ) *[Huang et al., 2010]*. POSS-NH_2 used as monomer in the Michael addition reaction with maleimide-containing polyamide leads to nanocomposites with a significant enhancement of mechanical properties, a low dielectric constant and a slight decrease of T_g (Scheme 8) *[Liu and Lee, 2006]*.

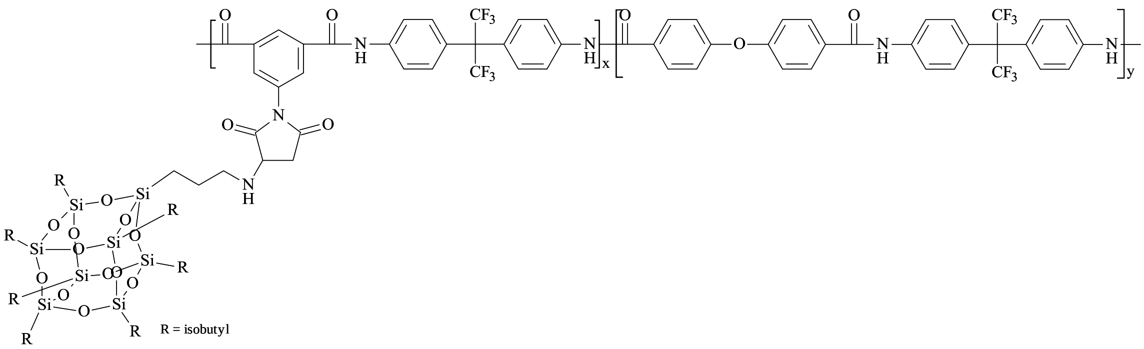

Scheme 8. Preparation of polyamide-tethered POSS nanocomposites

For improved integrated performance of the organic-inorganic hybrid based on BT resins (a resin containing BMI, diallyl bisphenol A and 2,2'-bis(4-cyanatophenyl) isopropylidene), the effects of POSS-NH_2 and its content on the integrated properties, including curing behaviour and dielectric and thermal properties of BT resin were studied *[Hu et al., 2011]*. The curing mechanism of BT prepolymer mainly consists of DA and ene reactions between BMI and diallyl bisphenol A as well as the cyclotrimerization of 2,2'-bis(4-cyanatophenyl) isopropylidene as shown in Scheme 9.

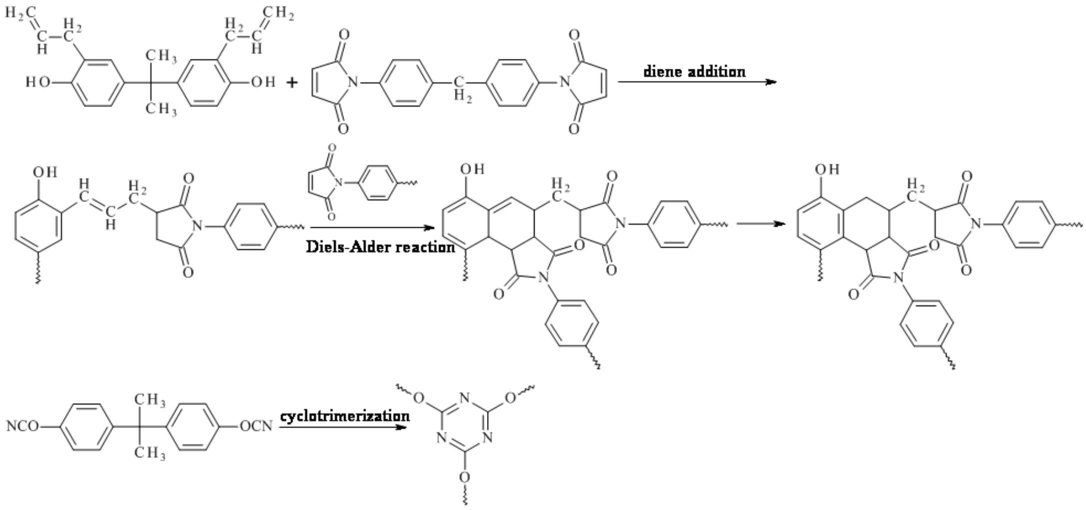

Scheme 9. The curing reactions of BT prepolymer

The curing reactions of POSS-NH_2/BT hybrids are more complicated than those of BT prepolymer. Besides above reactions during the curing of BT prepolymer, the curing reactions of POSS-NH_2/BT hybrids also include the Michael addition between POSS-NH_2 and BMI and the reaction between POSS-NH_2 and 2,2'-bis(4-cyanatophenyl) isopropylidene (Scheme 10). The reaction between maleimide and cyanate ester is still controversial. In this study, the decrement in curing temperature is ascribed to the reactions between -OCN and amine groups. Amine groups can react with -OCN groups upon mild heating or in the presence of base catalysts, interestingly, the product of the reaction is the catalyst for the formation of triazine rings. The amino groups on POSS-NH_2 can react easily by adding across the triple bond of -OCN in the molecules of 2,2'-bis(4-cyanatophenyl) isopropylidene (Scheme 10). This causes POSS-NH_2 macromer to react with cyanate ester monomer at temperatures far below the temperatures for curing cyanate ester.

Compared with BT resin, POSS-NH_2/BT hybrids exhibit significantly decreased curing temperature, improved dielectric properties, and thermal resistance. The decreased curing temperature may be ascribed to the reactions between -OCN with amine groups; the improved dielectric properties (lower dielectric constant and loss) can be attributed to the lower polarity of POSS.

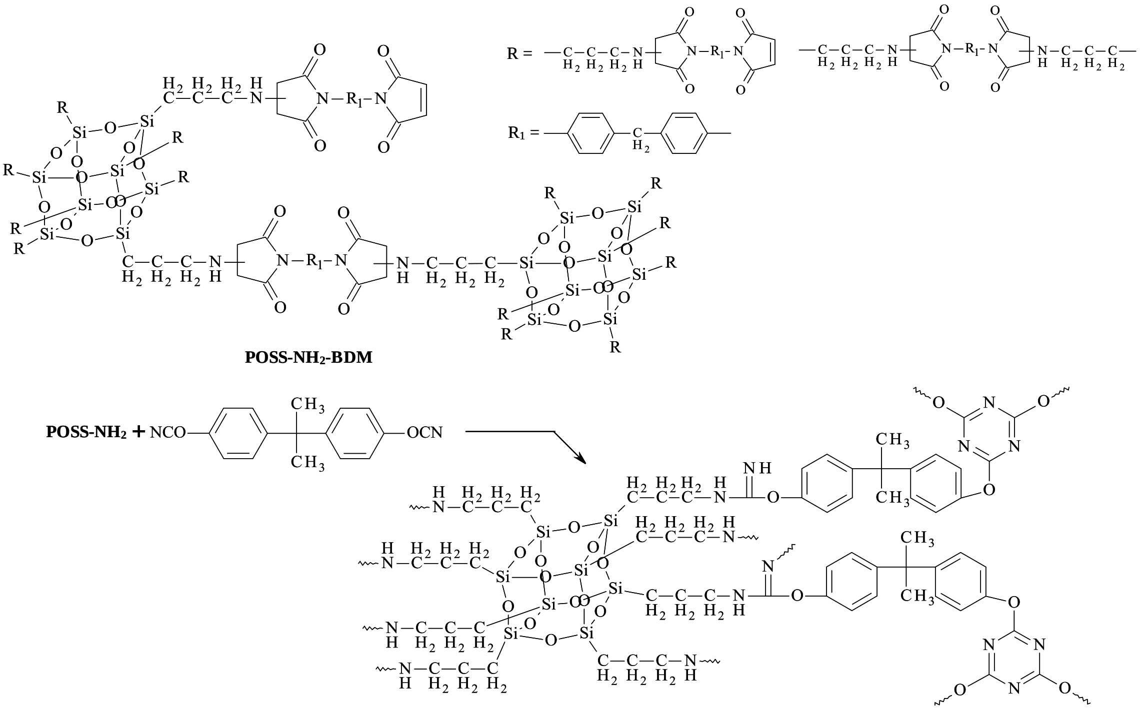

Scheme 10. Structure of POSS-NH_2-BDM and reaction between POSS-NH_2 and NCO groups

The effect of POSS-NH_2 on the thermal stability of BT resin is very complex by the contribution of the good thermal resistance of POSS, the change in cross-linking density, and the restriction of the macromolecular motion. The outstanding integrate properties of POSS-NH_2/BT hybrids supply a great potentiality for them to be used as matrix for advanced composites or high-performance adhesive in many cutting edge fields.

Advancements in semiconductor miniaturization have propelled an increasing interest in high performance insulating materials, which are characterized with outstanding integrated properties including high mechanical properties, low dielectric constant and loss, good thermal stability, and desirable lower coefficient of thermal expansion (CTE). Hu et al. reported a new composite based on a new organic/inorganic mesoporous silica (MPSA) with functional –NH_2 groups and 2,2'-diallylbisphenol A (DBA) modified 4,4'-bismaleimidodiphenylmethane (BMI) resin *[Hu et al., 2011]*. The structure of MPSA is illustrated in Figure 6. Starting from TEOS and tetraethylammonium hydroxide, a cubic octameric silicate anion is obtained, which reacts with dimethyldichlorosilane. The white solid product reacts with γ-aminopropyl triethoxy silane and leads to MPSA.

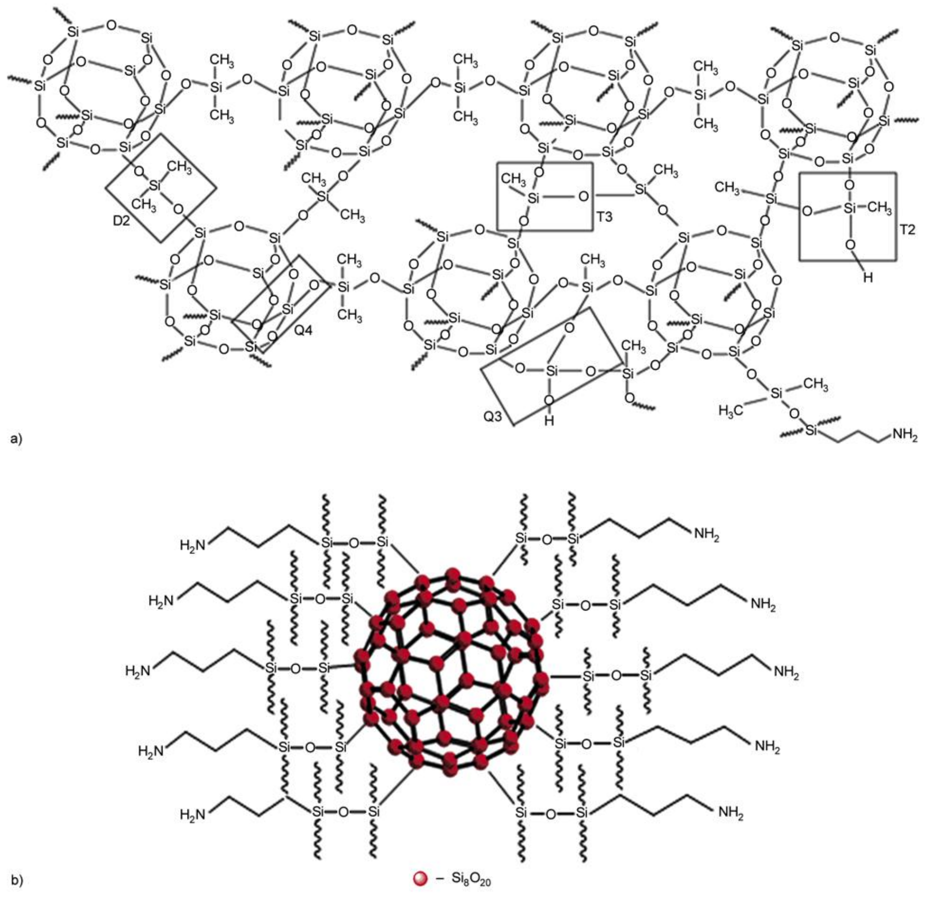

Figure 6. The chemical connection of MPSA (a), and chemical structure of MPSA (b)

The composites have different curing mechanism from DBA/BMI resin. For DBA/BMI resin, the curing mechanism contains multiple reactions, for example "ene" and Diels-Alder reactions between maleimide group of BMI and allyl group of DBA, and the self-polymerization of BMI *via* C=C bonds (Scheme 11a); while in the case of MPSA/DBA/BMI system, besides above reactions of DBA/BMI, there is a Michael reaction between maleimide and -NH_2 groups. This additional reaction not only supplies a chemical bonding between MPSA and DBA/BMI (Scheme 11b) to guarantee a good dispersion of MPSA in the matrix, but also leads to a different structure of the crosslinked network. Specifically, the effect of MPSA on the crosslinked structure is complicated, because MPSA is an organic/inorganic hybrid containing flexible Si–O–Si bonds and aliphatic chains, rigid SiO_2 with cage structure as well as functional -NH_2 groups. First of all, because the Michael reaction between BMI and -NH_2 takes place at a lower temperature than the homopolymerization of BMI does, so the addition of MPSA to DBA/BMI resin will produce flexible segments, and decrease the amount of the rigid polybismaleimide. Secondly, although the content of MPSA is small, there are a lot of –NH_2 groups on the surface of MPSA, meaning that the presence of MPSA tends to shorten the distance between the crosslinking points, and thus increases the crosslinking density of the resultant network. Third, the cage units of MPSA connect with each other to form a compact network, as one part of the whole crosslinked network of composites, tending to improve the crosslinking density of the composites.

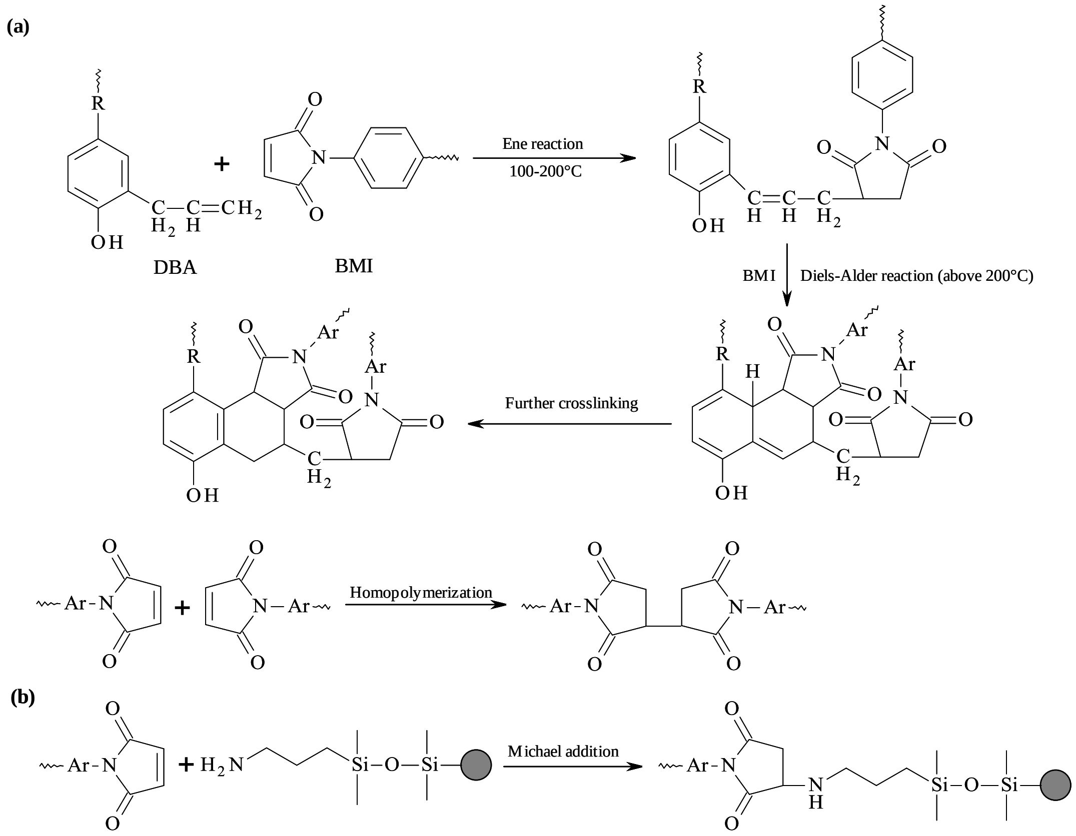

Scheme 11. The chemical reactions among BMI, DBA (a) and MPSA (b)

The addition of MPSA to DBA/BMI resin does not change the curing profile of DBA/BMI resin, but varies the curing mechanism, leading to different crosslinked networks, and thus the integrated performance of cured composites. Apparently, the content of MPSA exhibits a great influence on the integrated performance of cured composites. The composites with suitable content of MPSA show obviously improved flexural strength and modulus as well as impact strength; in addition, all composites not only have lower dielectric constant and similar frequency dependence, more interestingly, they also exhibit better stability of frequency on dielectric loss. The outstanding integrated performance of MPSA/DBA/BMI composites with suitable content of MPSA show a great potentiality to be used as high performance insulators for applications needing harsh requirements in thermal, mechanical and dielectric properties.

3. Organic-inorganic hybrid materials with nanoparticles unmodified or modified with coupling agents

The sol-gel reactions have been used not only as a chemical route to ceramics of high purity and controlled microstructure, but also in conjunction with polymeric materials as a method for preparing organic–inorganic hybrid materials. There are several advantages in using sol-gel chemistry, including the low synthesis temperature, easiness of obtaining optically transparent nanocomposites, versatility of control over the nature of the organic-inorganic interface, as well as convenience of introducing new properties into the resulting materials. Alkoxysilanes have been widely used to modify the silica particle surfaces. The reaction mechanism generally involves the hydrolysis of the alkoxy groups of silane to form silanol groups, followed by the condensation reaction between the silanol groups of silane molecules and silica particles.

In this chapter we describe the general synthesis of organic-inorganic hybrid materials in terms of the nature of the nanoparticles used (SiO_2, TiO_2, SiC, ZrO_2, montmorillonite) and based, on these nanoparticles, their preparation method ((co)polymerization, Michael addition, DA reaction etc.).

The literature reported new organic-inorganic hybrid materials based on the modification of silica particle surface with *N*-γ-triethoxypropyl-maleamic acid *[Lu and Huang, 2002]* or vinyltriethoxysilane *[Su et al., 2007]* followed by its polymerization reaction or copolymerization reaction with BMI.

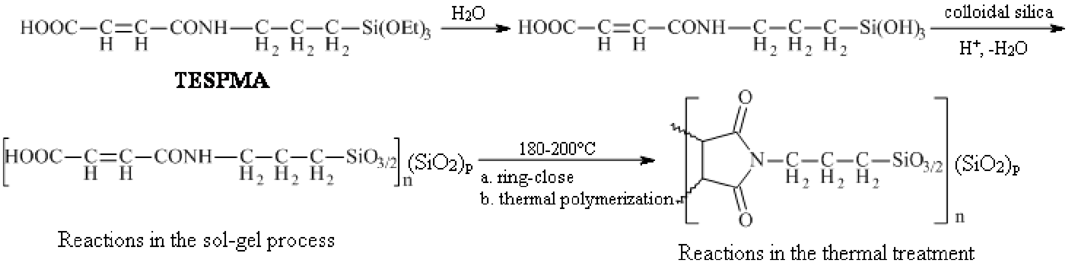

Scheme 12. Synthesis of polymaleimide/silica nanocomposite

Polymaleimide/silica nanocomposites synthesized from *N*-γ-triethoxysilylpropylmaleamic acid (TESPMA) through sol-gel process, imidation reaction of the maleamic acid functional groups and thermal polymerization of the formed maleimide at elevated temperature (Scheme 12), showed excellent thermal stability: high glass transition temperature and high decomposition temperatures *[Lu and Huang, 2002]*. The average particle size of the inorganic phase in these nanocomposites was in the range of 10–40 nm. Incorporation of colloidal silica did not make positive contributions to the thermal stability, although the weight fraction of inorganic part in the composite was increased significantly.

The vinyl groups of silane molecules grafted onto the silica nanoparticle surface can participate in the subsequent free radical polymerization of BMI molecules initiated by barbituric acid (Scheme 13) *[Su et al., 2007]*.

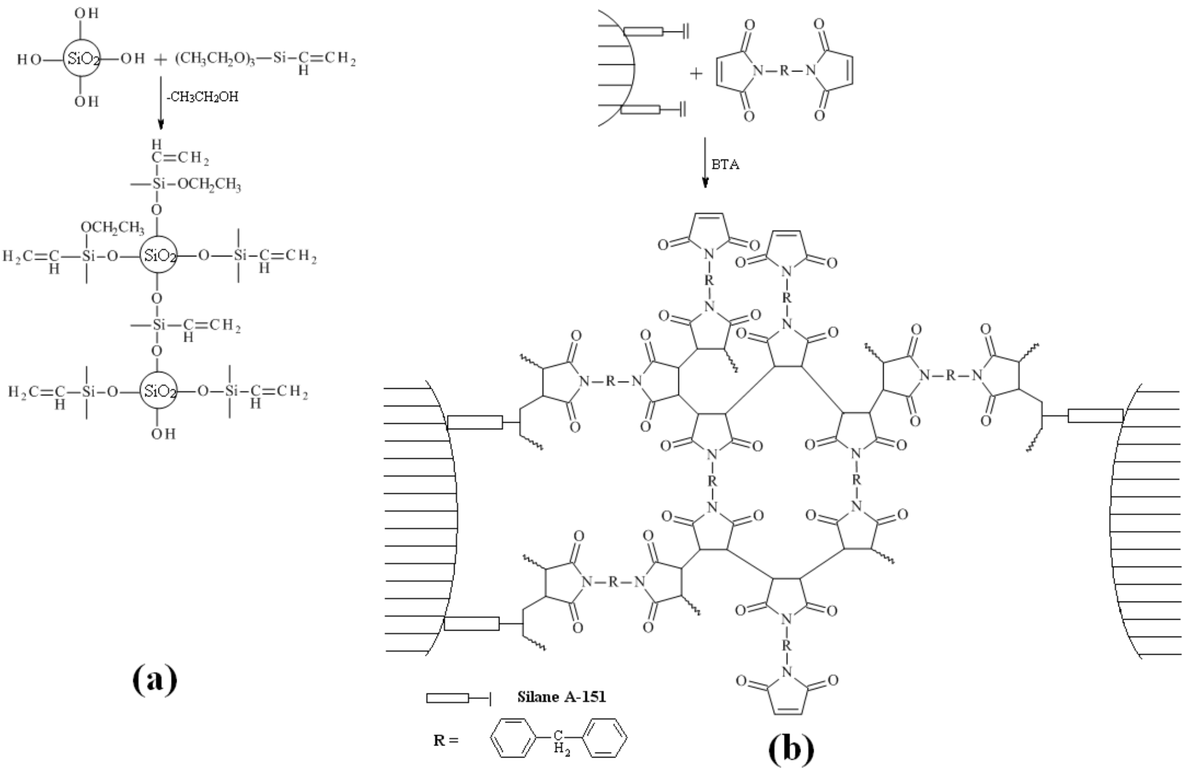

Scheme 13. (a) Modification of silica nanoparticles with vinyltriethoxysilane. (b) Polymerization of BMI initiated by barbituric acid (BTA) in the presence of the vinyltriethoxysilane-modified silica nanoparticles

The polymerization of BMI initiated by barbituric acid in the presence of the native or vinyltriethoxysilane-modified silica nanoparticles were carried out in γ-butyrolactone (total solids content = 20%). The BMI/silica particles with the weight percentage of silica based on total solids equal to 30 or 40 wt % completely failed to disperse in γ-butyrolactone. In contrast, the BMI/silane/silica colloidal systems with the weight percentage of silica based on total solids greater than 20 wt % still showed excellent fluidity. The vinyltriethoxysilane modified silica particles significantly improved their dispersion capability within the continuous BMI oligomer matrix. Moreover, the degree of dispersion of the vinyltriethoxysilane-modified silica particles in the BMI oligomer matrix decreased with the weight percentage of silica based on total solids being increased from 20 to 40 wt %.

The separation of a certain class of isomers that are important in the disciplines of environmental, clinical, and food science is one of the most challenging issues facing the analyst, because isomerism gives structurally similar compounds that sometimes differ negligibly in their physicochemical properties. However, their separation is essential. For example, carotenoids are thought to diminish the incidence of certain degenerative diseases, and though in common foods they are mostly found in the form of all trans-isomers, significant amounts of geometrical *cis*-isomers can be produced during processing. The *cis*-isomers of *β*-carotene have attracted attention because their bioavailability is different from that of their corresponding *trans*-isomers, and they may have specific functions. Separation of the isomers of polycyclic aromatic hydrocarbons, vitamin E (tocopherol), retinoids, vitamin A derivatives, etc., also involves similar challenges. One of the easiest methods of separating these isomers may be the direct use of biosystems such as enzymes, antibodies, and proteins; however, this method has its disadvantages, such as a too narrow selectivity, low stability, and limited scope of use. Another approach to isomer separation may be based on biomimetic approaches. For example, biomembrane systems are very attractive to mimic for a separation because their self-assembling structures yield various supramolecular functions. Alternating copolymerization mediated by electron donor-acceptor interactions remains a popular approach for achieving special materials with different functionalities in a wide range of scientific fields including nanotechnology and drug delivery. Mallik et al. have reported a new class of high-performance liquid chromatography (HPLC) stationary phase as the first application of alternating copolymerization on silica *[Mallik et al., 2010, 2011]*. This approach can be used to enhance the selective interaction *via* multiple interactions based on the precise arrangement of weak interaction groups. Also, Mallik et al. have reported the first complete baseline separation of *β*-and *γ*-isomers of tocopherol (vitamin E) with alternating copolymer, poly(octadecyl acrylate-*alt*-*N*-octadecylmaleimide)-grafted silica (Sil-*alt*-P) in reversed-phase high-performance liquid chromatography (RP-HPLC). For the hybridization of silica with the polymer, 3-mercaptopropyltrimethoxysilane (MPS) was introduced onto silica by using the reactive trimethoxysilyl groups and then the copolymerization with octadecyl acrylate (ODA) and *N*-octadecyl-*β*-alanyl maleimide was carried out through surface-initiated radical-chain transfer reaction (Scheme 14). The molecular recognition ability of Sil-*alt*-P was evaluated by liquid chromatographic separation with a packed column of copolymer-silica hybrids and compared with conventionally used C_{18} and C_{30} columns. The first examination was carried out with two nonplanar and planar polycyclic aromatic hydrocarbons (*o*-terphenyl and triphenylene, respectively) having the same number of carbon atoms and π-electrons. Newly developed alternating copolymer-grafted silica (Sil-*alt*-P) showed much higher molecular recognition ability than commercially available hydrophobized silica such as monomeric and polymeric C_{18} and C_{30} phases. One of the driving forces for the separation was derived from multiple carbonyl-π interaction due to the high interaction aspect ratio.

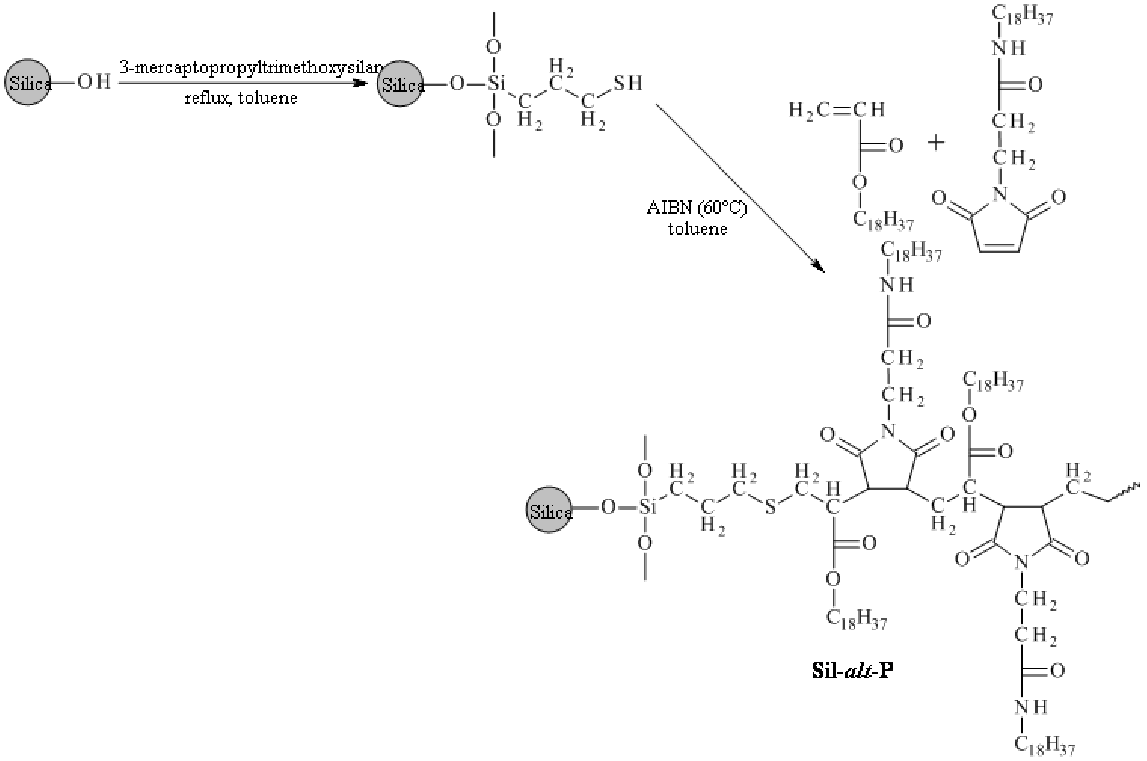

Scheme 14. Alternating copolymerization from MPS modified silica with octadecyl acrylate and *N*-octadecyl-*β*-alanyl maleimide

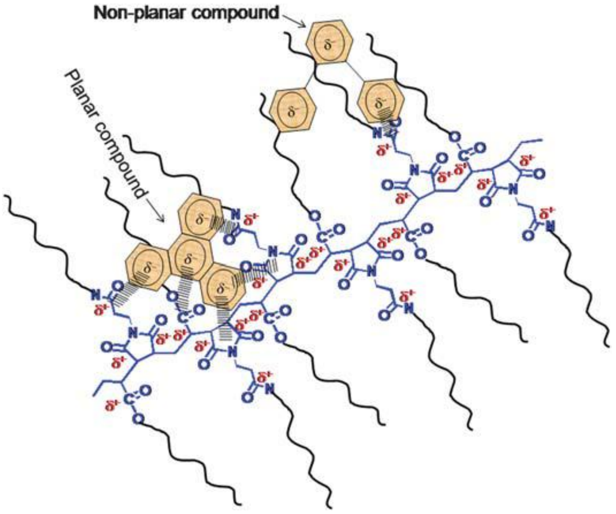

Figure 7. Schematic illustration to explain the molecular planarity selectivity of Sil-*alt*-P with a larger interaction aspect ratio of weak interaction sites (carbonyl–π interaction) for the planar triphenylene than the nonplanar *o*-terphenyl

The separation capability of Sil-*alt*-P can be described by direct interaction with the integrated π-electron containing carbonyl groups oriented by alternating copolymerization along the rigid polymer main chain, which is enhanced by increasing the interaction aspect ratio for planar molecules rather than the non-planar one. It is easy for the planar molecule to penetrate into the interaction sites of the stationary phase and elutes later than the non-planar compound due to less penetration as shown in Figure 7. The first baseline separation of tocopherol isomers by grafting the new phase on 5 μm particle size silica indicates this type of phase will open a new door in separation science to solve separation challenges for the isomers of bioactive compounds.

Reversible Diels–Alder chemistry was exploited to develop polymer films in which a change in optical clarity can be thermally triggered. SiO_2 nanoparticles of various sizes (100 and 40 nm in diameter) were functionalized with maleimide moieties. A furyl-terminated poly(ethylene glycol) linker was prepared and tethered to the SiO_2 nanoparticles via a DA linkage *[Costanzo and Beyer, 2007]* (Scheme 15).

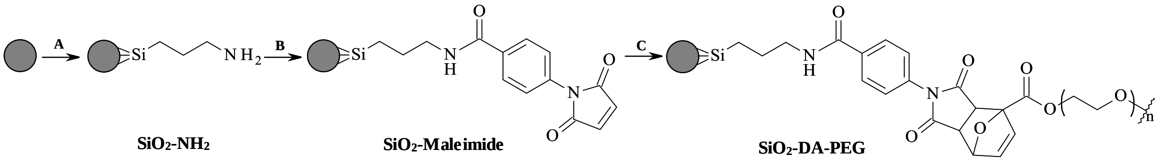

Scheme 15. Synthetic route for preparation of SiO_2-DA-PEG nanoparticles

The pegylated SiO_2 nanoparticles were randomly distributed within a poly(methyl methacrylate) matrix, resulting in an optically transparent film. Annealing the film cleaves the DA linkage and effectively renders the SiO_2 particles immiscible within the poly(methyl methacrylate) matrix creating a driving force for particle aggregation. The large aggregates were able to scatter light and resulted in an optically opaque film.

The bismaleimide nanocomposites filled with surface-modified SiO_2 nanoparticles by silane coupling agent *N*-(2-aminoethyl)-*γ*-aminopropylmethyl dimethoxy silane (JH-53) showed better wear resistance and lower frictional coefficient than that with the unmodified nanoparticles SiO_2 *[Yan et al., 2008]* (Scheme 16). The specific wear rate and the steady frictional coefficient of the composite with 1.0 wt % surface-modified SiO_2 nanoparticles are only 1.8×10^{-6} $mm^3/N\ m$ and 0.21, respectively. The severe fatigue wear of the neat resin matrix can be changed into slight adhesive wear with the addition of the suitable content of SiO_2 nanoparticles. The surface-modified of SiO_2 nanoparticles by *N*-(2-aminoethyl)-*γ*-amino-propylmethyl dimethoxy silane can distribute relative uniform in resin matrix. The different tribological behavior of the resin matrix and the filled composites should be dependent on their different mechanical properties and wear mechanism.

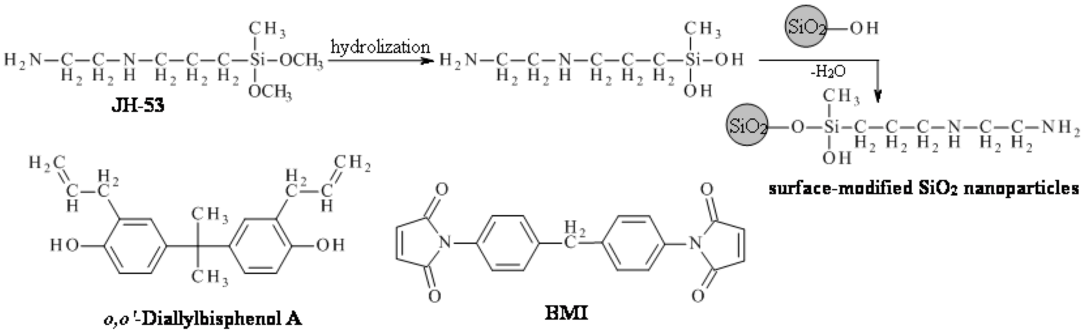

Scheme 16. The components of bismaleimide nanocomposites

Grafting free maleimide and epoxide pendant groups onto the surface of ~7-nm silica nanoparticles *via* a silylation condensation reaction using 3-glycidyloxypropyltrimethoxysilane (GPTS) and 3-aminopropyltrimethoxysilane (APTS) leads to advance nanocomposite materials *[Vejayakumaran et al., 2008]*. The maleimide groups were incorporated by nucleophilic addition of BMI monomers with amine groups grafted to the silica surface (Scheme 17). The epoxide groups and amine groups were grafted to the silica surface.

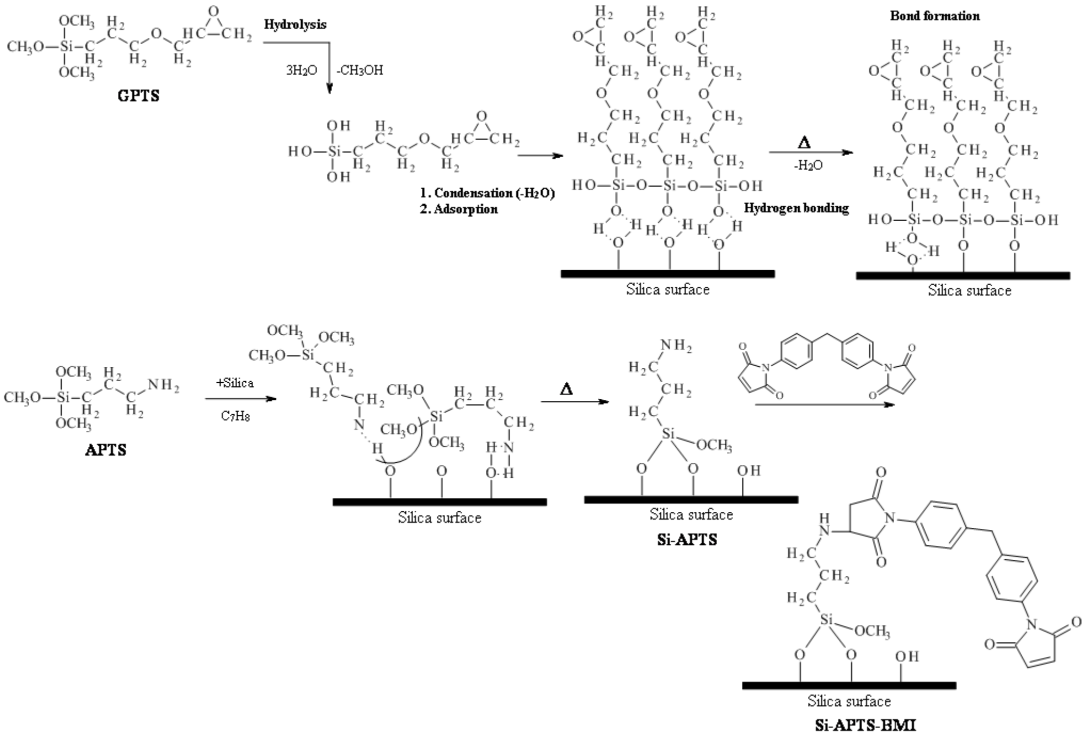

Scheme 17. Reaction scheme between APTA (GPTS) and silanol groups of silica, and Si-APTS and BMI

Compared to the precursor of SiO_2, the precursor of TiO_2, tetrabutyl titanate, is much more reactive, and its hydrolysis rate is much higher than that of TEOS; this makes its aggregation much easier during the sol-gel process. To overcome this problem, several methods have been developed to lower the hydrolysis rate of tetrabutyl titanate: (1) adding organic acids or β-diketones such as acetyl acetone as chelating agents to coordinate with tetrabutyl titanate and then reducing its hydrolysis rate; (2) dropwise adding acidified water and alcohol into tetrabutyl titanate to avoid aggregation; (3) hydrolyzing without adding water, that is, using water in air (humidity = 60%) to slowly hydrolyze tetrabutyl titanate; and (4) using the inverse-adding method, that is, adding tetrabutyl titanate to HCl-acidified water.

So, ternary hybrids of bismaleimide–polyetherimide–titania were synthesized by sol–gel reaction using dibutoxy bis(acetylacetonato) titanium (IV) *[Zhao et al., 2004]*. The bismaleimide resin was pre-polymerized with 2,2'-diallyl bisphenol A to improve its solubility before preparing hybrids and mixed with polyetherimide (PEI) prepared from bisphenol A dianhydride and 4,4'-[1,3-phenylenebis(1-methyl-ethylidene)]bisaniline. The titania particles dispersed in the hybrids uniformly and the titania content in BMI rich phase was higher than that in PEI rich phase. The introduction of titania did change the morphology of BMI–PEI blends. However, the final phase structure of BMI–PEI–TiO_2 hybrids was not affected apparently by the increasing content of titania under a given content of PEI. The mechanical properties of the hybrids were improved with increasing titania content, while the thermal decomposition temperatures of the hybrids deceased because of catalytic decomposition of titania to the BMI resin. These hybrids have the potential application of high-performance composites.

4,4'-Bismaleimidodiphenyl methane modified novolak resin/titania nanocomposites were prepared by the sol–gel process of tetrabutyl titanate in the presence of 4,4'-bismaleimidodiphenyl methane modified novolak resin prepolymers with acetyl acetone as a stabilizer *[Lu et al., 2006]*. Tetrabutyl titanate was transformed into TiO_2 through hydrolysis and condensation, and the inorganic phase was linked with the resin matrix through ether groups produced by a condensation reaction during the curing process. The involved reactions are shown in Scheme 18. The average diameter of the primary particles of the dispersed phase was about 150 nm, but there existed particle aggregates. The introduction of the TiO_2 inorganic nanophase did not enhance the *Tg*’s of the nanocomposites but lowered the thermal resistance of the material because of the incomplete decomposition of acetyl acetone coordinated with tributyl titanate; it improved the modulus of the material at lower temperatures (<200°C) but lowered the modulus of the material at higher temperatures (>250°C). The polymer composites filled with nanoparticles have good friction and wear properties and widely used in many fields. The performances of nanocomposites are influenced extensively by the nanoparticles morphology, size, volume fraction and dispersion.

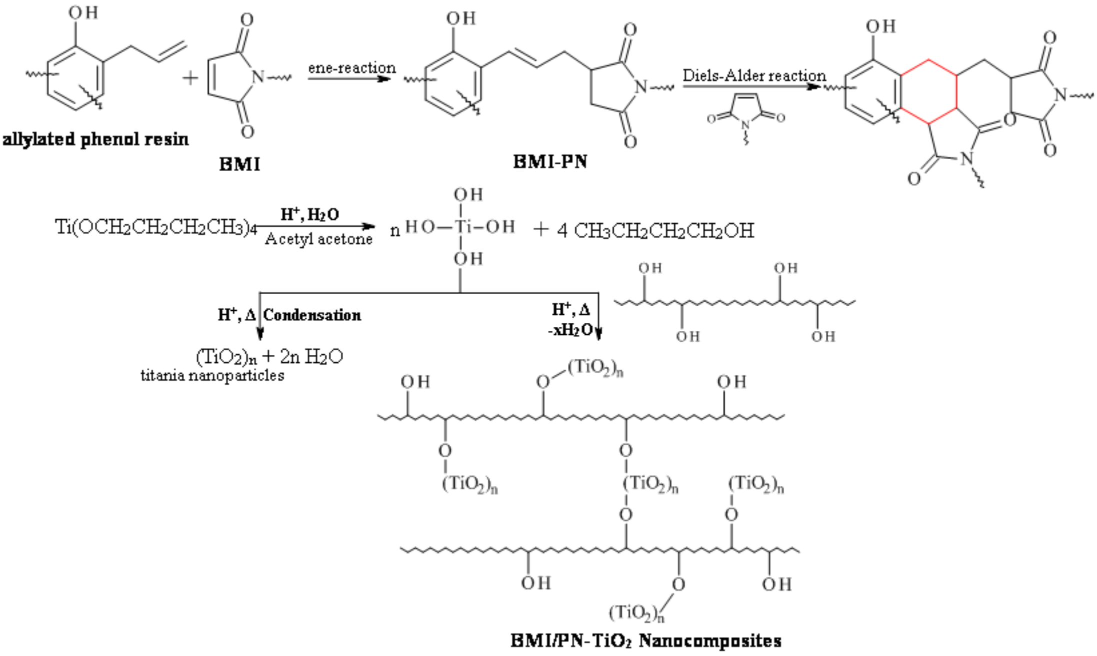

Scheme 18. Reactions involved in the preparation of the BMI-PN/TiO_2 nanocomposites

Nanometer SiC particles have good properties, lower prices and shows good foreground in resist-materials of polymer composites. Yan et al. have prepared nanocomposites of bismaleimide pre-polymer (consist of 4,4'-bismaleimido-diphenylmethane and 2,2'-diallyl bisphenol A) with different proportions of nanometer SiC, by a high shear dispersion process and casting method at elevated temperature *[Yan et al., 2005]*. The nanocomposite of BMI exhibited lower friction coefficient and wear loss as well as higher bending and impact strength than BMI resin under the same testing conditions. The lowest wear rate was obtained with the nanocomposite containing 6.0 wt % SiC, while the highest mechanical properties were obtained with the nanocomposite containing 2.0 wt % SiC. The wear mechanism of the nanocomposite is mainly adhesion wear, while that of pure BMI resin is mainly fatigue cracking with plastic deformation.

Continuing the research on nanocomposites based on the same bismaleimide pre-polymers, Yan et al. have studied the effect of nanometer ZrO_2 content and silane coupling agent (*N*-(2-aminoethyl)-γ-aminopropylmethyl dimethoxy silane) on the friction and wear properties of BMI composites filled with nanometer ZrO_2 *[Yan et al., 2007]*. The composites filled with untreated ZrO_2 and treated ZrO_2 are prepared by the same way of mechanical high shear dispersion process and casting method. The sliding wear performance of the nanocomposites is studied on an M-200 friction and wear tester. The experimental results indicate that the frictional coefficient and the wear rate of the composites can be reduced by filled with nanometer ZrO_2. The composites containing treated nanometer ZrO_2 have better tribological performance than that containing untreated nanometer ZrO_2. The results are explained from the SEM morphologies of the worn surface of matrix resin and the composites containing nanometer ZrO_2 and the TEM photographs of the nanometer ZrO_2 dispersion in the matrix.

Montmorillonite (a layered material with lamellar shape) has attracted intense research interest for the preparation of polymer-clay nanocomposites because its lamellar elements display high in-plane strength, stiffness, and high aspect ratio. Typically, the chemical structures of MMT consist of two fused silica tetrahedral sheets sandwiching an edge-shared octahedral sheet of either magnesium or aluminium hydroxide. The organic compounds and polymers could be intercalated into the MMT layers due to the easy exchange of these inorganic cations with organic cations. This intercalation increases the spacing between the MMT sheets and even leads to the complete dissociation of the sheets to form a MMT/organic composite with a nanometer scale.

Nanocomposites of organo(cetyltrimethylammonium bromide)-modified MMT (OMMT) and Na^+-MMT intercalated by styrene-*N*-phenyl maleimide copolymer were prepared by emulsion intercalative polymerization *[Liu et al., 2005]*. X-ray diffraction and transmission electron microscopy results show that the interaction between the clay layer and the copolymer was greatly strengthened by the incorporation of *N*-phenyl maleimide. The dispersability of OMMT in the matrix is much better than that of MMT. On the other hand, styrene-*N*-phenyl maleimide copolymer/MMT composites and styrene-*N*-phenyl maleimide copolymer/OMMT composites have nearly the same thermal, polymer loading, and rheological properties.

Wang et al. have used *p*-phenylenediamine as swelling agent for sodium-montmorillonite (Na–MMT) in the synthesis of bismaleimide-modified novolac resins/MMT nanocomposites *[Wang et al., 2005]*. One amine group of *p*-phenylenediamine was converted into cation by neutralization with hydrochloric acid. Intercalation of *p*-phenylenediamine to Na–MMT took place as the cations in the gallery were exchanged by the protonated molecules, which formed ionic bonds with the negatively charged clay layer, as shown in Figure 8. The remaining amine group of the swelling agent was reacted with maleic anhydride to form maleamic acid. Organoclay thus obtained was easily exfoliated in the bismaleimide-modified novolac resin. Maleamic acid was converted into maleimide and copolymerized with bismaleimide-modified novolac upon curing. TEM studies on the microstructure of bismaleimide-modified novolac resins/maleamic acid-modified MMT nanocomposite in comparison with bismaleimide-modified novolac resins/Na-MMT nanocomposite show that, in the first case, many exfoliated silicate layers of thickness about 1 nm, along with some thicker platelets, are dispersed in the polymer matrix.

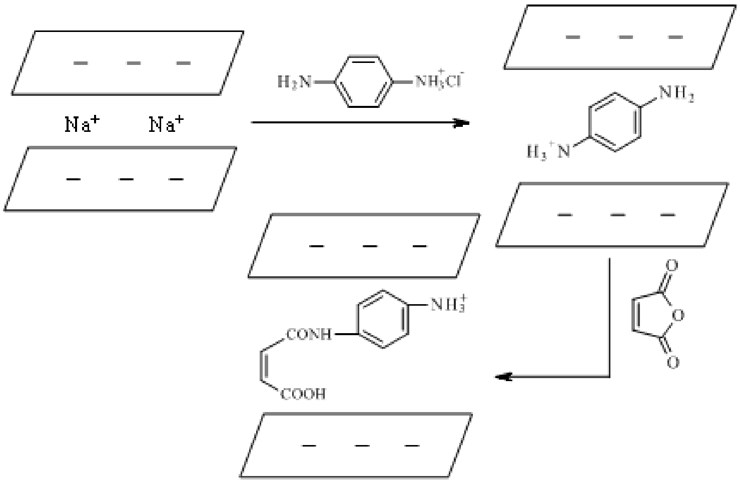

Figure 8. Intercalation of MMT by the swelling agents

The space between silicate layers appears to range from 10 to 30 nm. By contrast, fewer exfoliated clay layers and more multiples are present in the TEM micrographs for the bismaleimide-modified novolac resins/Na–MMT nanocomposite. Delamination of the organo-MMT in the resin gives rise to a tremendous increase in viscosity. Major improvements in thermal stability, mechanical strength, and stiffness have been achieved by incorporation of the exfoliated clay nanolayers.

Novel hybrid materials were reported by Soylemez et al. by interlamellar complex-radical (co)terpolymerization of intercalated monomer complexes of maleic anhydride (MA) and itaconic acid (IA) with dimethyl dodecylamine (DMDA) surface modified MMT, *n*-butyl methacrylate (BMA) and/or BMA/styrene monomer mixtures *[Soylemez et al., 2008]*. The complex formation of MA (or IA) and its (co)terpolymers with DMDA surface modified silicate layers plays an important role in the interlamellar co(ter)polymerization reactions and intercalation/exfoliation of polymer chains between silicate galleries. It was shown that the intercalation/exfoliation behaviour of functional (co)terpolymers, and therefore, the formation of nano-structure depend on the hydrophilic/hydrophobic balance in amphiphilic terpolymers, amount of flexible BMA linkages and interlayer complex-formation between anhydride/acid units and surface alkylammonium fragments (Figure 9). Addition of DMDA-MMT as a complex-forming agent has catalytic effect in the complex-radical polymerization by increasing copolymer yield. In order to increase the effectiveness of intercalation process and therefore, the formation of nanostructures in the studied system, MA or IA monomers were dispersed between silicate galleries before copolymerization reactions. So, two carbonyl or carboxylic groups of the MA or IA monomer molecule interact with two neighbouring silicate platelet surfaces having tetrahedral structures, which contain alkyl ammonium captions, through interlayer complex or strong H-bonding.

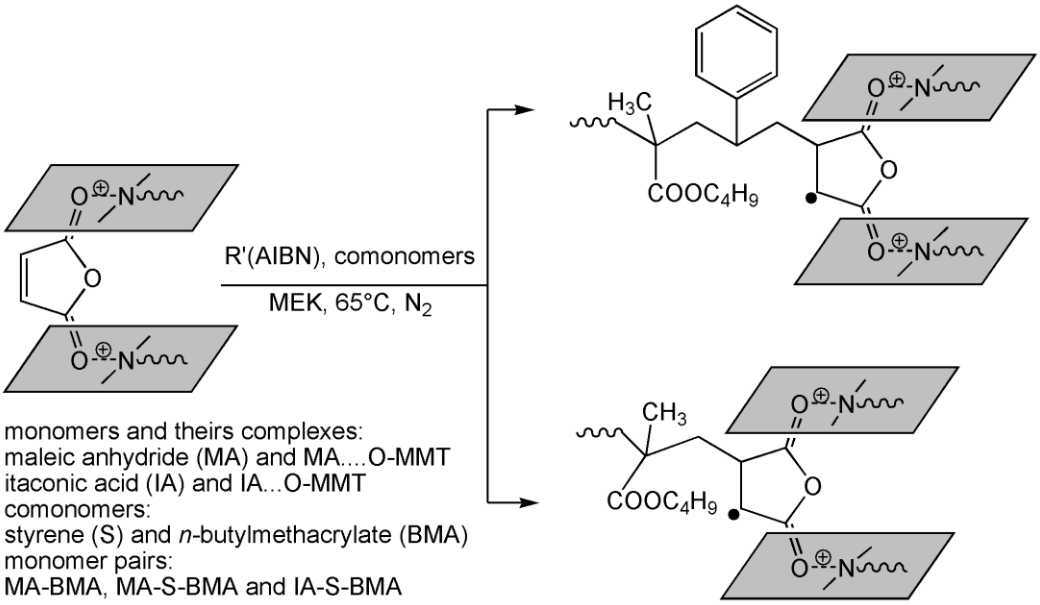

Figure 9. Schematic representation of interlamellar complex-radical (co)terpolymerization

The obtained hybrids show significant increase in the thermal and dynamic mechanical behaviour and crystallinity due to the homogeneous dispersion of the silicate nano-galleries in the functional (co)terpolymer matrix. Synthesized polymer hybrids may be also used as reactive compatibilizer-nanofillers for the thermoplastic polymer blends, especially for the acrylic and styrene polymer-based systems, and to prepare the various nanomaterials in melt by reactive extrusion *in situ* processing.

4. Organic-inorganic hybrid materials with functionalized organotrialkoxysylane

Regarding the coupling agents used for introducing covalent bonds in hybrid materials, several methods have been used for functionalizing the desired compounds with such agents. We can mention here Michael addition of aminotriethoxysilanes to the maleimidic double bond, Diels-Alder cycloaddition of a dienic triethoxysilane compound with the maleimidic group as a dienophile and ring opening reactions (e.g. epoxide ring opening by aminotriethoxysilanes).

For example, Michael addition reaction was used for preparing polystyrene/silica hybrids *[Jothibasu et al., 2007]*. For this purpose, polystyrene has been functionalized with maleimide groups and then, the organic–inorganic transparent polymer hybrids were obtained from the sol–gel reaction of TEOS in the presence of maleimide substituted polystyrene and APTES as coupling agent (according to scheme 19). In the absence of APTES only turbid films were obtained, since the uniform dispersion of maleimide substituted styrene in the siloxane network is influenced by the amino group of APTES (when used) which prevents the aggregation of the organic polymer.

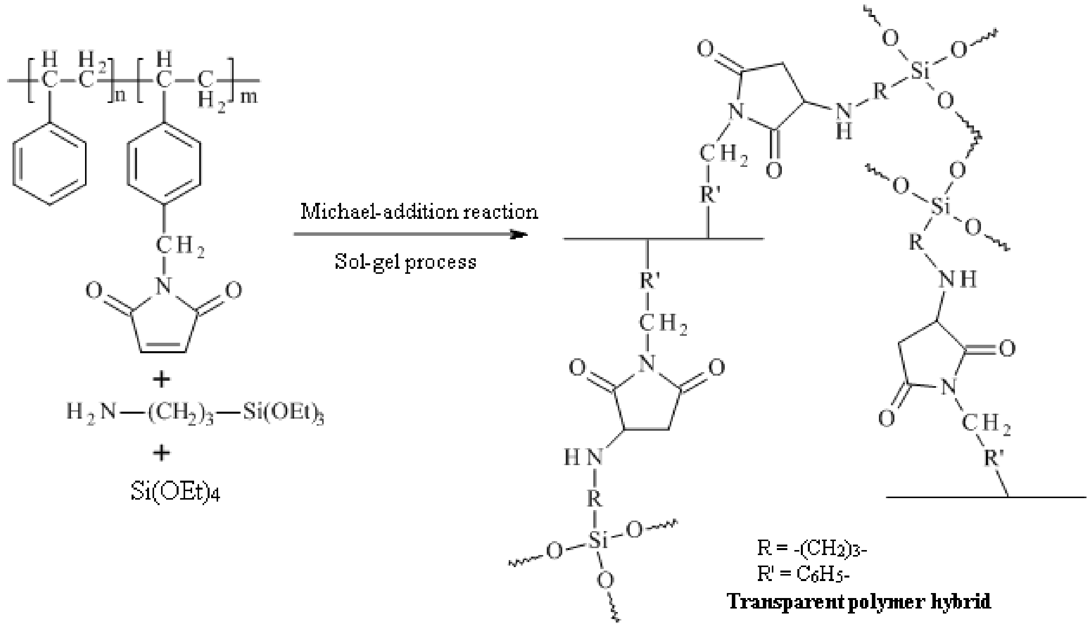

Scheme 19. The formation of organic-inorganic polymer hybrids by the sol-gel reaction of TEOS in the presence of maleimide functionalized polystyrene and APTES

The presence of bonding between polymer and siloxane network is also suggested by the increasing of T_g value in the case of hybrid polymers (the chemical bonding between these two phases retards the molecular relaxation of the organic polymer leading to a higher T_g value). The transparent hybrid polymer exhibits excellent solvent resistance towards THF. Normally, the thermal stability of the polymer hybrid is higher when compared with that of the individual polymer, but in the presented study, it was observed a decrease in thermal stability of the polymer hybrid. The authors ascribe this to the thermal instability of APTES. In addition, the presence of unreacted alkoxy groups, and the presence of weak amine linkages imparted by Michael-addition reaction during the formation of polymer hybrid may also be a cause for the lower initial degradation temperature. Nanometer sized dispersion of polymer in the siloxane matrix was confirmed by nitrogen porosimetry study and was found to be around 4 nm. The transparent polymer hybrids developed in this work were expected to find application in the field of optoelectronics and in solar cells.

Styrene based hybrid materials have been also obtained by the sol-gel reaction of TEOS in the presence of furyl functionalized polystyrene using as crosslinking agent a maleimide-modified alkoxysilane, M-TEOS *[Adachi et al., 2004]*. This crosslinking agent will introduce (by a DA reaction with the modified polystyrene) covalent bonds between the organic and inorganic phases (Scheme 20).

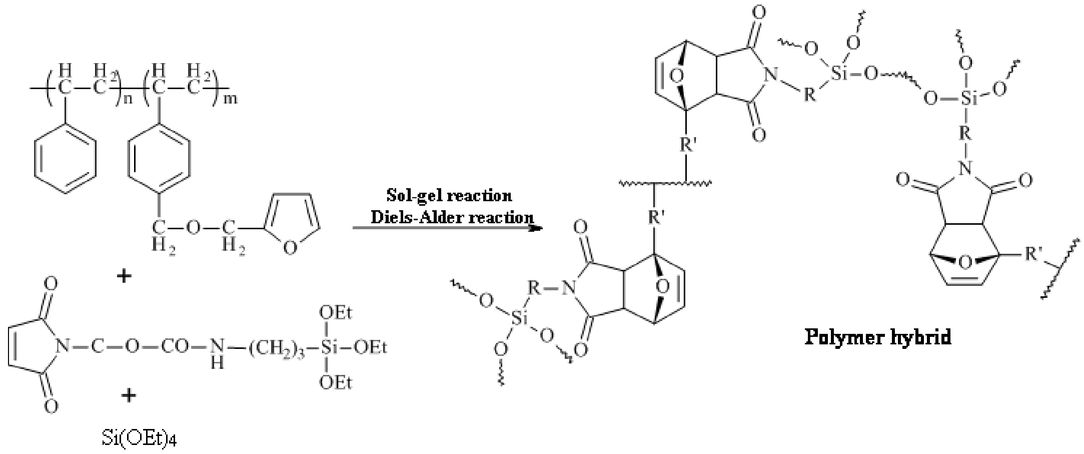

Scheme 20. Synthesis of polymer hybrids using DA reaction

The reaction was conducted in the presence or absence of the coupling agent and at different temperatures. In the absence of M-TEOS, just like in the case presented above, turbid films were obtained. Also, this phenomenon took place when M-TEOS was used, but the reaction was conducted at room temperature while at 60 and 90°C transparent films were obtained (Figure 10). The explanation given by the authors is the following: in solutions of furyl modified polystyrene, M-TEOS, TEOS and acid catalyst, both sol-gel and DA reaction occur simultaneously, the homogeneity of the obtained material being affected by the rate of these two reactions. The sol-gel reaction at room temperature is slower than at 60 or 90°C. At room temperature, the DA reaction between maleimide groups and furan groups might be much faster than gelation of alkoxysilanes. At 60 and 90°C, simultaneous DA reaction and gelation of alkoxysilanes which disperse maleimide groups into silica matrix might be carried out. This uniform dispersion of maleimide groups prevents aggregation of organic polymer by the DA reaction at various points in the polymer chain.

The thermal stability of these hybrid materials was comparable to the one of the hybrid materials described above (where a Michael addition reaction was used to functionalize the modified polystyrene with the coupling agent).

The ring opening reaction is used, for example, for functionalizing epoxy resins with coupling agent in order to obtain hybrid materials. Alagar et al. have synthesized various coupling agents and used them for coupling hydroxyl terminated polydimethylsiloxane with epoxy matrix and cured with hexamethylenediamine and diaminodiphenylmethane *[Alagar et al.]*. The

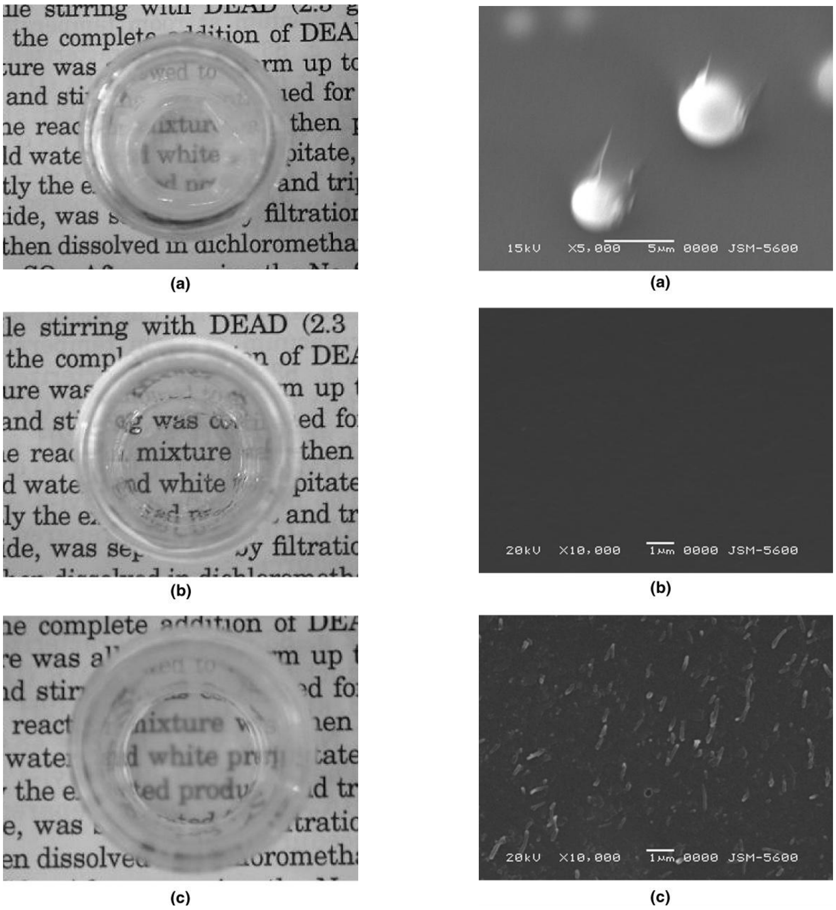

Figure 10. Optical (left) and SEM (right) images of transparent DA polymer hybrid and turbid composite: (a) prepared without M-TEOS; (b) prepared with M-TEOS at 60 °C; (c) prepared with M-TEOS at room temperature *[Reprinted with permission from Macromol. 2004, 37, 9793-9797 © 2004, American Chemical Society]*

coupling agents used were 3-[(2-aminoethyl)amino]propyltrimethoxysilane (AETMS), 3-[(2-maleicmonoamido)maleicmonoamido]propyltrimethoxysilane (MMTMS) and 3-[(2-maleicdiamido)maleicdiamido]propyltrimethoxysilane (MDTMS) and were obtained according to the scheme below (Scheme 21).

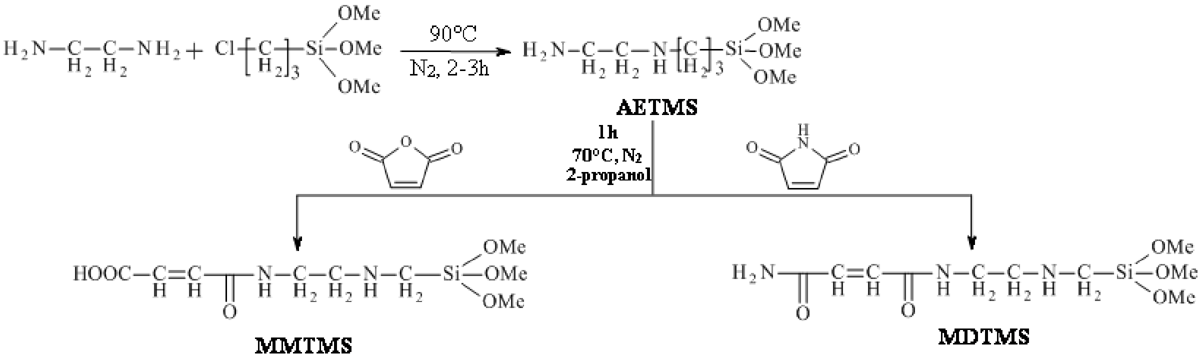

Scheme 21. Synthetic route for the preparation of silane coupling agents

Formation of siliconized epoxy interpenetrating polymer network with silane coupling agents in the presence of dibutyl tindilaurate catalyst may occur in two stages. The first stage involves the reaction between the epoxide ring of the epoxy resin and primary and secondary amino groups of AETMS and MDTMS, and secondary amino group and carboxyl group of MMTMS. In the second stage, the methoxy groups of silane coupling agents (AETMS, MMTMS and MDTMS) react with hydroxyl groups of hydroxyl terminated polydimethylsiloxane. The siliconized epoxy matrix systems prepared as described above have high crosslink density due to the presence of multifunctional reactive sites. Since MDTMS has the higher functionality (pentafunctional) among these coupling agents, it was an expecting thing that it exhibits a higher reactivity than AETMS and MMTMS. Also, using MDTMS as coupling agent and diaminodiphenylmethane for the curing process leads to a higher glass transition temperature and a better thermal stability of the hybrid system. The authors concluded that among the silane coupling agents developed in this study, MDTMS is more suitable for the development of advanced siliconized epoxy composites.

A coupling agent was also used for introducing covalent bonds, between the organic and inorganic parts, through a ring opening reaction which involves a succinimidic ring of a polyetherimide. Li et al. have synthesized bismaleimide-polyetherimide-silica (BMI/PEI/SiO_2) hybrids using APTES as coupling agent *[Li et al., 2005]*. First, they synthesized polyetherimide and a pre-polymerized BMI-resin (obtained from bis(4-maleimidodiphenyl)methane and o,o'-diallyl bisphenol A in a 57:43 weight ratio), which were further used, besides APTES and TEOS, for the preparation of BMI/PEI/SiO_2 hybrids. The BMI/PEI weight ratio was maintained constant (100:30) and so did the PEI/APTES weight ratio (10:1) when used, while the amount of TEOS was varied. When not using APTES transparent films were obtained only at a 0 and 5 wt% of TEOS while for 10, 15, 20 and 25 wt% of TEOS opaque films were obtained. If using APTES, except for 25 wt% of TEOS, all the films were transparent.

The thermal decomposition temperature of the hybrids increased with the content of silica from 382°C (0 % TEOS) to 418°C (20 wt% TEOS). Regarding the mechanical properties, the Young's moduli and tensile strength increased greatly with increasing the silica content while the elongations at break of the hybrids decreased when increasing the content of silica. The morphology of the films has been investigated using scanning electron microscopy. The PEI/BMI blend showed co-continues or phase-inversion structure with the BMI spherical particles dispersed in the PEI rich matrix when the content of PEI is 30 phr (per hundred of BMI resin) (Figure 11a). When silica is introduced into the blend PEI/BMI with 30 phr PEI content (Figure 11b), the hybrid maintains a phase inversion structure and the silica is dispersed uniformly in both PEI rich phase and BMI rich phase (Figure 11c and 11d). The molecular weight of PEI has a

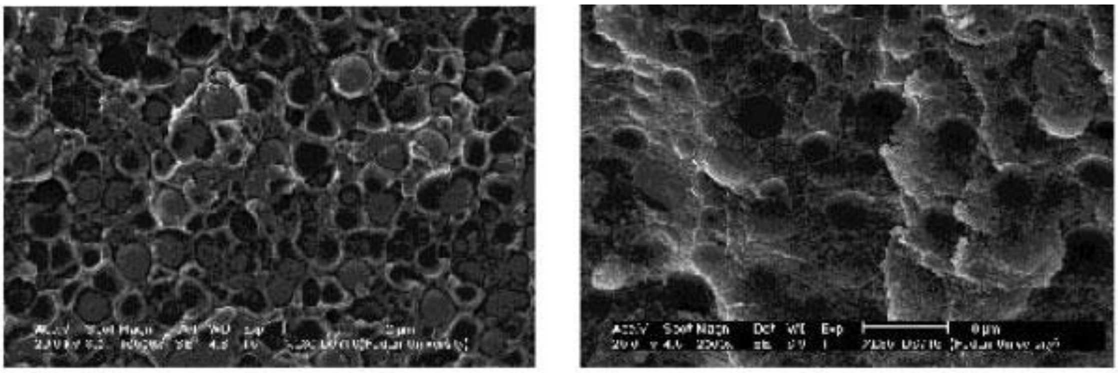

a. SEM photographs of the PEI/BMI blend, PEI 30phr M_w=26000

b. SEM photographs of the PEI/BMI/SiO_2 hybrid, PEI 30phr M_w=26000, TEOS 10wt %

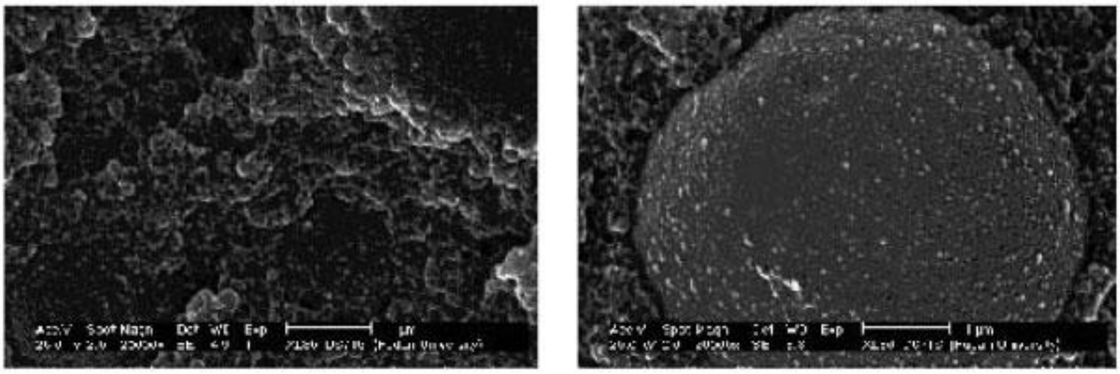

c. SEM photographs of PEI rich phase of the PEI/BMI/SiO_2 hybrid, PEI 30phr M_w=26000, TEOS 10wt %

d. SEM photographs of BMI rich phase of the PEI/BMI/SiO_2 hybrid, PEI 30phr M_w=26000, TEOS 10wt%

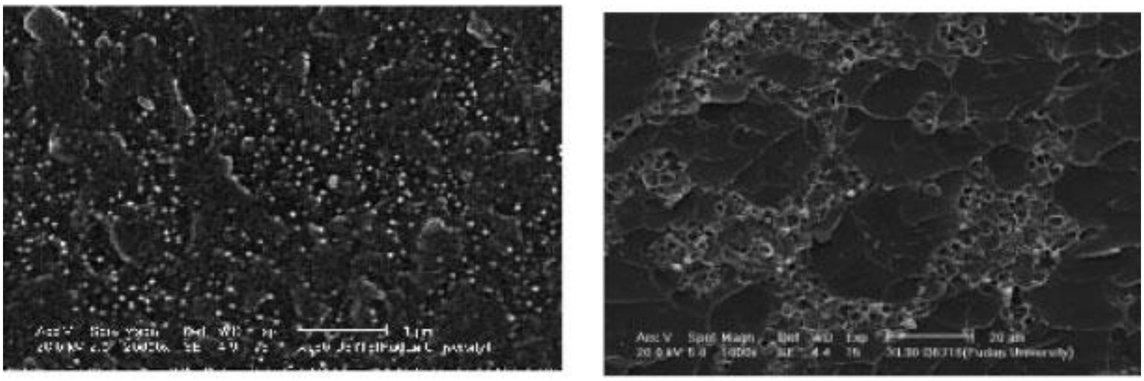

e. SEM photographs of the PEI/BMI/SiO2 hybrid, PEI 30phr M_w=5800, TEOS 10wt %

f. SEM photographs of the PEI/BMI/SiO2 hybrid, PEI 20phr M_w=26000, TEOS 10wt %

Figure 11. SEM micrographs of blend and hybrids *[Reprinted with permission from Polym. Adv. Technol. 2005, 16, 133-138 © 2005 John Wiley and Sons]*

great effect on the morphology of the blends of PEI/BMI, the same phenomena being observed for the BMI/PEI/SiO_2 hybrids. In the case of the hybrid with 30 phr PEI content the phase-inversion structure was observed in the sample with high molecular weight (M_w=26,000, Figure 11b), while the spherical structure could be observed in the sample with low molecular weight (M_w=5800, Figure 11e).

5. Conclusion

As has been discussed within this review, a very wide range of material properties can be generated by combining the appropriate features of a given inorganic metal moiety with those of appropriately selected organic species. In some cases, these two different types of moieties can be directly bonded to each other to build a hybrid network, while in other cases just strong seconding bonding interactions promote the miscibility of the different components.

It is expected that over the next decade, numerous such materials will enter into the marketplace and serve an important function in the ever growing field of materials science.

6. References

Adachi K., Achimuthu A. K., Chujo Y. (2004) Synthesis of organic-inorganic polymer hybrids controlled by Diels-Alder reaction, *Macromol.,* Vol. 37, No 26, pp. 9793-9797.

Alagar M., Ashok Kumar A., Anand Prabu A., Rajendran A. (2004) Modification of siliconized epoxy resin using multifunctional silanes, *Int. J. Polym. Mater.,* Vol. 53, No 1, pp. 45-58.

Altintas Z., Karatas S., Kayaman-Apohan N., Gungor A. (2011) The maleimide modified epoxy resins for the preparation of UV-curable hybrid coatings, *Polym. Adv. Technol.,* Vol. 22, No 2, pp. 270-278.

Brown Jr J. F., Vogt Jr L. H., Katchman A., Eustance J. W., Kiser K. M., Krantz K. W. (1960) Double chain polymers of phenylsilsesquioxane, *J. Am. Chem. Soc.*, Vol. 82, No 23, pp. 6194–6195.

Cao H., Xu R., Yu D. (2008) Thermal and dielectric properties of bismaleimide-triazine resins containing octa(maleimidophenyl)silsesquioxane, *J. Appl. Polym. Sci.,* Vol. 109, No 5, pp. 3114-3121.

Costanzo P. J., Beyer F. L. (2007) Thermoresponsive, optically active films based on Diels-Alder chemistry, *Chem. Mater.,* Vol. 19, No 25, pp. 6168-6173.

dell’Erba I. E., Fasce D. P., Williams R. J. J., Erra-Balsells R., Fukuyama Y., Nonami H. (2003) Poly(silsesquioxanes) derived from the hydrolytic condensation of organotrialkoxysilanes containing hydroxyl groups, *J. Organomet. Chem.*, Vol. 686, No 1-2, pp. 42-51.

Fasce D. P., Williams R. J. J., Méchin F., Pascault J. P., Llauro M. F., Pe´tiaud R. (1999) Synthesis and characterization of polyhedral silsesquioxanes bearing bulky functionalized substituents, *Macromolecules*, Vol. 32, No 15, pp. 4757-4763.

Gomez-Romero P., Sanchez C. (2004) In: *Functional hybrid materials*, Wiley-VCH Weinheim.

Hu J., Gu A., Liang G., Zhuo D., Yuan L. (2011) Preparation and properties of mesoporous silica/bismaleimide/diallylbisphenol composites with improved thermal stability, mechanical and dielectric properties, *Express Polym. Lett.*, Vol. 5, No 6, pp. 555-568.

Hu J. T., Gu A., Liang G., Zhuo D., Yuan L. (2011) Preparation and properties of high-performance polysilsesquioxanes/bismaleimide-triazine hybrids, *J. Appl. Polym. Sci.*, Vol. 120, No 1, pp. 360-367.

Huang F., Rong Z., Shen X., Huang F., Du L., Li Z. (2008) Organic/inorganic hybrid bismaleimide resin with octa(aminophenyl)silsesquioxane, *Polym. Eng. Sci.*, Vol. 48, No 5, pp. 1022-1028.

Huang F., Huang F., Zhou Y., Du L. (2010) Thermal properties of new bismaleimide resins containing hydrogen silsesquioxane and diallyl bisphenol A, *J. Appl. Polym. Sci.*, Vol. 117, No 5, pp. 2932-2936.

Imai Y., Itoh H., Naka K., Chujo Y. (2000) Thermally reversible IPN organic-inorganic polymer hybrids utilizing the Diels-Alder reaction, *Macromol.*, Vol. 33, No 12, pp. 4343-4346.

Jothibasu S., Ashok Kumar A., Alagar M. (2007) Synthesis of maleimide substituted polystyrene-silica hybrid utilizing Michael addition reaction, *J. Sol-Gel Sci. Tehnol.*, Vol. 43, No 3, pp. 337-345.

Jothibasu S., Premkumar S., Alagar M., Hamerton I. (2008) Synthesis and characterization of a POSS-maleimide precursor for hybrid nanocomposites, *High Perform. Polym.*, Vol. 20, No 1, pp. 67-85.

Judenstein P., Sanchez C (1996) Hybrid organic-inorganic materials: a land of multidisciplinarity, *J. Mater. Chem.*, Vol. 6, No 4, pp. 511-525.

Krishnan P. S. G., He C., Shang C. T. S. (2004) Synthesis, characterization, and curing kinetics of novel ladder-like polysilsesquioxanes containing side-chain maleimide Groups, *J. Polym. Sci. : Part A: Polym. Chem.*, Vol. 42, No 16, pp. 4036-4046.

Krishnan P. S. G., He C. (2005) Octa(maleimido phenyl) silsesquioxane copolymers, *J. Polym. Sci. : Part A: Polym. Chem.*, Vol. 43, No 12, pp. 2483-2494.

Li S., Tian J., Gan W., Zhao L., Li L., Wang J. (2005) Synthesis and characterization of bismaleimide-polyetherimide-silica hybrid by sol-gel process, *Polym. Adv. Technol.*, Vol. 16, No 2-3, pp. 133-138.

Li W., Liu F., Wei L., Zhao T. (2007) Allylated novolac/4,4’-bismaleimidodiphenylmethane resin containing polyhedral oligomeric silsesquioxane: preparation, morphology and thermal stability, *J. Appl. Polym. Sci.*, Vol. 104, No 6, pp. 3903-3908.

Liu G., Zhang L., Li Z., Qu X. (2005) Synthesize and characterization of styrene-*N*-phenyl maleimide/montmorillonite nanocomposites prepared through emulsion polymerization, *J. Appl. Polym. Sci.*, Vol. 98, No 3, pp. 1010-1015.

Liu Y. L., Chang G. P., Wu C. S., Chiu Y. S. (2005) Preparation and properties of high performance epoxy-silsesquioxane hybrid resins prepared using a maleimide-alkoxysilane compound as a modifier, *J. Polym. Sci.: Part A: Polym. Chem.*, Vol. 43, No 23, pp. 5787-5798.

Liu Y. L., Lee H. C. (2006) Preparation and properties of polyhedral oligosilsesquioxane tethered aromatic polyamide nanocomposites through Michael addition between maleimide-containing polyamides and amino-functionalized polyhedral oligosilsesquioxane, *J. Polym. Sci.: Part A: Polym. Chem.*, Vol. 44, No 15, pp. 4632-4643.

Lu G. T., Huang Y. (2002) Synthesis of polymaleimide/silica nanocomposites, *J. Mater. Sci.*, Vol. 37, No 11, pp. 2305-2309.

Lu G., Huang Y., Yan Y., Zhao T., Yu Y. (2006) 4,4'-Bismaleimidodiphenylmethane modified novolak resin/titania nanocomposites: preparation and properties, *J. Appl. Polym. Sci.*, Vol. 102, No 1, pp. 52-57.

Mallik A. K., Sawada T., Takafuji M., Ihara H. (2010) Novel approach for the separation of shape-constrained isomers with alternating copolymer-grafted silica in reversed-phase liquid chromatography, *Anal. Chem.*, Vol. 82, No. 8, pp. 3320-3328.

Mallik A. K., Qiu H., Takafuji M., Ihara H. (2011) Strategic achievement for the baseline separation of tocopherol isomers by integration of weak interaction sites on alternating copolymer, *Anal. Methods,* Vol. 3, No 6, pp. 1277-1279.

Materials Science Society of Japan, Molecular Hybridization and Hybrid Materials, Composite System in Materials, Shokabo Publishing Co., Tokyo, Japan (1993) pp. 336-343

Proupin-Perez M., Cosstick R., Liz-Marzan L. M., Salgueirino-Maceira V., Brust M. (2005) Studies on the attachment of DNA to silica-coated nanoparticles through a Diels-Alder reaction, *Nucleos. Nucleot. Nucleic Acids,* Vol. 24, No 5-7, pp. 1075-1079.

Shibata M., Teramoto N., Akiba T., Ogihara M. (2011) High-performance hybrid materials prepared by the thermo-reversible Diels-Alder polymerization of furfuryl ester-terminated butylene succinate oligomers and maleimide compounds, *Polym. J.*, Vol. 43, No 5, pp. 455-465.

Soylemez E., Caylak N., Rzayev Z. M. O. (2008) Synthesis and characterization of functional copolymer/organo-silicate nanoarchitectures through interlamellar complex-radical (co)terpolymerization, *Express Polym. Lett.,* Vol. 2, No 9, pp. 639-654.

Su H. L., Hsu J. M., Pan J. P., Chern C. S. (2007) Silica nanoparticles modified with vinyltriethoxysilane and their copolymerization with *N,N*'-bismaleimide-4,4'-diphenylmethane, *J. Appl. Polym. Sci.,* Vol. 103, No 6, pp. 3600-3608.

Vejayakumaran P., Rahman I. A., Sipaut C. S., Ismail J., Chee C. K. (2008) Structural and thermal characterizations of silica nanoparticles grafted with pendant maleimide and epoxide groups, *J. Coll. Int. Sci.,* Vol. 328, No 1, pp. 81-91.

Xie Z., He Z., Dai D., Zhang R. (1989) Study on the synthesis and characterization of the soluble, high molecular weight and ladder like polymethylsilsesquioxane, *Chin. J. Polym. Sci.*, Vol. 7, No 2, pp. 183-188.

Yan H., Ning R., Liang G., Ma X. (2005) The performance of BMI nanocomposites filled with nanometer SiC, *J. Appl. Polym. Sci.,* Vol. 95, No 5, pp. 1246-1250.

Yan H., Ning R., Liang G., Huang Y., Lu T. (2007) The effect of silane coupling agent on the sliding wear behaviour of nanometer ZrO_2/bismaleimide composites, *J. Mater. Sci.,* Vol. 42, No 3, pp. 958-965.

Yan H., Li P., Ning R., Ma X., Zhang Z. (2008) Tribological properties of bismaleimide composites with surface-modified SiO_2 nanoparticles, *J. Appl. Polym. Sci.,* Vol. 110, No 3, pp. 1375-1381.

Zhang J., Xu R. W., Yu D. S. (2007) A Novel and Facile Method for the Synthesis of Octa(aminophenyl)silsesquioxane and Its Nanocomposites with Bismaleimide-Diamine Resin, *J. Appl. Polym. Sci.,* Vol. 103, No 2, pp. 1004-1010.

Zhao L., Li L., Tian J., Zhuang J., Li S. (2004) Synthesis and characterization of bismaleimide-polyetherimide-titania hybrid, *Compos.: Part A,* Vol. 35, No 10, pp. 1217-1224.

Polymer Nanomaterials

Chapter 9

Thermoplastic Polymers Containing Nanofillers

Volodymyr LEVCHENKO[1,2]*, Yevgen MAMUNYA*[1]*,*
Gisele BOITEUX[2]*, Eugene LEBEDEV*[1]

[1] Institute of Macromolecular Chemistry of National Academy of Sciences of Ukraine, Kyiv 02160, Ukraine
[2] Universite de Lyon, CNRS, UMR 5223, IMP@Lyon 1; Universite Claude Bernard Lyon 1, F-69622, Villeurbanne, France

Summary

Polymer nanocomposites filled with nanofillers are intensively investigated during last years due to their valuable properties and the perspectives of application in the various areas. Their physical and electrical characteristics can be close to the properties of those for the nanofiller, whereas the mechanical properties and processing methods are typical for the plastics. The electrical properties of such nanocomposites based on polymers filled with conductive nanofillers are of great interest both for science and technology. In recent years, different kinds of nanoparticles are frequently used together as combined nanofiller to prepare multi-component polymer nanocomposites, in order to study the synergistic effects of different nanofillers. Such combination of two fillers may result in a successful integration of properties of the components in new nanomaterials based on thermoplastics which reveal new valuable characteristics.

Notations and acronyms

PC	polycarbonate
PVC	polyvinylchloride
PE	polyethylene
PP	polypropylene
MFI	melt flow index
PMMA	polymethylmethacrylate
UHMWPE	ultrahigh molecular weight polyethylene
PTFE	polytetrafluoroethylene
PVA	polyvinyl acetate
CPA	co-polyamide
POM	polyoxymethylene
CNT	carbon nanotubes
SWCNT	single-walled carbon nanotube
MWCNT	multi-walled carbon nanotubes
CF	carbon fibers
MMT	montmorillonite
THF	tetrahydrofurane
SEM	scanning electron microscopy
TEM	transmission electron microscopy
PTC	positive temperature coefficient
ε'	dielectric permittivity
$\tan \delta$	tangent of the dielectric loss angle
θ	chiral angle
φ_c	percolation threshold
σ	conductivity
ξ	correlation length
λ	thermal conductiviy
E'	elastic modulus
H	viscosity
χ_c	crystallinity degree

1. Introduction

Modern technologies demand new polymeric materials with the properties which are not inherent in conventional polymers. They are, for instance, materials with high electrical and thermal conductivity, with specific dielectric characteristics (high value of ε' and low value of $\tan \delta$), with high heat resistance and thermal stability. The problem of creation of such materials can be solved by three different ways: i) by a synthesis of new type of polymers, ii) via modification of conventional polymers through the changes in their chemical structure, iii) through the preparation of polymeric composites filled with both organic and inorganic fillers, which would provide the required properties. One of the most interesting goals is creation of electrically conductive polymer material. At the moment the class of polymers (such as polyaniline polyacetylene, polypyrrole, polythiophene, etc.), which are characterized by the intrinsic conductivity of the electronic type, is widely known. Their limitations are impossibility of processing by many methods typical for polymers (they process preferable through the solvents), fragility and inflexibility, and time instability of characteristics as a result of aging. They do not belong to thermoplastics and their industrial processing via conventional methods is practically impossible.

New type of thermoplastic conductive materials can be based on conventional thermoplastic polymers filled with conductive fillers such as carbon black, carbon fibbers, dispersed metals, metal fibbers, and ceramics.

Lately, composite materials, containing nanofillers, and, in particular, carbon nanotubes (CNT) seems to be very attractive for applications. Owing to the unique mechanical, electrical and thermal properties, CNTs are expected to be an ideal filler for the electroconductive polymer composites and the introduction of CNTs into the polymer matrix is the basis for the formation of the various functional materials. Polymers filled with CNTs are characterized by a wide range of unique physical properties and can be used as sensors, electrodes for batteries, supercapacitors, special coatings protecting from electromagnetic radiation etc.

New way allowing further modification and improving of properties of thermoplastic matrix is using of combined nanofillers, for example CNTs together with nanometal or nanoclay or with carbon black. Such combination of two fillers may result in a successful integration of properties of the components in new nanomaterials based on thermoplastics which reveal new valuable characteristics.

The problems of formation of such composites, their electrical thermal and mechanical properties and the dependence of their electrophysical characteristics on the morphological features will be reviewed in this chapter in detail.

2. General characteristics of the conductive polymer composites filled with carbon nanotubes

2.1 The properties of carbon nanotubes

As it was notice by different authors, first, carbon nanotubes were reported in 1991 by S. Iijima *[Mittal, 2010; Moniruzzaman and Winey, 2006; Thostenson et al., 2001]*. Carbon nanotubes are long cylinders of covalently bonded carbon atoms. The ends of the cylinders may be capped by hemi-fullerenes *[Moniruzzaman and Winey, 2006]*. In the nature there exist two types of carbon nanotubes: single-walled and multi-walled *[Dyachkov, 2006]*. Ideal single-walled carbon nanotube (SWCNT) is a graphene sheet rolled in a cylinder, i.e. the surface of CNTs contained regular hexagons of the carbon atoms. The various ways of rolling graphene into tubes are described by the tube chirality, i.e. the angle of the orientation of graphene sheet relative to the axis of the tube. Electrical properties of CNTs are defined by the chirality namely. Figure 1 shows the graphene sheet with marked possible directions of its rolling. The chirality of the nanotubes are identified by symbols (m, n) which indicate the number of steps along the unit vectors ($\vec{a}_1$ and $\vec{a}_2$) *[Moniruzzaman and Winey, 2006]*. The chirality of CNT can be also identified by the angle θ between the direction of nanotube rolling and the direction in which adjacent hexagons have a common side. Depending on the chirality single-wall carbon nanotubes are divided into three types: "armchair" (n, n); "zigzag" (n, 0); and "chiral" (n, m) (Figure 2). In the simplified model, the single-wall CNT does not form the seams during rolling and ending by hemi-fullerenes, which contain regular hexagons and six regular pentagons. However, idealized CNT structure differs from the experimentally observed.

Carbon nanotubes can be metallic or semiconductor, what depended on their diameter and chirality. During synthesis a mixture of nanotubes is usually received, two-thirds of which have semiconductor properties and one-third – metal ones. All the carbon atoms in nanotubes have ternary coordination, therefore nanotubes are conjugated aromatic systems. In such structure each three of four valent electrons of carbon atom form sp^2-hybrid orbitals with localized σ-bonds C-C and the fourth electron is involved in the formation of the delocalized π-system *[Dyachkov, 2006]*. These π-electrons are weakly connected with their atoms, so that they are involved in charge transport. High (metallic) conductivity appears when occupied π-states are not separated by energy gap from vacant π-states. If this condition is not fulfilled and the energy gap is quite narrow, the carbon nanotube is semiconductor; when a gap is wide, then a CNT is insulator. The conduction takes place along the nanotube, which makes the CNTs the functional quantum wires.

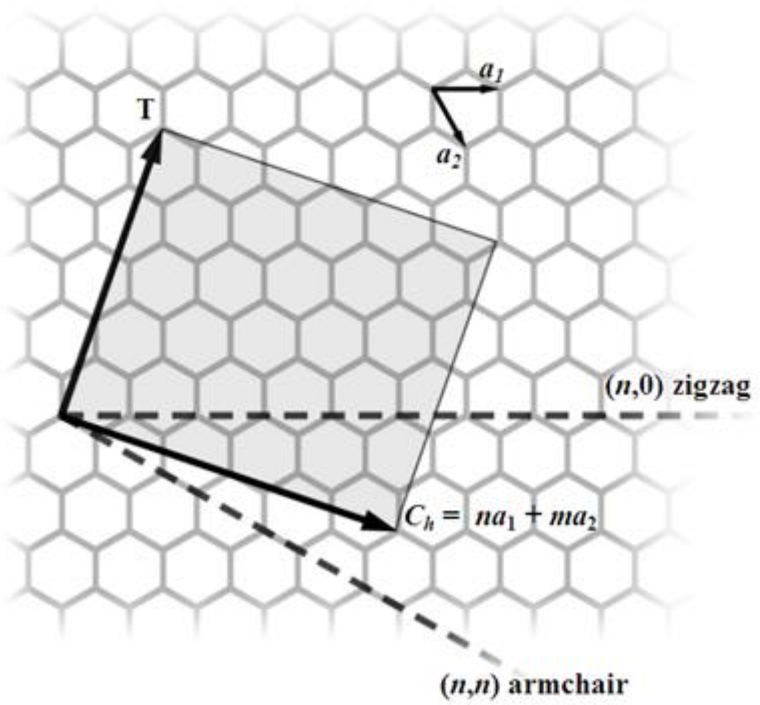

Figure 1. The graphene sheet with marked possible directions of its rolling *[http://en.wikipedia.org/wiki/Carbon_nanotubes]*

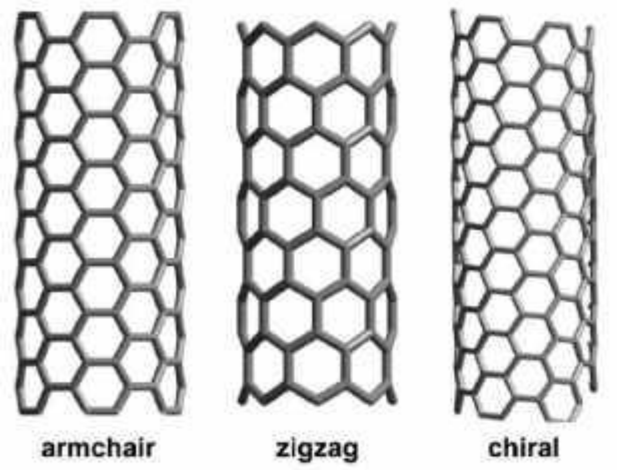

Figure 2. Carbon nanotubes are divided into three types: "armchair"; "zigzag"; and "chiral" *[http://www.robaid.com/tech/nanotechnologies-carbon-nanotubes.htm]*

All armchair SWCNTs are metallic with a band gap of 0 eV. SWCNTs with $n\text{-}m=3i$ (i being an integer and is not equal to 0) are semimetallic with a band gap about few meV, while SWCNTs with $n\text{-}m\neq 3i$ are semiconductors with a band gap of (0.5÷1) eV *[Moniruzzaman and Winey, 2006]*.

In the nature there are also multi-walled carbon nanotubes (MWCNTs) which differ from single-walled with wider variety of shapes and configurations

[Dai, 2002]. There are several types of multi-walled structures of CNTs. The first structure is known as the Russian dolls and the second structure is a roll

With the increase of the numbers of walls the deviation from the ideal cylindrical shape occurs. In some cases the outer wall of the nanotube takes a shape of polyhedrons. Also on the outer wall such defects as pentagons and heptagons can be formed, and they lead to the disruption of cylindrical form. The presence of similar defects leads to the appearance of curved and spiral carbon nanotubes [Dyachkov, 2006].

Carbon nanotubes are also characterized by unique mechanical properties, in particular - strength and stiffness. It is explained by the fact that CNTs have a high degree of structural perfection, i.e. a small number of structural defects. In addition, carbon rings of walls which form a regular hexagon, being bent can change its structure. This is caused by the fact that C-C bonds can be sp^2 -hybridized and change the hybridization during bending [Dyachkov, 2006]. This property of carbon nanotubes provides them with great values of Young modulus and ultimate tensile strength. In the polymer/carbon nanotubes composites external tensile loads were successfully transmitted to the nanotubes across the tube/polymer interface [Harris, 2004]. Thus, polymer composites filled with carbon nanotubes composites demonstrate excellent mechanical properties and high mechanical module values. For example the elastic modulus for SWCNTs is approcsimatly 1 TPa and for MWCNTs approcsimatly 0,3-1 TPa [Mittal, 2010].

Moreover, except unique mechanical and electrical properties, carbon nanotubes have very interesting magnetic, optical and thermal characteristics [Baibarac and Gomez-Romero, 2006; Baxendale et al., 1997; Bellucci, 2005; Bommeli et al., 1997; Breuer and Sundararaj, 2004; Dyachkov, 2006; Li H.J. et al., 2005; Mittal, 2010; Stetter et al., 2008; Tersoff, 1999; Zettl and Cumings, 2001].

Analyzing the above mentioned data, one can suggest that CNTs is exellent filler for making electrically conductive polymer systems.

2.2 The formation of the conductive cluster in the polymer composites

The conductive polymer composites are thermoplastic or thermoset polymers filled with dispersed conductive components such as metal, carbon black, carbon nanotubes etc. The composites which contain an electro-conductive filler in insulating polymer became electroconductive at certain value the so-called percolation threshold φ_c (i.e. the critical concentration of filler above which the conductivity appears) [Mamunya et al., 2010a; Vysotskiy and Roldughin, 1998]. The percolation threshold is very important parameter of such systems, and the lower it is, the better is the structural organization of conductive phase. In two-component system, some components of which are characterized by high and low conductivity, the distribution of filler particles in the volume of the polymer can be random or ordered. Formally, such systems can be characterized as a combination of conductive and non-conductive particles. The conductivity of the first one is indicated as σ_1, and another one as σ_2, ($\sigma_2 < \sigma_1$). During the growth of the filler content (from very small values) in the system small associates start to form, and then conductive separate clusters are formed. The average size of the clusters is characterized by the so-called correlation length ξ. At a certain concentration of conductive particles φ_c, between the isolated clusters conductive bridges are formed and they can consist both of individual particles and of their aggregates. This way the connection of the initially isolated clusters into the infinite conductive cluster takes place. At this moment a stepwise of transition system from the non-conductive to conductive state is observed. At further increase of the concentration of conducting phase the infinite cluster grows, absorbing some small clusters, what results in the monotonous increase of the system conductivity. Percolation threshold is characterized by the sharp change of the conductivity by several orders of magnitude, what is connected with the creation of three-dimensioned conductive network of the filler inside the matrix. In numerous reports there were presented different models, which characterize the dependence of percolation threshold on the composite conductivity and on the content of the conductive filler *[Chiteme and McLachlan, 2003; Fournier, 1997; Hu N. et al, 2008; McLachlan et al., 2005; McLachlan et al., 1998; McLachlan, 1999; McLachlan, 2000]*.

The composites polymer/CNTs are characterized by the low percolation threshold because of the great value of the ratio between the length and diameter of the CNTs, which reaches (100 ÷ 1000). The dependence of the composite conductivity on the CNTs content and polymer matrix conductivity and on the percolation threshold were introduced by D. S. McLachlan et al. *[McLachlan et al., 2005]*:

$$|\sigma_f| \to \infty : \quad \sigma_c = \sigma_i \left(\frac{\varphi_c}{(\varphi_c - \varphi)} \right)^S, \quad \varphi < \varphi_c \tag{1}$$

$$|\sigma_i| \to 0 : \quad \sigma_c = \sigma_f \left(\frac{\varphi - \varphi_c}{(1 - \varphi_c)} \right)^t, \quad \varphi > \varphi_c \tag{2}$$

where σ_c – is the conductivity of the composite, σ_f – is conductivity of CNTs, σ_i - is the polymer conductivity, φ_c – is the percolation threshold, φ – is CNT concentration, s and t – are critical exponents.

It should also be noted that polymer nanocomposites filled with CNTs are characterized by the electrical conductivity values which are significantly lower than the conductivity of individual carbon nanotubes. This is caused by the fact that a polymer can create a thin insulating layer in the contact point between nanotubes. This thin layer can not prevent the tunneling process between neighboring nanotubes, however, it can significantly increase the value of contact resistance between them.

3. Methods of formation of the conducting polymer composites

In general, the process of the CNT introduction into thermoplastic and thermoset polymers can be achieved by three methods, namely:

- solution mixing;
- "*in situ*"-polymerization;
- melt mixing;

Each of these methods has its advantages and disadvantages as well as certain restrictions in the formation of the polymer composites and in the achievement of uniform distribution of the nanotubes in a polymer matrix.

3.1 Conductive polymer composites prepared by solution mixing

The solution mixing is one of the commonly used methods of the preparation of polymer composites filled with CNTs *[Biercuk et al., 2002; Broza et al., 2007; Hu G. et al., 2006; Lee H.K. et al., 2007; Skakalova et al., 2005; So et al., 2007; Sterzynski et al, 2010; Suhr et al., 2006; Zhu et al., 2006]*. The advantage of this method is low viscosity of the system, what provides a high degree of random distribution of the nanotubes in a polymer matrix. This method is used to form a thermoset and thermoplastic composites. The principal stages of the formation of the polymer nanocomposites based on polycarbonate (PC) and prepared by solution mixing are as follows *[Suhr et al., 2006]*. First, nanotubes have been oxidized in nitric acid to from carboxyl groups on their surface, which can interact with the carbonate groups of the polymer. After that, the oxidized nanotubes have been dissolved in the tetrahydrofurane (THF) and mixed with the polycarbonate, also dissolved in THF. Further, the precipitate of the nanocomposite material, which was formed during introduction of the obtained suspension into methanol, was removed by filtration. The scanning electron microscopy (SEM) images have confirmed the uniform distribution of nanotubes in polycarbonate matrix. The introduction of CNTs into the PC matrix has provided the growth of the elastic modulus of the composites, compared to the pure PC.

The method of solution mixing was also used for the synthesis of the nanocomposites based on the epoxy matrix and filled with chemically modified carbon nanotubes *[Biercuk et al., 2002]*. The transmission electron microscopy (TEM) microimages have revealed that ultrasound treatment of the polymer solution, filled with modified CNTs, provide the random distribution of carbon nanotubes in the polymer matrix. The authors have found that the introduction of a small number of CNTs into the polymer matrix causes a significant increase of the thermal conductivity of the composites compared to the pure epoxy. Solution mixing is a quite effective method for the introduction of carbon nanotubes into the polymers which have high viscosity and can not be processed on extruders. The solutions of high viscose polymers have low viscosity, thus the filler can be easily distributed in the matrix. Particularly, there have been reported about the introduction of nanotubes in a solution of polyvinylchloride (PVC) *[Broza et al., 2007; Sterzynski et al, 2010]*. After that in order to obtain polymer composite the solvent was evaporated in a vacuum heater.

In addition, a significant advantage of this method is the possibility to treat by ultrasound a polymer solution filled with nanotubes *[Broza et al., 2007; Suhr et al., 2006; Sterzynski et al, 2010]*. G. Broza et al. *[Broza et al., 2007]* have noted that ultrasonic treatment of PVC dissolved in THF and filled with carbon nanotubes, provides a random distribution of CNTs in the composite. Obtained in such a way composites are characterized by low percolation threshold, as far as nanotubes have introduced into low viscous environment with further ultrasonication of the solution. For example, the composites based on polymethylmethacrylate filled with CNTs are characterized with low percolation threshold φ_c=0.11 vol. %. It has been also shown that when a content of nanotubes is such small, the mechanical properties of the composites improved significantly *[Broza et al., 2007]*.

Better dispersion of CNTs in the polymer solution can be realized by the functionalization of the carbon nanotubes surface. The modification of the CNT surface by functional groups can provide the increase of the interaction between the filler and the polymer chains, which will promote a more random dispersion of CNTs in the composite *[Lee H.K. et al., 2007; So et al., 2007; Suhr et al., 2006]*. H. K. Lee et al. *[Lee H.K. et al., 2007]* have found that the presence of diazo-compounds on the external wall of functionalized carbon nanotubes has significantly increased the interfacial interaction between the CNTs and polyisoprene matrix. A strong interaction between the filler and the polymer has been confirmed by a significant increase of the viscosity of the investigated composites.

Thus, the advantage of solution mixing method is the low viscosity of the polymer solution, what makes easier the distribution of CNTs in the polymer matrix. The disadvantage of this method is the requirement to dissolve the polymer, what is quite difficult for some types of polymers, such as polyethylene and polypropylene. Moreover, such a method demands to use a huge amount of solvents, which may be harmful for ecology. This factor is a significant disadvantage for this composite preparation method to be used in the industry.

3.2 Formation of conducting polymer composites by "in situ"-polymerization

The method of "*in-situ*"-polymerization is applied to improve the dispersion of nanofiller and to increase the interaction between the filler and the polymer matrix. Polymerization "*in-situ*" occurs at the simultaneous presence of carbon nanotubes and monomer in a solvent. A low viscosity of the system ensures the distribution of nanotubes in a polymer matrix and subsequent polymerization of monomer leads to a random polymer interaction with the surface of the nanotubes. In many cases the synthesized polymer can be chemically deposited on the surface of the CNTs through the functional groups or through direct grafting of the polymer chains on the surface of nanotubes in the presence of initiators *[Akbar et al., 2009; Barraza et al., 2002; Immonen et al., 2009; Kong et al., 2004; Koval'chuk et al., 2008a; Qin et al., 2004; Velasco-Santos et al., 2003]*. C. Velasco-Santos et al. *[Velasco-Santos et al., 2003]* have compared the properties of the composites filled with functionalized CNTs (f-CNTs) and non-functionalized CNTs (n-CNTs) obtained by "*in-situ*"-polymerization of methylmethacrylate. The results have revealed that n-CNTs can chemically interact with the polymer through the open π-bonds. However, the reaction groups of f-CNTs were more effective for the formation of the bonds with the polymer chains during polymerization. The investigation of the composite characteristics has revealed that the mechanical properties of composites with f-CNTs were much better than those, containing n-CNTs. This difference appears in enhance of the elastic modulus and increase of glass transition temperature by 33 ºC.

The growth of polymer chains from the surface of nanotubes has also been studied. S. Qin et al. *[Qin et al., 2004]* have investigated polymer composites based on *n*-butyl methacrylate obtained by controlled polymerization from the surface of carbon nanotubes. H. Kong et al. have described a similar method of composite preparation *[Kong et al., 2004]*, when methyl methacrylate was polymerized on the surface of CNTs by radical polymerization with the atom transfer. The use of "*in-situ*"-polymerization in the presence of nanotubes for the formation of the conductive composites has both advantages and disadvantages. On the one hand, the polymerization around CNTs provides better interaction between the filler and polymer matrix. On the other hand the polymer formed the layer around the surface of carbon nanotubes, which prevents the formation of contacts between them and reduces the conductivity of composites. It should be noted that the formation of composites by "*in-situ*"-polymerization requires the functionalization of CNTs surface, which can affect their properties negatively. In particular, S. M. Yuen et al. *[Yuen et al., 2007]* reported that prolonged modification of carbon nanotubes can reduce their length, as well as facilitate the formation of the defects on their surface.

3.3 Formation of the conducting polymer composites by melt mixing method

The melt mixing of polymer with inorganic filler and, in particular, with carbon nanotubes is a very attractive method for the formation of the nanocomposites based on a wide range of polymers. The advantage of this method is a direct mixing of the polymer with the filler at high temperature without the solvent. Thus melt mixing is easier to use and more environmentally friendly compared to the other methods. However, melt mixing requires high-quality mixing equipment what enables to apply high shear forces to blend the polymer melt with nanofiller.

The random distribution of the filler in the polymer matrix can be achieved, mainly due to high shear deformations in the extruder. Also, better mixing of the organic and inorganic components can be improved by the increase of the composite mixing time or by the regulation of the mixing temperature, which affects the viscosity of the polymer. Formation of composites by melt mixing has been described in *[Hobbie et al., 2006; Liang and Tjong, 2006; Pegel et al., 2008; Pötschke et al., 2003b; Valentino et al., 2008]*. P. Pötschke et al. *[Pötschke et al., 2002]* have obtained the nanocomposites based on polycarbonate by melt mixing in twin-screw mini extruder at the temperature of 240 °C and rotation speed of 280 rpm. The authors reported that such mixing parameters provided random distribution of CNTs in the polymer matrix. The parameters of the composite preparation influence significantly the final characteristics of the conductive systems. In particular, the prolonged mixing with high shear deformation applied can reduce the length of CNTs *[Andrews et al., 2002; Pötschke et al., 2004]*. Thus the value of the conductivity of nanocomposites can be decreased as well. R. Andrews et al. have reported that the length of CNTs decreased by 25%, when mixing of the material in the extruder was longer than 15 minutes *[Andrews et al., 2002]*.

The materials can be also received by the combining of several methods. In particular, M. X. Pulikkathara et al. have obtained the composites, combining the methods of the melt and solution mixing *[Pulikkathara et al., 2009]*. First, CNTs and PE powder of were dissolved in chloroform. The solvent was removed by the drying of the solution in the thermal heater. Then the obtained material was melt mixed in the extruder at 110 °C during 10 min.

In conclusion, it should be noted that melt mixing is the most appropriate method of the preparation of the nanocomposites based on thermoplastic polymers being filled with nanofillers. However, this method does not provide a uniform distribution of the filler particles in a thermoplastic matrix, particularly in polypropylene - due to the high viscosity of the polymer melt and low wettability of the filler by the polymer.

4. Conductive polymer composites based on polypropylene filled with CNTs

Polypropylene (PP), which belongs to the group of polyolefins and has a valuable complex of potential applications, is one of the mostly used polymers. Because of the low cost, low density, high thermal stability and corrosion resistance, PP is widely used in various fields of industry *[Bikiaris, 2010]*. The introduction of the fillers gives an opportunity to steer the properties of the materials, obtained from PP.

Last decade a great attention has been paid to the formation of the nanocomposites based on polypropylene and carbon nanotubes. Introduction of carbon nanotubes into polymer matrix results in the significant enhancement of thermophysical properties of the polypropylene matrix. It is well known that the properties of polymer composites strongly depend on the distribution of the filler, and, therefore, all properties of PP/CNTs composites depend on the morphology of the composites.

The effect of the CNT concentration on the electrical properties of PP/CNT composites was intensively studied *[Deng et al., 2009a; Deng et al., 2009b; Du et al., 2004; Mičušík et al., 2010; Kharchenko et al., 2004; King et al., 2009; Lee* S.H. *et al., 2007; Logakis et al., 2010; Seo and Park, 2004; Tjong et al., 2007; Zhou et al., 2006]*. It was found that the conductivity of the composites increased with the increase of the CNT content. The percolation threshold for the PP/CNTS composites was in the range of (0.6÷3) vol. % *[Du et al., 2004; Kharchenko et al., 2004; Lee* S.H. *et al., 2007 ; Logakis et al., 2010; Mičušík et al., 2010; Seo and Park, 2004]*. Electrical conductivity of PP/CNT composites depends on many factors, in particular - the types of CNT and PP *[Koval'chuk et al., 2008b]*, viscosity of PP *[Mičušík et al., 2010]* and parameters of the composite preparation *[Tjong et al., 2007]*. M. Mičušík et al. *[Mičušík et al., 2010]* have found that the content of CNT aggregates, and, thus, the value of the percolation threshold significantly depends on the viscosity of the polymer matrix. In particular, the increase of melt flow index $\mathrm{MFI}_{210/2.16}$ of polypropylene from 2 g/10 min to 12 g/10 min (i.e., viscosity is diminished) results in the percolation threshold decrease from 2 vol. % to 1.18 vol. % of CNT, that is less viscous the polymer the lower value of φ_c. The percolation threshold value also depends on the parameters of composite preparation, such as speed of mixing in extruders. S. C. Tjong et al. *[Tjong et al., 2007]* have observed a significant decrease of the percolation threshold when the mixing speed increased from 60 rpm to 200 rpm. The value of the percolation threshold at 200 rpm was only 0.22 vol. %. However, as it was mentioned above, a high speed of mixing may reduce the length of the nanotubes.

A huge amount of works have been devoted to the study of the influence of the carbon nanotubes on the crystallization of the polypropylene matrix *[Bao* *and Tjong, 2008; Bhattacharyya et al., 2003; Bikiaris et al., 2008; Causin et al., 2009; Logakis et al., 2010; Seo et al., 2005; Sandler et al., 2003; Valentini et al., 2004; Xu and Wang, 2008; Zhang H. and Zhang Z., 2007]*. In most of them it has been shown that when the content of carbon nanotubes in the composites increases, the crystallization temperature of PP shifts to higher values. This indicates that the CNTs act as the crystallization centers *[Bao and Tjong, 2008; Bhattacharyya et al., 2003; Bikiaris et al., 2008; Logakis et al., 2010]*. Also, the presence of CNTs leads to the growth of crystallinity degree χ_c of PP. In particular, the degree of crystallinity increased by 3 % and by 4 % at concentration of CNTs equal to 5 wt. % of CNTs *[Logakis et al., 2010]* and 1 wt. % of CNTs *[Zhang H. and Zhang Z., 2007]*, respectively. One can conclude that the improvement of mechanical properties of the PP/CNT composites is caused by two factors: the reinforcement effect of CNTs and increase of the crystallinity degree. The reverse effect of CNTs on the degree of crystallinity of PP was also observed *[Bao and Tjong, 2008; Bikiaris et al., 2008]*. D. Bikiaris et al. *[Bikiaris et al., 2008]* have found that when the concentration of carbon nanotubes was 6 vol. %, the degree of crystallinity χ_c have decreased by 5% compared to the pure polypropylene matrix. This effect can be attributed to the fact that the functionalized carbon nanotubes were used and they interact with the polymer chains preventing the formation of the crystal structure of PP. It has also been noted that CNTs, can act as crystallization centers and cause a faster growth of crystals and formation of large number of small-sized spherulites *[Bikiaris et al., 2008]*. H. Zhang and Z. Zhang *[Zhang H. and Zhang Z., 2007]* have also found the reduction of spherulites size with the introduction of CNTs into PP matrix.

A significant value of elasticity modulus of CNTs (~ 1 TPa) and a great value of the ratio between the length and diameter (100÷1000) make carbon nanotubes an effective filler for the enhancement of mechanical properties of polymers. It was found that Young's modulus, elastic modulus and strength of composites PP/CNT increased with the introduction of CNTs into the polymer matrix *[Bikiaris et al., 2008; Lee G.-W. et al., 2008; López Manchado et al., 2005; Prashantha et al., 2009; Razavi-Nouri et al., 2009; Teng et al., 2008]*. In particular, G.-W. Lee et al. *[Lee G.-W. et al., 2008]* have found that the introduction of CNTs into the PP matrix caused the increase of elastic modulus by 8 GPa at -140 °C and on 1 GPa at 100 °C. However, it should be noted that in some cases, the increase of the CNT content does not result in the change of the mechanical properties or they even can be retrogressed. This effect is due to the ability of CNTs to form the agglomerates. M. Mičušík et al. *[Mičušík et al., 2010]* have studied the PP/CNT composites and observed the presence of the aggregates of large sizes which were in some composites about 100 μm. Their presence was explained by the semicristalline structure of polymer matrix and weak interaction between non-polar PP and CNTs. In semicristalline polymers the CNTs are localized only in the amorphous phase.

The review of the methods of forming of the electro-conductive polymer systems has shown that a great amount of experimental reports is devoted to the formation of the polymer composites, filled with CNTs. Nevertheless, the uniform distribution of CNTs in polymer matrix is a very actual problem. The successful solution of this problem will give the possibility to use all unique properties of CNTs for the realization of desirable properties of the composites. In order to solve this problem a lot of methods were proposed and described, in particular, CNT functionalizing for the enhancement of the interaction with the polymer links; preparing of the composites by the solution mixing method; changing of the composite forming parameters, such as temperature and shearing deformation value. However, the mentioned above methods have also their significant shortcomings along with the advantages. Thus, there appears a problem to search new, economically sound ways to form the composites, which would be able to provide a uniform CNT distribution.

Another important problem is to search the regimes of formation of electro-conductive composites with rather high conduction level and low percolation threshold, which would affect the electro-physical properties of the composites. In order to reach low percolation threshold values, one has to obtain a uniform distribution of the CNT in polymer matrix, what is realized in so-called “segregated systems” and in the filled polymer blends.

5. The formation of the conductive phase of the filler in the different systems

Nowadays the investigations of conductive polymer composites filled with carbon nanotubes are mainly focused on the decreasing of the percolation threshold value and improving the processability. The electrical properties of the conductive polymer composites filled with carbon nanotubes and their percolation behaviour depend on many factors, particularly, on a kind of polymer matrix, type of CNT, spatial distribution of nanotubes, interfacial interaction polymer–filler, etc.

Experimental values of percolation threshold of CPC depending on the different parameters vary in a wide range, $\varphi_c = (0.0025 \div 10)$ % *[Mamunya et al., 2010a]*. The attained low values of φ_c are attractive because the conductive composites can be obtained at very low content of nanotubes. Such low values of percolation threshold are caused by high ratio length/diameter of nanotubes, which can be equal to (100÷1000) and provide the presence of contacts between individual nanotubes even at their small content in polymer matrix. However, the attainment of low φ_c values is impeded by experimental difficulties of separation of the curled and tangled long nanotubes and, as a result, leads to a presence of aggregates, which heightens the percolation threshold.

One of the ways to reduce the percolation threshold in the composite is to induce inhomogeneous distribution of the filler in polymer matrix. Such inhomogeneous distribution of the filler can be achieved in segregated polymer systems, polymer blends and composites filled with combined filler.

5.1 Segregated conductive nanocomposites

First the term "segregated system" was introduced by A. Malliaris and D.T. Turner *[Malliaris and Turner, 1971]* and referred to the electroconductive composites based on polymers and metal filler. So-called *"segregated systems"* differ from the usual filled systems by the fact, the filler is distributed not uniformly, but creates an ordered structure in the form of a framework (or lattice) in polymer matrix, wherewith one can achieve significantly lower φ_c value in comparison with common filled polymers *[Lebovka et al., 2006; Lisunova et al., 2007; Lux, 1993; Mamunya et al., 2002a]*. Such an ordered filler distribution is realized, for instance, in the polymer mixture, when a filler is localized in one polymer phase or on the interphase boundary *[Mamunya, 1999; Mamunya et al., 2002b, 2010b]*. Because of the presence of two phases, crystal and amorphous ones, semi-crystalline polymers can also be considered as segregated systems, as far as the filler is localized only in the amorphous phase, while diminishing the percolation threshold of the composite.

One of the available methods of the formation of the segregates system is compacting (pressing of the mixture of polymer and filler powders) on conditions that the size of polymer particles D exceeds the size d of the filler particles significantly ($D >> d$). Nowadays there are a lot of reports devoted to the study of the segregate systems obtained by compacting method. In particular, there were studied segregated composites based on the polymers filled with metal nanoparticles *[Bridge et al., 1990; Lebovka et al., 2006; Malliaris and Turner, 1971; Mamunya et al., 2001, 2002a, 2002c, 2003; Privalko et al., 2000; Zois et al., 2001]*, carbon-black *[Chan et al., 1997; Chiteme and Mclachlan, 2000; Yacubowicz et al., 1990]*, ceramics *[Bouchet et al., 2000]* and carbon nanotubes *[Lisunova et al., 2007; Mamunya et al., 2010a]*.

Structure model showing the evolution of structure of the PVC/MWCNT composite in a process of its forming is represented in Figure 3 *[Mamunya et al., 2010a]*. On the first stage the mechanical mixture of polymer/MWCNT contains rather agglomerated nanotubes in the space between polymer particles.

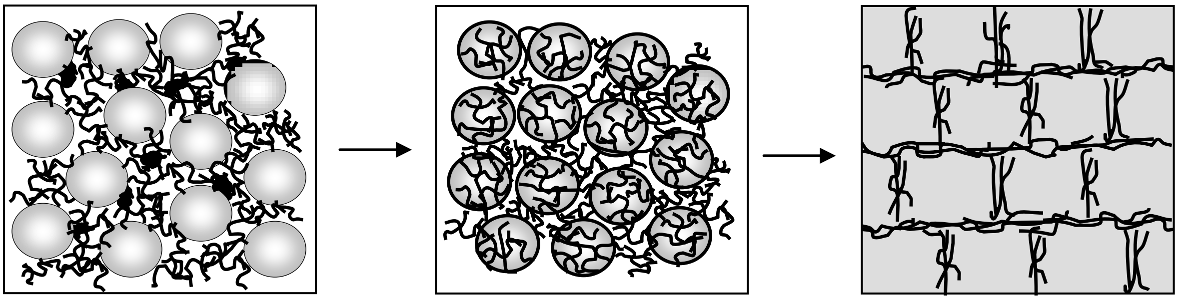

Figure 3. A model of evolution of the PVC/MWNT structure along a process of its forming by hot compacting method

Then it is necessary to cover the surface of polymer particles with smooth layer of filler without agglomerates of the filler particles. In this case one can expect to obtain the conductive composite with low value of the percolation threshold. On the last stage the mechanical mixture has to be compacted (to be pressed), at higher temperature, which leads to the deformation of polymer particles and the creation of solid polymer matrix.

The filler having such a segregated structure creates continuous nanotube framework inside the polymer matrix with location of the filler on the boundaries between polymer grainsThe main factors, which define the electrical properties of the segregated systems can be listed as follows.

- The ratio of the radii of polymer and filler R_p/R_f.
- The types of the filler and polymer matrix.
- The form of the filler and matrix particles.
- Viscosity and mechanical properties of polymer.
- Interaction between polymer and filler.
- Conditions and ways of composite forming.

A. Malliaris and D. T. Turner have shown that if the ratio of PE and Ni particles increases from 7.5 to 30, the percolation threshold of PE/Ni composites will decrease from 14 vol. % Ni to 6 vol. % Ni *[Malliaris and Turner, 1971]*. R. P. Kusy and R. D. Corneliussen have shown, that for PE/Ni composites at $R_p/R_f \approx 2$, the percolation threshold was extremely high and reached 36 vol. %, while at $R_p/R_f > 30$ the percolation threshold has decreased more than 10 times and was equal just 3 vol. % of Ni *[Kusy and Corneliussen, 1975]*. J. Bouchet et al. have compared the electrical properties of two segregated systems based on ultrahigh molecular weight polyethylene (UHMWPE) with the sizes of polymer particles – 30 μm and 150 μm and titanium carbide with the sizes of filler particles – 0.8 μm and 0.5 μm *[Bouchet et al., 2000]*. In the case when polymer particle size was 150 μm the percolation threshold was significantly lower.

The type of polymer matrix influences significantly the properties of the segregated systems and formation of the conductive cluster *[Bridge et al., 1990]*. B. Bridge et al. studied the segregated systems based on polymethylmethacrylate (PMMA) and polyethylene, which were filled with gold particles *[Bridge et al., 1990]*. It was found a significant difference between the formation of the conduting cluster for amorphous and semicrystalline polymer. It has also been shown that introduction of Au particles results in the gradual increase of the electroconductivity of PMMA/Au, and at filler content φ=34 vol. % it becomes 3 orders of magnitude more in comparison with the electroconductivity of pure polymer matrix *[Bridge et al., 1990]*. At the same time, PE/Au composites have demonstrated absolutely different conductivity character dependently on the content of the filler *[Bridge et al., 1990]*. The conductivity of the polymer decreased with filler content increase and reached minimum at φ=50 vol. %. For semicrystalline polymers filled with Au, metal particles can play a role of crystallization centers, and then the polymer layer, formed around the particles, will prevent the formation of the contacts between filler. Thus, it is necessary to have a great amount of conductivity filler for the formation of the conducting cluster. G. D. Liang et al. have found that in PP/Ag composites silver particles play a role of the crystallization centres for PP molecules *[Liang et al., 2007]*. Thus, the amorphous polymers are more effective to form the segregated systems filled with metal particles.

The filling of polymer with carbon-black results in the significant decrease of the percolation threshold of the segregated conducting composites, what is caused by the specific structure and by the form of the carbon-black particles *[Chan et al., 1997; Chiteme and Mclachlan, 2000; Yacubowicz et al., 1990]*. For PE/carbon black composites the percolation threshold value varied form 0.25 vol. % to 0.65 vol. % dependently on the carbon-black type *[Yacubowicz et al., 1990]*. Because of the low filler concentration and its selective localization a positive temperature coefficient of resistance was found for the PE/carbon-black composites. This effect is caused by the breaking of the conducting lattice due to the space widening of the polymer matrix at crystal melting process *[Chan et al., 1997]*. C.-M. Chan et al. have also shown the correlation between the parameters of composite forming and their morphology *[Chan et al., 1997]*. It has been found, that pressure change from 13.8 MPa to 44.2 MPa did not influence the composition morphology, whereas high temperatures and a prolonged pressing resulted in the mixture of carbon-black and polymer particles, what caused, in one’s turn, the resistance increase of the composites.

I. J. Youngs has investigated the dependence of the percolation threshold on the size ratio of polymer and filler particles in conductor-insulator composites *[Youngs, 2003]*. The composites were prepared by cold compacting method. The compacting process was carried out at pressure value of 500 MPa during 5 min from the mixture of polytetrafluoroethylene (PTFE) and carbon-black particles. The PTFE particle sizes varied in the range of (1÷100) µm. The lowest percolation threshold value was found to be 1 vol. %, when the size of the polymer matrix particles was 100 µm. And when the latter value was equal to 1 μm, the percolation threshold value was found to be 5 vol. %. The authors have found the discordance between the theoretical and experimental data, which has been explained by the possible change of the shape of matrix particles (from spherical to disc-shaped) during pressing *[Youngs, 2003]*. It is connected with the fact that surface area of the disc is larger than that of the sphere at equal volumes of these geometrical objects. Thus, in order to form the conducting network it is necessary to take a greater amount of the filler.

In order to form segregated conducting systems, polymer emulsions filled with carbon-black *[Grunlan et al., 2001; Kim et al., 2008; Miriyala et al., 2008]* and carbon nanotubes *[Grossiord et al., 2010; Ha et al., 2007]* are also often used. S. M. Miriyala et al. *[Miriyala et al., 2008]* have compared mechanical and electrical properties of the composites based on the emulsions and polyvinyl acetate (PVA) solution, filled with carbon-black. It has been shown, that during the emulsion drying, carbon-black particles segregated around the polymer particles, while forming the conducting network, what enabled to obtain a low percolation threshold value – 1.2 vol. % of carbon-black. In the case of formation of composite from the solution, the nanotubes were uniformly distributed in the polymer matrix, what resulted in the high value of the percolation threshold, which was equal to φ_c=8.18 vol. %. It has also been found that at filler concentrations below 5 vol. % the elastic modulus of the segregated system grows impetuously; however, it decreases at filler high content above 6.5 vol. %, what is related to the pore formation.

The composites, formed from the solution, revealed better mechanical properties, and elastic modulus increased in the whole range of the carbon-black content. The comparing of the composites, formed by two different ways has revealed that a segregated system formation enabled to decrease the percolation threshold of the PVA/carbon-black composites almost by 8 times. However, these systems at significant filler concentrations revealed worse mechanical properties as compared to the composites, obtained from a melt.

A similar comparison of the composites with the uniformly distributed Ni particles and segregated filler network was reported by Ye. Mamunya et al. *[Mamunya et al., 2002c]*. It has been found that for epoxy/Ni composites, in which Ni particles were uniformly distributed in the whole polymer matrix, the percolation threshold was about 10 vol. % of Ni, whereas for the PVC/Ni segregated systems φ_c value was much lower and equalled 5 vol. % of Ni.

Y. S. Kim et al. have analyzed the connection between the elastic modulus E' of the polymer matrix and formation of the conductive filler network in it *[Kim et al., 2008]*. There was investigated a series of co-polymers filled with carbon-black and synthesized on basis of butyl acrylate and methyl methacrylate. While changing the ratio between the initial components of the co-polymer, the authors obtained polymer matrixes, which were characterized by the different values of the elastic modulus. It has been shown, that a polymer with a high value of elastic modulus is more effective for the formation of the segregated network of the filler. However, the particles of the polymer, which has a low elastic modulus, are deformed easily by the carbon-black particles. Thus, the carbon-black migrates inside the polymer particles and the segregated structure of the filler undergoes destruction. A co-polymer, characterized by the elastic modulus of E'=640 MPa (at T=20 °C) had the percolation threshold value φ_c=1.5 vol. % of carbon-black, whereas for the matrix with E'=3.6 MPa, the percolation threshold was 4.9 vol. % of carbon-black.

While studying the segregated systems based on the ultra-high-molecular-weight polyethylene, filled with carbon nanotubes, C. Zhang et al. have found that the percolation threshold of such composites significantly depend on the viscosity of the polymer matrix *[Zhang C. et al., 2005]*. It has been found that in more highly viscosity systems a filler did not migrate into the polymer phase at composite formation, what resulted in low value of the percolation threshold.

For the segregated systems a non-typical dependence of the thermal conductiviy λ on the filler content was observed. First R. P. Kusy and R. D. Corneliussen found that for the segregated systems PVC/Cu even at low filler content a thermal conductivity increased by one order of magnitude in comparison with pure PVC *[Kusy and Corneliussen, 1975]*. In order to correct the equation, which described the concentration dependency of the segregated systems, the authors proposed to introduce the “coefficient of metal conductivity”. Ye. P. Mamunya et al. *[Mamunya et al., 2002a]* have observed a non-linear dependence of the thermal conductivity on the filler content and corrected the equation by the introduction of the exponent N. A non-typical character of the $\lambda=f(\varphi)$ dependence was explained by the fact that for the non-segregated conducting network for which $\varphi_{loc}>\varphi$, a filler compacting is more dense, what results in the best condition of the heat transfer.

The use of CNTs as a filler for segregated systems seems to be rather perspective. It is caused by the high length/diameter ratio, which can reach for CNTs, as it was mentioned above, (100÷1000), and due to this fact the contact between separate nanotubes can be achieved at their low concentration. Nowadays there are only some reports, devoted to the study of the segregated systems, filled with CNTs *[Grossiord et al., 2010; Lisunova et al., 2007; Mamunya et al., 2008, 2010a; Mierczyńska et al., 2004]*. The described in these papers investigations have shown that in segregated systems based on PVC and PE, filled with CNT it was succeeded to reach ultra-low percolation threshold value φ_c=0.04 % *[Lisunova et al., 2007]*. This effect was achieved both due the length/diameter ratio of nanotubes and due to the ordered distribution of the filler in the polymer matrix. While having such interesting properties, segregated systems, filled with nanotubes demand more detailed investigation of their electrical, dielectric and mechanical characteristics.

5.2 Polymer blends, filled with electro-conductive filler

One can significantly decrease the percolation threshold of the composites by means of introduction of the conductive filler into the polymer matrix, what is realized due to the so-called “double percolation” effect, which was proposed by M. Sumita et al. for the first time *[Sumita et al., 1991]*. This effect is caused by the formation of the co-continuous morphology of the phases of two polymers, where the conductive filler is localized in one polymer phase or on the boundary of the phases *[Al-Saleh et al., 2008; Boiteux et al., 2007; Gubbels et al., 1995; Mamunya, 1999; Mamunya et al., 2010b; Rybak et al., 2010; Sumita et al., 1992; Tchoudakov et al., 1996; Zhang C. et al., 1998; Zois et al., 2003a; Zois et al., 2003b; Zois et al., 2003c]*.

On the other hand, the polymer blend composites are of interest due to the possibility to obtain the materials with combination of properties of both blended components. Co-continuous structure of polymer blends can give the maximum contribution of the mechanical modulus from each component simultaneously.

A lot of factors influence the distribution of the conducting filler in the heterogeneous polymer matrix. In particular, the viscosity of the blend components, the wettability of the filler with the polymers, the parameters of the conduction blend formation and the order of the introduction of the components into the composite *[Fenouillot et al., 2009; Mamunya, 1999; Tchoudakov et al., 1996]*.

The distribution of the conducting filler in the polymer blend dependently on the ratio of the surface tensions of the composite components was investigated in *[Baudouin et al., 2010; Mamunya, 1999; Naficy and Garmabi, 2007; Sumita et al., 1991; Zhang L. et al., 2009]*. A.-C. Baudouin et al. have shown that during the dilution of the concentrate based on the co-polyamide (CPA) by the co-polymer ethylene-methacrylate (EMA) the nanotubes remained in the in CPA phase, what did not correlate with the thermodinamical calculations *[Baudouin et al., 2010]*. At the same time, when the concentrate based on EMA and CNT was diluted with CPA, the nanotubes were localized on the boundary of the phases of two polymers, what correlated to the theoretical calculations. Thus, the authors have found that the localization of CNTs in the composite depends both on the thermodynamic factor (the ratio between the values of interphase tensions polymer$_1$–filler, polymer$_2$–filler, polymer$_1$–polymer$_2$) and on the technological one (the way of introduction of the filler into the heterogeneous polymer matrix).

A significant influence of the technological factor on the filler distribution was fixed by Ye. P. Mamunya *[Mamunya, 1999]*. Thus, it has been shown that at the dilution of the conducting concentrate PE/carbon-black with the polypropylene, the carbon-black particles remained in the PE phase, whereas in the composites, obtained by the dilution of the PP/carbon-black concentrate with the polyethylene, the filler was uniformly distributed by the whole heterogeneous polymer matrix.

In order to decrease the interphase tension between the polymers and to reach the stability of the polymer blend, the compatibilizers are often used. In particular, maleated polypropylene (mPP) was introduced into the PA6/PP blend filled with CNTs *[Zhang L., 2009a]*. It was shown, that the thermal stability of the blend had increased significantly at the introduction of CNT and mPP. In addition the rheological investigations have shown that both fillers – CNT and mPP – increase the viscosity and mechanical modulus of the composites.

In the review, devoted to the filled polymer blends F. Fenouillot et al. *[Fenouillot et al., 2009]* have noted that the transition of the filler from one phase into another one occurs more slowly, when the particles are localized first in the more viscous polymer. But at the significant difference of the thermodynamic interactions of the filler with each polymer, such regularity may not be fulfilled. It has also been noted *[Fenouillot et al., 2009]* that at approximately equal values of viscosity of both polymers of the blend the key factor, which determines the space distribution of the filler is the values of the polymer/filler surface tension. In ones turn, F. Gubbels et al. came to a conclusion that the influence of viscosity on the distribution of the filler in the heterogeneous polymer matrix is weaker in comparison with the effect of the polar interactions between the system components *[Gubbels et al., 1995]*.

As concerns the electrical characteristics of the composites, a low percolation threshold occurs, when the conducting filler is localized on the boundary of the polymer phases *[Baudouin et al., 2010; Gubbels et al., 1995; Mamunya, 1999]*. Thus, Ye. P. Mamunya *[Mamunya, 1999]* has shown, that for the composites based on the polyoxymethylene (POM) and for the PE, filled with carbon-black, the percolation threshold was φ_c=4 vol. %. At the same time for PE/carbon-black and POM/carbon-black composites the percolation threshold was 9 vol. % and 12 vol. %, respectively.

A low percolation threshold value φ_c=3 wt. % was also found for PE/PS/carbon-black composites, in which the filler particles localized on the boundary of the phases *[Gubbels et al., 1995]*.

The dependence of the electro-conductivity of the PS/PE blend, filled with carbon-black on blending time is reported by F. Fenouillot et al. *[Fenouillot et al., 2009]*. At the beginning stage of the blending of PE with PS/carbon-black concentrate, the carbon black particles began to migrate from PS to PE phase. This resulted in the increase of the electro-conductivity of the composite, which has its maximum at the localization of the carbon-black on the boundary of the polymers. At further mixing carbon-black totally migrated into PE phase, what caused the conductivity decrease. Thus, while regulating the time of mixing of the polymer blend, one can obtain a composite at non-equilibrium state with a high value of conductivity, which can be achieved at low filler content due to its localization on the boundary of polymer phases.

D. Yan and G Yang *[Yan and Yang 2009]* have investigated the electrical properties and morphology of the PA6/PS polymer blend, filled with CNTs dependently on the ratio of the composite components. SEM and TEM micropictures have revealed that CNTs localized on the boundary of the polymer phases only. It was found, that at the introduction of the nanotubes into PA6/PS blend the resistivity of the composites decrease by 7 orders of magnitude. Besides, this effect was observed only for the samples with PA6 and PS ratio of 70 wt. % and 30 wt. %, respectively. As far as CNTs were localized only on the boundary of the phases, the continuous conducting network of the filler can be formed only in the composites with the continuous polymer structure in the blend, what was achieved at the component ratio 70:30.

Y. Li and H. Shimizu *[Li Y. and Shimizu, 2008]* found that the value of the rate of mixing during preparing of the filled blend influences significantly the distribution of CNTs in the polymer matrix and the electrical characteristics of the composite. TEM images have shown that in the composites based on the polyvinylidene fluoride (PVDF) and PA6, which were mixed at low rates, CNTs created aggregates and localized only in PA6 phase. However, at high mixing rates the nanotube aggregates were not formed, and nanotube distribution in the PA6 turned out to be more homogeneous, what, in one’s turn, resulted in the enhancement of the electrical properties of the composites. The investigation of the mechanical properties of the filled blends, treated at different mixing rates revealed that the mechanical modulus remain almost invariable, whereas elongation at break was 200% more for the composites, treated at higher mixing rates. Y. Li and H. Shimizu have also noted the influence of CNTs on the composite morphology and on the parameters of component interactions *[Li Y. and Shimizu, 2008]*. It has been shown, that at the introduction in the polymer blend CNTs are localized in the PA6 phase only, what increases its viscosity significantly. Due to this fact the sizes of the particles decreased, and the composite transformed from the structure with isolated spherical inclusions PA6 in PVDF matrix to the co-continuous structure of both components. This, in one’s turn, increased the polymer compatibility, and such a change of the structure also results in the enhancement of the mechanical properties of the composite.

Some papers were devoted to the investigation of the CNT distribution in the polymer matrix based on the PA6/PP *[Zhang L. et al., 2009a, 2009b]* and PE/PC *[Pötschke et al., 2003a]*, and to the influence of CNTs on the electro-conductivity of the compositions. It has been found, that when the content of the conducting filler PC-2% CNT in PE/PC blend reached 30 vol. %, a co-continuous structure formed in the composite, and its conductivity increased by 7 orders of magnitude *[Pötschke et al., 2003a]*. At such ratio of the components a general content of the nanotubes in the composites was 0.41 vol. % of CNTs, whereas the percolation threshold for the individually filled PE or PC is more, than 1 vol. % of CNT. It is interesting, that the composite remained conductive after the removing of the PC phase with a dissolvent. P. Pötschke et al. have proposed to use such composites as conducting/antistatic membranes *[Pötschke et al., 2003a]*. L. Zhang et al. reported about the initiation of the conductivity, connected with the double percolation effect and selective localization of CNTs in the PA6 phase *[Zhang L. et al., 2009b]*. When PP content increased from 50 wt. % to 80 wt. %, the structure of the conductive phase changed from co-continuous to the dispersed one, what was accompanied by the conductivity decrease.

Carbon nanotubes, due to their specific properties, turned to be rather effective filler for polymer blends. O. Meincke et al. *[Meincke et al., 2004]* have compared the mechanical properties of both PA6 blends and acrylonitrile/butadiene/styrene (ABS), filled with CNT and carbon-black. For the unfilled blend the Young's modulus was 1.97 GPa, whereas the introduction of 7 wt. % of CNT resulted in the increase of its value up to 2.51 GPa (i. e. 27% more in comparison with the initial value). In the case of the blend, filled with 7 wt. % of carbon-black, the Young's modulus increased up to 2.08 GPa only. Break elongation decreases for both composites PA6/ABS/carbon-black and PA6/ABS/CNT, though in the latter case this decrease is not such pronounced, what illustrates the higher strength of the systems, filled with CNT.

Due to high ratio between the length and diameter, a nanotube can belong to every phase of the blend simultaneously, what increases the mechanical properties of the composite significantly. In several papers *[Pötschke et al., 2003a, 2007; Zhang L. et al., 2009a; Zhang L. et al., 2009b]* the authors described a so-called "bridging"-effect, at which nanotubes localized simultaneously in two polymer phases, while forming singular "bridges" between them.

Some interesting results were also obtained for the blends of polycarbonate (PC) and PP, filled with CNT and montmorillonite (MMT) *[Pötschke et al., 2007]*. When PC/CNT and PP/MMT concentrates are mixed, montmorillonite localized on the boundary of the polymer phases, and prevented this way the migration of CNT from PC to PP phase. Thus, montmorillonite has provided the decrease of percolation threshold of the composites, while protecting the transition of CNT from one phase into another one.

CNTs also have a significant influence on the rheological properties of the polymer blends *[Abbasi et al., 2010; Bose et al., 2009; Pötschke et al., 2003a; Zhang L. et al., 2009a, 2009b]*. The presence of CNT in the PA6/PP blend resulted in the increase of the of the complex viscosity value (η^*), elastic modulus (G') and viscosity modulus (G'') in the whole frequency range *[Zhang*

L. et al., 2009a]. Such a behaviour is connected with the fact that CNTs prevent the relaxation process of the polymer chains.

Temperature dependences of the conductivity revealed that electroconductive polymer blends are characterized by positive *[Boiteux et al., 2007; Mamunya et al., 2007; Mironi-Harpaz and Narkis, 2001a; Rybak et al., 2010]* and negative *[Feng and Chan, 2000a, 2000b]* temperature coefficients (PTC and NTC, respectively). The basic factors, which influence PTC and NTC are the ratios between the composite components, the conducting filler content and the size of its particles. Thus, J. Feng and C.-M. Chan have shown, that the blends, filled with large particles of carbon-black reveal stronger PTC effect, besides, their room-temperature resistance is usually higher *[Feng and Chan, 2000a]*. It has been shown, that one can reach the NTC of the composites, while using a semiconductor polymer with a high viscosity as one of the component. For the UHMWPE/PP/carbon-black systems it has been found a double PTC effect *[Mironi-Harpaz and Narkis, 2001]*. The initial growth of the resistance of the composite was connected with the melting of the UHMWPE particles, and the following PTC was related to the melting of the PP matrix.

I. Mironi-Harpaz and M. Narkis *[Mironi-Harpaz and Narkis, 2001b]* have studied the influence of γ-radiation on the electric properties of UHMWPE/PE/carbon-black properties. In the case of non-irradiated composite the carbon-black particles were segregated on the surface of the UHMWPE particles due to its high viscosity. The investigations have revealed that the irradiation of tree-component blend resulted in the increase of the composite conductivity, what was caused by the growth of the crystal phase of PE due to cross-linking of the macromolecules.

A polymer with inherent conductivity can also play a role of a conductive filler. M. Zilbermann et al. *[Zilberman et al., 2000]* have studied the composites based on the CPA and polystyrole (PS), filled with polyaniline (PANI). It has been found that PAN is more compatible with CPA, what provides more conductive structure with low percolation threshold in comparison with polymer blend based on the PS. When PAN is introduced into the blend of two CPA/PC polymers, PAN is localized in the co-polymer what results in the double percolation effect.

5.3 Polymer composites filled with combined nanoparticles

Recently, the idea of simultaneous introduction of different type of fillers into polymer matrix seems very promising. The properties of such polymer nanocomposites depend greatly on the dimensions of nanofillers. The different dimensions of nanofiller determine the dispersion, interface, and distribution of nanofiller in polymer matrix. It is expected that the positive synergistic effect of these nanoparticles will improve the properties of polymer matrix. In contrast to conventional composites, in the systems filled with binary filler, the interaction between the nanoparticles should be also taken into account as well as the interaction between nanoparticles and matrix. In such composites, one type of nanofiller will affect the dispersion and distribution of another one, that may result in new synergistic effects in nanocomposites.

A fabrication of polymer nanocomposites is one of the most important applications of CNTs. Carbon nanotubes, due to their specific properties, may be a unique filler for conductive polymer composites with low percolation threshold. However, poor CNTs dispersion and weak interface interaction between CNTs and polymer matrix result in the limitation of the improvement of various properties, and, thus the unique characteristics of CNTs can not be efficiently used in the nanocomposites. The ability to form the large aggregates also leads to the growth of the percolation threshold.

In order to form polymer nanocomposites it was proposed to use such combinations of the filler as clay/carbon black *[Etika et al., 2009; Feller et al., 2004; Konishi and Cakmak, 2006]* and CNT/clay. Polymer/CNT/clay composite is one of the most important multiphase systems with an interesting synergistic effect, in which sodium based montmorillonite (MMT) is the most commonly used layered clay.

An interesting effect was observed for electrically conductive composites filled with carbon black and clay *[Etika et al., 2009; Feller et al., 2004; Konishi and Cakmak, 2006]*. K. C. Etika et al. *[Etika et al., 2009]* have found that the adding of 0.5 vol. % of clay into epoxy/carbon black composites provided to the growth of the conductivity by more than one order. TEM micrographs have shown that around the clay particles a halo of carbon black particles was formed. The appearance of such halo is caused by the interaction between two types of filler. The interaction between the clay and carbon black leads to the improvement of the electrical properties of the composites. The similar effect was observed for the thermoplastic matrix filled with combination of carbon black/clay fillers *[Feller et al., 2004]*. In particular, in the composites based on PE/carbon black filled with clay, the electrical conductivity increased significantly. This effect was explained by the fact that clay interacted simultaneously with the polymer chains and with carbon black. On the one hand, the interaction between the organic components of the clay and the polymer chains results in the decay of interaction between the polymer particles of carbon black. On the other hand, the network of clay particles with the adsorbed carbon black particles on their surface owing to the interactions between the fillers was formed. Such interaction provides more uniform distribution of the fillers.

The incorporation of 3 vol. % of clay into composites PA6/carbon black results in the decrease of the percolation threshold φ_c from 0.155 vol. % to 0.058 vol. % of carbon black *[Konishi and Cakmak, 2006]*. Besides, for the studied composites it was also found the disappearance of aggregates and a uniform distribution of carbon black in the polymer matrix. The interaction of clay platelets with carbon black prevented its aggregation and has provided the formation of the continuous conductive network.

L. Liu and J. C. Grunlan *[Liu and Grunlan, 2007]* have investigated various epoxy/carbon nanotubes composites filled with clay, which were obtained by a mixture in solution. The presence of clay in composites epoxy/CNT provided the reduction of percolation threshold from 0.05 vol. % to 0.01 vol. % of CNTs. In addition, the introduction of clay resulted in the increase of the composite conductivity. For instance, for the composite containing 0.05 vol. % of carbon nanotubes the conductivity increased by more than four orders with the adding of 0.2 vol. % of clay. The photos of the optical microscopy showed that in the epoxy/CNT composites, the carbon nanotubes were present as isolated structures, while the introduction of the clay resulted in the formation of three-dimensional CNTs conductive network. The authors suggest several possible reasons, why the presence of the clay improves the electrical characteristics of the composite epoxy/CNT and provides the formation of the CNT network. First, the clay increases the viscosity of the composite mixture what complicates the re-agglomeration of CNTs in the solution after the ultrasound treatment. Second, CNTs interact stronger with the clay than with the polymer matrix, what results in the formation of segregated carbon nanotubes network.

A significant improvement in the mutual distribution of the fillers in the polymer matrix, and the absence of the aggregates leads to the improvement of not only electrical, but also the mechanical properties of the composites. In particular, Z. Wang and X. Y. Meng *[Wang et al., 2009]* have observed the effect of the clay/CNT filler combination on the mechanical properties of composites based on the polyethyleneoxide (PEO). The values of the yield strength, tensile strength at break and elongation at break for the composites PEO/clay/CNT were significantly higher than those for the composites PEO/clay and PEO/CNT. TEM micrographs have shown that the sizes of the clay particles in the composites filled with binary clay/CNT filler were significantly lower than in the PEO/CNT composite. It was found that the strong interaction between the clay platelets and CNTs prevented the formation of CNT and clay aggregates, and resulted in the formation of the specific network created by both fillers *[Wang et al., 2009]*. The results of dynamic-mechanical analysis of the composites *[Liu and Grunlan, 2007]* showed that the introduction of a small number of SHS composites in clay/CNT, significantly increases their modulus of elasticity, which value was greater than for the composites filled only with clay or CNTs. A similar effect of fillers combination on the elastic modulus of the composites was reported by K. C. Etika et al. *[Etika et al., 2009]*.

The influence of the clay on the carbon nanofibers (CNF) distribution in the polymer matrix was studied by J. A. Johnson et al. *[Johnson et al., 2003]*. The authors have supposed that the effect of the improvement of CNF dispersion in the polymer matrix was caused by the penetration of the clay platelets into the pores of CNF aggregates.

A new type of materials based on the ethylene-vinyl acetate, filled with CNTs and clay and obtained by melt mixing were introduced by P. C. Ma et al. *[Ma et al., 2008]*. The thermal and mechanical properties of composites were significantly changed in the presence of both fillers. It was found that the thermal properties and fire resistance of the material had to be better in the presence of the filler combination.

The combination of CNT and carbon black particles were also found to be very effective. A low percolation threshold was achieved when the hybrid filler content of CNT and carbon black reached 0.2 wt. % and 0.2% wt. %, respectively *[Ma et al., 2009]*. Different shape and aspect ratio and different dispersion characteristics of two conductive fillers result in a unique synergy effect, which provides the improvement of the electrical properties of the nanocomposites. The conductivity of the composites based on PP and PE filled with carbon black has grown significantly after the introduction of a small amount of carbon fibers (CF) *[Dang et al., 2009]*. Such an effect was caused by the fact that CF has connected the divided particles of carbon black, while forming more conductive network in the composite. It has been also established that the composites filled with a hybrid filler show a higher value of the positive temperature coefficient effect, (so-called “PTC-effect”), compared to the composites filled with carbon black. The expansion of the polymer matrix during melting breaks the conductive bridges of CF which connect the carbon black particles. A similar effect of a hybrid filler on the PTC effect was found by W. Di et al. *[Di et al., 2003]*.

During the several previous years there were reported the experimental works, which show that the combination of metal nanofiller and CNTs can improve the electrical properties of the polymer composites. Nanotubes provide the decrease of the percolation threshold, and metal particles result in the appearance of the high conductivity of the composites. Thus, the combining of carbon nanotubes and metal nanofiller makes it possible to obtain the composites with low percolation threshold and high conductivity.

The combination of these two classes of materials (CNTs and metal nanoparticles) may result in a successful integration of properties of two components in new hybrid materials. The CNTs surface serves as a template, where metal particles are absorbed or, when they bear some functional groups, CNTs may be linked through the organic fragments. The composites of CNTs with metal nanoparticles can be formed by two different ways. Pure metal particles are grown and/or deposited directly onto the CNTs surface.

Alternatively, metal particles can be pre-formed and connected to CNTs using covalent bonding of organic fragments, located on the both particles.

During the last decade the idea of decorating of metal nanoparticles on the surface of carbon nanotubes have been reported in some papers *[Dai et al., 2007; Guo and Li, 2005; Kauffman and Star, 2007; Pietrzak and Jeszka, 2009; Reddy et al., 2009; Tang et al., 2009; Tzitzios et al., 2006]*. Due to the integration of the properties of two types of nanoparticles the new nanoscale fillers are obtained, which exhibit new properties, not inherent to pure carbon nanotubes or metal particles. P. C. Ma et al. *[Ma et al., 2009]* have compared the properties of three types of composites based on epoxy resin, filled with: 1) CNTs; 2) functionalized CNTs; 3) CNTs decorated with particles of Ag (CNT/Ag). In the process of decoration metal nanoparticles with the average size of (2 ÷ 4) nm were uniformly distributed on the surface of nanotubes. The conductivity of the composites filled with the decorated carbon nanotubes was significantly higher than that for the composites with pure and functionalized CNTs. The lowest conductivity was observed for the composites with the functionalized CNTs. The presence of the functional groups on the surface of CNTs decreases the number contacts between the nanotubes and prevents the charge transfer between them. Also the length of CNTs can be reduced directly during their functionalization. In addition, the composites filled with CNT/Ag have shown a significant improvement of their thermal conductivity. This value for the epoxy/CNT/Ag composites increased by 94% compared to the pure epoxy, while for the epoxy/CNT composites it increased by 71% only. In addition, all three fillers revealed the improvement of mechanical properties of the composites and the best result were obtained for the samples filled with functionalized NTD, because of their better interaction with polymer matrix.

Metal nanoparticles can be linked to the CNTs surface by the intermolecular or covalent bonds. In the beginning, the surface of metal nanoparticles should be modified by functional groups. They can form covalent bonds with functional groups on the surface of CNTs, or CNTs can interact with the surface by intermolecular or electrostatic interactions *[Georgakilas et al., 2007]*. The filler, formed by the interaction of CNTs with metallic species can be used for the production of composites with several potential applications, such as gas sensors, biosensors, electronic nanodevices, polymer electrolyte fuel cells, etc. In many recent reports metal metal–CNTs are involved in catalytic systems *[Georgakilas et al., 2007]*.

A simple method for decorating the surface of the CNTs with gold particles without modifying of CNTs by the functional groups was reported by N. Salah et al. *[Salah et al., 2009]*. CNTs and solution of metal particles were irradiated by gamma rays. TEM images have shown that Au nanoparticles where localized on the surface of carbon nanotubes. K.-P. Lee et al. *[Lee K.-P. et al., 2007]* have also used gamma-rays for the distribution of gold nanoparticles in the composites based on polyaniline and carbon nanotubes. Interesting results were presented by H. Yu et al. *[Yu et al., 2007]*. The suspension of water solution of CNT-$AgNO_3$ in the presence of 2-propanol were irradiated. The authors received silver nanofibers with the length of several microns, which were localized inside the carbon nanotubes.

The modification of carbon black surface with the particles of Ni and Au was very effective as well *[Pourabbas and Peighambardoust, 2007]*. Nanometal particles filled holes and defects on the surface of carbon black, thereby significantly changing their properties. Such changes of the surface properties of carbon black particles resulted in the changes of the filler-matrix interactions, what influenced the characteristics of the resulting composite. The measurements of the electrical parameters of the composites have shown that the modification of carbon black with metallic particles caused a reduction of resistivity of such systems in comparison with the composites, which contain carbon black only.

A significant improvement of electrical characteristics of PP/Ag composites was achieved by the introduction of CNTs *[Liang et al., 2007]*. At nanometal content below percolation threshold, the addition of nanotubes resulted in the increase of conductivity via a so-called "bridging"-effect, which means the following. The nanoparticles of metal connect the individual nanotubes and form, in such a way, a conductive network.

6. Conclusion

Polymer composites filled with nonofillers are intensively investigated due to their valuable properties and perspectives of the application both for the research purposes and in the industry.

Owing to the unique mechanical, electrical and thermal properties, carbon nanotubes are very promising nanofiller for creation of the electro-conductive polymer composites. Incorporation of CNTs with their excellent properties into polymer matrix becomes a greatly attractive route for the fabrication of various advanced functional materials. However, all the improvements which can be achieved with the presence of CNTs in a polymer composite greatly depend on the amount of CNTs added into the polymer matrix and mainly on the structure organization of the conductive nanofiller and its interaction with polymer phase.

The structural organization of carbon nanotubes in the composites based on thermoplastic polymers plays one of the crucial roles in the manifestation of specific electrical, mechanical and thermal properties. Thus, one can conclude, that a possibility to control the structure formation of the filler conductive phase becomes especially important when this process determines the electro-physical properties of the polymer composite and enables to create the composites with predefined electro-physical properties.

7. References

Abbasi S., Carreau P.J., Derdouri A. (2010) Flow induced orientation of multiwalled carbon nanotubes in polycarbonate nanocomposites: Rheology, conductivity and mechanical properties. *Polymer*, Vol. 51, pp. 922–935.

Akbar S., Beyou E., Cassagnau P., Chaumont P., Farzi G. (2009) Radical grafting of polyethylene onto MWCNTs : A model compound approach. *Polymer*, Vol. 50, pp. 2535–2543.

Al-Saleh M.H., Sundararaj U. (2008) Nanostructured carbon black filled polypropylene/ polystyrene blends containing styrene–butadiene–styrene copolymer: Influence of morphology on electrical resistivity. *European Polymer Journal*, Vol. 44, pp. 1931–1939.

Andrews R., Jacques D., Minot M., Rantell T. (2002) Fabrication of carbon multiwall nanotube/polymer composites by shear mixing. *Macromolecular Materials and Engineering*, Vol. 287, pp. 395–403.

Baibarac M., Gomez-Romero P. (2006) Nanocomposites based on conducting polymers and carbon nanotubes from fancy materials to functional applications. *Journal of Nanoscience and Nanotechnology*, Vol. 6, pp. 1–14.

Bao S.P., Tjong S.C. (2008) Mechanical behaviors of polypropylene/carbon nanotube nanocomposites: The effects of loading rate and temperature. *Materials Science and Engineering A*, Vol. 485, pp. 508–516.

Barraza H.J., Pompeo F., O'Rear E.A., Resasco D.E. (2002) SWCNT-filled thermoplastic and elastomeric composites prepared by miniemulsion polymerization. *Nano Letters*, Vol. 2, pp. 797–803.

Baudouin A.-C., Bailly C., Devaux J. (2010) Interface localization of carbon nanotubes in blends of two copolymers. *Polymer Degradation and Stability*, Vol.95, pp. 389–398.

Baxendale M., Mordkovich V.Z., Chang R.P.H., Yoshimura S. (1997) Magneto-oscillatory behavior of carbon nanotube bundles. *Synthetic Metals*, Vol. 86, pp. 2001–2002.

Bellucci S. (2005) Carbon nanotubes: physics and applications. *Physica Status Solidi*, Vol. 2**,** No 1, pp. 34–47.

Bhattacharyya A.R., Sreekumar T.V., Liu T., Kumar S., Ericson L.M., Hauge R.H., Smalley R.E. (2003) Crystallization and orientation studies in polypropylene/single wall carbon nanotube composite. *Polymer*, Vol. 44, pp. 2373–2377.

Biercuk M.J., Llaguno M.C., Radosavljevic M., Hyun J.K., Johnson A.T., Fischer J.E. (2002) Carbon nanotube composites for thermal management. *Applied Physics Letters*, Vol. 80, pp. 2767–2770.

Bikiaris D. (2010) Microstructure and properties of polypropylene/carbon nanotube nanocomposites. *Materials*, Vol. 3, pp. 2884–2946.

Bikiaris D., Vassiliou A., Chrissafis K., Paraskevopoulos K.M., Jannakoudakis A., Docoslis A. (2008) Effect of acid treated multi-walled carbon nanotubes on the mechanical, permeability, thermal properties and thermo-oxidative stability of isotactic polypropylene. *Polymer Degradation and Stability*, Vol. 93, pp. 952–967.

Boiteux G., Mamunya Ye.P., Lebedev E.V., Adamczewski A., Boullanger C., Cassagnau P., Seytre G. (2007) From conductive polymer composites with controlled morphology to smart materials. *Synthetic Metals*, Vol. 157, pp. 1071–1073.

Bommeli F., Degiorgi L., Wachter P., Bacsa W.S., Heer W.A., Forro L. (1997) The optical response of carbon nanotubes. *Synthetic Metals,* Vol. 86, pp. 2307–2308.

Bose S., Bhattacharyya A.R., Kulkarni A.R., Pötschke P. (2009) Electrical, rheological and morphological studies in co-continuous blends of polyamide 6 and acrylonitrile-butadiene-styrene with multiwall carbon nanotubes prepared by melt blending. *Composites Science and Technology,* Vol. 69, pp. 365–372.

Bouchet J., Carrot C., Guillet J., Boiteux G., Seytre G., Pineri M. (2000) Conductive composites of UHMWPE and ceramics based on the segregated network concept. *Polymer Engineering and Science*, Vol. 40, pp. 36–45.

Breuer O., Sundararaj U. (2004) Big returns from small fibers: A review of polymer/carbon nanotube composites. *Polymer composites,* Vol. 25, No 6, pp. 630–645.

Bridge B., Folkes M.J., Wood B.R. (1990) Investigation into the DC conductivity of colloidally dispersed gold/polymer composites. *Journal Of Physics D: Applied Physics,* Vol. 23, pp. 890–898.

Broza G., Piszczek K., Schulte K., Sterzynski T. (2007) Nanocomposites of poly(vinyl chloride) with carbon nanotubes (CNT). *Composites Science and Technology,* Vol. 67, pp. 890–894.

Causin V., Yang B.-X., Marega C., Goh S.H., Marigo A. (2009) Nucleation, structure and lamellar morphology of isotactic polypropylene filled with polypropylene-grafted multiwalled carbon nanotubes. *European Polymer Journal,* Vol. 45, pp. 2155–2163.

Chan C.-M., Cheng C.-L., Yuen M.M.F. (1997) Electrical properties of polymer composites prepared by sintering a mixture of carbon black and ultra-high molecular weight polyethylene powder. *Polymer Engineering and Science*, Vol. 37, No 7, pp. 1127–1136.

Chiteme C., Mclachlan D.S. (2000) Measurements of universal and non-universal percolation exponents in macroscopically similar systems. *Physica B,* Vol. 279, pp. 69–71.

Chiteme C., McLachlan D.S. (2003) AC and DC conductivity, magnetoresistance, and scaling in cellular percolation systems. *Physical Review B,* Vol. 67, pp. 1–18.

Dai H. (2002) Carbon nanotubes: opportunities and challenges. *Surface Science,* Vol. 500, pp. 218–241.

Dai K., Shi L., Fang J., Zhang Y. (2007) Synthesis of silver nanoparticles on functional multi-walled carbon nanotubes. *Materials Science and Engineering A*, Vol. 465, pp. 283–286.

Dang Z.-M., Li W.-K., Xu H.-P. (2009) Origin of remarkable positive temperature coefficient effect in the modified carbon black and carbon fiber cofilled polymer composites. *Journal Applied Physics,* Vol. 106, pp. 0249131–0249135.

Deng H., Skipa T., Zhang R., Lellinger D., Bilotti E., Alig I., Peijs T. (2009a) Effect of melting and crystallization on the conductive network in conductive polymer composites. *Polymer,* Vol. 50, pp. 3747–3754.

Deng H., Zhang R., Bilotti E., Loos J., Peijs T. (2009b) Conductive polymer tape containing highly oriented carbon nanofillers. *Journal of Applied Polymer Science,* Vol. 113, pp. 742–751.

Di W., Zhang G., Xu J., Peng Y., Wang X., Xie Z. (2003) Positive-temperature-coefficient/negative-temperature-coefficient effect of low-density polyethylene filled with a mixture of carbon black and carbon fiber. *Journal of Polymer Science: Part B: Polymer Physics,* Vol. 41, pp. 3094–3101.

Du F.M., Scogna R.C., Zhou W., Brand S., Winey K.I. (2004) Nanotube networks in polymer nanocomposites: Rheology and electrical conductivity. *Macromolecules,* Vol. 37, pp. 9048–9055.

Dyachkov P.N. (2006) Carbon nanotubes, Binom, Moscow; Russia.

Etika K.C., Liu L., Hess L.A., Grunlan J.C. (2009) The influence of synergistic stabilization of carbon black and clay on the electrical and mechanical properties of epoxy composites. *Carbon,* Vol. 47, pp. 3128–3136.

Feller J.F., Bruzaud S., Grohens Y. (2004) Influence of clay nanofiller on electrical and rheological properties of conductive polymer composite. *Materials Letters,* Vol. 58, pp 739–745.

Fenouillot F., Cassagnau P., Majesté J.-C. (2009) Uneven distribution of nanoparticles in immiscible fluids: Morphology development in polymer blends. *Polymer,* Vol. 50, pp. 1333–1350.

Feng J., Chan C.-M. (2000a) Double positive temperature coefficient effects of carbon black-filled polymer blends containing two semicrystalline polymers. *Polymer,* Vol. 41, pp. 4559–4565.

Feng J., Chan C.-M. (2000b) Positive and negative temperature coefficient effects of an alternating copolyumer of tetrafluoroethylene-ethylene containing carbon black-filled HDPE particles. *Polymer,* Vol. 41, pp. 7279–7282.

Fournier J., Boiteux G., Seytre G., Marichy G. (1997) Percolation network of polypyrrole in conducting polymer composites. *Synthetic Metals,* Vol. 84, pp. 839–840.

Georgakilas V., Gournis D., Tzitzios V., Pasquato L., Guldi D.M., Prato M. (2007) Decorating carbon nanotubes with metal or semiconductor nanoparticles. *Journal of Materials Chemistry,* Vol. 17, pp. 2679–2694.

Grossiord N., Wouters M.E.L., Miltner H.E., Lu K., Loos J., Mele B.V., Koning C.E. (2010) Isotactic polypropylene/carbon nanotube composites prepared by latex technology: Electrical conductivity study. *European Polymer Journal,* Vol. 46, pp. 1833–1843.

Grunlan J.C., Gerberich W.W., Francis L.F. (2001) Lowering the percolation threshold of conductive composites using particulate polymer microstructure. *Journal of Applied Polymer Science,* Vol. 80, pp. 692–705.

Gubbels F., Blacher S., Vanlathem E., Jerome R., Deltour R., Brouers F., Teyssie Ph. (1995) Design of electrical conductive composites: key role of the morphology on the electrical properties of carbon black filled polymer blends. *Macromolecules,* Vol. 28, No 5, pp. 1559–1566.

Guo D.J., Li H.L. (2005) Highly dispersed Ag nanoparticles on functional MWNT surfaces for methanol oxidation in alkaline solution. *Carbon,* Vol. 43, pp. 1259–1264.

Ha M.L.P., Grady B.P., Lolli G., Resasco D.E., Ford W.T. (2007) Composites of single-walled carbon nanotubes and styrene-isoprene copolymer lattices. *Macromolecular Chemistry and Physics,* Vol. 208, pp. 446–456.

Harris P.J.F. (2004) Carbon nanotube composites. *International Materials Reviews,* Vol. 49, No 1, pp. 31–43.

Hobbie E.K., Obrzut J., Kharchenko S.B. (2006) Charge transport in melt-dispersed carbon nanotubes. *The Journal of Chemical Physics,* Vol. 125, pp. 125–127.

Hu G., Zhao C., Zhang S., Yang M., Wang Z. (2006) Low percolation thresholds of electrical conductivity and rheology in poly(ethylene terephthalate) through the networks of multi-walled carbon nanotubes. *Polymer,* Vol. 47, pp. 480–488.

Hu N., Masuda Z., Yan C., Yamamoto G., Fukunaga H., Hashida T. (2008) The electrical properties of polymer nanocomposites with carbon nanotube fillers. *Nanotechnology,* Vol. 19, pp. 215701–215711.

Immonen K., Nattinen K., Sarlin J., Hartikainen J. (2009) Conductive plastics with hybrid materials. *Journal of Applied Polymer Science,* Vol. 114, pp. 1494–1502.

Johnson J.A., Barbato M.J., Hopkins S.R., O'Malley M.J. (2003) Dispersion and film properties of carbon nanofiber pigmented conductive coatings. *Progress in Organic Coatings,* Vol. 47, pp. 198–206.

Kauffman D.R., Star A. (2007) Chemically induced potential barriers at the carbon nanotube-metal nanoparticle interface. *Nano Letters,* Vol. 7, No 7, pp. 1863–1868.

Kharchenko S.B., Douglas J.F., Obrzut J., Grulke E.A., Migler K.B. (2004) Flow-induced properties of nanotube-filled polymer materials. *Nature Materials,* Vol. 3, pp. 564–568.

Kim Y.S., Wright J.B., Grunlan J.C. (2008) Influence of polymer modulus on the percolation threshold of latex-based composites. *Polymer,* Vol. 49, pp. 570–578.

King J.A., Johnson B.A., Via M.D., Ciarkowski C.J. (2009) Electrical conductivity of carbon-filled polypropylene-based resins. *Journal of Applied Polymer Science,* Vol. 112, pp. 425–433.

Kong H., Gao C., Yan D. (2004) Controlled functionalization of multiwalled carbon nanotubes by in situ atom transfer radical polymerization. *Journal of American Chemistry Society,* Vol. 126, pp. 412–413.

Konishi Y., Cakmak M. (2006) Nanoparticle induced network self-assembly in polymer–carbon black composites. *Polymer,* Vol. 47, pp. 5371–5391.

Koval'chuk A.A., Shchegolikhin A.N., Shevchenko V.G., Nedorezova P.M., Klyamkina A.N., Aladyshev A.M. (2008a) Synthesis and properties of polypropylene/multiwall carbon nanotube composites. *Macromolecules,* Vol. 41, pp. 3149–3156.

Koval'chuk A.A., Shevchenko V.G., Shchegolikhin A.N., Nedorezova P.M., Klyamkina A.N., Aladyshev A.M. (2008b) Isotactic and syndiotactic polypropylene/multi-wall carbon nanotube composites: Synthesis and properties. *Journal of Material Science,* Vol. 43, pp. 7132–7140.

Kusy R.P., Corneliussen R.D. (1975) The thermal conductivity of nickel and copper dispersed in poly(vinyl chloride). *Polymer Engineering & Science,* Vol. 15, No 2, pp. 107–112.

Lebovka N., Lisunova M., Mamunya Ye.P., Vygornitskii N. (2006) Scaling in percolation behavior in conductive-insulating composites with particles of different size. *Journal of Pysics D: Applied Pysics,* Vol. 39, pp. 1–8.

Lee G.-W., Jagannathan S., Chae H.G., Minus M.L., Kumar S. (2008) Carbon nanotube dispersion and exfoliation in polypropylene and structure and properties of the resulting composites. *Polymer,* Vol. 49, pp. 1831–1840.

Li H.J., Lu W.G., Li J.J., Bai X.D., Gu C.Z. (2005) Multichannel ballistic transport in multiwall carbon nanotubes. *Physical Review Letters,* Vol. 95, pp. 0866011–0866014.

Lee H.K., Pejanovic S., Mondragon I., Mijovic J. (2007) Dynamics of single-walled carbon nanotube (SWNT)/polyisoprene (PI) nanocomposites in electric and mechanical field. *Polymer,* Vol. 48, pp. 7345–7355.

Lee K.-P., Gopalan A.I., Santhosh P., Lee S.H., Nho Y.C. (2007) Gamma radiation induced distribution of gold nanoparticles into carbon nanotube-polyaniline composite. *Composites Science and Technology,* Vol. 67, pp. 811–816.

Lee S.H., Cho E., Jeon S.H., Youn J.R. (2007) Rheological and electrical properties of polypropylene composites containing functionalized multi-walled carbon nanotubes and compatibilizers. *Carbon,* Vol. 45, pp. 2810–2822.

Li Y., Shimizu H. (2008) Conductive PVDF/PA6/CNTs nanocomposites fabricated by dual formation of cocontinuous and nanodispersion structures. *Macromolecules,* Vol. 41, pp. 5339–5344.

Liang G.D., Tjong S.C. (2006) Electrical properties of low-density polyethylene/multiwalled carbon nanotube nanocomposites. *Materials Chemistry and Physics,* Vol. 100, pp 132–137.

Liang G.D., Bao S.P., Tjong S.C. (2007) Microstructure and properties of polypropylene composites filled with silver and carbon nanotube nanoparticles prepared by melt-compounding. *Materials Science and Engineering B,* Vol. 142, pp. 55–61.

Lisunova M.O., Mamunya Ye.P., Lebovka N.I., Melezhyk A.V. (2007) Percolation behaviour of ultrahigh molecular weight polyethylene/multi-walled carbon nanotubes composites. *European Polymer Journal,* Vol. 43, pp. 949–958.

Liu L., Grunlan J.C. (2007) Clay assisted dispersion of carbon nanotubes in conductive epoxy nanocomposites. *Advanced Functional Materials,* Vol. 17, pp. 2343–2348.

Logakis E., Pollatos E., Pandis Ch., Peoglos V., Zuburtikudis I., Delides C.G., Vatalis A., Gjoka M., Syskakis E., Viras K., Pissis P. (2010) Structure–property relationships in isotactic polypropylene/multi-walled carbon nanotubes nanocomposites. *Composites Science and Technology,* Vol. 70, pp. 328–335.

López Manchado M.A., Valentini L., Biagiotti J., Kenny J.M. (2005) Thermal and mechanical properties of single-walled carbon nanotubes–polypropylene composites prepared by melt processing. *Carbon,* Vol. 43, pp.1499–1505.

Lux F., Review. (1993) Models proposed to explain the electrical conductivity of mixtures made of conductive and insulating materials. *Journal of Material Science,* Vol. 28, pp. 285–301.

Ma P.C., Tang B.Z., Kim J.-K. (2008) Effect of CNT decoration with silver nanoparticles on electrical conductivity of CNT-polymer composites. *Carbon,* Vol. 46, pp. 1497–1505.

Ma P.C., Liu M.-Y., Zhang H., Wang S.-Q., Wang R., Wang K., Wong Y.-K., Tang B.-Z., Hong S.-H., Paik K.-W., Kim J.-K. (2009) Enhanced electrical conductivity of nanocomposites containing hybrid fillers of carbon nanotubes and carbon black. *Applied Materials and Interfaces,* Vol. 1, No 5, pp. 1090–1096.

Malliaris A., Turner D.T. (1971) Influence of particle size on the electrical resistivity of compacted mixtures of polymeric and metallic powders. *Journal of Applied Physics,* Vol. 42, No 2, pp. 614–618.

Mamunya Ye.P. (1999) Morphology and percolation conductivity of polymer blends containing carbon black. *Journal of Macromolecular Science, Part B: Physics,* Vol. 38, No 5-6, pp. 615–622.

Mamunya Ye.P., Privalko E.G., Lebedev E.V., Privalko V.P., Balta Calleja F.J., Pissis P. (2001) Structure-dependent conductivity and microhardness of metal-filled PVC composites. *Macromolecular Symposia,* Vol. 169, pp. 297–306.

Mamunya Ye.P., Davydenko V.V., Pissis P., Lebedev E.V. (2002a) Electrical and thermal conductivity of polymers filled with metal powders. *European Polymer Journal,* Vol. 38, pp 1887–1897.

Mamunya Ye.P., Muzychenko Yu., Pissis P., Lebedev E.V., Shut M.I. (2002b) Percolation phenomena in polymers contained dispersed iron. *Polymer Engineering and Science,* Vol. 42, No 1, pp. 90–100.

Mamunya Ye.P., Davydenko V.V., Zois H., Apekis L., Snarskii A.A., Slipchenko K.V. (2002c) Dielectric properties of polymers filled with dispersed metals. *Polymer and Polymer Composites,* Vol. 10, No 3b, pp. 219–227.

Mamunya Ye.P., Vasylenko S.L., Paraschenko I.M., Lebedev E.V., Shut M.I. (2003) Structure and electrical properties of electro-conductive polymer composites. *Composite polymer materials,* Vol. 25, No 1, pp.36–42.

Mamunya Y.P., Muzychenko Y.V., Lebedev E.V., Boiteux G., Seytre G., Boullanger C., Pissis P. (2007) PTC effect and structure of polymer composites based on polyethylene/polyoxymethylene blend filled with dispersed iron. *Polymer Engineering and Science,* Vol. 47, No 1, pp. 34–42.

Mamunya Ye., Boudenne A., Lebovka N., Ibos L., Candau Y., Lisunova M. (2008) Electrical and thermophysical behaviour of PVC-MWCNT nanocomposites. *Conposites Science and Technology,* Vol. 68, pp. 1981–1988.

Mamunya Ye.P., Levchenko V.V., Rybak A., Boiteux G., Lebedev E.V., Ulanski J., Seytre G. (2010a) Electrical and thermomechanical properties of segregated nanocomposites based on PVC and multiwalled carbon nanotubes. *Journal of Non-Crystalline Solids,* Vol. 356 pp. 635–641.

Mamunya Ye.P., Levchenko V.V., Boiteux G., Lebedev E.V., Zanoaga M., Tanasa F. (2010b) Electrical and mechanical properties of novel nanocomposites based on copolyamide-polypropylene polymer blends containing carbon nanotubes. *Polymer Journal (Ukraine),* Vol. 32, No 4, pp. 313–320.

McLachlan D.S. (1999) Complex AC conductivity of a carbon black composite as a function of frequency, composition, and temperature. *Physical Review B,* Vol. 60, No 18, pp. 12746–12751.

McLachlan D.S. (2000) Analytical functions for the DC and AC conductivity of conductor-insulator composites. *Journal of Electroceramics,* Vol. 5, No 2, pp. 93–110.

McLachlan D.S., Heiss W.D., Chiteme C., Wu J. (1998) Analytic scaling functions applicable to dispersion measurements in percolative metal-insulator system. *Physical Review B,* Vol. 58, No 20, pp. 13558–13564.

McLachlan D.S., Chiteme C., Park C., Wise K.E., Lowther S.E., Lillehei P.T., Siochi E.J., Harrison J.S. (2005) AC and DC percolative conductivity of single wall carbon nanotube polymer composites. *Journal of Polymer Science: Part B: Polymer Physics,* Vol. 43, pp. 3273–3287.

Meincke O., Kaempfer D., Weickmann H., Friedrich C., Vathauer M., Warth H. (2004) Mechanical properties and electrical conductivity of carbon-nanotube filled polyamide-6 and its blends with acrylonitrile/butadiene/styrene. *Polymer,* Vol. 45, pp. 739–748.

Mičušík M., Omastová M., Krupa I., Prokes J., Pissis P., Logakis E., Pandis C., Pötschke P., Pionteck J. (2009) A comparative study on the electrical and mechanical behaviour of multi-walled carbon nanotube composites prepared by diluting a masterbatch with various types of polypropylenes. *Journal of Applied Polymer Science,* Vol. 113, pp. 2536–2551.

Mierczyńska A., Friedrich J., Maneck H.E., Boiteux G., Jeszka J.K. (2004) Segregated network polymer/carbon nanotubes composites. *Central European Journal of Chemistry,* Vol. 2, No 2, pp. 363–370.

Miriyala S.M., Kim Y.S., Liu L., Grunlan J.C. (2008) Segregated networks of carbon black in poly(vinyl acetate) latex: influence of clay on the electrical and mechanical behavior. *Macromolecular Chemistry and Physics,* Vol. 209, pp. 2399–2409.

Mironi-Harpaz I., Narkis M. (2001a) Electrical behavior and strtucture of polypropylene/ultrahigh molecular weight polyethylene/carbon black immiscible blends. *Journal of Applied Polymer Science,* Vol. 81, pp. 104–115.

Mironi-Harpaz I., Narkis M. (2001b) Thermoelectric behavior (PTC) of carbon black-containing TPX/UHMWPE and TPX/XL-UHMWPE blends. *Journal of Polymer Science: Part B: Polymer Physics,* Vol. 39, pp. 1415–1428.

Mittal V. (Ed.) (2010) Polymer nanotube nanocomposites. Synthesis, properties and applications, Wiley, New Jersey, USA.

Moniruzzaman M., Winey K.I. (2006) Polymer nanocomposites containing carbon nanotubes. *Macromolecules,* Vol. 39, pp. 5194–5205.

Naficy S., Garmabi H. (2007) Study of the effective parameters on mechanical and electrical properties of carbon black filled PP/PA6 microfibrillar composites. *Composites Science and Technology,* Vol. 67, pp. 3222–3241.

Pegel S., Pötschke P., Petzold G., Alig I., Dudkin S.M., Lellinger D. (2008) Dispersion, agglomeration, and network formation of multiwalled carbon nanotubes in polycarbonate melts. *Polymer,* Vol. 49, pp. 974–98.

Pietrzak Ł., Jeszka J. K. (2009) Gold nanoparticles grown on multiwall carbon nanotubes. Materials Science (Poland), Vol. 27, No 3, pp. 693-698.

Pourabbas B., Peighambardoust S.J. (2007) PTC effect in HDPE filled with carbon blacks modified by Ni and Au metallic particles. Journal of Applied Polymer Science, Vol. 105, pp. 1031–1041.

Pötschke P., Fornes T.D., Paul D.R. (2002) Rheological behavior of multiwalled carbon nanotube- polycarbonate composites. *Polymer,* Vol. 43, pp. 3247–3255.

Pötschke P., Bhattacharyya A.R., Janke A. (2003a) Morphology and electrical resistivity of melt mixed blends of polyethylene and carbon nanotubes filled polycarbonate. *Polymer,* Vol. 44, pp. 8061–8069.

Pötschke P., Dudkin S.M., Alig I. (2003b) Dielectric spectroscopy on melt processed polycarbonate–multiwalled carbon nanotube composites. *Polymer,* Vol. 44, pp. 5023–5030.

Pötschke P., Bhattacharyya A.R., Janke A. (2004) Carbon nanotube-filled polycarbonate composites produced by melt mixing and their use in blends with polyethylene. *Carbon,* Vol.42, pp. 965–969.

Pötschke P., Kretschmar B., Janke A. (2007) Use of carbon nanotube filled polycarbonate in blends with montmorillonite filled polypropylene. Composites Science and Technology, Vol. 67, pp. 855–860.

Prashantha K., Soulestin J., Lacrampe M.F., Krawczak P., Dupin G., Claes M. (2009) Masterbatch-based multi-walled carbon nanotube filled polypropylene nanocomposites: Assessment of rheological and mechanical properties. *Composites Science and Technology,* Vol. 69, pp. 1756–1763.

Privalko E.G., Mamunya E.P., Lebedev E.V., Privalko V.P., Balta Calleja F.J., Pissis P. (2000) Structure-dependent microhardness of metal-filled polyvinyl chloride composites. *Letters of National Academy of Science of Ukraine,* Vol. 5, pp. 159–162.

Pulikkathara M.X., Kuznetsov O.V., Peralta I.R.G., Wei X., Khabashesku V.N. (2009) Medium density polyethylene composites with functionalized carbon nanotubes. *Nanotechnology,* Vol. 20, pp. 195602–195607.

Qin S., Qin D., Ford W.T., Resasco D.E., Herrera J.E. (2004) Polymer brushes on single-walled carbon nanotubes by atom transfer radical polymerization of n-butyl methacrylate. *Journal of American Chemistry Society,* Vol. 126, pp. 170–176.

Razavi-Nouri M., Ghorbanzadeh-Ahangari M., Fereidoon A., Jahanshahi M. (2009) Effect of carbon nanotubes content on crystallization kinetics and morphology of polypropylene. *Polymer Testing,* Vol. 28, pp. 46–52.

Reddy K.R., Sin B.C., Ryu K.S., Kim J.-C., Chung H., Lee Y. (2009) Conducting polymer functionalized multi-walled carbon nanotubes with noble metal nanoparticles: Synthesis, morphological characteristics and electrical properties. *Synthetic Metals,* Vol. 159, pp. 595–603.

Rybak A., Boiteux G., Melis F., Seytre G. (2010) Conductive polymer composites based on metallic nanofiller as smart materials for current limiting devices. *Composites Science and Technology,* Vol. 70, pp. 410–416.

Salah N., Habib S.S., Khan Z.H., Al-Hamedi S., Djouider F. (2009) Functionalization of gold and carbon nanostructured materials using gamma-ray irradiation. *Radiation Physics and Chemistry,* Vol. 78, pp. 910–913.

Sandler J., Broza G., Nolte M., Schulte K., Lam Y.-M., Shaffer M.S.P. (2003) Crystallization of carbon nanotube and nanofiber polypropylene composites. *Journal of Macromolecular Science Part B—Physics,* Vol. 42, No (3&4), pp. 479–488.

Seo M.-K., Park S.-J. (2004) Electrical resistivity and rheological behaviors of carbon nanotubes-filled polypropylene composites. *Chemical Physics Letters,* Vol. 395, pp. 44–48.

Seo M.-K., Lee J.-R., Park S.-J. (2005) Crystallization kinetics and interfacial behaviors of polypropylene composites reinforced with multi-walled carbon nanotubes. *Materials Science and Engineering A,* Vol. 404, pp. 79–84.

Skakalova V., Dettlaff-Weglikowska U., Roth S. (2005) Electrical and mechanical properties of nanocomposites of single wall carbon nanotubes with PMMA. *Synthetic Metals,* Vol. 152, pp. 349–352.

So H.H., Cho J.W., Sahoo N.G. (2007) Effect of carbon nanotubes on mechanical and electrical properties of polyimide/carbon nanotubes nanocomposites. *European Polymer Journal,* Vol. 43, pp. 3750–3756.

Sterzynski T., Tomaszewska J., Piszczek K., Skorczewska K. (2010) The influence of carbon nanotubes on the PVC glass transition temperature. *Composites Science and Technology*, Vol. 70, pp. 966–969.

Stetter A., Vancea J., Back C.H. (2008) Determination of the intershell conductance in a multiwall carbon nanotube. *Applied Physics Letters,* Vol. 93, pp. 1721031–1721033.

Suhr J., Zhang W., Ajayan P.M., Koratkar N.A. (2006) Temperature-activated interfacial friction damping in carbon nanotube polymer composites. *Nano Letters,* Vol. 6, pp. 219–223.

Sumita M., Sakata K., Asai S., Miyasaka K., Nakagawa H. (1991) Dispersion of fillers and the electrical conductivity of polymer blends with carbon black. *Polymer Bulletin,* Vol. 25, pp. 265–271.

Sumita M., Sakata K., Hayakawa Y., Asai S., Miyasaka K., Tanemura M. (1992) Double percolation effect on the electrical conductivity of conductive particles filled polymer blends. *Colloid Polymer Science,* Vol. 270, pp. 134–139.

Tang Y., Yang D., Qin F., Hu J., Wang C., Xu H. (2009) Decorating multi-walled carbon nanotubes with nickel nanoparticles for selective hydrogenation of citral. *Journal of Solid State Chemistry,* Vol. 182, pp. 2279–2284.

Tchoudakov R., Breuer O., Narkis M. (1996) Conductive polymer blends with low carbon black loading: polypropylene/polyamide. *Polymer Engineering and Science,* Vol. 36, No 10, pp. 1336–1346.

Teng C.-C., Ma C.-C.M., Huang Y.-W., Yuen S.-M., Weng C.-C., Chen C.-H., Su S.-F. (2008) Effect of MWCNT content on rheological and dynamic mechanical properties of multiwalled carbon nanotube/polypropylene composites. *Composites: Part A,* Vol. 39, pp. 1869–1875.

Tersoff J. (1999) Contact resistance of carbon nanotubes. *Applied Physics Letters,* Vol. 74, No 15, pp. 2122–2124.

Thostenson E.T., Ren Z., Chou T.-W. (2001) Advances in the science and technology of carbon nanotubes and their composites: a review. *Composites Science and Technolog*y, Vol. 61, pp. 1899–1912.

Tjong S.C., Liang G.D., Bao S.P. (2007) Electrical behavior of polypropylene/multiwalled carbon nanotube nanocomposites with low percolation threshold. *Scripta Materialia,* Vol. 57, pp. 461–464.

Tzitzios V., Georgakilas V., Oikonomou E., Karakassides M., Petridis D. (2006) Synthesis and characterization of carbon nanotube/metal nanoparticle composites well dispersed in organic media. *Carbon,* Vol. 44, pp. 848–853.

Valentini L., Biagiotti J., Lopez-Manchado M.A., Santucci S., Kenny J.M. (2004) Effects of carbon nanotubes on the crystallization behavior of polypropylene. *Polymer Engineering and Science,* Vol. 44, No 2, pp. 303–311.

Valentino O., Sarno M., Rainone N.G., Nobile M.R., Ciambelli P., Neitzert H.C., Simon G.P. (2008) Influence of the polymer structure and nanotube concentration on the conductivity and rheological properties of polyethylene/CNT composites. *Physica E,* Vol. 40, pp. 2440–2445.

Velasco-Santos C., Martinez-Hernandez A.L., Fisher F.T., Ruoff R., Castano V.M. (2003) Improvement of thermal and mechanical properties of carbon nanotube composites through chemical functionalization. *Chemistry of Materials,* Vol. 15, pp. 4470–4475.

Vysotskiy V.V., Roldughin V.I. (1998) Structure and percolation properties of conductive film composites. *Journal of colloid (Russian),* Vol. 60, No 6, pp. 729–745.

Wang Z., Meng X.Y., Li J.Z., Du X.H., Li S.Y., Jiang Z.W., Tang T. (2009) A simple method for preparing carbon nanotubes/clay hybrids in water. *Journal of Physical Chemistry C,* Vol. 113, pp. 8058–8064.

Xu D., Wang Z. (2008) Role of multi-wall carbon nanotube network in composites to crystallization of isotactic polypropylene matrix. *Polymer,* Vol. 49, pp. 330–338.

Yacubowicz J., Narkis M., Benguigui L. (1990) Electrical and dielectric properties of segregated carbon black-polyethylene systems. *Polymer Engineering and Science,* Vol. 30, No 8, pp. 459–468.

Yan D., Yang G. (2009) An innovative method to improve the electrical conductivity of multi-walled carbon nanotubes filled polyamide 6/ polystyrene blends. *Materials Letters,* Vol. 63, pp. 1900–1903.

Youngs I.J. (2003) A geometric percolation model for non-spherical excluded volumes. *Journal of Physics D: Applied Physics,* Vol. 36, pp. 738–747.

Yu H., Peng J., Zhai M., Li J., Wie G. (2008) Silver nanowires formed within multi-walled carbon nanotubes by radiation-induced reduction of silver ions. *Physica E,* Vol. 40, pp. 2694–2697.

Yuen S.M., Ma C.C., Chiang C.L., Lin Y.Y., Teng C.C. (2007) Preparation and morphological, electrical, and mechanical properties of polyimide-grafted MWCNT/polyimide composite. *Journal of Polymer Science Part A: Polymer Chemistry,* Vol. 45, pp. 3349–3358.

Zettl A., Cumings J. (2001) Electromechanical Properties of Multiwall Carbon Nanotubes. *Nanonetwork Materials: Fullerenes, Nanotubes, and Related Systems,* Vol. 590, pp. 107–112.

Zhang C., Yi X.S., Yui H., Asai S., Sumita M. (1998) Selective location and double percolation of short carbon fiber filled polymer blends: high-density polyethylenerisotactic polypropylene. *Materials Letters,* Vol. 36, pp. 186–190.

Zhang C., Ma C.-A., Wang P., Sumita M. (2005) Temperature dependence of electrical resistivity for carbon black filled ultra-high molecular weight polyethylene composites prepared by hot compaction. *Carbon,* Vol.43, pp. 2544–2553.

Zhang H., Zhang Z. (2007) Impact behaviour of polypropylene filled with multi-walled carbon nanotubes. *European Polymer Journal,* Vol.43, pp. 3197–3207.

Zhang L., Wan C., Zhang Y. (2009a) Investigation on the multiwalled carbon nanotubes reinforced polyamide 6/polypropylene composites. *Polymer Engineering and Science,* Vol. 49, pp. 1909–1917.

Zhang L., Wan C., Zhang Y. (2009b) Morphology and electrical properties of polyamide 6/polypropylene / multi-walled carbon nanotubes composites. *Composites Science and Technology,* Vol. 69, pp. 2212–2217.

Zhou Z., Wang S., Zhang Y., Zhang Y. (2006) Effect of different carbon fillers on the properties of PP composites: comparison of carbon black with multiwalled carbon nanotubes. *Journal of Applied Polymer Science,* Vol. 102, pp. 4823–4830.

Zhu B.-K., Xie S.-H., Xu Z.-K., Xu Y.-Y. (2006) Preparation and properties of the polyimide/multi-walled carbon nanotubes (MWNTs) nanocomposites. *Composites Science and Technology,* Vol. 66, pp. 548–554.

Zilberman M., Siegmann A., Narkis M. (2000) Conductivity and structure of melt-processed polyaniline binary and ternary blends. *Polymers for Advanced Technologies,* Vol. 11, pp. 20–26.

Zois H., Apekis L., Mamunya Ye.P., Lebedev E.V. (2001) The influence of the filler spatial distribution on the dielectric properties of metal-polymer composites. *Composite polymeric materials,* Vol. 23, No 2, pp. 92–95.

Zois H., Apekis L., Mamunya Ye.P. (2003a) Structure-electrical properties relationships of polymer composites filled with Fe-powder. *Macromolecular Symposia*, Vol. 194, pp. 351–359.

Zois H., Apekis L., Mamunya Ye.P. (2003b) Dielectric properties and morphology of polymer composites filled with dispersed iron. *Journal of Applied Polymer Science,* Vol. 88, pp. 3013–3020.

Zois H., Mamunya Ye.P., Apekis L. (2003c) Structure and dielectric properties of a thermoplastic blend containing dispersed metal. *Macromolecular Symposia,* Vol. 198, pp. 461–472.

Chapter 10

Thermosetting Cyanate Ester Resins filled with CNTs

Alexander FAINLEIB[1], Liubov BARDASH[1],
Gisèle BOITEUX[2], Olga GRIGORYEVA[1]

[1] Institute of Macromolecular Chemistry of the National Academy of Sciences of Ukraine, 48, Kharkivske shose, 02160 Kyiv, Ukraine
[2] Université de Lyon, Lyon, F-69003, France; Université Lyon 1, IMP/LMPB Laboratoire des Matériaux Polymères et Biomatériaux, Bât ISTIL, 43 Bld du 11 Novembre, Villeurbanne, F-69622, France; CNRS, UMR 5223, Ingénierie des Matériaux Polymères, Villeurbanne, F-69621, France

---

Summary

In this chapter, a review on synthesis, structure and properties of the novel nanocomposites based on high performance thermosetting polymer matrix, polycyanarate, from Cyanate Ester Resins and the nanofiller, Carbon Nanotubes, is given and the own results of the authors are discussed.

Notations and acronyms

PCN	polycyanurates
CE	cyanate esters
POSS	polyhedral oligomeric silsesquioxane
MMT	montmorillonite
CNTs	carbon nanotubes
SWCNTs	single-walled carbon nanotubes
MWCNTs	multi-walled carbon nanotubes
DCBA	dicyanate ester of bisphenol A
FR-4 diepoxide	glass-reinforced epoxy material
DGEBA	diglycidyl ether of bisphenol A
FTIR	Fourier transform infrared spectroscopy
SEM	scanning electron microscopy
TEM	transmission electron microscopy
TGA	thermogravimetric analysis
DMTA	dynamic mechanical thermal analysis
DSC	differential scanning calorimetry
AFM	atomic force microscopy
$tg\ \delta$	loss tangent
E'	storage modulus, MPa
E	elasticity modulus, Psi
E_{flex}	flexural modulus, GPa
σ_{flex}	flexural strength, GPa
σ_{compr}	compression strength, GPa
σ_{b}	tensile strength at a break, MPa
σ	electric conductivity, S/cm
p_c	percolation threshold, weight %
ΔC_{p}	heat capacity, J/(K· g)
T_{∂}	degradation temperature, K
α	conversion, %

1. Introduction

Polycyanurates (PCN) offer a variety of excellent thermal and good mechanical properties, which commend them for use in high performance technology (e.g. as matrices for composites for high-speed electronic circuitry and transportation). For the electronics market, attractive features of PCN are their low dielectric loss characteristics, dimensional stability at molten solder temperatures (220-270 °C), high purity, inherent flame-retardancy (giving the potential to eliminate brominated flame retardants) and excellent adhesion to conductor metals at temperatures up to 250 °C *[Penczek and Kaminska, 1990]*.

Since the late 1970s, Cyanate Ester (CE) resins have been used with glass or aramid fiber in high-speed multilayer circuit boards and this remains their primary application. Several reviews *[Fainleib et al., 1991a, 1991b, 2006, 2010; Fang and Shimp, 1995; Hamerton and Hay, 1998; Nair et al., 2000, Snow, 1994]* collected the numerous publications (papers and patents) in the field of PCN synthesis, processing, characterization, modification and application have appeared since 1990s. In addition, like conventional FR-4 diepoxides, cyanate ester laminates retain the desirable (ketone) solution processing characteristics and the ability to be drilled, making it possible to employ them in printed circuit board manufacture. In the last two decades, aerospace composites have evolved into damage-tolerant primary and secondary structures utilizing both thermoset and thermoplastic resins. PCN homopolymers develop approximately twice the fracture toughness of multifunctional epoxies while qualifying for service temperatures of at least 150 °C, intermediate between epoxy and bismaleimides capabilities. PCN have already flown in prototype radomes and high gain antennae, with possible applications in primary and secondary structures of the High Speed Civil Transport and European Fighter Aircraft. PCN are also being qualified for satellite truss and tube structures and cryogenic, radiation-resistant components in the Superconducting Supercollider *[Fang and Shimp, 1995]*.

This is indeed the problem, to convince a traditionally conservative industry that the superior performance of PCN (which surpass the glass transition temperature and hydrophobicity of epoxies while matching their processability and are easily toughened) makes them worthy of further investigation in spite of their price, which is currently higher than the price of the epoxies. PCN must be traditionally cured at high temperatures in order to achieve complete conversion, which increases manufacturing cost, but reactive modification of PCN allows decreasing the high temperature of PCN post-curing. The primary drawback of PCN, which hinders more extensive application of the cured materials, however, is low room temperature toughness.

PCN are synthesized by a polycyclotrimerization reaction of cyanate esters (CE) of bisphenols (cf. Fig. 1).

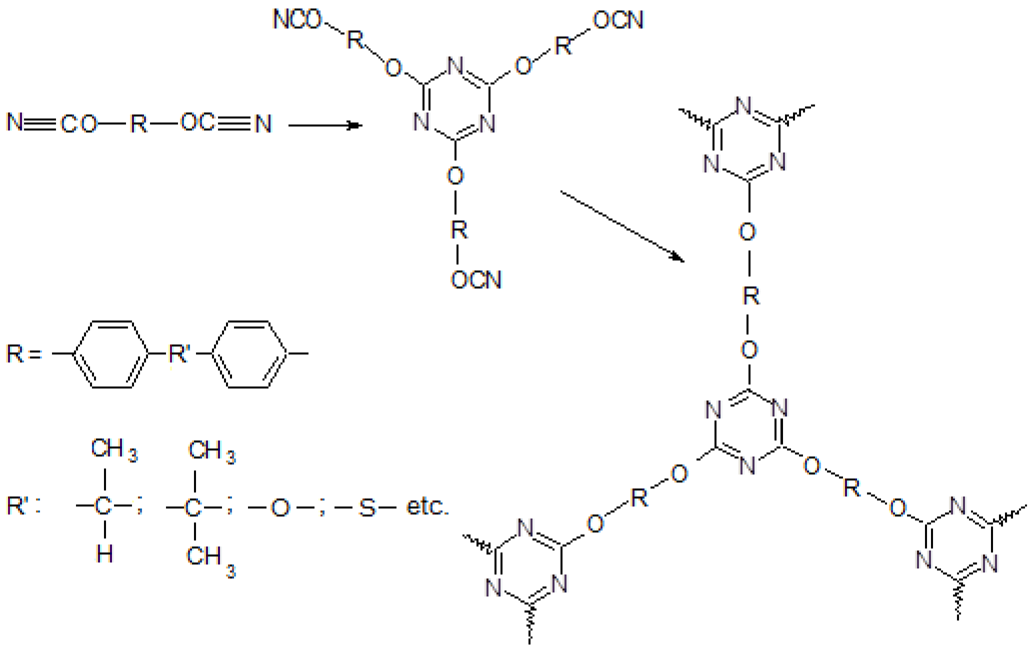

Figure 1. Generalized monomer structure and polycyanurate network formation

High-performance thermostable polycyanurates with the combination of outstanding properties exhibit brittleness as the only drawback restricting their possibilities for more extensive applications. Two basic routes for PCN modification to partially overcome this shortage are of significance, namely, formation of PCN-flexible chain hybrid networks and PCN-based nanocomposites. Recently the book, edited by A. Fainleib, on modification of polycyanurates was published *[Fainleib, 2010]* where the papers on methods of reactive (chemical) and physical modification of PCN are analyzed and the structure and properties of the modified polycyanurates and nanocomposites based on them are discussed. As the nanofillers montmorillonite (MMT) and polyhedral oligomeric silsesquioxanes (POSS) were used in PCN-based nanocomposites leading to materials of high mechanical and thermal properties *[Bershtein et al., 2010]*.

A special dynamics in matrix interfacial layers in nanocomposites was registered *[Bershtein et al., 2010]*. Finally, the development of microplasticity in modified PCN at low temperatures was evidenced as a result of the local decrease in crosslink density and increasing free volume in a system. As a result, the possibilities for (a) the further enhancing high-temperature mechanical properties, thermal stability and other properties of PCN, and (b) improving the fracture toughness, crack resistance and strength at the room temperature, as compared to those for the neat PCN, could be demonstrated. Due to the pronounced dynamic heterogeneity, these opposite changes might be observed simultaneously in some PCN-based nanocomposites. Two mechanisms of enhancing toughness in modified PCN materials at low temperatures are discussed *[Bershtein et al., 2010]*: (a) crack tip blunting due to the development of some relaxation abilities and relaxation of local overstresses under loading, and (b) crack hindering due to a "pinning" impact of nanoparticles; covalent PCN-nanoparticle interactions may strongly contribute to this effect. The large effects of adding low contents of 3-D nanofillers, chemically incorporated into PCN network, e.g., 1 wt. % POSS or 0.3 wt. % of silica, or 1-2 wt. % of 2-D MMT and bentonite, on the enhancement of PCN performance are worthy to be mentioned.

Thus, the modified hybrid PCN-based materials, especially nanocomposites, may consider as the perspective materials for applications, and the further developments in this field are of significance.

Recently, much attention has been given to the use of Carbon Nanotubes (CNTs) in composite materials to improve their exceptional mechanical and electric properties. Basically, for obtaining conductive CNTs-polymer composites, the highly electrical conductive CNTs filler is dispersed into the polymer matrix. Hence, a three-dimensional conductive network of the CNTs in the polymer matrix is formed.

In this chapter, the first scientific articles, including the own ones, that recently appeared on synthesis and investigation of structure-properties relationships for composites based on thermostable polycyanurate networks and different types of carbon nanotubes (single-walled, multi-walled, non-functionalized, functionalized) have been analyzed.

2. Nanocomposites based on polycyanurates and single-walled carbon nanotubes (SWCNTs)

So far we know only two works *[Che and Chan-Parc, 2008; Hopkins and Lipeles, 2005]* where polycyanurate networks filled by SWCNTs were synthesized and investigated.

Recently Latypov and Pozdnyakova *[Latypov and Pozdnyakova, 2006]* have published an interesting and important theoretical work where they calculated the optimal conditions of synthesis of ordered dendrymer polymer networks (PCN-based films) containing an ordered structure of SWCNTs. Authors supposed that as CNTs are highly polarized particles, using electrostatic field, one can determine the conditions of preparing a stable homogeneous suspension of the oriented SWCNTs in the melt (at $T \sim 100$ °C) of cyanate ester and also control the movement of SWCNTs in CE, and even growing up the SWCNTs during the synthesis of PCN matrix.

In 2005 *[Hopkins and Lipeles, 2005]* obtained the nanocomposites based on PCN and SWCNTs for the first time. Incorporation of SWCNTs (0.5 wt. %)/

acetone suspension into the dicianate ester of bisphenol A (DCBA) with subsequent sonication for 40 minutes yielded the mixture stable for 2 months without any signs of phase separation, unsheathing layers and overall inhomogeneity. Furthermore, the resulting composite exhibited a marked improvement in homogeneity without decreasing elastic modulus (E) or glass transition temperature (T_g) of the PCN matrix. Optimum sonication time (defined here as the shortest time to disperse SWCNTs into the cyanate monomer) was experimentally found to be 40 minutes. According to *[Hopkins and Lipeles, 2005]* excessive mixing time did not improve physical-mechanical properties of PCN/SWCNTs nanocomposites, obtained by thermal curing of DCBA in the presence of SWCNTs, and even had a potential both to introduce defects into the carbon nanotubes and degrade the polycyanurate matrix. We should note here that the authors called “polycyanurate” correctly for PCN network and incorrectly for cyanate monomer (for example DCBA). The monomer one can only call cyanate, dicyanate, or dicyanate ester (dicyanate ester of bisphenol), or, generally, Cyanate Ester Resins. The latter can be also used for PCN network, but with a note that it is crosslinked (cured) product.

It is worth to describe here in more details the specificity of preparing method used by the authors. Using the SWCNTs/acetone stock solutions, a series of DCBA/acetone mixtures were prepared under sonication with SWCNTs concentration ranging from 0.01 to 2.00 wt. %. Control samples were prepared in a similar way. Since nanotube additions caused the monomer solution to become optically opaque, the dispersion homogeneity was evaluated in dilute solutions visually. All the compositions were cast onto a metal tin pan and cured using step-by-step temperature schedule up to 300 °C. It should be noted that SWCNTs/acetone solutions were allowed to sit idle for a period of 2-3 months to allow for heavy rope/bundle sedimentation to occur and tubes to become solubilized. The upper 75-80 % of supernatant (upper layer) was carefully decanted, leaving suspended nanotube solutions at a typical mass concentration of 0.56 wt. %.

The elastic modulus E calculated from a linear correlation for neat PCN and PCN/SWCNTs composite thin film with 0.54 vol. % of SWCNTs were 303,400 Psi and 690,000 Psi, respectively. This represents a 127 % increase in stiffness for a 0.54 vol. % loading of SWCNTs compared to that for neat PCN. Using rule of mixtures, the predicted value for this PCN/SWCNTs nanocomposite was obtained higher. This indicates that dispersing procedure was not optimized *[Hopkins and Lipeles, 2005]*. Decreasing the SWCNTs loading to 0.01 % gives the lower value of modulus (313,000 Psi) which is close to the 317.800 Psi predicted value. As nanotubes concentration increases, they are bundling, that yield E values markedly lower compared to the predicted values.

PCN/SWCNTs nanocomposites and PCN/graphite and PCN/(carbon black) composites (with the same filler content of 0.5 wt. %) were compared (cf. Table 1). It was determined that such fillers as carbon black (particle size 0,5÷5 μm) and graphite (particle size 2÷15 μm) increased the modulus *E* of composites (in comparison with individual PCN), but less efficiently than SWCNTs that the authors explained by specific properties of the structure of CNTs.

Table 1. Elastic modulus *E* for individual polycyanurate and various PCN-based composites with filler content equal 0.5 wt. %

Composition	***E*, Psi**
PCN	302
PCN/SWCNTs	690
PCN/graphite	484
PCN/carbon black	407

In our opinion, the authors of this paper have achieved their goal, since by reinforcing of polycyanurate matrix with SWCNTs they managed to improve significantly its adhesive strength to metal (probably aluminum or titanium) used in aircraft and airspace industries *[after Hamerton, 1994]*.

2.1 Reactive spinning of cyanate ester fibers reinforced with aligned amino-functionalized SWCNTs

The tensile modulus and strength of one-dimensional SWCNTs have been estimated experimentally and theoretically to be of the order of 1 TPa and 30 GPa, respectively, making them excellent candidates as fillers in high performance polymer nanocomposites *[Bugachenko, 2003; Fischer, 2003; Jordan, 2005; Paul and Robeson, 2008; Silberglitt, 2004; Trefilov, 2001]*.

However, present approaches to bulk production of carbon nanotubes based composites often result in a dense entangled network of nanotube bundles with rather unimpressive increase in mechanical properties. Alignment of CNTs in micro-sized fibers has been confirmed to be a highly effective way of exploiting the anisotropic superior mechanical properties of CNTs *[May and Gong, 2008; Mittal, 2010]*. As it is reviewed in *[Che and Chan-Parc, 2008]* polymer matrix composite fibers can be produced by solution-based methods *[Miaudet et al., 2005]*, traditional melt-spinning *[McIntosh et al. 2006]*, or electrospinning *[Zussman et al., 2006]*.

High viscosity makes it difficult to disperse CNTs in the polymer matrix and/or to remove the solvent. The alternative approach of processing CNTs reinforced fibers using thermosetting oligomers would promote the dispersion of CNTs and removal of solvent from the blend after fiber spinning due to their lower molecular weight and thus viscosity. Also, reactive groups in thermosets would enable their covalent bonds with functional groups on the CNTs surfaces to improve interfacial adhesion *[Moniruzzaman and Winey, 2006]*.

First the thermoset composite fibers with aligned CNTs have been reported *[Che and Chan-Parc, 2008]*. It was noted that since thermosets have low viscosity, control of reactivity and hence viscosity during spinning is necessary. During curing, thermosets transform from a liquid state to a gel state, before reaching a solid state. During the liquid stage, it is relatively easy to get a uniform dispersion of CNTs. The polymer builds up its viscosity before it begins to gel. For condensation curing, the rate can be controlled to obtain an appropriate viscosity over a period of time sufficient for spinning. Then the spun fibers can be further cured to obtain improved properties. In their study polycyanurate composite micro-sized fibers reinforced with aligned SWCNTs were fabricated by reactive spinning. Two types of fibers were produced from neat cyanate CE resin: pristine SWCNTs (p-SWCNTs)/CE composite, and amino-functionalized SWCNTs (f-SWCNTs)/CE composite. Dicyclopentadienyl bisphenol CE and 2,2-Diallyl bisphenol A hardener (DBA) were used for PCN synthesis. f-SWNTs were amine-functionalized using ethylenediamine (EDA) via bridging isocyanate to improve nanotube dispersion and enable covalent bonding with the CE matrix *[Che and Chan-Parc, 2008]*.

The resin, together with or without the SWCNTs, was prepolymerized to increase viscosity, and then spun to produce fibers. The mixture was forced to flow through a spinneret and then drawn into a much finer fiber at an elevated temperature. The high drawing of the spun strand is expected to align the nanotubes along the draw direction. The spun fibers were then cured in stages to achieve good mechanical and thermal properties. The viscosity and degree of cure of the composite during reactive spinning were characterized by rheometry, FTIR spectroscopy, and softening point measurements. The SWCNTs and composite fibers were characterized by SEM, optical microscopy, tensile measurement, Raman spectroscopy and TGA. Unless otherwise stated, the SWCNTs contents were 1 wt. %.

For the purpose of reinforcement, a mild acid treatment was employed in order to avoid severe damage but obtain micrometer lengths of disentangled small nanotube bundles *[Che and Chan-Parc, 2008]*. As far as the viscosities of neat CE resin and 1 wt. % f-SWNTs/CE mixtures are too low for fiber spinning the SWCNTs/PCN composite fibers were made by a three-stage curing: (I) pre-polymerization before spinning to raise the viscosity for improving spinnability; (II) pre-curing of spun fibers at a temperature below the softening point to increase curing degree and softening point without fiber conglutination; and (III) curing and post-curing at higher temperatures to achieve good thermal and mechanical properties.

During prepolymerization at 120 ^{o}C the viscosity initially remained low for about an hour. The viscosity increases only marginally from 0.8 Pa·s to 1.3

Pa·s, 1.9 Pa·s, and 2.3 Pa·s (at 120 °C) as SWCNTs content increases from 0 to 0.5, 1.0 and 2.0 wt. %, respectively. However, at around the gel point, the viscosity increased dramatically. All the mixtures attain a high enough viscosity (about 30 Pa·s) to achieve spinnability with extended pre-polymerization time. Hence, the pre-polymerization time can be controlled to achieve almost the same starting viscosity before fiber spinning. Che and Chan-Parc *[Che and Chan-Parc, 2008]* have observed that the gelation of f-SWCNTs/CE blend was retarded with higher f-SWCNTs content.

They noted that the π-stacking interaction between the aryl group of DBA and f-SWCNTs can cause the DBA molecules to easily immobilize onto f-SWCNTs sidewalls making them difficult to diffuse into the blend. If the curing is catalyst diffusion controlled or impeded by lower catalyst content in the bulk, then the lower polymerization rate of CE resin with increased SWCNTs is reasonable.

The degree of polymerization during the pre-polymerization of the f-SWCNTs/CE composition at 120 °C was also monitored by FTIR *[Che and Chan-Parc, 2008]*. FTIR spectra showed that the cyanate ester group absorption peak at 2260 cm^{-1} decreased, and two peaks at 1560 and 1370 cm^{-1}, characteristic for cyanurate cycle appeared. The ratio of the normalized area of the cyanate ester absorption peak at 2260 cm^{-1} to its original peak area was used to calculate the degree of polymerization at various stages of polymerization. Authors used the unusually low temperature for polymerization of cyanate monomer, it is usually >150 °C. However, at this temperature the pre-polymerization cannot sequentially be precisely controlled to obtain suitable spinnability. After 100 min of the pre-polymerization at 120 °C the viscosity and the softening point had increased sufficiently but the polymerization degree of CE was still low (about 17.7 %) so that the mixture was still spinnable. It was found experimentally that the optimum condition for spinning was when the melt viscosity was 50-80 Pa·s. The temperature of the spinning process should be adjusted so that the polymer has sufficiently high fluidity at the spinneret and almost-constant viscosity.

The optimum fixed temperature for the spinning is about 100 °C since the pot life is long at this temperature and the viscosity is mostly in the suitable range; the lower reaction speed at this temperature makes viscosity stable for an extended time period to improve spinning control. After spinning, the fibers were further pre-cured in order to achieve shape stability during subsequent higher temperature curing. To avoid the fiber melting after spinning, with attendant loss of SWCNTs alignment and fiber shape, the spun fibers must be cured at sufficiently low temperature: 80 °C was chosen as it was lower than the achieved softening temperature of the spun fibers (90 °C). The polymerization progress of CE in f-SWCNTs/CE during pre-curing at 80 °C was monitored by FTIR. At this stage (pre-curing) the polymerization degree reached 33.9 %.

The fibers were then post-cured at 120, 140, and 160 ^{o}C consecutively each for 2 h in an air-circulating oven. After these curing steps, the polymerization level of CE in f-SWCNTs/CE, measured by FTIR, increased to 70 %. Che and Chan-Parc *[Che and Chan-Parc, 2008]* noted that it was difficult to further increase the polymerization degree at 160 ^{o}C, even with prolonged curing time. Post-curing was completed at a higher temperature of 250 ^{o}C for 4 h to achieve maximum conversion of cyanate groups into crosslinked triazine structures. The synthesis of carbon nanotube composites with enhanced mechanical properties requires strong interfacial bonding for load transfer between matrix and filler. Authors have confirmed chemical grafting of the polycyanurate formed onto the f-SWCNTs surface using FTIR technique. The amount of the polymer grafted onto the nanotube surface was estimated as ~100 % based on f-SWCNTs. Using SEM analysis it was observed a good dispersion of nanotubes, they also found that the nanotubes are oriented in the longitudinal direction of the fibers. The alignment of SWCNTs in the composite fibers was also confirmed by Raman spectroscopy. It was found that the reinforcement of PCN-fibers by SWCNTs and especially f-SWCNTs increased the values of tensile strength by 85÷140% (depending on CNTs content); impact strength of PCN-fibers micro-reinforced with f-SWCNTs increased by 420%; elongation at break increased by ~36÷144%.

Similar results have been obtained for CNTs/epoxy composites *[Tseng et al., 2007]*. This result contradicts the general phenomena of micro-sized fiber-reinforced composites, i.e., the elongation at failure typically drops drastically when short fibers are added to the matrix *[Koo, 2006]*. However, carbon nanotubes present a peculiar form of reinforcement with high aspect ratio and highly flexible elastic behavior during loading.

3. Structure-property relationships for nanocomposites based on polycyanurates and multi-walled carbon nanotubes (MWCNTs)

Search in electronic databases of scientific libraries (Science Direct-www.sciencedirect.com, Wiley - www3.interscience.wiley.com, Springer Link - www.springerlink.com, SciFinder - www.scifinder.com and Scopus - www.scopus.com), has shown that up to now there are only a few works *[Fang et al., 2006; Okotrub et al., 2007; Tang et al., 2009]*, where the synthesis and study of nanocomposites based on PCN and MWCNTs are described.

Fang et al. *[Fang et al., 2006]* present mechanical and thermal properties as well as microstructure characterization of PCN/MWCNTs nanocomposites containing MWCNTs (or their functionalized analogue, f-MWCNTs) of different structure: single MWCNTs or MWCNTs grouped in bundles. Okotrub et al. *[Okotrub et al., 2007]* described in detail synthesis of MWCNTs (L=40÷400 nm and $D_{external}$=10÷15 nm) using the method of electroarc evaporation of graphite and method of MWCNTs oxidation (for their purification out of graphite particles and amorphous carbon) and presented the results of thermal and mechanical properties of PCN/MWCNTs nanocomposites (unfortunately the chemical composition of the cyanate ester is not given) depending on the content of the oxidized MWCNTs. Tang et al. *[Tang et al., 2009]* described a method of synthesis of nanocomposites based on blends of DCBA and diglycidyl ether of bisphenol A (DGEBA) in the presence of functionalized MWCNTs. The influence of nanotubes content on the reaction kinetics of polycyclotrimerization of cyanate ester and on physical and mechanical properties of the nanocomposites obtained was investigated. The above work will be reviewed in detail below.

3.1 In situ reactive formation and dispersion of MWCNTs

Since polycyanurates are high crosslink density polymer networks the only high-tech way to prepare CNTs-containing nanocomposites is the reaction of polycyclotrimerization of cyanate esters in the presence of nanofiller (CNTs) i.e. under the conditions of *in situ* reactive formation at high temperature (T~390÷570 K) *[Che and Chan-Parc, 2008; Fang et al., 2006; Hopkins and Lipeles, 2005; Okotrub et al., 2007; Tang et al., 2009]*. Physical and chemical properties of CNTs-containing nanocomposites are controlled, primarily, by the level of dispersion of CNTs in a matrix. Thus the best mechanical properties are measured for the nanocomposites, where CNTs are dispersed to individual nanotubes. The presence of CNTs aggregates leads to less effective influence of nanofiller on final properties of nanomaterials based on them *[Gibson, 1992; Harris, 1999; Iijima, 1991; Koo, 2006; Saito et al., 1998; Tanaka et al., 1999; Wei et al., 2001; Zhang et al., 2003]*. The most effective way of CNTs introduction to oligomeric or polymer matrixes known is their dispersing using ultrasonic equipment of different capacity (from 12 to 500 W) and frequency (20÷55 kHz) *[Harris, 1999; Tanaka et al., 1999]*. In a number of works for the dispersing CNTs a high-speed mechanical mixers (500÷3000 rpm *[Fang et al., 2006; Wei et al., 2001])* or calenders (rolls speed 20 - 180 rpm *[Fiedler et al., 2006]*) were used.

It is interesting to note that Okotrub et al. *[Okotrub et al., 2007]* prepared a filled thermosetting composition by simple grinding in a mortar of initial or oxidated (by a specially developed technique) MWCNTs with cyanate resin (cyanate monomer) at ambient temperature to obtain a homogeneous mixture (content of nanotubes was 20.0; 33.3 or 50.0%). The authors believed that the degree of dispersing of nanotubes was good, but the experimental confirmation of this fact is absent in the work. Note that only for one sample, obtained with oxidized and annealed (in argon atmosphere at T=400 °C) MWCNTs (the content is not specified), the structure of surface cracking was investigated by atomic force microscopy (AFM). It was found that anisotropic grooves of a height less than 20 nm only are present on the surface (authors believe that they are the CNTs embedded into the PCN-matrix).

So, it was concluded that aggregates of CNTs are absent in this sample. Note that in order to improve dispersing of MWCNTs authors used their original developed method of oxidation and purification of nanotubes, based on a different ability to interact of individual carbon phases with solution of potassium permanganate in concentrated sulfuric acid *[Okotrub et al., 2007]*.

The structure of purified MWCNTs was studied by transmittance electron microscope and it was found that the material has only pipe and polyhedral multilayer structures. By means of X-ray analysis it was found that two or three surface layers of MWCNTs only undergone oxidation while the inner layers of nanotubes were not chemically modified.

It is known that chemical functionalization of CNTs promotes the chemical interaction between CNTs and polymer matrix that enhances the interfacial adhesion between components and prevents phase separation *[Fang et al., 2006; Fiedler et al., 2006; Goh et al., 2003; Gojny et al., 2003, 2004]*. So Fang et al. *[Fang et al., 2006]* described a preparing method of nanocomposites based on cyanate ester (the concrete name was not given, but one can assume it was DCBA) and two types of functionalized (using triethylene tetraamine) MWCNTs of different morphological structure: single nanotubes (f-MWCNTs$_1$) and grouped in bundles nanotubes (f-MWCNTs). Authors found that after functionalization nanotubes became of shorter size and were better dispersed than their non-functionalized analogues. Also, it was shown that the chemical functionalization of MWCNTs led to unbundling and their better dispersing in comparison with f-MWCNTs$_1$.

In this paper, dispersing of CNTs was carried out for 15 minutes at a temperature higher than the melting temperature of the cyanate monomer ($T \geq 363$ K) using high-speed mixer (rotation speed of ~ 500 rpm). Then the PCN/MWCNTs mixture was dried in vacuum and after this it was cured.

3.2 Influence of MWCNTs on mechanical and thermal properties of nanocomposites

Fang et al. *[Fang et al., 2006]* basic on the results of mechanical tests of PCN/MWCNTs$_1$ and PCN/f-MWCNTs$_1$ as well as PCN/MWCNTs and PCN/f-MWCNTs nanocomposites (MWCNTs$_1$ - single nanotubes with $D \approx 20 \div 50$ nm; MWCNTs - grouped in bundles nanotubes, D of one CNT was ≈ 10 nm) concluded that the morphology of MWCNTs (isolated or grouped in bundles) and the presence of functional groups on a surface of the nanotubes affected the final mechanical properties of nanocomposites obtained.

It was shown that the nanocomposites filled with the non-functionalized and functionalized nanotubes grouped in bundles (MWCNTs and f-MWCNTs) have a higher value of flexibility modulus and impact strength (Table 2) than nanocomposites of PCN/MWCNTs$_1$ and PCN/f-MWCNTs$_1$ (non-functionalized and functionalized isolated nanotubes). Authors explained that fact by lower entanglement of MWCNTs and f-MWCNTs and lower content of agglomerates (in comparison with isolated MWCNTs$_1$ and f-MWCNTs$_1$) according to SEM data.

Table 2. Mechanical properties of PCN and PCN-based nanocomposites with 0,5 wt. % of different type MWCNTs *[after Fang et al., 2006]*

Composition	**Flexibility modulus, GPa**	**Impact strength, kJ/m^2**
PCN	3.04	3.24
PCN/MWCNTs$_1$	2.95	3.08
PCN/MWCNTs	3.13	3.49
PCN/f-MWCNTs$_1$	3.38	3.20
PCN/f-MWCNTs	3.47	3.66

It was also found that the nanocomposites, obtained from functionalized f-MWCNTs, had better physical-mechanical parameters (Table 2) than analogous samples obtained with non-functionalized MWCNTs$_1$ and MWCNTs. Enhancement of physical-mechanical properties of nanocomposites obtained from functionalized f-MWCNTs$_1$ or f-MWCNTs authors associated with increasing interfacial adhesion between the components through the chemical reaction of amine-groups grafted onto a surface of nanotubes with cyanate groups of the forming PCN (this chemical reaction was studied and described before *[Fife et al., 1995; Hamerton, 1994]*). This conclusion was based on FTIR data shown that the intensity of the band of stretching vibration of NH-groups (with a maximum at $\nu \approx 610$ cm^{-1}) significantly reduced during the synthesis of PCN-matrix in the presence of carbon nanotubes.

It was also shown *[Fang et al., 2006]* that the introduction of nanotubes slightly improves the thermal stability of the obtained nanocomposites, especially with f-MWCNTs. It is concluded that better dispersing of f-MWCNTs and its covalent (chemical) bonding to the PCN-matrix slow down the decomposition of the nanocomposites obtained. However, it was found that in all the nanocomposites obtained the glass transition temperature (T_g) of PCN matrix was lower by ~ 9 ÷ 11 °C than the T_g for non-filled PCN. Authors explained this fact by decreasing crosslink density of PCN-network caused by introduction of CNTs. It is noteworthy that in general the authors of this paper failed to improve significantly physical-mechanical properties of PCN/CNTs nanocomposites prepared.

Tang et al. *[Tang et al., 2009]* investigated the mechanical and thermal properties of nanocomposites prepared by *in situ* synthesis of PCN from the mixture of DCBA and diglycidyl ether of bisphenol A, DGEBA, with the functionalized MWCNTs (MWCNTs content was 1.0, 1.5 and 2.0 wt. %). MWCNTs of $D_{\text{intern}} \approx 10 \div 30$ nm, $D_{\text{extern}} \approx 40 \div 60$ nm and $L/D \approx 1000$ were used.

Functionalization of MWCNTs was carried out by pyrolysis (at $T = 580$ °C for 1 h) followed by treatment (during 40 min) with acids HCl, HNO_3 (65%) or with mixture of acids HNO_3/H_2SO_4 (1/2 or 1/3). Using FTIR it was found that after treating by acid carboxyl, carbonyl and hydroxyl groups appeared on the surface of MWCNTs. It has been determined that the introduction of 1 wt. % of the functionalized MWCNTs obtained increases flexural strength from 132 to 147 MPa and impact strength from 14.0 to 16.5 kJ/m^2 (compared with initial PCN). However, further increasing of nanotubes content in the composite caused the lowering the above mentioned parameters (almost to the level of initial PCN). It was found that loading of 1 % of nanotubes decreased by ≈ 30% water absorption of nanocomposites. Increasing storage modulus (E') in the temperature range of 50÷300 ºC at introduction of up to 1.5 wt. % of nanotubes was detected by DMTA, however at the concentration of nanotubes ≥ 2 wt % some drop in value of E' was observed. Unfortunately the authors did not give any explanations of these non-monotonic dependencies. In our opinion, such non-monotonic mechanism can be explained by the fact that at increasing of nanotubes content agglomerates are formed and hinder stress transfer between MWCNTs and matrix, so nanotubes become the centers of crack formation that leads to reducing physical-mechanical properties of nanocomposite.

Okotrub et al. have been studied *[Okotrub et al., 2007]* the effect of oxidated MWCNTs content on mechanical properties of new carbon fiber reinforced plastic materials based on CE resins and carbon fibers "ELUR" (fiber content is not mentioned). These polymer composites were obtained by multiple impregnations of carbon fibers with a diluted solution of oxidized MWCNTs/CE/acetone achieving the content of CNTs on the fibers surface of 0.25÷1.00 %. The sample was then formed by direct pressing at a special temperature conditions (the details are not specified) to achieve the highest curing degree of the polymer matrix. Mechanical properties of carbon fiber reinforced composites obtained were studied at temperatures $T = 20$ and 180 °C: flexural strength (σ_{flex}), compression strength (σ_{compr}), and flexural modulus (E_{flex}) were measured. It was found that at above mentioned temperatures the original carbon fiber reinforced composites (without nanotubes) had the following parameters: $\sigma_{flex} = 1.12$ (1.10) GPa, $\sigma_{compr} = 8.95$ (7.90), $E_{flex} = 102.64$ (96.66) GPa (the values at $T = 180$ °C are indicated in brackets). It was found that treatment of fibers by nanotubes enhanced physical-mechanical properties of carbon fiber reinforced composites, especially at elevated temperatures; the greatest effect was observed at MWCNTs content of 0.25%: $\sigma_{flex} = 1.42$ GPa, $E_{flex} = 134.43$ (125.3) GPa and for composite, containing 0.5 % of MWCNTs: $\sigma_{compr} = 9.97$ (8.99) GPa (the values at $T = 180$ °C are indicated in the brackets).

As in the previous work the authors *[Okotrub et al., 2007]* do not give explanations of the non-monotonic effect of MWCNTs content on the basic properties of the investigated nanocomposites. However, from DMTA data, namely temperature dependence of storage modulus (E') and loss tangent ($tg\ \delta$), one can conclude that already at 1 % of nanotubes content in the investigated samples a significant decline (compared with the original carbon fiber) of material stiffness (modulus E' decreases from ~95 to ~70 GPa at $T \approx 50 \div 200$ °C, and from ~75 to ~35 GPa for $T \geq 250$ ^{o}C) and increasing intensity of α-relaxation transition (at $T_g \approx 250$ °C) of PCN-matrix occurs. These facts can be associated with decreasing crosslink density and appearance of defects in the structure of PCN-network, i.e. increasing content of oxidized MWCNTs hinders the polycyclotrimerization of cyanate monomer.

This conclusion is in a good agreement with the one reported by dynamic DSC, since it was found that with increasing concentration of the oxidized MWCNTs (from 20 to 50%) enthalpy of PCN formation decreased non-additively and exothermal peak at 70÷130 ^{o}C simultaneously appeared that the authors attributed to chemical interaction of cyanate groups of the monomer and oxygen-containing functional groups on the surface of oxidized MWCNTs (no doubt that this assumption requires further experimental confirmation). It is shown that at content of 50 % of the oxidized MWCNTs the first peak becomes dominant and curing of polycyanurate matrix almost not occurs. However, after annealing of oxidized MWCNTs in an inert atmosphere authors managed to obtain nanocomposites (nanotubes content is not specified) with a uniformly glossy black surface.

4. Catalytic effect of Carbon Nanotubes on the polycyclotrimerization process of dicyanate ester of bisphenol A at in situ synthesis of PCN-based nanocomposites

This section presents the results of investigation of structure and basic physical-chemical properties of nanocomposites of polycyanurate networks and multi-walled carbon nanotubes MWCNTs. These nanocomposites were obtained in the presence of different content of carbon nanotubes by *in situ* polycyclotrimerization: 1) oligomer of dicyanate ester of bisphenol A, DCBA previously synthesized from monomer DCBA ("Primaset BADCy") with conversion of cyanate groups α ~ 28 %, or 2) industrial oligomer DCBA ("Primaset BA-230S 75") with conversion of cyanate groups α ~ 52 %. In the first series of samples polycyanurate component was marked as PCN_1, in the second series of samples - as PCN_2.

For the first time, the catalytic effect of unfunctionalized MWCNTs on kinetics of polycyclotrimerization reaction of DCBA was established by us *[Fainleib et al., 2010]*, and this work has been patented *[Fainleib et al., 2009]*. The conversion of cyanate groups was determined by changes of absorbance of the band with maximum at $\nu \approx 2236\text{-}2272\ cm^{-1}$, corresponding to the valence vibrations of the −O−C≡N group. As a standard band the band at $\nu \approx 2968\ cm^{-1}$ of the valence vibrations of CH_3-group in FTIR spectra of the reactive composition.

In Figure 2 the FTIR spectra of DCBA monomer, DCBA oligomer and PCN_1 synthesized without using any catalyst are shown. It is seen that at polymerization of the DCBA an intensity of the peaks of cyanate groups at $\nu \approx 2236\text{-}2272\ cm^{-1}$ decreases and the peaks at $\nu \approx 1367$ and $\nu \approx 1564\ cm^{-1}$ corresponding to polycyanurate cycle *[Fainleib, 2010; Hamerton, 1994]* appear in the FTIR spectra.

The conversion (α) of the CE resin was calculated using the Equation 1:

$$\alpha(t) = 1 - \frac{A_{(t)2236-2272}/A_{(0)2236-2272}}{A_{(t)2968}/A_{(0)2968}} \qquad (1)$$

where $A_{(t)2236\text{-}2272}$ is the area under absorbance peak of −O−C≡N at $\nu \approx 2236\text{-}2272\ cm^{-1}$ at time *t*; $A_{(t)2968}$ is the area under absorbance peak of $-CH_3$ at $\nu \approx 2968\ cm^{-1}$ at time *t*; $A_{(0)}$ are the areas under absorbance peaks of corresponding groups in initial DCBA monomer.

The conversion of cyanate groups in DCBA oligomer was found to be α ~ 28% and that in PCN sample - α~ 92.5 %. It should be noted here that for

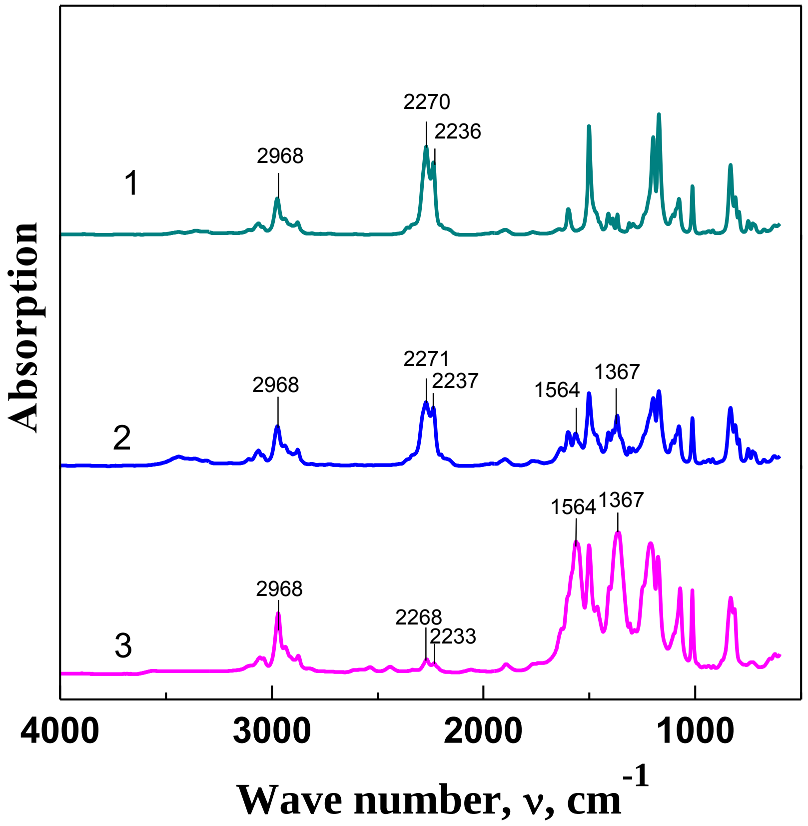

Figure 2. FTIR-spectra: 1 – DCBA monomer; 2 – DCBA oligomer; 3 – individual PCN_1 *[Printed with permission from eXPRESS Polymer Letters Vol.3, No.8, 2009, p. 479. Copyright 2009]*

achieving full conversion post-curing is needed at 270-300 °C even at using conventional catalysts *[Fainleib, 2010; Hamerton, 1994]*. For kinetic measurements the system based on DCBA oligomer (with conversion of the cyanate groups, $\alpha \sim 28$ %) containing 0.01 and 0.1 wt. % of MWCNTs was used. The kinetics of polycyclotrimerization of DCBA oligomer as well as in the presence of MWCNTs through the schedule with step by step temperature increase was studied by FTIR method (Figs. 3 and 4). In Figure 5 the conversion of cyanate groups of DCBA oligomer as well as in the presence of the small amounts of MWCNTs *versus* time is shown.

The FTIR data evidence an acceleration effect of MWCNTs on kinetics of the early stages of PCN formation. The higher the MWCNTs content in the system, the higher the conversion of the cyanate groups into cyanurate cycles at least in the range of the concentrations used. The attempt to study the system with 0.5 wt. % of MWCNTs resulted in vitrification as early as in a stage of components blending in 2 min after starting ultrasound action.

However, as can be seen from Table 3, in spite of the higher reaction speed of the polycyclotrimerization process of the cyanate ester in the presence

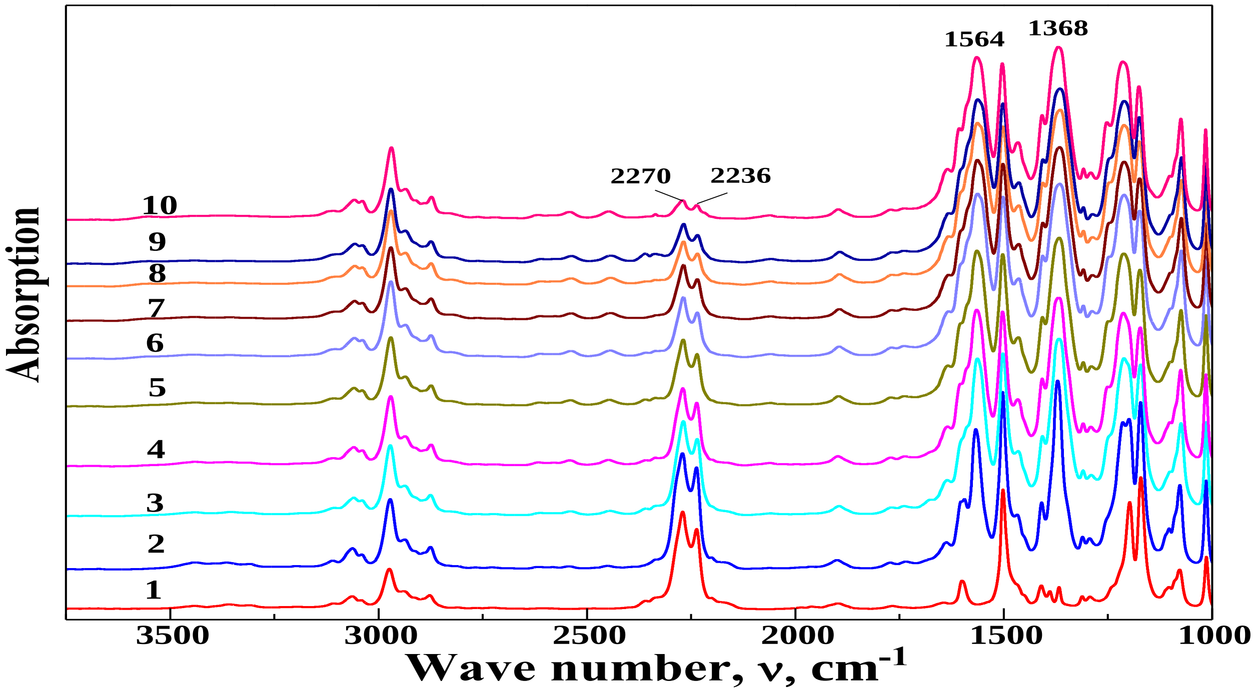

Figure 3. FTIR–spectra of polycyclotrimerization process of DCBA oligomer, synthesis schedule (with step by step temperature increase): 1 – 423 K, 40 h; 2 – 453 K, 1 h; 3 – 453 K, 2 h; 4 – 453 K, 3 h; 5 – 483 K, 30 min; 6 – 483 K, 1 h; 7 – 503 K, 30 min; 8 –503 K, 1 h; 9 – 523 K, 30 min; 10 –523 K, 1 h

of MWCNTs the final conversion of −O−C≡N groups for the temperature/time schedule used was some lower compared to that for neat PCN_1.

One can suppose that the acceleration effect of carbon nanotubes on polymerization of cyanate ester is due to adsorption of DCBA oligomer molecules on highly developed surface of MWCNTs. However, this phenomenon can play negative role in the final stage of PCN_1 network formation, when some unreacted molecules are not easy accessible, and the probability of elementary reaction act is very low (as can be seen from Fig. 1 three molecules of cyanate ester have to meet each other to react with cyanurate

Table 3. Influence of MWCNTs content on conversion of cyanate groups of DCBA and activation energy E_a at formation of PCN_1/MWCNTs nanocomposites *[Printed with permission from eXPRESS Polymer Letters Vol.3, No.8, 2009, p. 480. Copyright 2009]*

MWCNTs content , wt. %	**Conversion of −O−C≡N groups, %**	**E_a (kJ/mol)**
0.00	92.5	32.7
0.01	89.1	27.3
0.10	88.8	16.9

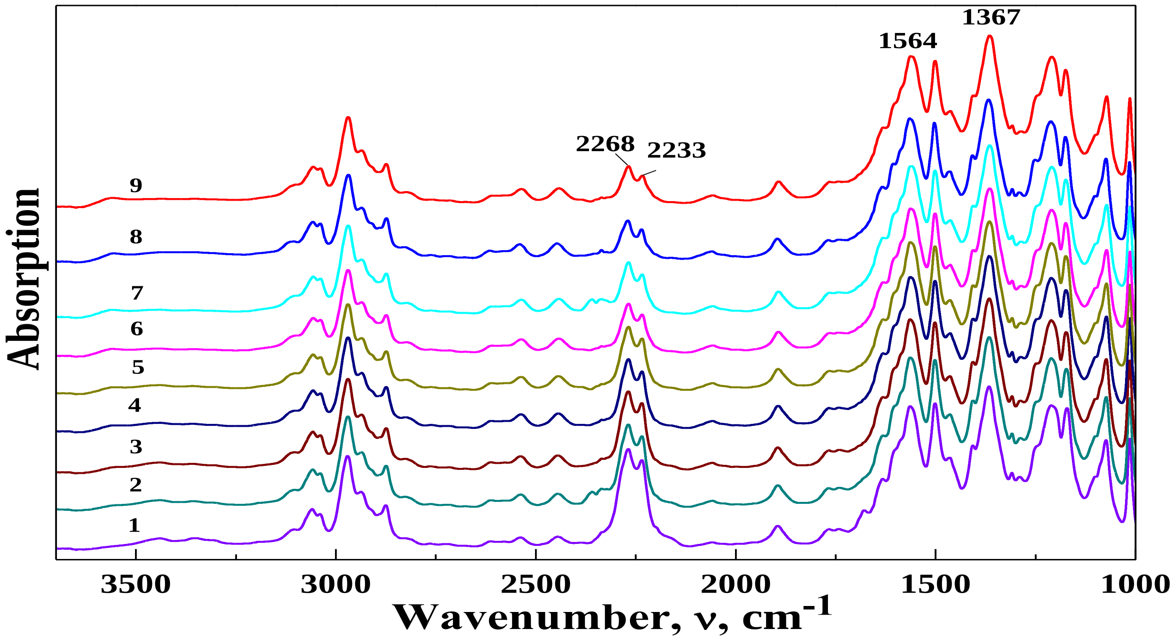

Figure 4. FTIR–spectra of polycyclotrimerization process of DCBA oligomer *in situ* in the presence of MWCNTs (0.01 wt. %), synthesis schedule (with step by step temperature increase): 1 – 423 K, 5 h (individual DCBA oligomer); 2 – 453 K, 1 h; 3 – 453 K, 2 h; 4 – 453 K, 3 h; 5 – 483 K, 30 min; 6 – 483 K, 1 h; 7 – 503 K, 1 h; 8 – 523 K, 30 min; 9 – 523 K, 1 h

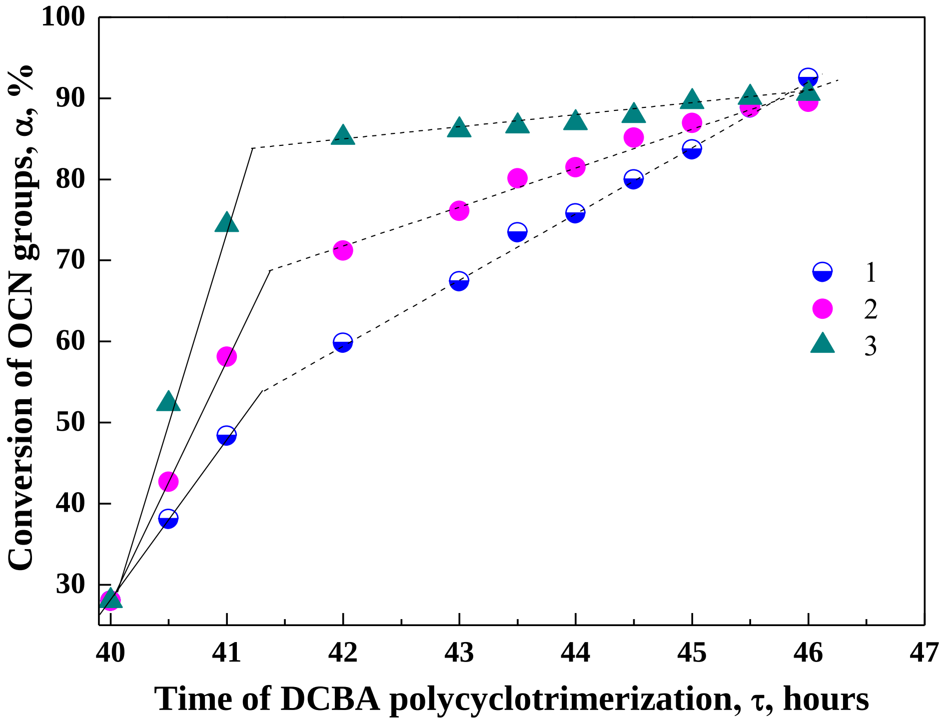

Figure 5. Kinetic curves of PCN formation from DCBA at MWCNTs content, wt. %: 1 – 0.00; 2 – 0.01; 3 – 0.10 *[Printed with permission from eXPRESS Polymer Letters Vol.3, No.8, 2009, p. 479. Copyright 2009]*

As it was above mentioned this problem can be solved by post-curing of the polymer product at higher temperatures, when the mobility of the reactive molecules and polymer fragments is higher.

The manufacturer of MWCNTs used in this study reports that catalyst residue in MWCNTs is the mixture of SiO_2, Al_2O_3, Fe_2O_3, MoO_3. For the moment, there are no references in the literature that describe the catalytic action of such oxides on reaction of cyclotrimerization of cyanate esters. Normally, reaction of cyclotrimerization of the aryl dicyanates can be catalyzed by the mixture of catalyst and co-catalyst. The most common types of catalyst are carboxylate salts and chelates of transition metal ions (Cu^{2+}, Co^{2+}, Zn^{2+}, Mn^{2+}...) *[Hamerton, 1994]* that facilitate the reaction of cyclotrimerization by formation of coordination complexes. The co-catalyst serves a dual purpose of acting as a solvent for catalyst and completing ring closure of the triazine ring via hydrogen transfer. The most commonly used co-catalyst is nonylphenol. The data obtained from FTIR studies for DCBA oligomer as well as filled with 0.01 and 0.1 wt. % of MWCNTs were analyzed using an empirical Equation 2 *[Fainleib, 2010; Hamerton, 1994]:*

$$\frac{\partial \alpha}{\partial t} = k(1-\alpha)^n , \tag{2}$$

where k is the rate constant and n is the order of overall reaction.

The parameters k and n are evaluated from the data region where the reaction rate depends on monomer concentration and sharp increase in conversion is observed. Equation 2 was integrated and fitted to experimental concentration profiles of both the unfilled and the filled with MWCNTs systems. It was observed that the data calculated from FTIR spectra is in a good agreement with Equation 2, when the order of reaction $n = 1$. This means that DCBA oligomer or DCBA oligomer/MWCNTs systems can be described by a first-order autocatalytic rate law. The values of the observed rate constants obtained from the first-order reaction analysis for DCBA and DCBA/MWCNTs nanocomposites are listed in the Table 4. The values of kinetic constants for unfilled DCBA are lower than the values reported for the catalyzed DCBA *[Li et al., 2004]*. The results show that the kinetic constant increases with the addition of MWCNTs on each isothermal step of polymerization of DCBA oligomer.

The activation energies E_a (cf. Table 3) were determined from Arrhenius plots. The activation energies E_a for the reaction ranged from 32.7 to 16.9 kJ/mol for pure DCBA oligomer and for that filled with MWCNTs and agree with the values reported earlier *[Li et al., 2004; Osei-Owusu and Martin, 1992]*. The E_a values for the samples of DCBA oligomer cured in the presence of MWCNTs

Table 4. Rate constant of polycyclotrimerization reaction for individual DCBA oligomer and that in a mixture of DCBA oligomer/MWCNTs *[Printed with permission from eXPRESS Polymer Letters Vol.3, No.8, 2009, p. 480. Copyright 2009]*

Temperature, K	**Reaction rate constant, k x 10^4 (conc. sec)$^{-1}$**		
	DCBA	**DCBA oligomer / MWCNTs (0.01 wt. %)**	**DCBA oligomer / MWCNTs (0.1 wt. %)**
423	0.02	0.02	0.02
453	0.05	0.06	0.09
483	0.08	0.10	0.12
503	0.10	0.12	0.14

are much lower than the values obtained for virgin DCBA oligomer and they decrease with increasing MWCNTs content. This effect is quite similar to the decrease of activation energy with adding catalysts in reactive systems *[Carey and Sundberg, 2007]*. Presence of low molar mass compounds (for example, conventional catalysts) in polymer networks can influences negatively on thermal properties of the final material. In this work we have shown that synthesis of PCN/CNTs nanocomposites can be effectively realized without using the conventional catalysts.

Tang et al. *[Tang et al., 2009]* using method of dynamic DSC has fixed acceleration of polycyclotrimerization process of cyanate esters of bisphenols at additions of MWCNTs too. At that, shifting of maximum of the exothermic peak to the lower temperatures has been observed. The authors have explained the catalytic effect found by the presence on the surface of carbon nanotubes of reactive OH-groups, which, as known *[Hamerton, 1994; Haman et al., 2009; Fainleib, 2010]*, can catalyze polycyclotrimerization reaction. As far as the existence of OH-groups on a surface of MWCNTs used was confirmed in our work by methods of FTIR and TGA, one can suppose the same nature of the catalysis.

5. Study of morphological features of PCN_2/MWCNTs nanocomposites depending on the nanofiller content

Using SEM and TEM methods the changes of morphological features of PCN_2/MWCNTs nanocomposites were investigated depending on the content of the nanofiller *[Bardash, 2011]*, the corresponding microphotographs are presented in Figs. 6 and 7.

From the analysis of the SEM microphotographs one can conclude that in these nanocomposites the MWCNTs are effectively dispersed throughout the sample. The isolated nanotubes (the thread like light includings) as well as the

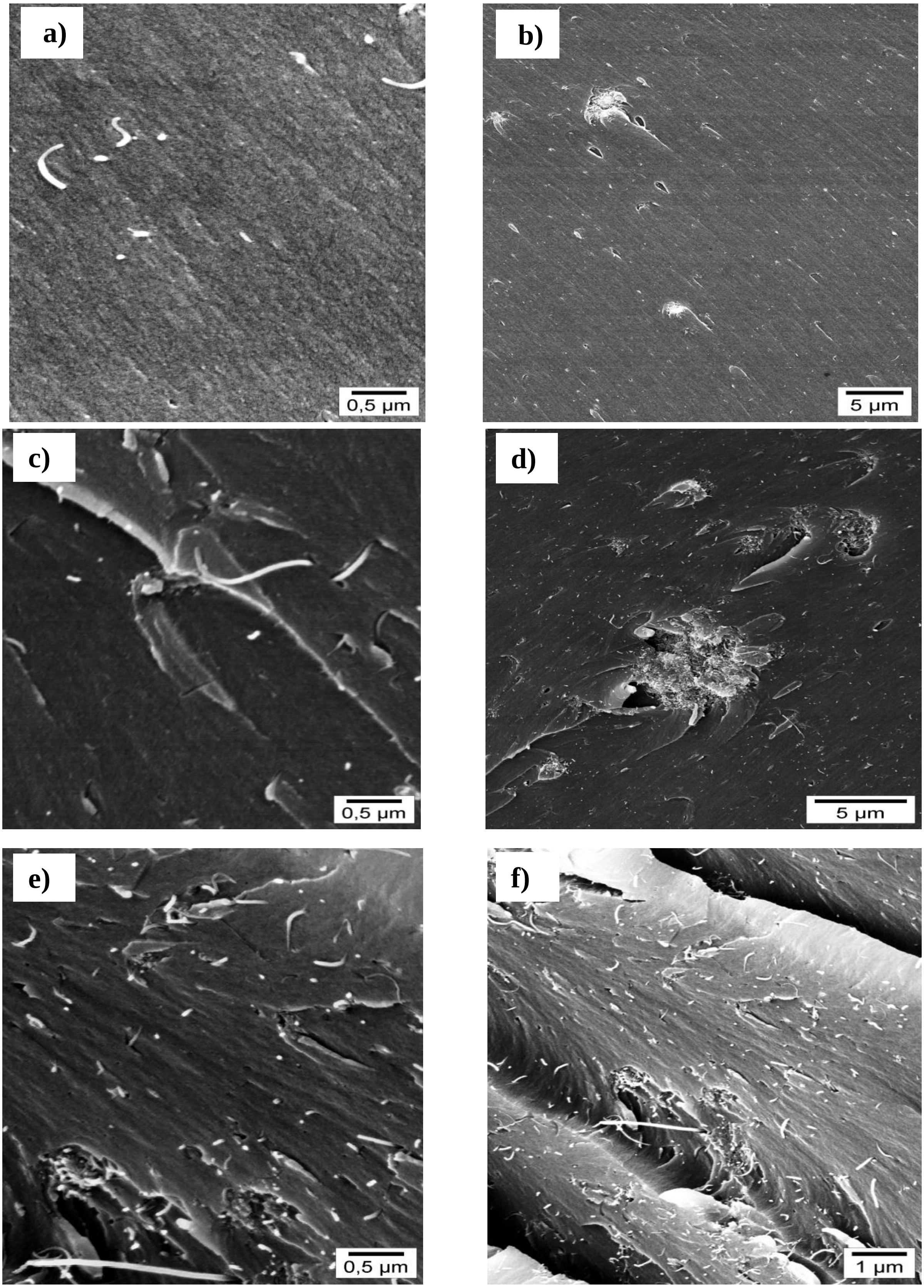

Figure 6. SEM microphotographs of the PCN$_2$/MWCNTs nanocomposites with the MWCNTs content, wt. %: a, b - 0.08; c, d - 0.50; e, f - 1.20

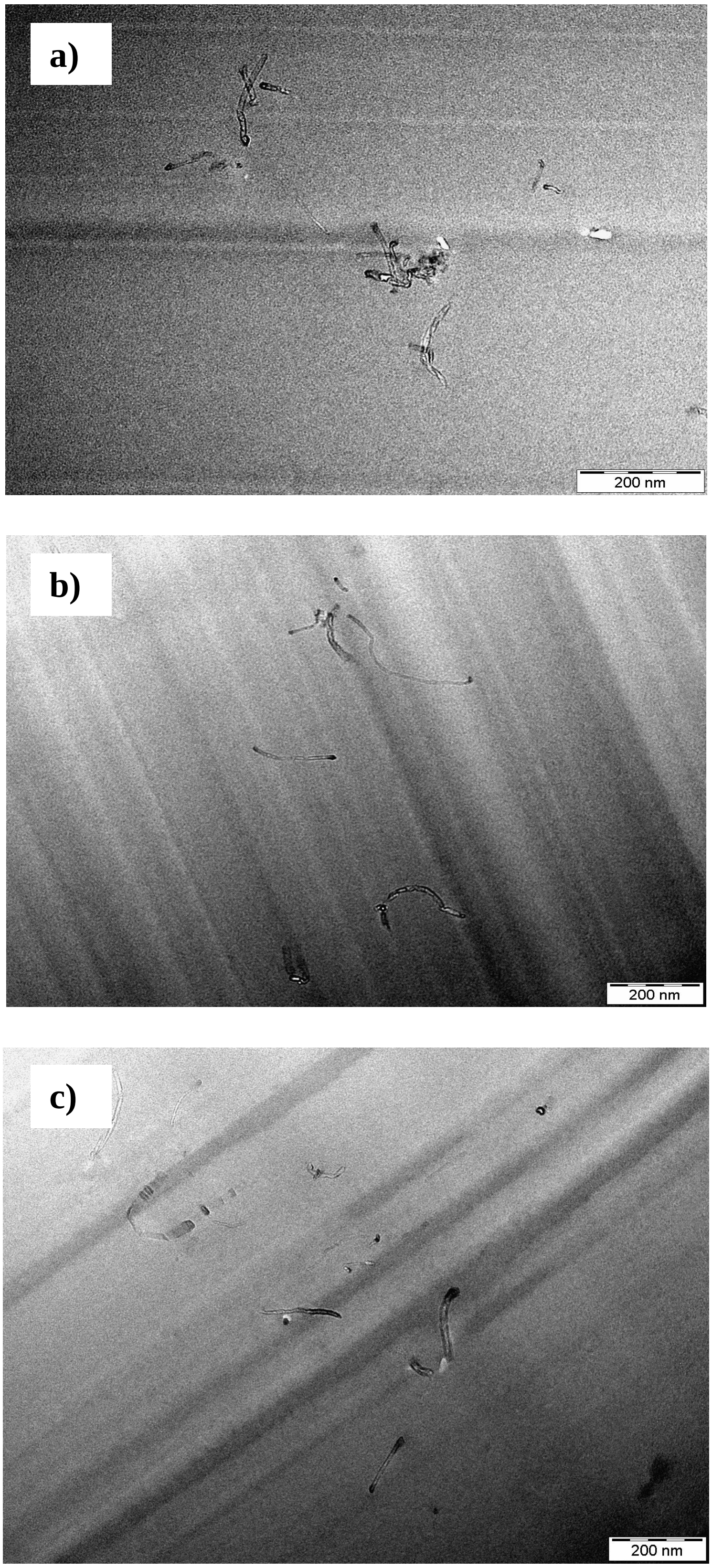

Figure 7. TEM microphotographs of the PCN_2/MWCNTs nanocomposites with the MWCNTs content, wt. %: a - 0.05; b - 0.10; c - 0.20

nanotubes broken during preparation of samples for their study by SEM method (at cracking of the sample in liquid nitrogen) are observed too. The latter is confirmed by the presence of a large number of cross cutover of nanotubes (light points). There dark spherical areas, which refer to the voids formed after pulling (at breaking sample) the nanotubes out, are also observed. Thus one can conclude of high adhesion between the polymer matrix and the carbon nanotubes.

This conclusion is confirmed by the estimations carried out using the computer program "Image J", which allows measuring precisely the size of any visible inclusions on the microphotographs. The estimations carried out using SEM and TEM microphotographs of nanocomposite samples have shown that the diameters of the nanotubes is larger than that the initial MWCNTs by ~ 5 ÷ 45 nm *[Bardash, 2011]*. This evidences wrapping of carbon nanotubes by the polymer that is only possible in systems with high adhesion between the polymer matrix and CNTs.

However, as it is seen from the SEM (Fig. 6) and TEM microphotographs (Fig. 7), there are agglomerates of CNTs in all the samples along with the isolated CNTs: in the SEM pictures one can observe the clusters of light points or threads, in the TEM microphotographs the clear clews of CNTs can be seen.

It has been found that with increasing content of MWCNTs from 0.08 to 1.20 wt. % the content of agglomerates increases too (Fig. 6 d, e). This can be explained by 2 reasons: 1) an inclination of carbon nanotubes to self-agglomeration at increasing their content in the nanocomposite sample due to their extended surface and significant Van der Waals forces; 2) during high-temperature synthesis of polymer (here polycyanurate) matrix the reaggregation of the dispersed carbon nanotubes occurs, probably because at high temperature CNTs have higher mobility that promotes their reaggregation.

As it will be shown below in sections 6 ÷ 9, such change in the morphology of the nanocomposite samples studied leads to some improvement in their physical-chemical properties.

6. Effect of MWCNT on viscoelastic properties of the nanocomposites and their mechanical characteristics

Viscoelastic characteristics of the original polycyanurate network and the nanocomposites based on them with different content of carbon nanotubes were investigated by DMTA technique *[Bardash, 2011]*, the experimental results are presented in Figures 8, 9 and in Table 5. Two series of nanocomposite samples were investigated: 1) the samples of PCN_1/MWCNTs prepared from DCBA oligomer synthesized at the lab; 2) the samples of PCN_2/MWCNTs prepared from the industrially available oligomer DCBA.

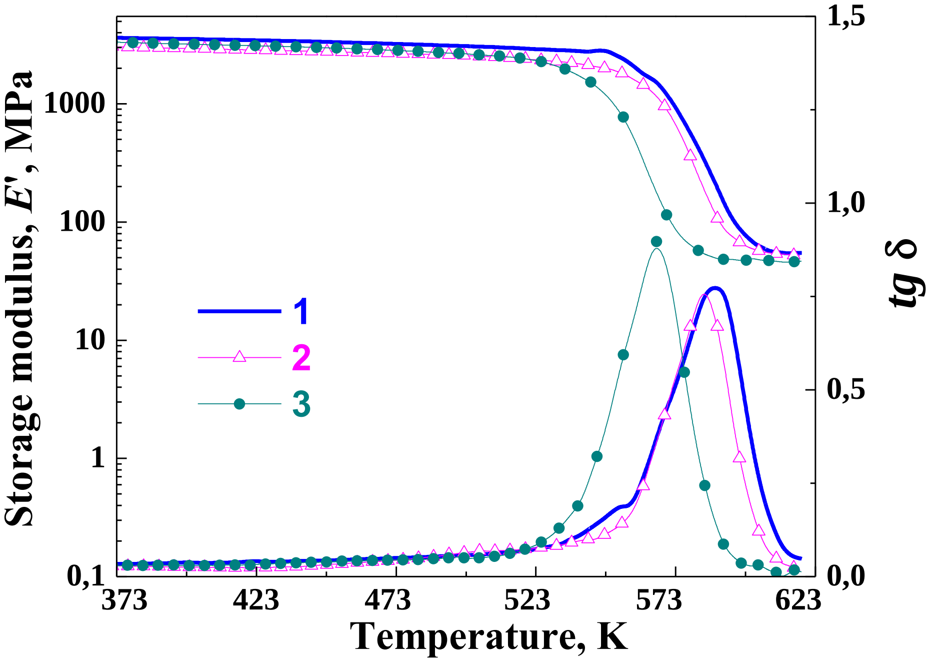

Figure 8. Temperature dependence of storage modulus *E'* and *tg* δ (at frequency 1 Hz) for the PCN_1/MWCNTs nanocomposites with MWCNTs content, wt. % 1 – 0.00; 2 – 0.01; 3 – 0.10

It is seen (Fig. 8) that addition of even a small amount of carbon nanotubes (0.01 ÷ 0.1 wt. %) changes viscoelastic properties of the PCN-matrix (in comparison with unfilled PCN_1). In the dependencies $E' = f(T)$ and $tg\,\delta = f(T)$ one can see redistribution of intensities and shift of the *tg* δ peak maxima along the temperature axis, narrower glass transition temperature interval (ΔT_g), *E'*. It should be noted here that the introduction of the nanofiller (MWCNTs) and increase of its content leads to decreasing glass transition temperature (T_g) value of the amorphous polycyanurate matrix (Table 5).

As it is well known *[Georjon et al., 1993; Georjon and Galy, 1998]* the T_g value for the polycyanurate networks depends directly on the network crosslink degree and, therefore, depends on the conversion of cyanate groups,: the lower the value of the conversion α, the lower the crosslink degree of PCN-network and lower T_g (Table 6). It was shown above (sect. 4) that despite the catalytic effect of CNTs in the initial stages of the DCBA polycyclotrimerization process, the ultimate conversion of cyanate groups in the nanocomposites is slightly lower than in the individual PCN_1 (Table 3), and for all the samples $\alpha < 100$ %.

Table 5. Viscoelastic properties of PCN_1/MWCNTs and PCN_2/MWCNTs nanocomposites

MWCNTs content, wt. %	T_g, **K**	ΔT_g, **K**	E', **MPa (at 373 K)**	$h_{tg\,\delta}$
PCN_1/MWCNTs				
0.00 (PCN_1)	552; 588	92	3632	0.40; 0.77
0.01	583	73	3034	0.76
0.10	566	70	3336	0.90
PCN_2/MWCNTs				
0 (PCN_2)	545; 560; 578	79	2876	0.16; 0.19; 0.29
0.03	534; 546; 566	85	4226	0.11; 0.14; 0.37
0.04	524; 545; 565	93	3654	0.11; 0.12; 0.32
0.10	552; 572	81	3652	0.32; 0.24
1.20	560	63	3301	0.46

So the study of PCN-containing samples by methods (for example DMTA, DSC, etc.) that provide some heating at temperatures > T_g, the properties of the samples may change due to chemical interactions of cyanate groups of PCN-matrix, which were not able to react at lower temperature because of steric hindrance.

Table 6. Glass transition temperature T_g *versus* conversion of cyanate groups for DCBA curing process *[after Hamerton, 1994]*

Conversion $\alpha_{C\equiv N\rightarrow PCN}$	T_g, °C
0.60	38
0.65	52
0.70	82
0.75	105
0.80	134
0.82	155
0.85	175
0.87	196
0.90	226
0.92	242
0.95	257
0.98	283
1.00	296

During step by step synthesis at temperatures > T_g the mobility of kinetic segments in the polycyanurate network increases and the unreacted cyanate groups can react to each other with further formation of cyanurate cycles providing post-curing process *[Hamerton, 1994; Haman et al., 2009]*. Occurrence of post-curing in the PCN_1 sample is evidenced by an appearance of a small peak in the curve of $E' = f(T)$ dependence in the temperature range of $T = 540 \div 550$ K, and a similar maximum on the curve of $tg\ \delta = f(T)$ dependence (cf. Fig. 8), which indicates increasing mobility of kinetic segments of macromolecules of the PCN_1 in this temperature region. At further heating of the sample the crosslink degree of polycyanurate network increases (due to post-curing), and a new higher glass transition temperature T_g is fixed for this PCN_1 (Table 6) *[Georjon et al., 1993]*.

The lower values of T_g and E' for the nanocomposites investigated are explained, first of all, by the formation during synthesis in the presence of MWCNTs of more defective and less crosslinked PCN_1 matrix (in comparison with the sample of individual PCN_1).

In Figure 9 the temperature dependences of E' and $tg\ \delta$ for nanocomposites of PCN_2/MWCNTs with different MWCNTs content are shown, it is clear seen that for the individual PCN_2 synthesized from the industrial oligomer DCBA three T_gs are clearly fixed (cf. Table 5) and in the curve of its temperature dependence of E' at temperatures $T > 540$ K a new broad maximum is observed. Both of these facts evidence the above mentioned post-curing process, which occur at heating of the sample at the temperature $T > T_g$, providing increasing crosslink density of PCN_2 and, as a result, increasing value of glass transition temperature T_g.

Note that during the second study (heating) of the same sample (the plot is not shown) the single glass transition temperature $T_g \sim 578$ K is found *[Bardash, 2011]* that obviously evidences achieving complete conversion of cyanate groups and maximal degree of crossliking (according to Table 6).

As it was shown above in sect. 4 the carbon nanotubes hinder achieving higher conversion of cyanate groups of PCN_1 matrix that cause formation of the less crosslinked network. The formation of the network of lower crosslink density is confirmed by an increasing intensity of the $tg\ \delta$ maximum (at T_g, cf. Fig. 9, curve 3) that reflects the greater mobility of kinetic segments in the less-crosslinked PCN_1 matrix of the nanocomposites. However in general, the results indicate that the nanocomposites of PCN_1/MWCNTs have high glass transition temperature T_g and E' that is important in terms of their possible practical application.

It can be seen from the curves of $E' = f(T)$ and $tg\ \delta = f(T)$ for PCN_2/MWCNTs nanocomposites (Fig. 9) that at addition of carbon nanotubes MWCNTs into the polycyanurate matrix and increase of their content from 0.03 to 1.2 wt. % the visible changes in viscoelastic properties occur: redistribution of intensities and shift of the maxima for $tg\ \delta$ along the temperature axis (decreasing T_g value), changing the glass transition temperature interval (ΔT_g), increase of E' in a wide temperature range, and etc.

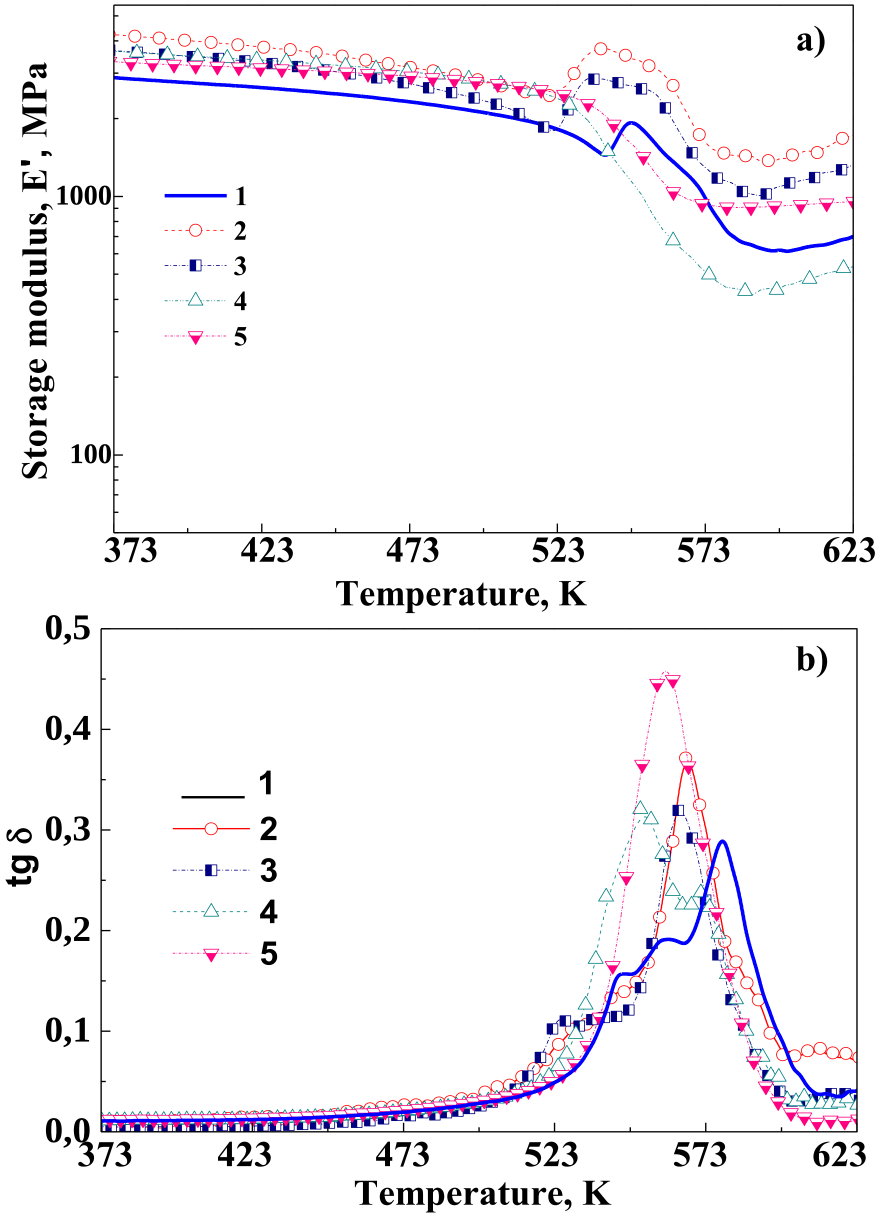

Figure 9. Temperature dependences of (a) modulus *E'* and (b) *tg* δ (at frequency 3 Hz) for the PCN$_2$/MWCNTs nanocomposites with MWCNTs content, wt. %: 1 – 0.00; 2 – 0.03; 3 – 0.04; 4 – 0.10; 5 – 1.20

It can be concluded that increasing concentrations of carbon nanotubes in PCN$_2$/MWCNTs nanocomposites cause reduced crosslink density of PCN$_2$ formed in their presence that leads to lower values of T_g. This conclusion is confirmed by the growth of the intensity maxima for *tg* δ (Fig. 9 b, curves 2-5). In other words, the carbon nanotubes in the synthesis of these nanocomposites to some extent prevent the formation of a regular three-dimensional polycyanurate matrix. This is also confirmed by the fact that at increase in nanocomposites the MWCNTs content to 0.1 ÷ 1.20 wt. % simultaneously with decreasing T_g values, the number of relaxation transitions is reduced (from three to one, Table. 5), indicating impediments in the process of post-curing in samples with high content of carbon nanotubes.

Note that during the second study (heating) of all the nanocomposite samples the only single T_g (the highest value for each sample, Table. 5) is observed. However, because the value of T_g is less than that for the unfilled PCN_2 sample, we believe that due to the presence of carbon nanotubes in PCN_2 matrix the complete conversion of cyanate groups is not achieved and the polycyanurate network of lower regularity is formed.

Unlike the series of samples PCN_1/MWCNTs for all the PCN_2/MWCNTs nanocomposites a significant increase in the values of E' is observed (Fig. 9 a). For example, the value of E' at T ~ 273 K for the nanocomposite sample with small MWCNTs content (0.03 wt. %) is ~ 63 % higher than the E' value for unfilled PCN_2 that, as it is known, indicates reinforcement of PCN-matrix by carbon nanotubes, which are effectively dispersed into individual nanotubes (Fig. 6).

Additionally, perhaps the increase in E' in these nanocomposites is related to the nanostructuring of the samples (the appearance of the structures of the type, which can be called as "nano hot dog"), since it is clear that reinforcing effect of carbon nanotubes is increased with contributions in some way of the oriented thin polymer layer wrapping the carbon nanotubes. In other words in covalently crosslinked polycyanurate network the physical network of carbon nanotubes "wrapped" by the polymer is formed that, as known *[Nilsen, 1978]*, promotes growing storage modulus values.

Increasing concentrations of nanofiller leads to lower values of E' in the whole temperature range (Fig. 9 a), but the values of E' modulus for the nanocomposites synthesized are larger than that for the pure PCN_2. As it was noted above, in these nanocomposites during high-temperature synthesis of PCN-matrix a secondary reaggregation of carbon nanotubes occurs, resulting in reduced uniformity of dispersion of carbon nanotubes in a polymer matrix, there are areas where there is no physical network of carbon nanotubes "wrapped" by the polymer (sect. 5) that leads to decreasing values of E' modulus *[Nilsen, 1978]*.

Comparison of viscoelastic properties of two series of the investigated nanocomposites based on crosslinked polycyanurates indicates that using of the industrial oligomer DCBA for synthesis of PCN_2-matrix allows to obtain of the nanocomposites with high E' that is important in terms of their possible practical application.

Using the "TA Instruments DMTA 2980" equipment the "stress-strain" dependence for samples of the nanocomposites PCN_2/MWCNTs was recordered

[Bardash, 2011] and the value of tensile strength at break, σ_b was determined depending on the content of the nanofiller (cf. Fig. 10 and Table 7).

It is obvious that with the introduction of the nanofiller to the unfilled polymer matrix the value of the ultimate strength σ_b significantly increases, the higher content of MWCNTs, the greater the value of σ_b: for example, introduction of 0.03 and 0.06 wt. % of MWCNTs increases the value of σ_b by ~ 62 % and ~ 94%, respectively (compared to the value for pure PCN_2, Table. 7).

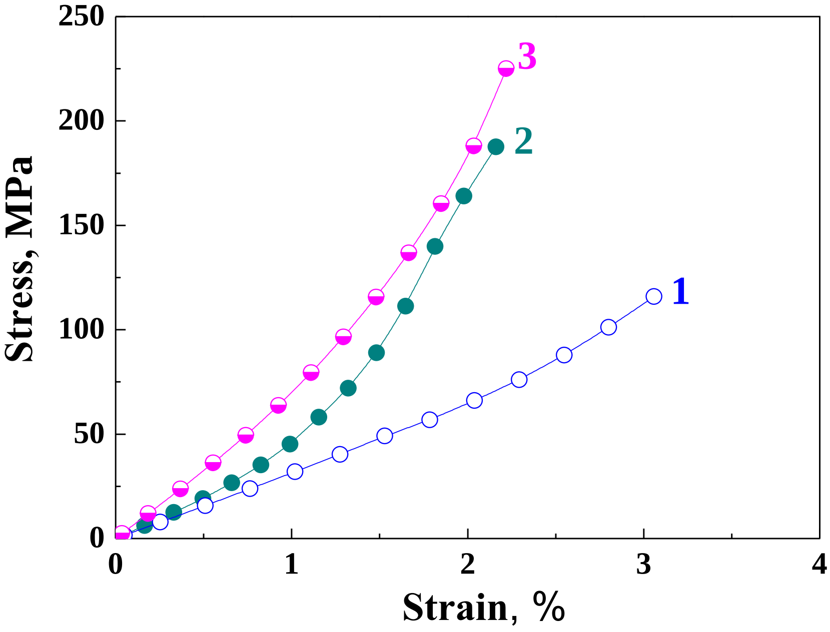

Figure 10. Stress - strain curves for samples of the nanocomposites based on PCN_2 with MWCNTs content, wt. %: 1 – 0.00; 2 – 0.03; 3 – 0.06

Table 7. The impact of the nanofiller on the value of tensile strength at break σ_b for PCN_2/MWCNTs nanocomposites

MWCNTs content, wt. %	**σ_b, MPa**
0.00 (PCN_2)	115.9
0.03	187.6
0.06	225.1

It can be concluded that at the conditions of forming PCN_2-matrix used even a small amount (0.03 ÷ 0.06 wt. %) of MWCNTs significantly improves the strength of the nanocomposites obtained that is associated with features of the structure of carbon nanotubes as nanofiller.

7. Study of the effect of MWCNTs on the thermophysical characteristics of nanostructured composites

As it was found (sect. 4-6), the presence of the nanofiller significantly affects the kinetics of the DCBA polycyclotrimerization process, it was interesting to investigate thermophysical properties of the PCN_1/MWCNTs and PCN_2/MWCNTs nanocomposites.

The profile of DSC-thermograms (cf. Fig. 11) obtained during the first scan (heating) of the samples of the nanocomposites PCN_1/MWCNTs allows to determine that in all the samples studied the formation process of polycyanurate matrix is incomplete, it is clear seen that after the endothermic transition, corresponding to T_g of PCN_1-matrix, an intensive exothermic process starts, which is known *[Haman et al., 2009]* to appear when the reaction of post-curing of PCN-matrix through the interactions of unreacted (at the synthesis of the matrix) cyanate groups occur. This finding correlates with the above kinetic data (sect. 4) and the results of DMTA study (sect. 6).

From the DSC-thermograms recordered during the second heating of the same samples it can be seen (Fig. 11, curves at number 2) that the exothermic effects on thermograms disappear, indicating the absence of chemical reactions in these systems *[Bershtein and Egorov, 1990]*. The thermophysical parameters are summarized in Table 8, it is seen that the values of T_g for PCN-matrix are slightly higher for the nanocomposite samples after their second scan (heating), certainly due to the increase of the crosslink density of PCN network after chemical reactions (interactions) of cyanate groups of PCN-matrix during the first scan (heating). It is also established *[Bardash, 2011]* that with increasing content of carbon nanotubes in the samples the value of heat capacity jump ΔC_p increases, indicating some disordering in highly regular polycyanurate matrix under the influence of the nanofiller. This conclusion is consistent with the above presented DMTA data (sect. 6).

For samples of the nanocomposites PCN_2/MWCNTs the similar DSC-thermograms have been obtained, they are shown in Figure 12. It is found that, as for the previous series of samples in these nanocomposites the formation of polycyanurate matrix was not complete, it is evidenced by the appearance in the temperature region $T > 500$ K an intensive exothermic peak, which, as noted above (sect. 4), corresponds to post-curing polycyclotrimerization reaction of the residual cyanate groups of the PCN-matrix, which were not able to react during the matrix synthesis. It should be noted that in comparison with the first series of samples of PCN_1/MWCNTs in the series of PCN_2/MWCNTs nanocomposites the exothermic effect is somewhat higher (Fig. 12) and it even makes impossible to fix the T_g value of the nanocomposites after first heating of the samples.

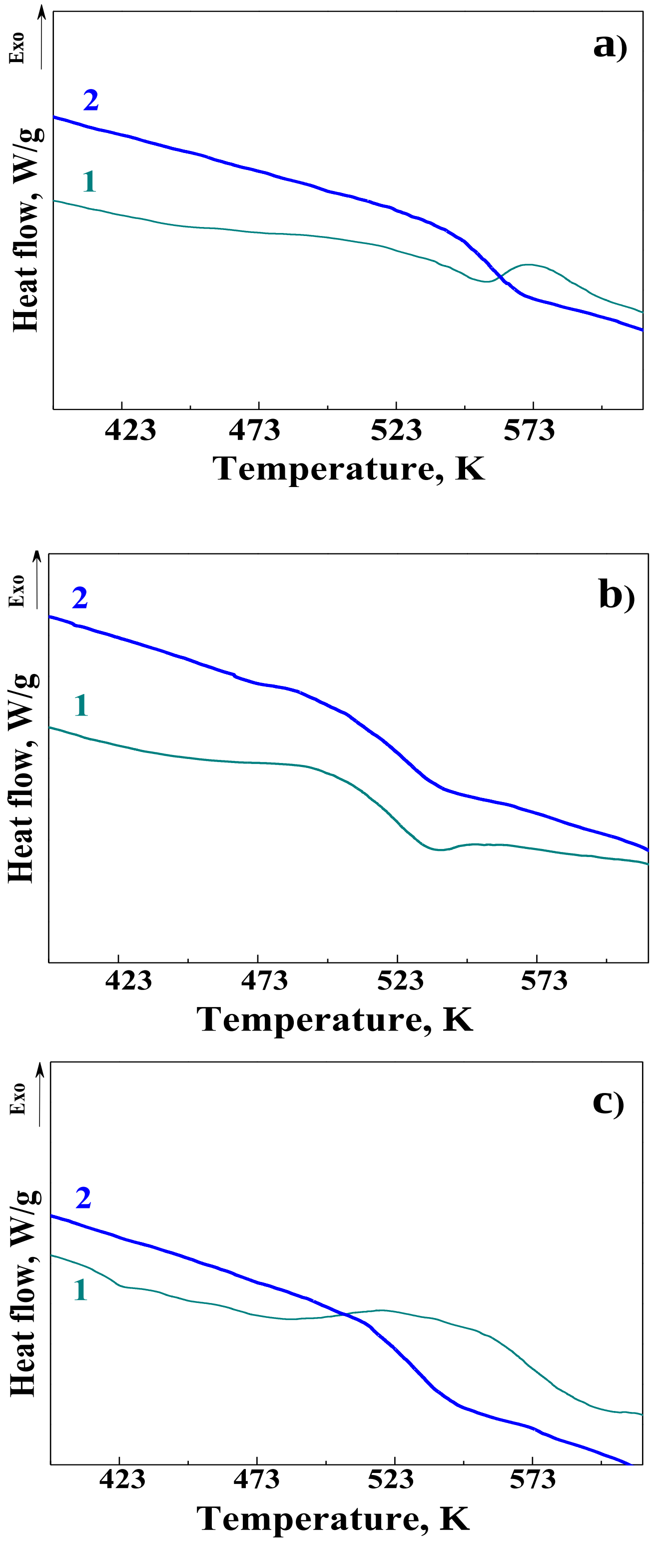

Figure 11. DSC-thermograms for the PCN$_1$/MWCNTs nanocomposites with MWCNTs content, wt. %: a – 0.00; b – 0.01; c – 0.10; 1 – first heating scan; 2 – second heating scan

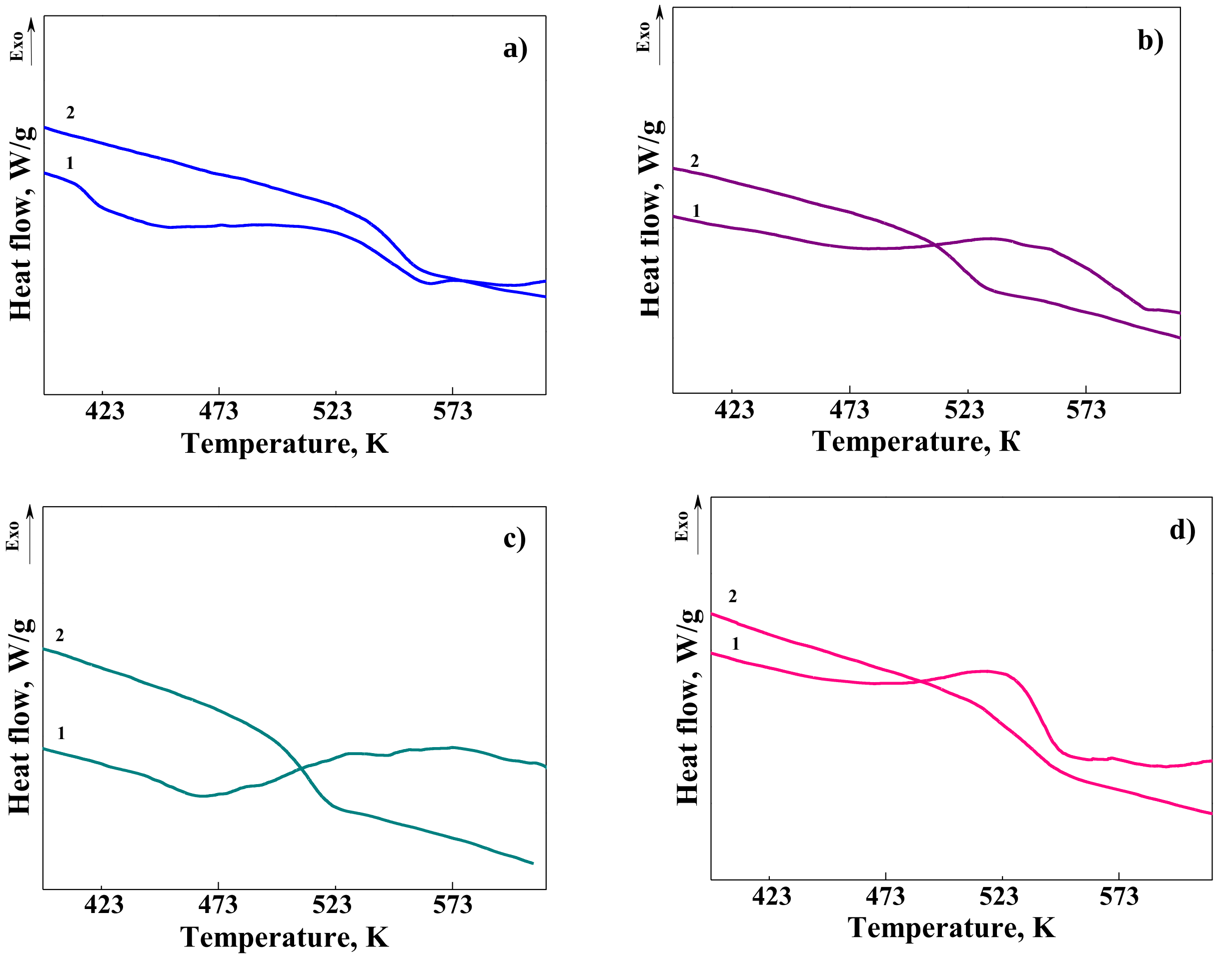

Figure 12. Typical DSC-thermograms for PCN_2/MWCNTs nanocomposites with MWCNTs content, wt. %: a – 0.00; b – 0.03; c – 0.50; d – 1.20; curve 1 – first heating scan; curve 2 – second heating scan

Thus, we can conclude that the basic thermophysical characteristics, such as glass transition temperature T_g, the heat capacity jump ΔC_p, glass transition interval ΔT_g of PCN-matrix in the nanocomposites PCN_1/MWCNTs and PCN_2/MWCNTs change non-monotonically and non-additively under the influence of carbon nanotubes that evidences a complex reorganization of the phase structure of the nanocomposites during their synthesis.

Comparison of the T_g values for post-cured individual PCN_1 and PCN_2 (Tables 8 and 9) has shown that the value of glass transition temperature T_g for the latter is lower by 6.7 K. This finding correlates with the above results of the DMTA study of the nanocomposites (sect. 6). As it was discussed above the lower T_g value of the PCN network is explained by the lowering of its crosslink density arising from the lower final conversion of the cyanate groups in the resulting network. We suppose that at synthesis of the industrial DCBA

Table 8. Thermal-physical parameters for PCN$_1$/MWCNTs nanocomposites

MWCNTs content, wt. %	**T_g, K**		**ΔT_g, K**		**ΔC_p, J/(K· g)**	
	1 scan	**2 scan**	**1 scan**	**2 scan**	**1 scan**	**2 scan**
0.00 (PCN$_1$)	538.5	557.8	16.7	20.0	0.106	0.224
0.01	522.6	525.8	25.7	32.8	0.282	0.304
0.10	-	529.7	-	26.4	-	0.299

oligomer the producer used a special catalyst, and it is known that catalyst accelerates the reaction of polycyclotrimerization of cyanate ester monomers in first steps of curing, but leads to formation of the final network with lower conversion of the cyanate groups. The higher rate of network formation hinders formation of the network regular structure.

Table 9. Thermal-physical parameters for PCN$_2$/MWCNTs nanocomposites

MWCNTs content, wt. %	**T_g, K**		**ΔT_g, K**		**ΔC_p, J/(K· g)**	
	1 scan	**2 scan**	**1 scan**	**2 scan**	**1 scan**	**2 scan**
0.00 (PCN$_2$)	416.2; 542.5	551.1	17.8; 33.3	17.1	0.200; 0.276	0.204
0.03	-	545.5	-	29.0	-	0.249
0.10	-	538.3	-	11.2	-	0.291
0.50	-	512.4	-	17.0	-	0.227
1.20	-	537.1	-	29.5	-	0.218

In the DSC-thermograms for all the PCN$_2$/MWCNTs studied nanocomposites, obtained during the second scan (heating), there are no exothermic peaks (Fig. 12, curves at number 2), indicating the completion of the post-curing process *[Bershtein and Egorov, 1990]*. It has been found (Table 9) that with increasing content of carbon nanotubes in the samples the value of heat capacity jump ΔC_p increases (non-monotonically) indicating some disordering of polycyanurate matrix under the influence of the nanofiller. This conclusion is consistent with the above data obtained using DMTA technique (sect. 6).

8. Influence of MWCNT on resistance to thermooxidative destruction of nanocomposites PCN$_1$/MWCNTs and PCN$_2$/MWCNTs

Since the polycyanurate networks are thermostable polymers, it was certainly interesting to evaluate the influence of carbon nanotubes on thermal behaviour of PCN-matrix in air, the corresponding experimental TGA-curves, obtained for nanocomposites PCN$_1$/MWCNTs and PCN$_2$/MWCNTs, are shown in Figures 13 and 14. The appropriate thermal characteristics for the nanocomposite samples studied have been summarized in Tables 10 and 11.

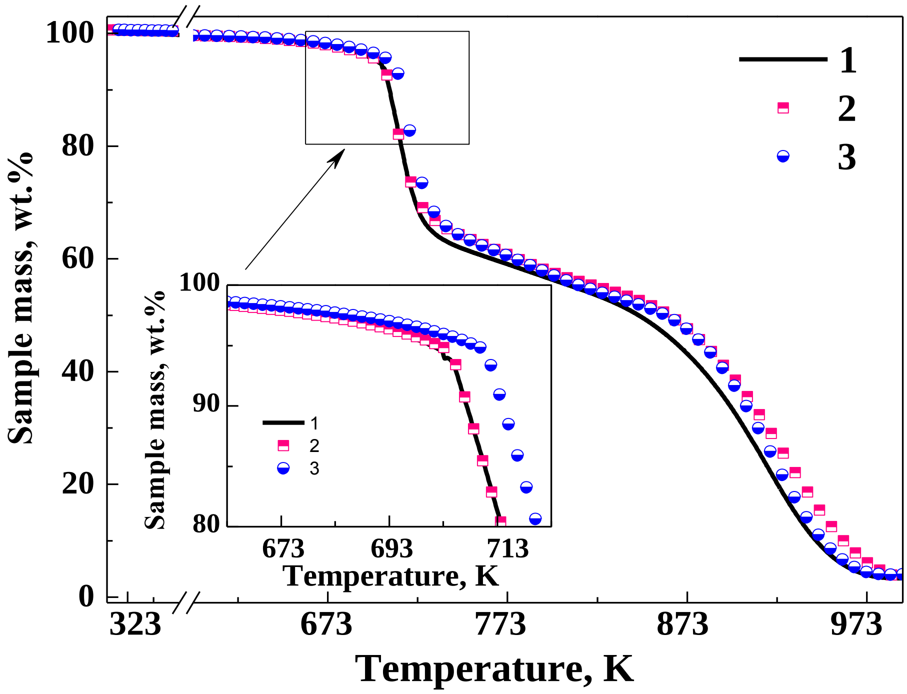

Figure 13. TGA curves (in air) for the PCN_1/MWCNTs nanocomposite samples with MWCNTs content, wt. %: 1 – 0.00; 2 – 0.01; 3 – 0.10

Table 10. Influence of MWCNTs on resistance to thermooxidative destruction of PCN_1/MWCNTs nanocomposites

MWCNTs content, wt. %	$T_{\partial\ (5\%)}$, **K**	$T_{\partial\ (50\%)}$, **K**	$T_{\partial 1\ (max)}$, **K**	$T_{\partial 2\ (max)}$, **K**	**Δ*m*, wt. %**		m_{char}, **wt. %**
					at $T_{\partial 1\ (max)}$	**at** $T_{\partial 2\ (max)}$	
0.00 (PCN_1)	701	846	714	912	20	74	3.11
0.01	702	863	715	926	20	74	3.57
0.10	709	861	720	920	19	74	4.25

It should be noted that the character of the TGA curves does not change at introduction of carbon nanotubes to the PCN-matrix since the trend of curves, the number of degradation stages for PCN_1/MWCNTs nanocomposites are similar to that for individual PCN_1. For all the TGA curves the intense mass loss is observed in the temperature range of 700-750 K, which is associated with the destruction of the carbon backbone of PCN network. Samples of the nanocomposites of series PCN_1/MWCNTs as well as the individual PCN_1 show a slightly higher resistance to thermooxidative destruction than the corresponding samples from the second series (PCN_2/MWCNTs), certainly due to the difference in the structure formed of polycyanurate matrix. As it was discussed above in section 7, in the samples based on PCN$_1$ the degree of polycyclotrimerization completeness and, correspondingly, the crosslink density of the resulting PCN-matrix are higher and thermal stability is higher too.

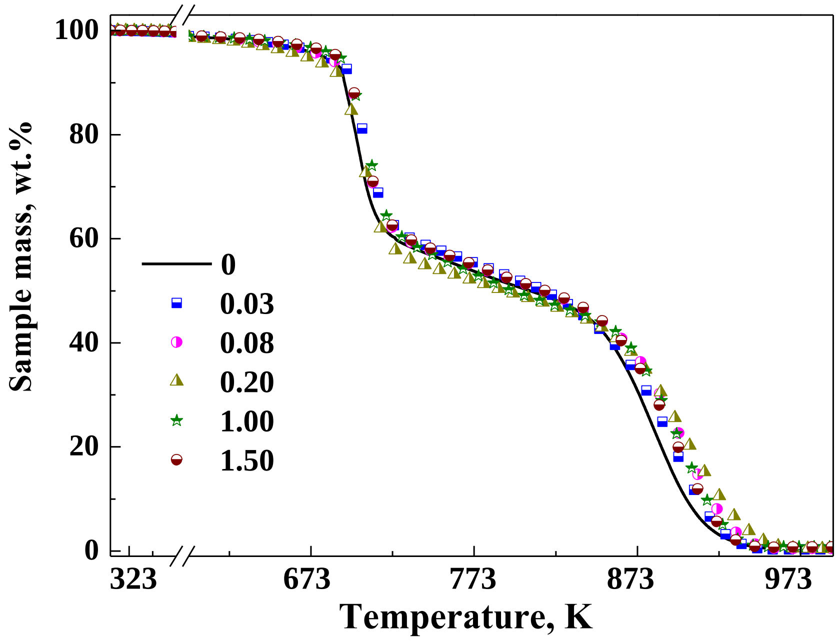

Figure 14. Typical TGA curves (in air) for samples of the PCN$_2$/MWCNTs nanocomposites with MWCNTs content, wt. %: 1 – 0.00; 2 – 0.03; 3 – 0.08; 4 – 0.20; 5 – 1.00; 6 – 1.50

Table 11. Influence of MWCNTs on resistance of PCN$_2$/MWCNTs nanocomposites to thermooxidative degradation

MWCNTs content, wt. %	$T_{\partial (5\%)}$, **K**	$T_{\partial (50\%)}$, **K**	$T_{\partial 1 (max)}$, **K**	$T_{\partial 2 (max)}$, **K**	**Δ*m*, wt. %**		m_{char}, **wt. %**
					at $T_{\partial 1 (max)}$	**at** $T_{\partial 2 (max)}$	
0.00 (PCN$_2$)	680	807	702	884	22	77	0.63
0.03	683	816	708	890	24	82	0.34
0.08	682	816	706	899	23	78	0.54
0.20	670	792	704	903	24	78	0.47
1.00	663	766	699	883	25	80	0.56
1.20	689	796	708	899	23	78	0.98
1.50	690	816	706	894	22	77	0.79

It has been found *[Bardash, 2011]* that for the series of samples PCN$_1$/MWCNTs the presence of carbon nanotubes dispersed in polymer matrix in an amount of 0.01 and 0.10 wt. % slightly increases the resistance of these nanocomposites to thermal degradation in air. As it is seen from the data of Table 10, destruction of these samples starts at higher temperatures compared to the pure PCN_1 (the values of $T_{\partial(5\%)}$, $T_{\partial(\max)}$ and $T_{\partial(50\%)}$ are higher). This is connected with some contribution of CNTs themselves, which have very high own thermal stability *[Bardash, 2011]*. However, on the other hand it is known that the polycyanurate networks have higher heat resistance and resistance to thermooxidative destruction at higher crosslink density *[Hamerton, 2004]*.

In section 4 it was shown that the increase of MWCNTs content in samples of the nanocomposites slightly decreased the final conversion value of cyanate groups, resulting to lower crosslink density of the final PCN network. Therefore it was logical to assume that the thermal properties of the nanocomposites would be worse than that of the individual PCN. Surprisingly, the experimental results show the opposite. Thus it can be assumed that the improved resistance to thermooxidative degradation in these nanocomposite samples is associated not only with a certain additive contribution of thermally resistant CNTs, but probably also with the post-curing process of PCN-matrix due to additional heating to high temperatures ($T > T_g$) during TGA measurements (the same observations were fixed by DMTA and DSC methods, sect. 6 and 7, correspondingly), increasing the density of PCN-matrix and hence the stability of nanocomposites to thermooxidative destruction.

Investigation of resistance to thermooxidative degradation for series of samples PCN_2/MWCNTs has shown that their thermal stability in air depends non-monotonically on the MWCNTs content (Fig. 14 and Table. 11). For example, the presence of 0.03 ÷ 0.08 wt. % of the dispersed in the polymer matrix MWCNTs increases the resistance to thermooxidative destruction of these nanocomposites: increasing degradation temperatures $T_{\partial(5\%)}$, $T_{\partial(\max)}$ and $T_{\partial(50\%)}$, simultaneously the reduced mass loss for these samples has been fixed in comparison with the individual PCN_2). In general we can conclude that the synthesized nanocomposites PCN_1/MWCNTs and PCN_2/MWCNTs have high resistance to thermooxidative destruction.

9. Study of influence of carbon nanotubes on electrical properties of PCN_2/MWCNTs

As it was noted above, carbon nanotubes in addition to the unique thermal and mechanical properties possess high electrical conductivity, thus they are very attractive for use as conductive filler for creation of conductive polymer nanocomposites. Therefore it is interesting to assess, first, in which limits the electrical properties of polycyanurates (which are recognized as dielectrics with low dielectric constant, 2.5 ÷ 3.2) can be purposefully altered; secondly, it is useful to determine the percolation threshold, p_c, above which the PCN$_2$/MWCNTs nanocomposites exhibit properties of conductive material.

According to the percolation theory, at low filler content, a conductivity of material is determined by a polymer matrix *[Kirkpatrick, 1973; Lisunova et al., 2007; Stauffer and Aharony, 1992]*, while at certain critical volume fraction of conductive filler a percolation threshold, p_c, is achieved. As a result, the conductivity grows by many orders instantly and rapidly, even with very small increase in filler content. When content of nanofiller is lower as compared with the value of p_c, the system has no conductive CNTs pathways, but when the filler content is higher than the p_c, a great number of continuous conductive pathways is formed, resulting in generation of conductive composite. Classical percolation theory assumes that the conductivity (σ) of systems above p_c should be described by exponential law as follows *[Sahimi, 1994]*:

$$\sigma = \sigma_0 (p - p_c)^t \tag{3}$$

where σ_0 – scaling factor, p_c– the value of percolation threshold, t – universal exponent, depending on dimensionality and topology of the system (t = 1.33 for two-dimensional systems, t = 2.0 for three-dimensional systems*[Sahimi, 1994]*).

It is known, that experimental values of t described for the CNT-filled polymer nanocomposites are within the range $t = 0.7 \div 7.5$ *[Bauhofer and Kovacs, 2009]*. It should be noted that since the density of carbon nanotubes can be determined only approximately (according to *[Hu et al., 2006]* $\rho_{CNT} \approx 1.4 \div 1.9$ g/cm^3, and in *[Lisunova et al., 2007]* $\rho_{CNT} \approx 2.045$ g/cm^3), it is reasonable for calculations to use mass fraction (instead of volume one) of MWCNTs.

Figure 15 shows the concentration dependence of conductivity measured under direct currant (σ_{DC}) for PCN$_2$/MWCNTs nanocomposites, it is clear that the σ_{DC} value demonstrates percolation behavior *[Kirkpatrick, 1973; Sahimi, 1994; Stauffer and Aharony, 1992]*, namely: at low concentrations of MWCNTs from 0 to ~ 0.3 wt. % in nanocomposites σ_{DC} value does not change and is equal ≈ 10^{-16} S/cm; with increasing content of nanotubes in composites the value of σ_{DC} conductivity sharply increases by ~ 10 orders of magnitude in a narrow concentration range of MWCNTs ~ 0.3 – 0.5 wt. %.

A further increase in concentration of MWCNTs in these samples causes slow growth of σ_{DC} value by ~ 3 orders of magnitude in the concentration range ~ 0.3-1.5 wt. %. Experimental dependence of $\sigma_{DC} = f\,(C_{MWCNTs})$ shown in Fig. 15 was theoretically approximated using Equation 3, the dependence of $\lg \sigma = f \lg (p - p_c)$ was built and step by step by changing the value of p_c the best linear approximation of the experimental data was achieved. As shown in Figure 15, theoretical and experimental data agree well with each other. The percolation threshold p_c and the value of t are given in Table 12.

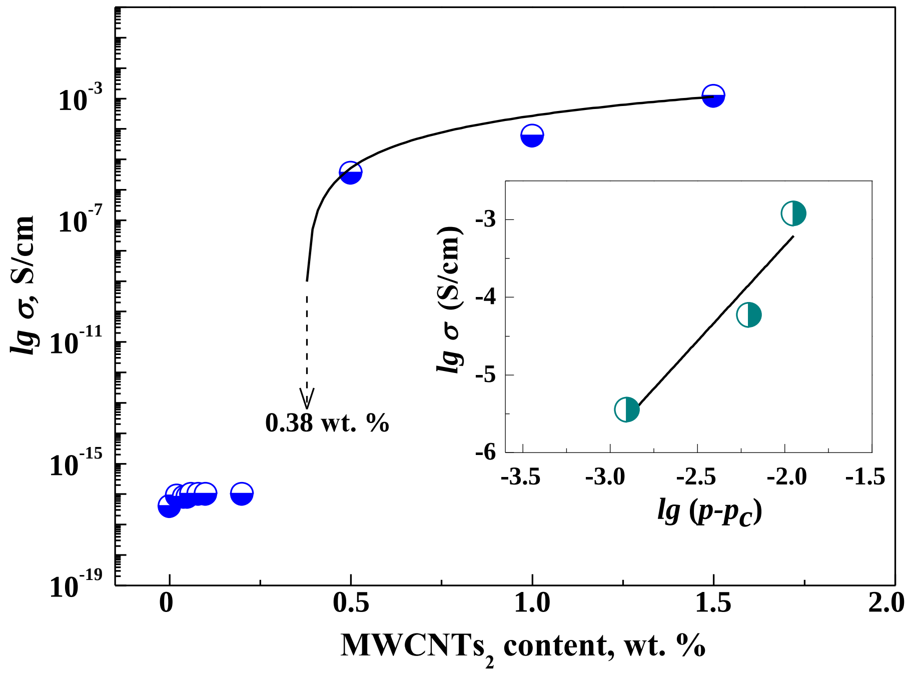

Figure 15. Dependence of conductivity σ_{DC} (direct current) for PCN_2/MWCNTs nanocomposites on MWCNTs content; dots represent experimental data; lines shows theoretical values (according to Equation 3); insertion reflects the dependence curve of $lg\sigma_{DC} = f(lg)(p - p_c)$ for $p > p_c$

Table 12. Percolation threshold p_c and critical exponent t for PCN_2/MWCNTs nanocomposites

Percolation parameters	**PCN_2/MWCNTs**
p_c	0.0038
t	2.46

One can see that the percolation area for PCN_2/MWCNTs system is fixed in the concentration range of MWCNTs content of 0.38 – 0.50 wt. %. Therefore the percolation behavior of this system can be characterized by two critical values of concentration: $p_c \approx 0.38$ wt. % when the conducting cluster begins to form and $p_c^* \approx 0.50$ wt. %, corresponding to the end of formation of spatial conducting cluster.

It was also interesting to determine the mechanism of conductivity in PCN_2/MWCNTs nanocomposites. In the reviews *[Gibson et al., 2007; Ulanski and Kryszewski, 1995]* electrical properties in heterogeneous organic polymer systems as well as basic concepts and equations for mechanisms of charge transport controlled by percolation processes are discussed in details.

Authors present theoretical models from the point of view of their experimental implications. Among the many possible conduction mechanisms, including hopping and tunneling, especial attention is paid to Fluctuation-

Induced Tunneling (FIT) model proposed by Sheng *[Sheng, 1980]*. The theory was applied for description of charge carrier transport in our material. Generally, this can be applied to heterogeneous materials, in which relatively large conducting islands (or long conducting pathways) are separated by small insulating barriers. The main idea of this model is that thermal noise can induce strong voltage fluctuations over a tunnel junction, which effectively narrow and lower the barrier analogous to the effect of an externally applied electric field. The analytical expression for the temperature dependence of the Fluctuation-Induced Tunneling conductivity is presented by the following equations *[Sheng, 1980]*:

$$\sigma = \sigma_0 \exp\left(\frac{-T_1}{T+T_0}\right) \quad , \tag{4}$$

where

$$T_1 = \frac{wA\varepsilon_0^2}{8\pi k_B} \tag{5}$$

$$T_2 = \frac{2T_1}{\pi w \chi} \quad , \tag{6}$$

where σ_0 is a constant, T is the absolute temperature, T_0 is a temperature below which the tunneling is a simple elastic and temperature independent process, and T_1 is the temperature above which the conductivity is thermally activated, k_B is the Boltzmann constant, $\chi = (2mV_0/h^2)^{1/2}$, $\varepsilon_0 = 4V_0/ew$, m is the electron mass, V_0 is the potential barrier height, w is the insulating layer width, and A is the aria of capacitance formed at the junction.

In order to determine the mechanism of conductivity in PCN_2/MWCNTs nanocomposites for the samples with the MWCNTs content higher than the percolation threshold found, the temperature dependence of DC conductivity at temperatures close to the temperature of 0 K was investigated.

In Figure 16 the experimental temperature dependence of DC conductivity of nanocomposites with different $MWCNT_2$ content is shown and the theoretical values of σ_{DC} calculated using the FIT theory (equations 4-6) are given. The calculations have shown that the experimental and theoretically calculated values of σ_{DC} obtained with a help of FIT model agree well in the whole temperature range measured, it is seen that at temperatures close to 0 K a weak temperature dependence of σ_{DC} is observed.

It is explained by the above mentioned contribution to σ_{DC} of electrical conductivity of metallic carbon nanotubes (observed in used MWCNTs by Raman spectroscopy *[Bardash, 2011]*), because at so low temperatures the semiconducting CNTs cannot conduct electrical current *[Kymakis and Amaratunga, 2006; Harris, 1999]*.

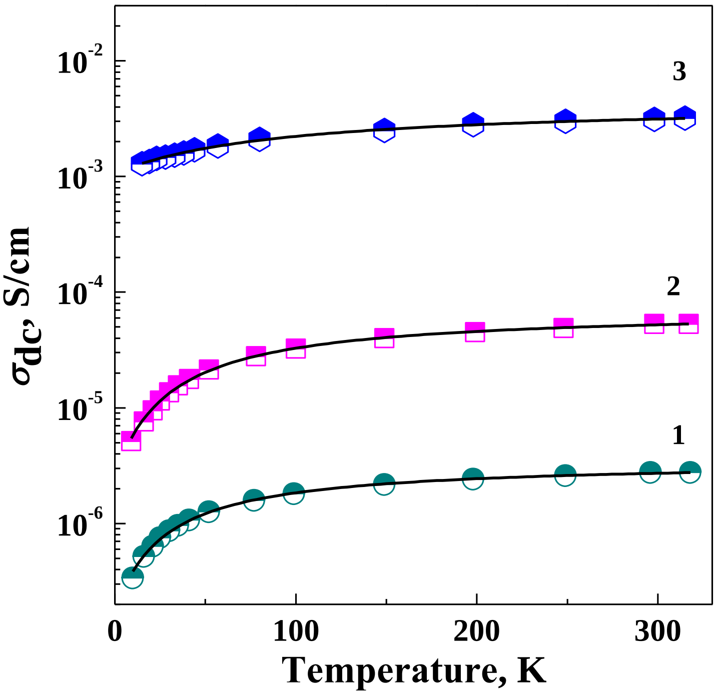

Figure 16. Temperature dependence of dc conductivity of PCN$_2$/MWCNTs nanocomposites with MWCNTs content, wt. %: 1 – 0.5; 2 – 1.0; 3 – 1.2; symbols – experimental data, lines – theoretically calculated using FIT model

Finally, we can conclude that the conductivity in these nanocomposites is mainly created by electrons through the tunneling mechanism, and the "wrapping" of carbon nanotubes with polymer described in section 5 does not hinder this process. Increasing concentration of MWCNTs in PCN$_2$/MWCNTs nanocomposites causes growth in dc conductivity that is certainly explained by increasing number of the conducting channels *[Stauffer and Aharony, 1992]*.

10. Conclusions

Thus, the literature review shows that to date investigations on the synthesis and structure-property relationships of nanostructured polymer composites based on heterocyclic esters and carbon nanotubes are just at the beginning *[Bardash and Fainleib, 2010]*. So far the studies of effect of CNTs on the kinetics of polycyclotrimerization of cyanate esters of bisphenols was not carried out. There is also a lack of information in the literature about the effect of CNTs on thermal, viscoelastic and electrical properties of PCN/CNTs. Thus one can say that today there is an absolute need for comprehensive investigation of *in situ* synthesis of polymer nanocomposites based on CE in the presence of carbon nanotubes and to establish the regularities of the influence of nanofiller on basic physical-chemical properties of nanocomposites synthesized.

The comprehensive study of determination of the impact of multi-walled carbon nanotubes on structure and basic physical-chemical and electric properties of polymer composites synthesized from oligomers of dicyanate ester of bisphenol A by *in situ* polycyclotrimerization of DCBA in the presence of MWCNTs, using the method of reaction forming was carried out by our group. For the first time it is found that at synthesis of the crosslinked polycyanurate matrix the presence of MWCNTs in the first stages of the process accelerates the reaction of polycyclotrimerization of DCBA oligomer, but in the final stages of the process the nanofiller hinders achieving high conversion of DCBA cyanate groups, leading to the formation of PCN-matrix with a lower degree of crosslinks. This conclusion is confirmed by the results of measurements by DMTA technique, as for the nanocomposites with higher content of MWCNTs a significant reduction in T_g values for PCN-matrix has been fixed. Using TGA method it was determined that all the synthesized PCN_2/MWCNTs nanocomposite samples retained high resistance to thermal-oxidative degradation inherent to this class of polymers, some increase in thermal performance of the nanocomposites compared to the individual PCN_2 was observed. It has been found that in these nanocomposites the value of tensile strength at break σ_b increases by 62 and 94% for the samples with 0.03 and 0.06 wt. % of MWCNTs, respectively, compared with unfilled PCN_2 ($\sigma_b \approx 115.9$ MPa). It is found that by introducing of carbon nanotubes into the dielectric PCN-matrix the electrical properties of the nanocomposite can be purposefully alter from insulator to the conductor by varying conductivity in a wide range (depending on the CNTs content). It has been determined that the percolation threshold for PCN_2/MWCNTs nanocomposites is low and equal ~ 0.38 wt. % of MWCNTs indicating the formation of three-dimensional percolation conducting network of carbon nanotubes in the system. In summary, the efficient methods of synthesis of PCN/MWCNTs nanocomposites with improved physical-chemical properties were developed.

11. Acknowledgements

The authors would like to acknowledge French Government for the grant for PhD students as well as to Région Rhône-Alpes (the grant of initiative international mobility for PhD students EXPLORA’DOC 2008-2009) for the financial support. Authors thank Professor Jacek Ulanski, a head of the Department of Molecular Physics of Technical University of Lodz, of for many useful discussions. This work was supported through the State Target Scientific-Technical Program "Nanotechnologies and nanomaterials (2010-2014)", project No 6.22.3.31.

12. References

Bardash L., Fainleib A. (2010) Nanocomposites based on polycyanurates filled by carbon nanotubes. *Polym. J.* (Kyiv, Ukraine), Vol. 32, No 4, pp. 287–298 (in Ukrainian).

Bardash L. (2011) Synthesis and Investigation of Nanostructured Polymer Composites Based on Heterocyclic Esters and Carbon Nanotubes. *Diss. PhD, Institute of Macromolecular Chemistry of NAS of Ukraine*, Kyiv, Ukraine, University Claude Bernard – Lyon1 – Lyon, France.

Bershtein V. A., Egorov V. M. (1990) *Differential scanning Calorimetry in physical chemistry of polymers*, Khimiya, Leningrad, Russia (in Russian).

Bershtein V., Fainleib A., Yakushev P**.** (2010) Polycyanurate-based Hybrid Networks and Nanocomposites: Structure-Glass Transition Dynamics-Dynamic Heterogeneity-Properties Relationships**,** In: *Thermostable polycyanurates: synthesis, modification, structure and properties*, Nova Science Publishers Inc., New York, USA.

Bauhofer W., Kovacs J. Z. (2009) A review and analysis of electrical percolation in carbon nanotube – polymer composites. *Compos. Sci. Technol*., Vol. 69, pp. 1486–1498.

Bugachenko F. L. (2003) Nanochemistry – the direct way to high technologies of the new century. *Uspekhi khimii***,** Vol. 72, pp. 419–437 (in Russian).

Carey F. A., Sundberg R. J. (2007) *Advanced organic chemistry A*: *structure and mechanisms,* Springer Science + Business Media, Inc., New York, USA.

Che J., *Chan-Park* M. B. (2008) Reactive spinning of cyanate ester fibers reinforced with aligned amino-functionalized single wall carbon nanotubes. *Adv. Funct. Mater.*, Vol. 18, pp. 888–897.

Fainleib A. M., Sergeeva L. M., Shantalii T. A. (1991) Triazinecontaining interpenetrating polymer networks. *Compos. Polym. Mater,* (Kiev, in Russian), Vol. 50, pp. 63–72.(in Russian).

Fainleib A. M., Shantalii T. A., Pankratov V. A. (1991) Copolymers of cyanate esters and plastics based on them. *Compos. Polym. Mater.* (Kiev, in Russian), Vol. 49, pp. 39–53. (in Russian).

Fainleib A., Grigoryeva O., Pissis P. (2006) Modification of Polycyanurates by Polyethers, Polyesters and Polyurethanes. Hybrid and Interpenetrating Polymer Networks, In: *Focus on Natural and Synthetic Polymer Science,* Nova Science Publishers: New York, USA.

Fainleib A., Bardash L., Boiteux G. (2009) Catalytic effect of carbon nanotubes on polymerization of cyanate ester resins. *eXPRESS Polym. Lett.,* Vol. 3, pp. 477–482.

Fainleib A. (Ed) (2010) *Thermostable polycyanurates: synthesis, modification, structure and properties,* Nova Science Publishers Inc., New York, USA.

Fainleib O. M., Bardash L. V., Grigoryeva O. P., Boiteux G., Ulanski J. (2010) Method of producing of polycyanurates, *Pat. 52506 Ukraine,* C08G 73/00.

Fang T., Shimp D. A. (1995) Polycyanurate esters: science and application. *Prog. Polym. Sci.*, Vol. 20, No 1, pp. 61–118.

Fang Z., Wang J., Gu A. (2006) Structure and properties of multiwalled carbon nanotubes/cyanate ester composites, *Polym. Eng. Sci.,* Vol. 46, pp. 670–679.

Fiedler B., Gojny F. H., Wichmann M. H. G., Nolte M. C. M., Schulte K. (2006) Fundamental aspects of nano-reinforced composites. *Compos. Sci. Technol*., Vol. 66, pp. 3115–3125.

Fife C. A., Niu J., Mok K. J. (1995) Synthesis and characterization of polyfunctional crosslinking agents for cyanate resins. J. *Polym. Sci. A: Polym. Chem*., Vol. 33, pp. 1191–1202.

Fischer H. (2003) Polymer nanocomposites: from fundamental research to specific applications*. Mater. Sci. Eng.*, *C*, Vol. 23, pp. 763–772.

Hopkins A. R., Lipeles R. (2005) Preparation and characterization of single wall carbon nanotube-reinforced polycyanurate nanocomposites. *Polym. Prepr.*, Vol. 46, pp. 787–793.

Georjon O., Galy J., Pascault J. P. (1993) Isothermal curing of an uncatalyzed dicyanate ester monomer: kinetics and modeling. *J. Appl. Polym. Sci.*, Vol. 49, pp. 1441–1452.

Georjon O., Galy J. (1998) Effects of crosslink density on the volumetric properties of high Tg polycyanurate networks. Polymer. Vol. 39, pp. 339 – 345.

Gibson J. A. E. (1992) Early nanotubes. *Nature*, Vol. 359**,** pp. 347–364.

Gibson R. F., Ayorinde E. O., Wen Y.-F. (2007) Vibrations of carbon nanotubes and their composites: A review, *Comp. Sci. Technol*., Vol. 67, pp. 1–28.

Goh H. W., Goh S. H., Xu G. O., Pramoda K. P., Zhang W. D. (2003) Dynamic mechanical behavior of *in situ* functionalized multi-walled carbon nanotube/phenoxy resin composite*. Chem. Phys. Lett*., Vol. 373, pp. 277–283.

Gojny F. H., Nastalczyk J., Roslaniec Z., Schulte K. (2003) Surface modified multi-walled carbon nanotubes in CNT/epoxy-composites. *Chem. Phys. Lett*., Vol. 370, pp. 820–824.

Gojny F. H., Schulte K. (2004) Functionalisation effect on the thermo-mechanical behaviour of multi-wall carbon nanotube/epoxy-composites. *Compos. Sci. Technol.*, Vol. 64, pp. 2303–2308.

Haman K., Badrinarayanan P., Kessler M. R. (2009) Effect of a zirconium tungstate filler on the cure behavior of cyanate ester resin. *Appl. Mat. Interfaces*, Vol. 1, No 6, pp. 1190–1195.

Hamerton I. (1994) *Chemistry and Technology of Cyanate Ester Resins*, Chaman & Hall, Glasgow, Scotland.

Hamerton, I., Hay J. N. (1998) Recent Technological Developments in Cyanate Ester Resins.*High Perform. Polym*., Vol. 10, No 2, pp. 163–174.

Harris P. J. F. (1999) *Carbon nanotubes and related structures: new materials for the twenty–first centur*, Cambridge University Press, Cambridge, UK.

Hu G., Zhao C., Zhang S., Yang M., Wang Z. (2006) Low percolation thresholds of electrical conductivity and rheology in poly(ethylene terephthalate) through the networks of multi-walled carbon nanotubes, *Polymer*, Vol. 47, pp. 480–488.

Iijima S. (1991) Helical microtubules of graphitic carbon. *Nature* Vol. 354, pp. 56–58.

Jordan J., Jacob K. I., Tannenbaum R., Sharaf M.A., Jasiuk I. (2005) Experimental trends in polymer nanocomposites – a review. *Mater. Sci. Eng.*, *A*, Vol. 393, pp. 1–11.

Kirkpatrick S. (1973) Percolation and conduction. R*ev. Modern Phys.,* Vol. 45, pp. 574–588.

Koo J. H. (2006) *Polymer nanocomposites. Processing, characterization and applications*, McGraw-Hill, New York, USA.

Kymakis E., Amaratunga G. A. J. (2006) Electrical properties of single-wall carbon nanotube-polymer composite films. *J. Appl. Phys*., Vol. 99, No 8, pp. 084302.1 – 084302.7.

Latypov Z. Z., Pozdnyakov O. F. (2006) Determination of conditions of producing of polymer films containing ordered structure of carbon nanotubes and fullerenes. *Letters to JTF,* Vol. 32, pp. 28–33. (in Russian).

Li W., Ling G., Xin W. (2004) Triazine reaction of cyanate ester resin systems catalyzed by organic tin compound: kinetics and mechanism. *Polym. Int*., Vol. 53, pp. 869–876.

Lisunova M. O., Mamunya Ye. P., Lebovka N. I., Melezhyk A. V. (2007) Percolation behaviour of ultrahigh molecular weight polyethylene/multi-walled carbon nanotubes composites. *Eur. Polym. J.*, Vol. 43, pp. 949–958.

May Y. Y., Gong Y. G. (Eds.) (2008) *Polymer nanocomposites*, Technosfera, Moscow, Russia (translation to Russian).

McIntosh D., Khabashesku V. N., Barrera E. V. (2006) Processing and mechanical properties of continuous fiber systems made from fluorinated single-walled carbon nanotube-polypropylene composites. *Chem. Mater.*, Vol. 18, pp. 4561–4569.

Miaudet P., Badaire S., Maugey M., Derré A., Pichot V., Launois P., Poulin P., Zakri C. (2005) Hot-drawing of single and multiwall carbon nanotube fibers for hightoughness and alignment. *Nano Lett.*, Vol. 5, pp. 2212–2215.

Mittal V. (2010) *Polymer Nanotube nanocomposites: synthesis, properties, and applications,* Wiley, New Jersey, USA.

Moniruzzaman M., Winey I. K. (2006) Polymer nanocomposites containing carbon nanotubes. *Macromolecules*, Vol. 39, pp. 5194–5205.

Nair C. P. R., Mathew D., Ninan K. N. (2000) Cyanate ester resins, recent developments. *Adv. Polym. Sci.*, Vol. 155**,** pp. 1–99.

Nilsen L. (1978) *Mechanical properties of polymers and polymer compositions*, Khimiya, Moscow, Russia (translation to Russian).

Oberlin A., Endo M., Koyama T. (1976) *High resolution electron microscope observations of graphitized carbon fibers*. *Carbon*, Vol. 14, pp. 133–135.

Okotrub A. V., Yudantsov N. F., Aleksashin V. M. (2007) Study of thermal and mechanical properties of composites from electroarc carbon nanotubes and thermostable binder based on cyanate ester. *Vysokomol. Soed. A.* Vol. 49, pp. 1049–1055. (in Russian).

Osei-Owusu A., Martin G. C. (1992) Catalysis of cyclotrimerization of cyanate ester resin systems. *Polym. Eng. Sci.,* Vol. 32, pp. 535–541.

Paul D., Robeson L. M. (2008) Polymer nanotechnology: nanocomposites. *Polymer***,** Vol. 49, pp. 3187–3204.

Penczek P., Kaminska W. (1990) Polyfunctional cyanate monomers as components of polymer systems, In: *Adv. Polym. Sci.*, Springer-Verlag, Berlin, Germany, Vol. 97, pp. 41–60.

Radushevich L. V., Luk’yanovich V. M. (1952) Structure of carbon formed at thermal decomposition of carbon oxide on iron contact. *Jurnal Fizicheskoy Khimii*, Vol. 26, pp. 88–95. (in Russian).

Saito R., Dresselhaus G., Dresselhaus M. S. (1998) *Physical properties of carbon nanotubes*, Imperial College Press, London, UK.

Sahimi M. (Ed.) (1994) *Applications of percolation theory*, Taylor & Francis, London, UK.

Snow A. W. (1994) The synthesis, manufacture and characterization of cyanate ester monomers, In: *Chemistry and Technology of Cyanate Ester Resins*, Chapman & Hall: Glasgow, UK.

Silberglitt R. (2004) Nanomaterials: new trends, In: *Dekker encyclopedia of nanoscience and nanotechnology*, Dekker Inc., New York, USA.

Sheng P. L. (1980) Fluctuation-Induced tunneling conduction in disordered materials. *Phys. Rev., B***,** Vol. 21, No 6, pp. 2180–2195.

Stauffer D., Aharony A. (1992) *Introduction to percolation theory*, Taylor & Francis, London, UK.

Tanaka K., Yamabe T., Fukui K. (1999) *The science and technology of carbon nanotubes*, Elsevier, Amsterdam, The Netherlands.

Tang Y. S., Kong J., Gu J. W., Liang G-Z. (2009) Reinforced cyanate ester resins with carbon nanotubes: surface modification, reaction activity and mechanical properties analyses. *Polym.-Plast. Technol. Eng.*, Vol. 48, pp. 359–366.

Trefilov V. I., Shchur D. V., Tarasov B. P. (2001) *Fullerenes – the base for future materials,* ADEF-Ukraine, Kyiv, Ukraine (in Russian).

Tseng C. H., Wang C. C., Chen C. Y. (2007) Functionalizing Carbon Nanotubes by Plasma Modification for the Preparation of Covalent-Integrated Epoxy Composites. *Chem. Mater.*, Vol. 19, pp. 308–315.

Zhang Z. F., Liu T., Sreekumar T. V., Kumar S., Moore V. C., Hauge R. H., Smalley R. E. (2003) Poly(vinyl alcohol)/SWNT composite film. *Nano Lett.*, Vol. 3, pp. 1285–1288.

Zussman E., Yarin A. L., Bazilevsky A.V., Avrahami R., Feldman M. (2006) Electrospun polyaniline/poly(methyl methacrylate)-derived turbostratic carbon micro-/nanotubes. *Adv. Mater.,* Vol. 18, pp. 348–353.

Ulanski J., Kryszewski M. (1995) Electrical conductivity in heterogeneous organic polymeric systems. *Polish J. Chem.,* Vol. 69**,** pp. 651–673.

Wei B. Q, Vajtai R., Ajayan P.M. (2001) Reliability and current carrying capacity of carbon nanotubes. *Appl. Phys. Lett*., Vol. 79, pp. 1172–1174.

Yevgen MAMUNYA

Dr. Yevgen Mamunya was graduated as PhD (with a speciality - polymer chemistry), and afterwards as Dr Sci (with a speciality - physics of polymers) in the Institute of Macromolecular Chemistry (IMC) of National Academy of Sciences of Ukraine (NASU). He is currently Head of the research group in IMC and Director of the Centre of Collective Use of scientific Equipment (CCUE) in NASU. During his scientific career he embraced a broad range of research topics, namely the investigations of the effect of gamma-radiation and cold plasma on polymers, and the radical reactions induced; the study of polymer blends, filled polymer blends and polymer composites – mechanical properties, structure, morphology, rheology; the investigations of electrical and physical properties of polymer composites, nanocomposites and organic-inorganic systems – electrical and thermal conductivity, dielectric properties, morphology, rheology, surface characteristics. He engaged as an active member of the New York Academy of Sciences (1995), a member of American Chemical Society (2006), a laureate of the NASU prize in polymer chemistry (2009); he is a member of the editorial board of two Ukrainian scientific journals. Part of his efforts is devoted to the reviewing activity in many international scientific journals and to the work as a member of juries for confering on scientific degrees in the Ukrainian Academic institutions. He is an author of more than 180 publications in scientific journals and a numerous presentations on international conferences.

Maksym IURZHENKO

Dr. Maksym Iurzhenko is the senior staff scientist in the Institute of Macromolecular Chemistry (IMC) of the National Academy of Sciences of Ukraine (NASU), and Deputy Director of the Center of Collective Use of scientific Equipment (CCUE) of the National Academy of Scinces of Ukraine that is specialized in thermophysical investigations and analysis of polymer, composites and biomaterials, and assistant coordinator of the Central and East European Polymer Network (CEEPN) in Ukraine. He is PhD in Polymer Physics (Ukraine) and Docteur en Physique in Materiaux Polymeres et Composites (University Claude Bernard Lyon 1, France). Among his wide scientific interests the main part is taken by investigations of hybrid organic-inorganic composites and nanocomposites, electroactive polymer systems and nanosystems, their synthesis, rheology, structure and morphology, thermo and electrophysical properties, namely thermal, mechanical, thermomechanical, electrical (on DC and AC measurements) and dielectric (using microDielectric Spectroscopy, Broadband Dielectric Spectroscopy and Impedance spectroscopy); computer modeling of their structure and properties. Due to his scientific activity he is a laureate of the Eiffel Doctorant Grant of the French Government in SDV-BIO-NANO (2007), NASU Grant in chemistry (2009) and Grant of the President of Ukraine (2011). More than 50 publications, including papers in the high ranked scientific journals are in his professional account.

"If you have no fundamental investigations today you will have nothing to apply tomorrow..."

Prof. N. Bogolyubov,
Director of JINR - Dubna (1966—1988)

ISBN 978-973-702-902-7

9 789737 029027

Published
in EU

Open access:

http://www.tehnopress.ro

http://www.macromol.kiev.ua/CCUE/